The role of Notch1 N-glycans and their impact on myogenic differentiation of resident vascular stem cells.

A dissertation submitted for the degree of Ph.D

by

Eoin Corcoran

BSc. Genetics and Cell Biology

Under the supervision of

Prof. Paul A. Cahill

School of Biotechnology

Dublin City University

August 2021

DECLARATION

I hereby certify that this material, which I now submit for assessment on the programme of study leading to the award of PhD is entirely my own work, and that I have exercised reasonable care to ensure that the work is original, does not to the best of my knowledge breach any law of copyright, and has not been taken from the work of others save and to the extent that such work has been cited and acknowledged within the text of my work.

Signed:  ID No.: 16213692 Date: 24/08/2021

Acknowledgements

First and foremost, I would like to thank my supervisor Prof. Paul Cahill. From the moment I stepped into the lab and became part of your research group, you never stopped encouraging me and pushing me to reach my potential. You always showed unwavering faith in me and never doubted my ability to accomplish my goals. For this, and everything else, I will be forever grateful.

I would also like to express my gratitude towards the rest of the academic staff in the School of Biotechnology, in particular Dr. Brendan O'Connor and Dr. Dermot Walls, who would have given me all of the hours in their day if they felt it would help me. Your guidance and kindness pulled me out of a few deep ruts throughout the last 5 years.

To the unsung heroes of the School of Biotechnology, the technical staff, I cannot thank you enough for all of the times you bailed me out of seemingly impossible situations. No problem was ever too large that you couldn't fix and every one of you went above and beyond to make life easier for myself and all of the other postgrads in the School. Graham, Monica, Deirdre, David, Janice, Teresa, Kasia, Allison and Carmen, my experience over the last five years would have been a lot less enjoyable without your help and generosity.

Next, I would like to acknowledge the members of my lab group who supported me so regularly throughout this experience. Abi, Roya, Mariana and Claire, you welcomed me into the lab and showed unnatural levels of patience to teach me everything I know today. Each one of you inspired me and stood out as a shining example of how to be a great researcher and mentor.

A PhD can often be a very isolating experience, especially when things are going wrong. I was very lucky to have friends in the same position as myself with whom I could share both my failures and my victories. I fully believe that I would not have made it even close to finishing this project and this thesis without my good friends Denise, Susan, Arabelle, Conor and Yusof. You made every day more manageable and enjoyable. My fondest memories of this experience will be of the laughing we did together and the ferocious ranting sessions that sometimes had the effect of abating my frustration, but more often ended with us winding each other up even more (especially when Denise was involved)!

I would also like to thank all of my friends outside the bubble of DCU, especially Jack, Butch, Andy, Paul and Lowry. I could count on every single one of you for advice and

support whenever I needed it, even if it was often accompanied by a few sneery digs! The last 5 years were only made possible by the craic that we had, the pints that we drank and the rot that we talked. All of the slagging kept me grounded, the sessions kept me sane and your complete and utter indifference to all things science kept my life in balance. Thanks lads.

Another person who played no small part in the completion of this project is my girlfriend, Amie. You've been my own personal cheerleader for the last two years and it's safe to say that the size of my head has at least doubled in that time thanks to your unyielding belief in my abilities. Whenever something went wrong, I felt safe in the knowledge that one conversation with you would make things better, whether that was by making me laugh, finding a silver lining or just flat out planning entire experiments for me! Thanks for everything.

Finally, I would like to thank my family. For Joey and Siún, it must have been a living nightmare to have a brother who spent 80% of his time complaining about the PhD (and the other 20% complaining about injuries), but you managed to bear it without killing me and even chipped in with the odd few words of wisdom or advice. There is no combination of words that could do justice to the debt of gratitude I owe to my parents, Vinny and Teresa, for all the ways in which they helped me to succeed in this endeavour. The support I received from you, both financially and emotionally, will never be forgotten. It is the most comforting thought in the world to know that no matter what happens in life there are two people out there who are directing every fibre of their being towards making sure you are happy and healthy and have the means to achieve the absolute limits of your potential.

Table of Contents

Chapter 1: Introduction 1

1.1 Structure of the Artery 2

1.2 Cardiovascular Disease 3

1.2.1 Atherosclerosis 4
1.2.2 Primary Artery Calcification 5
1.2.3 Fibromuscular Intimal Thickening 5

1.3 Current treatments for CVD 7

1.3.1 Drug treatments for CVD 7
1.3.1.1 Statins 7
1.3.1.2 Anti-coagulants 8
1.3.1.3 Beta blockers and ACE inhibitors 8
1.3.2 Surgical Interventions 9
1.3.2.1 In-stent Restenosis 9

1.4 Origin of Neointimal Cells 11

1.4.1 De-differentiated SMCs 11
1.4.2 Endothelial cells 13
1.4.3 Bone marrow-derived Stem Cells 13
1.4.4 Resident Vascular Stem Cells 15

1.5 Notch Signalling 16

1.5.1 History of Notch 16
1.5.2 Notch receptors and ligands 17
1.5.2 Notch Signalling and Stem Cell Fate 19
1.5.3 Notch in Disease 21
1.5.4 Notch in Vascular Remodelling 22
1.5.5 Regulation of Notch Signalling 23

1.6 Glycosylation 24

1.6.1 N-linked Glycosylation 25
1.6.2 O-linked Glycosylation 26

1.7 Glycosylation and Notch Signalling 27

1.7.1 Notch O-glycosylation 27
1.7.2 Notch N-glycosylation 29

1.8 Detecting N-glycans 30

1.8.1 Structural Analysis 31
1.8.2 Lectin Technology 31
1.8.2.1 Lectin Microarrays 32
1.8.2.2 Serial Lectin Affinity Chromatography 32
1.8.2.3 Enzyme-linked Lectin Assay 32

1.9 Methods for Investigating the Effect of N-glycosylation ... 34

1.9.1 Chemical Inhibitors 34
1.9.2 siRNA Technology 35
1.9.3 DNA Mutation Methods 36

1.10 Aims and Objectives 37

Chapter 2: Materials and Methods 38

2.1 Materials 39

2.2 Methods 45

2.2.1 Genetic Lineage Tracing of S100β Stem cells and assessment of their contribution to neointimal lesions *in vivo* 45
2.2.2 Isolation of MVSCs from mouse aorta by enzymatic dispersion 46
2.2.3 Cell Culture Methods 46
2.2.3.1 MVSCs 46
2.2.3.2 mSMC 47
2.2.3.3 mC3H 47
2.2.3.4 Subculturing 47
2.2.3.5 Viable Cell Counting 47
2.2.3.6 Cryopreservation 48
2.2.4 Plasmid Amplification and Purification 48
2.2.4.1 Transformation 48
2.2.4.2 Plasmid DNA Purification 49
2.2.4.3 Agarose Gel Electrophoresis 49
2.2.5 Notch1 Activation using Jagged1 (Jag1) 50
2.2.6 Transient Transfections 50
2.2.6.1 Plasmid Transfection 50
2.2.6.2 siRNA Transfection 51
2.2.7 Immunocytochemistry 51
2.2.8 RNA Extraction 52
2.2.9 Genomic DNA Extraction 53
2.2.10 Quantitation of Nucleic Acid Concentration 53
2.2.11 Quantitative Reverse-Transcription Polymerase Chain Reaction (qRT-PCR) 53
2.2.12 Protein Isolation and Quantitation 55
2.2.13 Membrane Protein Isolation 56
2.2.14 Telomerase Activity Assay 56
2.2.15 Immunoprecipitation 57
2.2.16 Western Blot 58
2.2.17 Enzyme-Linked Lectin Assay (ELLA) 59
2.2.18 Site-directed mutagenesis 61
2.2.19 Data Analysis and Statistics 62

Chapter 3: Characterisation of MVSCs and their response to Jag-1 treatment 63

3.1 Introduction 64

3.2 Strategy 65

3.3 Results 68

3.3.1 Identification of Neointimal Cells Derived from an S100β^{+} Parent Population 68
3.3.2 Characterisation of MVSCs and C3Hs 70
3.3.3 Measurement of Telomere Length in MVSCs 72
3.3.4 Measurement of Telomerase Activity in MVSCs 72
3.3.5 Adipogenic and Osteogenic Differentiation of MVSCs 75

3.3.6 Jag-1 activation of Notch Signalling and Myogenic Differentiation in MVSCs 77
3.3.6 Inhibition of Jag-1 mediated Notch activation using DAPT 83
3.3.7 Measurement of siRNA transfection efficiency in MVSCs 85
3.3.8 Effect of Notch1 knockdown on Jag-1-mediated Notch signalling and Myogenic differentiation 88
3.4 Discussion 93
Chapter 4: The Effect of Small-molecule N-glycosylation Inhibitors on Notch Signalling and Myogenic Differentiation 102
4.1 Introduction 103
4.2 Strategy 104
4.3 Results 107
4.3.1 Purification of Notch1 by Immunoprecipitation 107
4.3.2 Ectopic Expression of Myc-tagged Notch1 and NICD 109
4.3.3 N-glycosylation Profile of Purified Notch1 110
4.3.4 Effect of TNC and DMJ Inhibitors on global N-glycosylation 113
4.3.5 Effect of TNC and DMJ on Notch1 N-glycosylation 114
4.3.6 TNC Treatment of Jag-1-stimulated MVSCs and C3Hs 120
4.3.7 DMJ Treatment of Jag-1-stimulated MVSCs and C3Hs 120
4.3.8 TNC and DMJ Treatment of NICD-stimulated MVSCs 129
4.3.9 Effect of TNC and DMJ on Notch1 Expression in MVSCs 129
4.3.10 Membrane Fractionation of MVSC Protein Lysate 136
4.3.11 Effect of TNC and DMJ on Membrane Localisation of Notch1 138
4.3.12 Effect of TNC and DMJ on Trafficking of Notch1 Receptor 140
4.4 Discussion 142
Chapter 5: The Effect of GnT-III and Fut8 knockdown on Notch Signalling and Myogenic Differentiation 149
5.1 Introduction 150
5.2 Strategy 151
5.3 Results 153
5.3.1 Confirmation of *Mgat3* and *Fut8* transcript knockdown 153
5.3.2 Effect of *Mgat3* and *Fut8* knockdown on global N-glycosylation 158
5.3.3 Effect of *Mgat3* and *Fut8* knockdown on Notch1 N-glycosylation 161
5.3.4 *Mgat3* knockdown in Jag-1-stimulated MVSCs and C3Hs 163
5.3.5 *Fut8* knockdown in Jag-1-stimulated MVSCs and C3Hs 163
5.3.6 *Mgat3* and *Fut8* Knockdown in NICD-stimulated MVSCs 172
5.3.7 Effect of *Mgat3* and *Fut8* Knockdowns on Notch1 Expression in MVSCs 172
5.3.8 Effect of *Mgat3* and *Fut8* Knockdowns on Membrane Localisation of Notch1 179

5.3.9 Effect of *Mgat3* and *Fut8* Knockdowns on Trafficking of Notch1 Receptor....181
5.4 Discussion....183
Chapter 6: Effect of N-glycosylation site mutation on Notch1 signalling and myogenic differentiation....189
6.1 Introduction....190
6.2 Strategy....191
6.3 Results....194
6.3.1 Puromycin Cytotoxicity Titration in MVSCs and C3Hs....194
6.3.2 Plasmid Transfection Optimisation in MVSCs and C3Hs....197
6.3.3 Validation of Puromycin Selection in C3Hs....200
6.3.4 Site-directed Mutagenesis of Plasmid-encoded Notch1....202
6.3.5 Effect of Asparagine Mutations on Notch1 N-glycosylation....204
6.3.6 Effect of Asparagine Mutations on Jag-1 activation of C3Hs....206
6.3.7 Effect of Asparagine Mutations on Plasmid Transfection Efficiency....209
6.3.8 Effect of Asparagine Mutations on Notch1 Protein Levels....211
6.4 Discussion....213
Chapter 7: Final Discussion....219
7.1 Notch1 mediates myogenic differentiation in S100β⁺ MVSCs....221
7.2 N-glycosylation Profile of the Notch1 Receptor....223
7.3 N-glycans on Notch1 Regulate its Degradation and its Control of Myogenic Differentiation....225
7.4 Future Work....229
7.5 Conclusions....234
Bibliography....235
Appendices....271
Appendix A....272
Appendix B....274
Appendix C....276
Appendix D....276

Publications

Journal Articles

Fitzpatrick, E., Han, X., Liu, W., Corcoran, E., Burtenshaw, D., Morrow, D., Helt, J., Cahill, PA., Redmond, E., (2017) 'Alcohol reduces arterial remodeling by inhibiting Sonic Hedgehog-stimulated Stem Cell Antigen-1 positive progenitor cell expansion', *Alcoholism: Clinical and Experimental Research.* 41 (12). 2051-2065. DOI: 10.1111

Liu, W., Harman, S., Di Luca, M., Burtenshaw, D., Corcoran, E., Cahill, PA. and Redmond E., (2020) 'Moderate Alcohol Consumption Targets S100β+ Vascular Stem Cells and Attenuates Injury-Induced Neointimal Hyperplasia', *Alcoholism: Clinical and Experimental Research*. Blackwell Publishing Ltd, 44(9), pp. 1734–1746. doi: 10.1111/acer.14415.

Di Luca, M., Fitzpatrick, E., Burtenshaw, D., Liu, W., Helt, J., Hakimjavadi, R., Corcoran, E., Gusti, Y., Sheridan, D., Harman, S., Lally, C., Redmond, E. and Cahill, PA., (2021) 'The calcium binding protein S100β marks hedgehog-responsive resident vascular stem cells within vascular lesions', *npj Regenerative Medicine*. Nature Publishing Group, 6(1), p. 10. doi: 10.1038/s41536-021-00120-8.

Posters/Abstracts

Corcoran, E., Olayinka, A., O'Connor, B. and Cahill, PA., (2019) 'Abstract 476: The Role of N-glycosylation in the Myogenic Differentiation of Stem Cells to Vascular Smooth Muscle Cells', *Arteriosclerosis, Thrombosis, and Vascular Biology*. 38(Suppl_1), A476-A476. Doi: 10.1161/atvb.38.suppl_1.476

Corcoran, E., Olayinka, A., O'Connor, B. and Cahill, PA., (2019) 'Poster: The Role of N-glycosylation in the Myogenic Differentiation of Stem Cells to Vascular Smooth Muscle Cells' , *Scottish Cardiovascular Forum 2019*, University of the Highlands and Islands, Inverness, Scotland.

Corcoran, E., Olayinka, A., O'Connor, B. and Cahill, PA., (2019) 'Poster: N-glycosylation of Notch1 and the Regulation of Vascular Stem Cell Fate', *The Notch Meeting 2019*, Athens, Greece

Oral Presentations

'The Role of N-glycosylation in the Myogenic Differentiation of Stem Cells to Vascular Smooth Muscle Cells', *DCU School of Biotechnology Research Day 2018, 2019 and 2021*, Dublin City University, Glasnevin, Co. Dublin, Ireland.

List of Figures

Fig 1.1 Structure of the Artery

Fig 1.2 Vascular Remodelling

Fig 1.3 In-stent Restenosis

Fig 1.4 Origin of Neointimal Cells

Fig 1.5 Structure of the mammalian Notch receptor

Fig 1.6 Notch Signalling Pathway

Fig 1.7 O-linked and N-linked Glycosylation

Fig 1.8 Glycosylation of the Notch Receptor

Fig 1.9 Enzyme-linked Lectin Assay (ELLA)

Fig 2.1 Immunocytochemistry

Fig 2.2 qRT-PCR

Fig 2.3 Telomerase Activity Assay

Fig 2.4 Western Blot

Fig 2.5 ELLA

Fig 3.1 S100β Lineage Tracing Model

Fig 3.2 Characterisation of MVSCs and C3Hs

Fig 3.3 Relative Telomere Length in Different Cell Lines

Fig 3.4 Telomerase Activity in Aortic Tissue and MVSCs

Fig 3.5 MVSC Multipotency

Fig 3.6 Expression of *Hey1* in Jag-1-treated MVSCs

Fig 3.7 Expression of *Myh11* in Jag-1-treated MVSCs

Fig 3.8 Expression of *Hey1* in Jag-1-treated C3Hs

Fig 3.9 Expression of *Myh11* in Jag-1-treated C3Hs

Fig 3.10 Protein expression of Cnn1 in Jag1-treated MVSCs

Fig 3.11 DAPT inhibition of Jag-1 response in MVSCs

Fig 3.12 siRNA Transfection Efficiency of MVSCs

Fig 3.13 siRNA Transfection Efficiency of C3Hs

Fig 3.14 Expression of *Notch1* transcript in MVSCs following Notch1 siRNA knockdown

Fig 3.15 Expression of Notch1 protein in MVSCs following Notch1 siRNA knockdown

Fig 3.16 Effect of Notch1 knockdown on *Hey1* expression in Jag-1-treated MVSCs

Fig 3.17 Effect of Notch1 knockdown on *Myh11* expression in Jag-1-treated MVSCs

Fig 4.1 Optimisation of Notch1 Immunoprecipitation

Fig 4.2 Ectopic expression of myc-tagged Notch1 and NICD in MVSCs

Fig 4.3 N-glycosylation profile of the purified Notch1 receptor

Fig 4.4 Effect of TNC on N-glycosylation in MVSCs

Fig 4.5 Effect of TNC on N-glycosylation in C3Hs

Fig 4.6 Effect of DMJ on N-glycosylation in MVSCs

Fig 4.7 Effect of DMJ on N-glycosylation in C3Hs

Fig 4.8 Effect of TNC and DMJ on N-glycosylation of the Notch1 receptor

Fig 4.9 Effect of TNC on *Hey1* expression in Jag1-treated MVSCs

Fig 4.10 Effect of TNC on *Hey1* expression in Jag1-treated C3Hs

Fig 4.11 Effect of TNC on *Myh11* expression in Jag1-treated MVSCs

Fig 4.12 Effect of TNC on *Myh11* expression in Jag1-treated C3Hs

Fig 4.13 Effect of DMJ on *Hey1* expression in Jag1-treated MVSCs

Fig 4.14 Effect of DMJ on *Hey1* expression in Jag1-treated C3Hs

Fig 4.15 Effect of DMJ on *Myh11* expression in Jag1-treated MVSCs

Fig 4.16 Effect of DMJ on *Myh11* expression in Jag1-treated C3Hs

Fig 4.17 Effect of TNC on NICD-activated *Hey1* expression in MVSCs

Fig 4.18 Effect of DMJ on NICD-activated *Hey1* expression in MVSCs

Fig 4.19 Effect of TNC on NICD-activated *Myh11* expression in MVSCs

Fig 4.20 Effect of DMJ on NICD-activated *Myh11* expression in MVSCs

Fig 4.21 Effect of TNC and DMJ on *Notch1* transcript expression in MVSCs

Fig 4.22 Effect of TNC and DMJ on Notch1 protein expression in MVSCs

Fig 4.23 Validation of Membrane Fractionation Method

Fig 4.24 Effect of TNC and DMJ on Membrane Localisation of Notch1

Fig 4.25 Effect of TNC and DMJ on Notch1 Receptor Trafficking

Fig 5.1 Expression of *Mgat3* transcript in MVSCs following *Mgat3* siRNA knockdown

Fig 5.2 Expression of *Fut8* transcript in MVSCs following *Fut8* siRNA knockdown

Fig 5.3 Expression of *Mgat3* transcript in C3Hs following *Mgat3* siRNA knockdown

Fig 5.4 Expression of *Fut8* transcript in C3Hs following *Fut8* siRNA knockdown

Fig 5.5 Effect of *Mgat3* and *Fut8* knockdowns on N-glycosylation in MVSCs

Fig 5.6 Effect of *Mgat3* and *Fut8* knockdowns on N-glycosylation in C3Hs

Fig 5.7 Effect of *Mgat3* and *Fut8* knockdowns on N-glycosylation of the Notch1 receptor

Fig 5.8 Effect of *Mgat3* knockdown on *Hey1* expression in Jag-1-treated MVSCs

Fig 5.9 Effect of *Mgat3* knockdown on *Hey1* expression in Jag-1-treated C3Hs

Fig 5.10 Effect of *Mgat3* knockdown on *Myh11* expression in Jag-1-treated MVSCs

Fig 5.11 Effect of *Mgat3* knockdown on *Myh11* expression in Jag-1-treated C3Hs

Fig 5.12 Effect of *Fut8* knockdown on *Hey1* expression in Jag-1-treated MVSCs

Fig 5.13 Effect of *Fut8* knockdown on *Hey1* expression in Jag-1-treated C3Hs

Fig 5.14 Effect of *Fut8* knockdown on *Myh11* expression in Jag-1-treated MVSCs

Fig 5.15 Effect of *Fut8* knockdown on *Myh11* expression in Jag-1-treated C3Hs

Fig 5.16 Effect of *Mgat3* knockdown on NICD-activated *Hey1* expression in MVSCs

Fig 5.17 Effect of *Mgat3* knockdown on NICD-activated *Myh11* expression in MVSCs

Fig 5.18 Effect of *Fut8* knockdown on NICD-activated *Hey1* expression in MVSCs

Fig 5.19 Effect of *Fut8* knockdown on NICD-activated *Myh11* expression in MVSCs

Fig 5.20 Effect of *Mgat3* and *Fut8* knockdowns on *Notch1* transcript expression in MVSCs

Fig 5.21 Effect of *Mgat3* and *Fut8* knockdowns on Notch1 protein expression in MVSCs

Fig 5.22 Effect of *Mgat3* and *Fut8* knockdowns on Membrane Localisation of Notch1

Fig 5.23 Effect of *Mgat3* and *Fut8* knockdowns on Notch1 Receptor Trafficking

Fig 6.1 Puromycin cytotoxicity titration in MVSCs

Fig 6.2 Puromycin cytotoxicity titration in C3Hs

Fig 6.3 Plasmid transfection efficiency in MVSCs

Fig 6.4 Plasmid transfection efficiency in C3Hs

Fig 6.5 Validation of Puromycin Selection in C3Hs

Fig 6.6 Mutant plasmid sequence alignment

Fig 6.7 Effect of asparagine mutations on N-glycosylation of Notch1

Fig 6.8 Effect of asparagine mutations on *Hey1* expression in Jag-1-treated C3Hs

Fig 6.9 Effect of asparagine mutations on *Myh11* expression in Jag-1-treated C3Hs

Fig 6.10 Effect of asparagine mutations on Plasmid Transfection Efficiency in C3Hs

Fig 6.10 Effect of asparagine mutations on Notch1 protein levels

Fig 7.1 Example of Glycan Structural Analysis by MS

List of Tables

Table 2.1 Mammalian Cell Lines used in this study

Table 2.2 Bacterial Cell Lines used in this study

Table 2.3 Primers used in this study from Qiagen

Table 2.4 Primers used in this study from Integrated DNA Technologies

Table 2.5 Plasmid Vectors used in this study

Table 2.6 siRNA molecules used in this study

Table 2.7 Antibodies used in this study

Table 2.8 Chemicals, Reagents, Proteins and Kits used in this study

Table 2.9 Plasmid Transfection Complex Tube setup with Mirus TransIT-X2

Table 2.10 siRNA Transfection Complex Tube setup with Mirus TransIT-X2

Table 2.11 qRT-PCR reaction tube setup with Bioline Sensifast Kit

Table 2.12 qRT-PCR programme setup with Bioline Sensifast Kit

Table 2.13 qRT-PCR reaction tube setup with Qiagen SYBR Green Kit

Table 2.14 qRT-PCR programme setup with Qiagen SYBR Green Kit

Table 2.15 Carbohydrate binding specificity of lectins used in this study

Table 2.16 PCR reaction tube setup with QuikChange Lightning Kit

Table 2.17 PCR programme setup with QuikChange Lightning Kit

Table 5.1 Summary of findings from small-molecule inhibitor and siRNA knockdown experiments

Table 7.1 N-Glycan Structures and Possible Roles on the Notch1 Receptor

Abbreviations

ACE	Angiotensin Converting Enzyme
ADAM10	Disintegrin and metalloproteinase domain-containing protein 10
ADCC	Antibody-dependent Cellular Cytotoxicity
Alpl	Alkaline Phosphatase Biomineralisation Associated
ANK	Ankyrin
ANOVA	Analysis of Variance
ASM	Acid Sphingomyelinase
Asn	Asparagine
BCA	Bicinchoninic Acid
BFA	Brefeldin A
BMD-SC	Bone Marrow Derived Stem Cell
BMS	Bare Metal Stent
BSA	Bovine Serum Albumin
CAV	Cardiac Allograft Vasculopathy
CBF1	Cp-binding factor 1
cDNA	Complementary DNA
CNN1	Calponin 1
ConA	Concanavalin A
CRISPR	Clustered Regularly Interspersed Short Palindromic Repeats
CSL	CBF1, Suppressor of Hairless, Lag-1
CVD	Cardiovascular Disease
DAPI	4′,6-diamidino-2-phenylindole
DAPT	N-[N-(3, 5-difluorophenacetyl-L-alanyl)]-S-phenylglycine t-butyl ester
DEPC	Diethyl Pyrocarbonate
DES	Drug-eluting Stent
DLL	Delta-like ligand
Dlk-1	Delta-like non-canonical Notch ligand 1
DMEM	Dulbecco's Modified Eagle's Medium
DMJ	1-deoxymannojirimycin
DMSO	Dimethyl Sulfoxide
DNA	Deoxyribonucleic acid
DON	6-diazo-5-oxo-L-norleucine

DPBS	Dulbecco's Phosphate Buffered Saline
DPPIV	Dipeptidylpeptidase IV
EC	Endothelial Cell
ECL	*Erythrina critagalli* lectin
EDTA	Ethylenediaminetetraacetic acid
EEL	External Elastic Lamina
EGF	Epidermal Growth Factor
ELISA	Enzyme-linked Immunosorbent Assay
ELLA	Enzyme-linked Lectin Assay
EMEM	Eagle's Modified Essential Medium
EndMT	Endothelial to Mesenchymal Transition
E-PHA	Phaseolus Vulgaris Erythroagglutinin
ER	Endoplasmic Reticulum
ESI	Electrospray Ionization
Fabp4	Fatty acid binding protein 4
FBS	Fetal Bovine Serum
FGF	Fibroblast Growth Factor
FIT	Fibromuscular Intimal Thickening
FSH	Follicle-Stimulating Hormone
FSP-1	Fibroblast-specific Protein-1
FUT	Fucosyltransferase
GA	Golgi Apparatus
GalNAc	N-acetylgalactosamine
Galnt11	Polypeptide N-acetylgalactosaminyltransferase 11
Glc	Glucose
GlcNAc	N-acetylglucosamine
GnT	N-acetylglucosaminyltransferase
HBSS	Hanks Balanced Salt Solution
HD	Hydrophobic Domain
Hes	Hairy/enhancer of split
Hey	Hairy/enhancer-of-split related with YRPW motif protein 1
HPC	Hematopoietic Progenitor Cell
HPLC	High-performance Liquid Chromatography
HPRT	Hypoxanthine phosphoribosyltransferase 1
HRP	Horseradish Peroxidase

IEL	Internal Elastic Lamina
IgG	Immunoglobulin
IP	Immunoprecipitation
ISR	In-stent Restenosis
LAMP1	Lysosomal-associated membrane protein 1
LB	Lysogeny Broth
LBD	Ligand-binding domain
LCA	Lens Culinaris Agglutinin
LCA	Left Carotid Artery
LCAT	Lecithin:cholesterol acyltransferase
LDL-C	Low Density Lipoprotein Cholesterol
LIF	Leukaemia Inhibitory Factor
LNR	Lin12 repeat
L-PHA	Phaseolus Vulgaris Leucoagglutinin
Lpl	Lipoprotein lipase
Man	Mannose
MEM	Minimum Essential Medium
Mesp2	Mesoderm Posterior BHLH Transcription Factor 2
Mgat3	Mannosyl (Beta-1,4-)-Glycoprotein Beta-1,4-N-Acetylglucosaminyltransferase
Mib	Mindbomb
MINT	Msx2-interacting nuclear target protein
MM1	Maintenance Medium 1
mRNA	Messenger RNA
MS	Mass Spectrometry
MVSC	Multipotent Vascular Stem Cell
Myh11	Myosin Heavy-chain 11
NECD	Notch Extracellular Domain
Neu	Neuralized
NICD	Notch Intracellular Domain
NRR	Negative Regulatory Region
NTM	Notch1 Transmembrane Domain
OD	Optical Density
Ofut1	O-fucosyltransferase 1
OST	Oligosaccharyltransferase

PBS	Phosphate Buffered Saline
PCR	Polymerase Chain Reaction
PEST	Proline (P), Glutamic Acid (E), Serine (S), Threonine (T)
PNGase F	Peptide: N-glycosidase F
Pofut1	Protein O-fucosyltransferase 1
Poglut1	Protein O-glucosyltransferase 1
PTEN	Phosphatase and tensin homolog
PTM	Post-translational modification
PVA	Polyvinyl alcohol
qRT-PCR	Quantitative Reverse Transcriptase Polymerase Chain Reaction
RAM	RBP-Jkappa associated module
RBP-Jκ	Recombination signal sequence-binding protein Jkappa
RCA	Right Carotid Artery
RER	Rough Endoplasmic Reticulum
RIP	Regulated Intramembrane Proteolysis
RIPA	Radioimmunoprecipitation assay
RNA	Ribonucleic acid
RPMI	Roswell Park Memorial Institute
RTK	Receptor Tyrosine Kinase
S100β	S100 Calcium-binding protein β
Sca1	Stem Cell Antigen 1
scRNA-Seq	Single cell RNA Sequencing
SDS	Sodium Dodecyl Sulphate
SEM	Standard Error Margin
Ser	Serine
shRNA	Short hairpin RNA
siRNA	Short interfering RNA
SLAC	Serial Lectin Affinity Chromatography
SMC	Smooth Muscle Cell
SM-MHC	Smooth Muscle Myosin Heavy Chain
SOC	Super Optimal broth with Catabolite repression
Sost	Sclerostin
Sox10	Sry-related HMg-box gene 10
Sox17	Sry-related HMg-box gene 17
SRF	Serum Response Factor

SRP	Signal Recognition Particle
STL	*Solanum tuberosum* lectin
TE	Tris-EDTA
TG	Thioglycerol
TGF-β	Transforming Growth Factor Beta
Thr	Threonine
TMB	3,3',5,5'-Tetramethylbenzidine
TMD	Transmembrane domain
TNC	Tunicamycin
TRAP	Telomerase Repeated Amplification Protocol
VEGF	Vascular Endothelial Growth Factor
VSMC	Vascular Smooth Muscle Cell
VWF	von Willebrand Factor
WGA	Wheat Germ Agglutinin
Wnt	Wingless-related integration site
WT	Wild-type

Units of measurement

^{o}C	Degrees Celsius
cm	centimetre
g	grams
hr	hour
L	litre
M	molar
mg	milligram
min	minute
mL	millilitre
mM	millimolar
nm	nanometre
nM	nanomolar
rpm	revolutions per minute
sec	second
TPG	Total Protein Generated
µL	microlitre
µg	microgram
µm	micrometre
µM	micromolar
x g	G force

Abstract

The role of Notch1 N-glycans and their impact on myogenic differentiation of resident vascular stem cells

Eoin Corcoran

Hypothesis: N-glycosylation of the Notch1 receptor regulates Notch signalling and Notch-dependent myogenic differentiation in S100β$^+$ multipotent vascular stem cells

Cardiovascular disease (CVD) is characterized by a thickening of blood vessel walls. This leads to the formation of a neointima, which occludes the lumen and restricts blood flow to vital organs. Mounting evidence suggests that resident stem cells in the vasculature may give rise to the smooth muscle-like cells which make up this neointima. In particular, a group of S100β$^+$ cells, termed multipotent vascular stem cells (MVSCs), have been reported to contribute significantly to neointimal formation. Recent studies have shown that activation of Notch signalling, and Notch1 in particular, may be pivotal in this process as it is heavily involved in regulating stem cell fate and in directing myogenic differentiation. The Notch signalling pathway is highly regulated by a number of mechanisms including glycosylation. While the importance of O-linked glycosylation has been extensively described, the structures and roles of N-glycans on the Notch1 receptor have yet to be defined.

The current study presents novel findings which confirm that activation of the Notch1 receptor by its ligand, Jag-1, stimulates myogenic differentiation in S100β$^+$ MVSCs isolated from a mouse aortic arch. Furthermore, N-glycosylation intervention strategies, including small-molecule inhibition (using tunicamycin and 1-deoxymannojirimycin), siRNA knockdown of the GnT-III and Fut8 glycosyltransferases, and site-directed mutagenesis of N-glycosylation sites, revealed that this process is heavily regulated by N-glycans which reside at six consensus sequences along the extracellular domain of Notch1. A number of key oligosaccharides at these sites were found to contain bisecting or core fucosylated structures. Notch1 expression and trafficking analysis indicated that N-glycans at asparagine (N) 1241 and 1587 protect the receptor from accelerated degradation, while the oligosaccharide at N888 directly affects signal transduction. Conversely, N-linked glycans at the other three sites do not impact canonical Notch1 signalling but still play a role in

Notch-mediated myogenic differentiation, possibly via a non-canonical Notch signalling pathway. The findings in the current study provide novel insights into the location and structure of N-glycans on the Notch1 receptor, as well as illuminating some of the likely mechanisms by which they regulate Notch signalling and myogenic differentiation in a CVD-relevant vascular stem cell population.

Chapter 1:

Introduction

1.1 Structure of the Artery

In mammals the vascular system is made up of an intricate network of vessels whose job it is to transport blood around the body. Arteries carry blood away from the heart to a range of different tissues in order to provide the cells in those tissues with the necessary components required to survive. In order to do this, an artery is made up of a number of different layers (Fig 1.1).

The tunica intima/endothelium is the innermost layer of the artery. It surrounds the lumen and consists of a monolayer of endothelial cells and a sub-endothelial support structure. As the point of contact between the artery and the blood, endothelial cells possess a number of characteristics to aid normal blood flow and prevent disease development. For example, the smooth, flat structure of these cells allows for frictionless flow of blood through the vessel to reduce shear stress on vascular cells (Gimbrone *et al.*, 2000). Additionally, endothelial cells express high levels of anti-inflammatory and anti-thrombotic proteins in response to changes in blood flow dynamics (Berk *et al.*, 2008).

The intimal layer is separated from the tunica media by a layer of connective tissue and elastic fibres known as the internal elastic lamina (Roostalu and Wong, 2018). The tunica media is the middle layer and consists mainly of smooth muscle cells which contract to narrow the lumen and create pressure for blood flow. In addition to these contractile smooth muscle cells, the medial layer contains pericytes, proteoglycans and a small population of resident stem cells (Tang *et al.*, 2012; Potter *et al.*, 2014).

The external elastic lamina separates the tunica media from the outermost layer: the tunica adventitia (also known as the tunica externa). The adventitia largely consists of connective tissue and collagen fibre but is also home to a number of sub-populations, including stem cells, mast cells, macrophages and adipocytes (Martini and Nath, 2011).

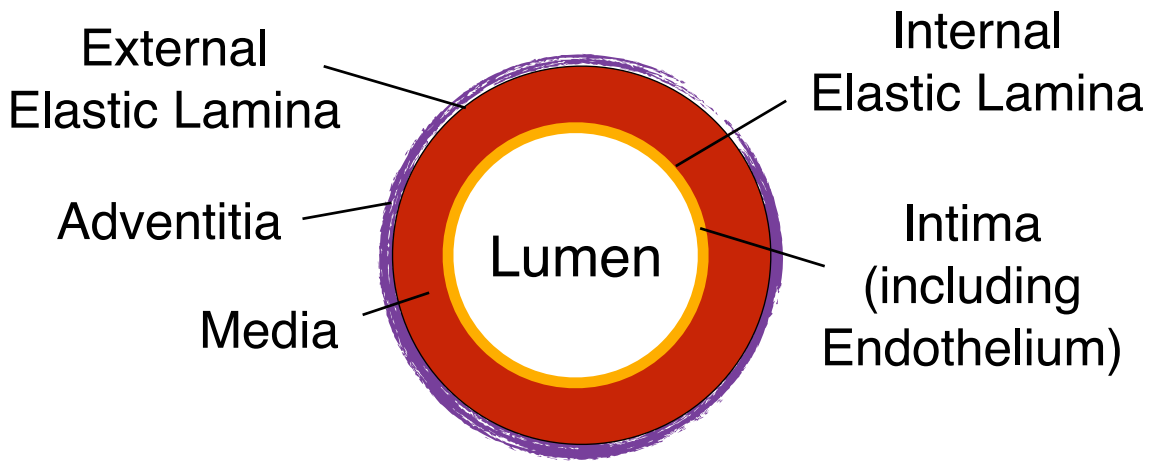


Fig 1.1 Structure of the Artery. Arteries transport oxygenated blood from the heart to all of the various organs and tissues of the body. They are composed of a series of well-defined layers with specialised functions and varying cell populations. Connective tissue and elastic fibres combine to form a number of lamina which separate these layers. The lumen refers to the space in the centre of the artery through which the blood flows.

1.2 Cardiovascular Disease

According to the World Health Organisation, cardiovascular disease (CVD) refers to any disorder of the heart or blood vessels and can often lead to a myocardial infarction (heart attack) or stroke. CVD is currently the most common cause of death worldwide with ischemic heart disease alone accounting for 16% of global deaths in 2019 (World Health Organisation, 2020).

The vast majority of CVD results from arterial remodelling where the flow of blood through the artery is blocked due to the thickening of the vessel wall. This prevents oxygen and nutrients from reaching cells in the body and can be fatal if the blockage is significantly large and not immediately treated. This thickening of the artery wall has been given the term arteriosclerosis. It can be difficult to categorise and distinguish between different forms of arteriosclerosis due to a large number of shared characteristics and a tendency for several forms to develop simultaneously. For a long period of time, the most widely used classification for arteriosclerotic lesions denoted three categories: atherosclerosis, Mönckeberg medial calcific sclerosis, and arteriolosclerosis (Robbins and Cotran, 2010). However, further study of the variation in instances of CVD has shown this classification to

be quite reductive. In 2009, a new classification was proposed to address this issue. Three main categories were described: atherosclerosis, primary artery calcification and fibromuscular intimal thickening which make up the majority of cases (albeit with further sub-types in each of those categories). A number of other less common categories were also identified, such as arterial hyalinosis, amyloidosis and oxalosis, but these will not be discussed in depth in this study (Fishbein and Fishbein, 2009).

1.2.1 Atherosclerosis

Atherosclerosis is the most common form of arteriosclerosis. It is classed as a chronic inflammatory disease and is characterised by the formation of a plaque known as an atheroma which occludes the lumen and leads to restricted blood flow (Andersson, Libby and Hansson, 2010). This atheroma forms asymmetrically in the vessel wall when a complex mixture of components such as cholesterol, lipids, foam cells and endothelial cells are deposited in the endothelium (Galkina and Ley, 2009). A fibrous cap forms over this core plaque and if the disease is left untreated this fibrous cap can rupture, resulting in an ischemic event that can be fatal (Ross, 1999). Hypertension can accelerate this process and lifestyle factors such as smoking, alcohol consumption and lack of exercise can increase the risk of atherosclerosis.

Subclinical atherosclerosis defines the initiation and progression of early atherosclerotic plaques and can be present in a number of different forms. Pathological intimal thickening (PIT) is one of the most widespread forms of subclinical atherosclerosis and has been widely reported to give rise to more advanced plaque lesions. It is characterised by macrophage infiltration, loss of intimal SMCs and the formation of an extracellular lipid pool (Kolodgie *et al.*, 2007). Adaptive intimal thickening (AIT), is generally present from birth and involves mild luminal occlusion involving only SMCs and the proteoglycan matrix, but without immune cell infiltration. However, AIT is often seen as a precursor to PIT as it allows for increased lipid retention in the vessel wall (Otsuka *et al.*, 2015). There are also multiple, less frequently observed forms of subclinical atherosclerosis which are not considered to be progression-prone. One such form is known as an intimal xanthoma (Sakamoto *et al.*, 2018). Intimal xanthomas are mostly composed of fat-laden macrophages and form a “fatty streak” in the vessel wall. They do not share many of the features associated with more advanced atherosclerotic plaques and usually regress over time (Virmani *et al.*, 2000).

Subclinical atherosclerosis is routinely modelled in rodents following surgical interventions, usually through partial ligation of a carotid artery which has been reported to result in full or partial flow obstruction with resultant hemodynamic perturbations (Korshunov and Berk, 2003). These injury models elicit vascular remodelling patterns characterized by PIT and the formation of non-atherosclerotic AIT intimal lesions that can further develop into advanced atherosclerotic lesions in *ApoE* gene-deficient mice when placed concurrently on a western diet (Nam *et al.*, 2009; Liu *et al.*, 2011). These models provide valuable approaches to analyse subclinical atherosclerosis and AIT lesions under *in vivo* conditions that can be used to validate and substantiate *in vitro* results.

1.2.2 Primary Artery Calcification

Primary artery calcification usually occurs concomitantly with atherosclerosis and can be an indicator of advanced stage plaque formation (Wexler *et al.*, 1996). This form of arteriosclerosis can occur most often in coronary and temporal arteries and involves the asymmetric accumulation of calcific deposits in the vessel wall which can reduce elasticity and subsequently contribute to flow restriction and increased blood pressure (Madhavan *et al.*, 2014). Calcification can occur in the intima, the internal elastic lamina (IEL) or the media. Intimal and IEL calcification take place most regularly in coronary arteries and are therefore deemed to be the most pathogenic forms (Mori *et al.*, 2018). Meanwhile, medial calcification, often termed Mönckeberg medial calcific sclerosis, is usually observed in peripheral arteries where it can lead to further complications such as renal failure and hypercalcemia (Lanzer *et al.*, 2014).

1.2.3 Fibromuscular Intimal Thickening

Fibromuscular intimal thickening (FIT) occurs when symmetrical thickening of the intimal and medial layers of an artery takes place. This results in the formation of a fibrous lesion known as a neointima. This neointima occludes the artery, hardens the vessel walls and reduces elasticity, preventing normal blood flow which in turn can lead to a myocardial infarction or stroke (Fishbein and Fishbein, 2009).

FIT can develop naturally with ageing and this usually manifests through adaptive intimal thickening resulting from endothelial dysfunction or changes in tensile stress within the vessel (Tesauro *et al.*, 2017). This often gives rise to only a small occlusion of the artery,

but the risk of atherosclerotic plaque formation at this site is drastically increased (Stary, 1992).

Some variations of FIT stem from treatments of atherosclerosis. Transplant arteriosclerosis, also known as cardiac allograft vasculopathy (CAV), is a form of FIT which can occur following heart transplantation. This condition is believed to develop as a result of an immunological response against the transplanted tissue and is characterised by endothelial dysfunction, infiltration of immune cells into the grafted vessel wall and formation of a fibrous neointimal lesion which narrows the lumenal space (Weis and Von Scheidt, 1997; Rahmani *et al.*, 2006; Xu, 2008). Occurrences of FIT are also common following vein-graft bypass procedures. Autogenous vein grafts are often surgically inserted as conduit vessels to bypass heavily damaged areas of an artery (Zou *et al.*, 1998). In order for the vein graft to adapt to the increased flow rate and pressure of arterial blood, a certain level of desirable outer remodelling of the vessel must occur. However, this must be tightly regulated as it can easily lead to uncontrolled remodelling and subsequent occlusion of the vein-graft (Davies and Hagen, 1995; Muto *et al.*, 2010).

Numerous other variations of FIT can occur both naturally and due to surgical interventions, such as in-stent restenosis which is discussed at length in Section 1.3.2.1, and so it is very difficult to develop treatments which are suitable for all variations.

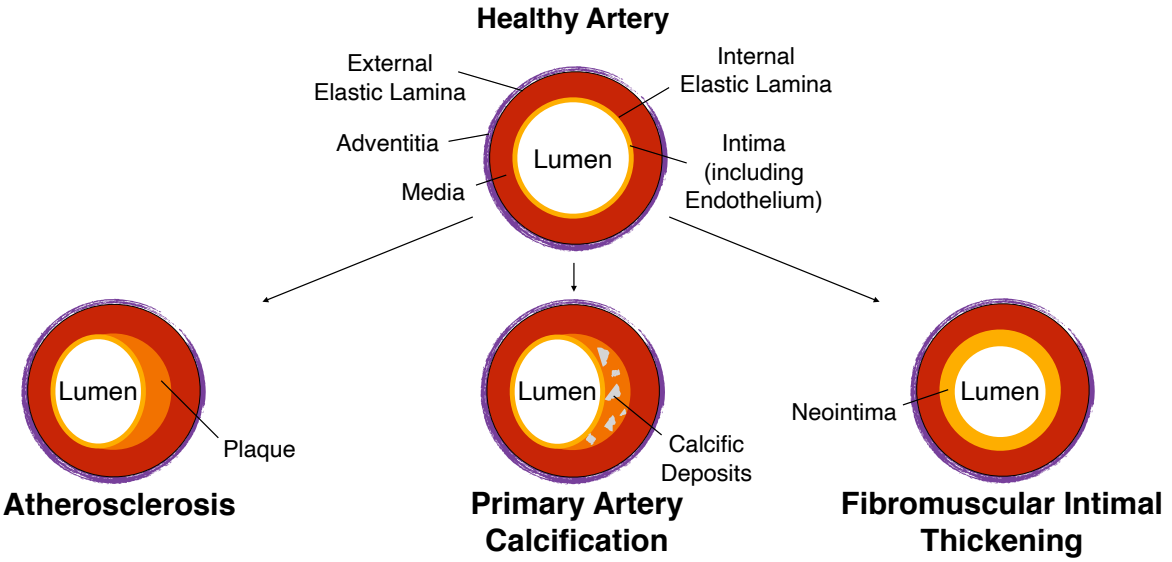


Fig 1.2 Vascular Remodelling. Inward arterial remodelling can occur symmetrically or asymmetrically. Symmetrical remodelling is most often observed in fibromuscular intimal thickening (FIT) where a fibrous neointima forms. Asymmetrical remodelling is seen in atherosclerotic or calcified lesions where a plaque (lipid-based or calcific) extends from one side of the vessel wall, occluding the lumen.

1.3 Current treatments for CVD

The type of treatment applied to a patient with CVD is obviously going to be dependent on the type of CVD they are suffering from, but it must also be tailored to the severity and stage of progression. Mild cases can be treated with lifestyle changes which can reduce risk factors and help to mitigate progression of CVD. Obesity, smoking, alcohol consumption and poor diet have all been implicated as risk factors for CVD. Reducing or eliminating these risk factors can substantially improve a patient's disease prognosis (Anderson *et al.*, 1991; Lavie, Milani and Ventura, 2009; Yusuf *et al.*, 2020). Meanwhile, cases of moderate severity require ongoing medication, while the most severe cases may require surgical intervention.

1.3.1 Drug treatments for CVD

1.3.1.1 Statins

High levels of low density lipoprotein cholesterol (LDL-C) have been widely implicated in the onset of CVD (Fernández-Friera *et al.*, 2017). LDL-C circulating in the blood can become lodged in the vessel wall and contribute to plaque formation. Statins have been

extensively used to combat high levels of LDL-C by inhibiting the HMG-CoA Reductase enzyme which plays a vital role in the cholesterol synthesis pathway (Wadhera *et al.*, 2016). While many other drug groups have an indirect effect on the development of an atheroma, statins are usually the first choice for treatment of atherosclerosis as they work directly to reduce plaque formation.

1.3.1.2 Anti-coagulants

Anti-coagulants are routinely used to treat various forms of CVD. Members of this drug group can reduce the risk of stroke and myocardial infarction by preventing the formation of blood clots in the vasculature (McNeil *et al.*, 2018). The most commonly used anti-coagulant is Aspirin, which inhibits platelet aggregation by acetylating the cyclo-oxygenase enzyme, thus blocking the synthesis of the clotting hormone thromboxane (Reilly and FitzGerald, 1988). Other anti-coagulants act as receptor antagonists to prevent clotting. Clopidogrel, for example, binds to the ADP receptor on platelets, which subsequently inhibits their ability to aggregate (Savi *et al.*, 2002). Due to their blood-thinning properties, the use of anti-coagulants must be strictly regulated to avoid haemorrhaging, but numerous studies have concluded that the benefits to patients far outweigh the risks (McNeil *et al.*, 2018).

1.3.1.3 Beta blockers and ACE inhibitors

High blood pressure, or hypertension, is widely accepted as one of the most significant risk factors for the onset of CVD (Yusuf *et al.*, 2020). Two drug groups which are routinely prescribed to combat this condition are beta blockers and ACE inhibitors. Beta blockers act as antagonists for beta-adrenergic receptors which, when activated, significantly increase cardiac contraction output (Martínez-Milla *et al.*, 2019; Oliver, Mayor Jr and D'Ocon, 2019). Some newer forms of beta-blockers, such as Carvedilol, have been engineered to also have a strong vasodilating effect (Diaconu *et al.*, 2019). Angiotensin Converting Enzyme-(ACE-) inhibitors are also classed as vasodilators but utilise a different mechanism of action. They bind and inactivate ACE which prevents the synthesis of angiotensin II, a potent vasoconstrictor (Dzau, 1990). Beta blockers or ACE inhibitors are often used in conjunction with other drug groups to provide a more comprehensive treatment strategy.

1.3.2 Surgical Interventions

In the most severe cases of CVD, invasive action must be taken to treat the patient. For treatment of CVD in coronary arteries, bypass grafts have been the method of choice for a number of years. This process involves taking a blood vessel from elsewhere in the body and using it to direct blood flow around the blockage in the coronary artery (NIH, 2014). In more recent times, balloon angioplasty and stenting have become very popular techniques for treating patients who have developed a severe atheroma. In balloon angioplasty, a catheter is threaded up through the obstructed artery to the site of plaque formation. A small balloon is then inflated to break down the plaque and widen the lumen. In order to reduce the possibility of elastic recoil a stent is often inserted. A stent is a short metal mesh used to maintain the opening created by the angioplasty (Haery, Sachar and Ellis, 2004). However, this can lead to a number of other challenges, most notably the occurrence of in-stent restenosis (ISR) due to vessel damage.

1.3.2.1 In-stent Restenosis

Upon insertion of a stent into the artery wall, mechanical stress can cause the endothelial lining to rupture. As with most tissue injuries, platelet aggregation and local inflammation are upregulated at the site of injury. However, an additional side effect can occur whereby a neointima begins to form as cell migration to the area increases along with exaggerated proliferation, this is often referred to as neointimal hyperplasia (Haery, Sachar and Ellis, 2004). What results is a new remodelling event that is clinically and pathologically similar to the original atherosclerotic event, but is completely different on the molecular level (Hoffmann *et al.*, 1996). Rather than a lipid-based plaque, as is seen in atherosclerosis, the neointimal lesion that forms is fibrous in nature, made up of cells that are similar to vascular smooth muscle cells (VSMCs), a characteristic which is indicative of fibromuscular intimal thickening. The growth of this neointima is also not characterised by a build-up of lipids and cell debris, but rather by the division, migration and proliferation of the neointimal cells (Yin, Yang and Wu, 2014).

To combat this issue of in-stent restenosis (ISR), researchers sought to improve upon the bare metal stent (BMS) that was classically deployed to treat ISR. Drug eluting stents (DESs) have since been developed whereby the stent is coated with a particular drug which is then released at the site of stenting to prevent ISR developing (Farooq, Gogas and Serruys, 2011).

Several anti-thrombotic, anti-mitotic and anti-proliferative drugs (eg. Sirolimus, Paclitaxel) have been used in this way, with varying degrees of efficacy (Yin, Yang and Wu, 2014).

However, a number of issues continue to plague the use of drug-coated stents. Due to rapid delivery of the drug, anti-thrombotic and anti-proliferative effects often only last for a couple of days or weeks, merely postponing the eventual development of ISR. Another problem is the ability of these drugs to partition through tissues. Depending on the reactive properties of the drug, tissues in the vicinity may have varying degrees of drug uptake, often leading to very low potency. In recent years, biodegradable nanoparticles have been developed to combat these issues. Their ability to release the drug slowly over time and their tissue penetration success have shown promising results in the prevention of ISR (Panyam and Labhasetwar, 2003). However, in order to develop highly effective and highly specific drugs to treat neointimal hyperplasia and ISR, it is imperative that we gain a greater understanding of the molecular mechanisms that are occurring in these conditions. One such area of uncertainty and a source of ongoing debate is the origin of the cells that make up the neointima.

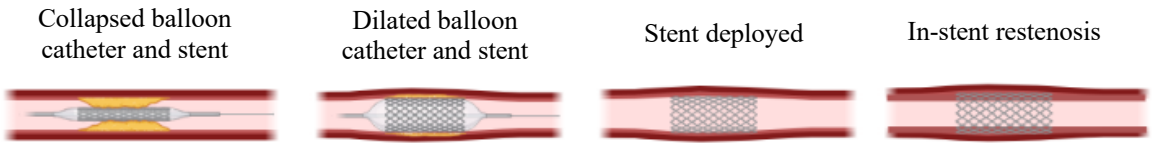


Fig 1.3 In-stent Restenosis. Balloon angioplasty is regularly used to widen the lumen of an artery after an atherosclerotic plaque has caused the lumen to narrow. A metal mesh stent can be inserted around the balloon to prevent elastic recoil and re-occlusion of the lumen. However, this can injure the artery wall and cause artery wall hardening and neointima formation which restricts blood flow. This is called in-stent restenosis.

1.4 Origin of Neointimal Cells

1.4.1 De-differentiated SMCs

The long-standing assumption for the origin of cells in the neointima was that they arise from the de-differentiation of smooth muscle cells (SMCs) in the medial layer. Differentiated SMCs have been shown in numerous studies to have a high level of plasticity. Multiple studies described the down-regulation of SMC markers such as smooth muscle α-actin (SM α-actin) and smooth muscle myosin heavy chain (SM-MHC) in neointimal cells post vessel ligation, which led to these cells being termed SMC-like rather than SMC (Ross and Glomset, 1973; Chamley-Campbell, Campbell and Ross, 1979). It has also been shown that SMCs express different markers at different stages of maturation (Owens, Kumar and Wamhoff, 2004). Numerous reports also went on to further describe the ability of SMCs to not only de-differentiate but also to take on a new phenotype. This process, known as phenotypic modulation, was shown to occur in vascular SMCs following vessel injury with contractile SMCs spontaneously switching to a synthetic SMC phenotype with higher levels of proliferation and inflammatory cell recruitment (Rensen, Doevendans and van Eys, 2007). This all led to a generally accepted model of SMC de-differentiation giving rise to neointimal cells. However, a lot of evidence for this model was circumstantial and based on previously held assumptions.

In an attempt to address these issues, researchers began to use cell fate mapping techniques to trace the lineage of a given cell and determine its origin. Lineage tracing involves the indelible genomic marking of a cell with a specific reporter construct, such that all of its progeny will also be marked (Kretzschmar and Watt, 2012). In this way, the number of progeny and their migration patterns can be assessed, regardless of subsequent phenotypic changes. Multiple different genetic cassettes have been developed, mostly using Cre recombinase-based systems, to improve the stringency of this technology over the years (Das and Yaniv, 2020). One such cassette is the Confetti model which allows cells (and therefore their parent cell) to be identified by one of four different fluorescent reporters (Snippert *et al.*, 2010). Furthermore, these systems can not only be constitutively expressed, but can also be inducible, whereby cells only begin expressing their reporter genes when an activating stimulus is administered, eg. Tamoxifen activation of a Cre recombinase controlled by an estrogen receptor (ER) gene (Pucella, Upadhaya and Reizis, 2020).

Many research groups have employed lineage tracing techniques to attempt to determine the origin of cells present in an arteriosclerotic lesion. In one such instance, a lineage tracing study was performed where PTEN-knockout mice were bred with a Cre recombinase system driven by a *Myh11* promoter and induced by Tamoxifen treatment after wire-injury. The resulting data suggested that cells in the ligation-induced neointima arose from a cell which, before vessel injury, was positive for Myh11 expression, ie. a SMC (Nemenoff *et al.*, 2011). This approach was expanded and improved upon in subsequent studies which reported that a small sub-population of highly plastic SMCs in the medial layer of the artery was the source of the cells making up the neointima (Herring *et al.*, 2014; Chappell *et al.*, 2016). However, concerns have persisted regarding the lack of relevant negative controls and, more significantly, the possibility that the tamoxifen can remain in the tissue and still be labelling cells for at least 4 weeks post treatment (Reinert *et al.*, 2012).

Single-cell RNA-sequencing (scRNA-Seq) has, in recent years, been combined with lineage tracing to address some of the shortcomings of the technology. Using scRNA-Seq, researchers have reported that a subpopulation of SMCs which are $Myh11^{+}$, but which also express Stem Cell Antigen 1 (Sca1), may contribute significantly to the formation of a neointima and that increased Sca1 expression is a hallmark of SMC phenotypic switching both *in vivo* and *in vitro* (Dobnikar *et al.*, 2018). It is becoming more and more apparent that the complexity and variety of cell types in the vasculature suggests that in fact neointimal cells may arise from one or several rare subpopulations that have yet to be fully characterised. This is supported by recent scRNA-Seq data which identified multiple novel cell subtypes in the mouse aorta, some of which are more prevalent in diseased vessels and therefore may play a role in the development of arteriosclerotic lesions (Kalluri *et al.*, 2019). Furthermore, it has been recently reported that a heterogeneous population of both SMCs and non-SMCs may be responsible for the formation of the neointima and that the make-up of the cell population in the lesion may also be dependent on the extent of the ligation injury (Yuan *et al.*, 2017; Roostalu *et al.*, 2018). The involvement of non-SMC cells in the development of a neointimal hyperplasia is not necessarily a new concept and this is reflected in the literature as many different cell types have been previously implicated to varying extents in the process.

1.4.2 Endothelial cells

As far back as 1997 it has been shown that endothelial cells (ECs) have the ability to transition to a SMC progenitor cell expressing myogenic markers (DeRuiter *et al.*, 1997). Since then, this process of trans-differentiation has been demonstrated on a number of occasions, with the progenitor cell being classed as a mesenchymal stem cell. This has given rise to the term, endothelial-to-mesenchymal transition (EndMT), a process which is characterised by not only the loss of morphological features such as tight junctions, but also the loss of endothelial markers such as CD31 and von Willebrand factor (VWF) and the gain of mesenchymal markers such as fibroblast-specific protein 1 (FSP-1) and vimentin (P. Y. Chen *et al.*, 2015). Several research groups have reported that EndMT occurs during neointimal hyperplasia and that SMC-like cells in the neointima are derived from cells which have undergone this transition process (Frid, Kale and Stenmark, 2002; Cooley *et al.*, 2014; Moonen *et al.*, 2015; Chen *et al.*, 2021).

1.4.3 Bone marrow-derived Stem Cells

A substantial body of evidence also exists which supports the role of circulating bone marrow-derived stem cells (BMD-SCs) and hematopoietic progenitor cells (HPCs) in the development of stenotic lesions. Most of these studies involved bone marrow transplantation into a mouse which subsequently underwent vessel ligation. A large portion of the neointimal cells were then shown to have originated from the donor mouse (Shimizu *et al.*, 2001; Sata, 2003). Some human studies have also been carried out and it has been reported that SMCs in an atherosclerotic lesion may be derived from donor bone-marrow stem cells (Caplice *et al.*, 2003). However, it has been suggested on a number of occasions that these circulating cells are indeed recruited to the ligation site but do not go on to differentiate into neointimal cells (Hoofnagle *et al.*, 2006).

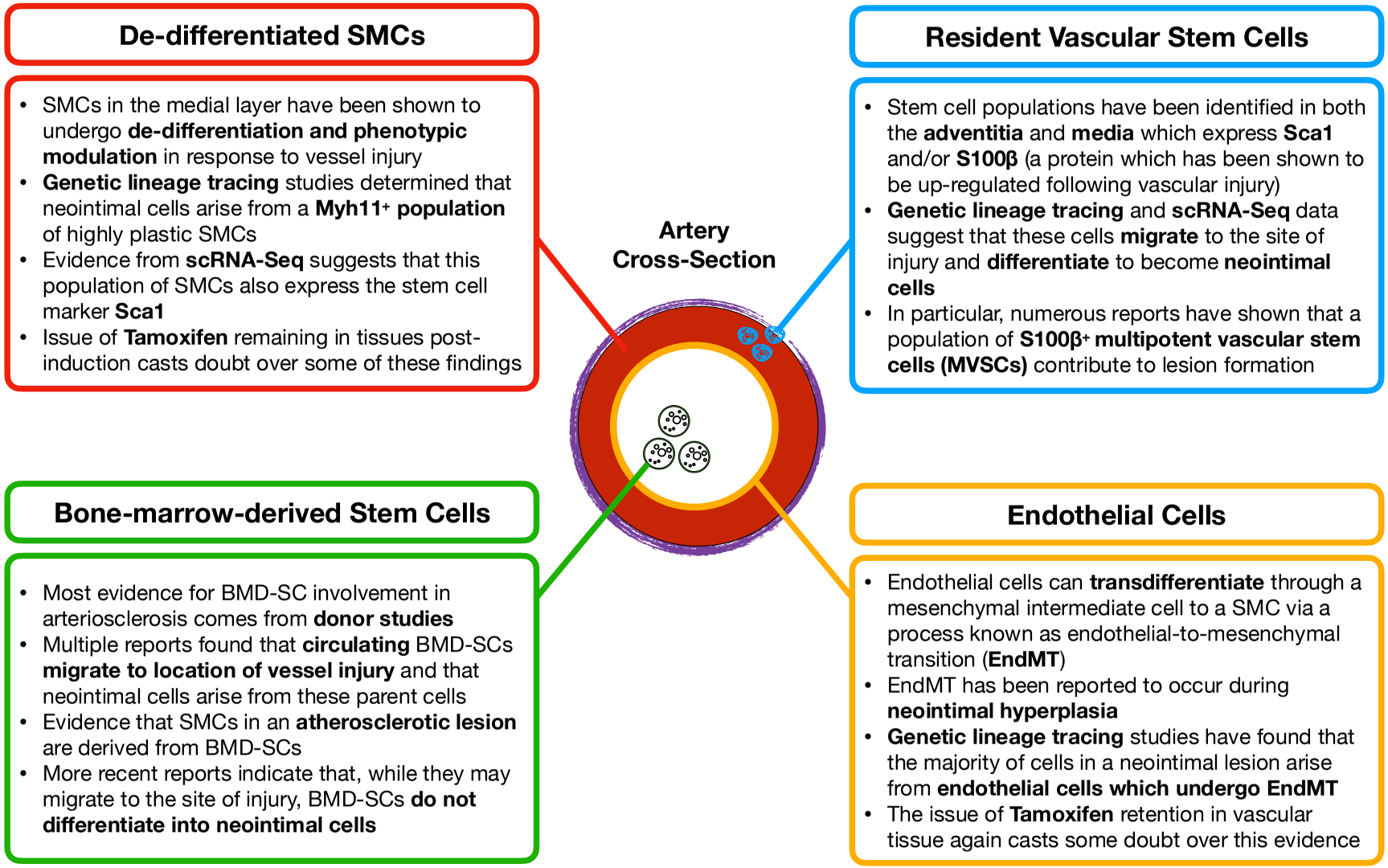


Fig 1.4 Origin of Neointimal Cells. Recent advances in technologies such as genetic lineage tracing and scRNA-Seq have given rise to a number of different theories regarding the origins of SMC-like cells found in a neointimal lesion. This figure summarises the main findings in this debate.

1.4.4 Resident Vascular Stem Cells

More recently, a new model has been proposed whereby resident stem cells in the vessel wall differentiate to give rise to the SMC-like cells of the neointima. A population of Stem cell antigen 1 (Sca1)-positive cells was discovered in the adventitia which could be stimulated to differentiate through a myofibroblast intermediate into a SMC population. It was also shown that these cells could migrate through the media *in vivo* and contribute to the neointima (Sartore *et al.*, 2001; Torsney, Hu and Xu, 2005). Data from cell fate mapping studies suggests that adventitial stem cells may indeed play a role in lesion formation, but only in cases of severe vessel injury (Roostalu *et al.*, 2018). This evidence has been further supported by recent lineage tracing and scRNA-Seq data which indicates that a population of adventitial $Sca1^+$ stem cells migrate into the medial layer and differentiate into SMC-like cells following severe vascular injury to initiate vessel repair (Tang *et al.*, 2020).

Although vascular stem cells are most abundant in the adventitia, populations of multipotent cells have also been identified in the tunica media (Tintut *et al.*, 2003). $Sca1^+$ cells have previously been isolated from the medial layer and shown to have the ability to differentiate into both SMC and EC lineages following appropriate stimulus (Sainz *et al.*, 2006). It wasn't until 2012 that a real breakthrough was observed for this model when members of the Song Li research group identified a new population of $Sca1^-$ cells in the tunica media of rat carotid arteries, termed multipotent vascular stem cells (MVSCs) (Tang *et al.*, 2012). Due to the fact that the carotid artery develops from a neuroectodermal lineage (Hempleman and Warburton, 2013), MVSCs were immunostained for neural crest stem cell markers. They were shown to be positive for a number of these markers, such as Sox10, Sox17 and Nestin. Furthermore, this subpopulation of cells expressed the calcium-binding protein S100β. Although S100β is extensively used as a marker for mature glial cells and astrocytes, it has been shown on multiple occasions to be expressed by several types of neural stem cell (Seri *et al.*, 2004; Ihrie and Alvarez-Buylla, 2008; Higuchi *et al.*, 2014). S100β has also been shown to contribute to neointima formation following ligation-induced injury (Cao *et al.*, 2017). In addition, MVSCs were found to be negative for myogenic markers such as SM-MHC and Calponin1 (Cnn1) and demonstrated high levels of proliferation and telomerase activity (an indicator of stemness). This study also carried out lineage tracing to show that, following wire injury, neointimal cells did not arise from the de-differentiation of medial SMCs, but rather medial and/or adventitial MVSCs (Tang *et al.*, 2012). This prompted Song Li's group to proclaim that despite decades of evidence to the contrary, it was resident vascular stem cells and not de-differentiated SMCs that contributed to neointima formation.

These claims were somewhat diluted when a number of issues with the study were subsequently pointed out in a response paper, including the fact that a constitutive lineage tracing model was used, rather than an inducible one, so the reliability of cell specific tagging was compromised (Nguyen *et al.*, 2012). Nonetheless, the discovery of these MVSCs as a potential contributor to neointima formation was still of great significance.

In two papers in 2014, research from our group went on to further characterise these MVSCs in culture and provide additional evidence that SMCs in culture also begin to express neural stem markers, such as Sox10, but do not have the same multipotency as MVSCs (E. Kennedy, Hakimjavadi, *et al.*, 2014; E. Kennedy, Mooney, *et al.*, 2014). These data suggest that SMCs in culture that were classically seen as de-differentiated may be in fact stem-cell derived and predominate within these cultures over time (Yuan *et al.*, 2017). Further studies from our group, using lineage tracing and discrete photonic signatures, have reported that SMC-like cells in vascular lesions may be derived from an S100β^+ resident vascular stem cell which can undergo myogenic differentiation via the Hedgehog signalling pathway (Molony *et al.*, 2020; Di Luca *et al.*, 2021). This evidence supports the theory that MVSCs may contribute, at least to some degree, in the formation of a neointimal lesion following vessel injury. However, in order to understand the exact mechanisms by which these events might occur, further investigation is required regarding the involvement of key signalling pathways such as that of Notch signalling.

1.5 Notch Signalling

1.5.1 History of Notch

The *notch* gene was first discovered in *Drosophila melanogaster* around 100 years ago when partial loss of gene function was shown to produce notches at the wing margin (Mohr, 1919). Mutations that gave rise to total loss-of-function resulted in a lethal neurogenic phenotype whereby cells were directed to differentiate down a neural lineage rather than an epidermal lineage (Poulson, 1937; Artavanis-Tsakonas, Rand and Lake, 1999). Notch has a pivotal role in development and embryogenesis as it is involved in controlling a number of fundamental cellular processes such as cell fate mapping, proliferation, differentiation and apoptosis (Gazave *et al.*, 2009). One of its most important roles is the regulation of "lateral-inhibition", a process whereby equivalent cells in a developing embryo differentiate down

alternate lineages to ensure equal patterning of different cell types (Greenwald, 1998). Notch has also been shown to regulate adult stem cell fate and maintenance (Perdigoto and Bardin, 2013) and its signalling pathway has been shown to be highly conserved across a large number of species (Guruharsha, Kankel and Artavanis-Tsakonas, 2012).

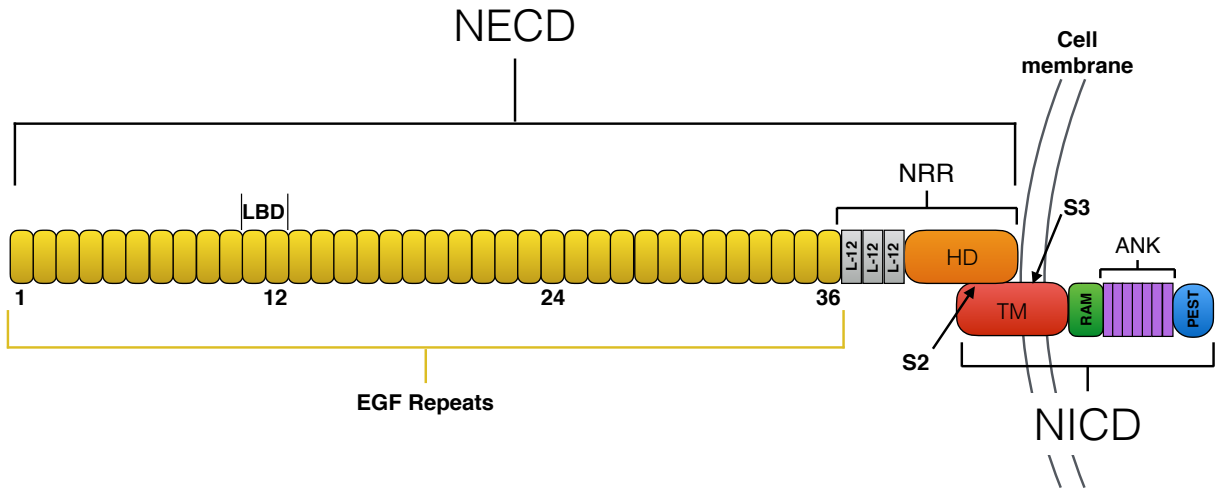


Fig 1.5 Structure of the mammalian Notch receptor. In this diagram the receptor is broadly separated into the extracellular domain (NECD) and intracellular domain (NICD). The extracellular domain consists of EGF repeats and a negative regulatory region (NRR) which contains Lin-12 (L-12) repeats and a hydrophobic domain (HD). The ligand binding domain (LBD) resides in EGF 11 and 12. The transmembrane (TM) domain, RAM domain, ankyrin (ANK) repeats and the terminal PEST domain make up the NICD. Cleavage sites S2 and S3 are also indicated in the diagram. All of these sites and domains are highly conserved across species and serve specified roles in the Notch signalling process.

1.5.2 Notch receptors and ligands

The Notch receptor is a ~300kDa single-pass transmembrane protein. Although the *Drosophila melanogaster* species only possess one form of Notch, mammalian cells have been shown to express four types of Notch receptor (named Notch 1-4) which all share a similar structure with only a few small differences (Weinmaster, Roberts and Lemke, 1992; Lardelli, Dahlstrand and Lendahl, 1994; Uyttendaele *et al.*, 1996).

The Notch extracellular domain (NECD) is dominated by epidermal growth factor (EGF)-like repeats. Each EGF-like repeat is about 40-45 residues in length (Gordon, Arnett and Blacklow, 2008).

The extracellular domain of mammalian Notch1 and Notch2 contain 36 EGF-like repeats, while Notch3 contains 34 repeats and Notch4 contains 29 (Meng *et al.*, 2016). Many of these EGF-like repeats have calcium-binding capabilities. The binding of Ca^{2+} ions is believed to play a role in maintaining the structure of the receptor (Sala *et al.*, 2012). As we move toward the membrane, the NECD contains a negative regulatory region (NRR) which consists of 3 Lin12-repeat (LNR) domains and a hydrophobic domain (HD) which mediates heterodimerisation (Baron, 2003). The Notch intracellular domain (NICD) consists of a number of smaller sub-domains with the most notable being the RBP-Jkappa-associated module (RAM), a sequence of seven ankyrin repeats and a PEST domain (named for the abundance of Proline (P), Glutamic Acid (E), Serine (S) and Threonine(T)) which is involved in NICD proteolysis (Chillakuri *et al.*, 2012).

In mammals, Notch receptors can be activated by 5 different types of ligand: Jagged-1 and -2, and Delta-like ligand (DLL)-1, -3 and -4. These ligands are all membrane bound proteins (Guruharsha, Kankel and Artavanis-Tsakonas, 2012). Notch signalling is initiated through a *trans* activation process whereby a ligand located on a neighbouring cell binds to the Notch receptor at the ligand-binding region, EGF 12 (Bray, 2006). This causes a small conformational change that exposes an S2 cleavage site which was previously protected by the NRR. A regulated intramembrane proteolysis (RIP) event is put into motion as the ADAM10 metalloprotease cleaves the Notch receptor at S2 (Gordon, Arnett and Blacklow, 2008). This is followed by a γ-secretase cleavage at S3 in the transmembrane domain (TMD) (van Tetering and Vooijs, 2011). Subsequently, the NICD is released from the membrane while the NECD is simultaneously endocytosed into the ligand-expressing cell. The NICD translocates to the nucleus where a number of transcription factors bind at the RAM domain and ankyrin repeats. Among these transcription factors is the Cp-binding factor 1 (CBF-1), also known as Recombination signal sequence-binding protein Jκ (RBP-Jκ) in mice, which is converted from a transcriptional repressor to an activator (Sala *et al.*, 2012). This transcription complex activates the expression of Notch target genes, most notably those of the Hairy Enhancer of Split (Hes) family which includes *Hey1*, *Hey2* and *HeyL* (Iso, Kedes and Hamamori, 2003). These target genes can then go on to initiate a wide range of processes (differentiation, proliferation, apoptosis, etc.) depending on the cell type, tissue type, epigenetic state, activating ligand and many other factors (Guruharsha, Kankel and Artavanis-Tsakonas, 2012).

Non-canonical modes of Notch signalling also exist, but have not been thoroughly researched and therefore their exact mechanisms are poorly understood. Some of these modes involve alternate ligands such as Delta-like non-canonical Notch ligand 1 (Dlk-1), while others arise from NICD interaction with intracellular proteins other than RBP-Jκ (Dongre *et al.*, 2014; Traustadóttir *et al.*, 2019). Many forms of non-canonical Notch signalling are actually ligand- or cleavage-independent and occur when the full-length receptor interacts with proteins from other signalling pathways, such as the Wnt pathway, at the membrane (D'Souza, Meloty-Kapella and Weinmaster, 2010; Andersen *et al.*, 2012).

1.5.2 Notch Signalling and Stem Cell Fate

During development, Notch has a vital role in directing stem cells down specific differentiation pathways in order to ensure that tissue generation occurs correctly. For the most part, this occurs in three ways: lateral inhibition, asymmetric lineage determination and boundary formation (Bray, 1998).

Lateral inhibition, as mentioned earlier, occurs in neighbouring cells where a slight increase in Notch signalling in one cell becomes amplified as a result of feedback loops (Lewis, 1998). Ligand production in that cell is reduced and Notch signalling between the neighbouring cells becomes unidirectional. In this way, only one of the two cells differentiates down a particular pathway and this leads to equal spatial patterning of differentiated cells (Schweisguth, 2004). This is most notably seen in the development of the neural tube (Sjöqvist and Andersson, 2019).

Asymmetric lineage determination can occur when a parent cell divides during development and only one of the daughter cells inherits a particular signalling component (Guo, Jan and Jan, 1996). Notch signalling is often regulated by such occurrences, such as when the Notch inhibitor, Numb, is asymmetrically segregated in daughter cells, leading to Notch signalling only taking place in one cell. This can result in daughter cells differentiating down separate lineages, eg. neuronal or glial cell lineage (Berdnik *et al.*, 2002).

Boundary formation is essential for the correct segregation of organs and tissues. Notch signalling can become active at the point where two different groups of cells meet (Perdigoto and Bardin, 2013). This activation induces specific target gene expression to stimulate differentiation of cells either side of this meeting point into a new cell type. This new cell

type goes on to form a boundary between the two original cell types and effectively compartmentalises each group. An example of this is seen in zebrafish hindbrain segmentation (Bray, 1998).

Notch signalling is also essential for maintenance of tissue and organ homeostasis in adults. One of the major mechanisms by which this is achieved is through the proper fate determination of adult stem cells. This is a process that is occurring constantly in a range of different tissue types, and is very often escalated following injury or disease (Chiba, 2006). In skin tissue, for example, Notch signalling plays a crucial role in the sequential differentiation of progenitor cells in the basal layer to spinous cells and subsequently to granular cells, thereby renewing each layer as terminally differentiated cells die off (Panelos and Massi, 2009). This process is dependent upon expression of Notch target genes such as p21 which are involved in cell-cycle arrest and terminal differentiation (Blanpain *et al.*, 2006; Williams *et al.*, 2011). Notch signalling has also been shown to activate stem cells in skeletal muscle (known as satellite cells) following injury (Carlson and Conboy, 2007). This is achieved through the down-regulation of the Notch inhibitor, Numb, post-injury, which results in increased Notch signalling, followed by expansion and differentiation of satellite cells to initiate tissue repair (Conboy and Rando, 2002). Throughout the literature there are many more examples of Notch control of stem cell fate, including that of hematopoietic stem cells, intestinal crypt cells and vascular stem cells, emphasising the role of Notch signalling as an essential element in normal function and maintenance of tissues and organs in the body.

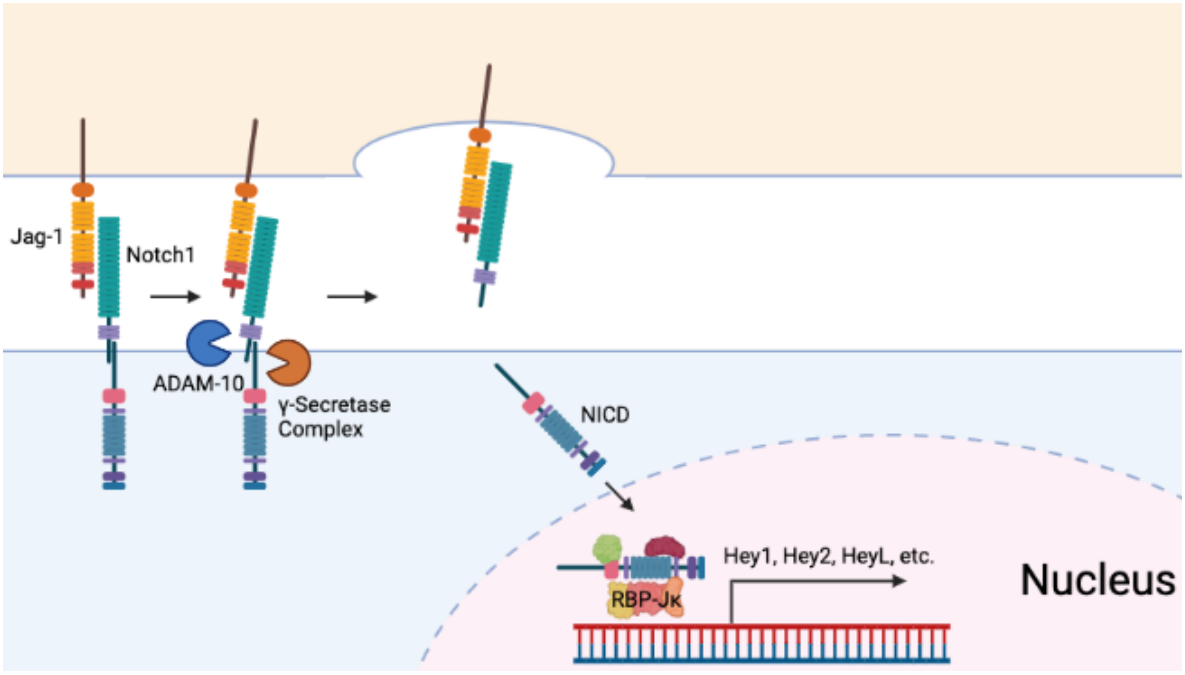


Fig 1.6 Notch Signalling Pathway. The Notch receptor binds to its cognate ligand (Jag-1 in this case) on a neighbouring cell. A conformational change occurs which exposes the S2 site which is subsequently cleaved by a metalloprotease called ADAM10. The NECD-Jag-1 complex is *trans*-endocytosed into the ligand-expressing cell. A second cleavage at S3 by γ-secretase releases the NICD which translocates to the nucleus and forms a transcription complex with a number of factors, including RBP-Jκ. Expression of target genes such as *Hey1* and *Hey2* is subsequently activated.

1.5.3 Notch in Disease

Notch signalling has been heavily implicated in a large number of human diseases and disorders, mostly those of a developmental nature, but also in cancers, cardiovascular disease, cerebrovascular disease, kidney disease, and many more (Talora *et al.*, 2008).

Due to the significant role of Notch in embryonic development, mutations in associated genes have been shown to cause congenital disorders such as Alagille Syndrome which is characterised by the development of physical anomalies in the heart, liver, eye, face and vertebrae (Penton, Leonard and Spinner, 2012; Stittrich *et al.*, 2014; Mašek and Andersson, 2017). Skeletal disorders can also arise from mutation of Notch pathway components, as is seen in Spondylocostal dysostosis, and a related condition called Spondylothoracic dysostosis, which are both associated with rib abnormalities and short trunk dwarfism and have been repeatedly linked to mutations in DLL3 and Mesp2 (a Notch-associated transcription factor) (Bulman *et al.*, 2000; Turnpenny *et al.*, 2003; Whittock *et al.*, 2004; Cornier *et al.*, 2008). Numerous studies have also implicated Notch in the development of a

range of cancers due to its role as a cell fate regulator. Mutations in Notch can give rise to colorectal, skin, breast and cervical cancer, as well as several different forms of T-cell leukaemia (Ellisen *et al.*, 1991; Jhappan *et al.*, 1992; Talora *et al.*, 2008; Fortini, 2012). Studies have also reported elevated levels of Notch in lung and cervical cancer (Zagouras *et al.*, 1995; Dang *et al.*, 2000). Additionally, Notch can act as both an oncogene and a tumour suppressor gene in different tissue types (Nicolas *et al.*, 2003). As well as contributing to the onset of leukaemia, dysregulation of T-cell fate due to mutations in Notch signalling components can also give rise to a number of autoimmune diseases (Talora *et al.*, 2008).

1.5.4 Notch in Vascular Remodelling

There is mounting evidence that Notch signalling is heavily involved in arterial remodelling following vascular injury. In 2001, Lindner *et al*. were the first to show that Notch and Jagged family genes were upregulated in injured rat carotid arteries. The role of these genes in vascular lesion formation was supported by evidence from Sakata *et al*. in 2004 who demonstrated the attenuation of neointimal hyperplasia in a *Hey2*-deficient mouse model. Furthermore, in 2009, Li *et al.* found that neointima formation was substantially reduced in Notch1 knockout mice compared to wild-type. Redmond *et al.* (2014) observed a similar effect when transient Notch1 knockdown inhibited arterial remodelling in a ligated vessel. It has also been reported that inhibition of Notch signalling using soluble Jag-1 can lead to a reduction in neointima formation *in vivo* following balloon angioplasty (Caolo *et al.*, 2011). Notch signalling has been shown to inhibit SMC differentiation (Proweller, Pear and Parmacek, 2005), promote proliferation following vascular injury (Morrow *et al.*, 2005), induce EndMT in vascular endothelial cells (Noseda *et al.*, 2004) and increase neointima formation in arteriovenous fistulas when activated in fibroblast-specific protein 1 (FSP-1) expressing BMD-SCs (Liang *et al.*, 2019). Multiple studies also reported the ability of Notch signalling to induce myogenic differentiation in stem cell populations such as C3H 10T1/2 embryonic fibroblasts, mesenchymal stem cells and neural crest stem cells (Doi *et al.*, 2006; High *et al.*, 2007; Kurpinski *et al.*, 2010). Hence, while the exact mechanism by which Notch and its target genes affect neointima formation is poorly understood, there is substantial evidence suggesting that Notch signalling, and Notch1 in particular, plays a vital role in this process.

1.5.5 Regulation of Notch Signalling

The Notch signalling pathway is tightly regulated by a vast array of mechanisms which work together to maintain a sustainable level of cell differentiation and proliferation. As previously mentioned in Section 1.5.1, an essential role for Notch in embryological development is in the process of lateral-specification. This can be seen as a self-regulating role for Notch as it involves increasing or decreasing the ratio of expression between receptor and ligand in neighbouring cells. A cell may become a signal-sender or signal-receiver depending on this ratio which is regulated by feedback loops resulting from activation of Notch target genes (Fortini, 2009).

Up-regulation of Notch ligands such as Jagged can also serve to activate *cis*-inhibition whereby ligands on the same cell as the Notch receptor bind the extracellular domain without activating signalling (Kopan and Ilagan, 2009). However, it has been shown that ligand-binding alone is not sufficient for receptor activation (Cordle *et al.*, 2008). A number of studies have demonstrated the importance of endocytosis of the Notch ligand and NECD into the ligand-expressing cell following binding, a process which again is highly regulated by the expression of ubiquitin ligases such as Neuralized (*Neu*) and Mindbomb (*Mib*) (Bray, 2006).

Although there is still debate on whether or not full *trans*-endocytosis of the NECD is required for signal activation (Sala *et al.*, 2012) it is clear that the pulling force of ligand-binding is an essential element of Notch activation. Upon binding of the ligand to Notch, a "catch-bond" is formed, whereby the strength of the bond increases due to tensile forces (Vincent C. Luca *et al.*, 2017). This results in a conformational change that causes the NRR domain of the Notch receptor to open up and expose the S2 site for cleavage (Gordon, Arnett and Blacklow, 2008; Meloty-Kapella *et al.*, 2012). Mutations in this NRR site have been shown to result in ligand-independent signalling and dysregulation of cell proliferation (Sanchez-Irizarry *et al.*, 2004; Malecki *et al.*, 2006). Further dysregulation can occur when mutation of the γ-secretase cleavage protein causes proteolysis of the PEST domain which usually shortens the half-life of the NICD by directing it towards autophagy (Wesley and Saez, 2000; Cao *et al.*, 2015).

Other forms of regulation include: extracellular Ca^{2+} concentration (Rand *et al.*, 2000), suppression of NICD signalling by Msx2-interacting nuclear target protein (MINT) and Numb (Spana and Doe, 1996; Kuroda *et al.*, 2003), endocytosis and degradation of Notch

receptors (Kooh, Fehon and Muskavitch, 1993) and interaction of downstream Notch targets with Smad proteins (Blokzijl *et al.*, 2003). In addition to all of these modes of regulation, an area that has been the subject of extensive research, especially in the last two decades, is that of glycosylation and its effect on Notch signalling.

1.6 Glycosylation

Protein glycosylation is the most common form of posttranslational modification (PTM), with almost every functional protein in a cell being glycosylated to some degree. This process involves the attachment of a carbohydrate polymer (or glycan) to a specific site on a polypeptide molecule. It is usually carried out by glycohydrolase or glycosyltransferase enzymes located in the endoplasmic reticulum (ER) or in the Golgi apparatus (Campbell and Yarema, 2005; Ohtsubo and Marth, 2006). A protein which has attached carbohydrates is often referred to as a glycoprotein.

The incredible complexity and diversity of glycans means that a vast range of variability can be observed among proteins with a similar primary sequence. Proteins with the same amino acid sequence but that differ in their glycosylation are known as glycoforms. Different glycoforms of the same protein can have completely different folding, function, activity and specificity (Rudd *et al.*, 2005).

Glycans have been found to influence an astonishing number of cellular processes and characteristics, ranging from single protein solubility and small protein-protein interactions, to cell signalling and recognition (Solá and Griebenow, 2009). Since glycosylation is a non-templated process, ie. is not specifically coded by the genome, variability is achieved by the use of tissue-specific genes, compartmentalisation and enzyme competition which influence the formation, composition and attachment of glycans (Dennis, Granovsky and Warren, 1999). There are a number of different types of glycosylation, with the most common being O-linked and N-linked glycosylation (Sinclair and Elliott, 2005).

1.6.1 N-linked Glycosylation

N-linked glycosylation is a co-translational process, meaning that it occurs while the nascent (unmodified) polypeptide chain is still being constructed by the ribosome. This process takes place first in the lumen of the rough endoplasmic reticulum (RER) and then in the Golgi apparatus (GA) (Helenius and Aebi, 2002). N-glycosylation can only take place at an asparagine (Asn) residue located in a consensus sequence of Asn-X-Ser/Thr where X can be any amino acid other than proline and the third residue can be a serine (Ser) or a threonine (Thr) (Ghazarian, Idoni and Oppenheimer, 2011). The reason this process is referred to as 'N-linked' is because it involves the binding of carbon 1 (C1) of a N-acetylglucosamine (GlcNAc) monosaccharide to the nitrogen (N) in the amide group of the Asn residue (Walsh, 2009).

While translation is still ongoing, the nascent polypeptide is guided into the RER by a signal recognition particle (SRP), which is released once the polypeptide has bound to the RER (Walsh 2009). As the growing polypeptide is passed through the lumen of the RER, a 14-sugar precursor dolichol oligosaccharide (Glc3Man9GlcNAc2) is attached to the appropriate recognition sequence on the peptide chain via a GlcNAc phosphotransferase (GPT) enzyme (Aaron Heifetz, Keenan and Elbein, 1979). Further reactions in the RER and later in the GA serve to trim down this precursor molecule using glucosidase and mannosidase enzymes (Dennis, Granovsky and Warren, 1999). The result is a trimannosyl core (Man3GlcNAc2) which is common to all N-linked glycans. This core carbohydrate sequence is then elongated through the addition of other monosaccharides by a vast number of highly specific glycosyltransferases such as FUT1-11 and GnT1-5 (Helenius and Aebi, 2002; Brockhausen, 2014). The addition of extra monosaccharide residues is usually terminated by the addition of a sialic acid or fucose.

The length, composition, linking and branching of the final glycan are all highly variable. However, it has been generally accepted that there are three distinct subsets of N-glycan: high-mannose, complex and hybrid (Solá & Griebenow 2009). High-mannose oligosaccharides contain an extra 2-6 mannose residues on top of the three already present in the trimannosyl core. These often occur when the precursor molecule is not fully trimmed down, leaving some or all of the original nine mannose residues. Complex oligosaccharides have been fully trimmed to the trimannosyl core and subsequently elongated. These type of glycans are often heavily branched and highly complex in their monosaccharide

composition. Hybrid oligosaccharides are the least plentiful of the N-glycans and contain a mix of structural features from the two more common types (Walsh 2009).

1.6.2 O-linked Glycosylation

O-linked glycosylation is a post-translational process, meaning that it occurs after the polypeptide chain has been completed and has left the ribosome. In fact, O-glycosylation takes place almost entirely in the GA after other modifications such as protein folding have been carried out. There are a few different types of O-glycosylation, but the one that is by far the most prominent in mammals is termed "mucin-type" and involves the attachment of a N-acetylgalactosamine (GalNAc) residue to a Ser/Thr residue (Sinclair and Elliott, 2005; Christiansen *et al.*, 2014). The reason this process is referred to as 'O-linked' is that the C1 of the GalNAc binds to the oxygen in the hydroxyl group of the Ser/Thr (Ghazarian, Idoni and Oppenheimer, 2011).

Since the polypeptide has already been folded in the endoplasmic reticulum (ER), possible O-glycosylation sites are limited to those Ser or Thr residues that are sterically accessible by the necessary glycozymes. Unlike N-glycosylation, there is no precursor molecule ready to be attached to the peptide chain. Therefore, only a single GalNAc is added at the Ser/Thr site by a member of the GALNT family of glycosyltransferases (Brockhausen, 2014). Elongation then takes place via numerous other glycosyltransferases. The glycans formed are highly complex but are often shorter and less branched (often bi-antennary) compared to N-glycans (Walsh, 2009).

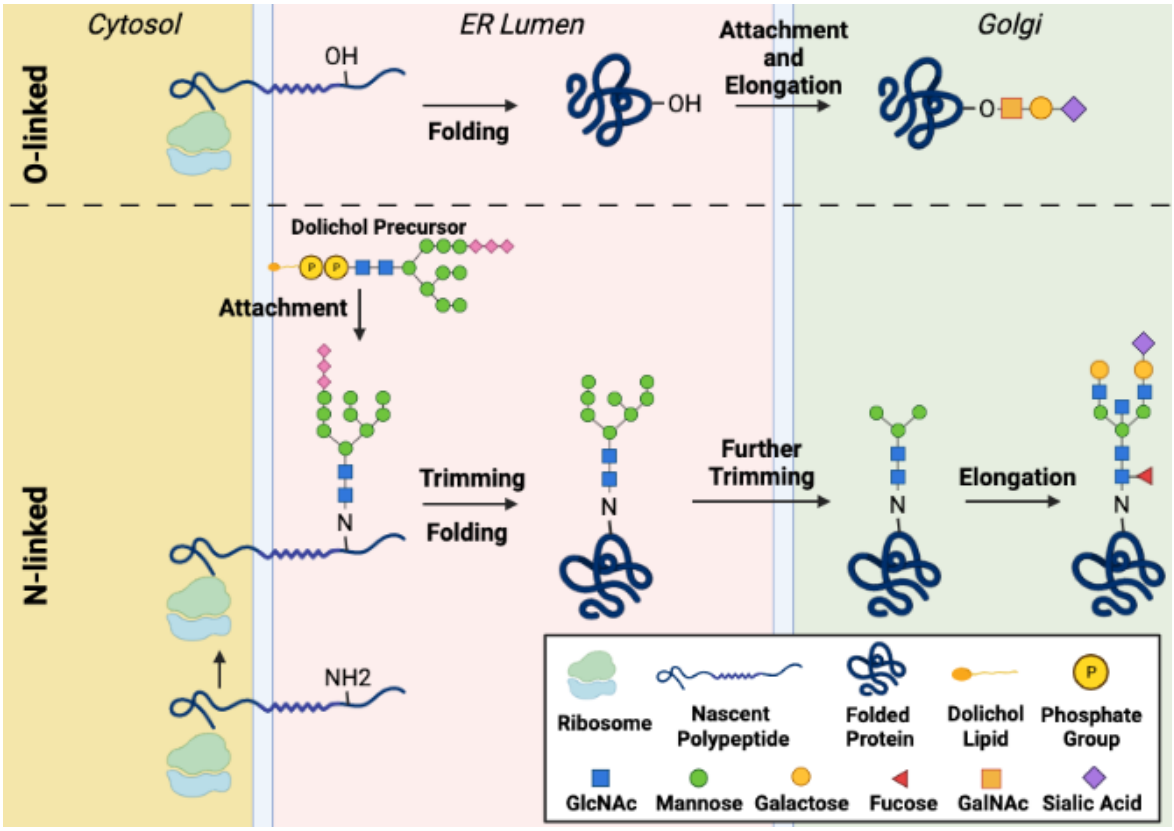


Fig 1.7 O-linked and N-linked Glycosylation. There are two main types of glycosylation in mammalian cells: O-linked and N-linked. O-linked glycosylation involves the attachment of a short oligosaccharide to the oxygen (O) of a hydroxyl group on a Serine or Threonine residue. This takes place in the Golgi Apparatus (GA). N-linked glycosylation, on the other hand, involves the transfer of a dolichol precursor oligosaccharide to the nitrogen (N) of an amino group on an Asparagine residue. This begins while the nascent polypeptide is still being translated in the cytosol and is followed by a number of trimming and elongation steps which occur throughout the endoplasmic reticulum (ER) and into the GA to form a long, complex oligosaccharide structure.

1.7 Glycosylation and Notch Signalling

1.7.1 Notch O-glycosylation

The Notch receptor harbours an array of O-glycans which all appear on its extracellular domain. A large number of the EGF repeats are modified with O-glucose and O-fucose, and to a lesser extent, O-xylose and O-GlcNAc (Pakkiriswami *et al.*, 2016). The O-fucosylation and O-glucosylation of Notch was first observed in 2000 by members of Robert Haltiwanger's research group in a study on *Drosophila melanogaster* in which a number of O-glycosylation consensus sites were also identified (Moloney, Shair, *et al.*, 2000). In a short space of time a large body of evidence was formed regarding the mechanisms and consequences of these glycosylation events. A family of glycosyltranferases called Fringe was shown to enhance Notch binding to Delta (Drosophila) and Delta-like (mammalian)

ligands but to reduce binding to Serrate (Drosophila) and Jagged-1 (mammalian) ligands (Brückner *et al.*, 2000; Hicks *et al.*, 2000). However, the mechanism of this enhancement was still unknown until, in a follow-up study, it was discovered that Fringe acts by adding GlcNAc to O-fucose residues on the EGF repeats of the NECD (Moloney, Panin, *et al.*, 2000). This modulation occurs at a number of EGF repeats and is essential for Delta and DLL binding and activation of Notch (Xu *et al.*, 2007). In particular, the elongation of the O-fucose residue by *Lunatic fringe* (*Lfng*) at EGF 12 has been shown to significantly enhance the binding of DLL1 in mammalian Notch signalling (Kakuda and Haltiwanger, 2017).

A number of other glycosyltransferases also regulate Notch signalling through addition of individual sugar residues. *O-fucosyltransferase 1* (*Ofut1*) in Drosophila and *Protein O-fucosyltransferase 1* (*Pofut1*) in mammals are responsible for O-fucosylation of Notch. Not only does this provide the primer for Fringe modulation but also aids in the secretion of Notch from the ER and trafficking of the receptor to the membrane (Panin *et al.*, 2002; Okajima *et al.*, 2008; Matsumoto *et al.*, 2016).

O-glucosylation is facilitated by *rumi* in Drosophila and *Protein O-glucosyltransferase1* (*Poglut1*) in mammals and has also been observed to modulate the essential domain EGF12 and enhance certain ligand-receptor interactions (Acar *et al.*, 2008). Additions of xylose, GalNAc and GlcNAc residues have also been reported in the literature with varying degrees of importance (Matsuura *et al.*, 2008; Sethi *et al.*, 2010; Boskovski *et al.*, 2013).

O-glycosylation of the Notch receptor and the dysregulation of this process has also been implicated in a number of diseases and disorders. The GALNT11 glycosyltransferase facilitates O-glycosylation at a number of sites on the NECD and has been shown to enhance S2 cleavage. GALNT11 dysfunction has been reported to cause embryological heterotaxy (Boskovski *et al.*, 2013). Similarly, mutation of *Pofut1* and *Poglut1* have been implicated in Dowling-Degos disease (Li *et al.*, 2013; Basmanav *et al.*, 2014) while deficiency in *Lunatic fringe* expression can contribute to malignancy in breast and prostate cancer (Xu *et al.*, 2012; Zhang *et al.*, 2014).

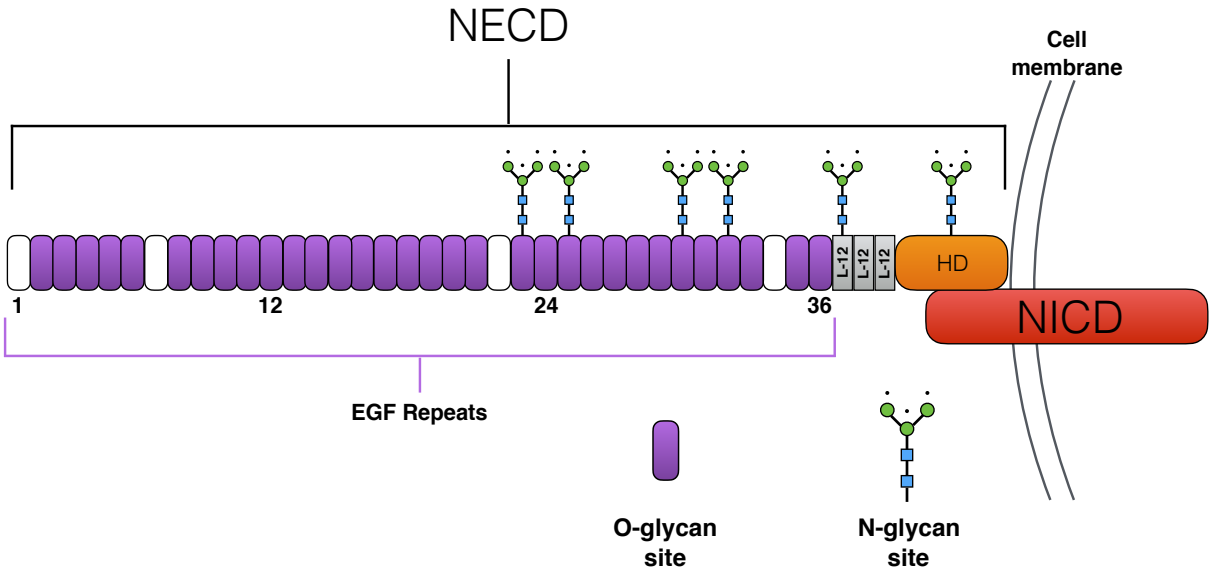


Fig 1.8 Glycosylation of the Notch Receptor. The Notch Receptor is heavily glycosylated. All glycosylation occurs on the extracellular domain (NECD), while there are no glycosylation sites on the intracellular domain (NICD). This figure details the EGF repeats that contain glycosylation sites, but it must be noted that glycosylation can also occur on the Lin-12 (L-12) repeats and in the hydrophobic domain (HD). These sites are highly conserved across species.

1.7.2 Notch N-glycosylation

While there is a substantial body of evidence to support the role of O-glycosylation in Notch signalling, there is very little regarding that of N-glycosylation. In 1989 Johansen et al., used a lentil lectin affinity column to show that the Notch receptor is modulated with high-mannose N-glycans. The sensitivity of Notch1 to peptide N-glycosidase F (PNGase F) further demonstrated the presence of N-glycans (Shao, Moloney and Haltiwanger, 2003). Research groups have identified six N-glycosylation consensus sites on the mammalian Notch1 receptor: one each at EGF 23, 25, 30 and 32, one in the LNR region and one adjacent to the S2 cleavage site (Takeuchi and Haltiwanger, 2014).

Although these consensus sites have been identified, it is not known how many of them actually harbour N-linked glycans. This is mostly due to the fact that, as previously stated, very little research has been directed towards deciphering the N-glycosylation profile of Notch and the role of these glycans. The main reason for this lack of research is that many review papers have cited N-glycosylation as non-critical for Notch signalling (Stanley, 2007; Takeuchi and Haltiwanger, 2014). This assumption is largely based on a single paper which reported that Lec1 CHO cells, which have the ability to form high-mannose N-glycans but

not complex or hybrid-type N-glycans, exhibited the same level of Jagged-1-induced Notch signalling as its wild-type equivalent (Moloney, Panin, *et al.*, 2000).

It was not until 2017 that strong evidence was published supporting the role of N-glycosylation in the activation and regulation of Notch signalling. Allam et al. had, in previous papers, described the mechanism and importance of N-acetylglucosaminyltransferase-III (GnT-III) in the process of Notch N-glycosylation. GnT-III is coded by the *Mgat3* gene and forms bisecting N-glycans by adding β1,4-linked GlcNAc to the mannosyl core which is common to all N-linked glycans (Allam *et al.*, 2015). In a follow-up study, the presence of bisecting N-glycans on the Notch receptor was confirmed via binding of the Phaseolus Vulgaris Erythroagglutinin (E-PHA) lectin. *Mgat3* was then stably knocked down in human ovarian cancer cell lines using shRNA. This led to a reduction in Notch, NICD and Hey1 protein levels and a decrease in γ-secretase cleavage activity. It was also observed that, following *Mgat3* knockdown, Notch1 co-localised with LAMP1, a lysosomal degradation protein, suggesting that the loss of GnT-III activity was resulting in increased endocytosis and degradation of the Notch1 receptor. This was further supported by data that showed an increase in Notch1 protein levels following inhibition of lysosomal enzymes in the *Mgat3* knockdown population, compared to no change in protein levels in the wild type population (Allam *et al.*, 2017). This evidence indicates that bisecting N-glycans may serve some role in maintaining Notch signalling. This may be through protection against endocytosis as, in addition to this data, it has previously been noted that N-glycosylation aids interaction of membrane-bound receptors with the extracellular matrix (Dennis *et al.*, 2009). However, it must be taken into account that N-glycan specific glycosyltransferases such as GnT-III modulate an enormous number of proteins in the cell and so complex signalling pathways such as that of Notch may be affected by GnT-III inhibition at a number of stages and not just at the receptor activation point.

1.8 Detecting N-glycans

The method of glycan analysis is usually determined by the type of information that one wishes to obtain. For structural analysis of the glycans in a sample the most commonly used methods are mass spectrometry (MS) and high performance liquid chromatography (HPLC) and in many cases these techniques are used in tandem to achieve optimum results. Alternatively, lectin technologies can be used to determine the presence or absence of particular oligosaccharides on the cell or protein surface.

1.8.1 Structural Analysis

These methods require the enzymatic or chemical removal of glycans from the surface of the glycoprotein. For N-glycosylation this can usually be achieved using the PNGase enzyme. In HPLC, released glycans can then be fluorescently labelled using a fluorescent molecule such as 2-aminobenzamide (2-AB) for enhanced detection of a particular carbohydrate structure. Relative quantification of that structure in a given sample can then be determined (Bigge *et al.*, 1995; Roth, Yehezkel and Khalaila, 2012).
MS involves the conversion of the glycans to gas-phase ions, often through electrospray ionization (ESI). These ions are then accelerated into a mass analyser and separated based on their mass to charge ratio. Interpretation of the mass spectrum can then reveal the structure of the glycans in the sample based on their mass to charge ratio (Kebarle, 2000).

Both methods are high throughput and can quite accurately describe the structure of individual glycans. However, these procedures can be expensive and laborious due to the need for the glycans to be removed from the protein before analysis, which can lead to information about glycosylation sites and linkages being lost (Geyer and Geyer, 2006). Additionally, the interpretation of the final mass spectrum requires a certain level of expertise to assess the link between the MS graph and actual structural information (Brooks, 2009).

1.8.2 Lectin Technology

Sharon and Lis (1998) describe lectins as proteins which can reversibly bind mono- and oligosaccharides with a high level of specificity, but are not enzymes or antibodies as they possess no catalytic activity and are not produced as part of the immune response. Lectin binding was originally believed to be quite broad and relatively weak. This was mainly due to the fact that most early studies concentrated on binding to monosaccharides. In the past decade however, lectin-carbohydrate binding has been shown to actually be highly specific and depends as much on the linkages, branching and orientation of sugars in the carbohydrate chain as it does on the individual monosaccharides (Ambrosi, Cameron and Davis, 2005; Ghazarian, Idoni and Oppenheimer, 2011). This has led to a number of lectin technologies being developed for the purpose of glycan analysis.

1.8.2.1 Lectin Microarrays

Microarrays have been developed using lectin-coated 'chips' where a glycoprotein sample is added to wells on the chip which each contain a different lectin. In order to detect and quantify the levels of bound glycoprotein, fluorescent labelling of either the proteins themselves or antibodies specific for that protein, is carried out (Rosenfeld et al. 2007). This process is used for the rapid, high-throughput analysis of the type of glycans present on the sample glycoprotein.

1.8.2.2 Serial Lectin Affinity Chromatography

Serial lectin affinity chromatography (SLAC) differs from lectin microarray technology in that it isolates specific glycoproteins in a sample based on the presence or absence of one or more particular glycans, rather than investigating the entire glycan make-up of the sample proteins. This is often referred to as a 'glyco-catch' approach as it involves the retention of a group of glycoproteins which share a common determinant (Walsh 2009). In this process, several columns, each containing a different lectin bound to the stationary phase beads, are used one after the other to sequentially isolate the target glycoforms (Qiu, Zhang and Regnier, 2007).

1.8.2.3 Enzyme-linked Lectin Assay

The enzyme-linked lectin assay (ELLA) is a simple and rapid technique that was conceived in the early 1980s (McCoy, Varani and Goldstein, 1983) but has only really come to prominence and been optimised in the last decade, thanks in no small part to a number of studies conducted by Brendan O'Connor's and Paul Clarke's research groups. ELLA is very similar in method to the enzyme-linked immunosorbent assay (ELISA) in that it involves the probing of immobilized proteins on the surface of a multi-well, but uses specific conjugated lectins rather than antibodies. Data is obtained in the form of a detectable colour change that can be spectrophotometrically measured and used to calculate the level of lectin-glycoprotein binding (Thompson *et al.*, 2011).

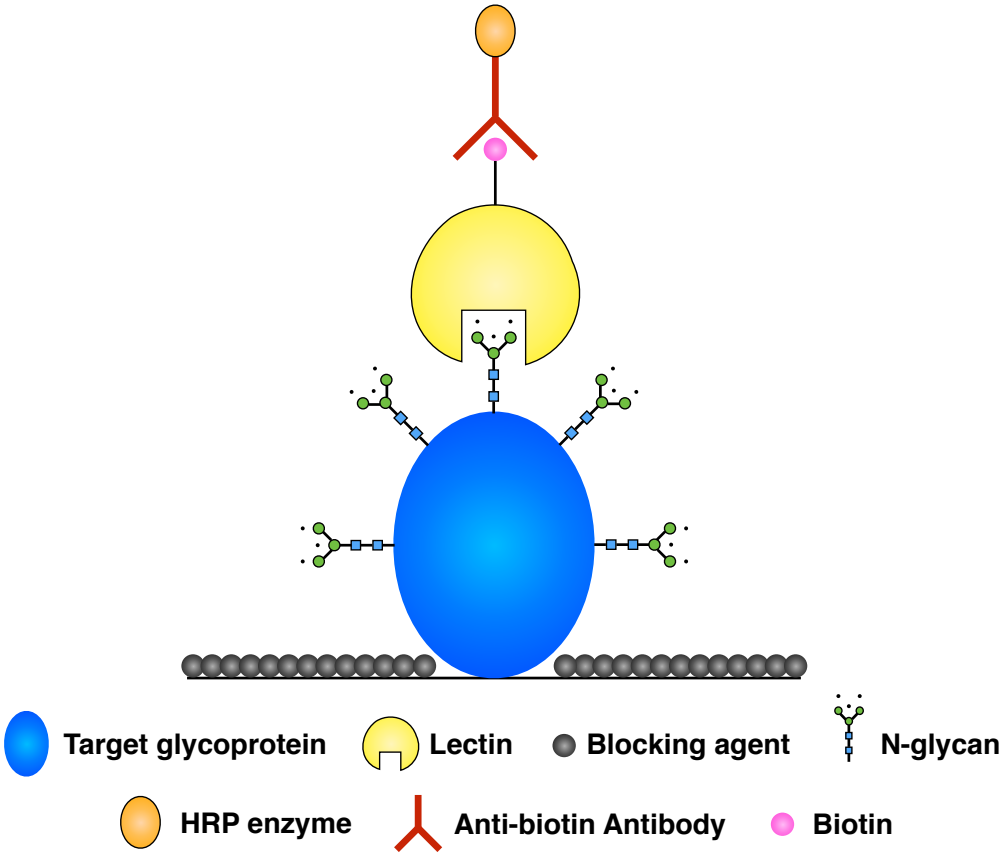


Fig 1.9 Enzyme-linked Lectin Assay (ELLA). This figure details the mechanism involved in the detection of glycans using ELLA. Target proteins are immobilised onto the surface of a well and probed with specific biotinylated lectins. Anti-biotin antibodies bind to these lectins. A conjugated horse radish peroxidase (HRP) enzyme acts on a TMB substrate to produce a detectable colour change.

1.8.2.4 Limitations of Lectin Technologies

Although lectins provide a promising alternative to the laborious processes of HPLC and MS, there are a number of limitations which must be taken into account when using lectin-based technologies. The main drawback is the lack of commercial lectins available for researchers. Only a small number have been studied, tested and purified for commercial use, and this number is far below what is required to investigate and analyse the wide variety of glycan structures that exist (Haab, 2012). The advent of recombinant lectin technology in recent years has provided a possible solution for this issue, with a number of recombinant lectins being developed which display high levels of avidity and specificity (Ribeiro et al., 2018).

However, this is a technology still in its very early stages and is yet to overcome multiple obstacles facing it, such as the need for developing a reliable, high-throughput screening method for lectin libraries (Hirabayashi and Arai, 2019; Tommasone et al., 2019). Another significant limitation to the use of lectin technology is the low binding affinity of many currently available lectins. Despite the fact that lectin affinity for specific glycans *in vivo* is very high (in the nanomolar range), this is most likely due to formation of homo-oligomeric lectin structures which create deep binding pockets (Bewley and Otero-Quintero, 2001). Meanwhile, lectin affinity *in vitro* is quite often restricted to the micromolar range, limiting the sensitivity of many lectin-based assays (Weis and Drickamer, 1996; Stowell et al., 2008).

1.9 Methods for Investigating the Effect of N-glycosylation

Due to the immense complexity and variety of N-glycosylation in mammalian cells, it can often be difficult for researchers to pinpoint the exact role of N-glycans in a given cellular process or pathway. While gene knockouts are regularly used as a starting point for elucidating protein or RNA function, the task becomes more difficult in a non-templated process like glycosylation. To overcome these challenges, an arsenal of strategies have been developed over the past few decades, making use of small-molecule inhibitors, siRNA technology and DNA mutation methods to investigate the role and effect of N-glycosylation in molecular mechanisms.

1.9.1 Small-molecule Inhibitors

First discovered in *Streptomyces lysosuperificus* in 1970 by Takatsuki *et al.*, Tunicamycin (TNC) is by far the most widely used inhibitor of N-glycosylation. It is a nucleoside antibiotic which acts by inhibiting GlcNAc Phosphotransferase (GPT), an essential enzyme in N-glycosylation which catalyses the addition of a dolichol precursor to the nascent polypeptide (Aaron Heifetz, Keenan and Elbein, 1979; Brandish *et al.*, 1996). Through this mechanism of action, TNC can inhibit global N-glycosylation in a cell. It has therefore been used extensively to study the effect of N-glycosylation on cellular mechanisms, such as the processing and activation of receptor tyrosine kinases (RTKs) (Klaver *et al.*, 2019). N-glycosylation has even emerged as a possible therapeutic target for cancer due to the ability of TNC to attenuate RTK signalling and induce ER stress in cancer cells (Contessa *et al.*, 2008; Wu *et al.*, 2018; Wang *et al.*, 2020).

Another small-molecule inhibitor being used to investigate the effects of N-glycosylation is 1-deoxymannojirimycin (DMJ). Unlike TNC, it does not suppress the formation of all types of N-glycans, only complex and hybrid types. As a mannosidase I inhibitor, DMJ blocks the trimming process of the 14-sugar precursor dolichol oligosaccharide (Glc3Man9GlcNAc2) to the trimannosyl core (Man3GlcNAc2), meaning that only high-mannose type N-glycans can be formed (Elbein, 1987). DMJ has been used to study the importance of N-glycosylation in processes such as cell recognition in T-cells (Bagriaçik, Kirkpatrick and Miller, 1996) and, similarly to TNC, has been shown to induce ER stress in cancer cells (Lu *et al.*, 2006), again emphasising the value of targeting glycosylation in cancer therapy.

A range of alternative small-molecule inhibitors also exist which are used to a lesser extent. Naturally occurring plant alkaloids such as Swainsonine can be potent suppressors of glycosidases, while metabolic inhibitors such as 6-diazo-5-oxo-L-norleucine (DON), which blocks glucosamine production, can indirectly reduce the capacity of the cell to form N-glycans (Esko, Bertozzi and Schnaar, 2015).

1.9.2 siRNA Technology

Since the discovery of siRNA as gene silencers in 1999, the technology has been rapidly developed and widely utilised to temporarily knock down specific gene transcripts in a multitude of cell types (Hamilton and Baulcombe, 1999). As previously mentioned, glycosylation is a non-coded process and so glycans cannot be targeted directly using this technology. Glycosyltransferases are defined as a "group of enzymes that catalyse the transfer of a sugar moiety from an activated sugar donor onto saccharide or non-saccharide acceptors" (Coutinho *et al.*, 2003). They are the builders of glycans and, as such, are ideal targets for siRNA knockdown as each type of glycosyltransferase is highly specific, not only for the monosaccharide it transfers, but also for the type of acceptor it transfers to and the linkage it forms (Jafar-Nejad, Leonardi and Fernandez-Valdivia, 2010).

Knockdown of glycosyltransferase genes using siRNA has been extensively implemented in the last 20 years to decipher the role of glycan sub-types in cellular mechanisms. For example, one study in 2004 used targeted siRNA to knock down the α1,6-fucosyltransferase Fut8 in CHO cells and this led to the production of defucosylated antibodies with greatly increased antibody-dependent cellular cytotoxicity (ADCC) (Mori *et al.*, 2004). Furthermore, it has been demonstrated that siRNA knockdown of glycosyltransferase

complex subunits can also be used to investigate the process of N-glycosylation. In this way, a study in 2012 examined the function of three subunits of the oligosaccharyltransferase (OST) complex and found each one to have specific selective modulatory functions (Roboti and High, 2012). These studies and many more provide substantial evidence that glycosyltransferase inhibition via targeted siRNA transfection can be a useful tool in analysis of the effect of N-glycosylation.

1.9.3 DNA Mutation Methods

Although N-linked glycosylation is a non-templated process, it does require, as described in Section 1.6.1, a consensus sequence including an asparagine residue to which the oligosaccharide precursor can be attached. Multiple research groups have targeted this consensus sequence, mutating the Asn residue to block the addition of a glycan at that site. A widely used approach is to carry out site-directed mutagenesis on a plasmid-encoded glycoprotein, transfect this plasmid into a cell population and observe the effect of the mutant glycoprotein compared to the wild-type. In the early 1990s, a number of ground-breaking studies showed that different glycoforms of the cytokine erythropoietin (EPO) had significantly different activity levels (Wasley *et al.*, 1991; Delorme *et al.*, 1992). One of the methods employed to investigate these differences was the site-directed mutagenesis of N-glycosylation sites in a plasmid-encoded EPO gene, which led to a substantial decrease in binding affinity of EPO to its receptor *in vivo* (Yamaguchi *et al.*, 1991). Other groups have applied this same approach to investigate the role of N-glycosylation in mechanisms such as tyrosinase activity, lactoferrin utilisation, processing of human acid sphingomyelinase (ASM) and binding affinity and signal transduction of follicle-stimulating hormone (FSH) (Flack *et al.*, 1994; Van Berkel *et al.*, 1996; Ferlinz *et al.*, 1997; Branza-Nichita *et al.*, 2000).

1.10 Aims and Objectives

The main aims of this study are to investigate the role of Notch1 in the myogenic differentiation of an S100β$^+$ resident vascular stem cell population, characterise the profile of N-glycosylation on the Notch1 receptor and explore the impact of this N-glycosylation on Notch signalling and Notch-mediated myogenic differentiation.

The specific objectives are as follows:

- To isolate and characterise an S100β$^+$ multipotent vascular stem cell (MVSC) population from a mouse aortic arch
- To demonstrate that Jag-1 activates Notch signalling and myogenic differentiation in MVSCs
- To determine whether this activation is dependent on the Notch1 receptor
- To confirm the presence and location of N-glycans on the Notch1 receptor extracellular domain
- To examine the effect of global N-glycosylation inhibition on Jag-1 activation of the Notch1 receptor and myogenic differentiation
- To examine the effect of specific glycosyltransferase knockdown on Jag-1 activation of the Notch1 receptor and myogenic differentiation
- To successfully carry out site-directed mutagenesis on specific N-glycosylation sites on the Notch1 extracellular domain
- To examine the effect of this site-directed mutagenesis on Jag-1 activation of the Notch1 receptor and myogenic differentiation
- To investigate how altered N-glycosylation affects the expression and localisation of Notch1

Chapter 2:

Materials and Methods

2.1 Materials

Table 2.1 Mammalian Cell Lines used in this study

Cell Line	Cell Type	Description
MVSC	Adult Stem Cell	Multipotent Vascular Stem Cells isolated from the medial layer of a mouse aortic arch by enzymatic dispersion and sequential plating on non-adherent and adherent tissue culture plates
MOVAS (ATCC® CRL-2797™)	Differentiated Smooth Muscle Cell	Commercial cell line of terminally differentiated mouse aortic smooth muscle cells. Immortalised with SV40 large T-antigen
C3H/10T1/2, Clone 8 (ATCC® CCL-226™)	Embryonic fibroblast	Commercial cell line of fibroblasts isolated from the embryo of C3H mice.

Table 2.2 Bacterial Cell Lines used in this study

Cell Line	Cell Type	Genotype
E.coli JM109	Bacterial Cell	endA1, recA1, gyrA96, thi, hsdR17 (rk–, mk+), relA1, supE44, Δ(lac-proAB), [F′ traD36, proAB, laqIqZΔM15]
XL-10 Gold	Ultracompetent Bacterial Cell	TetrΔ (mcrA)183 Δ(mcrCB-hsdSMR-mrr)173 endA1 supE44 thi-1 recA1 gyrA96 relA1 lac The [F' proAB lacIqZΔM15 Tn10 (Tetr) Amy Camr]

Table 2.3 Primers used in this study from Qiagen

Product	Target Gene	Catalog No.
Mm_Hprt_1_SG QuantiTect Primer Assay	*Hprt*	QT00166768
Mm_*Mgat3*_1_SG QuantiTect Primer Assay	*Mgat3*	QT00297073
Mm_*Fut8*_3_SG QuantiTect Primer Assay	*Fut8*	QT00115094

Table 2.4 Primers used in this study from Integrated DNA Technologies

Target Gene	Sequence
Hprt	Forward 5'- GGC TAT AAG TTC TTT GCT GAC CTG C -3'
	Reverse 5'- GCT TGC AAC CTT AAC CAT TTT GGG -3'
Hey1	Forward 5'- ACT CCG ATA GTC CAT AGC CA -3'
	Reverse 5'- GTA CCC AGT GCC TTT GAG AA -3'
Cnn1	Forward 5'- TCC ATG AAG TTG TTC CCG ATG -3'
	Reverse 5'- GCT TGT CTG CTG AAG TAA AGA AC -3'
Myh11	Forward 5'- ATT GTC ATT TAG CGG GTC CAT -3
	Reverse 5'- AAC AGA GTT CTC CAT CAT CCA C -3'
Notch1	Forward 5' – AGG ATC AGT GGA GTT GTG C – 3'
	Reverse 5' – CGT TAC ATG CAG CAG TTT CTG – 3'

Table 2.5 Plasmid Vectors used in this study

Plasmid	Description
pCS2 Notch1 Full Length-6MT	Plasmid encoding for the full length mouse Notch1 protein with a hexameric myc-tag at the C-terminus end. Prof. Raphael Kopan (Addgene plasmid No. 41728)
pCS2 Notch1 ICv-6MT	Plasmid encoding for the intracellular domain of mouse Notch1 protein (aa1744 – 2184) with a hexameric myc-tag at the C-terminus end. Prof. Raphael Kopan (Addgene plasmid No. 41730)
pEGFP-N1	Plasmid encoding for Enhanced Green Fluorescent Protein. Dr. Ronan Murphy, Dublin City University, Ireland.
pPGKpuro	Plasmid encoding a Puromycin Resistance gene. Dr. Dermot Walls, Dublin City University, Ireland
pCDNA3.1	Empty plasmid vector containing only bacterial resistance genes and restriction sites (Addgene plasmid no. V790-20)

Table 2.6 siRNA molecules used in this study

Product	Target Gene	Catalog No.
Silencer® Select siRNA, Notch1 (s70700)	*Notch1*	4390771
Silencer® Select siRNA, *Mgat3* (s69837)	*Mgat3*	4390771
Silencer® Select siRNA, *Fut8* (s79249)	*Fut8*	4390771
Silencer® Select GAPDH Positive Control siRNA	*Gapdh*	4390849
Silencer® Select Negative Control No. 1 siRNA	No Target	4390843
Silencer® Select Negative Control No. 2 siRNA	No Target	4390846
IDT TYE 563 Transfection Control DsiRNA	No Target	51-01-20-19

Table 2.7 Antibodies used in this study

Supplier	Product	Description	Catalog No.
Abcam	Anti-Calponin Antibody (EP798Y)	Rabbit monoclonal	ab46794
	Anti-smooth muscle Myosin heavy chain 11 antibody (1G12)	Mouse monoclonal	ab683
	Anti-myc-tag Antibody (9E10)	Mouse monoclonal	ab32
	Anti-S100β Antibody (EP1576Y)	Rabbit monoclonal	ab52642
	Anti-Nestin Antibody (196908)	Mouse monoclonal	ab6320
	Anti-pan Cadherin Antibody [EPR1792Y]	Rabbit monoclonal	ab51034
	Anti-Notch1 Antibody [EP1238Y]	Rabbit monoclonal	ab52627
Biosciences	Anti-Golgin-97 Antibody	Mouse Polyclonal	PA530048
	Anti-Notch1 Antibody (A6)	Mouse Monoclonal	MA511961
	AlexaFluor® 488 Anti-Rabbit IgG	Goat polyclonal secondary antibody	A11008
	AlexaFluor ® 488 Anti-Mouse IgG	Goat polyclonal secondary antibody	A11001

Brennan & Co	Anti-Notch1 Antibody (D1E11) XP®	Rabbit Monoclonal	3608S
Sigma-Alrich	Anti-β-actin Antibody (AC-74)	Mouse Monoclonal	A2228
	HRP-conjugated Anti-Mouse IgG (Fab specific)	Goat polyclonal secondary antibody	A9917-1ML
	HRP-conjugated Anti-Rabbit IgG (whole molecule)	Goat polyclonal secondary antibody	A0545-1ML
	HRP-conjugated Anti-biotin IgG	Goat polyclonal	A4541

Table 2.8 Chemicals, Reagents, Proteins and Kits used in this study

Product	Supplier	Catalog No.
Abcam	TEO-Tricine Precast Gels – RunBlue™ 10%	ab119202
Accuscience	Bio-Rad SureBeads™ Protein G Magnetic Beads	1614023
	Bio-Rad SureBeads™ Protein A Magnetic Beads	1614013
Agilent	QuikChange Lightning Site Directed Mutagenesis Kit	210518
Biosciences	TrypLE Select	A1217701
	Opti-MEM	11058021
	N2	A1370701
	B27	17504-044
	2-mercaptoethanol	31350-010
	UltraPure™ 0.5M EDTA, pH 8.0 (4 x 100ml per box)	15575020
	Pierce™ BCA Protein Assay Kit	23227
	Invitrogen PureLink™ HiPure Plasmid Filter	K210014
	Pierce™ ECL Western Blotting Substrate	32209
	1kb Plus DNA Ladder	10787018
	Mem-PER™ Plus Membrane Protein	89842

Bio-Techne	Recombinant Rat Jagged-1 Fc	599-JG-100
	Recombinant Human IgG1	110-HG-100
Fisher Scientific	Day Impex™ Disinfectant Virkon Virucidal Tablets	12328667
	PBS Tablets	12821680
Fluka	Calcium Chloride Solution	21114-1L
Lennox	Industrial Methylated Spirits	CRTSI0330716
LGC Standards	Fetal Bovine Serum, ES Qualified	ATCC SCRR-30-2020
Medical Supply Company	TransIT-X2® Dynamic Delivery System 0.3ml	MIR6003
	SensiMix SYBR No-ROX Kit (500 rxn)	QT650-02
	SensiFAST™ SYBR® No-ROX One-Step Kit	BIO-72005
	Bioline ISOLATE II Genomic DNA Kit	BIO-52067
	Protein G	21193-5mg
MyBio	Promega Reliaprep RNA cell mini prep system	Z6012
Qiagen	Rotor-Gene SYBR Green RT-PCR Kit (400)	204174
ScienCell	Relative Mouse Telomere length quantification qPCR	SC-M8908
Seralab	Chick Embryo Extract	CE-650-J
Sigma-Aldrich	DAPI	D9542-5MG
	Formaldehyde Solution	252549-100ML
	Polyvinyl Alcohol	P8136-250g
	Trizma base	T1503-1kg
	Sodium Chloride	S3014-5KG
	Hydrochloric Acid	H1758-500ML
	Manganese(II) Chloride Solution	M1787-100ML

Sigma-Aldrich (contd.)	DPBS	D5773-1L
	Magnesium Chloride Solution	M1028-100ML
	D-(+) Glucose	47829
	Magnesium Sulfate	M7506-500G
	Puromycin	P8833-10mg
	Ampicillin sodium salt	A9518-5G
	Trypan Blue	T8154-100ML
	Sodium Citrate	W302600
	Citric Acid	C2404
	TMB Tablets	T3405
	Hydrogen Peroxide	18312
	RIPA Buffer	R0278-50ml
	Protease inhibitor cocktail	P8340
	2-propanol	I9516
	Ethanol	E7023-500ML-D
	Penicillin-Streptomycin	P4333-100ML
	Bovine Serum Albumin	A4503-50G
	RPMI	R8758-500ML
	EMEM	M4655-500ML
	Fetal Bovine Serum	F9665-500mL
	DMEM	D5796-500mL
	DAPT	D5942-5MG
	DMSO	41639-500ML

Sigma-Aldrich (contd.)	Glycine	G8898-1kg
	Tween-20	P1379-500ML
	Retinoic Acid	R2656
	Agar	A1296-100G
	Agarose	A9414-5G
	TE Buffer	93283-100ML
	TRAPeze® XL Telomerase Detection Kit	S7707
	Triton X-100	T8787
	Fluoromount Aqueous Mounting Medium	F4680
Vector Laboratories	Concanavalin A	B1005
	Lens Culinaris Agglutinin	B1045
	Wheat Germ Agglutinin	B1025
	Phaseolus Vulgaris Erythroagglutinin	B1125
	Phaseolus Vulgaris Leucoagglutinin	B1115

2.2 Methods

2.2.1 Genetic Lineage Tracing of S100β Stem cells and assessment of their contribution to neointimal lesions *in vivo*

The methods for treatment and analysis of this mouse model are outlined in detail in previous publications from our research group (Di Luca *et al.*, 2021). Briefly, S100β-EGFP/Cre/ERT2 transgenic mice were crossed with Ai9 reporter mice to produce a S100β-eGFP/Cre/ERT2–dTomato double transgenic offspring. In this mouse model, tdTomato expression indicated a genomically marked S100β cell, while eGFP expression indicated constitutive expression of S100β. Tamoxifen injections were carried out for 5 consecutive days to induce Cre activation. Corn oil was used as a negative control for Tamoxifen. Four weeks after the final injection of Tamoxifen, ligation of the left carotid artery was performed

using a 6-0 silk suture. The neck incision was sutured closed and, after 21 days of observation, both the right and left carotid arteries were harvested. Arteries were sectioned and deparaffinised via immersion in xylene, before being rehydrated through sequential immersion in decreasing concentrations of ethanol. Sections were washed before nuclear staining with DAPI and mounting using Fluoroshield. All samples were imaged using a FV1000 Olympus or a Nikon A1R HD laser scanning confocal microscope.

2.2.2 Isolation of MVSCs from mouse aorta by enzymatic dispersion

The use of animals in this study was carried out in accordance with the EU legislation (Directive 2010/63/EU) for the protection of animals used in research. Furthermore, ethical permission was granted for this work by the DCU Research Ethics Committee (REC). Female Bl/tgtgt Thy1 YFP mice were anesthetized with an overdose of pentobarbital sodium (0.1mg/g), and death was confirmed by exsanguination by an authorised professional. After removal of aorta from the animal, the vessel was washed in PBS before incubation in 2.5 mg/mL Collagenase at 37^{o}C for 20min. Adventitia was then carefully removed. Aorta was cut into small pieces and incubated at 37^{o}C in Elastase Type III for 2.5h with vortexing every 10 minutes. Following two washes with PBS, cells were added to a non-adherent 6-well plate in MM1 and incubated at 37^{o}C and 5% CO_2 for 72h. Suspension cells were then transferred to an adherent 6-well plate and cultured as detailed in Section 2.2.3.1 (Tang *et al.*, 2012).

2.2.3 Cell Culture Methods

All mammalian cell culture was carried out under sterile conditions in a Biosciences Air 2000 Mac laminar air flow cabinet. Cells were grown in a water-jacketed Hera incubator at 37^{o}C and 5% CO_2. A Nikon Eclipse TS100 phase contrast microscope was used to visualize cells. All mammalian cells were grown in 25, 75 or 175 cm^2 tissue culture-treated flasks or in 6-well plates.

2.2.3.1 MVSCs

Grown in MM1 maintenance media which consisted of DMEM supplemented with 2% Chick Embryo Extract, 2% B27, 1% N2, 1% FBS, 1% Penicillin Streptomycin, 20ng/mL rFGF, 100nM Retinoic Acid and 50nM 2-mercaptoethanol (Tang *et al.*, 2012). Cells were

used at passage numbers below P25. Freezing media consisted of MM1 with FBS concentration increased to 15% and supplemented with 10% DMSO.

2.2.3.2 mSMC

Grown in RPMI basal media supplemented with 10% FBS and 1% Penicillin Streptomycin. Cells were used at passage numbers below P25 (Mackenzie *et al.*, 2011). Freezing media consisted of RPMI with 10% FBS, 1% Pen-Strep and 10% DMSO.

2.2.3.3 C3H10T1/2

Grown in EMEM basal media supplemented with 10% heat-inactivated FBS and 1% Penicillin Streptomycin. Cells were used at passage numbers below P20. Cells were always subcultured before confluency surpassed 70% in order to prevent post-confluence inhibition. Freezing media consisted of EMEM with 10% FBS, 1% Pen-Strep and 5% DMSO.

2.2.3.4 Subculturing

Growth media was removed from the culture vessel and cells were washed once with HBSS (stem cell lines) or PBS (differentiated cell lines). An appropriate volume of 0.5X TrypLE (stem cell lines) or 1X Trypsin (differentiated cell lines) was added to the culture vessel, which was then incubated at 37ºC for 5 minutes. Dissociation of cells from the base of the culture vessel was confirmed by visualisation under the bright field microscope. Growth media containing FBS was added to deactivate the TrypLE/Trypsin. This cell suspension was then transferred to a 15ml centrifuge tube and centrifuged at 300 x g for 5 minutes. The supernatant was discarded and the cell pellet was resuspended in 1mL of fresh growth media. This cell suspension was then divided into two or more flasks/wells with an appropriate amount of growth media and incubated at 37ºC.

2.2.3.5 Viable Cell Counting

Following trypsinisation and centrifugation, the cell pellet was resuspended in 1-3mL of fresh growth media. 20µL of this cell suspension was diluted 1:1 with 0.4% Trypan Blue and incubated at room temperature for 2-5 minutes. 20µL of this dilution was then added to the counting chamber of a haemocytometer. The haemocytometer was then viewed under the microscope at 20x magnification. Trypan blue can enter and stain the cytoplasm of a

dead cell but cannot cross the membrane of a viable cell. Due to this, dead cells appeared stained dark blue while live cells were unstained. Viable cells were counted in four of the major grid boxes on the haemocytometer and an average cell count was calculated. The following equation was used to estimate the viable cell concentration in the total cell suspension:

Average cell count x 10^4 (area under the cover slip) x 2 (dilution factor) = no. of viable cells/mL

2.2.3.6 Cryopreservation

Cells were trypsinised and pelleted as previously described. The cell pellet was then resuspended in freezing media which varied depending on the cell line. This cell suspension was divided into 1mL aliquots in sterile cryopreservation vials. These vials were placed in a Mr. Frosty™ freezing container which was then stored overnight at -80°C. The vials were then transferred to liquid nitrogen for long-term storage.

2.2.4 Plasmid Amplification and Purification

2.2.4.1 Transformation

LB Agar (20g/L LB, 12g/L Agar) was made up in dH_2O and autoclaved to sterilise. After cooling to 55°C, appropriate antibiotics were added (Ampicillin at 100µg/mL or Kanamycin at 50µg/mL). The agar was poured into sterile petri dishes, allowed to harden and stored at 4°C.

100ng of plasmid DNA was mixed with 50µL of competent JM109 bacterial cells in a sterile microfuge tube. Tube was placed on ice for 30 mins. Cells were then heat-shocked at 42°C for 45secs to allow plasmid DNA to cross the cell membrane. Tube was placed back on ice for 2 mins. 500µL of SOC medium (20% tryptone, 5% yeast extract, 0.5% NaCl, 1% 0.25M KCl, 2% 1M glucose) was added to the tube which was then incubated at 37°C for 45 mins. The contents of the tube were transferred to a LB Agar plate with appropriate antibiotics. Plates were incubated overnight at 37°C.

A single colony was picked from the transformation plate and inoculated in 5mL of LB broth (20g/L LB) with appropriate antibiotic. This culture was incubated at 37°C in a shaking

incubator for 6-8 hours. 1.2mL of this culture was then transferred to a sterile conical culture flask containing 250mL of LB broth with appropriate antibiotic. Flask was incubated at 37°C overnight in a shaking incubator. 50mL was removed from the flask for plasmid purification. The rest was used to make stocks by supplementing with 50% glycerol and storing at -80°C.

2.2.4.2 Plasmid DNA Purification

Plasmid DNA was purified from transformed bacterial cells using the Invitrogen PureLink™ HiPure Plasmid Filter Midiprep Kit. Standard kit protocol was followed. Briefly, 25mL of the overnight LB culture was centrifuged at 4,000 x g for 10 minutes. The supernatant was discarded and the pellet was resuspended in 10mL of Resuspension Buffer. 10mL of Lysis Buffer was added and the contents were incubated at room temperature for 5 minutes. 10mL of Precipitation Buffer was added and mixed thoroughly before transferring the tube contents to the filter column and allowing the solution to pass through the filter and binding column by gravity flow. After two wash steps, 5mL Elution buffer was passed through the column to elute the plasmid DNA. 3.5mL of isopropanol was added to the eluate and the contents were centrifuged at 12,000 x g for 30 minutes at 4°C. The supernatant was discarded and the pellet was resuspended in 3mL of 70% ethanol. The contents were centrifuged at 12,000 x g for 5 minutes at 4°C. The supernatant was discarded and, after air-drying for 10 minutes, the pellet was resuspended in 100µL of TE Buffer. The Nanodrop® ND-1000 Spectrophotometer was used to quantitate the DNA concentration as described in Section 2.2.8.

2.2.4.3 Agarose Gel Electrophoresis

Agarose gel was made by dissolving agarose powder at 1% in 1X TAE Buffer (40mM Tris, 20mM Glacial Acetic Acid, 1mM EDTA, pH to 8.5). 6X Loading Dye was mixed with 1kb Plus DNA Ladder and each plasmid DNA sample. 10µL of DNA Ladder and 20µL of each sample was added to a well in the agarose gel. Gel was run at 80V for approximately 90 minutes. SynGene G-Box was used to visualise and image bands on the gel.

2.2.5 Notch1 Activation using Jagged1 (Jag1)

Protein G was added to each well in a sterile 6-well plate at a concentration of 50µg/mL. Parafilm was used to seal the edges and the plate was stored overnight at 4°C. Protein G was discarded and wells were washed 3 times with sterile PBS. 1mL of blocking buffer (1% BSA in PBS) was added to each well. Plate was incubated at room temperature for 2 hours. Blocking buffer was discarded and wells were washed 3 times with PBS. 1mL of either Recombinant Rat Jagged-1-Fc or Recombinant Human IgG1-Fc (negative control) was added to each well. Plate was incubated at room temperature for 2 hours. Jag-1 and IgG1 were discarded and wells were washed once with PBS (Sukarawan *et al.*, 2016). Cells were seeded into wells with an appropriate volume of maintenance media.

2.2.6 Transient Transfections

2.2.6.1 Plasmid Transfection

Transfection of plasmid DNA into mammalian cells was achieved through the use of the Mirus Bio TransIT-X2® Dynamic Delivery System. Cells were grown to approximately 80% confluence in normal maintenance media with an appropriate concentration of FBS. Just before transfection, old media was removed and fresh maintenance media was added. The transfection mix was made up in a sterile microfuge tube according to kit protocol and optimization experiments (see example in Table 2.9) and incubated at room temperature for 30 minutes to allow transfection complexes to form. This mixture was then added dropwise to the cell culture. Cells were incubated at 37°C for 48 hours before harvesting.

Table 2.9 Plasmid Transfection Complex Tube setup with Mirus TransIT-X2

Component	Volume
OptiMEM Serum-free Media	200µL
Plasmid DNA (500ng/µL)	1.0µL
TransIT-X2	1.5µL
Add dropwise to cell culture with 2mL maintenance media	

2.2.6.2 siRNA Transfection

Transfection of single strand siRNA into mammalian cells was achieved through the use of the Mirus Bio TransIT-X2® Dynamic Delivery System. Cells were grown to approximately 80% confluence in normal maintenance media with an appropriate concentration of FBS. Just before transfection, old media was removed and fresh maintenance media was added. The transfection mix was made up in a sterile microfuge tube according to kit protocol (see example in Table 2.10) and incubated at room temperature for 30 minutes to allow transfection complexes to form. This mixture was then added dropwise to the cell culture. Cells were incubated at 37ºC for 48 hours before harvesting.

Table 2.10 siRNA Transfection Complex Tube setup with Mirus TransIT-X2

Component	Volume
OptiMEM Serum-free Media	200µL
siRNA (10µM)	5.6µL
TransIT-X2	6.0µL
Add dropwise to cell culture with 2mL maintenance media	

2.2.7 Immunocytochemistry

Cells were seeded on sterile cover slips in a 6-well plate at a low density (5,000 cells/well). When cells were ready to be stained and analysed, growth media was removed and cells were washed with PBS. Cells were fixed by incubating with 3.7% formaldehyde at room temperature for 15 minutes. PBST (PBS w/ 1% Tween-20) was used to wash the cells 3 times. For intracellular staining, cells were permeabilised by incubating with 0.1% Triton X-100 at room temperature for 15 minutes. Cells washed 3 times with PBST. Wells were blocked for 1hr at room temperature with PBS containing 5% BSA, 0.3M glycine and 1% Tween-20. Samples were incubated overnight at 4ºC with the primary antibody diluted to an appropriate concentration with 1% BSA in PBS. Cells washed 3 times with PBST. Samples were incubated at room temperature for 1hr with the secondary antibody (diluted with 1% BSA in PBS) and protected from light. Cells washed 3 times with PBST. Nuclear staining was carried out by incubating cells for 15 minutes at room temperature with DAPI which was diluted to 1µg/mL (3.6µM). Cells washed 3 times with PBST. Cover slips were mounted

on clean microscope slides using mounting media and the edges were sealed using nail varnish (Eimear Kennedy *et al.*, 2014). Cell nuclei and antibody staining could then be visualised and imaged using the Olympus DP-50 fluorescent microscope.

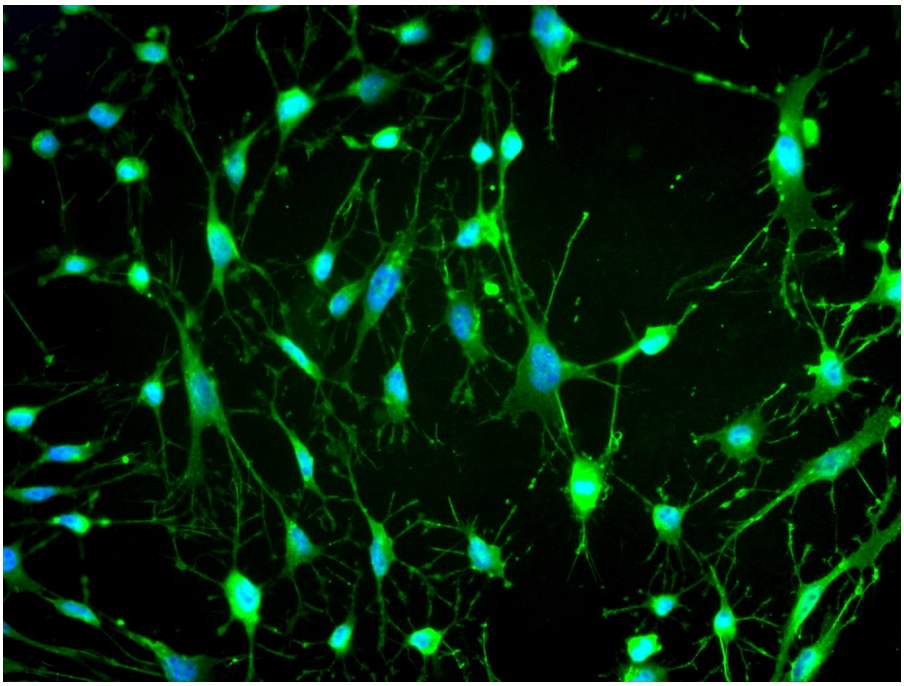


Fig 2.1 Immunocytochemistry. Immunocytochemistry involved the staining of specific protein markers using a combination of target-specific primary antibodies and host-specific secondary antibodies. Nuclei were stained with DAPI and a fluorescence microscope was used to obtain images. This figure is a sample image of the data output generated from an immunocytochemistry experiment.

2.2.8 RNA Extraction

RNA was extracted from cells using the Promega Reliaprep™ RNA Miniprep System. Kit instructions were followed. Briefly, cells were washed and scraped into PBS. Cells were pelleted by centrifugation at 1500 rpm for 5 minutes. The pellet was resuspended in an appropriate volume of BL+TG lysis buffer depending on the number of cells present. Isopropanol was added to the sample which was then mixed and transferred to a clean Reliaprep Minicolumn ™ in a collection tube. The contents were centrifuged at 13,000 x g for 30 seconds. A wash solution was added and the tube centrifuged again. DNase was added to the column to degrade any DNA present. After 3 more wash steps, an appropriate volume of nuclease-free water was added to the column. The tube was centrifuged at high speed to elute the purified RNA.

2.2.9 Genomic DNA Extraction

Genomic DNA was extracted from cells using the Bioline ISOLATE II Genomic DNA Kit. Kit instructions were followed. Briefly, cells were washed and scraped into PBS. Cells were pelleted by centrifugation at 1500 rpm for 5 minutes. The pellet was resuspended in Lysis Buffer GL. Proteinase K and Lysis Buffer G3 were then added to the sample before incubation at 70°C for 15 minutes. 99% ethanol was added to each sample to adjust DNA binding conditions. Samples were loaded into columns containing a silica membrane and centrifuged at 11,000 x g for 1 minute. The flow-through was discarded and columns were washed twice with Wash Buffer. Elution buffer was then added to each column. Samples were incubated at room temperature for 1 minute before centrifugation at 11,000 x g for 1 minute. The flow-through contained the purified DNA.

2.2.10 Quantitation of Nucleic Acid Concentration

Quantitation of both RNA and DNA concentrations were carried out using the Nanodrop® ND-1000 Spectrophotometer. The solution that the DNA or RNA had been eluted in was used to blank the instrument. A drop of sample was added to the stage and the absorbance of the sample was read at 260nm and 280nm. This gave a concentration of DNA/RNA in ng/μL. The ratio of OD260:OD280 provided an indication of the purity of the sample. It is generally accepted that a ratio of 1.8 indicates pure DNA while a ratio of 2.0 indicates pure RNA.

2.2.11 Quantitative Reverse-Transcription Polymerase Chain Reaction (qRT-PCR)

This technique was carried out using the Rotor Gene Q from Corbett Research. Sample RNA was first converted to cDNA by Reverse Transcriptase. Gene-specific primers and a Taq Polymerase enzyme then facilitated the amplification of a particular target gene over a number of temperature cycles. The complex formed between the cDNA and SYBR Green Dye led to the emission of a fluorescent signal. Therefore, fluorescence intensity was directly proportional to the starting amount of gene-specific mRNA in a given sample. A ubiquitously expressed reference gene (HPRT in murine cells) was used to give an indication of the expression levels of the target gene in the sample cell population. Two different kits were used for this method: Rotor-Gene SYBR® Green RT-PCR Kit (Qiagen, 204174) and SensiFAST™ SYBR® No-ROX One-Step Kit (BioLine, BIO-72001). The kit used depended on the type of primers needed. Samples were run in triplicate for each primer set.

Controls were included in each run to confirm functionality of the kit and instrument and to identify any possible contamination.

Table 2.11 qRT-PCR reaction tube setup with Bioline Sensifast Kit

Component	Volume
2x Sensifast ™ SYBR® No-ROX One-Step Mix	10µL
RNase Inhibitor	0.4µL
Forward Primer (10µM)	1.5µL
Reverse Primer (10µM)	1.5µL
Reverse Transcriptase	0.2µL
Nuclease-free H_2O	1.4µL
Template RNA (1-10 ng/µL)	5.0µL
Total	**20µL**

Table 2.12 qRT-PCR programme setup with Bioline Sensifast Kit

Step	Temperature	Time	Cycles
Reverse Transcription	45ºC	10 min	1
Polymerase Activation	95ºC	2 min	1
Denaturation	95ºC	5 secs	
Annealing	60ºC	10 secs	40
Extension	72ºC	5 secs	

Table 2.13 qRT-PCR reaction tube setup with Qiagen SYBR Green Kit

Component	Volume
2x Rotor-Gene SYBR Green RT-PCR Master Mix	12.5µL
QuantiTect Primers	2.5µL
Reverse Transcriptase	0.25µL
Nuclease-free H_2O	4.75µL
Template RNA (1-10 ng/µL)	5.0µL
Total	**25µL**

Table 2.14 qRT-PCR programme setup with Qiagen SYBR Green Kit

Step	Temperature	Time	Cycles
Reverse Transcription	55ºC	10 min	1
Polymerase Activation	95ºC	5 min	1
Denaturation	95ºC	5 secs	40
Annealing and Extension	60ºC	10 secs	

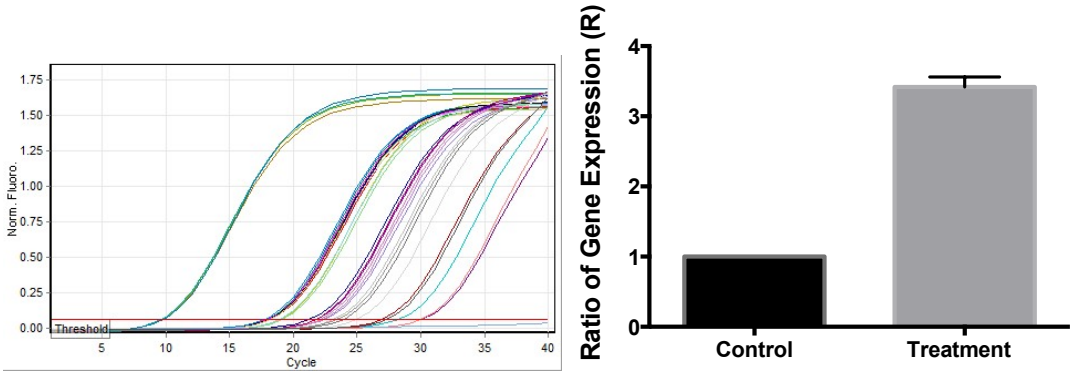


Fig 2.2 qRT-PCR. Relative levels of gene expression were measured by converting mRNA to cDNA and amplifying this cDNA using fluorescently-tagged primers specific for the target gene sequence. Fluorescence intensity data (sample on left) could be interpreted to allow gene expression ratios to be calculated and graphed (sample on right).

2.2.12 Protein Isolation and Quantitation

Cells were grown in a culture vessel to >80% confluency. Cells were scraped into the culture media and centrifuged at 300 x g for 5 minutes. The supernatant was discarded, cells were resuspended in 1mL of PBS and centrifuged at 300 x g for 5 minutes. The supernatant was discarded, cells were resuspended in an appropriate volume of RIPA buffer and incubated on ice for 30 minutes to induce cell lysis. The lysate was then clarified by centrifugation at 8,000 x g for 20 minutes at 4ºC. The supernatant containing cellular proteins was retained while the cell debris pellet was discarded. The Pierce™ BCA Protein Assay Kit was used to quantitate the concentration of protein in the clarified cell lysate. Kit instructions were followed. Briefly, 25µL of each sample or standard was added to each well of a 96-well plate. 200µL of Working Reagent was added to each well. The plate was then incubated at 37ºC for 30 minutes. Absorbance was read at 562nm in a plate reader. Sample readings were compared against a standard curve of BSA to determine protein concentration.

2.2.13 Membrane Protein Isolation

Isolation of proteins from the cell membrane was carried out using the Mem-PER Plus Membrane Protein Extraction Kit. Kit instructions were followed. Briefly, cells were grown in a culture vessel to >80% confluency. Cells were scraped into the culture media and centrifuged at 300 x g for 5 minutes. The supernatant was discarded, cells were resuspended in Cell Wash Solution and centrifuged again. The supernatant was discarded, cells were resuspended once more in Cell Wash Solution, transferred to a microfuge tube and centrifuged a third time. The supernatant was discarded, cells were resuspended in Permeabilisation Buffer (with protease inhibitors) and incubated on a rocker for 10 minutes at 4°C. Samples were then centrifuged at 16,000 x g for 15 minutes at 4°C. The supernatant which contained cytoplasmic proteins was transferred to a fresh microfuge tube and stored at -80°C. The pellet was resuspended in Solubilisation Buffer (with protease inhibitors) and incubated on a rocker at 4°C for 30 minutes. Samples were then centrifuged at 16,000 x g for 15 minutes at 4°C. The supernatant which contained membrane proteins was transferred to a fresh microfuge tube and stored at -80°C. The pellet was discarded.

2.2.14 Telomerase Activity Assay

Cell lysates were made using the RIPA buffer method and protein concentration was quantitated using a BCA assay (Section 2.2.10). Lysates were all diluted to a protein concentration of 10-750 ng/µL. The TRAPeze® XL Telomerase Detection Kit protocol was followed to assess telomerase activitity. Briefly, a PCR was carried out using fluorescein-labelled primers to amplify telomeric repeats in the sample DNA. Higher telomerase activity meant that there were more telomeric repeats to be amplified by the Taq polymerase, resulting in more fluorescent product. The PCR products were then analysed in a Tecan Safire II fluorescent plate reader. Telomerase activity was calculated by comparing the level of fluorescence detected in each sample to a standard curve generated from a set of telomeric repeat standards. The telomerase activity of a sample was given in TPG units.

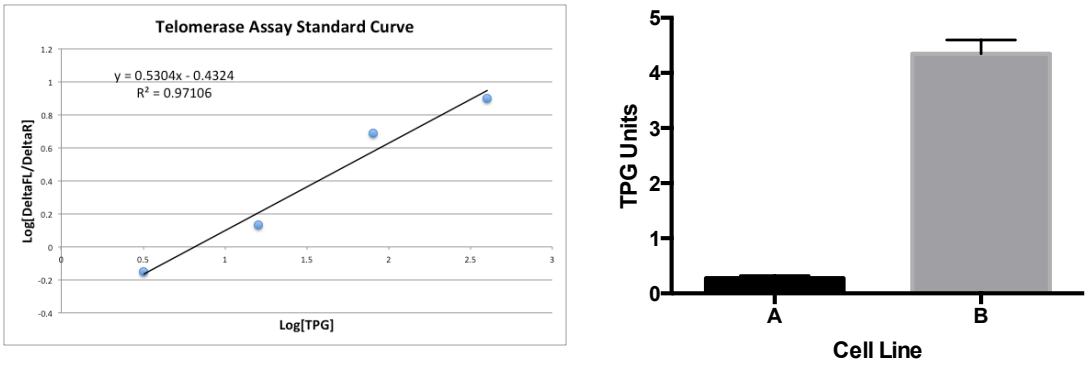


Fig 2.3 Telomerase Activity Assay. A TRAP assay was used to determine telomerase activity in a given sample population of cells. In this assay, telomerase in a sample protein lysate adds telomeric repeats to a substrate oligonucleotide sequence. Using target-specific primers, a DNA polymerase then elongates and amplifies these sequences via PCR. The Total Product Generated (TPG) can be calculated from a standard curve and this is directly proportional to the amount of telomerase in a sample. This figure shows a sample image of the data output generated from a telomerase activity assay. The standard curve generated from telomeric repeat standards (left) and telomerase activity of unknown samples in TPG units (right).

2.2.15 Immunoprecipitation

Cell lysates were made using the RIPA buffer method (Section 2.2.10). Target proteins could then be isolated through immunoprecipitation using Protein A or Protein G magnetic beads (depending on target antibody host species). 100µL of the magnetic bead solution was added to a microfuge tube which was then magnetised in a magnetic stand and the supernatant was removed following adherence of beads to the side of the tube. Beads were washed 3 times with PBS-Tween. The tube was removed from the magnetic stand and 1-5µg of target antibody was added to the tube and mixed thoroughly with the beads. This mixture was rotated for 10 minutes at room temperature. Beads were magnetised and washed 3 times with PBS-Tween. The clarified sample lysate was added to the tube and rotated for 1hr at room temperature. Beads were magnetised and washed 3 times with PBS-Tween. To elute the target protein, beads were resuspended in 0.1M Glycine buffer (pH 2.0) and incubated at room temperature for 5 minutes before magnetising the beads and transferring the eluate to a fresh tube. 1M Tris buffer (pH 9.0) was used to neutralise the purified protein fraction. Alternatively, if sample was to be used for SDS-PAGE, target protein was eluted by adding 40µL of 1X Laemmli buffer and incubating at 70°C for 10 minutes, before magnetising beads and collecting eluate.

2.2.16 Western Blot

Following protein isolation and quantitation (Section 2.2.10), samples were prepared for SDS-PAGE. 5µL of 1X sample buffer (Laemmli Buffer containing β-mercaptoethanol) was added to 15µL of sample. This mixture was incubated at 70°C for 10 minutes before transferring the full 20µL to a precast SDS 10% polyacrylamide gel to perform electrophoresis. This gel was run at 50mA for approx. 90 minutes. The gel was then removed from the electrophoresis cassette and soaked in Pierce™ One-Step Transfer Buffer for 15 minutes. Filter paper and a nitrocellulose membrane were also soaked in transfer buffer. The blotting "sandwich" was made up with the filter paper, membrane and gel and placed in the Pierce™ G2 Fast Blotter for protein transfer. The program settings used for protein transfer was dependent on the molecular weight of the target protein. Following transfer of proteins, the nitrocellulose membrane was washed with dH_2O and stained with Ponceau S to confirm that the transfer had been successful. The Ponceau S stain was washed off using dH_2O. Blocking buffer (5% dried milk in TBS with 0.1% Tween) was added to the membrane which was then incubated at room temperature for 1-2h on a rocker. Blocking buffer was removed and the membrane was subsequently incubated with the primary antibody (diluted with 5% BSA in TBST) overnight on a rocker at 4°C. Primary antibody was removed and the membrane was washed 3 times (5 minutes each) with TBST. The membrane was then incubated with a HRP-conjugated secondary antibody (diluted with 5% BSA in TBST) on a rocker for 1hr at room temperature. Membrane was washed 3 times with TBST. Fresh TMB was added to the membrane which was then incubated on a rocker at room temperature for approx. 10 minutes. The blot was imaged using BioRad GelDoc EZ Gel System. Alternatively, Pierce™ ECL Western Blotting Substrate was added to the membrane which was then incubated on a rocker at room temperature for 5 minutes. The blot was then imaged using Syngene G-Box (Eimear Kennedy *et al.*, 2014).

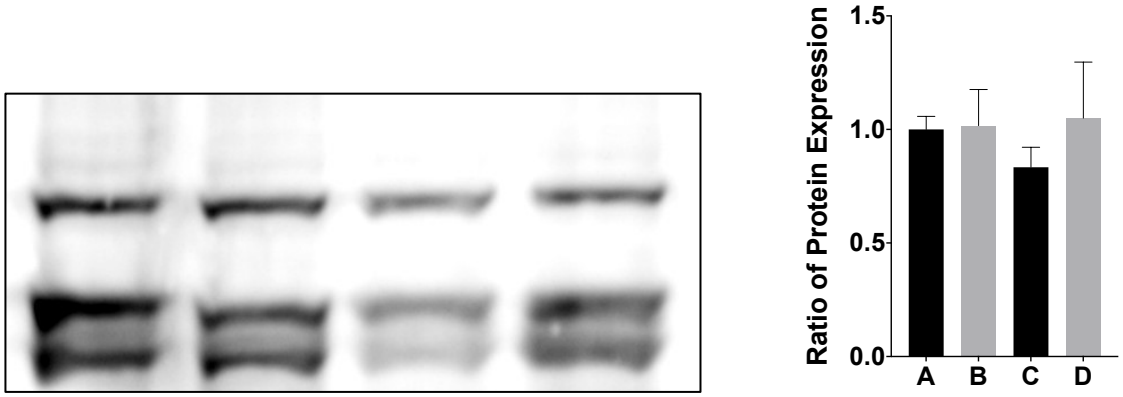


Fig 2.4 Western Blot. Relative protein expression levels were measured using Western Blot. Protein lysates were isolated and separated on an SDS-PAGE GEL before transfer to a nitrocellulose membrane. Sample lysates were then probed for specific markers using target-specific primary antibodies and host-specific secondary antibodies. Bands were visualized by chemiluminescence. This figure shows a sample image of the data output generated from Western Blot analysis. The blot image showing protein bands of similar molecular weight (left) and band intensities normalized to a loading control (right).

2.2.17 Enzyme-Linked Lectin Assay (ELLA)

All sample lysates diluted to the same concentration. 50µL of sample or control added in triplicate to each well in a 96-well plate. The plate was incubated overnight at 4°C with gentle shaking. Wells were emptied and 200µL of blocking buffer (0.5% PVA in PBS) was added to each well. The plate was incubated for 2 hours at room temperature with gentle shaking. Wells were emptied and washed 4 times with TBST (50mM Tris, 150mM NaCl, 1mM $MnCl_2$, 1mM $CaCl_2$, 1mM $MgCl_2$, 0.1% Tween-20). 50µL of biotinylated lectin (5µg/mL) was added to each well. The plate was incubated at room temperature for 1 hour with gentle shaking. Wells were emptied and washed again. 50µL of HRP-conjugated anti-biotin antibody (1:10,000) was added to each well. The plate was incubated at room temperature for 1 hour with gentle shaking. Wells were emptied and washed again. 90µL of TMB substrate solution was added to each well. The plate was incubated for 10 minutes at room temperature with gentle shaking. 50µL of stop solution (10% H_2SO_4) was added to each well. The absorbance of each well was measure at 450nm in a plate reader (Thompson *et al.*, 2011).

Table 2.15 Carbohydrate binding specificity of lectins used in this study

Lectin	Binding specificity
ConA	Internal α-linked mannose
LCA	Internal α-linked mannose. Strongest affinity for mannose core with α-1,6 linked fucose bound to primary GlcNAc residue
WGA	High affinity for terminal GlcNAc and dimers/trimers of GlcNAc. Also reacts with chitobiose core of N-linked glycans, specifically the Man β(1,4)GlcNAc β(1,4)GlcNAc trisaccharide. Can also bind GlcNAc in O-glycans
E-PHA	Binds complex N-glycans. Usually at branching point from mannose core, specifically Galβ4GlcNAcβ2Manα6; (GlcNAcβ4); (GlcNAcβ4Manα3). Strong affinity for complex bisecting N-glycan structure.

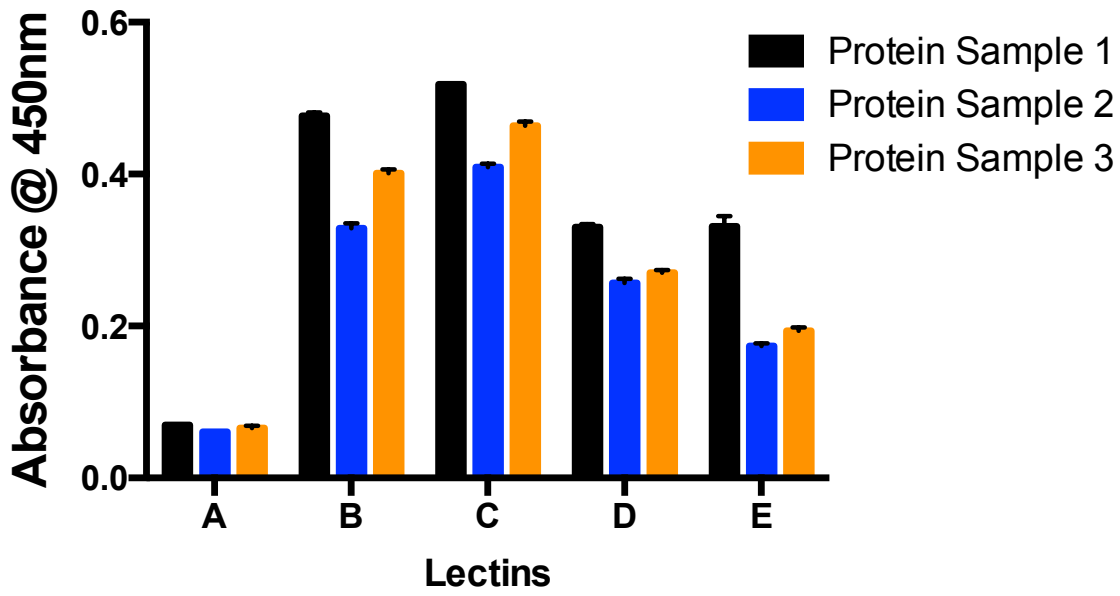


Fig 2.5 ELLA. N-glycosylation profiles were analysed by ELLA. Sample glycoproteins were immobilized in a 96-well plate and biotinylated lectins were used to probe for specific oligosaccharide structures. This figure shows a sample image of the data output generated from an enzyme-linked lectin assay. Data are presented as the absorbance at 450nm normalised to PBS control.

2.2.18 Site-directed mutagenesis

Mutation of N-glycosylation sites on a plasmid-encoded Notch1 receptor was achieved using the Agilent QuikChange Lightning Site Directed Mutagenesis Kit. Kit instructions were followed. Briefly, PCR tubes were set up as per Table 2.16 . Primers were specific for a region of the Notch1 gene containing an N-glycosylation site and were designed to incorporate a single base substitution in copies of the plasmid DNA template. PCR tubes were placed in an Applied Biosystems® Veriti® Thermal Cycler and the program in Table 2.17 was run. A *DpnI* restriction enzyme was added to each tube of PCR products to degrade any parental template DNA. Mutant plasmids were then transformed into ultracompetent XL10-Gold bacterial cells via heat-shock at 42ºC. After allowing the cells to recover for 1 hour in NZY^+ broth at 37ºC, each transformation reaction was spread on an LB agar plate with Ampicillin (50µg/mL) and incubated at 37ºC overnight. Colonies were picked and inoculated in liquid LB. As per section 2.2.8, transformed bacteria were grown and mutant plasmids were purified before sending them for sequencing with Source Biosciences to confirm that the correct single base substitution had been incorporated in each case.

Table 2.16 PCR reaction tube setup with QuikChange Lightning Kit

Component	Volume
10X Reaction Buffer	5.0µL
pCS2 Notch1 Full Length-6MT Plasmid (100 ng/µL)	1.0µL
Forward Primer (100 ng/µL)	1.25µL
Reverse Primer (100 ng/µL)	1.25µL
dNTP Mix	1.0µL
QuikSolution Reagent	1.5µL
ddH_2O	39.0µL
QuikChange Lightning Enzyme	1.0µL
Total	**25µL**

Table 2.17 PCR programme setup with QuikChange Lightning Kit

Step	Temperature	Time	Cycles
Polymerase Activation	95°C	2 min	1
Denaturation	95°C	20 secs	
Annealing	60°C	10 secs	18
Extension	68°C	5.5 mins	
Final Extension	68°C	5 mins	1

2.2.19 Data Analysis and Statistics

All statistical analysis was carried out using GraphPad Prism software. The mean and standard deviation (or standard error margin) was calculated for all of the technical and biological replicates in each experiment and these values were used to plot the data. The Kolmogorov-Smirnov normality test was used to analyse the spread of the data as it uses the most stringent conditions. The outcome of the normality test (along with the number of samples and parameters) dictated what type of significance test was carried out.

In the case of data containing only two samples, an unpaired t-test with Welch's correction was performed on normally distributed data. For non-parametric (skewed) data, the Wilcoxon test was carried out to calculate statistical significance.

For data containing more than two samples, ANOVA testing was used to perform multiple comparisons between all samples. This could be carried out using an ordinary one-way (one parameter to compare) or two-way (two parameters to compare) ANOVA for normalised data, or the Kruskal-Wallis test for non-parametric data. This would reveal the level of statistical significance for both the data as a whole and also between each sample.

Chapter 3:

Characterisation of MVSCs and their response to Jag-1 treatment

3.1 Introduction

The origin of neointimal cells has been a widely disputed matter for many years. The classic model to describe the formation of the neointima following vessel ligation involved the de-differentiation and migration of vascular smooth muscle cells (VSMCs) in the medial layer of the artery (Owens, Kumar and Wamhoff, 2004; Rensen, Doevendans and van Eys, 2007). In recent years, this assumption has been challenged and a number of other cell types have been reported to be involved in the development of the SMC-like cells of the neointima, such as vascular endothelial cells, bone-marrow derived mesenchymal stem cells and resident vascular stem cells (Sata, 2003; Torsney, Hu and Xu, 2005; Cooley *et al.*, 2014). Lineage tracing quickly became the gold standard for investigating the origin of neointimal cells as research groups engineered animal models with an indelibly tagged marker to track sub-populations of cells no matter where they migrated to or down what lineage they differentiated. Many of these studies supported the classic model of SMC de-differentiation and in fact identified a sub-population of highly plastic medial $Sca1^+$ $Myh11^+$ SMCs from which the majority of neointimal cells are derived (Nemenoff *et al.*, 2011; Herring *et al.*, 2014; Shankman *et al.*, 2015; Chappell *et al.*, 2016). However, lineage tracing models from Song Li's group have identified a sub-population of telomerically active $S100\beta^+$ resident stem cells in the media, termed multipotent vascular stem cells (MVSCs), which migrate and differentiate to become neointimal SMC-like cells (Tang *et al.*, 2012; Yuan *et al.*, 2017). Our own research group and collaborators have reported similar results, indelibly marking $S100\beta^+$ cells to demonstrate that the majority of neointimal cells are derived from a small parent population of stem cells in the media (Mooney *et al.*, 2015; Molony *et al.*, 2020; Di Luca *et al.*, 2021).

In order to effectively target the formation of vascular lesions and develop reliable therapeutics, it is essential to gain a deeper understanding of the molecular mechanisms by which their development and progression can occur. The Notch signalling pathway has been repeatedly flagged as a likely effector of this process (Li *et al.*, 2009; Redmond *et al.*, 2014). Notch is heavily involved in cell fate determination during embryogenesis and is essential for the proper development of arteries due to its role in the specification of both vascular endothelial cells and vascular smooth muscle cells (Liu *et al.*, 2003; Domenga *et al.*, 2004; Gridley, 2010). Multiple studies have linked Notch to the development of arteriosclerotic lesions, citing its increased expression in ligated vessels and ability to promote proliferation and myogenic differentiation in stem cells (Lindner *et al.*, 2001; Morrow *et al.*, 2005;

Kurpinski *et al.*, 2010). Although mammals possess four distinct forms of Notch receptor (Talora *et al.*, 2008), Notch1 has been the most widely implicated in vascular remodelling events. It was demonstrated in 2009 that Notch1-deficient mice experienced lower levels of SMC proliferation and neointima formation than their wild-type counterparts (Li *et al.*, 2009). Furthermore, Notch1 signalling was shown to be inhibited by miRNA-34a, resulting in decreased lesion formation and SMC migration and proliferation (Q. Chen *et al.*, 2015). It has also been reported that transient knockdown of Notch1 via perivascular delivery of targeted siRNA *in vivo* led to a significant reduction in arterial remodelling following vessel injury (Redmond *et al.*, 2014).

3.2 Strategy

In order to investigate the potential role of N-glycans in Notch signalling and myogenic differentiation, it was imperative to firstly identify, isolate and characterise a population of S100β^{+} multipotent stem cells from the medial layer of a mouse aorta and confirm their responsiveness to Jag-1 activation of the Notch1 receptor.

Several stem cell populations have been identified in the vasculature by a number of different research groups. Furthermore, many of these groups have reported, through lineage tracing studies, that cells in a neointimal lesion may arise, at least in part, from stem cell parent populations (Wang *et al.*, 2018). S100β^{+} stem cells have been shown to contribute to the development of a ligation-induced neointima through migration and differentiation (Tang *et al.*, 2012; Mooney *et al.*, 2015). As part of this study, genetic lineage tracing of neointimal cells was carried out using an inducible Cre reporter system controlled by S100β expression to further investigate the possible role of S100β^{+} multipotent vascular stem cells (MVSCs) in vascular lesion formation.

Medial SMCs within the aortic arch develop from a neuroectodermal embryological origin (Bacakova *et al.*, 2018) and this region is known to be a high risk site for vascular remodelling events, especially in ageing populations (Redheuil *et al.*, 2010, 2011; Lee *et al.*, 2014). Therefore, following dissection and harvesting of the mouse aortic vessel, MVSCs were isolated from the arch region of a Female Bl/tgtgt Thy1 YFP mouse using enzymatic dispersion following by sequential plating to create primary cultures (Section 2.2.2). MVSCs were grown and expanded in maintenance media type 1 (MM1). Immunocytochemistry (ICC) was then carried out in order to characterise the cell population by probing for the

calcium-binding protein S100β and the neural stem cell marker Nestin (Section 2.2.7). ICC was also used to investigate if these cells, isolated from an area rich in smooth muscle cells (SMCs), expressed SMC markers, such as Calponin1 (Cnn1) and Myosin heavy-chain 11 (Myh11). A second cell line, C3H10T1/2 (referred to here as simply C3H), was also characterised in this way. C3H cells are embryonic fibroblasts isolated from C3H mice that exhibit mesenchymal stem cell properties in culture (Reznikoff, Brankow and Heidelberger, 1973). For some of the more seminal experiments in this study, C3Hs were used as a comparative cell line to MVSCs. C3H cells have been shown to be functionally similar to mesenchymal stem cells and have the ability to differentiate down a myogenic lineage (Singh *et al.*, 2003; Tang, Otto and Lane, 2004; Zhou *et al.*, 2015). Unlike MVSCs though, C3Hs are not derived from a neuroectodermal lineage, but rather from the mesoderm, and do express Sca1, a marker of many other types of vascular stem cells, especially those found in the adventitial layer (Wu *et al.*, 2019).

As a measure of stemness, the telomerase activity and telomere length of MVSCs were evaluated and compared to terminally differentiated cell/tissue types (Section 2.2.14). Telomerase is an enzyme that catalyses the replication of specific repeat sequences found at the telomeres of chromosomes. The activity of telomerase maintains these telomeric repeats which are essential in the cell proliferation process (Wright *et al.*, 1996). For this reason, embryonic stem cells have very high telomerase activity. This activity is gradually reduced as the cell becomes more differentiated, resulting in shortening of the telomere length. Eventually, a terminal telomere length is reached and cell proliferation can no longer occur (Grimm *et al.*, 2004). The discovery of telomerase and its function in stem cell maintenance has led to a number of assays being developed to analyse both telomerase activity and telomere length as a method of determining the stemness of a particular cell or cell population. There are a number of different techniques that can be used to measure telomerase activity. One of the most widely used is the Telomerase Repeated Amplification Protocol (TRAP) assay. In this method, the telomerase enzyme adds telomeric repeats to specific sequences in the sample DNA. These repeats are then amplified using a PCR with fluorescently tagged primers. Telomerase activity can be calculated based on the level of fluorescence measured in the PCR products and given as a Total Protein Generated (TPG) unit (Mender and Shay, 2015). For the purpose of this study, telomerase activity was assessed using the TRAP assay, comparing a cell lysate of cultured MVSCs against a tissue lysate of a fresh mouse aorta (in which the majority of cells are terminally differentiated). Relative telomere length was also determined by qRT-PCR, using primers that are specific

to the telomeric repeat sequence. Telomere length of MVSCs was compared to that of a fresh mouse aortic lysate and a population of mouse primary vascular aortic SMCs (MOVAS).

The multipotency of the MVSCs was also evaluated by another member of our research group. MVSCs were cultured for 14 days in either adipogenic differentiation media, osteogenic differentiation media, or normal maintenance media (MM1). Among other analysis techniques, the mRNA was isolated and qRT-PCR (Section 2.2.11) was carried out to measure the expression of adipogenic markers (*Lpl* and *Fabp4*) or osteogenic markers (*Alpl* and *Sost*) in treated samples compared to untreated controls.

The responsiveness of MVSCs to the Notch ligand Jag-1 was subsequently assessed to ensure that both Notch signalling and myogenic differentiation was being activated by this stimulus. For Notch receptors to be activated *in vivo*, Jag-1 must be anchored to the plasma membrane of a neighbouring cell in order to create the tensile force of the "catch-bond" required for cleavage events to occur (Vincent C Luca *et al.*, 2017). To mimic this process *in vitro*, Jag-1 was immobilised on the surface of the cell culture vessel into which MVSCs were then seeded. After 48 h the transcript expression of Notch target gene *Hey1* and the myogenic marker *Myh11* were measured by qRT-PCR. The responsiveness of C3H cells to Jag-1 stimulation was also assessed in this way as a comparison. MVSCs were also subjected to a 7-day Jag-1 treatment, at which point the number of cells expressing the intermediate myogenic marker Cnn1 was measured by ICC. For both the qRT-PCR and the ICC analysis, Jag-1-treated samples were compared to samples treated with an immobilised IgG-Fc (referred to as simply Fc from this point on).

To confirm that the response being observed was Notch-dependent, the DAPT inhibitor was used to block γ-secretase cleavage of Notch. Furthermore, to investigate whether or not this response specifically involved the Notch1 receptor, siRNA transfection was used to transiently knock down the *Notch1* transcript (Section 2.2.6.2). It was necessary though to first confirm that MVSCs were amenable to siRNA transfection. MVSCs were transfected with TYE 563 Transfection Control DsiRNA, a fluorescently-tagged siRNA molecule. Cells were then imaged under a fluorescent microscope and the transfection efficiency of the cell line could be determined. Knockdown of *Notch1* could then be carried out using a targeted siRNA against the relevant sequence. This knockdown was confirmed by western blot and qRT-PCR before measuring the effect of the knockdown on transcript expression of *Hey1* and *Myh11*.

Data for all experiments in this section was gathered over at least three biological replicates. Normality tests were used to determine if data followed a parametric distribution pattern. Variation across samples was analysed by calculating p-values. The type of test used to calculate this was governed by the outcome of the normality test. Statistical significance was assigned to p-values less than 0.05 (Section 2.2.19).

3.3 Results

3.3.1 Identification of Neointimal Cells Derived from an S100β$^+$ Parent Population

Neointimal cell origin has been a widely disputed topic among the scientific community for the last couple of decades. Lineage tracing studies have recently arisen as the most promising tool for resolving this dispute. Members of Prof. Eileen Redmond's research group (our collaborators in University of Rochester, NY) utilised this approach to investigate the origin of cells in a murine vascular lesion. As described in Section 2.2.1, an inducible Cre reporter system was established by crossing S100β-eGFP/CreERT2 mice with Ai9 reporter mice. Tamoxifen induction of the Cre system was carried out and, 4 weeks after the last Tamoxifen injection, ligation of the left carotid artery (LCA) was performed. After 21 days, both the LCA and the right carotid artery (RCA) were harvested and sectioned. These sections were DAPI stained and mounted on slides before being imaged using a fluorescent microscope. This work was carried out by Dr. Weimin Liu.

The number of cells on the inner side of the internal elastic lamina (IEL) were counted for each image. The number of tdTomato-expressing cells in this area was also counted. There was a dramatic increase in the number of cells inside the IEL in the LCA compared to the RCA (Fig.3.1b), indicating the development of a neointimal lesion resulting from artery ligation. Furthermore, the proportion of these cells which are tdTomato$^+$ is significantly higher in the ligated LCA (Fig.3.1c), indicating that a substantial percentage of neointimal cells were derived from an S100β$^+$ parent population. A small number of tdTomato-expressing cells were also present in the medial and adventitial layers of both vessels.

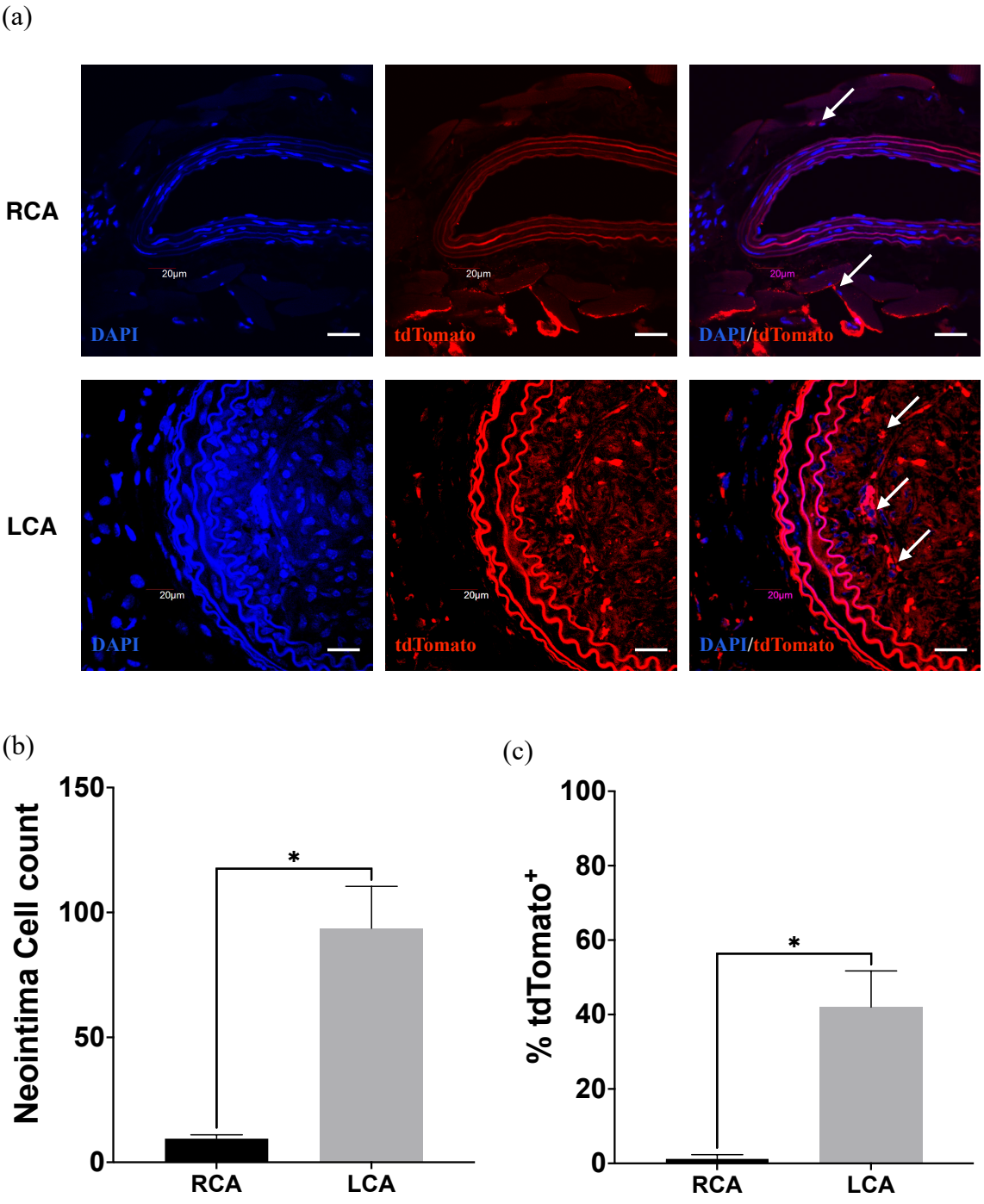


Fig.3.1 S100β Lineage Tracing Model. (a) Representative confocal fluorescence images of carotid artery sections from S100β-eGFP/Cre/ERT2–dTomato double transgenic mice treated with Tamoxifen or corn oil for 5 days. LCA was ligated after 4-week washout, RCA was left unligated. Images show DAPI-stained nuclei (blue) and tdTomato^{+} cells (red). Images taken using FV1000 Olympus confocal microscope and are representative of 10 individual animals. Scale bar = 20μm. Arrows highlight S100β-Tdt^{+} cells. (b) Mean number of DAPI nuclei inside the IEL. (c) Mean proportion of neointimal cells expressing tdTomato. Error bars representative of SEM. * $p < 0.05$

3.3.2 Characterisation of MVSCs and C3Hs

Female Bl/tgtgt Thy1 YFP mice were anesthetized and culled as per Section 2.2.1. The aortic arch was extracted and washed with PBS. The adventitial layer was then removed following Collagenase treatment. In order to break down the elastic lamina and release cells, physical cutting of the tissue was combined with Elastase treatment. Cells were then added to a non-adherent 6-well plate in MM1 and incubated at 37^{o}C for 72h. Suspension cells were then transferred to an adherent 6-well plate and cultured in MM1. ICC was carried out on this cell population and also on C3H cells to confirm the presence of specific protein markers. Cells were seeded onto sterile coverslips in a 6-well plate at a low density (5,000 cells/well) and incubated at 37^{o}C for 48 h. Cells were fixed with 3.7% formaldehyde and stained with primary antibodies for S100β, Nestin, Stem cell antigen 1 (Sca1), Cnn1 or Myh11. In order to generate a fluorescent signal for staining, fluorophore-conjugated secondary antibodies were added and nuclei were stained with DAPI. Using a fluorescent microscope, these stains were visualised, imaged and analysed to determine expression of each protein. IgG controls (secondary antibody probing without primary antibody staining) were used to account for background fluorescence or off-target binding of secondary IgGs. Cultured mouse SMCs (MOVAS) were used as a positive control for myogenic marker expression. MVSCs and C3Hs were both found to be positive for S100β and Sca1 expression, and MVSCs were also Nestin^{+} (Fig.3.2a). Both MVSCs and C3Hs were negative for Cnn1 and Myh11 expression (Fig.3.2b).

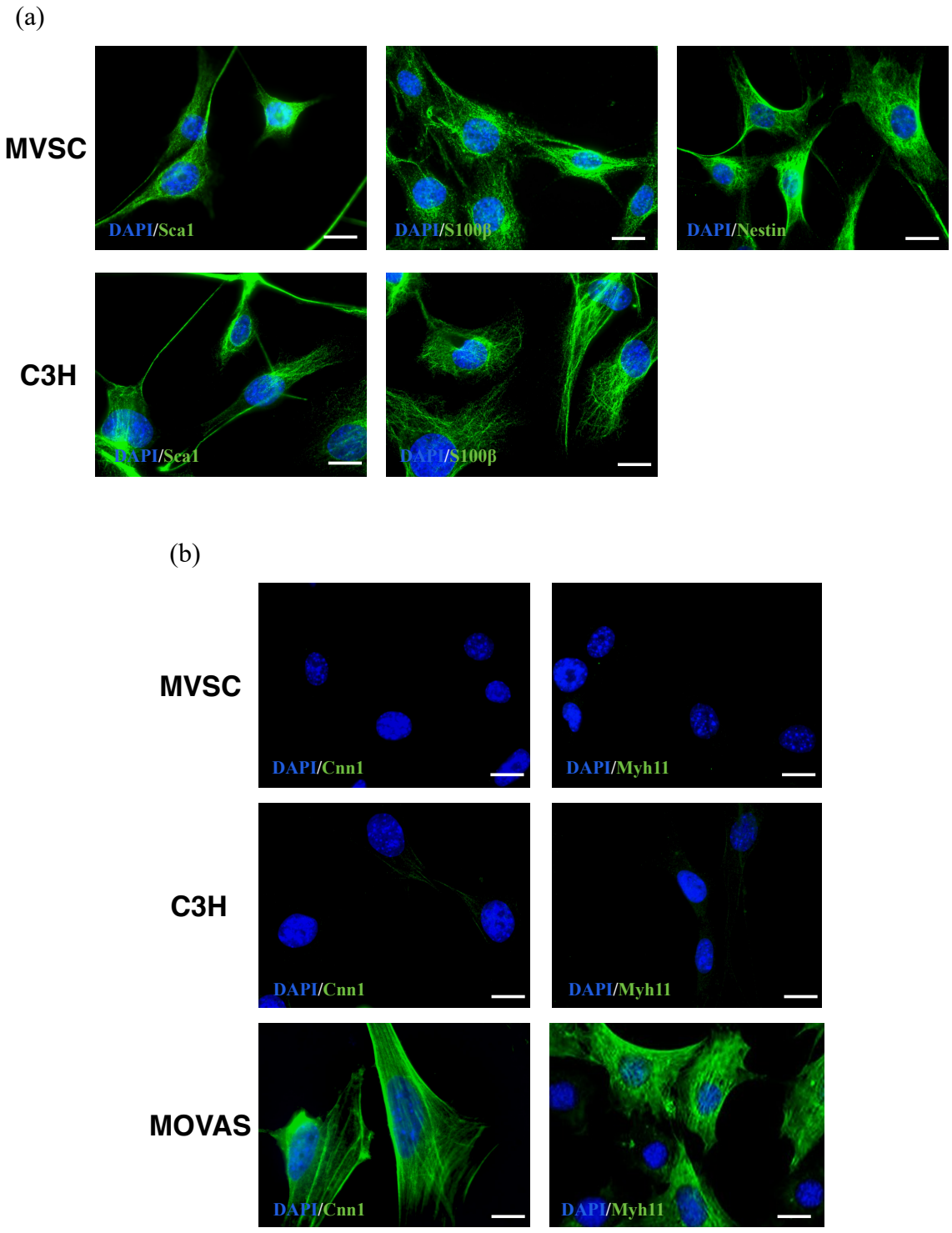


Fig.3.2 Characterisation of MVSCs and C3Hs. (a) Representative ICC images of MVSCs and C3Hs stained with DAPI, anti-S100β, anti-Sca1 or anti-Nestin primary antibody at 60X magnification. **(**b) Representative ICC images of MVSCs, C3Hs and MOVAS cells stained with DAPI, anti-Cnn1 or anti-Myh11 primary antibody at 60X magnification. All images taken using Olympus DP-50 fluorescent microscope. Images representative of 10 images taken per sample. AlexaFluor 488 secondary antibody used for visualisation of primary antibody binding. Control sample stained with secondary antibody but no primary antibody was used to determine level of background/off-target fluorescence. Scale bar = 10μm. Data representative of n=3.

3.3.3 Measurement of Telomere Length in MVSCs

As a confirmation of the stemness of isolated MVSCs, the average telomere length in a population was measured. Longer telomere lengths are characteristic of stem cells. DNA was isolated from mouse aortic tissue (composed primarily of differentiated SMCs), cultured mouse SMCs (MOVAS) and a population of mouse MVSCs as per Section 2.2.9. qPCR was carried out on these samples using two sets of primers: one primer set which targeted and amplified the murine telomeric repeat region, and another primer set which targeted a 100bp-long single copy reference (SCR) region on mouse chromosome 10. The average telomere length of each sample, relative to the fresh aorta control, could be calculated based on normalisation of fluorescence generated by telomere products to that generated by the SCR products. Telomere length was significantly longer in the MVSC sample when compared to both the fresh aortic tissue and the cultured mSMCs (Fig.3.3).

3.3.4 Measurement of Telomerase Activity in MVSCs

To further confirm the stemness of these MVSCs, telomerase activity was measured in a sample of the cells. Higher levels telomerase activity is characteristic of stem cells. A protein lysate was generated from MVSCs in culture as per Section 2.2.14, while a tissue lysate was generated from fresh mouse aorta by homogenisation and centrifugation. Protein concentration was quantified by BCA assay. A TRAP assay was then carried out using the TRAPeze® XL Telomerase Detection Kit to determine the telomerase activity in both samples. There was significantly higher level of telomerase activity in the MVSC sample compared to the aortic tissue sample (Fig.3.4).

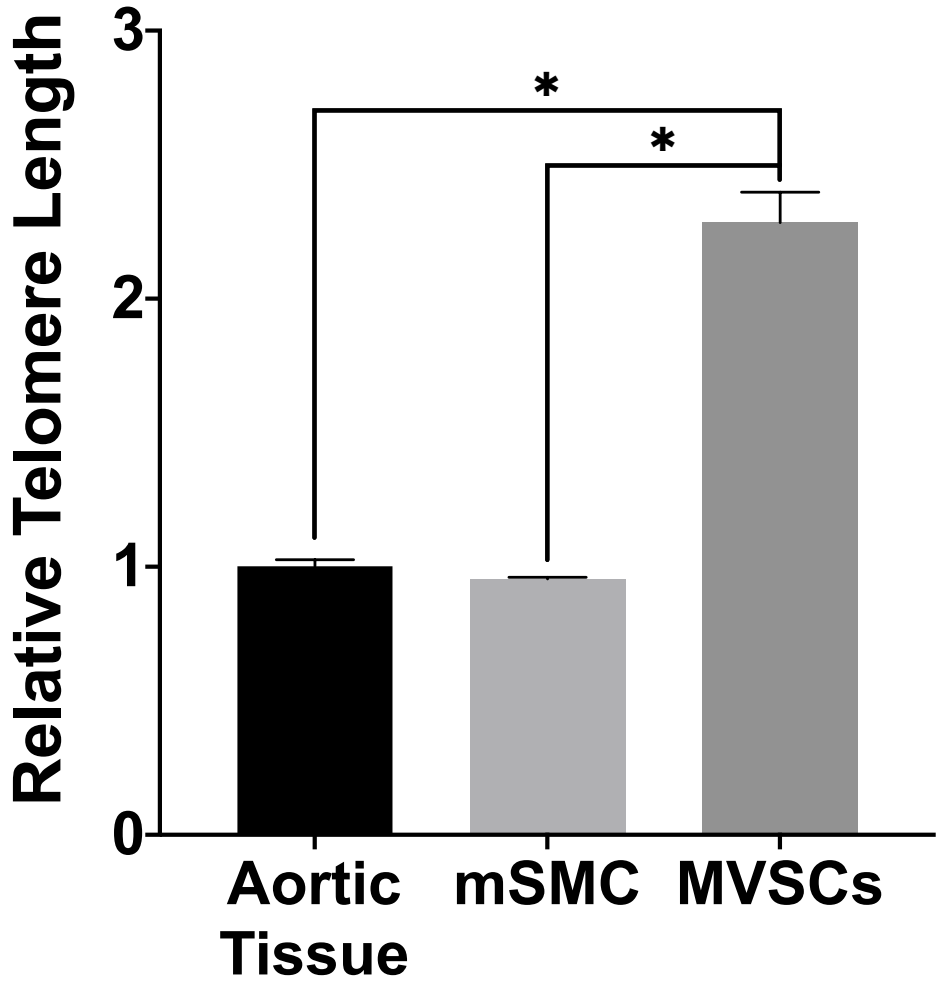


Fig.3.3 Relative telomere length in different cell lines. The relative telomere length of genomic DNA isolated from fresh aortic smooth muscle cells, SMCs cultured *in vitro* and MVSCs isolated from the aortic arch using real time PCR. Amplification was relative to a single copy reference (SCR) gene. Data are presented as the ratio of telomere length relative to the aortic SMC sample. Error bars based on SEM. Data is representative of n=3.
* $p < 0.05$

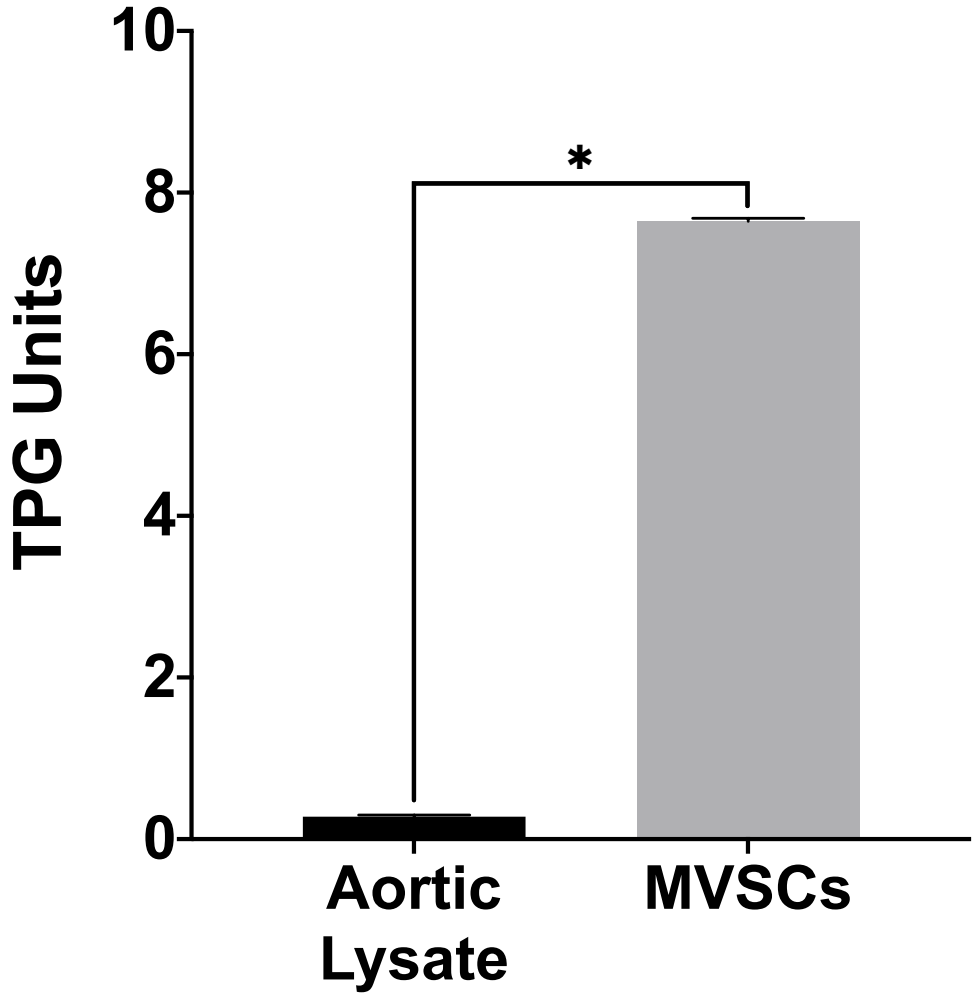


Fig.3.4 Telomerase activity in aortic tissue and MVSCs. The level of telomerase activity in protein lysates from sample tissue or cells analysed using the TRAPeze® XL Telomerase Detection Kit. PCR was performed to allow telomerase in the sample to amplify a telomeric repeat sequence. Amount of PCR product formed in each sample was compared against a standard curve to determine level of telomerase activity which is given as total protein generated (TPG) units. Error bars based on SEM. Data is representative of n=3. * $p < 0.05$

3.3.5 Adipogenic and Osteogenic Differentiation of MVSCs

As a measure of the multipotency of isolated MVSCs, adipogenic and osteogenic differentiation stimuli were used to demonstrate that, as well as the myogenic pathway, they could be driven down multiple other lineages of differentiation. The following work was carried out by Yusof Gusti, a member of Prof. Paul A. Cahill's lab in DCU. MVSCs were seeded in wells of a 6-well plate at 5000 cells/well and incubated at 37°C for 48 h. Media was discarded and replaced with either fresh MM1, StemPro® Adipogenesis Differentiation Medium or StemPro® Osteogenesis Differentiation Medium. Cells were incubated at 37°C for 14 days with media replacement every 3-4 days. Cells were harvested and RNA was isolated from each sample as per Section 2.2.8. RNA samples were analysed by qRT-PCR to measure the expression of adipogenic markers *Lpl* and *Fabp4*, or osteogenic markers *Alpl* and *Sost*, in treated samples relative to the MM1 control. In the samples treated with adipogenesis media, a significant increase was detected in the expression of both *Lpl* and *Fabp4* (Fig.3.5a-b), while in the samples treated with osteogenic media, there were significant increases in the expression of *Alpl* and *Sost* compared to the MM1 control (Fig.3.5c-d).

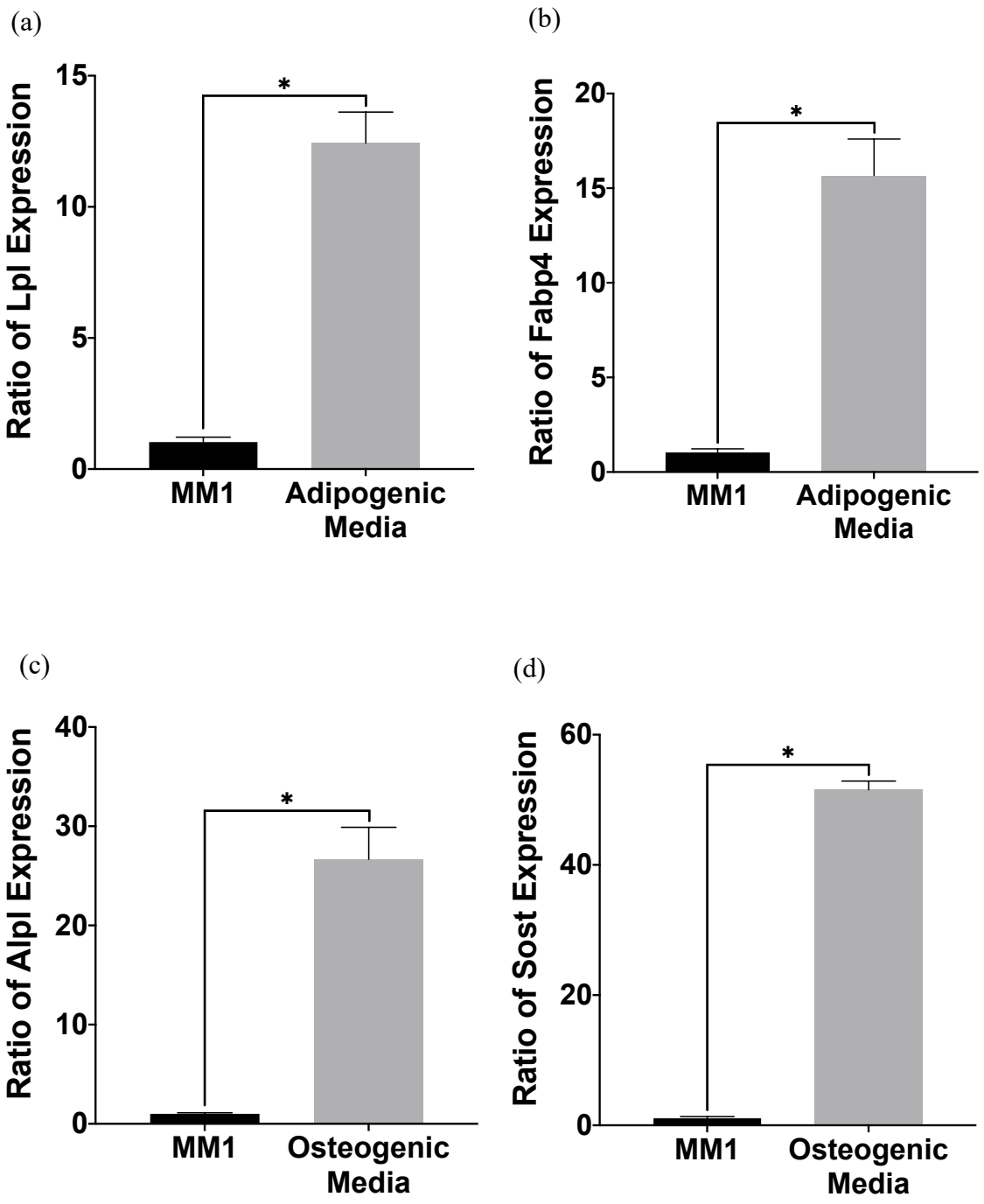


Fig.3.5 MVSC Multipotency. The relative expression of adipogenic marker genes (*Lpl* and *Fabp4*) and osteogenic markers (*Alpl* and *Sost*) by qRT-PCR in MVSCs treated for 14 days with appropriate differentiation media. Data are presented as the ratio of expression relative to the negative control sample treated with MM1. Error bars based on SEM. Data representative of n=3 , * $p < 0.05$.

3.3.6 Jag-1 activation of Notch Signalling and Myogenic Differentiation in MVSCs

As the Jag-1 ligand would be used throughout this project to stimulate Notch signalling, it was imperative to confirm early on that treatment with Jag-1 did indeed activate expression of Notch target genes and myogenic markers. Wells in a 6-well cell culture plate were coated with 1μg/mL of Jag-1 or a control Fc which does not activate the Notch receptor (Section 2.2.5). MVSCs were seeded into the Jag1-coated wells at a density of 200,000 cells per well in MM1 and incubated at 37^{o}C for 48 h. Cells were harvested and RNA was isolated from samples as described in section 2.2.8. Analysis by qRT-PCR was used to measure the change in expression of the Notch target gene *Hey1* (Fig 3.6) and of the myogenic differentiation marker *Myh11* (Fig 3.7). A significant increase was observed in the expression of both *Hey1* and *Myh11* following Jag-1 treatment. As a cell line comparison, C3H cells were treated and analysed in the same way (Fig. 3.8 and 3.9). A similar pattern of expression was achieved whereby *Hey1* and *Myh11* expression were upregulated following Jag-1 treatment.

Similarly, sterile glass cover slips were coated with Jag-1 or Fc and MVSCs were seeded onto these cover slips at a density of 5,000 cells per well. After incubation at 37^{o}C in MM1 for 7 days, cells were fixed and immunocytochemistry was carried out as detailed in Section 2.2.7. Cells were stained for expression of the intermediate myogenic differentiation marker Calponin1 (Cnn1). Nuclei were visualised via DAPI staining of cells. The number of positive cells was counted for each image and divided by the total number of cells in that image to give a ratio, and subsequently a percentage, of Cnn1-positive cells. Around 40% of cells in the Jag1-treated sample were found to be Cnn1^{+}, compared to 0% in the Fc-treated control(Fig.3.10a).

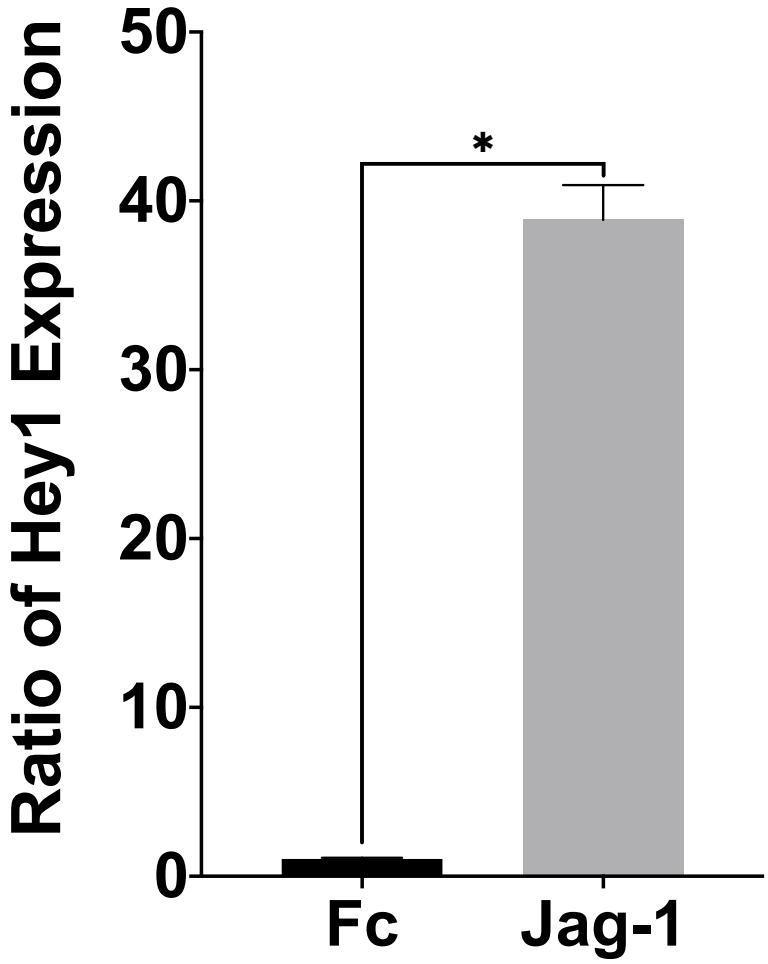


Fig.3.6 Expression of *Hey1* in Jag-1-treated MVSCs. The relative expression of *Hey1* mRNA levels by qRT-PCR in MVSCs treated for 48 h with recombinant rat Jagged-1 (Jag-1) at 1µg/mL in MM1. Data are presented as the ratio of *Hey1* expression relative to the negative control sample treated with Fc. Error bars based on SEM. Data representative of n=3, * $p < 0.05$

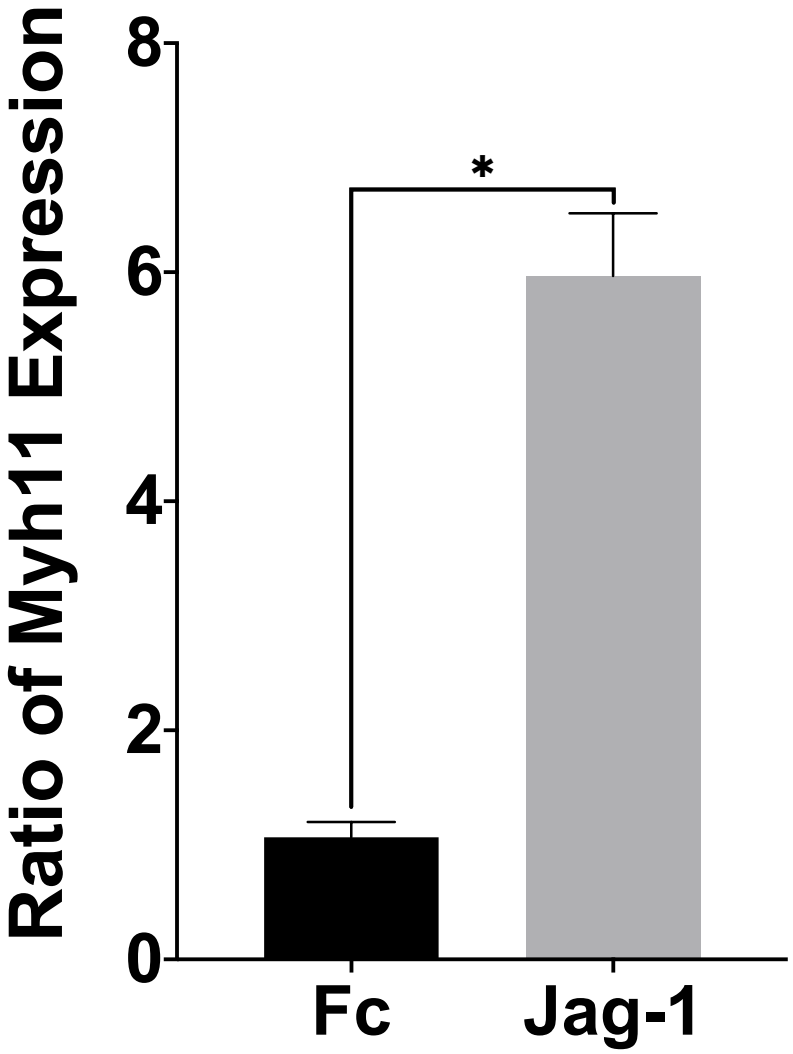


Fig.3.7 Expression of *Myh11* in Jag-1-treated MVSCs. The relative expression of *Myh11* mRNA levels by qRT-PCR in MVSCs treated for 48 h with recombinant rat Jag-1 at 1µg/mL in MM1. Data are presented as the ratio of *Myh11* expression relative to the negative control sample treated with Fc. Error bars based on SEM. Data representative of n=3, * $p < 0.05$

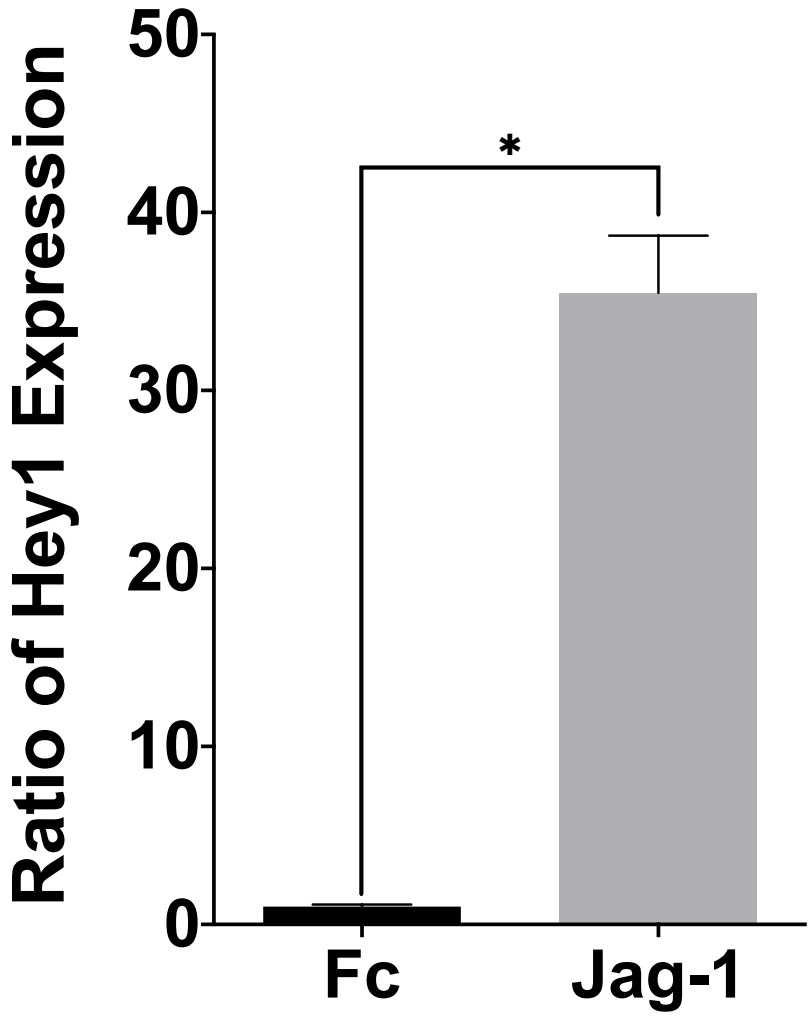


Fig.3.8 Expression of *Hey1* in Jag-1-treated C3Hs. The relative the expression of *Hey1* mRNA by qRT-PCR in C3Hs treated for 48 h with recombinant rat Jagged-1 (Jag-1) at 1μg/mL in MM1Analysis was used to measure. Data are presented as the ratio of *Hey1* expression relative to the negative control sample treated with Fc. Error bars based on SEM. Data representative of n=3.
* $p < 0.05$

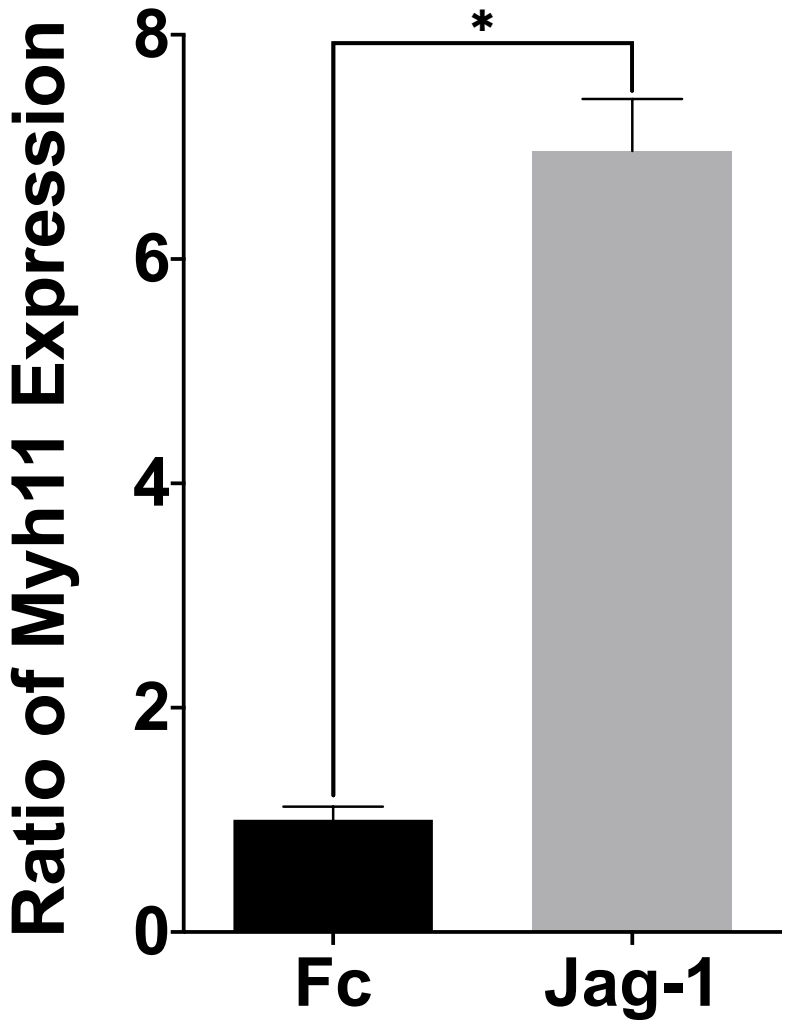
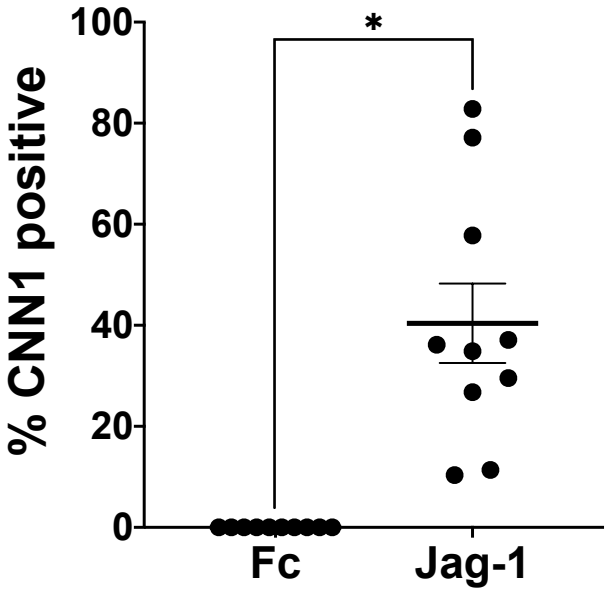


Fig.3.9 Expression of *Myh11* in Jag-1-treated C3Hs. The relative expression of *Myh11* mRNA levels by qRT-PCR in C3Hs treated for 48 h with recombinant rat Jag-1 at 1μg/mL in MM1. Data are presented as the ratio of *Myh11* expression relative to the negative control sample treated with Fc. Error bars based on SEM. Data representative of n=3 , * $p < 0.05$.

(a)



(b)

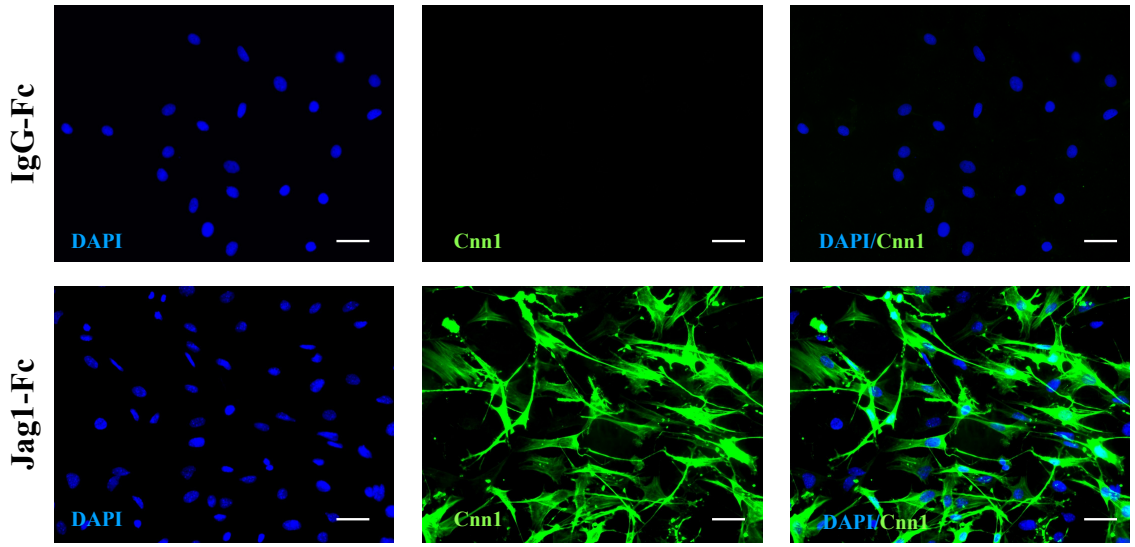


Fig.3.10 Protein expression of Cnn1 in Jag-1-treated MVSCs. Immunocytochemical analysis of Cnn1 protein expression in MVSCs treated for 7 days with recombinant rat Jag-1 at 1µg/mL in MM1. DAPI was used to stain nuclei. Anti-Cnn1 primary antibody and AlexaFluor 488 secondary antibody used to visualise Cnn1. Positive cells were counted and compared against total cell count. (a) Mean percentage of $Cnn1^{+}$ cells plotted for each sample. Error bars based on SEM. (b) Representative immunocytofluorescence images of Cnn1 expression in both samples. Scale bar = 25µm. Data representative of n=3. * $p < 0.05$

3.3.6 Inhibition of Jag-1 mediated Notch activation using DAPT

DAPT is a γ-secretase inhibitor which blocks Notch signalling following ligand-mediated activation. To confirm that the activation of Notch target gene expression following Jag-1 treatment was Notch-dependent, DAPT was used to suppress this activation. Wells in a 6-well cell culture plate were coated with 1µg/mL of recombinant rat Jagged-1 or a control Fc (Section 2.2.5). MVSCs were pre-treated with 10µM DAPT or equivalent volume of DAPT vehicle, DMSO, for 30 minutes before being seeded into the Jag1-coated wells at a density of 200,000 cells per well in MM1. The plate was incubated at 37^{o}C for 48 h. Cells were harvested and RNA was isolated from samples as described in section 2.2.8. The change in expression of the Notch target gene *Hey1* was measured by qRT-PCR in DAPT- or DMSO-treated samples and compared against samples treated with only Jag-1 or Fc (Fig.3.11). Jag-1 significantly increased *Hey1* expression compared to the Fc control. This response was entirely blocked by DAPT, while no significant change was seen in the Jag-1 response following DMSO treatment.

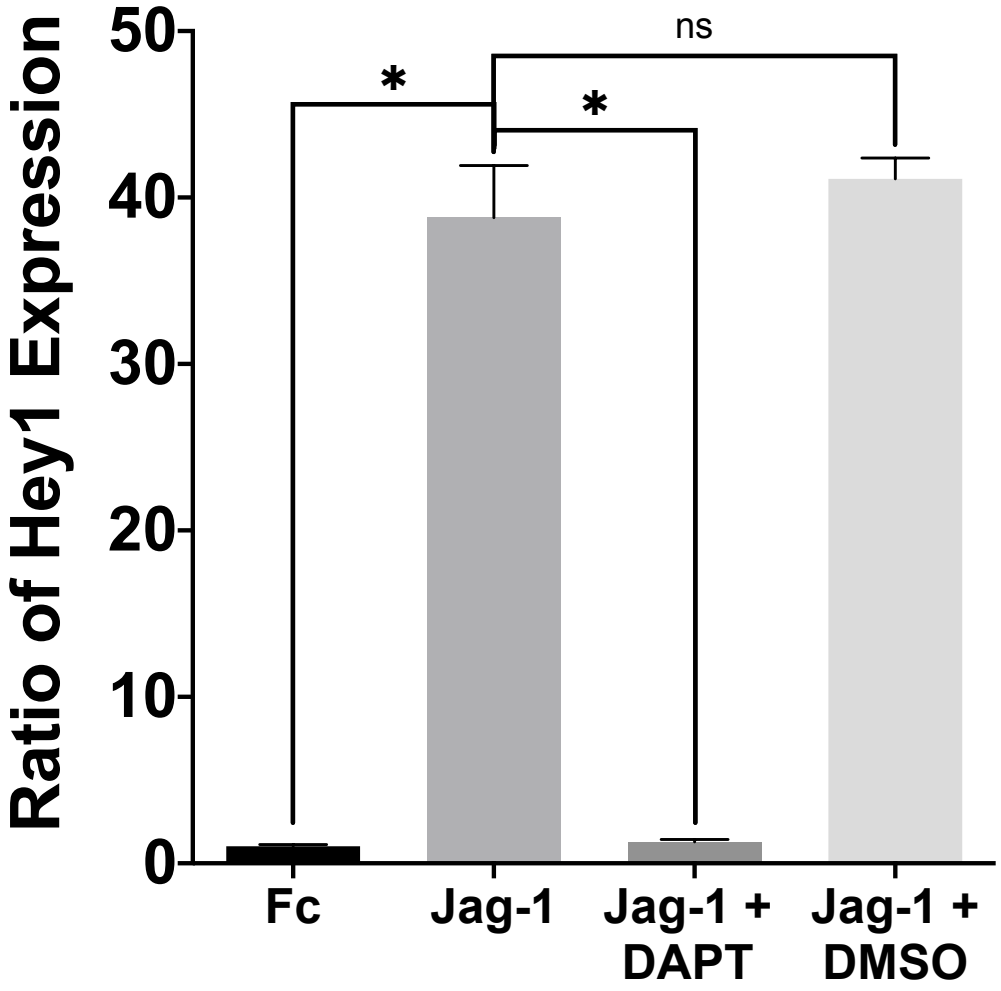


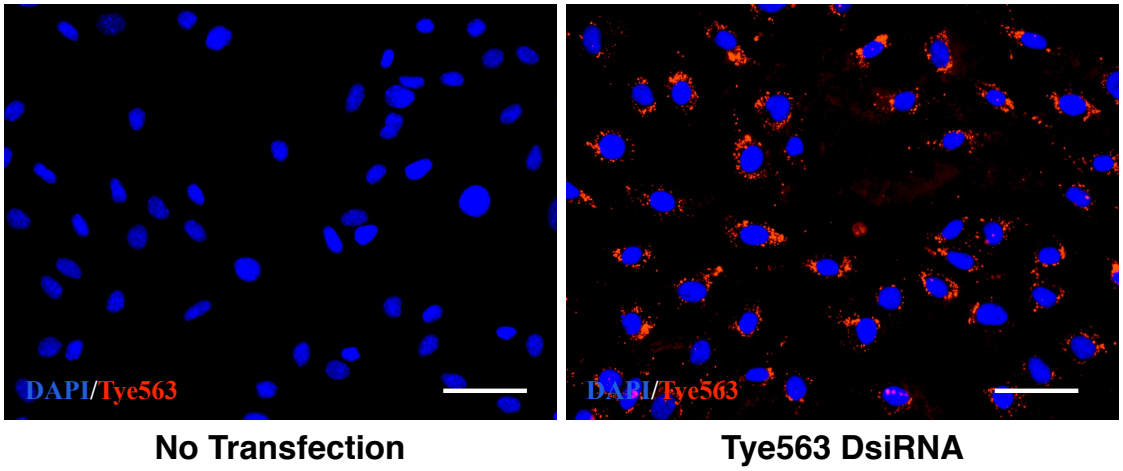
Fig.3.11 DAPT inhibition of Jag-1 response in MVSCs. The relative expression of *Hey1* mRNA levels by qRT-PCR in MVSCs treated for 48 h with recombinant rat Jag-1 at 1µg/mL ± DAPT or DMSO. Data are presented as the ratio of *Hey1* expression relative to the negative control sample treated with Fc. Error bars based on SEM. Data representative of n=3 , * $p < 0.05$.

3.3.7 Measurement of siRNA transfection efficiency in MVSCs

The Notch1 receptor in particular has been implicated in arterial remodelling (Li *et al.*, 2009; Redmond *et al.*, 2014; Q. Chen *et al.*, 2015). To investigate whether Jag-1-mediated activation of Notch signalling was Notch1-dependent, siRNA knockdown could be used to suppress expression of *Notch1*. In order for an siRNA intervention to elicit a measurable response, a large proportion of the cell population must take up the siRNA in the first place. In this study, the siRNA transfection efficiency refers to the percentage of a given cell population that allow passage of the siRNA molecule across their membrane and into the cytoplasm following chemical transfection. To visualise this, MVSCs were grown to ~80% confluency on sterile cover slips and transfected with TYE 563 DsiRNA, a fluorescently-tagged siRNA. A non-transfected sample was used as a negative control. Cells were incubated at 37^{o}C for 48 h before being fixed with 3.7% formaldehyde. Nuclei were stained with DAPI and cover slips were mounted onto slides before being imaged using a fluorescent microscope. The number of cells containing the dye were counted and graphed as a percentage of the total number of cells. A transfection efficiency of 99.6% was achieved in the dye-transfected sample, compared to 0% in the non-transfected sample (Fig.3.12).

The siRNA transfection efficiency of C3H cells was investigated in a similar manner. The C3H cell line is known to be highly amenable to transfection and could have therefore acted as a substitute for MVSCs in the event of a low transfection efficiency in that cell line. The siRNA transfection efficiency of C3Hs was determined to be 99.7% in the dye-transfected sample, compared to 0% in the non-transfected sample (Fig.3.13).

(a)



(b)

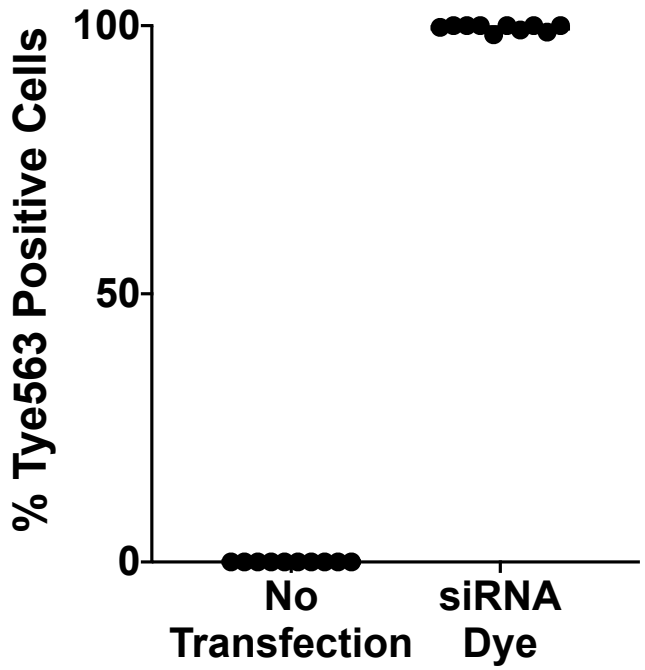
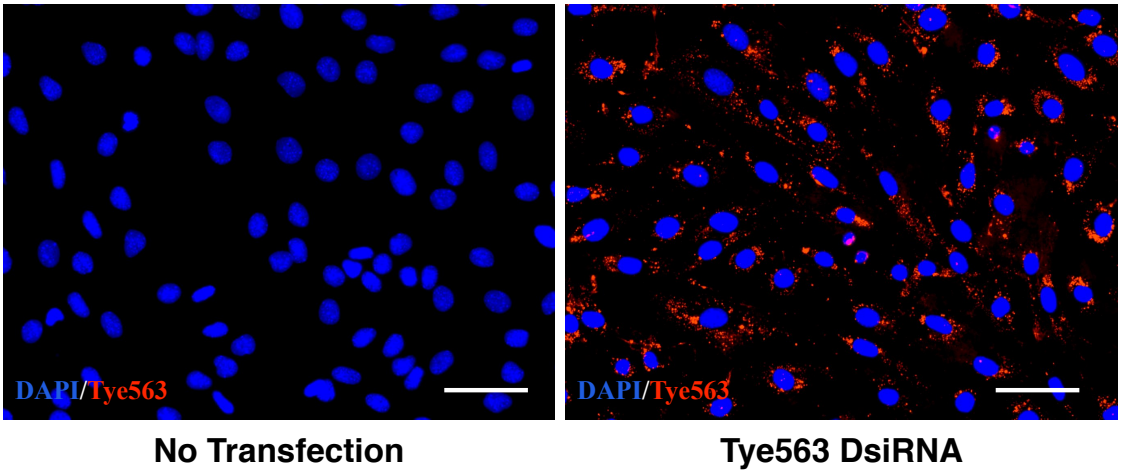


Fig.3.12 siRNA Transfection Efficiency of MVSCs. Fluorescence microscopic analysis of MVSCs transfected with Tye563 DsiRNA for 48 h. DAPI was used to stain nuclei. Tye563^{+} cells were counted and compared against total cell count. (a) Representative fluorescence images of Tye563 expression in both transfected and non-transfected samples. Scale bar = 25µm. (b) Mean percentage of Tye563^{+} cells plotted for each sample. Error bars based on SEM. Data representative of n=3.

(a)



(b)

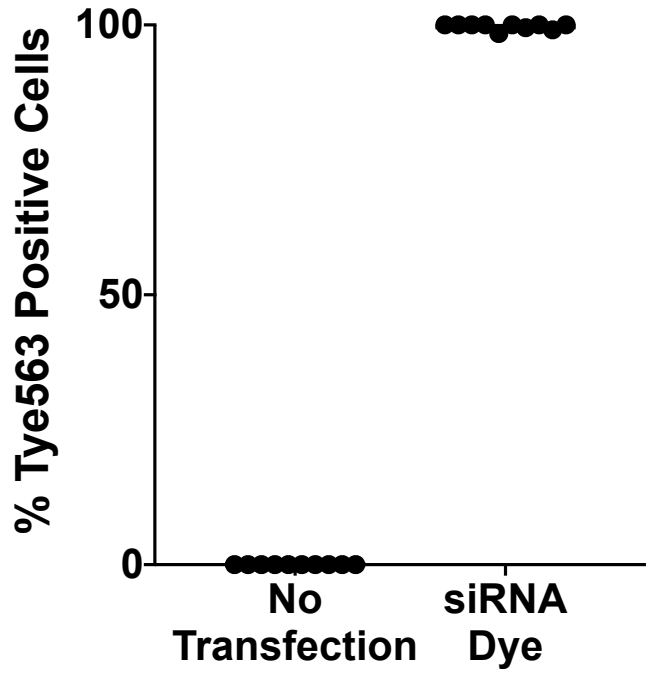


Fig.3.13 siRNA Transfection Efficiency of C3Hs. Fluorescence microscopic analysis of C3Hs transfected with Tye563 DsiRNA for 48 h. DAPI was used to stain nuclei. $Tye563^{+}$ cells were counted and compared against total cell count. (a) Representative fluorescene images of Tye563 expression in both transfected and non-transfected samples. Scale bar = 25µm. (b) Mean percentage of $Tye563^{+}$ cells plotted for each sample. Error bars based on SEM. Data representative of n=3.

3.3.8 Effect of Notch1 knockdown on Jag-1-mediated Notch signalling and Myogenic differentiation

After a high siRNA transfection efficiency had been established in MVSCs, targeted siRNA transfection was used to transiently inhibit the expression of Notch1. MVSCs were seeded into wells of a 6-well plate and incubated overnight at 37ºC. The following day, the TransIT-X2 Dynamic Delivery System was used to transiently transfect the cells with either a targeted siRNA against the *Notch1* transcript or a non-specific (Scrambled) control siRNA. Cells were then incubated for a further 48 h at 37ºC in MM1. Cells were harvested and both RNA and protein were isolated from each sample. The decrease in *Notch1* transcript was confirmed by qRT-PCR, while western blot was carried out to confirm the knockdown of Notch1 protein expression. A reduction of around 72% in *Notch1* transcript and a reduction of approximately 62% in Notch1 protein expression was observed following siRNA knockdown (Fig 3.14 and 3.15). It must also be noted that no physical/morphological impact was observed in the cell population following siRNA transfection.

This knockdown was then combined with Jag-1 stimulation to decipher whether or not Notch1 played a role in Jag-1 mediated activation of Notch signalling and myogenic differentiation. MVSCs were seeded into Jag-1- or Fc-coated wells at 100,000 cells/well. Following overnight incubation at 37ºC, the TransIT-X2 Dynamic Delivery System was used to transiently transfect the cells with either a *Notch1* siRNA or a Scrambled control siRNA. Cells were then incubated for a further 48 h at 37ºC in MM1. Cells were harvested and RNA was isolated from each sample. To examine the change in expression of the Notch target gene *Hey1* and the myogenic gene *Myh11,* qRT-PCR was carried out. There was a significant decrease in the expression of *Hey1* in the *Notch1* knockdown sample compared to the sample transfected with non-specific scrambled siRNA (Fig.3.16). Moreover, the expression of myogenic marker *Myh11* was also significantly reduced following *Notch1* siRNA knockdown and Jag-1 treatment (Fig 3.17).

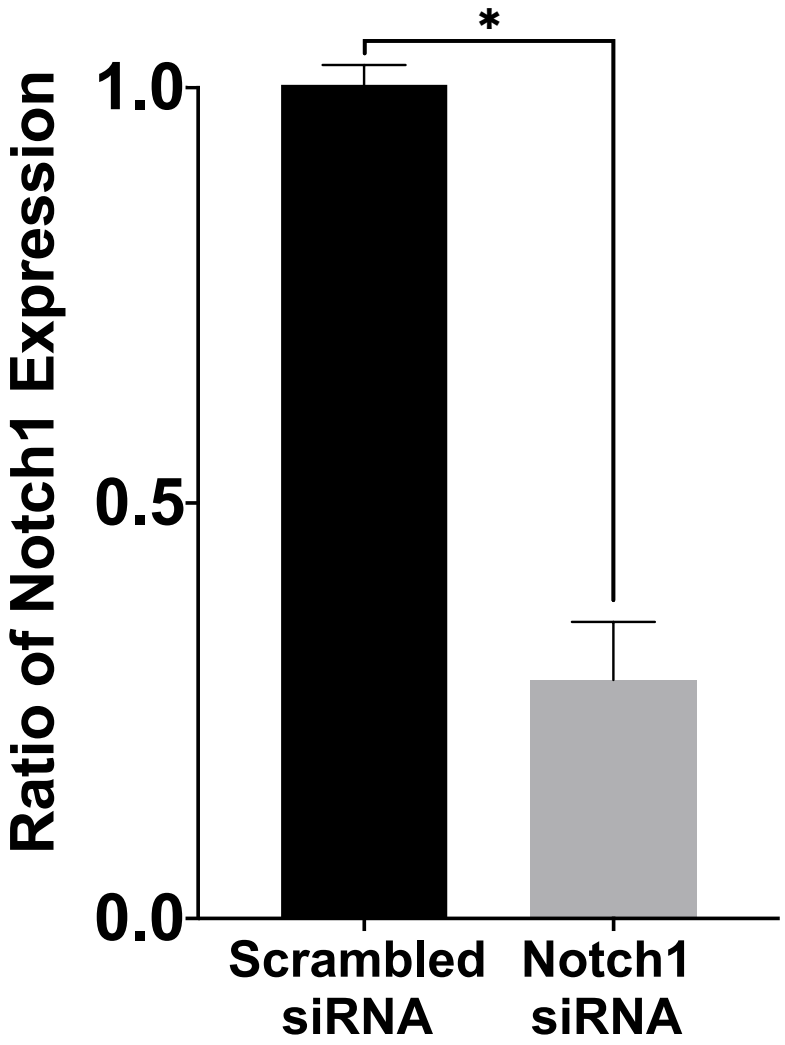
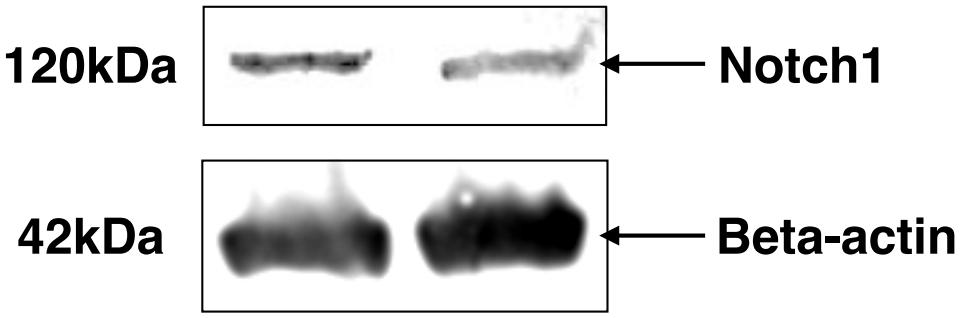


Fig.3.14 Expression of *Notch1* transcript in MVSCs following Notch1 siRNA knockdown. The relative expression of *Notch1* mRNA levels by qRT-PCR in MVSCs transfected with *Notch1* siRNA (25nM) or a scrambled control for 48 h at 37^{o}C in MM1. Data are presented as the ratio of expression relative to the negative control sample transfected with non-targeted (scrambled) siRNA. Error bars based on SEM. Data representative of n=3. * $p < 0.05$

(a)



(b)

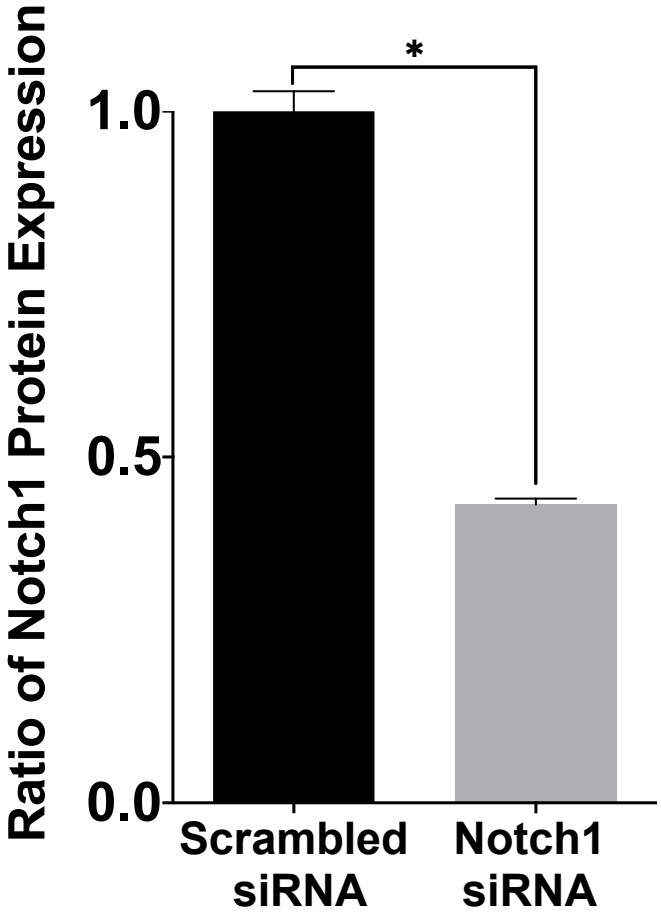


Fig.3.15 Expression of Notch1 protein in MVSCs following Notch1 siRNA knockdown. MVSCs were transfected with Notch1 siRNA (25nM) and scrambled control for 48 h at 37^{o}C in MM1 before Notch1 protein was assessed in cell lysates by immunoblot. (a) Representative immunoblot of Notch1 bands at 120kDa and β-actin bands at 42kDa. Densitometry was carried out on western blot samples to measure intensity of Notch1 bands normalised to the β-actin loading control. (b) Notch1 protein expression is presented as the ratio of expression relative to the negative control sample transfected with non-targeted (scrambled) siRNA. Error bars based on SEM. Data representative of n=3. * $p < 0.05$

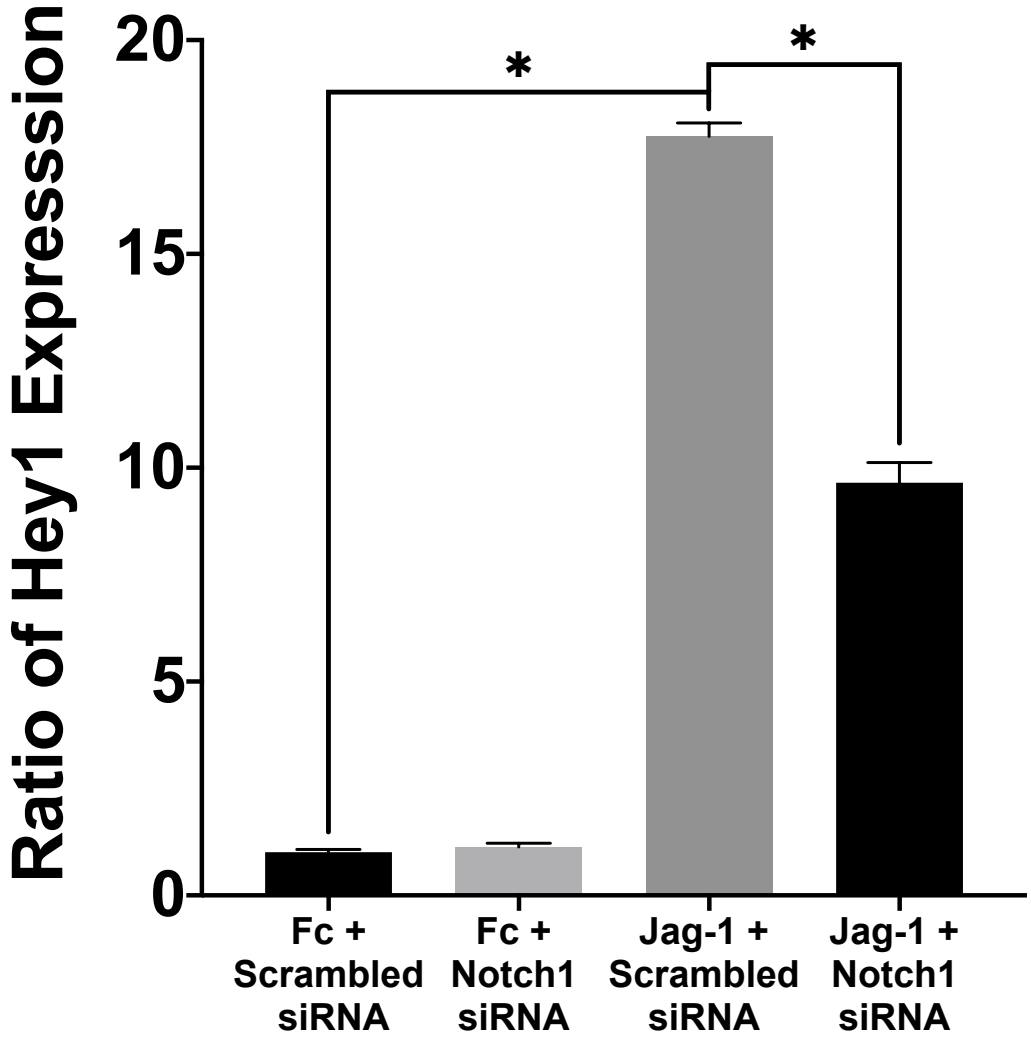


Fig.3.16 Effect of Notch1 knockdown on *Hey1* expression in Jag-1-treated MVSCs. The relative expression of *Hey1* mRNA levels by qRT-PCR following Notch1 knockdown and treatment with or without recombinant rat Jag-1 at 1μg/mL. MVSCs transfected with Notch1 siRNA (25nM) and a scrambled control were treated with or without recombinant rat Jag-1 for 48 h at 37ºC in MM1. Data are presented as the ratio of expression relative to the negative control sample treated with Fc and transfected with non-targeted (scrambled) siRNA. Error bars based on SEM. Data representative of n=3. * $p < 0.05$

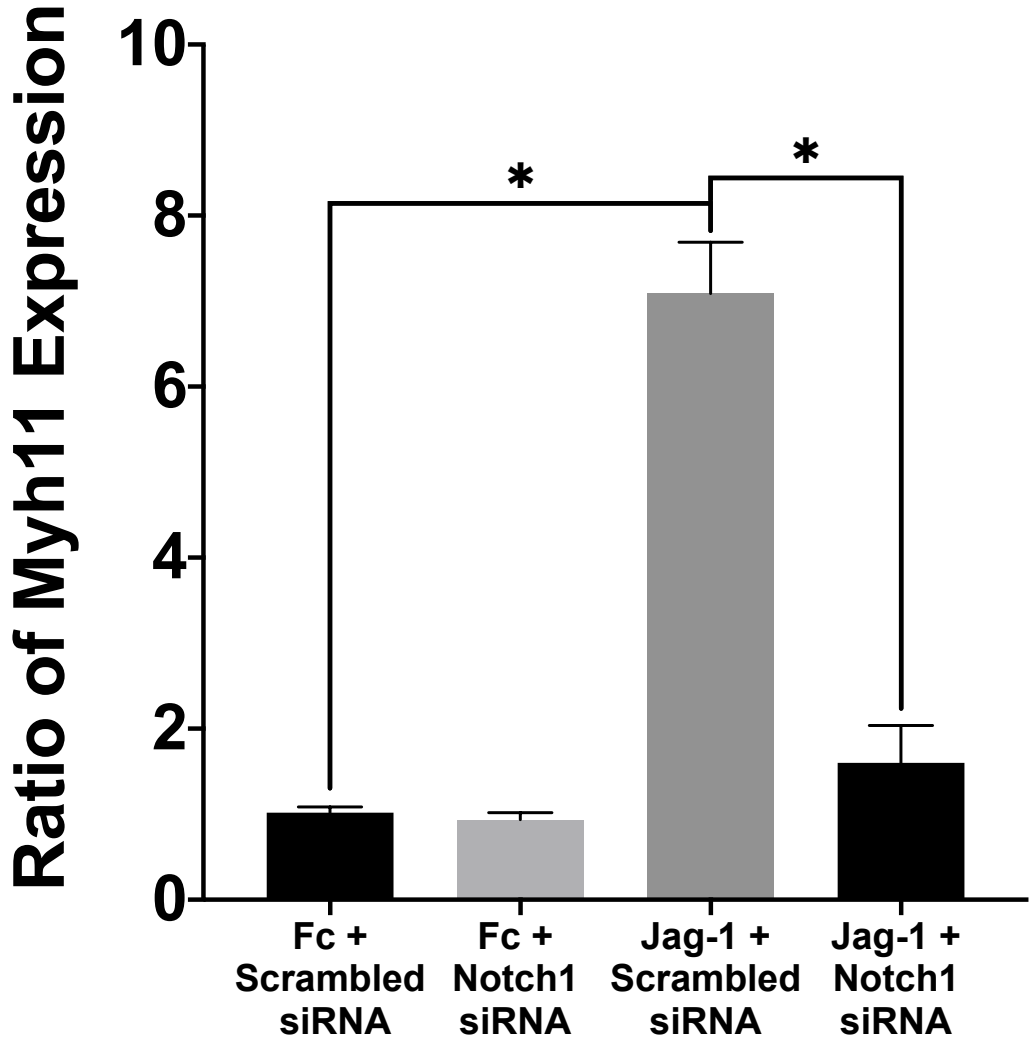


Fig.3.16 Effect of Notch1 knockdown on *Myh11* expression in Jag-1-treated MVSCs. The relative expression of *Myh11* mRNA levels by qRT-PCR following Notch1 knockdown. MVSCs transfected with Notch1 siRNA (25nM) and a scrambled control were treated with or without recombinant rat Jag-1 for 48 h at 37ºC in MM1. Data are presented as the ratio of expression relative to the negative control sample treated with Fc and transfected with non-targeted (scrambled) siRNA. Error bars based on SEM. Data representative of n=3.
* $p < 0.05$

3.4 Discussion

The formation of fibrous neointimal lesions in the vasculature is one of the most prevalent forms of cardiovascular disease (CVD) in humans (Fishbein and Fishbein, 2009). Moreover, the occurrence of such intimal thickening has become one of the major limiting factors for surgical interventions in CVD treatment as procedures such as stenting, balloon angioplasty and vein-graft bypass regularly lead to vessel injury and the emergence of arteriosclerotic lesions (Davies and Hagen, 1995; Haery, Sachar and Ellis, 2004). Therefore, the development of new drug treatments is required to combat this issue. In order for this to happen, further research must be carried out to understand the exact molecular mechanisms by which lesion formation occurs and from what source the SMC-like cells of the neointima are derived. The classic model of SMC de-differentiation to SMC-like cells has recently been challenged and it has been reported in numerous publications that other cell populations may play some part in the process (Yuan *et al.*, 2017). In particular, resident stem cells in the vasculature have repeatedly been shown, through genetic lineage tracing studies, to migrate to an injured site in the artery wall and differentiate to become SMC-like (Z. Tang *et al.*, 2012; Kramann *et al.*, 2016; J. Tang *et al.*, 2020). Evidence from our research group and several others has also suggested that neointimal cells originate from a medial stem cell parent population expressing Sca1 and/or S100β markers (Tang *et al.*, 2012; Cao *et al.*, 2017; Molony *et al.*, 2020; Di Luca *et al.*, 2021). Therefore, the first aim of this study was to identify, isolate and characterise a similar population of stem cells.

A lineage tracing mouse model was set up within our research group whereby S100β$^+$ cells were indelibly marked so that all of their progeny would express (upon Tamoxifen induction) the tdTomato red fluorescence protein. There was a significant increase in the number of cells on the inner side of the internal elastic lamina (IEL) in the ligated left carotid artery (LCA) compared to that of the contralateral right carotid artery (RCA) control. This indicates the formation of a neointima in the ligated vessel. It must be noted that the RCA control does not reflect a sham animal as the RCA is affected by the ligation of the LCA where blood flow dramatically increases with this contralateral vessel (Korshunov and Berk, 2003). This increase in blood flow in the RCA mitigates against the drop in the LCA due to the ligation and can result in outward remodelling. However, in this instance, only inward remodelling events were being analysed. A significant proportion of these neointimal cells were tdTomato$^+$ in the LCA. As S100β tdTomato-expressing cells were indelibly marked before injury, all tdT$^+$ cells in the neointima are derived from an S100β$^+$ parent population.

Cells expressing tdTomato in the medial and adventitial layers of the RCA may also be derived from this S100β$^+$ parent population and have arisen due to outward vascular remodelling, but it is also possible that they are themselves the parent population from which neointimal cells originate. In any case, from this data we can conclude that a subpopulation of S100β$^+$ cells within the lesion are derived from an S100β parent population and make a considerable contribution to vascular lesion formation. This, along with previously reported data, provided solid preliminary data to justify the use of an S100β$^+$ resident stem cell population for subsequent experiments in this study.

It is also important to note the time allowed for Tamoxifen washout before vessel ligation was performed. Tamoxifen induction has been regularly used in lineage tracing studies to initiate expression of a fluorescent tag in cells that have a target promoter activated. However, it has been reported that Tamoxifen can remain in tissues and induce fluorescent tag expression in cells for up to four weeks after the last injection has taken place (Reinert *et al.*, 2012). This casts doubt over many of the lineage tracing studies previously used to determine the origin of neointimal cells. The majority of these studies used an inducible Cre system which was activated by a Myh11 promoter and a ligation procedure that was carried out 1-14 days after Tamoxifen treatment (Nemenoff *et al.*, 2011; Herring *et al.*, 2014; Chappell *et al.*, 2016). Large portions of cells expressing the reporter tag led these research groups to conclude that SMC-like cells in the neointima were derived from de-differentiated SMCs, when in fact it could not be ruled out that these neointimal cells had been derived from a Myh11$^-$ population that had acquired the expression of Myh11 due to myogenic differentiation post-ligation and were subsequently marked by the Tamoxifen which remained in the tissue after treatment, confounding their results. This issue also applies to many studies which tracked the migration and differentiation of endothelial cells using Tamoxifen induced Cre systems controlled by a Cadh5 promoter (Chen *et al.*, 2021). To combat this issue, the current study used a lineage tracing model where vessel ligation was carried out four weeks post-Tamoxifen treatment and used an S100β promoter to activate the Cre system. This substantially reduced the chance of non-S100β derived neointimal cells being marked after vessel ligation.

In the future though, in order to circumvent the issues with inducible Cre systems, it will be necessary to develop and use new methods for determining the genetic lineage of cells. One such method which has gained popularity in recent years is that of single cell RNA-sequencing (scRNA-Seq) which can be utilised to identify discrete subpopulations in a large

pool of cells (Saliba *et al.*, 2014). Inducible Cre systems can be used in tandem with scRNA-Seq to provide an even more detailed analysis of the genetic lineage of a cell (Kester and van Oudenaarden, 2018). The combination of these technologies in recent years has yielded compelling evidence for discrete populations of SMCs, endothelial cells and resident stem cells in vascular remodelling (Kramann *et al.*, 2016; Dobnikar *et al.*, 2018; Kalluri *et al.*, 2019; Tang *et al.*, 2020). However, the issue of Tamoxifen persistence in the tissue must again be taken into account in such studies. For example, one study reported the existence of a $Sca1^{+}$ $Myh11^{+}$ SMC subpopulation from which a large proportion of neointimal cells were derived, but the Myh11 expression of this parent population was determined via a Tamoxifen-induced Cre system controlled by a *Myh11* promoter where vessel ligation was carried out only 1 week post-Tamoxifen treatment (Dobnikar *et al.*, 2018). Alternative technologies such as that of single cell photonics, which has previously been used to identify disease-relevant signatures in an $S100\beta^{+}$ resident stem cell population (Molony *et al.*, 2020), may provide more reliable insights into the origin of neointimal cells.

Enzymatic dispersion was used to isolate and culture a population of stem cells from the medial layer of a mouse aortic arch. The aortic arch was chosen as this is a high risk area for arteriosclerotic lesion formation (Redheuil *et al.*, 2010). These cells were subsequently referred to as multipotent vascular stem cells (MVSCs). Using immunocytochemistry (ICC), it was found that MVSCs expressed Sca1, S100β and Nestin. Sca1 has been previously reported to be upregulated in SMC phenotypic switching (Dobnikar *et al.*, 2018) and a number of stem cell populations in both the adventitial and medial layers of the artery have been shown to express Sca1 (Torsney, Hu and Xu, 2005; Sainz *et al.*, 2006; Tang *et al.*, 2020). Interestingly, when MVSCs were first characterised, they were determined to be $Sca1^{-}$ (Tang *et al.*, 2012). However, the growth media used for MVSCs in that instance consisted of DMEM with 10% FBS, as opposed to the 1% FBS MM1 used in this study, and this could have led to a loss of Sca1 expression. Nestin is regularly used as a marker for neural crest stem cells. The aortic arch has its embryological origin in the neuroectoderm and so many of the cells present in this area still express markers related to that origin (Bacakova *et al.*, 2018). Furthermore, neural crest stem cells have been previously shown to have the ability to differentiate down a myogenic lineage (High *et al.*, 2007). Therefore, this data suggests that the cells isolated from the mouse aortic arch were indeed stem cells derived from a neuroectodermal origin.

It was assumed that these cells were extracted from the medial layer due to the manner in which they were isolated whereby the endothelium was degraded by enzymatic digestion and the adventitial layer was physically removed following enzymatic treatment. However, S100β$^+$ cells have proven difficult to detect in the tunica media, with previous data from our research group finding no such cells in the medial layer of sham ligated vessels and only a very small number in the RCA contralateral artery which, as previously stated, could have arisen due to the occurrence of outward remodelling events (Di Luca *et al.*, 2021). It is possible that S100β$^+$ cells are extremely rare in the medial layer and therefore have not been identified in previously examined arterial sections. This appears to be the case with Sca1$^+$ cells which have been identified in the media but only at very low rates of occurrence (Sainz *et al.*, 2006; Di Luca *et al.*, 2021). An alternative possibility is that the isolated cells were in fact adventitial cells. Not only have S100β$^+$ and Sca1$^+$ cells been previously reported to be present in the adventitial layer of the artery (Torsney, Hu and Xu, 2005; Wu *et al.*, 2019; Liu *et al.*, 2020), but data from our research group has also confirmed that some adventitial cells remain attached to the external elastic lamina (EEL) following physical removal of the adventitia (Di Luca, 2019). It is therefore possible that the isolated MVSCs, which have previously been described as medial cells (Tang *et al.*, 2012), may in fact be derived from a population of S100β$^+$ Sca1$^+$ adventitial stem cells.

As the wall of the aorta is primarily comprised of differentiated SMCs, it was also appropriate to investigate whether the isolated cell population expressed myogenic markers. MVSCs did not express either the intermediate SMC marker, Calponin1 (Cnn1) or the terminal differentiation marker myosin heavy-chain 11 (Myh11) when interrogated by ICC. For comparison, cultured mouse SMCs were used as a positive control and shown to strongly express both myogenic markers. This confirms that the isolated medial cell population does not consist of SMCs. This is supported by previously reported data which noted that the epigenetic profile of an MVSC population does not contain the SMC-specific signature of di-methylation of lysine 4 on histone H3 (H3K4me2) and tri-methylation of lysine 27 on histone H3 (H3K27me3) at the *Myh11* locus (Di Luca *et al.*, 2021). Since SMCs retain much of their critical epigenetic signatures following phenotypic switching (Gomez, Swiatlowska and Owens, 2015), this data not only helps to confirm that the isolated stem cell population does not consist of SMCs, but also that it was not derived from de-differentiation of SMCs.

C3H cells were also characterised using ICC as they would be used as a comparison cell line for some of the more vital experiments in this study. C3Hs were shown to be positive for

both Sca1 and S100β, and negative for both Cnn1 and Myh11. Although C3Hs are a mesoderm-derived embryonic fibroblast cell line, this data, along with their previously reported ability to differentiate down a myogenic lineage (Singh *et al.*, 2003), make them a suitable candidate for comparison.

In order to further confirm the stemness of the MVSC population, telomere length and telomerase activity were measured. Telomeres, located at the end of each chromosome, serve a vital role in cell proliferation. As cells become more differentiated and lose proliferation potential, the length of their telomeres is reduced and there is decreased activity of the telomerase enzyme which elongates telomeres during cell division (Wright *et al.*, 1996; Grimm *et al.*, 2004). In this study, a TRAP assay was carried out which showed a significantly higher level of telomerase activity in mouse aortic MVSCs compared to fresh aortic tissue which is primarily comprised of differentiated SMCs. Additionally, the telomere length of MVSCs was measured using real-time PCR and compared against terminally differentiated cells. MVSCs were demonstrated to have telomere length of approximately 2.3 ± 0.114 fold greater than that of cells from a fresh aortic tissue. A similar increase was observed when compared to MOVAS cells. These results coupled together provide substantial evidence that these isolated MVSCs have a greater level of stemness than terminally differentiated cells in the mouse aorta.

As a final confirmation that the MVSCs isolated from the mouse aortic arch were in fact stem cells, their differentiation potential was examined. Following treatment with osteogenic differentiation media for 14 days, a significant increase in expression of osteogenic markers *Alpl* and *Sost* was recorded. Similarly, adipogenic media stimulated increased expression of adipogenic markers *Lpl* and *Fabp4*. This data indicates that MVSCs possess the ability to differentiate down an osteogenic or adipogenic pathway, depending on the stimulus. Coupled with previous data from our group (E. Kennedy, Hakimjavadi, *et al.*, 2014; Di Luca *et al.*, 2021) and others (Tang *et al.*, 2012) describing the ability of MVSCs to differentiate down a myogenic lineage, and later data in this study which demonstrates the same, this suggests that MVSCs have a high level of multipotency, an important characteristic of stem cells.

The molecular mechanisms by which resident vascular stem cells may differentiate into SMC-like cells is currently not fully understood and it seems as though a number of different signalling pathways may be involved, such as the Transforming Growth factor (TGF)-β and

Vascular Endothelial Growth Factor (VEGF) pathways (Wang *et al.*, 2015). A large body of evidence suggests that one of the principal pathways that may contribute to this process is the Notch signalling pathway. The role of the Notch receptor in regulation of both embryonic and adult stem cell fate has been extensively reported in literature (Guruharsha, Kankel and Artavanis-Tsakonas, 2012). This regulatory role, combined with a number of other factors, such as its ability to promote proliferation following vascular injury (Morrow *et al.*, 2005) and activate myogenic differentiation in stem cells (Kurpinski *et al.*, 2010), have identified Notch signalling as a potentially vital pathway in the development of CVD. Therefore, the next objective of this study was to investigate if activation of the Notch receptor by the Jagged-1 ligand could promote Notch signalling and myogenic differentiation in the previously isolated population of MVSCs *in vitro*.

Following Jag-1 treatment, expression of the Notch target gene *Hey1* and the myogenic marker *Myh11* were both significantly upregulated after 48 h in MVSCs. This data suggests that the myogenic differentiation pathway can be stimulated in MVSCs by activating Notch receptor signalling. This is supported by previously published data which recorded a significant increase in myogenic differentiation of MVSCs when co-cultured with OP-9-Delta1 feeder cells (Tang *et al.*, 2012). The response of MVSCs to Jag-1 stimulation was also mirrored in the C3H cell line, further supporting the role of Notch signalling in myogenic differentiation of stem cells. Expression of alternative Notch target genes, such as *Hey2* and *HeyL,* was not measured in this case but would certainly be interesting targets for future analyses, along with additional myogenic markers such as *Cnn1* and *SM22α.*

ICC data following a 7-day Jag-1 treatment of MVSCs exhibited the phenotypic effect that increased Notch target gene expression was having on the stem cell population. Approximately 40% of cells were observed to be expressing the myogenic marker Cnn1 following Jag1 treatment. This was compared to 0% Cnn1 expression in MVSCs treated with the Fc-control. This evidence suggests that activation of Notch signalling by the Jag-1 ligand can stimulate differentiation of MVSCs down a myogenic lineage. This further supports previous data which exhibited the multipotency of MVSCs. Cnn1 was used as the myogenic marker instead of Myh11 for this experiment. Cnn1 is an early stage marker of myogenic differentiation, while Myh11 is a marker of terminally differentiated SMCs (Cheung *et al.*, 2012). It has been reported that full myogenic differentiation can take anywhere between 10 days and 6 weeks and even terminally differentiated SMCs regularly lose the expression of the Myh11 protein when cultured *in vitro* (Mizuno *et al.*, 2002;

Yoshida, Kaestner and Owens, 2008; Wen *et al.*, 2014). Therefore, although Myh11 has previously been identified as the most specific marker for differentiated SMCs (Madsen *et al.*, 1998), Cnn1 was deemed to be the most suitable myogenic marker for this particular experiment.

As previously mentioned, signalling pathways involving TGF-β and VEGF have also been reported to influence stem cell differentiation to SMCs. In order to confirm that Jag-1 activation of target gene expression was Notch-dependent, the DAPT inhibitor (which blocks an essential cleavage event in Notch activation) was used to prevent Notch signalling. DAPT significantly reduced the expression of *Hey1* in response to Jag-1 activation, while its dissolving vehicle DMSO had no significant effect on *Hey1* expression, indicating that Jag-1 activation of target gene expression is in fact Notch-dependent. Previous work, carried out by Dr. Mariana Di Luca in our research group, demonstrated a similar trend in *Hey1* expression in MVSCs and also showed a significant reduction in *Myh11* expression following DAPT inhibition of Jag-1-treated MVSCs. Furthermore, this data included a control sample where DAPT treatment was carried out on Fc-treated MVSCs and this did not result in any significant reduction in *Hey1* or *Myh11* expression, indicating that DAPT only attenuates the expression of these target genes through inhibition of Notch receptor activation (Appendix D).

Further exploration of the exact mechanisms of Notch-dependent myogenic differentiation is required to identify the critical stages of the pathway that could be targeted in future therapies. It has been reported on numerous occasions that the activity of the Notch intracellular domain (NICD)-Centromere Binding Factor-1 (CBF-1)/Recombination signal sequence-binding protein Jκ (RBP-Jκ) complex is essential in the stimulation and regulation of myogenic differentiation (Morrow *et al.*, 2008). The NICD-CBF-1/RBP-Jκ complex can directly activate expression of myogenic genes such as smooth muscle α-actin (*SMA*) by binding to the promoter region (Manabe and Owens, 2001; Doi *et al.*, 2006), or it can interact with the serum response factor (SRF)- myocardin complex to stimulate binding to the CArG domain of myogenic markers such as *Myh11* to initiate transcription (Noseda *et al.*, 2006). These interactions are also tightly self-regulated as Notch target genes such as *Hey1* and *Hey2* inhibit the activity of the NICD-CBF-1/RBP-Jκ complex once their expression reaches a specific threshold level (Tang, Urs and Liaw, 2008). Furthermore, the activity of the NICD-CBF-1/RBP-Jκ complex has been shown to have a disease-relevant impact as previous studies have reported that knockout of RBP-Jκ in a mouse model for atherosclerosis led to

inhibition of myogenic differentiation and phenotypic switching of SMCs (Martos *et al.*, 2020). However, these mechanisms of activation and regulation have not yet been thoroughly investigated in resident vascular stem cells, and therefore future research in this area could help to decipher their impact on myogenic differentiation of stem cells during arteriosclerosis.

Although four types of Notch receptor exist in mammalian cells, Notch1 has been the most regularly implicated in the development of arteriosclerotic lesions. On numerous occasions, knockdown or knockout of Notch1 has been reported to reduce neointima formation following vascular injury (Li *et al.*, 2009; Redmond *et al.*, 2014; Q. Chen *et al.*, 2015). Therefore, it was of interest to this study to investigate whether the Jag-1 response observed in MVSCs would be affected by *Notch1* siRNA knockdown and if this would impact myogenic differentiation of MVSCs. A high siRNA transfection efficiency was established in MVSCs with almost 100% uptake of a fluorescent siRNA dye. A similar transfection rate was also observed in C3Hs which could therefore be used as a contingency cell line if knockdown levels were not sufficient in MVSCs. However, acceptable levels of *Notch1* knockdown were confirmed in MVSCs with a 72% reduction in *Notch1* transcript and a 62% reduction in Notch1 protein levels compared to a scrambled siRNA control. This knockdown was combined with Jag-1 treatment and this led to a considerable inhibition of the Jag-1 response, with expression of both *Hey1* and *Myh11* being significantly reduced. This data suggests that MVSCs treated with Jag-1 experience activation of Notch signalling and promotion of myogenic differentiation due, at least in part, to interaction of the Notch1 receptor with its ligand. It must be noted however, that the Jag-1 response in MVSCs may also be influenced by interactions between Jag-1 and the other three Notch receptors. Future research would require knockdown of each receptor individually to elicit information regarding the role of each one in this process and to determine what redundancies exist between the four Notch receptors. Additionally, stable knockout of Notch receptors *in vivo* could yield vital information about their impact on arterial remodelling. For example, an inducible Notch1 knockout mouse model could be set up and driven by an S100β-controlled Cre system to investigate the necessity of Notch1 in migration and differentiation of $S100\beta^{+}$ stem cells following vascular injury. Previous studies of this nature have mostly concentrated on the role of Notch receptors in SMC de-differentiation (Li *et al.*, 2009; Peterson *et al.*, 2018), so this would provide novel insights into the combined role of Notch and resident stem cells in neointima formation.

In summary, data in this chapter confirms that MVSCs isolated from the aortic arch of a mouse express a range of neural stem cell markers and are negative for SMC marker expression. Furthermore, these cells are telomerically active and have the capacity to differentiate down a number of lineages. These data sets support the hypothesis that MVSCs are indeed multipotent stem cells which are resident in the medial layer of the aorta and are derived from a neuroectodermal lineage. Therefore, they are highly similar to subpopulations of cells which have been previously reported to be heavily involved in the formation of the arteriosclerotic neointima (Tang *et al.*, 2012; Di Luca *et al.*, 2021). Numerous studies have indicated that the manner by which stem cells contribute to lesion formation is through differentiation to SMC-like cells (Wang *et al.*, 2018). This differentiation is likely controlled in some part by Notch signalling, as several elements of that pathway have been reported to be upregulated during injury-induced vascular remodelling and Notch target genes have the ability to induce myogenic differentiation in stem cells (Lindner *et al.*, 2001; Morrow *et al.*, 2005). This chapter provides evidence suggesting that MVSCs can be stimulated by the Notch ligand Jag-1 to express Notch target genes and to undergo myogenic differentiation. This activation process specifically involves the Notch1 receptor. In conclusion, this supports the hypothesis that MVSCs may undergo Notch1 signal activation and differentiate to become SMC-like cells in response to vascular injury, thus contributing to the formation of a neointimal lesion.

Chapter 4:

The Effect of Small-molecule N-glycosylation Inhibitors on Notch Signalling and Myogenic Differentiation

4.1 Introduction

Due to the substantial impact of Notch signalling on so many cellular and molecular processes, small changes in this signalling pathway can have meaningful consequences for the organism as a whole. For this reason, Notch signalling is tightly regulated by a number of mechanisms, including *cis*-inhibition, negative feedback loops and PEST ubiquitination (Fortini, 2009; Kopan and Ilagan, 2009). Another major regulating factor for Notch signalling is through glycosylation of the Notch receptor. There are a large number of highly conserved glycosylation sites along the extracellular domain of the Notch receptor. The vast majority of these sites harbour O-linked glycans. Conserved sites of O-glycosylation on Notch were first discovered at the turn of the century in *Drosophila melanogaster* (Moloney, Shair, *et al.*, 2000) and this gave rise to a wave of research centred on O-glycosylation of Notch, resulting in many more consensus sites and several important glycosyltransferases, such as Fringe, being identified (Shao, Moloney and Haltiwanger, 2003; Acar *et al.*, 2008; Okajima *et al.*, 2008). In contrast, very little is known about the specifics of N-linked glycosylation of Notch. It has been established that there are six N-glycosylation consensus sites along the extracellular domain of Notch (Takeuchi and Haltiwanger, 2014) and that N-glycans are certainly present on the Notch receptor (Moloney, Panin, *et al.*, 2000), but the number of these sites that are actually glycosylated, the structures of these N-glycans and their potential role in Notch signalling, remains a mystery.

One of the methods most regularly employed to investigate the impact of N-glycosylation on a given process is the use of small-molecule N-glycosylation inhibitors. The most widely used of these inhibitors is Tunicamycin (TNC), an antagonist for the GlcNAc phosphotransferase (GPT) enzyme which catalyses a critical step in the protein N-glycosylation pathway, linking the growing polypeptide to a dolichol precursor (A Heifetz, Keenan and Elbein, 1979). Another small-molecule inhibitor extensively used to block N-glycosylation is 1-deoxymannojirimycin (DMJ) which blocks the trimming of the 14-sugar dolichol precursor oligosaccharide by inhibiting the mannosidase I enzyme (Elbein, 1987). This allows for the production of high-mannose N-glycans, but prevents synthesis of complex or hybrid-type N-glycans. Although the specificities of these inhibitors are broad, they nonetheless represent an extremely useful tool in deciphering the role of N-glycans in Notch signalling.

When carrying out interventions against N-glycosylation, it is not only important to investigate the effect on the specific signalling pathway, but also to determine the

consequences of these interventions on the N-glycan profile of a cell population or that of a singular glycoprotein. Lectins have, in recent years, become powerful tools for the detection of glycans. Lectins are highly specific carbohydrate-binding proteins with no catalytic activity (Lis and Sharon, 2002). They can bind mono- or oligosaccharides and have the ability to recognise and distinguish between distinct branching and linkage patterns (Ghazarian, Idoni and Oppenheimer, 2011). A number of assays have been developed and optimised which exploit the high level of specificity seen in lectin-oligosaccharide binding to determine the glycosylation profile of a given glycoprotein sample. The enzyme-linked lectin assay (ELLA) is a simple and rapid method of glycan analysis that, unlike techniques such as mass spectrometry and HPLC, does not require the chemical or enzymatic removal of carbohydrates from proteins (Thompson *et al.*, 2011). In this way, lectins can be used to detect changes in N-glycosylation patterns following inhibitory interventions.

4.2 Strategy

Before proceeding to interfere with Notch1 N-glycosylation, it was imperative to first establish its baseline N-glycan profile in MVSCs. This could be achieved by carrying out an ELLA (Section 2.2.17) on a sample of purified Notch1 protein. Immunoprecipitation with Protein A-coupled magnetic beads was used to separate Notch1 from the rest of an MVSC cell lysate (Section 2.2.15). This, however, required a large volume of cultured cells to yield a usable quantity of purified Notch1. To overcome this issue, a new strategy was implemented to ectopically overexpress Notch1 in the cell population through transient transfection of a plasmid encoding a full-length myc-tagged Notch1 (Section 2.2.6.1). Through this approach, high levels of the myc-tagged Notch1 could be purified and ELLA was carried out to determine the N-glycan profile of the Notch1 receptor. This was achieved through the use of commercial lectins specific for different types of N-linked glycans (see Table 2.13 for list of lectin specificities).

When using small-molecule inhibitors such as TNC and DMJ, it is important to confirm that they carry out their function properly in a given cell line without causing cell cytotoxicity. In this case, proteins were isolated from MVSCs following treatment with TNC or DMJ at a range of concentrations and ELLAs were used to detect changes in the N-glycosylation profile of the whole cell lysate compared to a non-treated control. The activity of both inhibitors was similarly confirmed in C3H cells.

To further verify that TNC and DMJ could not only alter the N-glycan profile of the whole cell, but more specifically the N-glycosylation of the Notch1 receptor, it would be necessary to purify Notch1 from samples which had been treated with the inhibitors and use ELLAs to determine the resulting changes. The previously described tactic of overexpressing Notch1 using a transfected plasmid was attempted. However, extensive cell death was observed when plasmid transfection was combined with either of the inhibitors. Furthermore, the implications of ectopic overexpression of Notch1 on TNC and DMJ activity could not be predicted and therefore added another layer of variation that could cast doubt over the resulting data. Therefore, a more expensive but more suitable strategy was implemented whereby much larger volumes of cultured MVSCs were treated with TNC and DMJ, followed by immunoprecipitation of the native Notch1 protein and subsequent analysis of the N-glycan profiles via ELLA.

Once the effect of TNC and DMJ on both whole cell and Notch1 N-glycosylation had been established, Jag-1-stimulated MVSCs were then treated with each of the inhibitors to investigate how this change in N-glycosylation affected Notch signalling and myogenic differentiation. To achieve this, qRT-PCR was used to measure the expression levels of *Hey1* and *Myh11* across all samples (Section 2.2.11). C3H cells were used as a cell line comparison for this experiment.

The final set of experiments in this chapter were carried out to attempt to identify how TNC and DMJ were affecting Notch1 signalling, ie. what stage, in the Notch signalling pathway or in the processing of the Notch1 receptor itself, was being affected by these interventions. As described in Section 1.5.4, when Notch is activated by its corresponding ligand, the Notch intracellular domain (NICD) is cleaved and released, allowing it to translocate to the nucleus where it recruits a number of transcription factors and activates the expression of Notch target genes (Baron, 2003). Therefore, ectopic expression of the NICD by plasmid transfection could be used to stimulate Notch target gene expression and myogenic differentiation independent of Jag-1. A strategy was then developed whereby MVSCs transfected with NICD plasmid would be treated with TNC and DMJ to investigate whether these interventions were affecting elements of the Notch signalling pathway downstream of receptor activation. This could be determined again by qRT-PCR analysis of *Hey1* and *Myh11* expression. The same issue of cell death induced by combined transfection and inhibitor treatment, was not as significant a factor in this case as it was for the immunoprecipitation (IP) experiment. Certainly, high levels of cell death were again

observed but only a small amount of RNA was required for qRT-PCR compared to the high protein yield that was required for IP and ELLA.

The impact of both small-molecule inhibitors on Notch1 expression was subsequently assessed. MVSCs were treated with TNC and DMJ before carrying out qRT-PCR and western blot (Section 2.2.16) to measure their effect on Notch1 transcript and protein expression respectively.

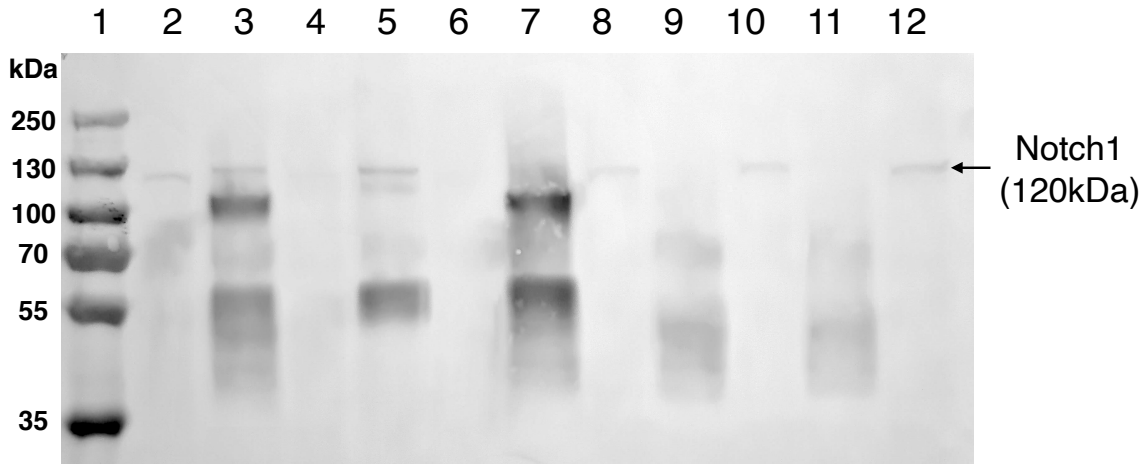
Lastly, the effect of TNC and DMJ on the trafficking of Notch1 in the cell was examined. One technique applied to achieve this was to carry out membrane fractionation on the protein lysate of MVSCs treated with each inhibitor (Section 2.2.13). Western blot was then used to measure the expression of Notch1 protein in the membrane fraction and determine whether this expression had been altered by the TNC or DMJ treatments. Another approach was to probe for Notch1 using immunocytochemistry (Section 2.2.7) in order to visualise changes in its localisation as a result of glycosylation interventions. With both techniques, a Brefeldin A (BFA) control was used. BFA is a potent inhibitor of protein transport in the Golgi apparatus (Takatsuki and Tamura, 1985) and is therefore useful as a positive control for the inhibition of Notch1 trafficking to the membrane.

Data for all experiments in this section was gathered over at least three biological replicates. Normality tests were used to determine if data followed a parametric distribution pattern. Variation across samples was analysed by calculating p-values. The type of test used to calculate this was governed by the outcome of the normality test. Statistical significance was assigned to p-values less than 0.05 (Section 2.2.19).

4.3 Results

4.3.1 Purification of Notch1 by Immunoprecipitation

In order to carry out analysis on a purified Notch1 protein, the purification method had to first be optimised. Protein lysates were made from a population of MVSCs and the protein concentration was measured by BCA assay, as per Section 2.2.12. Immunoprecipitation was carried out (Section 2.2.15) using Protein A-conjugated magnetic beads and either an anti-Notch1 rabbit monoclonal antibody from Brennan & Co (3608S), a rabbit IgG control antibody or a mouse IgG control antibody. Following incubation with the antibody, supernatants (containing unbound proteins) were transferred to a fresh tube and appropriately stored. Bound protein was eluted off the beads by either 1X Laemmli Buffer or a 0.1M Glycine buffer (pH 2.0). Sample eluted with the Glycine buffer were neutralised using a 1M Tris buffer (pH 9.0). Both eluted bound proteins and previously stored unbound protein samples were then run on an SDS-PAGE precast protein gel, transferred to a nitrocellulose membrane, immuno-probed using an anti-Notch1 rabbit monoclonal antibody from Abcam (ab52627) and visualised by TMB staining of the HRP-conjugated secondary antibody (Fig.4.1). Only a single band could be visualised in the whole cell lysate sample (Lane 2). This band appeared at the 120kDa mark and represented the Notch1 transmembrane (NTM) receptor. Notch1 bands were also observed in both samples that were immunoprecipitated with an anti-Notch1 antibody (Lanes 3 and 5) but not in their corresponding unbound protein fractions (Lanes 4 and 6). Conversely, Notch1 was not detected in the samples immunoprecipitated with the rabbit IgG control (Lane 7) or the mouse IgG control (Lane 9), or in the mock IP (Lane 11), but Notch1 was present in the unbound protein fractions of all three of those controls. Additionally, non-specific bands and smears were observed in all IP samples. In the only direct comparison of elution methods (Lane 3 v Lane 5), the glycine elution buffer appeared to yield a much lower level of non-specific staining than the Laemmli elution buffer.



Lanes

1- Molecular weight marker
2- Whole cell lysate (No IP)
3- Notch1 IP (Laemmli buffer elution)
4- Notch1 IP unbound (Laemmli buffer elution)
5- Notch1 IP (Glycine buffer elution)
6- Notch1 IP unbound (Glycine buffer elution)
7- Rb IgG Control IP
8- Rb IgG Control IP unbound
9- Ms IgG Control IP
10- Ms IgG Control IP unbound
11- Mock IP (No antibody)
12- Mock IP unbound (No antibody)

Fig.4.1 Optimisation of Notch1 Immunoprecipitation. Notch1 protein was purified from MVSC lysates using protein A-conjugated magnetic beads. Western blot was used to probe for Notch1 in eluted fraction with anti-Notch1 primary antibody from Abcam (ab52627). HRP-conjugated secondary antibody and TMB substrate used to visualise bands. Representative immunoblot image of Notch1 bands at 120kDa. All other bands represent off-target staining. Data representative of n=3.

4.3.2 Ectopic Expression of Myc-tagged Notch1 and NICD

As detailed in Section 4.2, the large volume of cells required to obtain an acceptable yield of purified Notch1 was not sustainable for all experiments and so a strategy of ectopic overexpression of a plasmid-encoded Notch1 was devised to address this issue. Ectopic expression of the Notch1 intracellular domain (NICD) would also be required for several experiments throughout this project. Therefore, amplification and purification of plasmids encoding the Notch1 full-length protein and NICD was required to establish reliable stocks going forward. The pCS2 Notch1 Full Length-6MT and pCS2 Notch1 ICv-6MT plasmids were purchased from Addgene as bacterial stabs. Plasmid-containing bacteria was transferred to a 5mL culture with selective antibiotic at 37ºC for 8 hours. 1.2mL of this culture was then transferred to a 250mL secondary culture with selective antibiotic which was incubated overnight at 37ºC. Plasmid DNA was isolated from this culture using the Invitrogen PureLink™ HiPure Plasmid Filter Midiprep Kit as per Section 2.2.4.2. To verify plasmid length and quality, plasmid DNA was digested with an appropriate restriction enzyme. This served to linearise the DNA before running plasmid samples through gel electrophoresis on an agarose gel as described in Section 2.4.3.3. Visualisation of this gel under UV light confirmed that plasmids were the correct length and that the stocks contained no contaminating DNA (see Appendix A).

In order to validate the ectopic expression of both proteins, MVSCs were grown to ~80% confluency in 3 wells of a 6-well plate and transfected with either the Notch1 full-length plasmid, the NICD plasmid or an empty vector plasmid (pCDNA3.1) using the TransIT-X2 Dynamic Delivery System. Cells were incubated at 37ºC for 48 h in normal maintenance media (MM1) before being harvested. Protein was isolated, as per Section 2.2.12, and quantified by BCA assay. Western blot was then carried out (as per Section 2.2.16), with all samples being immuno-probed using an anti-Myc-tag antibody from Abcam (ab32) to stain for either the myc-tagged Notch1 or myc-tagged NICD, and an anti-β-actin antibody from Sigma-Aldrich (A2228) which would serve as the loading control (Fig. 4.2).

At the 300kDa mark, a single band was observed in the Notch1 plasmid sample, but not in either of the other two samples. This band represents the full-length Notch1 receptor. At the 88kDa mark, again only a single band could be seen, this time in the NICD plasmid sample. This band represents the fully cleaved NICD. Finally, bands of similar size appeared at the 42kDa mark in all three samples. These bands represent the ubiquitously expressed β-actin. Densitometry was then carried out using ImageJ to determine the intensity of each band and

to therefore quantify the amount of myc-tagged Notch1 or myc-tagged NICD in each sample, relative to the amount of β-actin.

4.3.3 N-glycosylation Profile of Purified Notch1

Before employing any N-glycosylation interventions to alter the profile of N-glycans on Notch1, it was necessary to first establish what this baseline profile looked like. MVSCs were grown to ~80% confluency in 3 wells of a 6-well plate. One sample was not transfected while TransIT-X2 Dynamic Delivery System was used to transfect the other two samples either the Notch1 full-length plasmid or an empty vector control plasmid. Cells were incubated at 37ºC for 48 h in normal maintenance media (MM1) before being harvested. Protein was isolated, as per Section 2.2.12, and quantified by BCA assay. IP was carried out to purify the ectopically expressed Notch1 using Protein G-conjugated magnetic beads and an anti-Myc-tag antibody from Abcam (ab32). The non-transfected sample was immunoprecipitated with a mouse IgG control antibody. Bound proteins were eluted off the magnetic beads using a 0.1M Glycine buffer (pH 2.0) and a 1M Tris buffer (pH 9.0) was used to neutralise the purified protein fraction. BCA assay was carried out again to determine the concentration of protein in each sample post-IP. ELLA was then applied to detect the presence of N-glycans in all three samples. Control wells containing PBS rather than a protein sample were used to determine the baseline for non-specific absorbance, while the mouse IgG control sample acted as the baseline for non-specific lectin- or antibody-binding to the IP eluate. Both of these baseline values were subtracted from sample absorbance values to decipher the true level of specific lectin binding. TBST acted as the vehicle control for all lectins. Binding of the ConA, LCA and E-PHA lectins were all significantly increased in the sample transfected with the Notch1 plasmid, compared to the empty vector control, while no significant increase was observed in either sample with the WGA lectin (Fig.4.3).

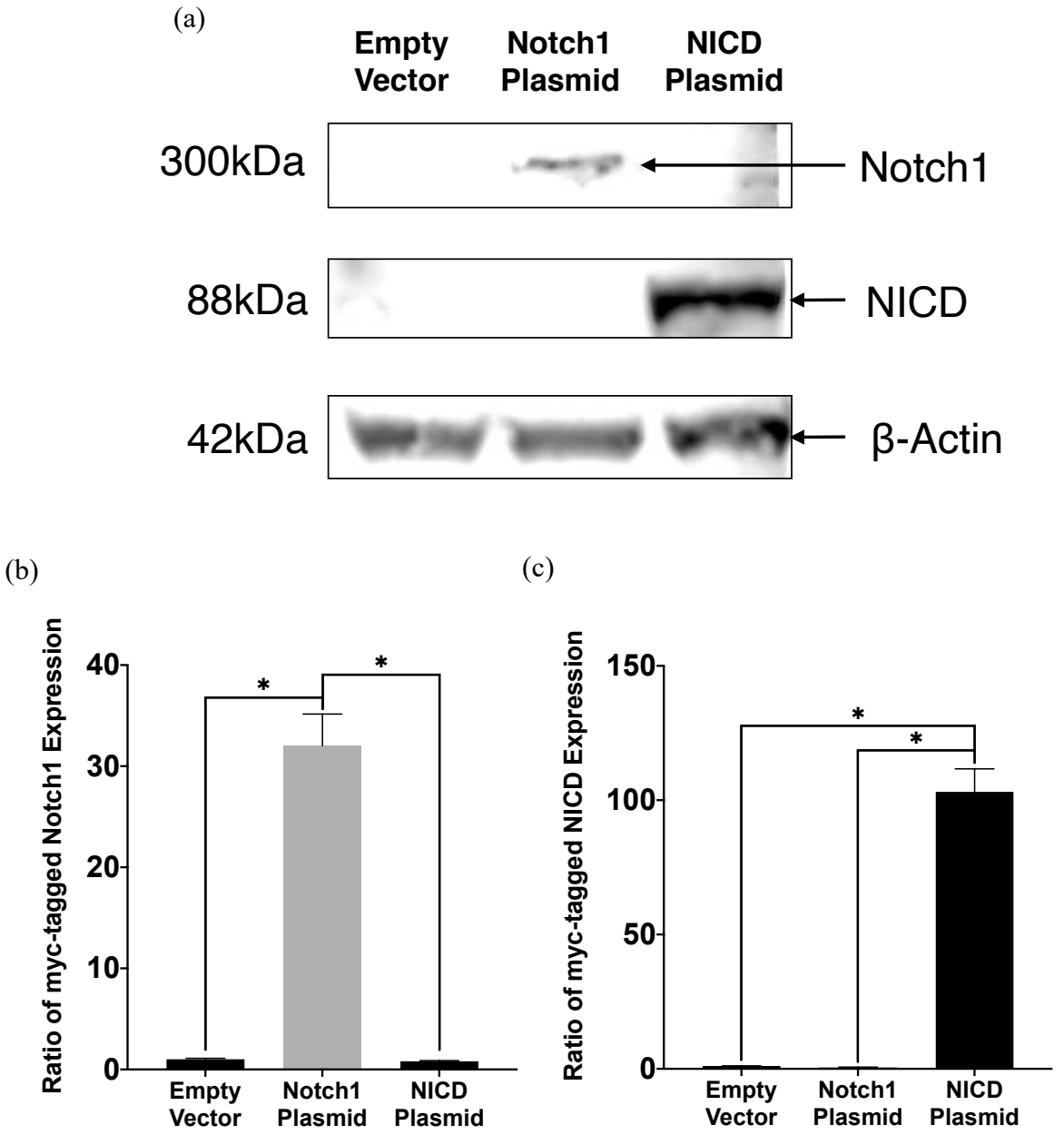


Fig.4.2 Ectopic expression of myc-tagged Notch1 and NICD in MVSCs. MVSCs transfected with either Notch1 plasmid, NICD plasmid or an empty vector and incubated for 48 h at 37°C in MM1 before ectopic expression of myc-tagged Notch1 and NICD was assessed by immunoblot. (a) Representative immunoblot image shows full-length Notch1 bands at 120kDa, NICD bands at 88kDa and β-actin bands at 42kDa. Densitometry was carried out on western blot samples to measure intensity of Notch1 and NICD bands normalised to the β-actin loading control. (b) Full-length Notch1 and (c) NICD protein levels given as ratio of expression relative to the negative control sample transfected with an empty vector plasmid. Error bars based on SEM. Data representative of n=3. * $p < 0.05$

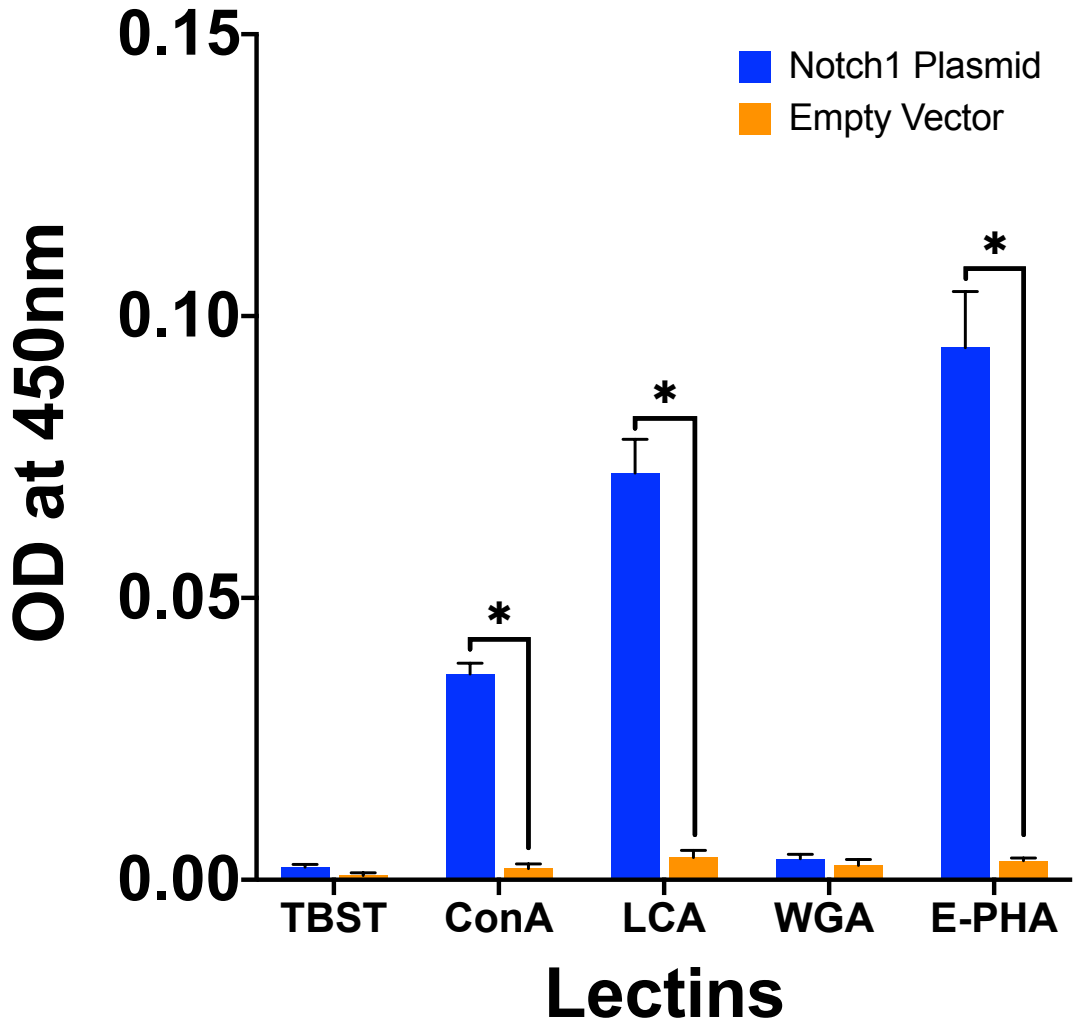


Fig.4.3 N-glycosylation profile of the purified Notch1 receptor. ELLA analysis of N-glycan specific lectin binding of MVSC lysates following ectopic expression of the Notch1 plasmid or empty vector plasmid for 48 h at 37ºC in MM1. Protein G-conjugated magnetic beads were used to immunoprecipitate the myc-tagged Notch1 receptor from MVSC lysates. Data are presented as the mean absorbance value at 450nm normalised to the negative control PBS sample and the IgG immunoprecipitation control. Error bars based on SEM. Data representative of n = 3. *$p < 0.05$

4.3.4 Effect of TNC and DMJ Inhibitors on global N-glycosylation

TNC and DMJ are both widely used inhibitors of N-glycosylation. As with any small-molecule inhibitor, their activity and optimum concentration can vary across cell lines and therefore it was important to established these factors in cell lines relative to this study. MVSCs and C3Hs were treated with different concentrations of TNC or DMJ. In MVSCs, five concentrations of TNC and DMJ were used, ranging from 0.3 - 0.7μg/mL TNC and 2.0 - 4.0μg/mL DMJ, while three different concentrations of each inhibitor were used in C3Hs, ranging from 0.25 - 1.0μg/mL TNC and 50 - 100μg/mL DMJ. Cells were incubated at 37^{o}C for 48 h before being harvested and lysed to isolate protein. BCA assay was used to quantify the concentration of protein in each sample before N-glycan analysis was carried out using ELLA. Control wells containing PBS rather than a protein sample were used to determine the baseline for non-specific absorbance and these baseline values were subtracted from sample absorbance values to decipher the true level of specific lectin binding. TBST acted as the vehicle control for all lectins.

In MVSCs, TNC treatment at all 5 concentrations caused a significant reduction in binding across all lectins compared to the non-treated control (Fig.4.4). In general there is a pattern of inverse correlation between TNC concentration and absorbance, indicating a reduction in lectin binding with each successive increase of TNC concentration. However, this reduction plateaus at concentrations higher than 0.5μg/mL in the cases of WGA and E-PHA. This data, coupled with the fact that significant cell death begins to occur in samples treated with 0.6μg/mL and 0.7μg/mL, indicates that the optimum concentration of TNC for N-glycosylation inhibition over 48 h in MVSCs is 0.5μg/mL (0.6μM).

With C3Hs, a similar pattern of inverse correlation was observed. All 3 concentrations of TNC significantly reduced binding across all lectins (Fig.4.5). The most substantial decrease was seen in the 1μg/mL sample, and concentrations above this level resulted in significant cell death. Therefore, 1μg/mL (1.2μM) was deemed to be the optimum concentration of TNC over 48 h in C3Hs.

DMJ treatment at all 5 concentrations in MVSCs also caused a significant reduction in binding across all lectins compared to the non-treated control (Fig.4.6). Once again, a pattern of inverse correlation between DMJ concentration and absorbance was observed. Concentrations above 4.0μg/mL were subsequently attempted but always resulted in a

significant increase in cell death. This indicates that the optimum concentration of DMJ for N-glycosylation inhibition over 48 h in MVSCs is 4.0μg/mL (20μM).

In the case of C3Hs, significant reductions in lectin binding were recorded across all 3 concentrations of DMJ, but only in WGA and E-PHA (Fig.4.7). No significant change in binding was detected at any DMJ concentration with ConA or LCA. Furthermore, the inverse correlation observed in MVSCs was not replicated here. In fact, slight increases in WGA and E-PHA binding were detected as DMJ concentration was increased. Therefore, this data indicates that 50μg/mL (250μM) is the optimum concentration of DMJ over 48 h in C3Hs.

It must also be noted that, at optimum concentrations of each inhibitor, no physical/morphological impact was observed in the cell population.

4.3.5 Effect of TNC and DMJ on Notch1 N-glycosylation

After establishing the effect of TNC and DMJ on the N-glycosylation of a whole cell lysate, the next logical step was to determine their effect on the N-glycan profile of the purified Notch1 receptor. MVSCs were grown to ~80% confluence in four T25 flasks. Two of the flasks were left untreated while the other two were treated with TNC (0.6μM) or DMJ (20μM). Cells were incubated at 37^{o}C for 48 h before being harvested and lysed to isolate protein. BCA assay was used to quantify the concentration of protein in each sample. IP was carried out on all samples using Protein A-conjugated magnetic beads and an anti-Notch1 rabbit monoclonal antibody from Brennan & Co. (3608S). One of the untreated samples was immunoprecipitated with a rabbit IgG control antibody. Following elution and neutralisation, using Glycine and Tris buffers respectively, another BCA assay was carried out to quantify protein concentration in the eluted fraction. ELLA was then used to detect N-glycans in all four samples. Control wells containing PBS rather than a protein sample were used to determine the baseline for non-specific absorbance, while the rabbit IgG control sample acted as the baseline for non-specific lectin- or antibody-binding to the IP eluate. Both of these baseline values were subtracted from sample absorbance values to decipher the true level of specific lectin binding. TBST acted as the vehicle control for all lectins. From Fig.4.8 it can be seen that lectin binding was significantly reduced by both TNC and DMJ across all lectins other than WGA. Inhibition by DMJ was not quite as pronounced as that of TNC, likely due to their differing mechanisms of action.

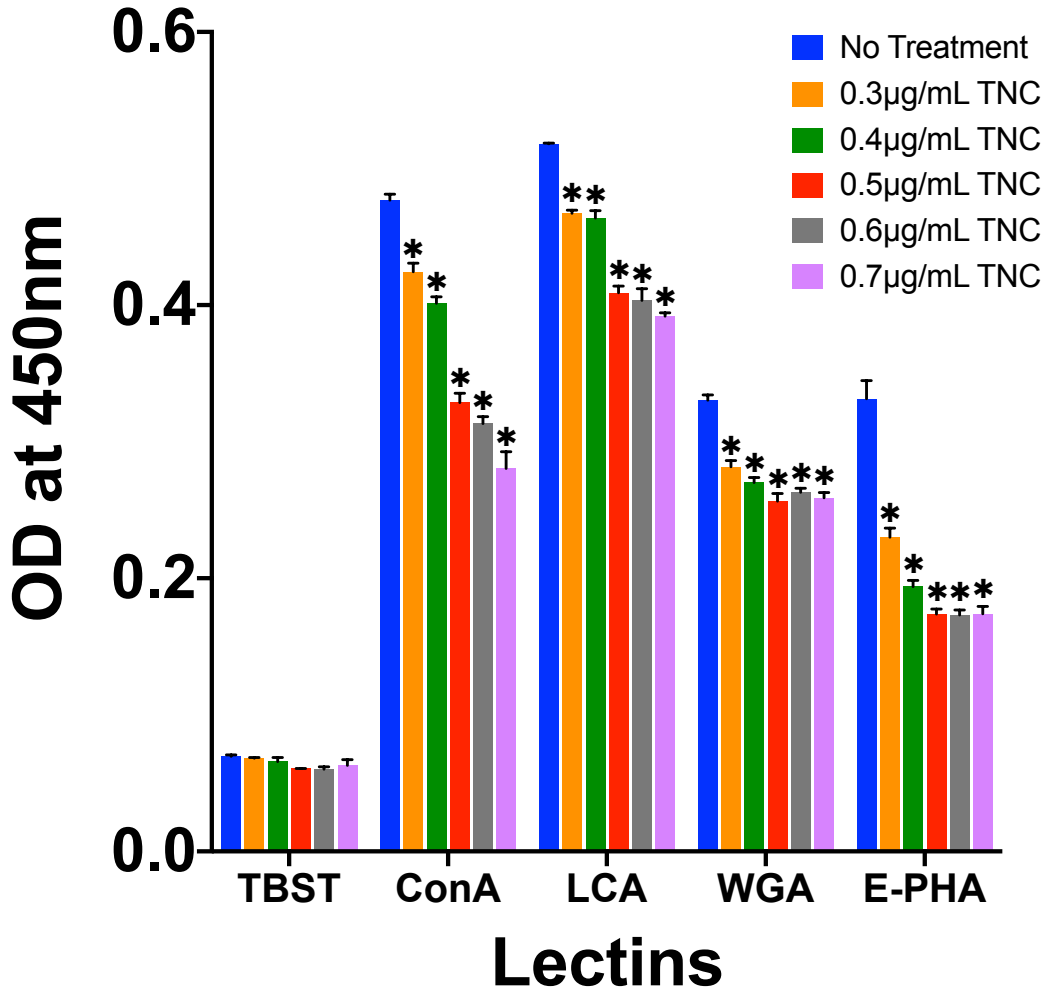


Fig.4.4 Effect of TNC on N-glycosylation in MVSCs. ELLA analysis of N-glycan specific lectin binding of MVSC lysates following treatment of cells with a range of TNC concentrations for 48 h at 37ºC. Data are presented as the mean absorbance value at 450nm normalised to the negative control PBS sample. Error bars based on SEM. Data representative of n = 3. *p < 0.05 compared to the non-treated sample probed with the same lectin

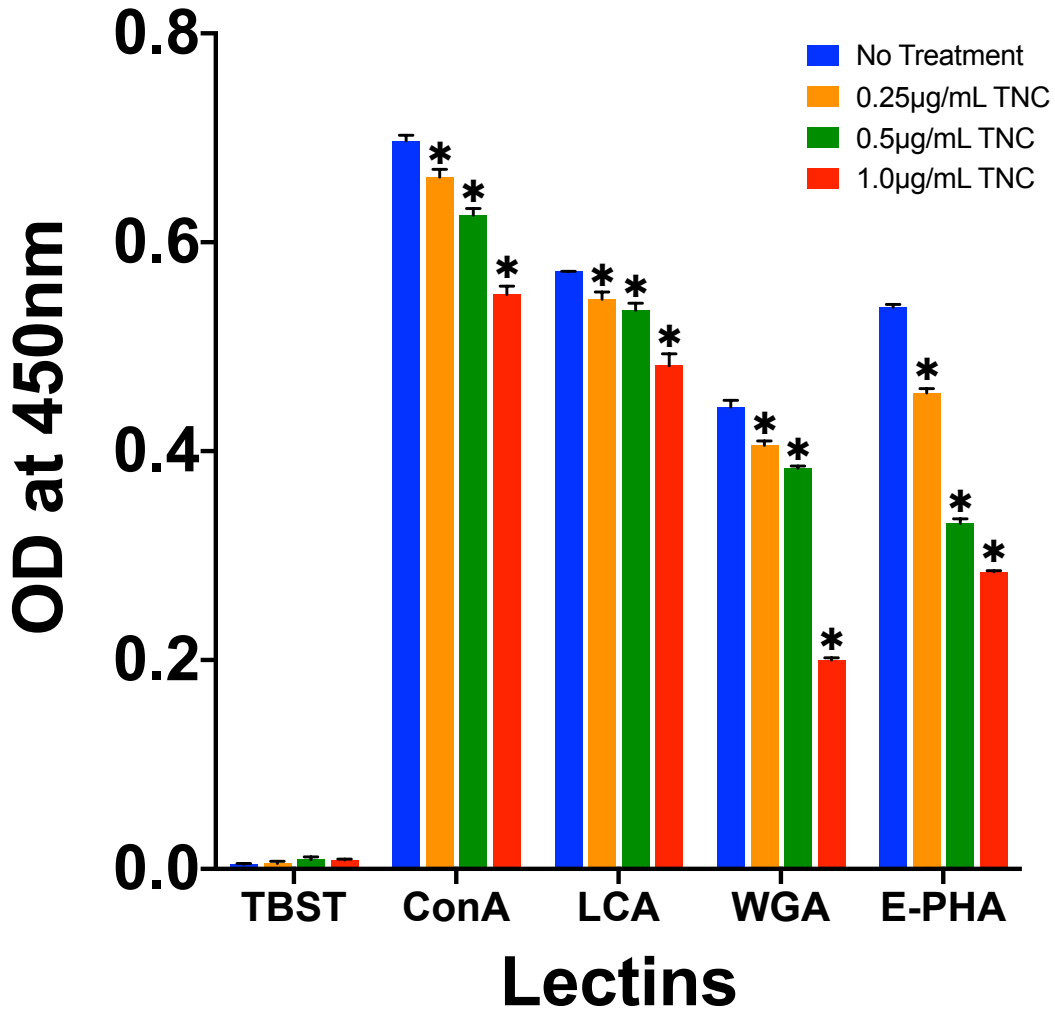


Fig.4.5 Effect of TNC on N-glycosylation in C3Hs. ELLA analysis of N-glycan specific lectin binding of C3H lysates following treatment of C3Hs with a range of TNC concentrations for 48 h at 37ºC. Data are presented as the mean absorbance value at 450nm normalised to the negative control PBS sample. Error bars based on SEM. Data representative of n = 3. *p < 0.05 compared to the non-treated sample probed with the same lectin

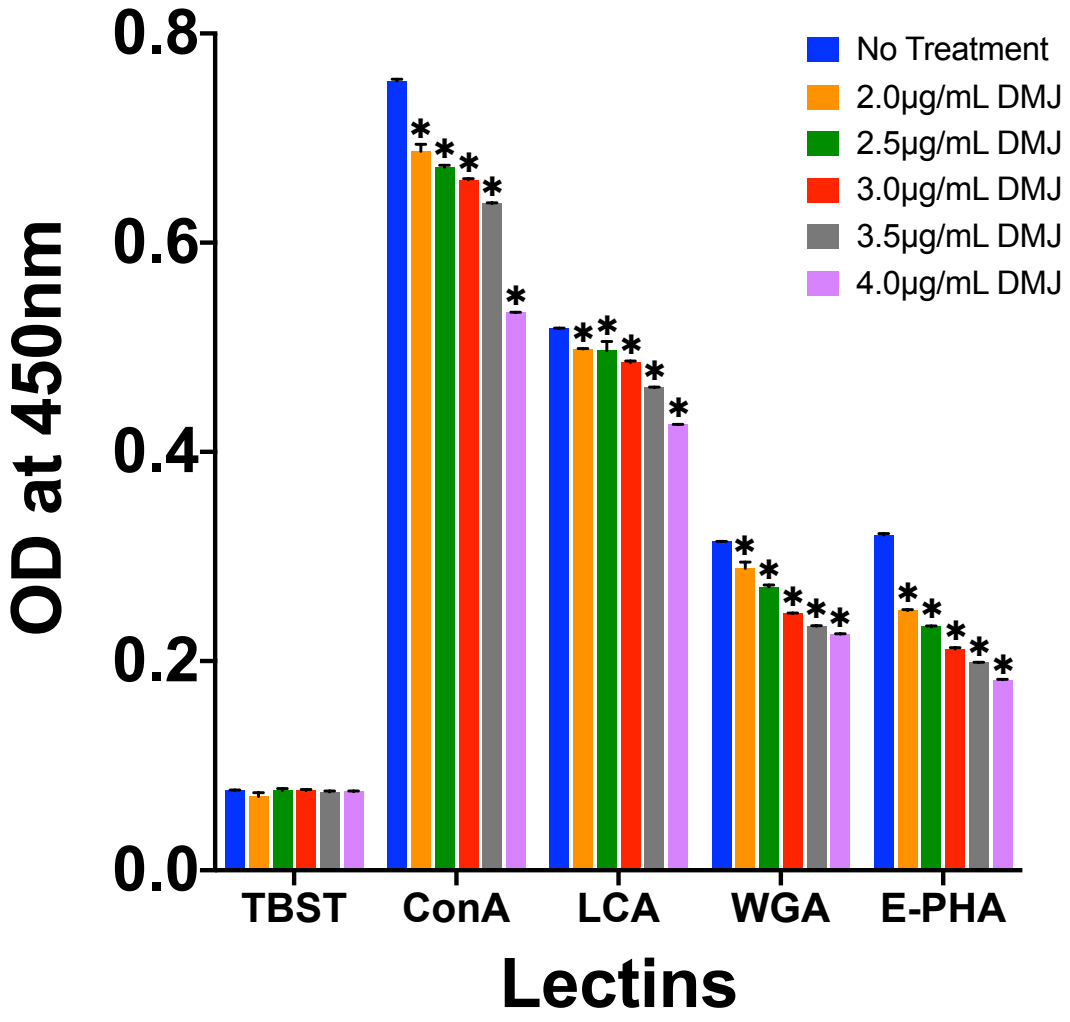


Fig.4.6 Effect of DMJ on N-glycosylation in MVSCs. ELLA analysis of N-glycan specific lectin binding of MVSC lysates following treatment of cells with a range of DMJ concentrations for 48 h at 37°C. Data are presented as the mean absorbance value at 450nm normalised to the negative control PBS sample. Error bars based on SEM. Data representative of n = 3. *p < 0.05 compared to the non-treated sample probed with the same lectin

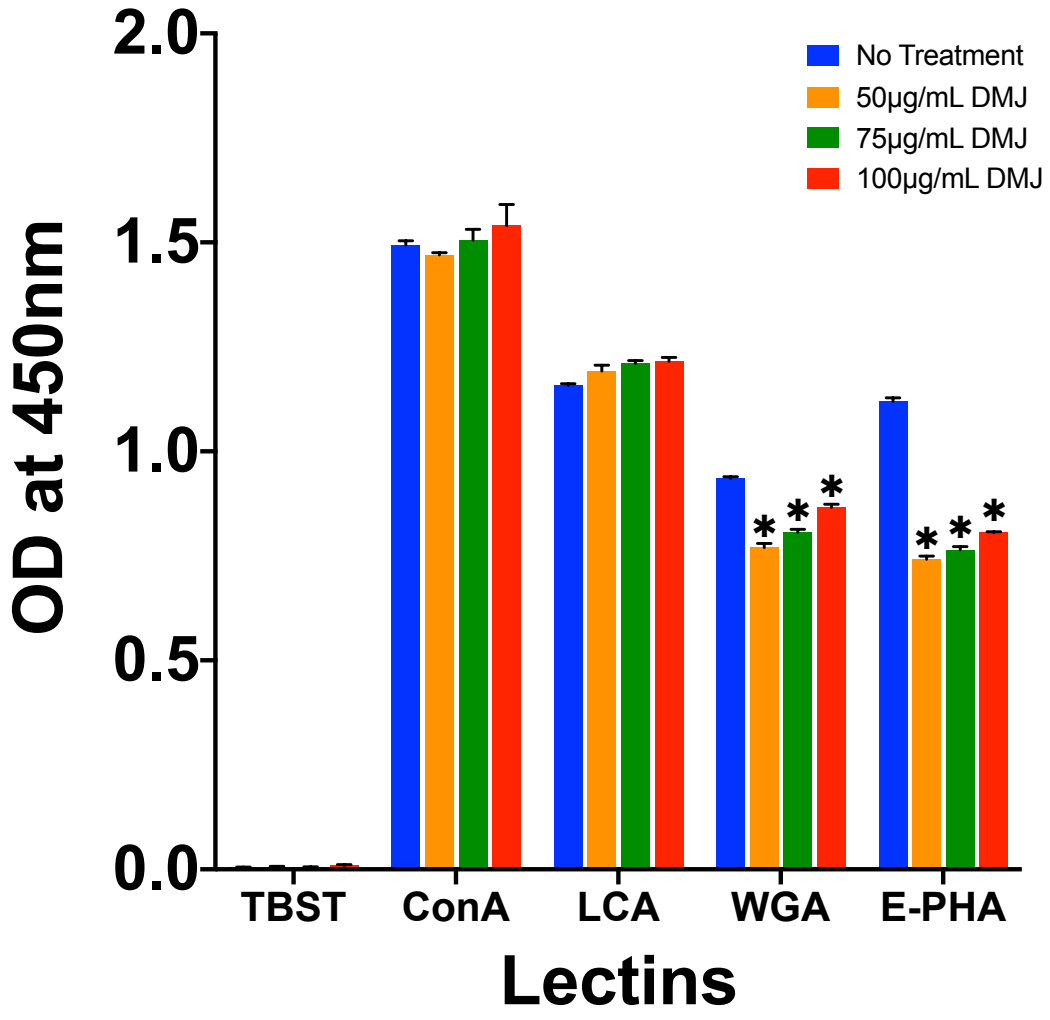


Fig.4.7 Effect of DMJ on N-glycosylation in C3Hs. ELLA analysis of N-glycan specific lectin binding of C3H lysates following treatment of cells with a range of DMJ concentrations for 48 h at 37ºC. Data are presented as the mean absorbance value at 450nm normalised to the negative control PBS sample. Error bars based on SEM. Data representative of n = 3. *p < 0.05 compared to the non-treated sample probed with the same lectin

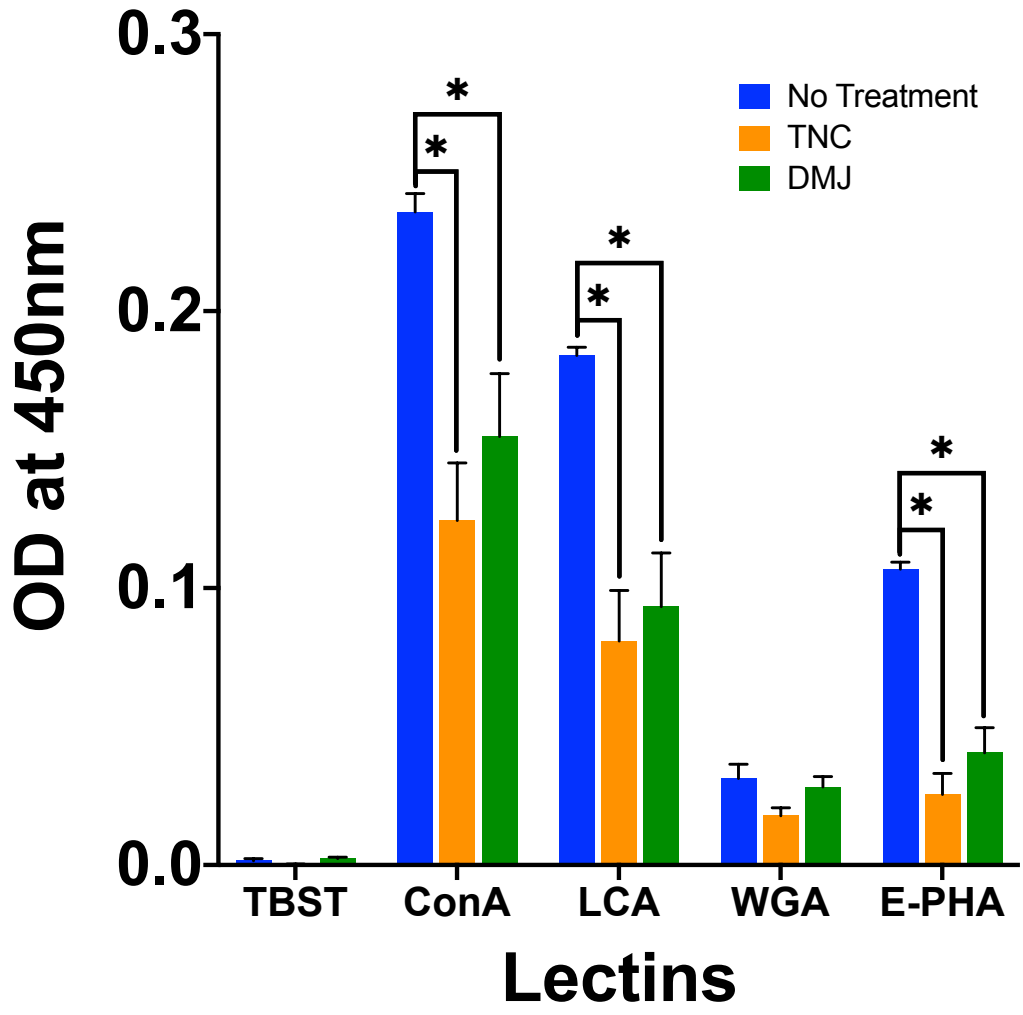


Fig.4.8 Effect of TNC and DMJ on N-glycosylation of the Notch1 receptor. ELLA analysis of N-glycan specific lectin binding of MVSC lysates following treatment of cells with TNC (0.5µg/mL) or DMJ (4µg/mL) for 48 h at 37ºC. Notch1 protein was then purified from sample lysates using protein A-conjugated magnetic beads. Data are presented as the mean absorbance value at 450nm normalised to the negative control PBS sample and the IgG immunoprecipitation control. Error bars based on SEM. Data representative of n = 3.
* $p < 0.05$

4.3.6 TNC Treatment of Jag-1-stimulated MVSCs and C3Hs

Having determined the optimum TNC concentration in both MVSCs and C3Hs, and shown the effect of TNC on Notch1 N-glycosylation, the next step was to investigate if this treatment affected Jag-1-mediated Notch signalling and myogenic differentiation. MVSCs or C3Hs were seeded into Jag-1- or Fc-coated wells and incubated overnight at 37ºC. The following day TNC was added to the media at 0.5µg/mL (MVSCs) or 1µg/mL (C3Hs) and the cells were incubated for a further 48 h at 37ºC. Cells were harvested and RNA was isolated from each sample as per Section 2.2.8. To evaluate the change in expression of the Notch target gene *Hey1* and the myogenic marker *Myh11,* qRT-PCR was carried out. In both cell lines, a substantial increase in *Hey1* expression was observed in the sample treated with Jag-1 as compared to the Fc-treated control. TNC treatment significantly attenuated this increase in Jag-1-treated samples (Fig.4.9-4.12). Interestingly, in C3Hs, TNC treatment also led to a decrease in *Hey1* expression in the Fc-treated sample. Upregulation of *Myh11* expression was also detected following Jag-1 treatment and again this response was significantly inhibited by TNC treatment in both MVSCs and C3Hs.

4.3.7 DMJ Treatment of Jag-1-stimulated MVSCs and C3Hs

Similarly to TNC, the effect of DMJ treatment on N-glycosylation had been demonstrated and so the next step was to investigate if this treatment affected Jag-1-mediated Notch signalling and myogenic differentiation. MVSCs or C3Hs were seeded into Jag-1- or Fc-coated wells and incubated overnight at 37ºC. The following day DMJ was added to the media at 4µg/mL (MVSCs) or 50µg/mL (C3Hs) and the cells were incubated for a further 48 h at 37ºC. Cells were harvested and RNA was isolated from each sample as per Section 2.2.8. To evaluate the change in expression of *Hey1* and *Myh11,* qRT-PCR was carried out. Fig.4.13-4.16 show that DMJ significantly inhibited the Jag-1 response of both MVSCs and C3Hs, leading to a reduction in *Hey1* and *Myh11* expression, both of which had been substantially increased by Jag-1 treatment compared to the Fc-treated control.

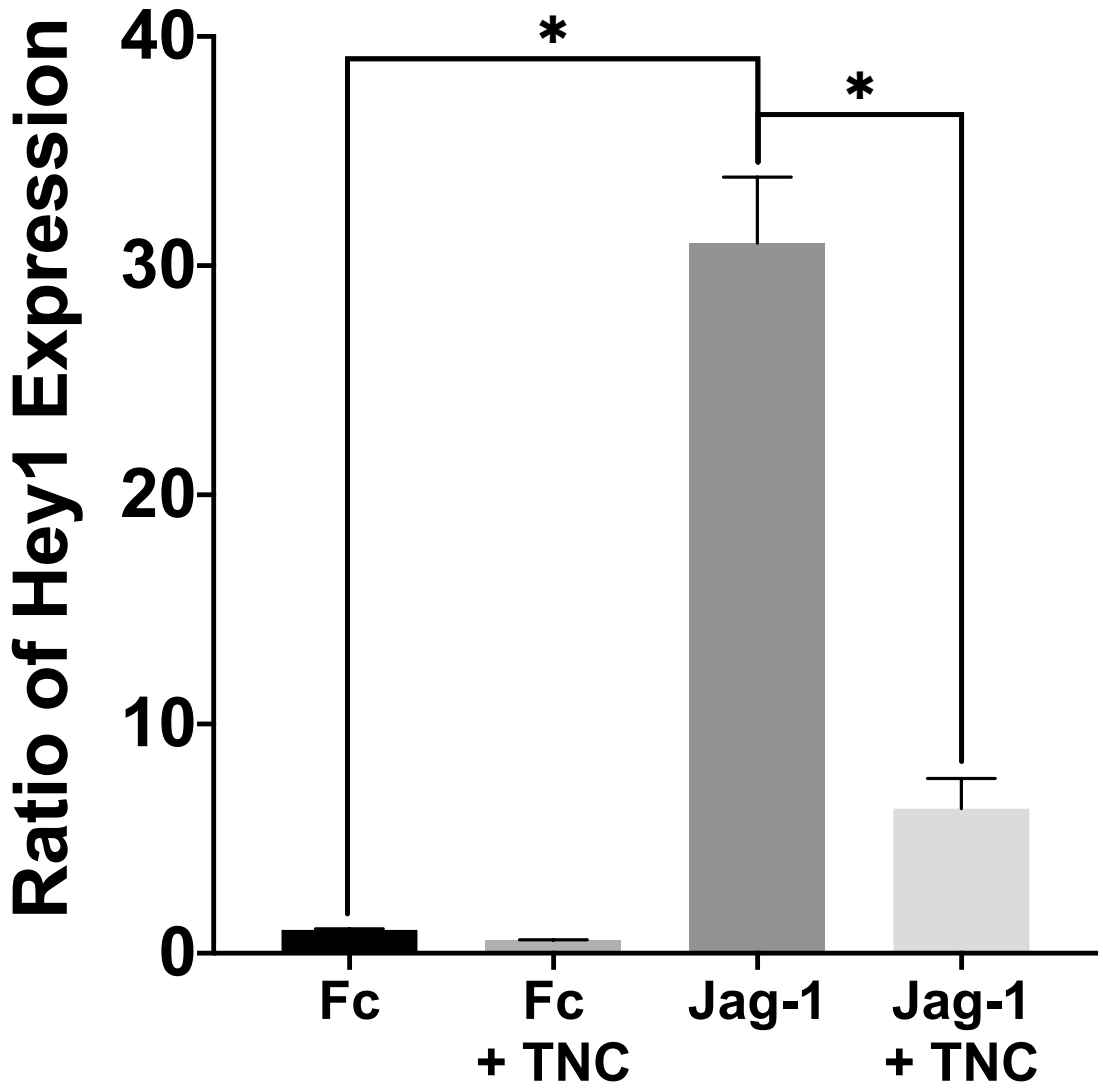


Fig.4.9 Effect of TNC on *Hey1* expression in Jag1-treated MVSCs. The relative expression of *Hey1* mRNA levels by qRT-PCR in MVSCs treated with Jag-1 (1µg/mL) ± TNC (0.5µg/mL) and incubated for 48 h at 37°C. Data are presented as the ratio of expression relative to the negative control sample treated with Fc. Error bars based on SEM. Data representative of n=3. * $p < 0.05$

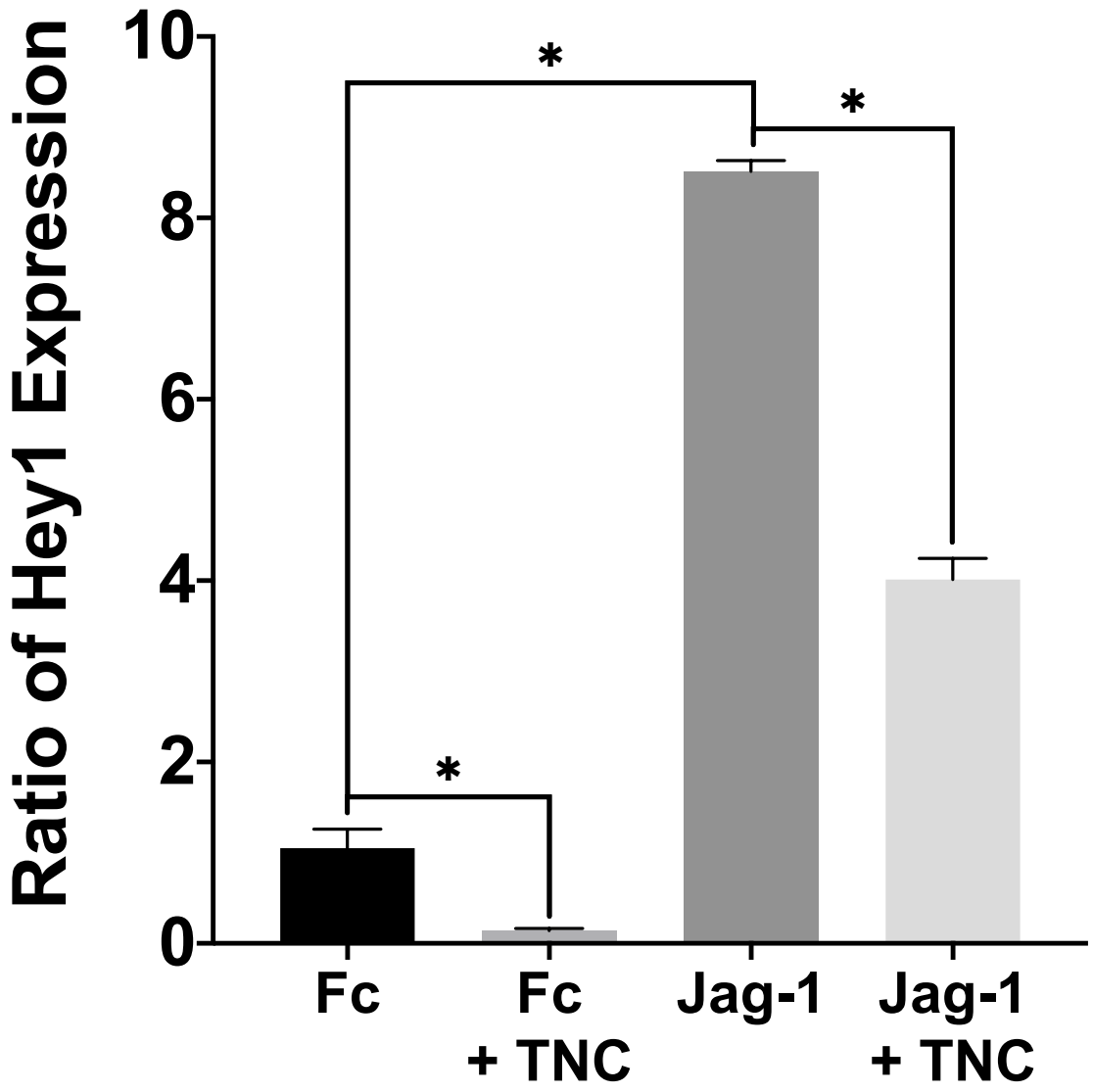


Fig.4.10 Effect of TNC on *Hey1* expression in Jag1-treated C3Hs. The relative expression of *Hey1* mRNA levels by qRT-PCR in C3Hs treated with Jag-1 (1µg/mL) ± TNC (0.5µg/mL) and incubated for 48 h at 37°C. Data are presented as the ratio of expression relative to the negative control sample treated with Fc. Error bars based on SEM. Data representative of n=3. * $p < 0.05$

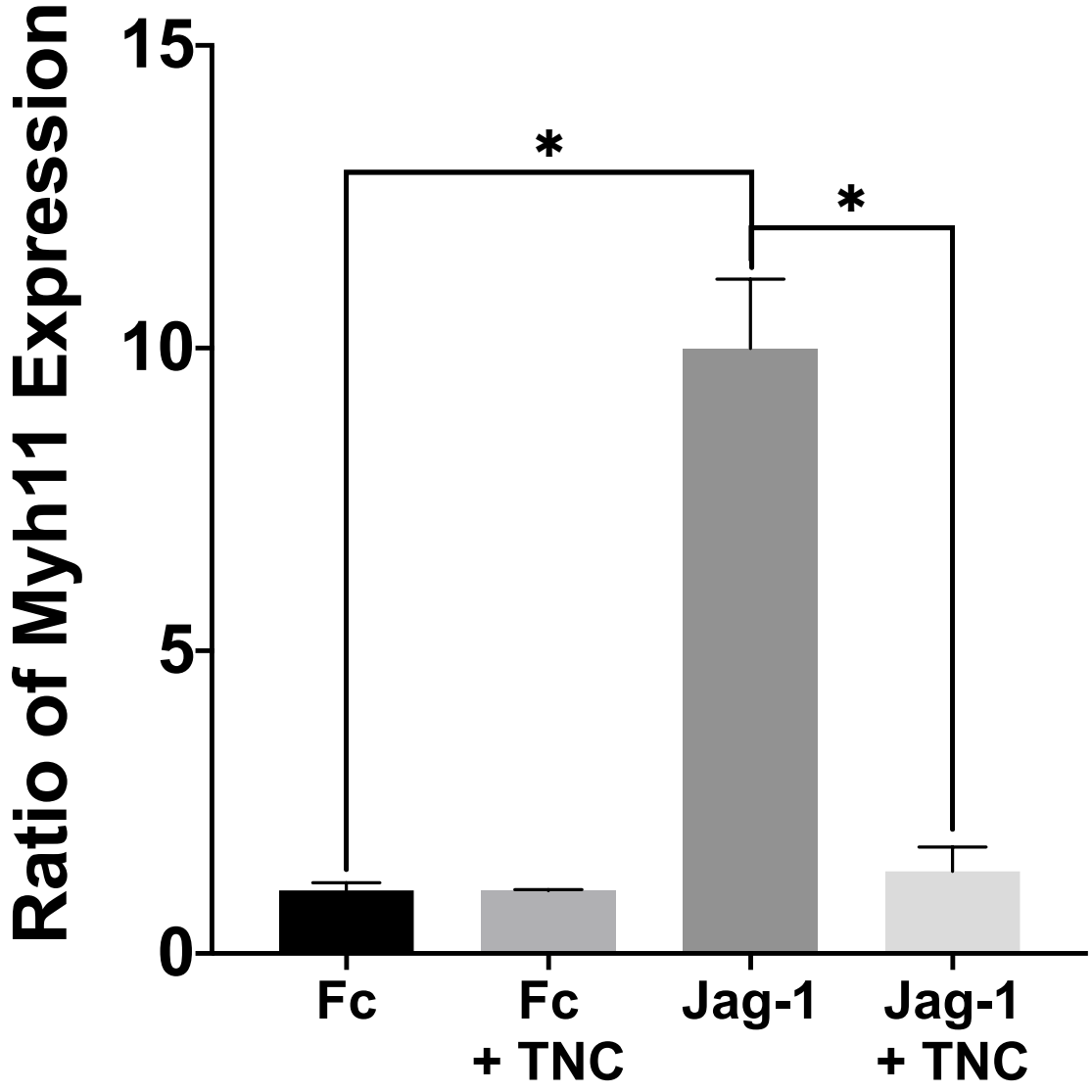


Fig.4.11 Effect of TNC on *Myh11* expression in Jag1-treated MVSCs. The relative expression of *Myh11* mRNA levels by qRT-PCR in MVSCs treated with Jag-1 (1µg/mL) ± TNC (0.5µg/mL) and incubated for 48 h at 37°C. Data are presented as the ratio of expression relative to the negative control sample treated with Fc. Error bars based on SEM. Data representative of n=3. * $p < 0.05$

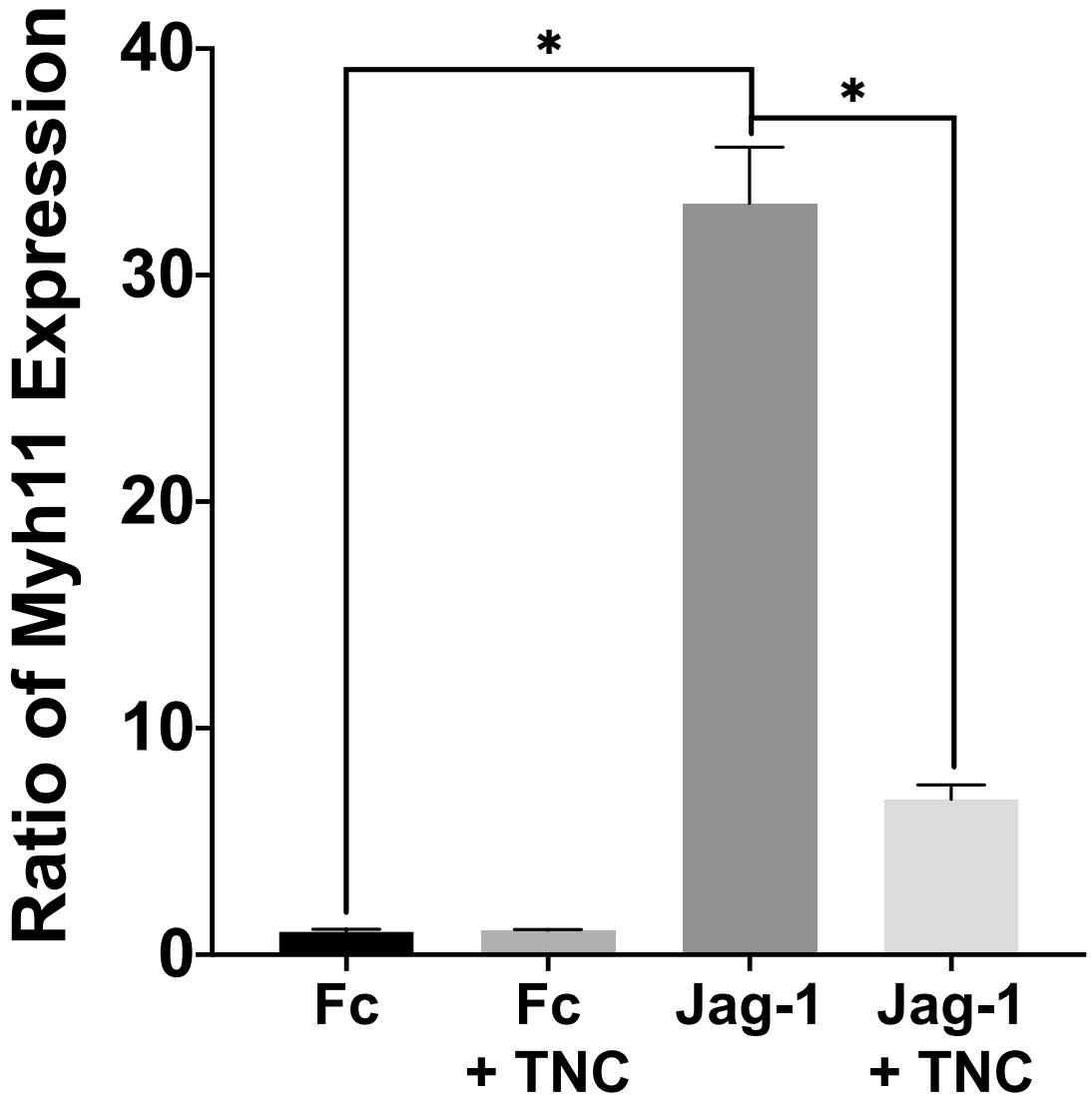


Fig.4.12 Effect of TNC on *Myh11* expression in Jag1-treated C3Hs. The relative expression of *Myh11* mRNA levels by qRT-PCR in C3Hs treated with Jag-1 (1µg/mL) ± TNC (0.5µg/mL) and incubated for 48 h at 37°C. Data are presented as the ratio of expression relative to the negative control sample treated with Fc. Error bars based on SEM. Data representative of n=3. * $p < 0.05$

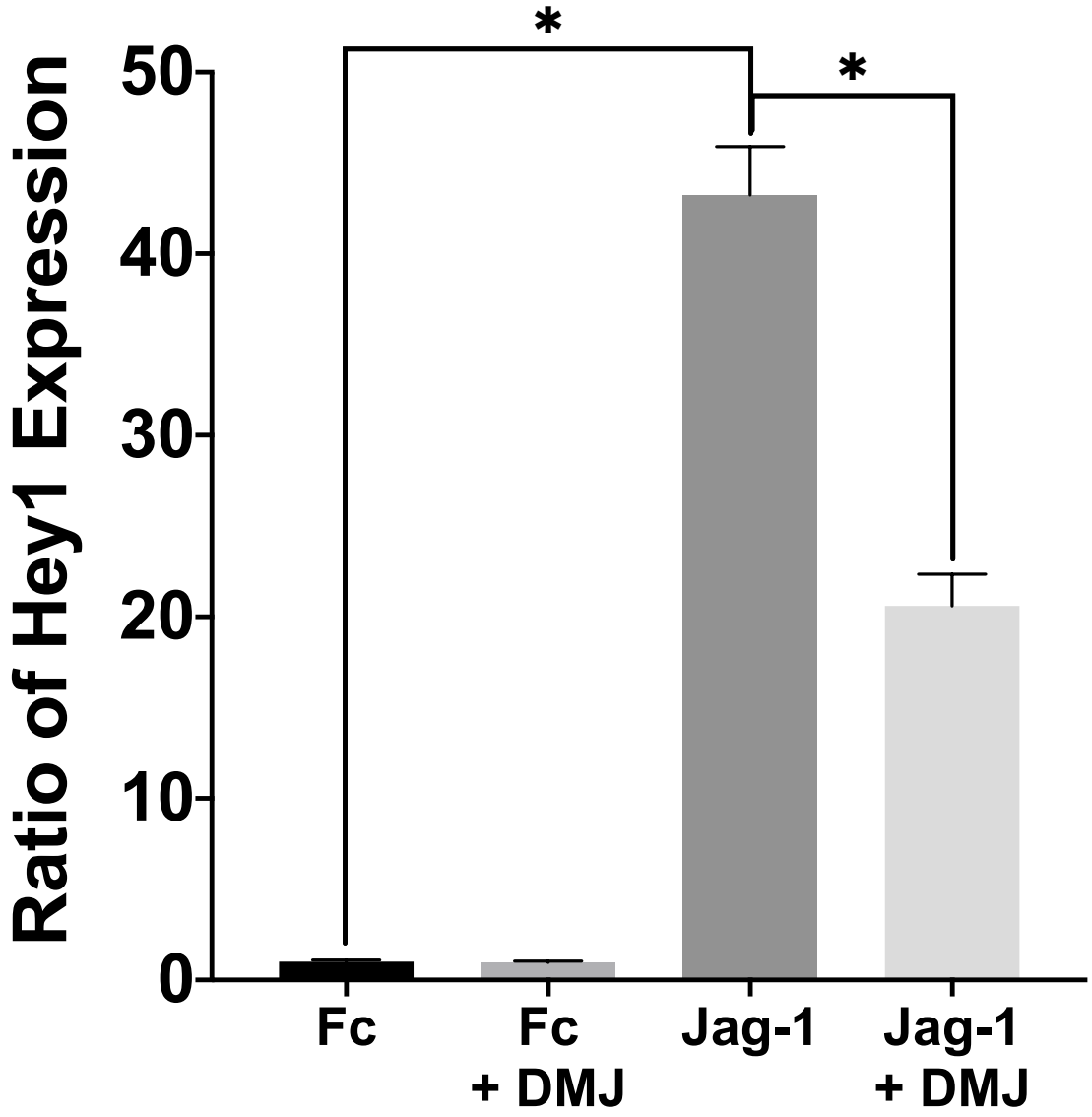


Fig.4.13 Effect of DMJ on *Hey1* expression in Jag1-treated MVSCs. The relative expression of *Hey1* mRNA levels by qRT-PCR in MVSCs treated with Jag-1 (1μg/mL) ± DMJ (4μg/mL) and incubated for 48 h at 37°C. Data are presented as the ratio of expression relative to the negative control sample treated with Fc. Error bars based on SEM. Data representative of n=3. * $p < 0.05$

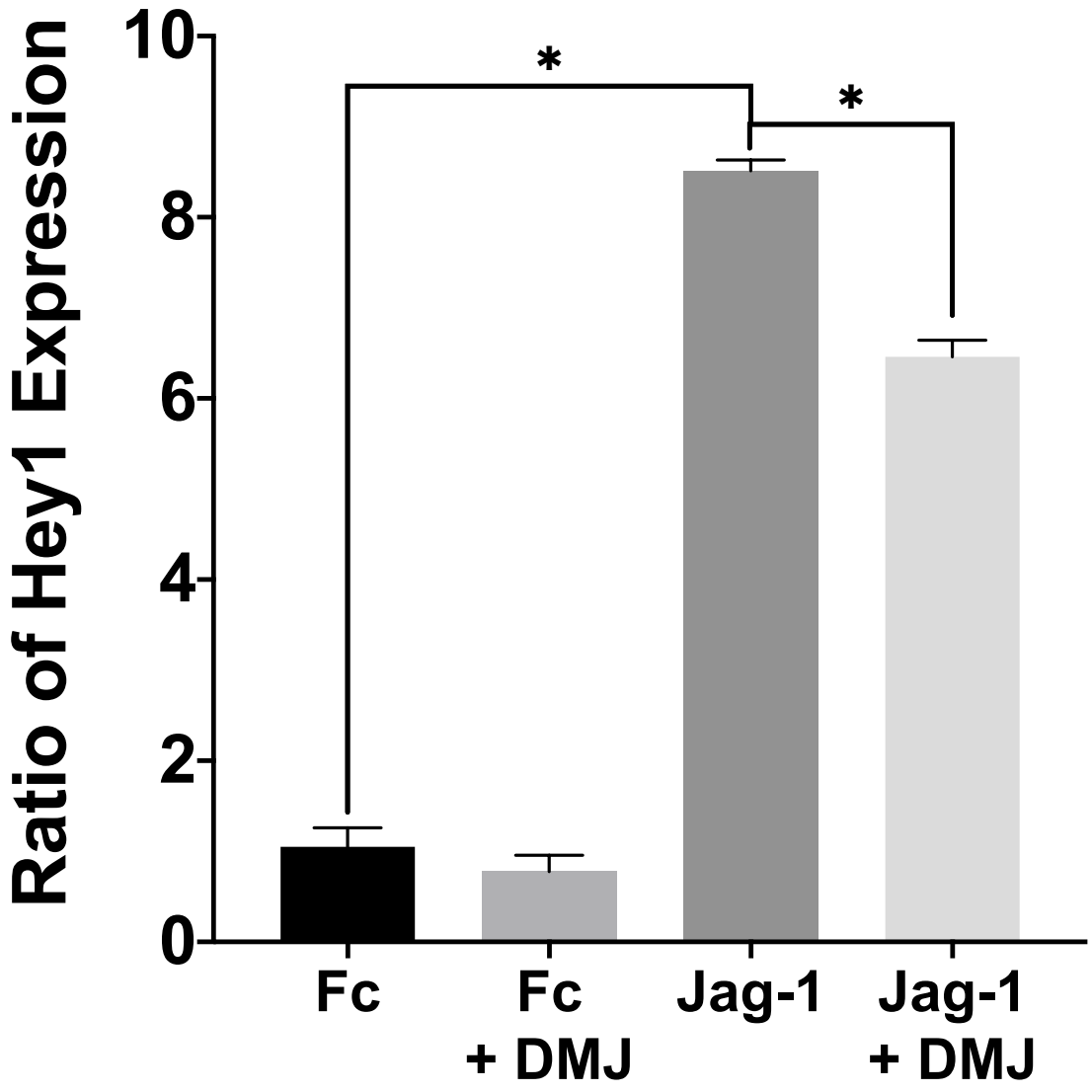


Fig.4.14 Effect of DMJ on *Hey1* expression in Jag1-treated C3Hs. The relative expression of *Hey1* mRNA levels by qRT-PCR in C3Hs treated with Jag-1 (1µg/mL) ± DMJ (4µg/mL) and incubated for 48 h at 37ºC. Data are presented as the ratio of expression relative to the negative control sample treated with Fc. Error bars based on SEM. Data representative of n=3. * $p < 0.05$

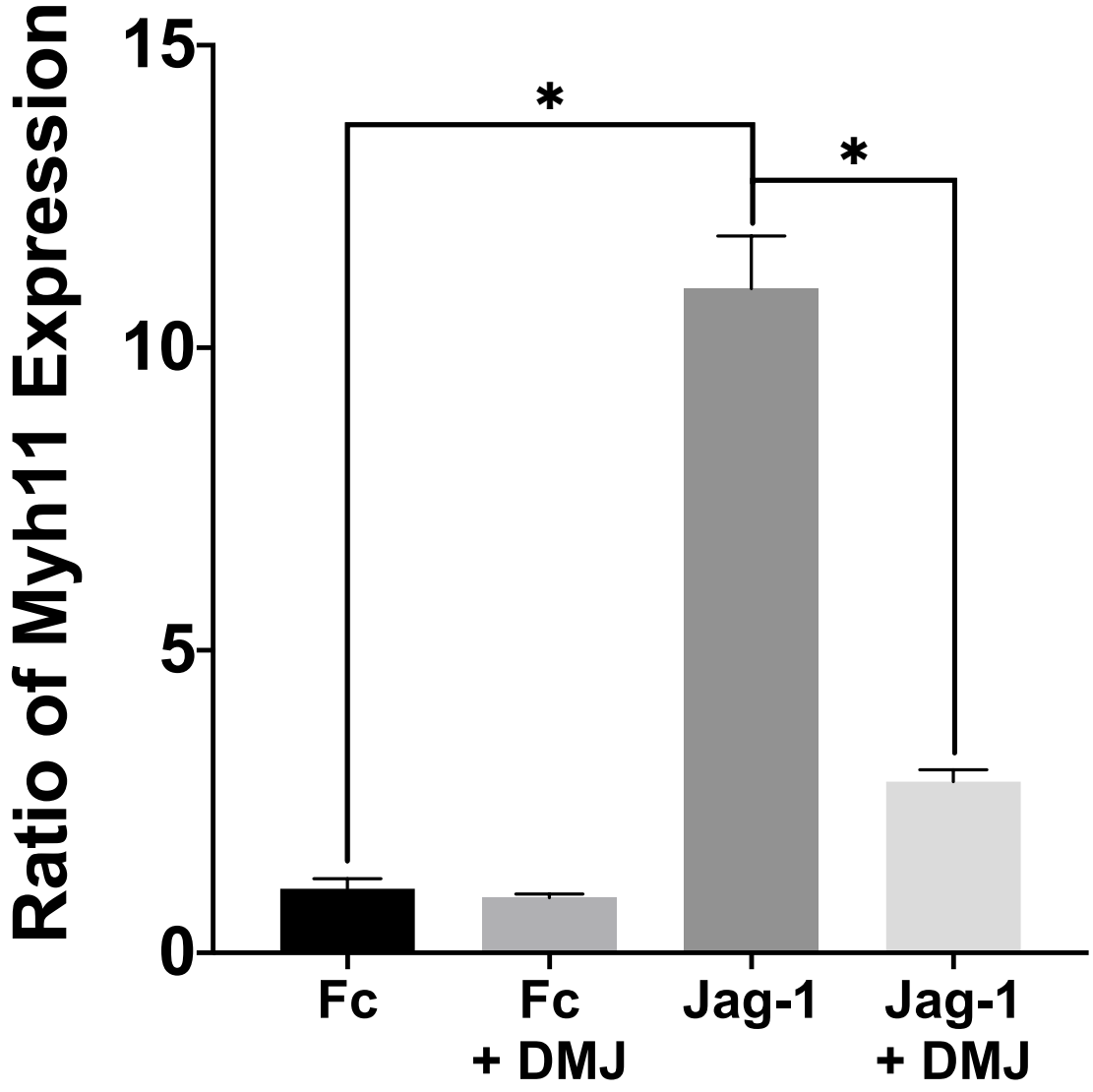


Fig.4.15 Effect of DMJ on *Myh11* expression in Jag1-treated MVSCs. The relative expression of *Myh11* mRNA levels by qRT-PCR in MVSCs treated with Jag-1 (1µg/mL) ± DMJ (4µg/mL) and incubated for 48 h at 37°C. Data are presented as the ratio of expression relative to the negative control sample treated with Fc. Error bars based on SEM. Data representative of n=3. * $p < 0.05$

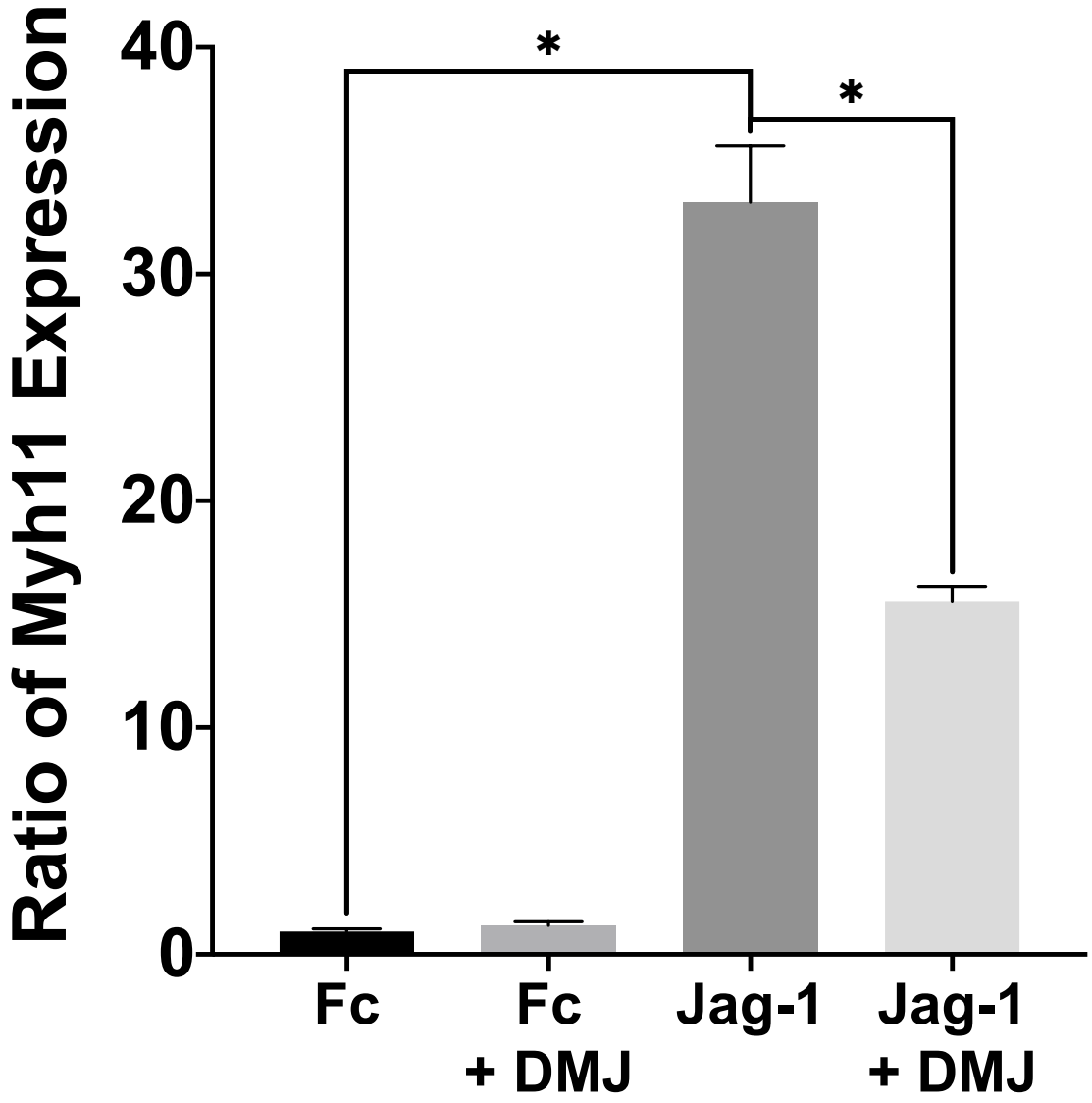


Fig.4.16 Effect of DMJ on *Myh11* expression in Jag1-treated C3Hs. The relative expression of *Myh11* mRNA levels by qRT-PCR in C3Hs treated with Jag-1 (1µg/mL) ± DMJ (4µg/mL) and incubated for 48 h at 37ºC. Data are presented as the ratio of expression relative to the negative control sample treated with Fc. Error bars based on SEM. Data representative of n=3. * $p < 0.05$

4.3.8 TNC and DMJ Treatment of NICD-stimulated MVSCs

Ectopically expressed NICD can activate Notch signalling independent of ligand binding. This process could be exploited to determine whether TNC and DMJ were having an effect on Notch pathway elements downstream of receptor activation. MVSCs were transfected with either the NICD-coding plasmid or an empty vector control using the TransIT-X2 Dynamic Delivery System. Simultaneously, these cells were either treated with TNC (0.5µg/mL), DMJ (4µg/mL) or not treated with any inhibitor. Cells were incubated at 37ºC for 48 h. RNA was isolated from all samples and qRT-PCR was carried out to measure the expression of *Hey1* and *Myh11*. The ectopically expressed NICD consistently increased the expression of the Notch target gene *Hey1*, and no significant change to this response was detected following TNC or DMJ treatment (Fig.4.17 and 4.18). Similarly, expression of the myogenic marker *Myh11* was invariably increased following NICD plasmid transfection compared to the empty vector control, but this response was significantly attenuated by treatment with either TNC or DMJ (Fig.4.19 and 4.20).

4.3.9 Effect of TNC and DMJ on Notch1 Expression in MVSCs

A change in baseline Notch1 expression in a cell population is very likely to have an effect on the expression of downstream target gene expression. Therefore, it was necessary to determine whether TNC and DMJ were affecting this baseline expression level. MVSCs were treated with either TNC (0.5µg/mL), DMJ (4µg/mL) or not treated with any inhibitor. Cells were incubated at 37ºC for 48 h. RNA and protein were isolated from all samples and their concentrations quantified using the Nanodrop® ND-1000 Spectrophotometer and a BCA assay respectively. To measure the expression of *Notch1* transcript qRT-PCR was carried out, while western blot was used to measure Notch1 protein expression. Densitometry was carried out on western blot samples to measure intensity of Notch1 bands relative to the β-actin loading control. No significant change in either *Notch1* transcript expression (Fig.4.21) or Notch1 protein expression (Fig.4.22) was observed following TNC or DMJ treatment, compared to the non-treated control.

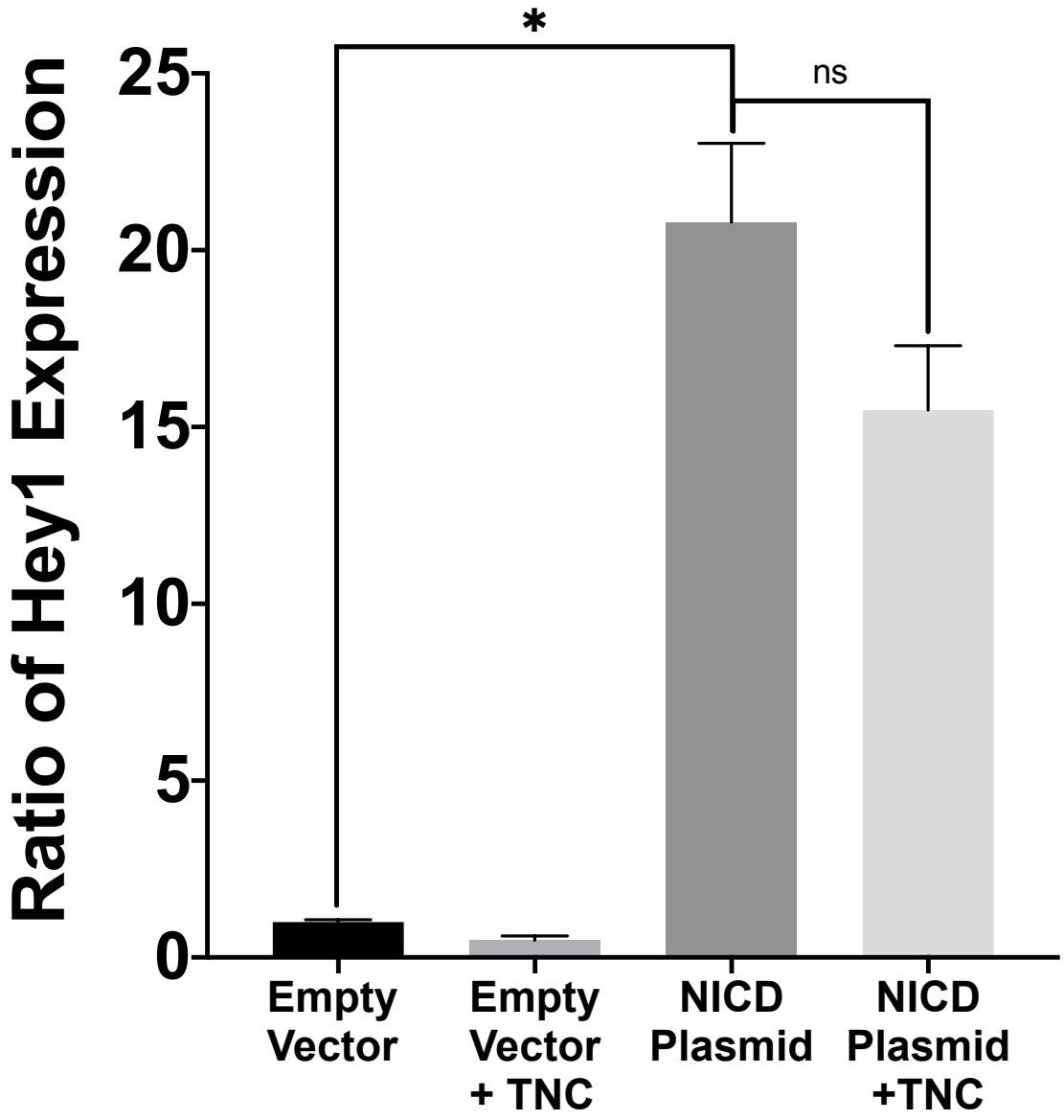


Fig.4.17 Effect of TNC on NICD-activated *Hey1* expression in MVSCs. The relative expression of *Hey1* mRNA levels by qRT-PCR in MVSCs transfected with NICD plasmid ± TNC (0.5μg/mL) and incubated for 48 h at 37ºC. Data are presented as the ratio of expression relative to the negative control sample transfected with empty vector plasmid. Error bars based on SEM. Data representative of n=3. * $p < 0.05$. ns – $p > 0.05$.

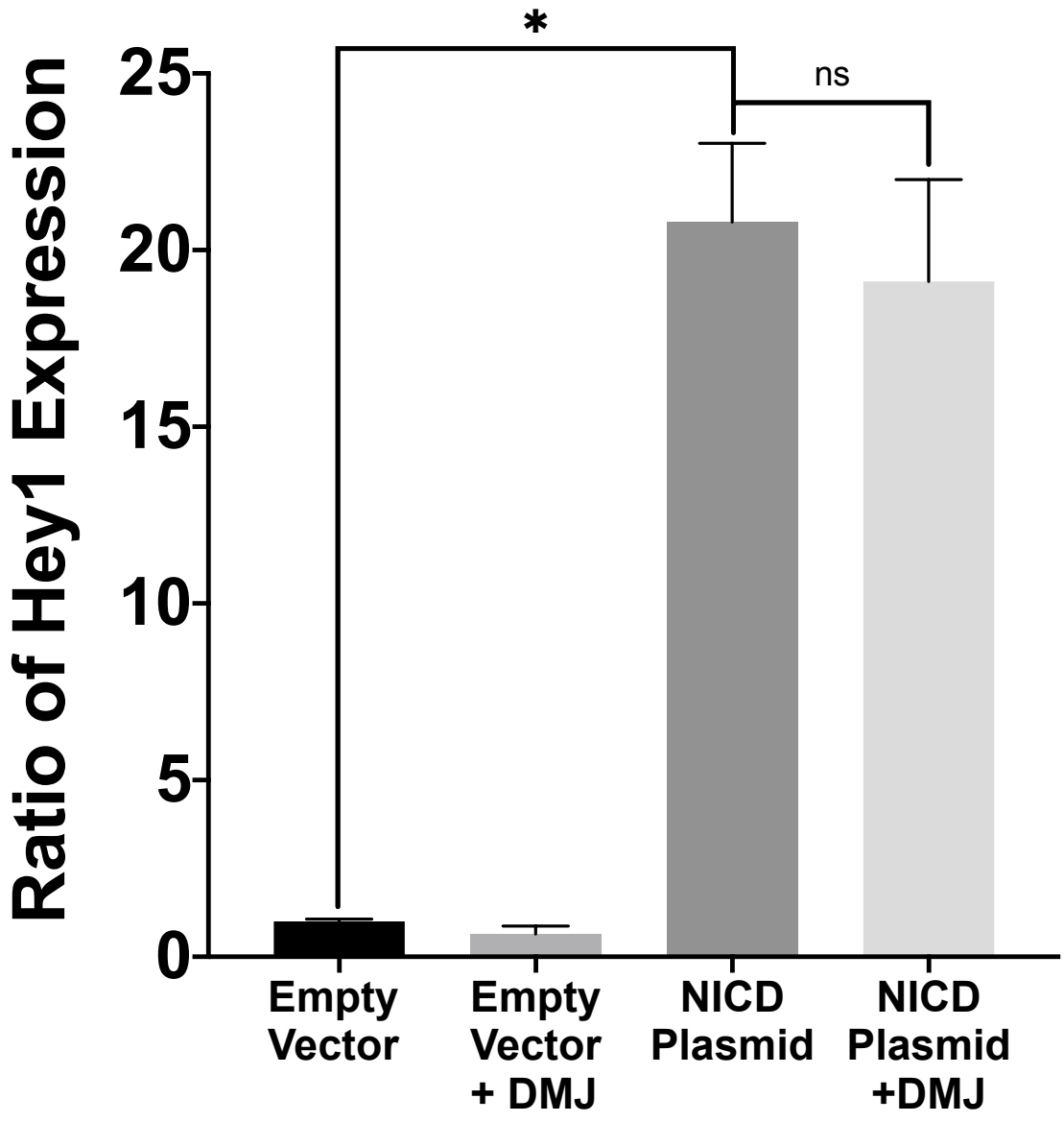


Fig.4.18 Effect of DMJ on NICD-activated *Hey1* expression in MVSCs. The relative expression of *Hey1* mRNA levels by qRT-PCR in MVSCs transfected with NICD plasmid ± DMJ (4μg/mL) and incubated for 48 h at 37°C. Data are presented as the ratio of expression relative to the negative control sample transfected with empty vector plasmid. Error bars based on SEM. Data representative of n=3. * $p < 0.05$. ns – $p > 0.05$.

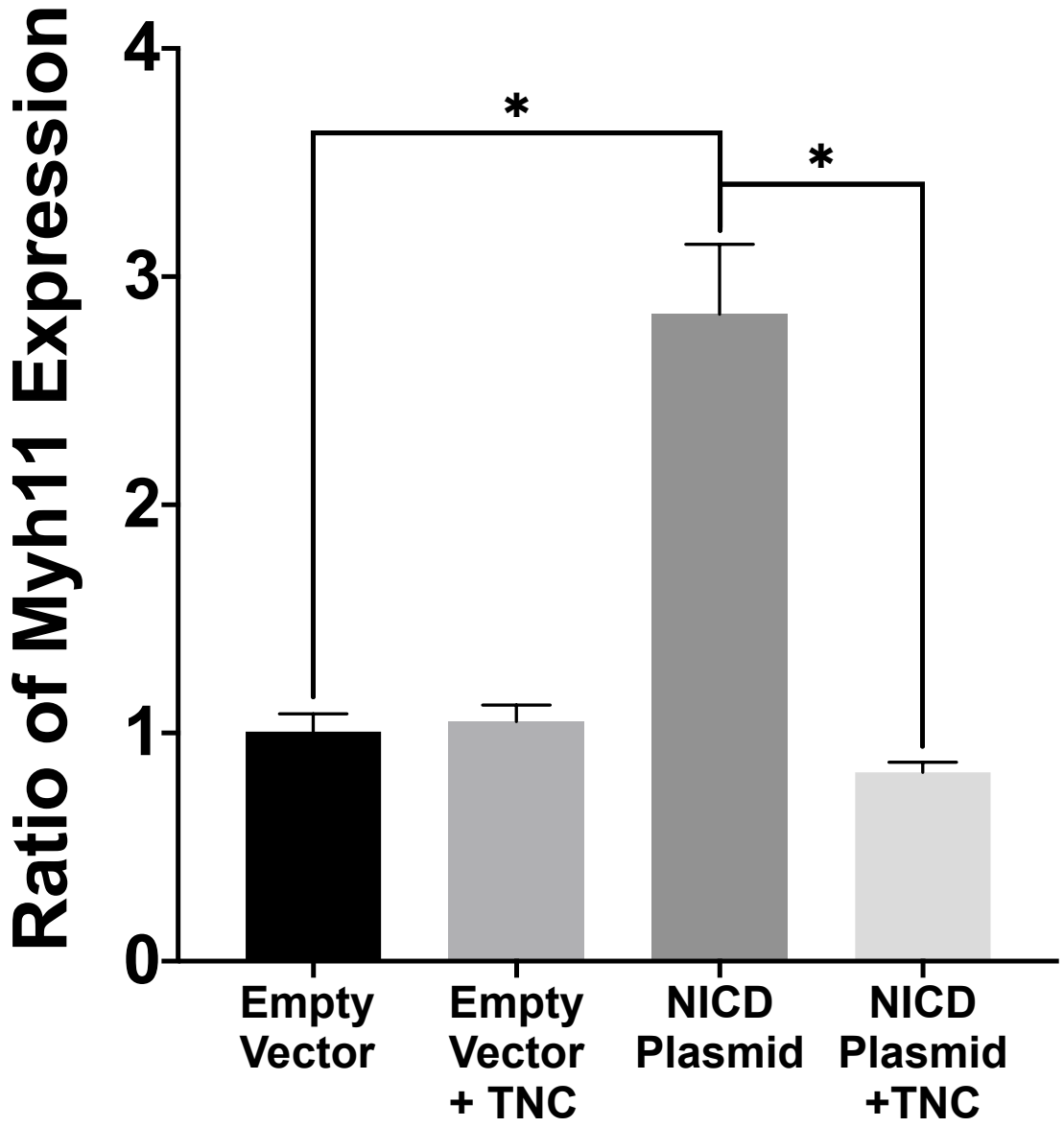


Fig.4.19 Effect of TNC on NICD-activated *Myh11* expression in MVSCs. The relative expression of *Myh11* mRNA levels by qRT-PCR in MVSCs transfected with NICD plasmid ± TNC (0.5μg/mL) and incubated for 48 h at 37ºC . Data are presented as the ratio of expression relative to the negative control sample transfected with empty vector plasmid. Error bars based on SEM. Data representative of n=3. * $p < 0.05$

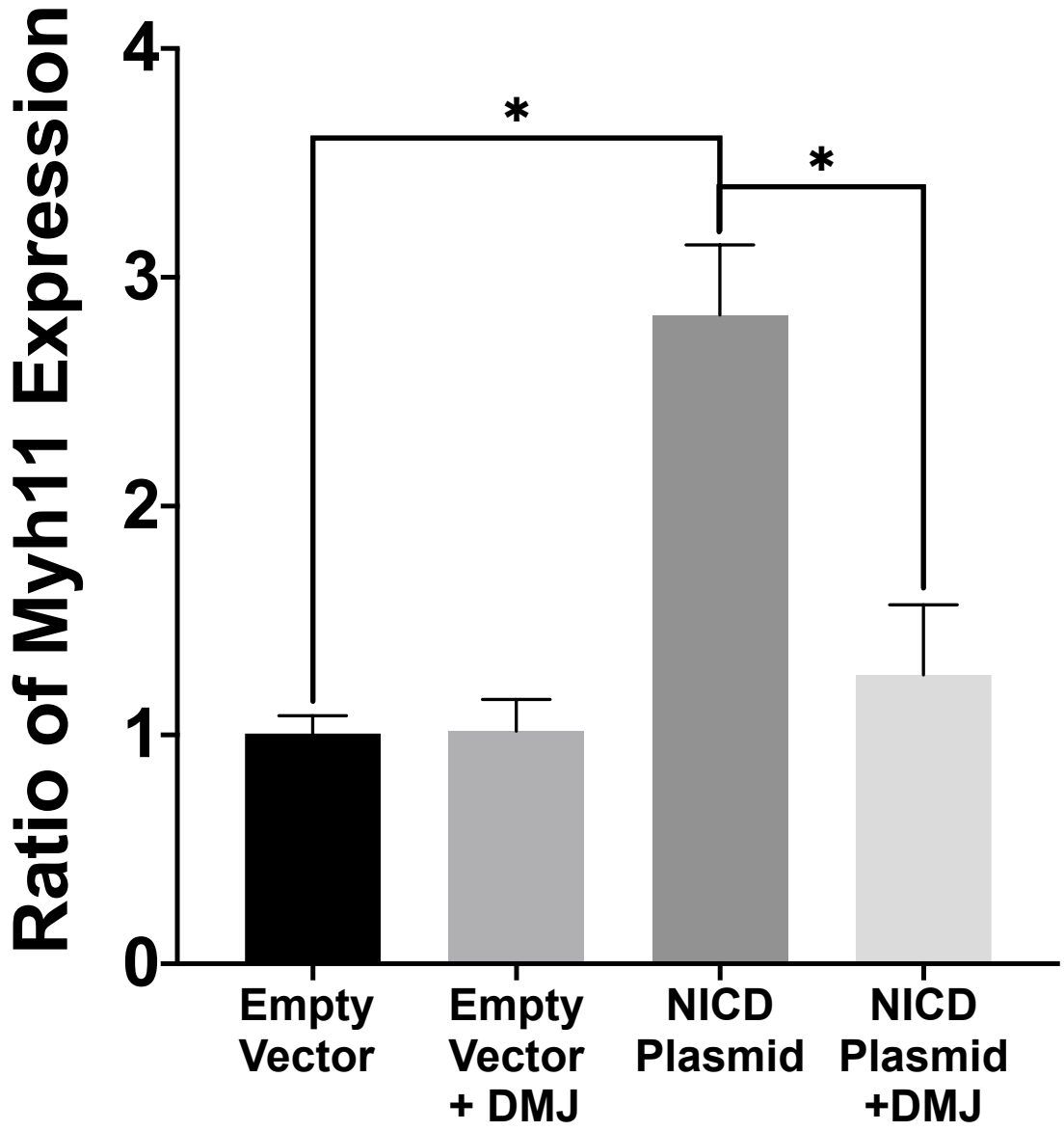


Fig.4.20 Effect of DMJ on NICD-activated *Myh11* expression in MVSCs. The relative expression of *Hey1* mRNA levels by qRT-PCR in MVSCs transfected with NICD plasmid ± DMJ (4μg/mL) and incubated for 48 h at 37°C. Data are presented as the ratio of expression relative to the negative control sample transfected with empty vector plasmid. Error bars based on SEM. Data representative of n=3. * $p < 0.05$

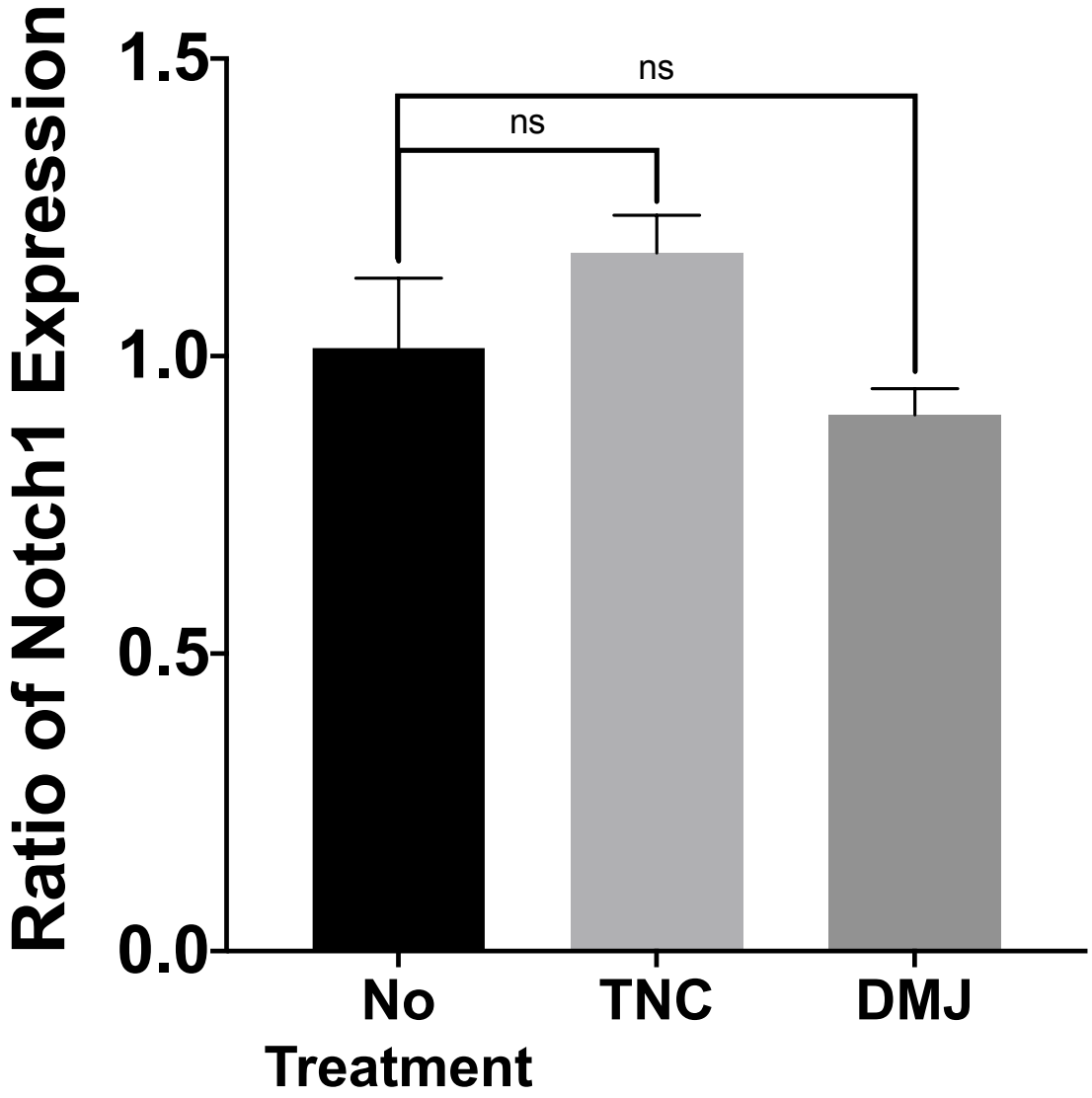


Fig.4.21 Effect of TNC and DMJ on *Notch1* transcript expression in MVSCs. The relative expression of *Notch1* mRNA levels by qRT-PCR in MVSCs treated with TNC (0.5µg/mL) or DMJ (4µg/mL) and incubated for 48 h at 37°C. Data are presented as the ratio of expression relative to the untreated negative control sample. Error bars based on SEM. Data representative of n=3. ns – $p > 0.05$

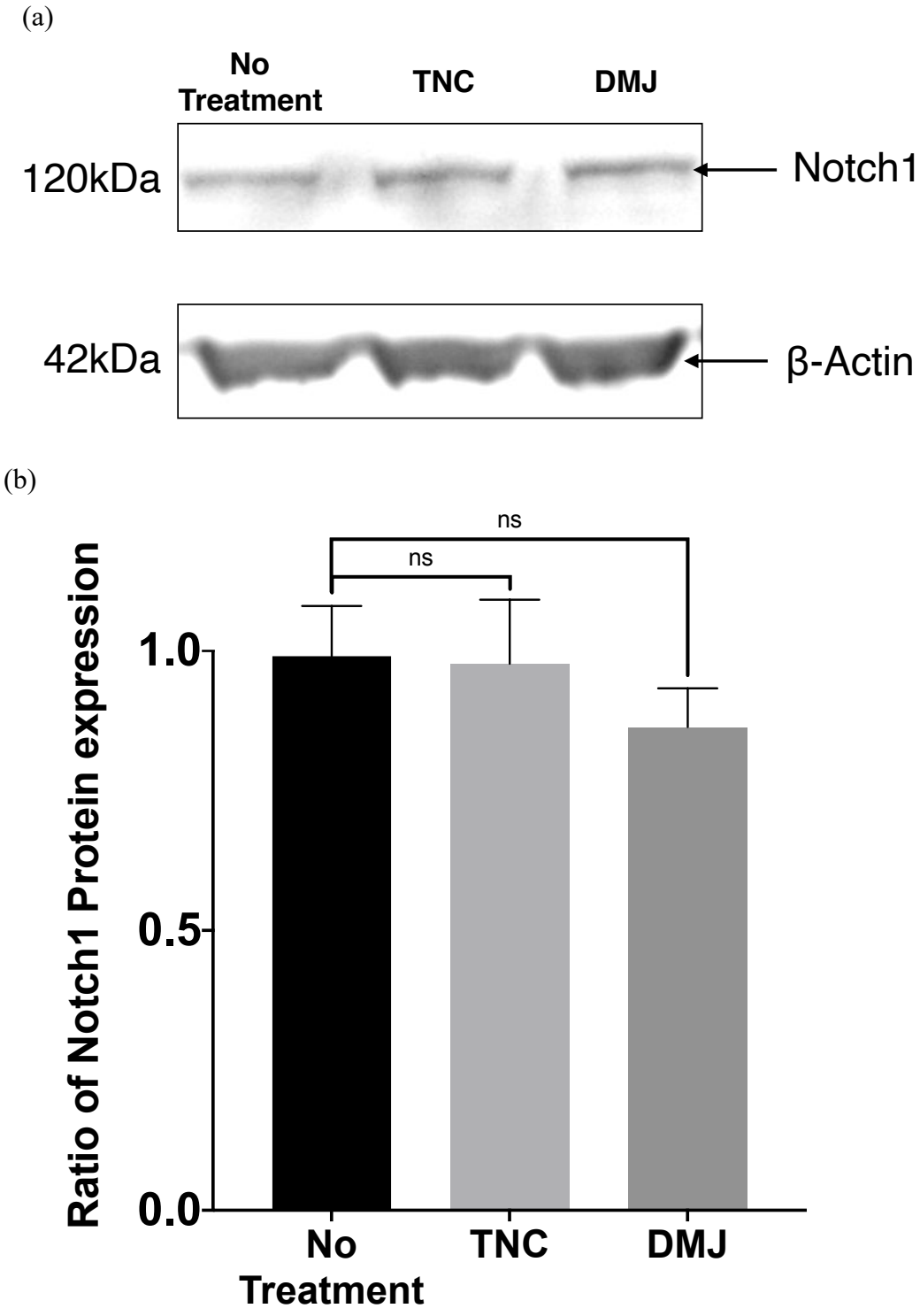


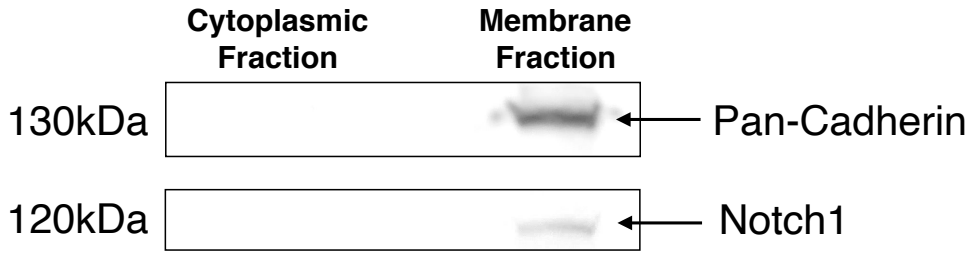
Fig.4.22 Effect of TNC and DMJ on Notch1 protein expression in MVSCs. MVSCs treated with TNC (0.5μg/mL) or DMJ (4μg/mL) for 48 h at 37°C were assessed for Notch1 protein expression in cell lsyates. HRP-conjugated secondary antibody and chemiluminescent staining used to visualise bands on the blot. (a) Representative immunoblot image of Notch1 bands at 120kDa and β-actin bands at 42kDa. Densitometry was carried out on western blot samples to measure intensity of Notch1 bands normalised to the β-actin loading control. (b) Notch1 protein levels given as ratio of expression relative to the untreated negative control sample. Error bars based on SEM. Data representative of n=3. ns – $p > 0.05$

4.3.10 Membrane Fractionation of MVSC Protein Lysate

In order to investigate changes in Notch1 membrane expression, the validity of the membrane fractionation method had to first be confirmed. A population of MVSCs was harvested and the Mem-PER™ Plus Membrane Protein Extraction Kit was used to carry out membrane fractionation on the crude lysate as per Section 2.2.13. Protein concentration in both the cytoplasmic fraction and membrane fraction was quantified by BCA Assay. Both samples were run on an SDS-PAGE precast protein gel and subsequently transferred to a nitrocellulose membrane. Staining with Ponceau S (Fig.4.23b) confirmed the presence of very different protein band profiles between the two samples. Immunoblotting was then carried out with an anti-Notch1 antibody (ab52627) and chemiluminescent staining was used to visualise bands.

A clear band was observed at the 120kDa mark in the membrane fraction, representing the transmembrane Notch1 protein, while no band was observed at the same mark in the cytoplasmic fraction. To further confirm the separation of membrane and cytoplasm proteins, the blot was stripped, re-blocked and re-probed, this time using an anti-Pan-Cadherin antibody (ab51034) which stains for members of the Cadherin family of proteins which are exclusively expressed on the plasma membrane. Once again a single band appeared at the 130kDa mark in the membrane fraction, representing the Cadherin group of proteins, while no band was observed at this mark in the cytoplasmic fraction (Fig.4.23a).

(a)



(b)

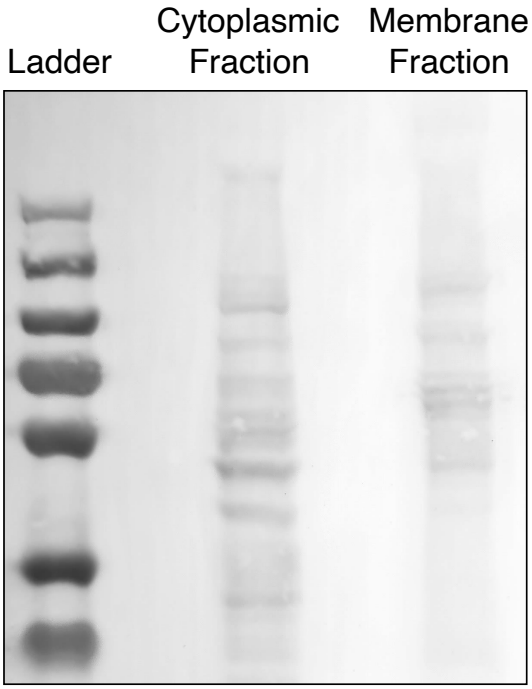


Fig.4.23 Validation of Membrane Fractionation Method. Membrane fractionation was carried out on MVSC lysates using Mem-PER™ Plus Membrane Protein Extraction Kit before Notch1 and Pan-Cadherin expression was assessed in cytoplasmic and membrane fractions. HRP-conjugated secondary antibody and chemiluminescent staining used to visualise bands on the blot. (a) Representative immunoblot image of Notch1 bands at 120kDa and Pan-Cadherin bands at 130kDa. (b) Ponceau S staining of protein band profiles in each fraction. Data representative of n=3.

4.3.11 Effect of TNC and DMJ on Membrane Localisation of Notch1

Once the method of membrane fractionation had been confirmed, this technique could be utilised to determine whether TNC and DMJ were affecting Notch1 localisation to the membrane. MVSCs were treated with either TNC (0.5µg/mL), DMJ (4µg/mL), 1X Brefeldin A (BFA) or not treated with any inhibitor. Cells were incubated at 37°C for 48 h before being harvested. Membrane fractions were isolated from all four samples using the Mem-PER™ Plus Membrane Protein Extraction Kit. Protein concentration in the membrane fractions was measured by BCA Assay. Western blot was then carried out and samples were immuno-probed using an anti-Notch1 antibody (ab52627). Chemiluminescent staining was used to visualise immunoblotting. Bands at the 120kDa mark represent the Notch1 transmembrane protein. The band in the non-treated sample is much more distinct and robust than those in either the TNC-, DMJ-, or BFA-treated samples. Densitometry was carried out using ImageJ to measure the intensity of Notch1 bands. As this was a membrane fraction, β-actin could not be used as a loading control as it is mostly expressed in the cytoplasm. Pan-Cadherin was considered as a loading control but through extensive research, personal communication and forum discussion it was concluded that the Ponceau S stain would be a more suitable loading control (Delaby *et al.*, 2005; Romero-Calvo *et al.*, 2010; Gilda and Gomes, 2013; Thacker *et al.*, 2016; Iwata *et al.*, 2017; Moritz, 2017). Therefore, Notch1 band intensities were calculated relative to the Ponceau S stain of the corresponding lane. A significant decrease in band intensity was observed following treatment with TNC, DMJ or BFA, indicating a reduction in Notch1 receptor at the plasma membrane in each case (Fig.4.24).

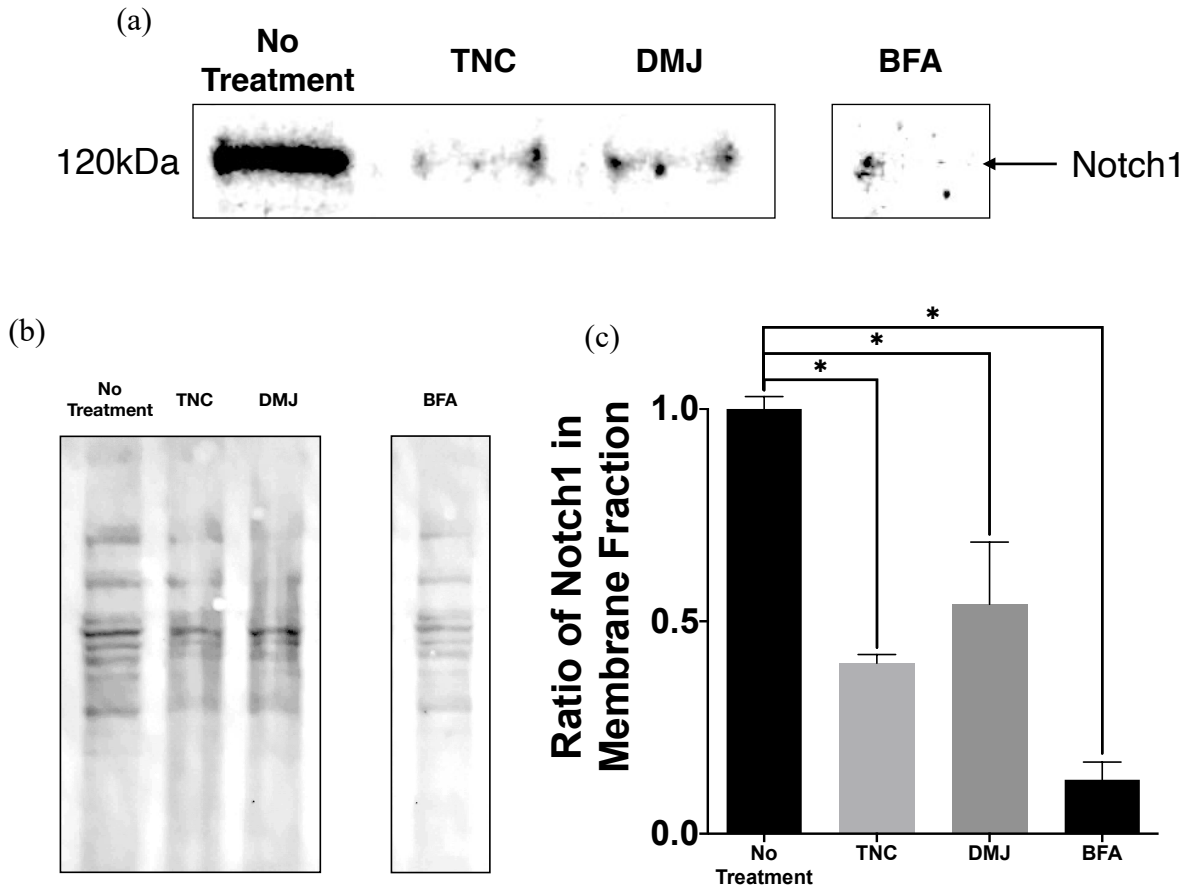


Fig.4.24 Effect of TNC and DMJ on Membrane Localisation of Notch1. MVSCs were treated with TNC (0.5μg/mL), DMJ (4μg/mL) or 1X BFA for 48 h at 37°C before membrane fractionation was carried out on lysates using Mem-PER™ Plus Membrane Protein Extraction Kit. HRP-conjugated secondary antibody and chemiluminescent staining was used to visualise bands on the blot. (a) Representative immunoblot image of Notch1 bands at 120kDa. (b) Ponceau S staining of protein band profiles in each fraction. Densitometry was carried out on western blot samples to measure intensity of Notch1 bands normalised to the Ponceau S loading control. (c) Notch1 protein levels in membrane fraction presented as the ratio of expression relative to the untreated negative control sample. Error bars based on SEM. Data representative of n=3. * $p < 0.05$

4.3.12 Effect of TNC and DMJ on Trafficking of Notch1 Receptor

N-glycosylation has been shown on numerous occasions to be an essential modification for correct protein trafficking from the endoplasmic reticulum (ER) and Golgi apparatus (GA) to their site of action in the cell (Fan *et al.*, 1997; Li *et al.*, 2004). Therefore, it was necessary to explore whether Notch1 trafficking was being affected by TNC and DMJ treatments as this would influence the activation of Notch target genes and myogenic differentiation. To investigate this, MVSCs were seeded at 5,000 cells/well onto sterile cover slips and treated with either TNC (c), DMJ (4µg/mL), 1X BFA or were left untreated. Cells were incubated at 37^{o}C for 48 h before being fixed with 3.7% formaldehyde. Immunocytochemistry was then carried out as per Section 2.2.6 and samples were stained using an anti-Notch1 antibody (ab52627). A control sample was also stained with an anti-Golgin-97 antibody (PA530048) to visualise the subcellular location of the GA. Nuclei were also stained with DAPI. One sample was only stained with an IgG control secondary antibody to account for background fluorescence. Samples were imaged using a fluorescent microscope. ImageJ was used to calculate the mean fluorescence intensity and the integrated density of fluorescence at both the cell membrane and in the perinuclear region (adjacent to nucleus, ie. where the GA is located). Samples were graphed as a ratio of the fluorescence at the membrane to the fluorescence in the perinuclear region. The ratio of both the fluorescence intensity and density significantly decreased following treatment with TNC, DMJ or BFA (Fig.4.25b and 4.25c). Lower ratios indicate a higher level of fluorescence in the perinuclear region compared to that at the membrane. Representative images, including the subcellular location of the GA, can be seen in Fig.4.25a.

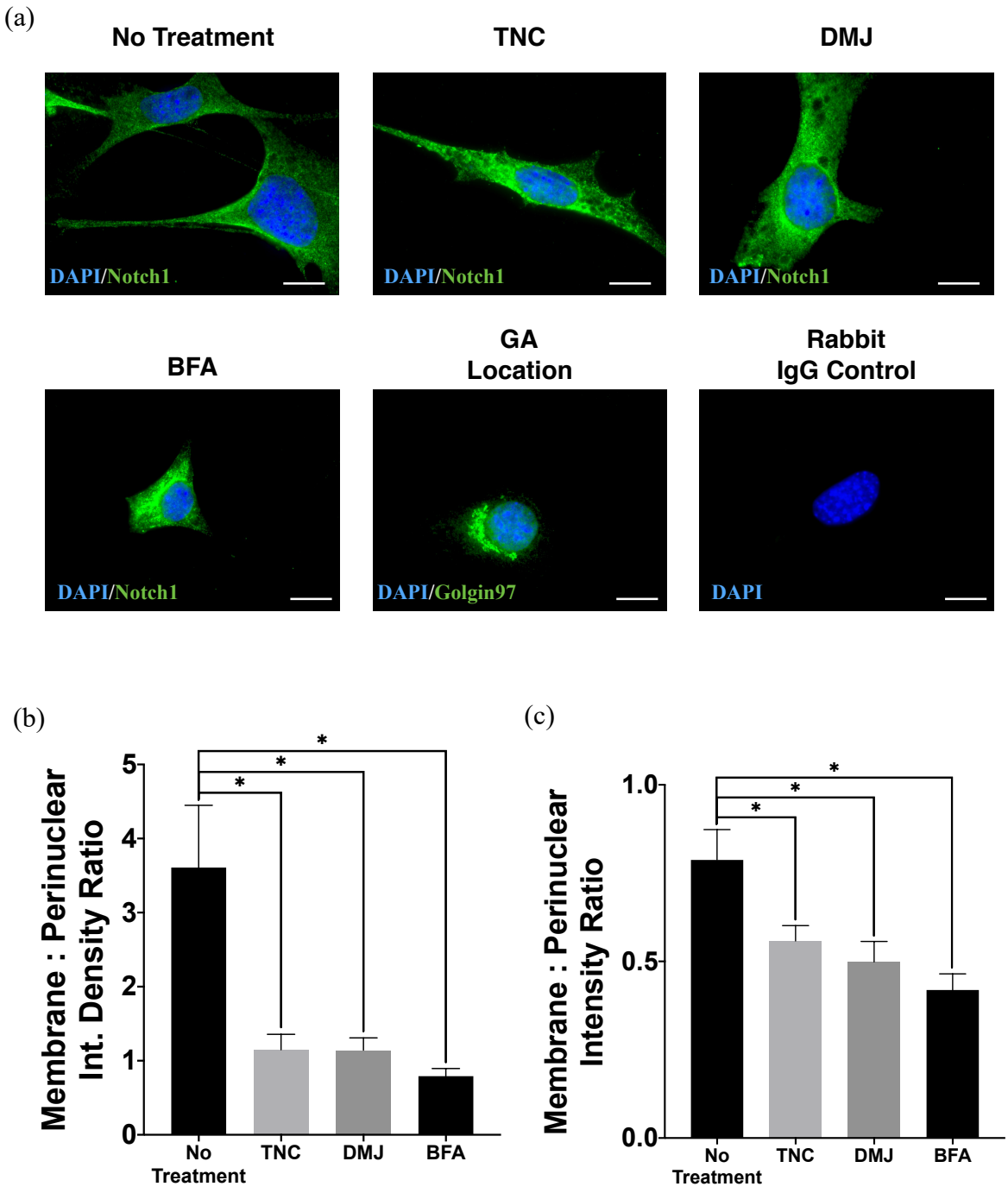


Fig.4.25 Effect of TNC and DMJ on Notch1 Receptor Trafficking. MVSCs were treated with TNC (0.5µg/mL), DMJ (4µg/mL) or 1X BFA for 48 h at 37ºC before ICC and fluorescence microscopy was performed to image the localisation of Notch1 in each sample. Nuclei were stained with DAPI and an AlexaFluor 488 secondary antibody used to visualise primary antibody staining. (a) Representative immunocytofluorescence images at 60X magnification of both treated and untreated samples, including a control sample demonstrating the location of the GA (using GA marker Golgin-97) and a rabbit IgG secondary antibody control. Scale bar = 10µm. ImageJ used to calculate ratio of Membrane : Perinuclear fluorescence using (b) integrated density and (c) mean fluorescence intensity values. Error bars based on SEM. Data representative of n=3. * $p < 0.05$

4.4 Discussion

The Notch signalling pathway is tightly regulated by a number of different mechanisms. One of the most widely reported is Notch receptor glycosylation. Both O-linked and N-linked glycosylation sites are highly conserved along the extracellular domain of the Notch receptor (Takeuchi and Haltiwanger, 2014). O-glycosylation of Notch has been extensively studied and has been shown to heavily impact processes such as receptor-ligand binding and receptor trafficking from the ER (Brückner *et al.*, 2000; Matsumoto *et al.*, 2016). Comparatively, very little research has been carried out to decipher the role of N-glycosylation in Notch signalling. Therefore, the overall aim of this project is to investigate the impact of Notch N-glycosylation on both Notch1 signalling and myogenic differentiation of MVSCs. To this end, a strategy to interfere with the process of N-glycosylation using pharmacological inhibitors and observe the resulting effects was developed and pursued.

Before employing strategies to inhibit Notch1 N-glycosylation, it was necessary to establish a baseline profile of the N-glycosylation present on the Notch1 receptor. This required purification of Notch1 by immunoprecipitation (IP). However, an early issue arose as western blot data showed a large amount of contaminating protein in supposedly purified Notch1 samples. In order to address this issue, a different elution strategy was implemented to improve stringency and several controls were carried out to decipher the nature of the contaminating protein. Interpretation of data in Section 4.3.1 suggests that the anti-Notch1 rabbit monoclonal antibody used to immunoprecipitate the Notch1 receptor was also being eluted and therefore contaminating the final fraction. In the mouse IgG and mock IP controls, there may also have been some alternative contaminating material present, possibly native antibodies in the lysate pulled down by the Protein A-conjugated beads or even some of the Protein A itself. Use of the glycine elution buffer in place of the Laemmli buffer improved the purity of the eluted fraction, however a fully purified fraction could not be obtained. Henceforth, any future analyses of purified Notch1 required an IgG control to determine the true baseline.

Another issue which presented itself during the optimisation of the IP technique was the unsustainably large volume of cells required to obtain acceptable yields of purified Notch1. To combat this issue, ectopic overexpression of a plasmid-encoded Notch1 was performed in some cases to increase the level of Notch1 protein in a smaller volume of cells. A Notch1-coding plasmid was therefore amplified and purified from bacterial cells, along with an

NICD-coding plasmid which would be required for later experiments in this project. The ectopic expression of Notch1 and NICD in MVSCs was validated by western blot. Both the Notch1 and NICD proteins produced in this case possess a C-terminal myc-tag and therefore an anti-myc tag antibody was used to probe for their presence. It must be noted that other western blot data in this study shows Notch1 bands at 120kDa while data in Section 4.3.2 shows the Notch1 band at 300kDa. Previous studies have reported that while Notch1 is translated as a 300kDa polypeptide, a cleavage event in the trans-Golgi network after protein glycosylation by a furin-like protease results in two fragments: a 120kDa Notch1 transmembrane domain (NTM) and a 180kDa Notch1 extracellular domain (NECD) which are tethered to each other by a disulfide bridge. This is the active form of Notch1 that is then trafficked to the membrane. However, the disulfide bridge is sensitive to degradation by reducing agents. Therefore, the 300kDa heterodimer is rarely detectable by western blot, which has led to the 120kDa NTM fragment becoming the most regularly used marker for Notch1 in western blot analysis (Blaumueller *et al.*, 1997; Logeat *et al.*, 1998). It is only with high levels of overexpression and an antibody-antigen bond with very high affinity (as seen with the anti-myc-tag antibody) that the 300kDa band of full-length Notch1 can be detected.

Having validated both the ectopic overexpression of plasmid-encoded Notch1 and the process of immunoprecipitation, an enzyme-linked lectin assay (ELLA) was then used to determine the N-glycosylation profile of the purified Notch1 receptor. ELLA data demonstrated significant levels of binding with the ConA, LCA and E-PHA lectins. This confirmed the presence of N-glycans on the Notch1 receptor and, using Table 2.13, some of the specific structures on these oligosaccharides could be deduced. ConA binds the ubiquitous tri-mannosyl core of N-glycans and therefore does not offer much insight into their structure. However, LCA is known to bind to an α-1,6 linked fucose attached to the core GlcNAc residue of an N-glycan, while E-PHA binds to complex N-glycans, especially those with a bisecting structure. Therefore, the data suggests that core fucosylated and complex bisecting N-linked oligosaccharides are present on the Notch1 receptor (Fig.3.18).

Broad spectrum N-glycosylation inhibitors such as tunicamycin (TNC) and 1-deoxymannojirimycin (DMJ) are useful tools in assessing the overall impact of N-glycosylation on a particular cellular process. TNC blocks all N-glycosylation by preventing the attachment of a 14-sugar dolichol precursor to the nascent polypeptide (Aaron Heifetz, Keenan and Elbein, 1979). DMJ on the other hand, inhibits the formation of complex and

hybrid-type N-glycans by inactivating a vital enzyme (α-mannosidase-I) involved in the trimming of the dolichol precursor oligosaccharide (Elbein, 1987). Once the N-glycosylation profile of the Notch1 receptor had been determined, these two inhibitors were then used to interfere with this profile. ELLA was used to confirm the effectiveness of both TNC and DMJ in MVSCs and C3Hs. In MVSCs, an inverse correlation between the concentration of TNC and the binding of all lectins was detected, with cell cytotoxicity eventually occurring when inhibitor concentration was increased past 0.5μg/mL (0.6μM). This data indicates that an increase in inhibitor concentration caused a reduction in all measured forms of N-glycosylation and, at a particular point, the cells could not survive any longer due to stress factors induced by low levels of N-glycosylation, such as ER dysfunction (Ling *et al.*, 2009). Previous studies support this data as it has been reported that TNC concentrations as low as 0.01μg/mL (12nM) can inhibit N-glycosylation (Aaron Heifetz, Keenan and Elbein, 1979), while higher concentrations (>1.2μM) are regularly used to induce ER stress *in vitro* (Abdullahi *et al.*, 2017; Wang *et al.*, 2020). In C3Hs, a similar pattern was observed with TNC treatment, albeit with a higher tolerance for inhibitor concentration, with substantial cell death only occurring at concentrations higher than 1μg/mL (1.2μM). This is in line with previously published studies which found TNC to be effective at 1μg/mL (1.2μM) in C3H cells and other embryonic fibroblast cell lines (Chen *et al.*, 2007; Takahata *et al.*, 2009). Increasing DMJ concentration also resulted in reduced N-glycosylation in MVSCs up to an optimal concentration of 4μg/mL (20μM). Higher concentrations gave rise to significant cell death. This data is supported by previous studies which report that DMJ can inhibit N-glycosylation at concentrations as low as 1.5μg/mL (7.5μM) (Shalel Levanon *et al.*, 2018), but can also cause cell cytotoxicity at higher concentrations (>1mM), possibly due to natural killer (NK) cells targeting and destroying cells with altered surface glycosylation (Rothman *et al.*, 1989; Yagita and Saksela, 1990).

In C3Hs, a rather different pattern of DMJ response was observed. Concentrations of DMJ below 50μg/mL (250μM) had no effect on N-glycosylation. Once this point was reached, a significant reduction in complex and hybrid-type N-glycosylation occurred (as detailed by the WGA and E-PHA binding in Fig.4.7). At concentrations higher than 50μg/mL (250μM), lectin binding began to increase again, indicating an increase in N-glycosylation. This seems to be counter-intuitive but is likely due to redundancies in the mannosidase family of enzymes (Ogen-Shtern *et al.*, 2016). Several other enzymes in this family possess the ability to hydrolyse mannose residues in the same way as α-mannosidase-I (Zhou *et al.*, 2009; Legler *et al.*, 2018). When inhibition of α-mannosidase-I reached a certain level as a result

of DMJ treatment, it is possible that alternative mannosidase enzymes took over to maintain the process of oligosaccharide trimming, thereby causing the increase in lectin binding at higher concentrations of DMJ. It must also be noted that this is the first time that the ELLA technique has been used to detect changes in N-glycosylation following TNC or DMJ treatment. Early studies used radio-labelling of components in the glycosylation pathway to confirm the effect of inhibitors on the process (Nakayasu *et al.*, 1980; Yodoi, Hirashima and Ishizaka, 1981), while more recent studies have employed techniques such as mass spectrometry, lectin biosensors and lectin-based western blotting to detect alterations in N-glycosylation resulting from TNC or DMJ treatment (Chen *et al.*, 2013; Xiao, Smeekens and Wu, 2016; Skrenkova *et al.*, 2018; Han *et al.*, 2019). Data from this section indicates that ELLA could be a viable alternative for rapid and cost-effective confirmation of the effectiveness of different N-glycosylation inhibitors.

The ability of TNC and DMJ to affect Notch1 N-glycosylation was also assessed. In this case, receptor overexpression could not be carried out as high levels of cell death were observed when inhibitor treatment was combined with plasmid transfection. Therefore, a large volume of cells was treated with TNC or DMJ for 48 h and the native Notch1 was immunoprecipitated using an anti-Notch1 antibody. ELLA was used to detect changes in N-glycosylation in inhibitor-treated samples compared to a non-treated control. TNC and DMJ significantly reduced binding with ConA, LCA and E-PHA. This data suggests that these inhibitors can effectively reduce the level of N-glycosylation on the Notch1 receptor and also supports previous data in this chapter which identified the presence of both core fucosylated and complex bisecting N-glycans on the Notch1 receptor. Published data regarding the effect of TNC or DMJ on Notch N-glycosylation is extremely scarce. One study from 1989 demonstrated that the WGA lectin binds to the *Drosophila* Notch receptor, and this binding is subsequently attenuated by treatment with TNC (Kidd *et al.*, 1989). This is at odds with the data from this section which indicates that WGA binding was unaffected by TNC treatment. This discrepancy is likely due to different glycosylation patterns between *Drosophila* and mammalian Notch, or possibly due to the low level of lectin sensitivity in some analytical assays.

TNC and DMJ were subsequently used to inhibit N-glycosylation in Jag-1 treated MVSCs and C3Hs. In both cell lines, Jag-1 treatment substantially increased transcript expression of both *Hey1* and *Myh11*, but this response was significantly reduced following treatment with either inhibitor. This attenuation was slightly less pronounced in DMJ-treated samples than

in TNC-treated samples. Interestingly, TNC treatment resulted in a significant decrease in *Hey1* expression in C3Hs treated with the Fc-control, indicating that baseline levels of Notch signalling are higher in C3Hs than in MVSCs, possibly due to their higher level of potency. Another potential reason for this discrepancy between MVSCs and C3Hs is that the two cell lines exhibit differential usage of canonical and non-canonical Notch signalling pathways (D'Souza, Meloty-Kapella and Weinmaster, 2010). TNC may affect these alternative pathways in different ways and it is common for cell types at different stages of differentiation to have different Notch signalling patterns (Mizutani *et al.*, 2007). There is currently no published data regarding the effect of small-molecule N-glycosylation inhibitors such as TNC and DMJ on Notch target gene expression or Notch-induced myogenic differentiation. Novel findings from this section confirmed that N-glycosylation has some role to play in Notch signalling and Notch-mediated myogenic differentiation, however more concrete evidence is required to determine whether this is specifically related to N-glycans on the Notch1 receptor, as treatments in this section would have affected all N-glycosylated proteins in the cell.

In an attempt to investigate whether TNC and DMJ were having an effect on downstream elements of the Notch signalling pathway, NICD ectopic expression was carried out in MVSCs in conjunction with inhibitor treatment. Ectopically expressed NICD successfully activated Notch target gene (*Hey1*) and myogenic marker (*Myh11*) expression. Treatment with TNC or DMJ incurred no significant change to this increase in *Hey1* expression, but both inhibitors significantly attenuated the increase in expression of *Myh11*. This evidence suggests that Notch pathway elements between the cleavage of the NICD and the activation of *Hey1* expression are unaffected by TNC or DMJ, but components of the myogenic differentiation pathway are altered by these treatments. As previously stated in Section 3.4, the NICD-CBF-1/RBP-Jκ complex can activate expression of both *Hey1* and *Myh11* through separate mechanisms. While *Hey1* activation occurs through direct binding of the complex to the target gene promoter region (Maier and Gessler, 2000), *Myh11* transcription is initiated through interaction with the serum response factor (SRF)-myocardin complex to stimulate binding to the CArG domain of the gene (Noseda *et al.*, 2006). Therefore it is possible that elements of the SRF-myocardin pathway are altered by TNC and DMJ treatments, leading to decreased *Myh11* expression.

It was also possible that TNC and DMJ treatment could be affecting Notch1 expression by altering the activity of transcription or translation machinery. To address this possibility,

qRT-PCR and western blot were carried out on MVSCs treated with TNC or DMJ for 48 h. No change in *Notch1* transcript or protein levels was detected, indicating that Notch1 expression was not being altered and was therefore not the cause of the reduction in signalling. It must be noted that *Notch1* itself is a Notch target gene (Borggrefe and Oswald, 2009). Since it has been demonstrated in this chapter that TNC and DMJ both reduce Notch target gene expression, it may seem that data in this section is contradictory to those findings and, in theory, *Notch1* expression should be attenuated by these treatments. However, MVSCs in this experiment have not been activated by Jag-1 like those in Sections 4.3.6 and 4.3.7. Therefore the level of baseline Notch signalling may be too low to detect a change in Notch-stimulated *Notch1* expression. It would be interesting to investigate whether *Notch1* expression would be altered in a cell line with higher levels of baseline Notch signalling, or in Jag-1-stimulated MVSCs.

The last possibility to be explored was that the TNC and DMJ treatments were affecting the trafficking of Notch1 either to or from the plasma membrane. This was investigated in two ways: through analysis of protein levels in the membrane fraction of a cell lysate; and through visualisation of Notch1 localisation in the cell. The membrane fractionation method was validated by western blot which confirmed that both Notch1 and Pan-Cadherin (a ubiquitously expressed membrane-bound protein) were present in the membrane fraction but not in the cytoplasmic fraction. BCA assay and Ponceau S stain confirmed the equal loading of protein in this case as a loading control such as β-actin could not be used due to the varying levels of expression between the membrane and cytoplasm (this is explained in greater detail in Section 4.3.11).

Membrane fractionation and western blot were then carried out on MVSCs treated for 48 h with TNC, DMJ or the Golgi trafficking inhibitor Brefeldin A (BFA). Significant decreases in Notch1 band intensity were observed in membrane fractions following treatment with each of the three inhibitors. This implies that in each instance, the amount of Notch1 on the membrane was decreased by the inhibitor. Reduction of Notch1 levels on the membrane could be due to inhibition of trafficking from the Golgi Apparatus (GA) or from endocytosis and degradation of Notch1 from the membrane. In the case of BFA, its mechanism of action is to inhibit trafficking from the GA and so this is almost certainly the reason for its effect on Notch1 membrane levels. With TNC and DMJ the reason is less certain, however if they were causing endocytosis and degradation of the receptor then total Notch1 protein levels in the cell would also be reduced, which was not the case according to data from Section 4.3.9.

Therefore the most likely scenario is that their effect is similar to that of BFA. This theory is further supported by immunocytochemistry data from Section 4.3.12 which shows a significant decrease in the ratio of Membrane : Perinuclear localisation of Notch1 following treatment with TNC, DMJ or BFA. This data is based upon analysis of ICC images using integrated density (the sum of all pixel intensities in a defined area) and mean fluorescence intensity (the average intensity of all pixels in a defined area), which indicates an accumulation of Notch1 in the perinuclear region of the cell in response to TNC and DMJ treatment, similar to what is observed following BFA treatment. This is supported by multiple published studies which reported a reduction of protein trafficking caused by both TNC and DMJ (Esapa *et al.*, 2003; Nacev *et al.*, 2011). In particular, these inhibitors have been shown to reduce migration of membrane-bound proteins from the ER-Golgi complex to the cell surface (Tordai, Brass and Gelfand, 1995; Skrenkova *et al.*, 2018). Furthermore, it has been previously reported that TNC treatment results in the intracellular accumulation of Notch3 receptors in CHO cells (Stahl *et al.*, 2008), and so it is likely that Notch1 receptors are affected in a similar manner.

In summary, data in this chapter confirms the presence of N-glycans on the Notch1 receptor and suggests that these N-glycans may contain core fucosylation and complex bisecting structures. Furthermore, protein N-glycosylation can be attenuated in MVSCs using the small-molecule inhibitors tunicamycin and 1-deoxymannojirimycin. This includes N-glycosylation of Notch1 specifically as both inhibitors can reduce the binding of certain lectins to its purified form. TNC and DMJ treatment can also reduce the level of Jag-1 mediated Notch signalling and myogenic differentiation in MVSCs and C3Hs, although it is not certain whether or not this is due to their effect on Notch1 or on other cellular proteins. These data sets have shown that Notch pathway elements between receptor cleavage and target gene expression are not altered by TNC or DMJ treatment, while it is likely that downstream components in the myogenic differentiation pathway are affected. Finally, although *Notch1* expression does not seem to be altered by treatment with either inhibitor, evidence from this chapter indicates that the trafficking of the Notch1 receptor from the GA to the membrane is substantially blocked by both TNC and DMJ activity.

Chapter 5:

The Effect of GnT-III and Fut8 knockdown on Notch Signalling and Myogenic Differentiation

5.1 Introduction

The data in Chapter 4, Section 4.3.3 using ELLA on the purified Notch1 receptor to determine its N-glycosylation profile revealed a significant level of lectin binding with the ConA, LCA and E-PHA lectins. Using Table 2.13 as a reference, it was determined that this binding pattern indicated the presence of both complex bisecting N-glycans and core fucosylated N-glycans on the extracellular domain of the Notch1 receptor. Therefore, in this Chapter, the specific glycosyltransferase enzymes responsible for the synthesis of these two types of N-glycans were assessed.

A family of glycosyltransferases known as N-acetylglucosaminyltransferases (GnT's) are responsible for the addition of GlcNAc residues to N-linked glycans. There are six members of this family (GnT-I to GnT-VI), all of which operate in the Golgi apparatus (Rademacher, Parekh and Dwek, 1988). GnT-III (coded by the *Mgat3* gene) catalyses the addition of a GlcNAc residue through a β-1,4 linkage to the β-mannose in the tri-mannosyl core of a growing N-linked oligosaccharide, creating a structure known as a bisecting N-glycan (Narasimhan, 1982). This structure has been shown to inhibit the addition of sugar residues by other glycosyltransferases such as GnT-II, GnT-IV and Fut8 (Longmore and Schachter, 1982; Schachter, 1986; Gu *et al.*, 1993). Bisecting N-glycans have been shown to be heavily involved in the regulation of a number of cellular processes, including cell adhesion, protein degradation and growth factor signalling (Zhao *et al.*, 2008; Song *et al.*, 2010). Changes in GnT-III activity can therefore lead to dysregulation of these processes and this has been reported on numerous occasions to influence the development of a range of cancer types, including breast cancer and leukaemia (Yoshimura *et al.*, 1995; Song *et al.*, 2010; Link-Lenczowski *et al.*, 2018). The presence of bisecting N-glycans on the Notch receptor was confirmed via binding of the Phaseolus Vulgaris Erythroagglutinin (E-PHA) lectin (Allam *et al.*, 2017). The same study found that cancer stem cell expansion was substantially reduced when *Mgat3* was stably knocked down in human ovarian cancer cell lines. This was attributed to a reduction in Notch1 signalling, seemingly due to the increased degradation of the Notch1 receptor (Allam *et al.*, 2017). This evidence indicates that bisecting N-glycans, synthesised by GnT-III, may serve some role in maintaining Notch signalling.

Members of the fucosyltransferase (FUT) family of enzymes facilitate the addition of fucose residues to the core N-glycan structure (Staudacher *et al.*, 1999). In a process known as core fucosylation, Fut8 catalyses the transfer of fucose from a donor substrate to the asparagine-

bound GlcNAc at the base of an N-glycan via an α1,6-linkage (Wilson, Williams and Schachter, 1976). Core-fucosylated N-glycans have been reported to regulate a wide array of cellular processes such as the expression of essential cadherins and the function of specific types of immunoglobulins (Okazaki *et al.*, 2004; Osumi *et al.*, 2009). Alterations in core fucosylation can lead to dysregulation of these processes and the onset of several forms of cancer, including liver and pancreatic cancer (Aoyagi *et al.*, 1998; Pinho and Reis, 2015). As of yet, it has not been established whether or not N-glycans on the Notch1 receptor are core fucosylated, though it has been noted that aberrant activity of both Fut8 and Notch is regularly observed in certain types of liver and breast cancer (Pakkiriswami *et al.*, 2016).

5.2 Strategy

The application of siRNA technology can be very useful when attempting to inhibit the activity of glycosyltransferases due to its versatility and high level of specificity, coupled with a very low level of cell cytotoxicity. Several research groups have utilised siRNA technology to investigate the role of N-glycans in a range of cellular mechanisms by knocking down specific glycosyltranferases such as Fut8 and ST3Gal-III (Mori *et al.*, 2004; Mo *et al.*, 2012). Therefore, this approach was used to inhibit the activity of Fut8 and GnT-III in MVSCs in order to examine the impact of bisecting and core-fucosylated N-glycans on Notch signalling and myogenic differentiation.

The first step in this process was to validate the knockdown of *Mgat3* and *Fut8* and to confirm that knockdown of each glycosyltransferase had a measurable functional effect. Targeted siRNA against *Mgat3* and *Fut8* transcripts were transiently transfected into MVSCs and C3Hs (Section 2.2.6.2). *Mgat3* and *Fut8* expression levels were then measured using qRT-PCR (Section 2.2.11) to confirm that the knockdown had been successful. To observe the functional effect of these knockdowns and to confirm their ability to alter N-glycosylation, ELLA was carried out on whole cell MVSC and C3H lysates using lectins specific for N-glycans (Section 2.2.17).

It was also necessary to determine the change in Notch1 N-glycosylation caused by knockdown of *Mgat3* and *Fut8*. ELLA was therefore carried out on IP-purified Notch1 following siRNA transfection in MVSCs.

Once the knockdown strategy had been validated, Jag-1-stimulated MVSCs and C3Hs were then transfected with *Mgat3* or *Fut8* siRNA to investigate how the change in N-glycosylation affected Notch signalling and myogenic differentiation. To achieve this, qRT-PCR was used to measure the expression levels of *Hey1* and *Myh11* across all samples.

As with Chapter 4, the final set of experiments in this chapter were carried out to attempt to identify how *Mgat3* and *Fut8* knockdown were affecting Notch1 signalling. MVSCs were co-transfected with NICD plasmid and either *Mgat3* or *Fut8* siRNA to investigate whether these interventions were affecting elements of the Notch signalling pathway downstream of receptor activation. This was again determined by qRT-PCR analysis of *Hey1* and *Myh11* expression.

The impact of both knockdowns on Notch1 expression was subsequently assessed. MVSCs were transfected with *Mgat3* or *Fut8* siRNA before carrying out qRT-PCR and western blot (Section 2.2.16) to measure their effect on *Notch1* transcript and Notch1 protein expression respectively.

Lastly, the effect of *Mgat3* and *Fut8* knockdowns on the trafficking of Notch1 in the cell was examined. To do this, membrane fractionation was carried out on the protein lysates of MVSCs transfected with each siRNA (Section 2.2.13). Western blot was then used to measure the expression of Notch1 protein in the membrane fraction and determine whether this expression had been altered by *Mgat3* or *Fut8* knockdown. A second approach was to probe for Notch1 using immunocytochemistry (Section 2.2.7) in order to visualise changes in its localisation as a result of glycosyltransferase inhibition. With both techniques, BFA was used as a positive control for the inhibition of Notch1 trafficking to the membrane.

Data for all experiments in this section was gathered over at least three biological replicates. Normality tests were used to determine if data followed a parametric distribution pattern. Variation across samples was analysed by calculating p-values. The type of test used to calculate this was governed by the outcome of the normality test. Statistical significance was assigned to p-values less than 0.05 (Section 2.2.19).

5.3 Results

5.3.1 Confirmation of *Mgat3* and *Fut8* transcript knockdown

Mgat3 and *Fut8* genes code for the glycosyltransferases GnT-III and Fut8 respectively. To inhibit their transcription, targeted siRNA transfection was carried out. MVSCs or C3Hs were seeded into wells of a 6-well plate and incubated overnight at 37^{o}C. The following day, the TransIT-X2 Dynamic Delivery System was used to transiently transfect the cells with siRNA targeting either the *Mgat3* transcript, *Fut8* transcript or a non-specific (Scrambled) control sequence. Cells were then incubated for a further 48 h at 37^{o}C in maintenance media. Cells were harvested and RNA was isolated from each sample. qRT-PCR was used to confirm the decrease in *Mgat3* and *Fut8* expression. In MVSCs, a reduction of around 70% was observed in *Mgat3* expression (Fig.5.1), while *Fut8* expression decreased by approximately 67% (Fig.5.2). Meanwhile, in C3H cells *Mgat3* expression decreased by 76% (Fig.5.3) and *Fut8* expression was reduced by 86% (Fig.5.4) following siRNA knockdown.

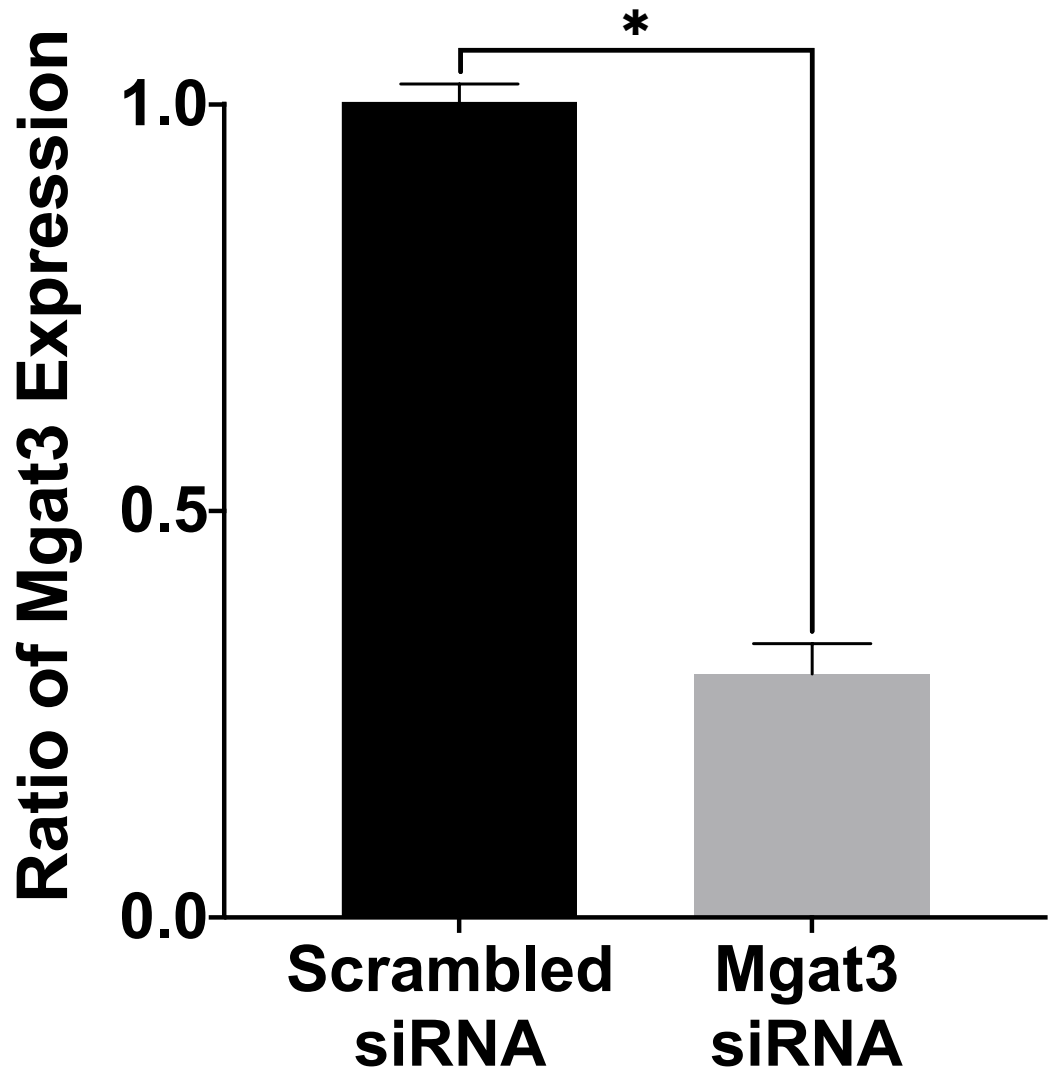


Fig.5.1 Expression of *Mgat3* transcript in MVSCs following *Mgat3* siRNA knockdown. The relative expression of *Mgat3* mRNA levels by qRT-PCR in MVSCs transfected with *Mgat3* siRNA (25nM) and the scrambled control for 48 h at 37°C. Data are presented as the ratio of expression relative to the negative control sample transfected with non-targeted (scrambled) siRNA. Error bars based on SEM. Data representative of n=3. * $p < 0.05$

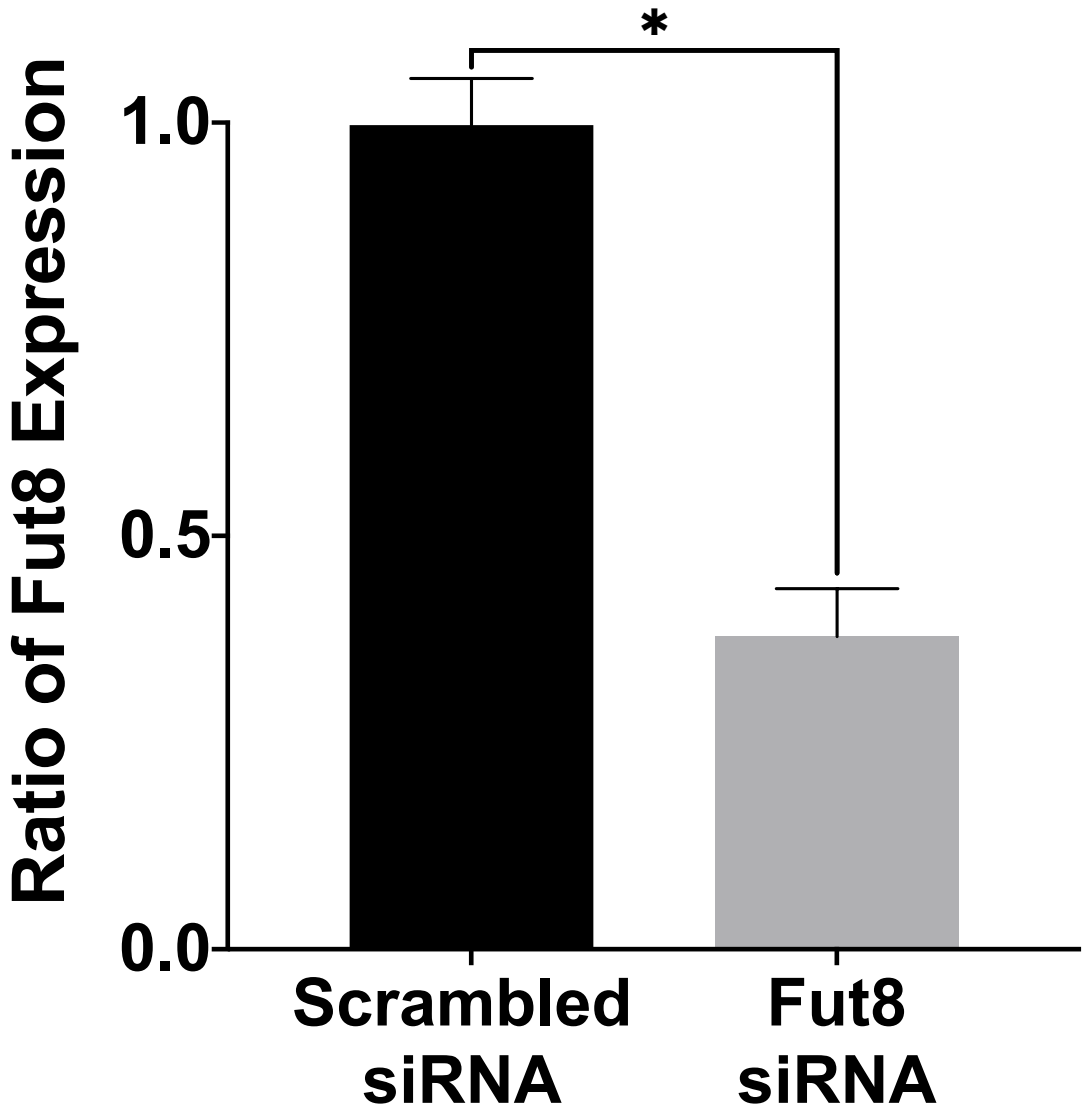


Fig.5.2 Expression of *Fut8* transcript in MVSCs following *Fut8* siRNA knockdown. The relative expression of *Fut8* mRNA levels by qRT-PCR in MVSCs transfected with *Fut8* siRNA (25nM) and scrambled control for 48 h at 37ºC. Data are presented as the ratio of expression relative to the negative control sample transfected with non-targeted (scrambled) siRNA. Error bars based on SEM. Data representative of n=3. * $p < 0.05$

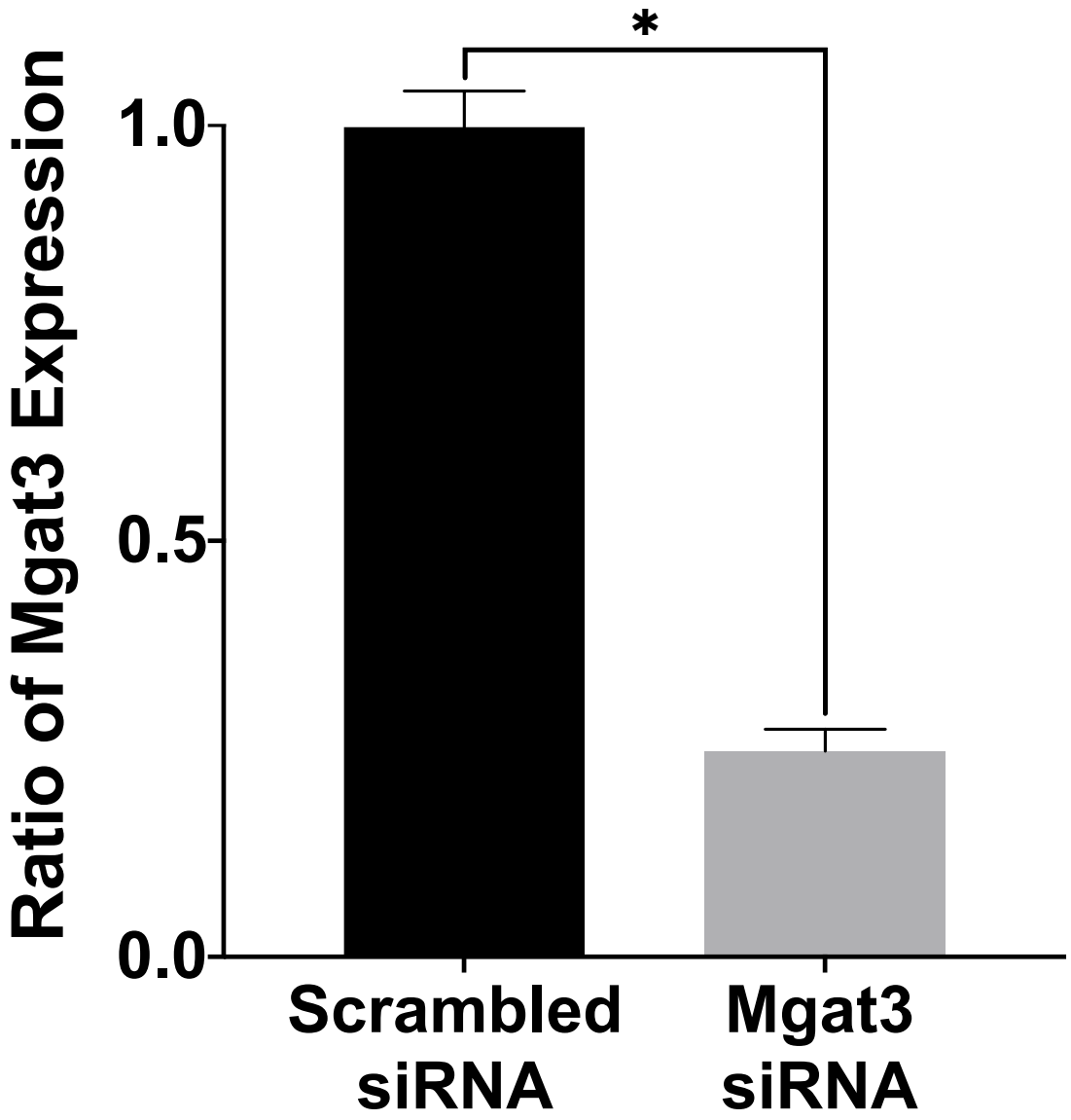


Fig.5.3 Expression of *Mgat3* transcript in C3Hs following *Mgat3* siRNA knockdown. The relative expression of *Mgat3* mRNA levels by qRT-PCR in C3Hs transfected with *Mgat3* siRNA (25nM) and scrambled control for 48 h at 37°C. Data are presented as the ratio of expression relative to the negative control sample transfected with non-targeted (scrambled) siRNA. Error bars based on SEM. Data representative of n=3. * $p < 0.05$

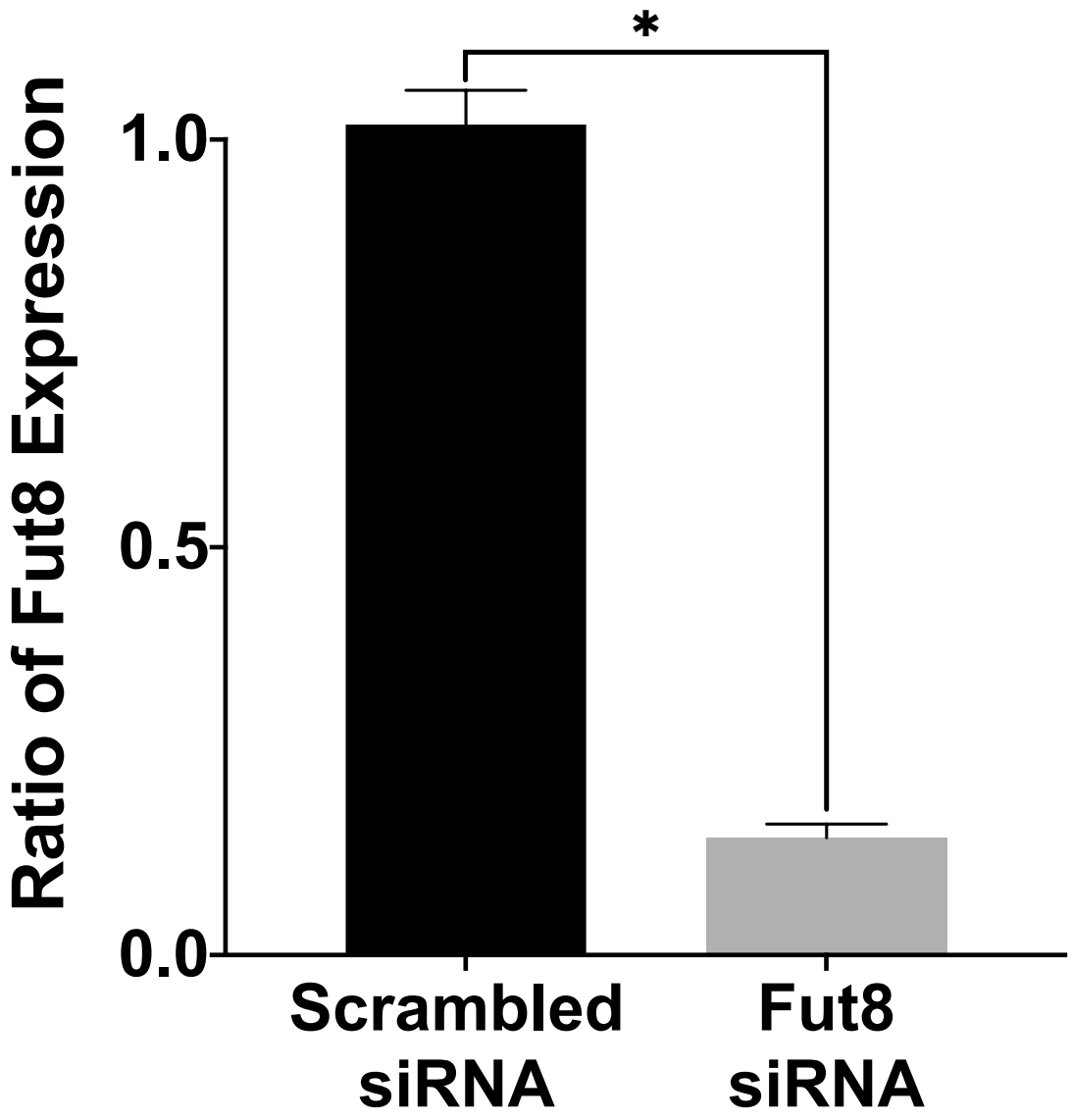


Fig.5.4 Expression of *Fut8* transcript in C3Hs following *Fut8* siRNA knockdown. The relative expression of *Fut8* mRNA levels by qRT-PCR in C3Hs transfected with *Fut8* siRNA (25nM) and scrambled control for 48 h at 37ºC. Data are presented as the ratio of expression relative to the negative control sample transfected with non-targeted (scrambled) siRNA. Error bars based on SEM. Data representative of n=3. * $p < 0.05$

5.3.2 Effect of *Mgat3* and *Fut8* knockdown on global N-glycosylation

GnT-III and Fut8 are critical enzymes in the synthesis of a vast array of N-glycans in mammalian cells. A reduction in expression of either of these enzymes should therefore have a measurable effect on the N-glycosylation profile of a cell's proteome. The ELLA platform was used to detect these changes in N-glycosylation. MVSCs or C3Hs were transfected with siRNA targeting either the *Mgat3* transcript, *Fut8* transcript or a non-specific (Scrambled) control sequence. Cells were incubated at 37^{o}C for 48 h before being harvested and lysed to isolate protein. BCA assay was used to quantify the concentration of protein in each sample before N-glycan analysis was carried out using ELLA. Control wells containing PBS rather than a protein sample were used to determine the baseline for non-specific absorbance and these baseline values were subtracted from sample absorbance values to decipher the true level of specific lectin binding. TBST acted as the vehicle control for all lectins.

There was a significant reduction in lectin binding following *Mgat3* knockdown with both the ConA and E-PHA lectins compared to the Scrambled siRNA control in both MVSCs (Fig.5.5) and C3Hs (Fig.5.6), while no significant reduction in binding was detected with the LCA or WGA lectins. In the case of the *Fut8* knockdown, this led to a significant decrease in LCA binding in both cell lines, while any changes in binding with the other three lectins was statistically insignificant.

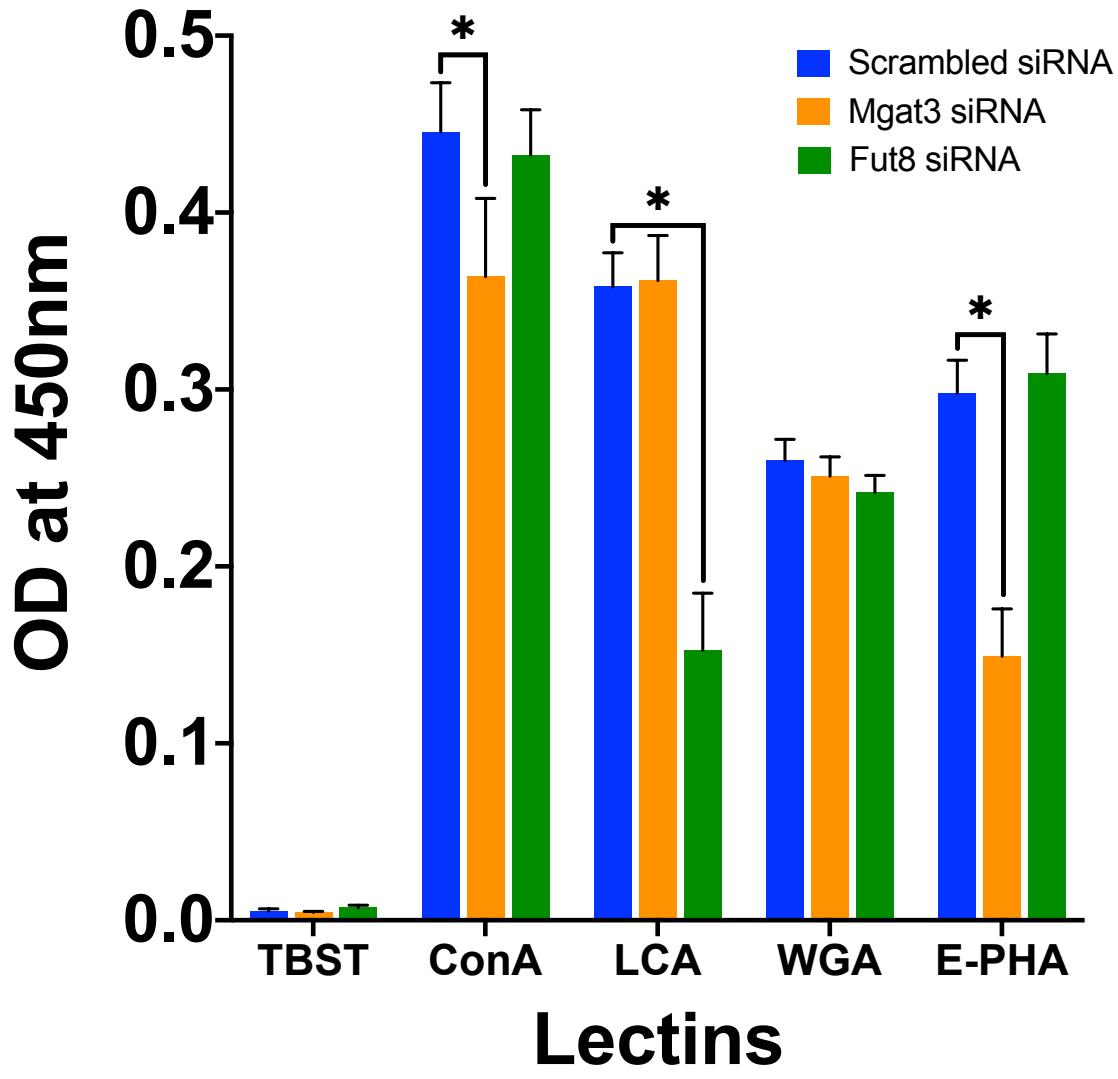


Fig.5.5 Effect of *Mgat3* and *Fut8* knockdowns on N-glycosylation in MVSCs. ELLA analysis of N-glycan specific lectin binding of MVSCs lysates following treatment with *Mgat3* siRNA, *Fut8* siRNA or a scrambled control siRNA (25nM) for 48 h at 37°C. Data are presented as the mean absorbance value at 450nm normalised to the negative control PBS sample. Error bars based on SEM. Data representative of n = 3. *$p < 0.05$

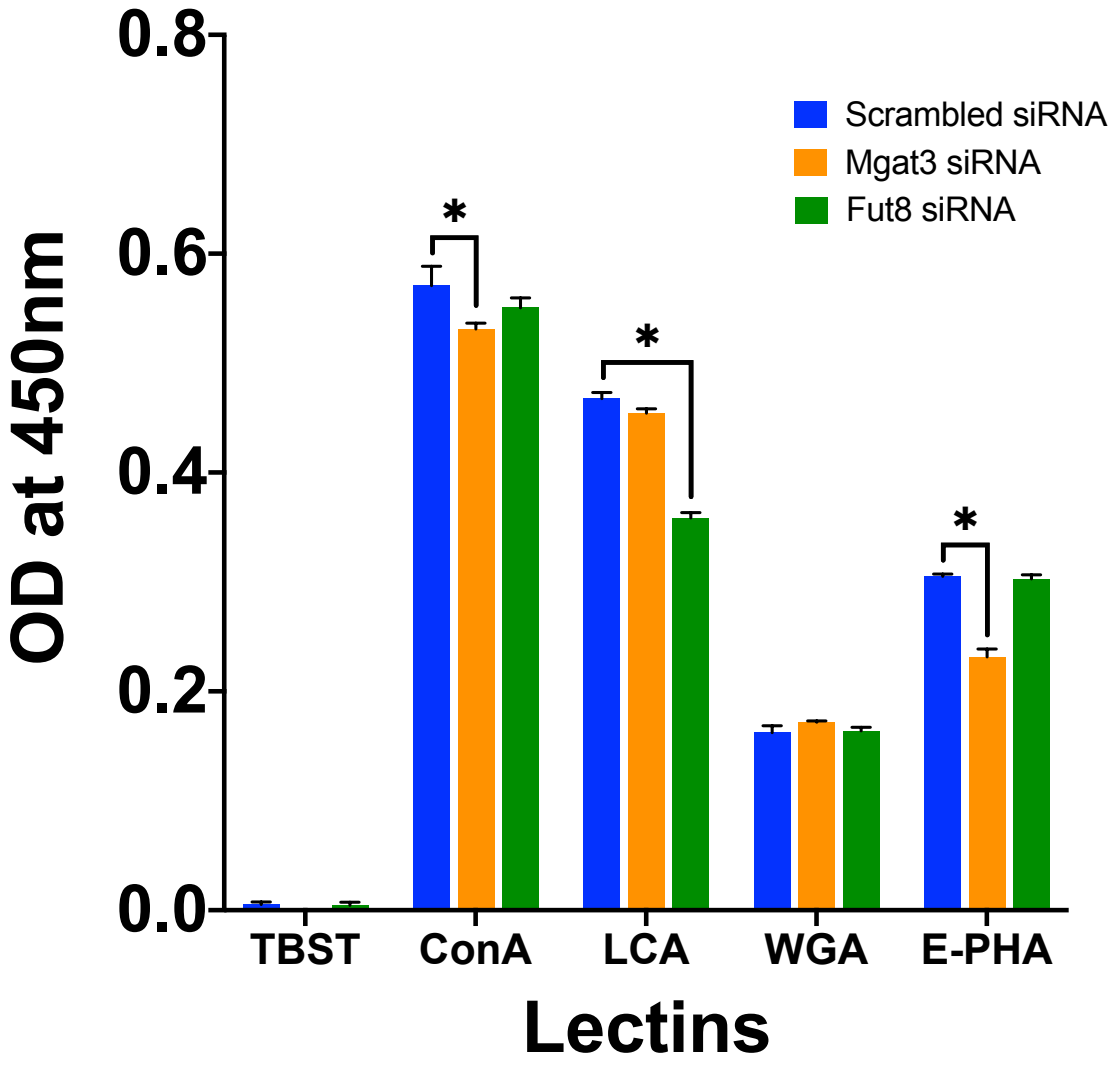


Fig.5.6 Effect of *Mgat3* and *Fut8* knockdowns on N-glycosylation in C3Hs. ELLA analysis of N-glycan specific lectin binding of C3H lysates following treatment with *Mgat3* siRNA, *Fut8* siRNA or a scrambled control siRNA (25nM) for 48 h at 37ºC. Data are presented as the mean absorbance value at 450nm normalised to the negative control PBS sample. Error bars based on SEM. Data representative of n = 3. *p < 0.05

5.3.3 Effect of *Mgat3* and *Fut8* knockdown on Notch1 N-glycosylation

After establishing the effect of *Mgat3* and *Fut8* knockdowns on the N-glycosylation of a whole cell lysate, the next step was to determine their effect on the N-glycan profile of the purified Notch1 receptor. MVSCs were grown to ~80% confluence in four T25 flasks. One of the flasks was left untreated while the other three were transfected with siRNA targeting either the *Mgat3* transcript, *Fut8* transcript or a non-specific (Scrambled) control sequence. Cells were incubated at 37^{o}C for 48 h before being harvested and lysed to isolate protein. BCA assay was used to quantify the concentration of protein in each sample. IP was carried out on all samples using Protein A-conjugated magnetic beads and an anti-Notch1 rabbit monoclonal antibody (3608S). The non-transfected sample was immunoprecipitated with a rabbit IgG control antibody. Following elution and neutralisation, using Glycine and Tris buffers respectively, another BCA assay was carried out to quantify protein concentration in the eluted fraction. ELLA was then used to detect N-glycans in all four samples. Control wells containing PBS rather than a protein sample were used to determine the baseline for non-specific absorbance, while the rabbit IgG control sample acted as the baseline for non-specific lectin- or antibody-binding to the IP eluate. Both of these baseline values were subtracted from sample absorbance values to decipher the true level of specific lectin binding. TBST acted as the vehicle control for all lectins. *Mgat3* knockdown resulted in a significant reduction in binding of both the ConA and E-PHA lectins compared to the Scrambled siRNA control, while no significant reduction in binding was detected with the LCA or WGA lectins (Fig.5.7). Meanwhile, *Fut8* knockdown led to significant decreases in ConA and LCA binding, but not in WGA or E-PHA binding (Fig.5.7).

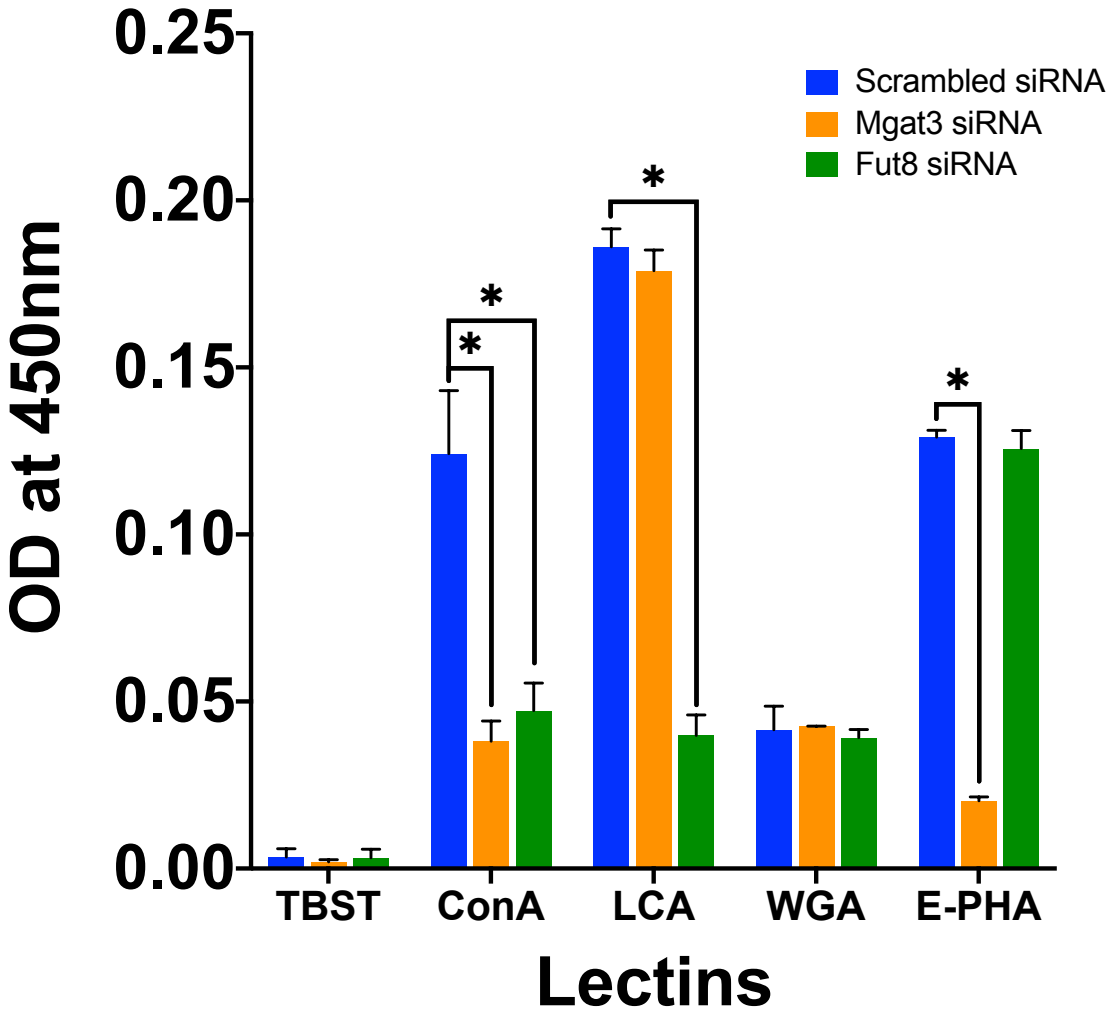


Fig.5.7 Effect of *Mgat3* and *Fut8* knockdowns on N-glycosylation of the Notch1 receptor. ELLA analysis of N-glycan specific lectin binding of the Notch1 receptor from MVSCs lysates following treatment with *Mgat3* siRNA, *Fut8* siRNA or a scrambled control siRNA (25nM) for 48 h at 37°C. Notch1 protein was purified from cell lysates using protein A-conjugated magnetic beads. Data are presented as the mean absorbance value at 450nm normalised to the negative control PBS sample and the IgG immunoprecipitation control. Error bars based on SEM. Data representative of n = 3, *p < 0.05

5.3.4 *Mgat3* knockdown in Jag-1-stimulated MVSCs and C3Hs

Having confirmed its effect on Notch1 N-glycosylation, the next step was to investigate if *Mgat3* knockdown affected Jag-1-mediated Notch signalling and myogenic differentiation. MVSCs or C3Hs were seeded into Jag-1- or Fc-coated wells and incubated overnight at 37ºC. The following day cells were transfected with *Mgat3* siRNA or a Scrambled control siRNA and were incubated for a further 48 h at 37ºC. Cells were harvested and RNA was isolated from each sample as per Section 2.2.8. qRT-PCR was used to evaluate the change in expression of the Notch target gene *Hey1* and the myogenic marker *Myh11.*

There was a substantial increase in *Hey1* expression in the sample treated with Jag-1 as compared to the Fc-treated control in both MVSCs (Fig.5.8) and C3Hs (Fig.5.9), respectively. This effect was then significantly decreased by *Mgat3* knockdown. Similarly, there was a substantial increase in *Myh11* expression in the sample treated with Jag-1 as compared to the Fc-treated control in both MVSCs (Fig.5.10) and C3Hs (Fig.5.11), respectively. This increase in *Myh11* expression following Jag-1 treatment was attenuated following *Mgat3* knockdown (Fig.5.10 and 5.11).

5.3.5 *Fut8* knockdown in Jag-1-stimulated MVSCs and C3Hs

Once its effect on Notch1 N-glycosylation had been determined, the next step was to investigate if *Fut8* knockdown affected Jag-1-mediated Notch signalling and myogenic differentiation. MVSCs or C3Hs were seeded into Jag-1- or Fc-coated wells and incubated overnight at 37ºC. The following day cells were transfected with *Fut8* siRNA or a Scrambled control siRNA and were incubated for a further 48 h at 37ºC. Cells were harvested and RNA was isolated from each sample as per Section 2.2.8. qRT-PCR was used to evaluate the change in expression of the Notch target gene *Hey1* and the myogenic marker *Myh11*.

There was a substantial increase in *Hey1* expression in the sample treated with Jag-1 as compared to the Fc-treated control, in both MVSCs (Fig.5.12) and C3Hs (Fig.5.13), respectively. This effect was then significantly decreased by *Fut8* knockdown. Similarly, there was a substantial increase in *Myh11* expression in the sample treated with Jag-1 as compared to the Fc-treated control in both MVSCs (Fig.5.14) and C3Hs (Fig.5.15), respectively. This increase in *Myh11* expression following Jag-1 treatment was attenuated following *Fut8* knockdown (Fig.5.14 and 5.15).

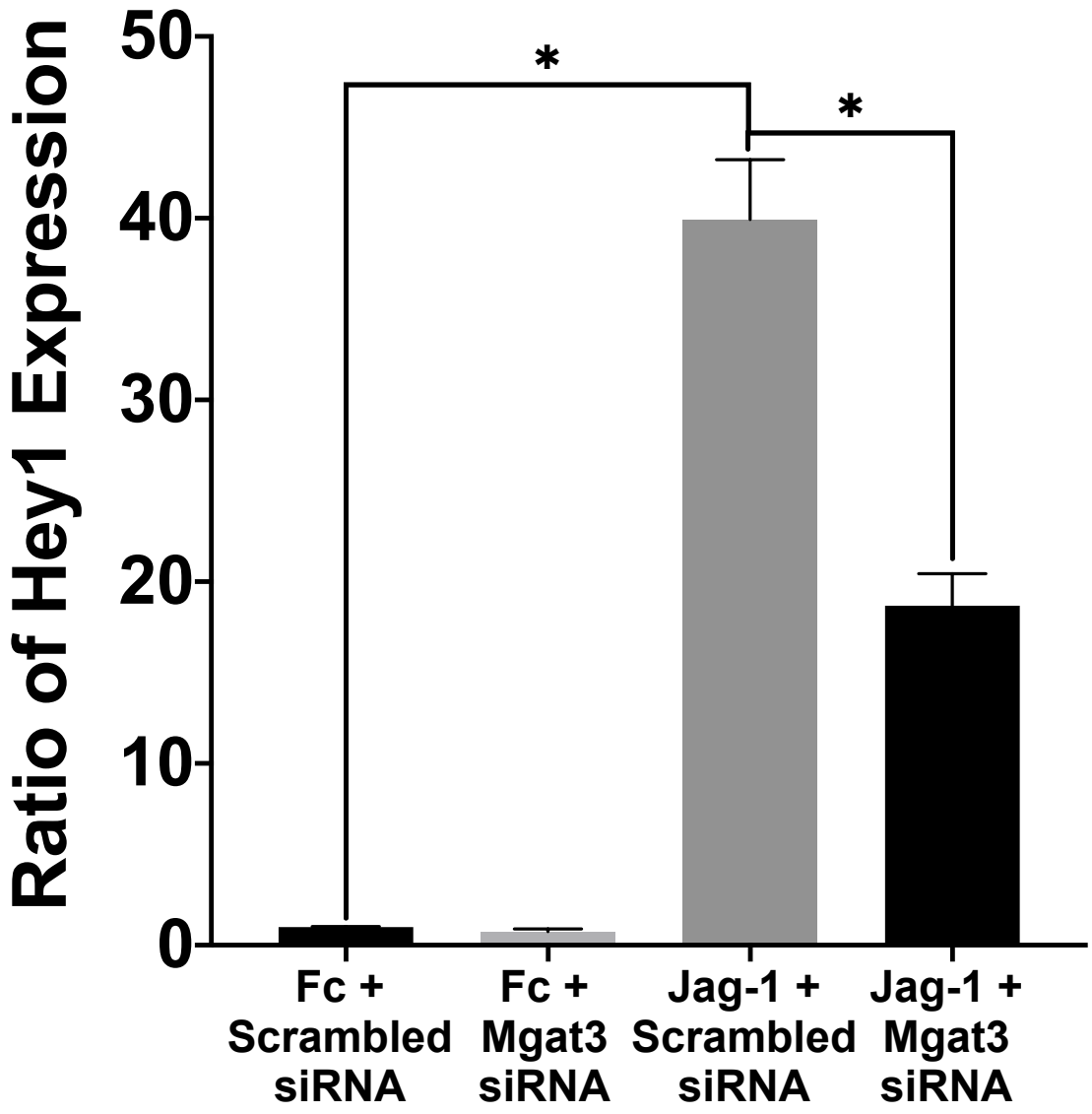


Fig.5.8 Effect of *Mgat3* knockdown on *Hey1* expression in Jag1-treated MVSCs. The relative expression of Jag1 (1μg/mL) stimulated *Hey1* mRNA levels by qRT-PCR in MVSCs following treatment with *Mgat3* siRNA (25nM) and the scrambled control for 48 h at 37°C. Data are presented as the ratio of expression relative to the negative control sample treated with Fc and transfected with non-targeted (scrambled) siRNA. Error bars based on SEM. Data representative of n=3. * $p < 0.05$

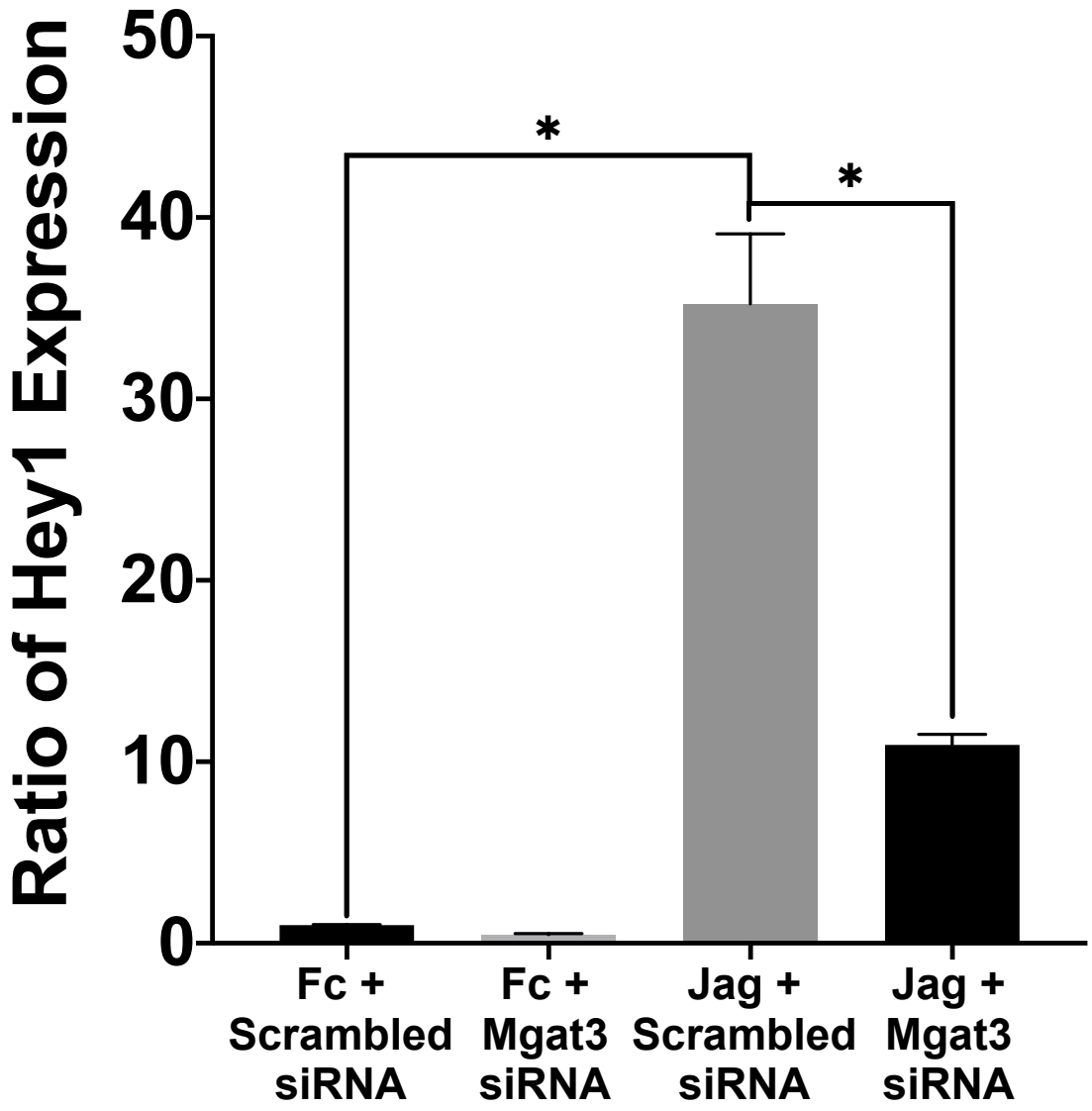


Fig.5.9 Effect of *Mgat3* knockdown on *Hey1* expression in Jag1-treated C3Hs. The relative expression of Jag-1 stimulated *Hey1* mRNA levels by qRT-PCR in C3Hs following treatment with *Mgat3* siRNA (25nM) and the scrambled control for 48 h at 37^{o}C. Data are presented as the ratio of expression relative to the negative control sample treated with Fc and transfected with non-targeted (scrambled) siRNA. Error bars based on SEM. Data representative of n=3. * $p < 0.05$

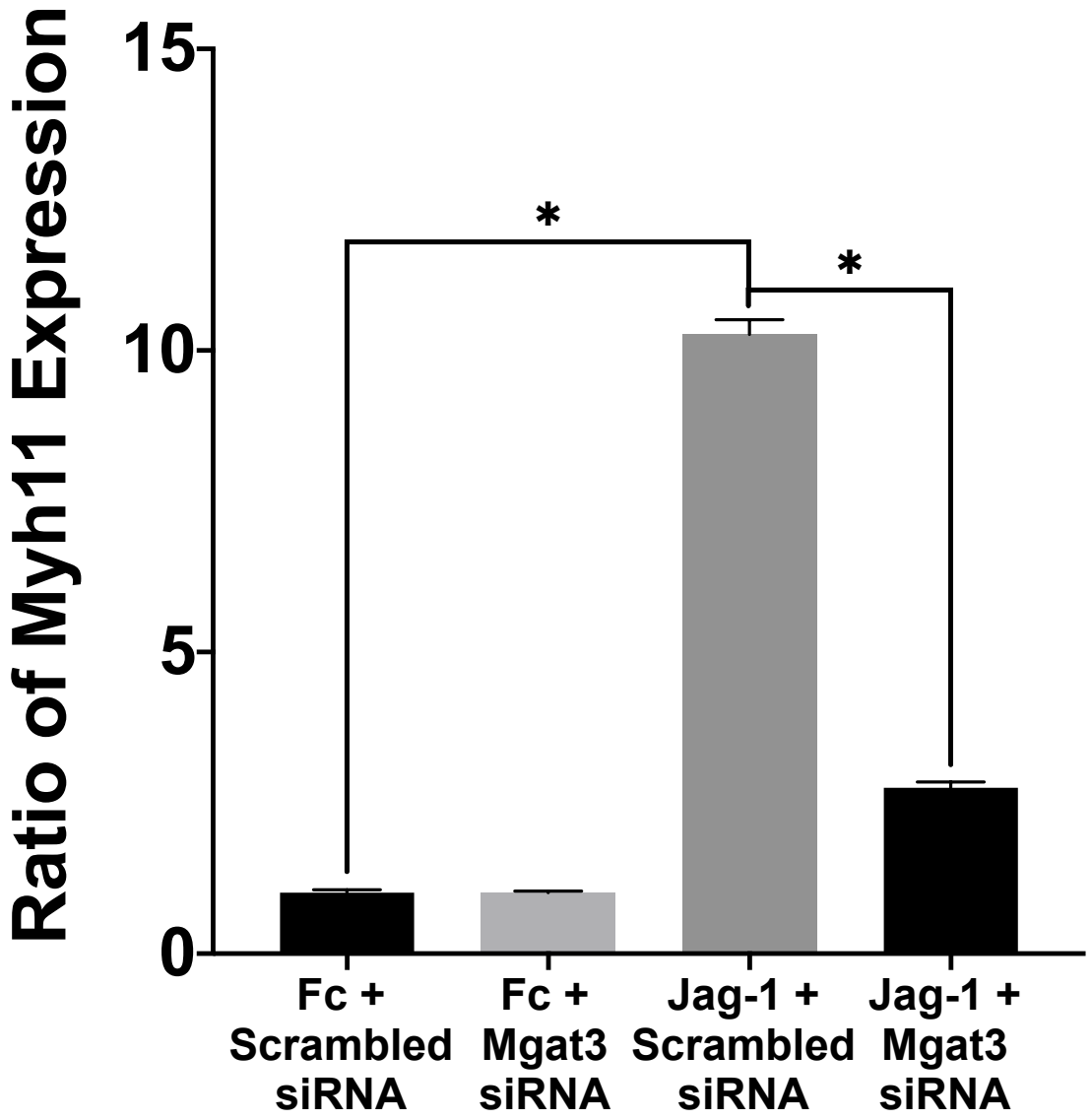


Fig.5.10 Effect of *Mgat3* knockdown on *Myh11* expression in Jag1-treated MVSCs. The relative expression of Jag-1 stimulated *Myh11* mRNA levels by qRT-PCR in MVSCs following treatment with *Mgat3* siRNA (25nM) and the scrambled control for 48 h at 37°C. Data are presented as the ratio of expression relative to the negative control sample treated with Fc and transfected with non-targeted (scrambled) siRNA. Error bars based on SEM. Data representative of n=3. * $p < 0.05$

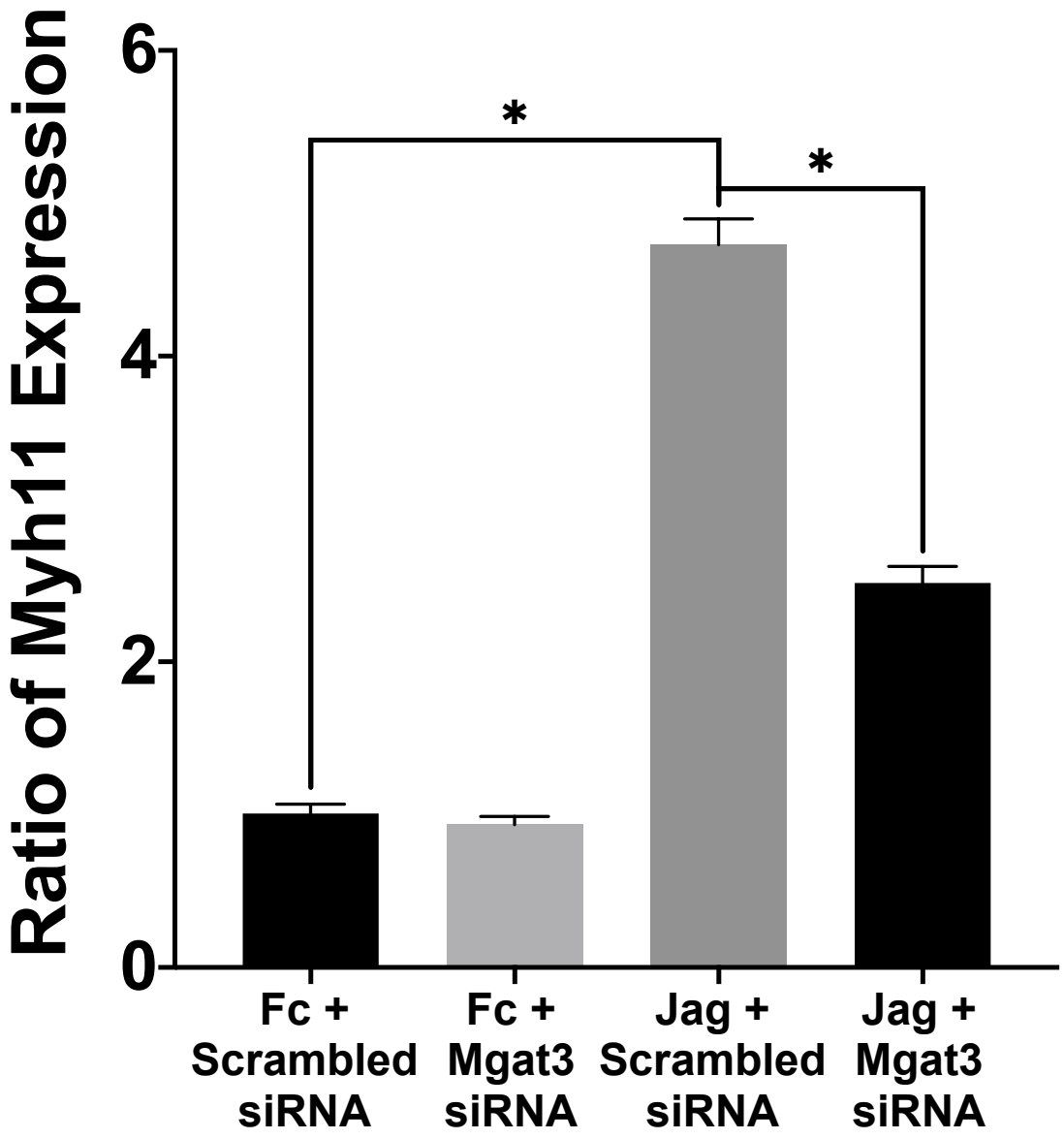


Fig.5.11 Effect of *Mgat3* knockdown on *Myh11* expression in Jag1-treated C3Hs. The relative expression of Jag-1 stimulated *Myh11* mRNA levels by qRT-PCR in C3Hs following treatment with *Mgat3* siRNA (25nM) and the scrambled control for 48 h at 37°C. Data are presented as the ratio of expression relative to the negative control sample treated with Fc and transfected with non-targeted (scrambled) siRNA. Error bars based on SEM. Data representative of n=3. * $p < 0.05$

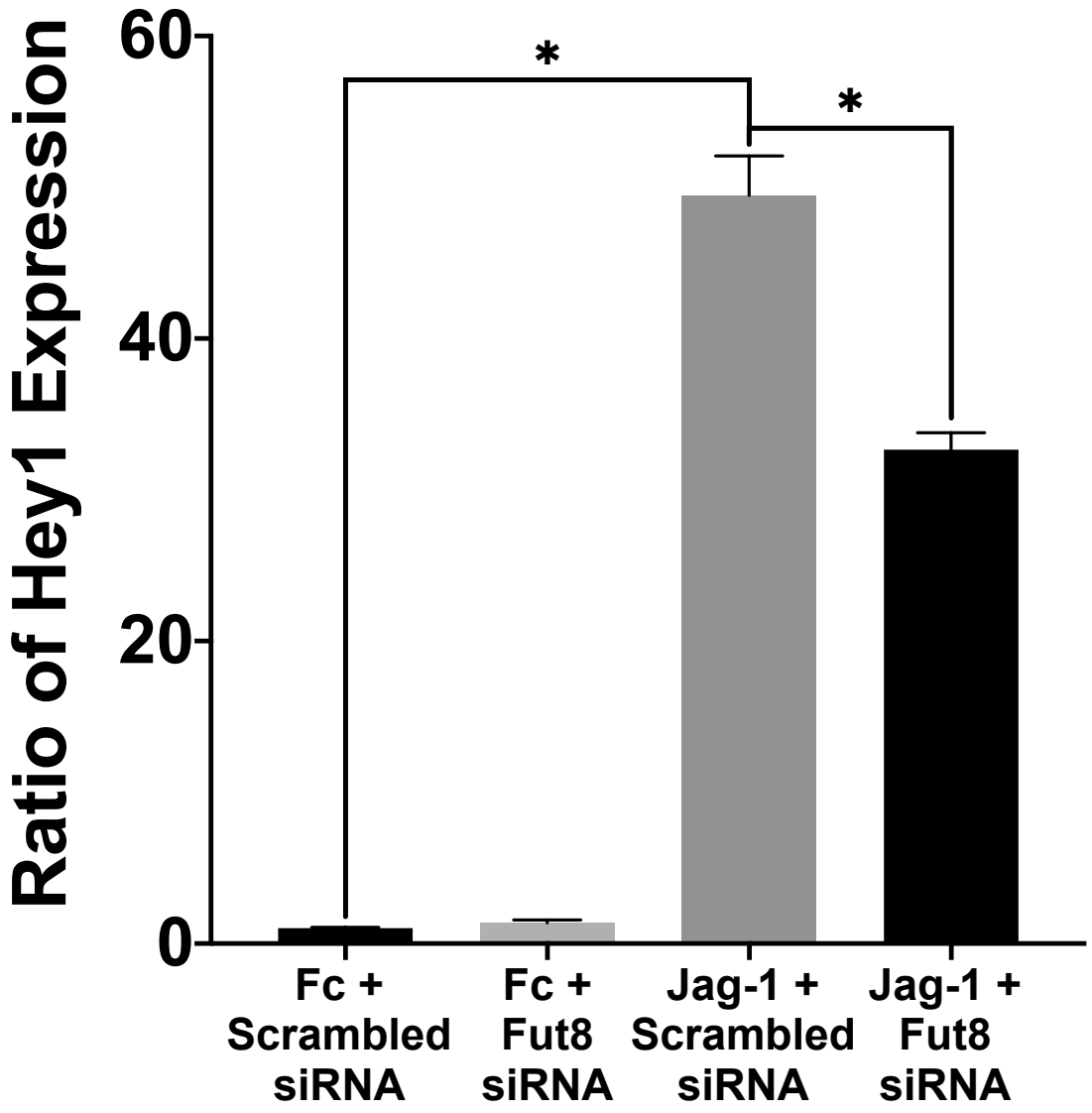


Fig.5.12 Effect of *Fut8* knockdown on *Hey1* expression in Jag1-treated MVSCs. The relative expression of Jag-1 stimulated *Hey1* mRNA levels by qRT-PCR in MVSCs following treatment with *Fut8* siRNA (25nM) and the scrambled control for 48 h at 37ºC Data are presented as the ratio of expression relative to the negative control sample treated with Fc and transfected with non-targeted (scrambled) siRNA. Error bars based on SEM. Data representative of n=3. * $p < 0.05$

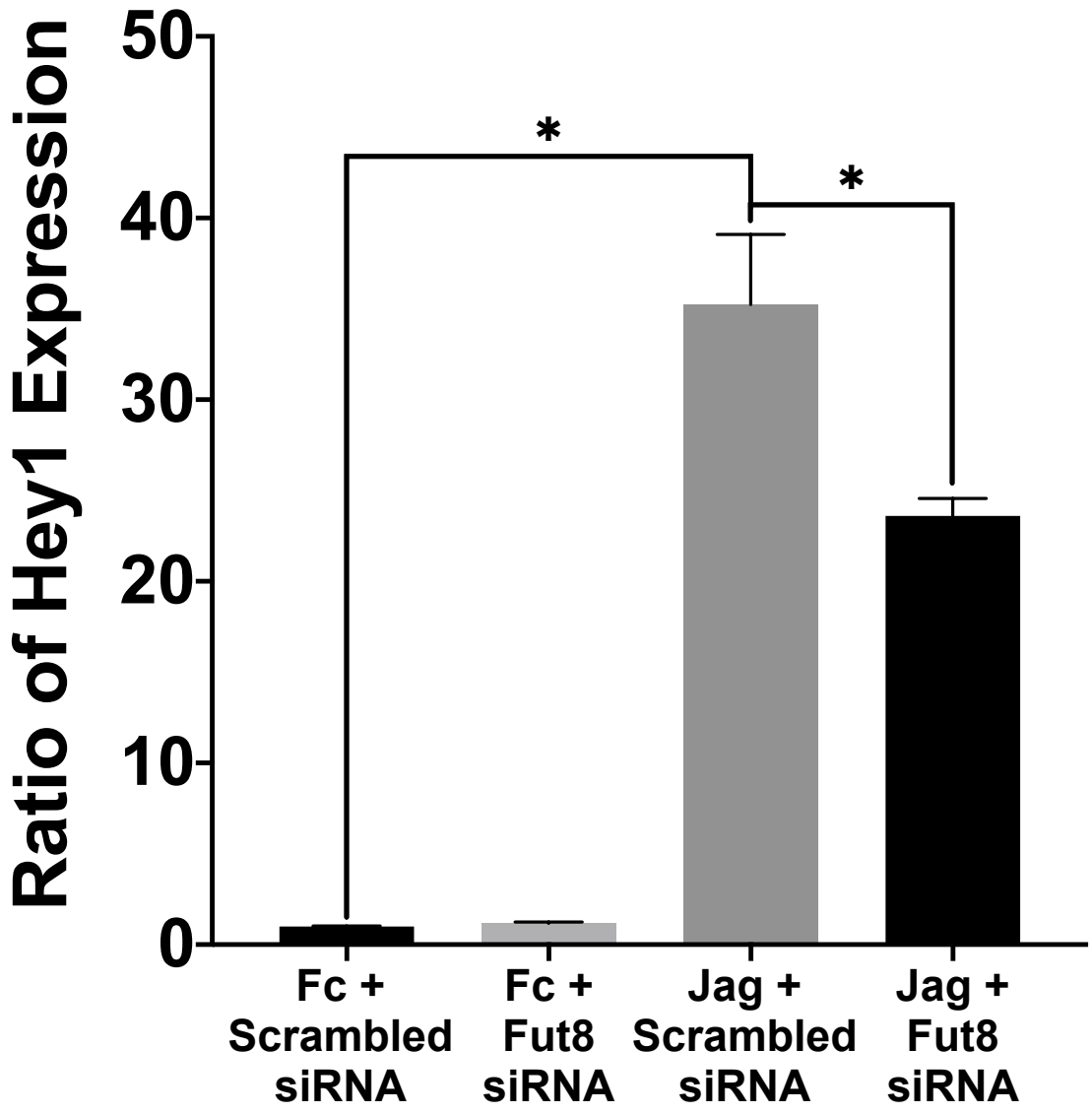


Fig.5.13 Effect of *Fut8* knockdown on *Hey1* expression in Jag1-treated C3Hs. The relative expression of Jag-1 stimulated *Hey1* mRNA levels by qRT-PCR in C3H cells following treatment with *Fut8* siRNA (25nM) and the scrambled control for 48 h at 37ºC Data are presented as the ratio of expression relative to the negative control sample treated with Fc and transfected with non-targeted (scrambled) siRNA. Error bars based on SEM. Data representative of n=3, * $p < 0.05$

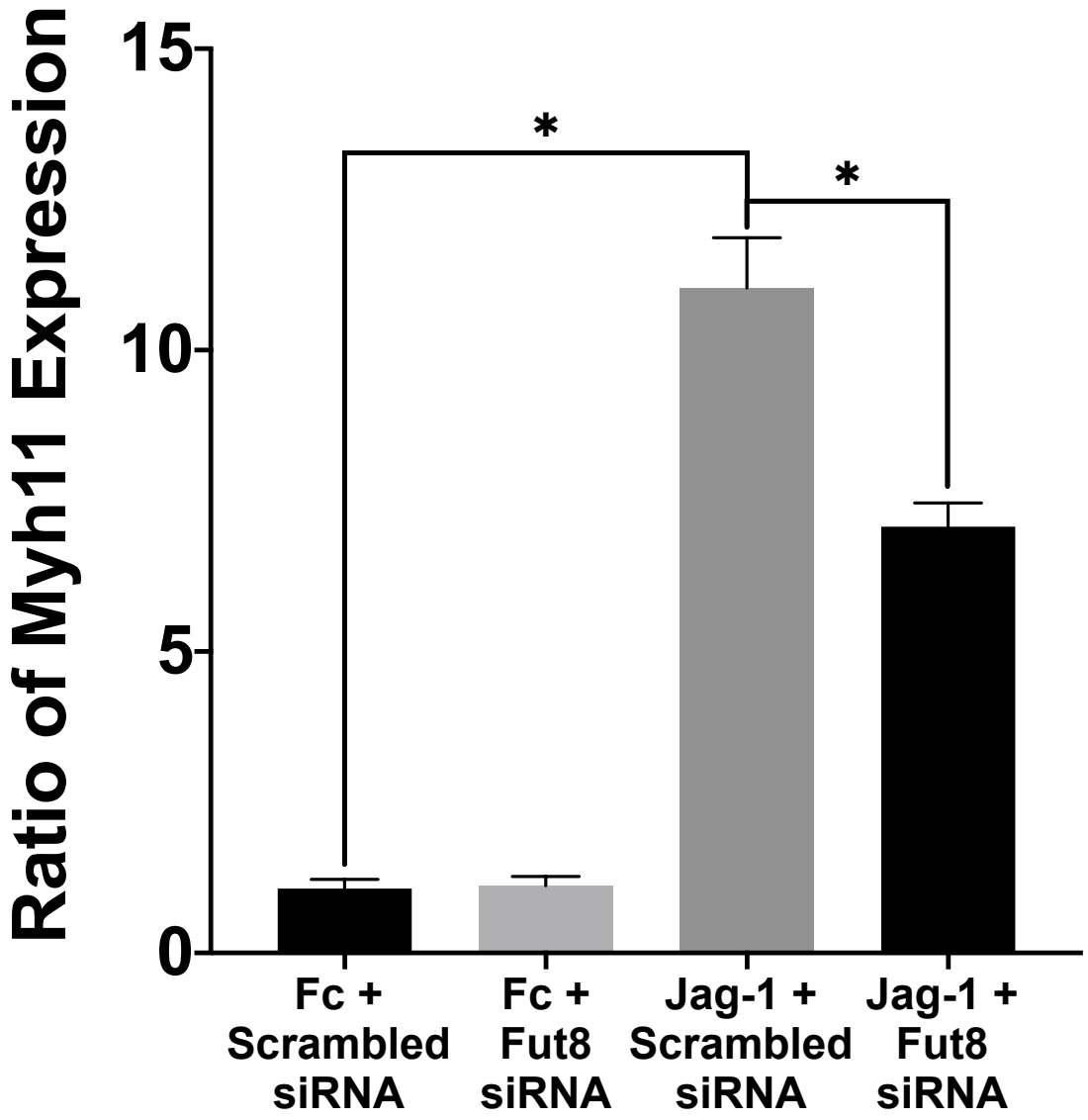


Fig.5.14 Effect of *Fut8* knockdown on *Myh11* expression in Jag1-treated MVSCs. The relative expression of Jag-1 stimulated *Myh11* mRNA levels by qRT-PCR in MVSCs following treatment with *Fut8* siRNA (25nM) and the scrambled control for 48 h at 37ºC. Data are presented as the ratio of expression relative to the negative control sample treated with Fc and transfected with non-targeted (scrambled) siRNA. Error bars based on SEM. Data representative of n=3. * $p < 0.05$

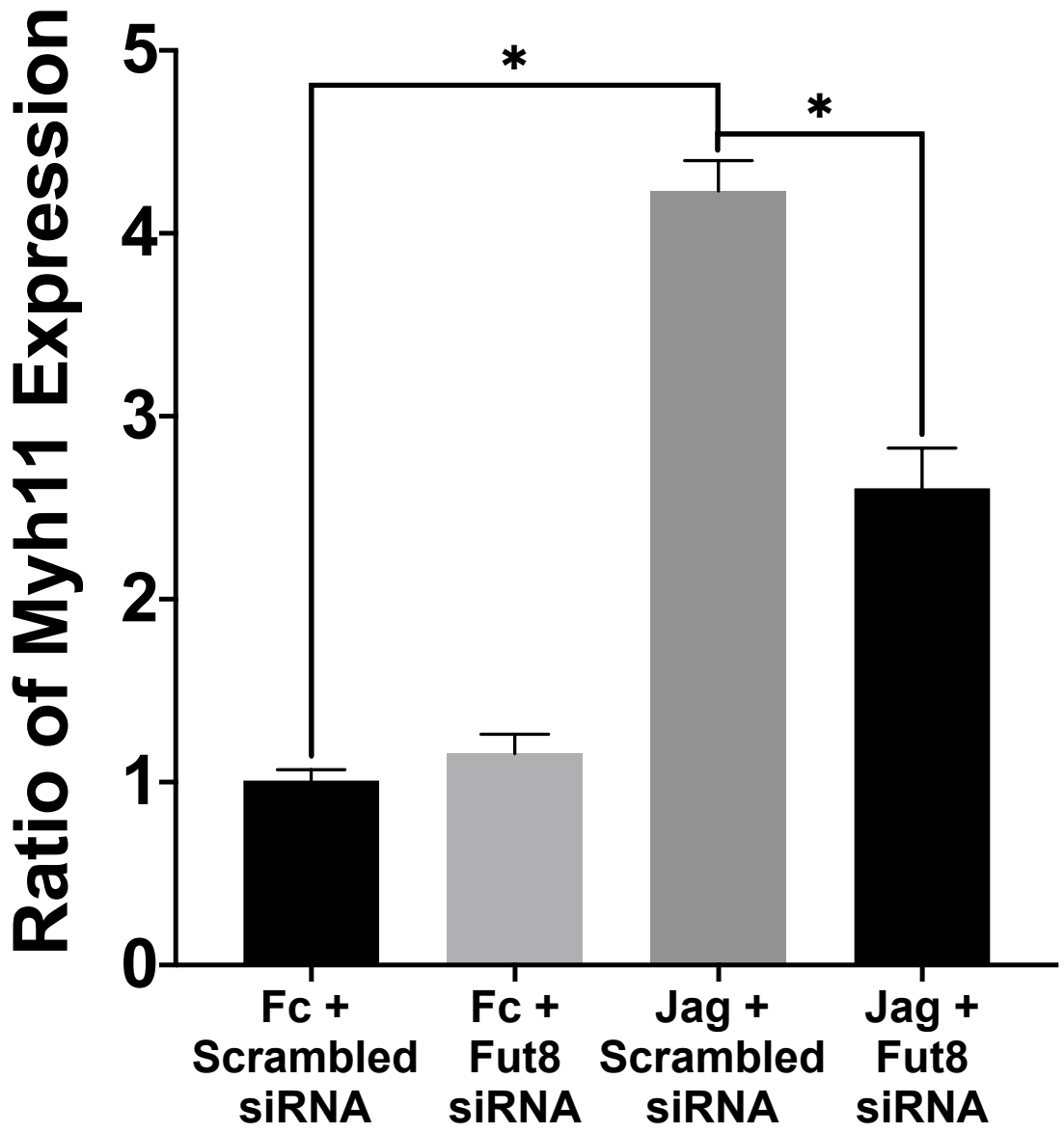


Fig.5.15 Effect of *Fut8* knockdown on *Myh11* expression in Jag1-treated C3Hs. The relative expression of Jag-1 stimulated *Myh11* mRNA levels by qRT-PCR in C3H cells following treatment with *Fut8* siRNA (25nM) and the scrambled control for 48 h at 37ºC. Data are presented as the ratio of expression relative to the negative control sample treated with Fc and transfected with non-targeted (scrambled) siRNA. Error bars based on SEM. Data representative of n=3, * $p < 0.05$

5.3.6 *Mgat3* and *Fut8* Knockdown in NICD-stimulated MVSCs

Ectopically expressed NICD can activate Notch signalling independent of ligand binding. This process could be exploited to determine whether *Mgat3* and *Fut8* knockdowns were having an effect on Notch pathway elements downstream of receptor activation. MVSCs were co-transfected with either the NICD-coding plasmid or an empty vector control, and either *Mgat3* siRNA, *Fut8* siRNA or Scrambled control siRNA using the TransIT-X2 Dynamic Delivery System. Cells were incubated at 37ºC for 48 h. RNA was isolated from all samples and qRT-PCR was carried out to measure the expression of *Hey1* and *Myh11*. The ectopically expressed NICD consistently increased the expression of the both the Notch target gene *Hey1* myogenic marker *Myh11* compared to the empty vector control. No significant change to this response was detected following *Mgat3* or *Fut8* knockdown (Fig.5.16 - 5.19).

5.3.7 Effect of *Mgat3* and *Fut8* Knockdowns on Notch1 Expression in MVSCs

A change in baseline Notch1 expression in a cell population is very likely to have an effect on the expression of downstream target gene expression. Therefore, it was necessary to determine whether knockdowns of *Mgat3* and *Fut8* were affecting this baseline expression level. MVSCs were transfected with either *Mgat3* siRNA, *Fut8* siRNA or Scrambled control siRNA using the TransIT-X2 Dynamic Delivery System. Cells were incubated at 37ºC for 48 h. RNA and protein were isolated from all samples and their concentrations quantified using the Nanodrop® ND-1000 Spectrophotometer and a BCA assay respectively. qRT-PCR was carried out to measure the expression of *Notch1* transcript, while western blot was used to measure Notch1 protein expression. Densitometry was carried out on western blot samples to measure intensity of Notch1 bands relative to the β-actin loading control. No significant change was detected in *Notch1* transcript expression following either knockdown (Fig.5.20). Similarly, the Fut8 knockdown displayed no significant effect on protein expression compared to the Scrambled siRNA control. However, a significant reduction was observed in Notch1 protein levels following *Mgat3* knockdown (Fig.5.21).

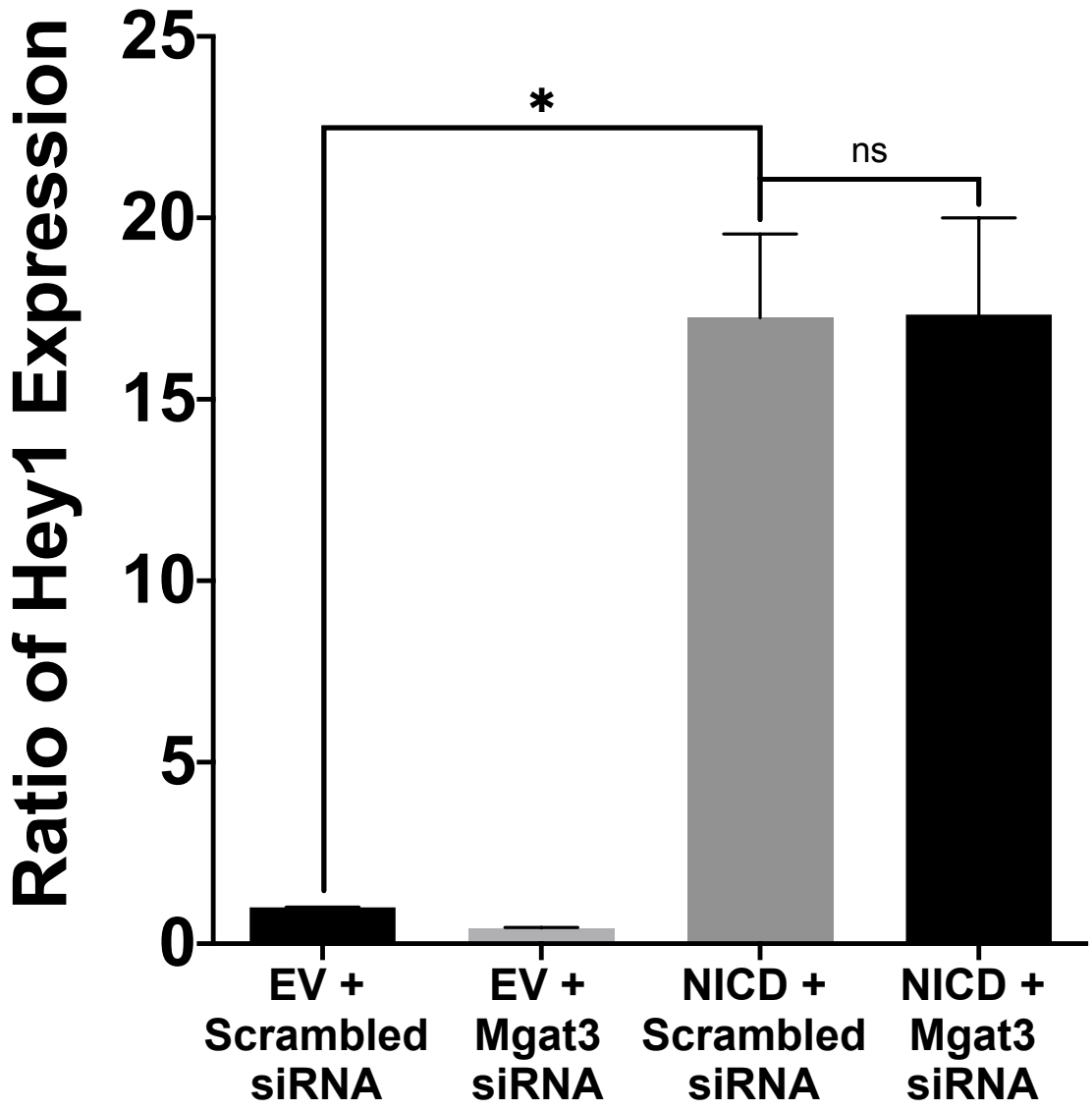


Fig.5.16 Effect of *Mgat3* knockdown on NICD-activated *Hey1* expression in MVSCs. The relative expression of NICD stimulated *Hey1* mRNA levels by qRT-PCR in MVSCs co-transfected with NICD plasmid and *Mgat3* siRNA (25nM) or the scrambled control for 48 h at 37ºC. Data are presented as the ratio of expression relative to the negative control sample co-transfected with empty vector plasmid and a non-targeted (scrambled) siRNA. Error bars based on SEM. Data representative of n=3. * $p < 0.05$. ns – $p > 0.05$.

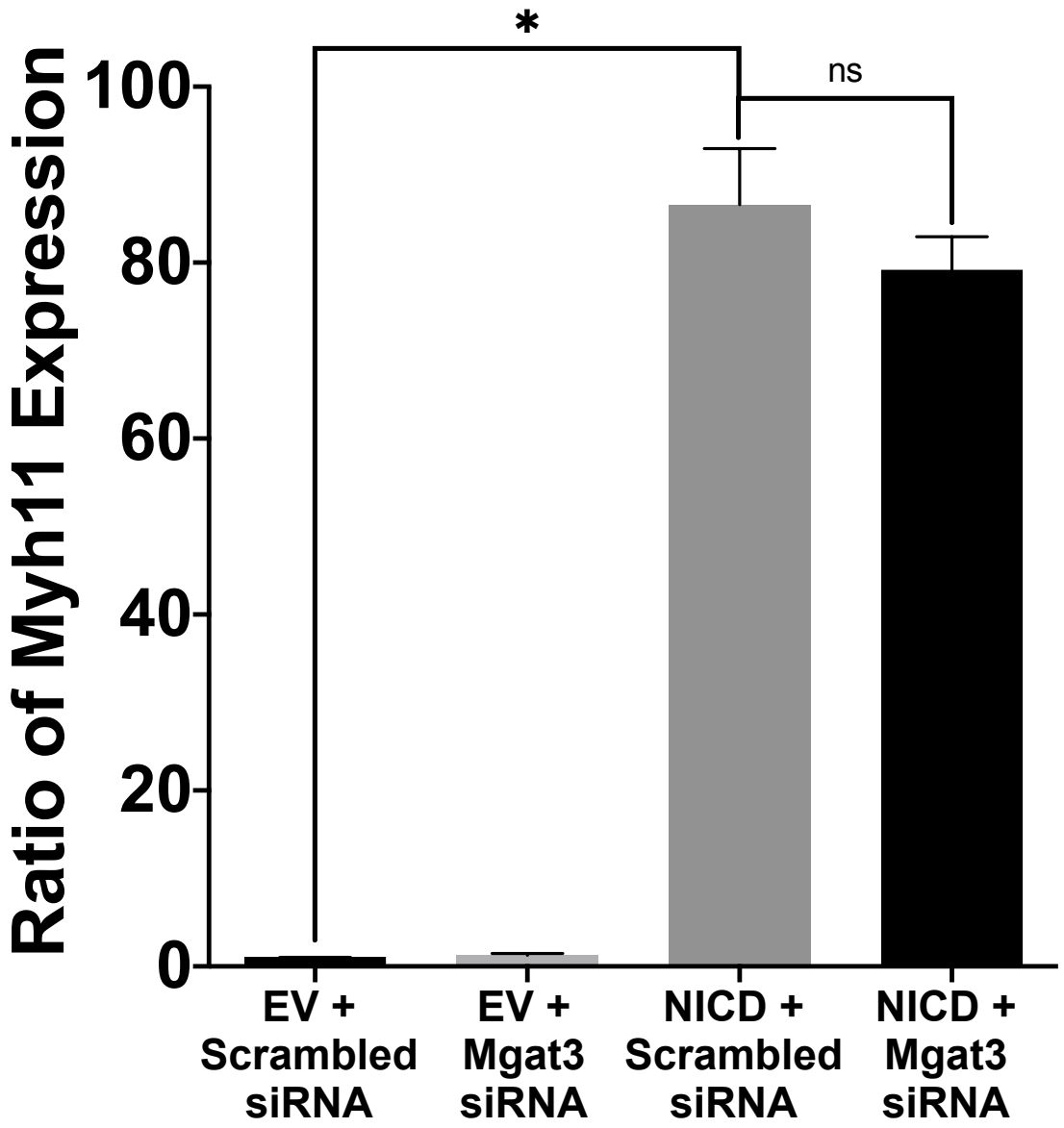


Fig.5.17 Effect of *Mgat3* knockdown on NICD-activated *Myh11* expression in MVSCs. The relative expression of NICD stimulated *Myh11* mRNA levels by qRT-PCR in MVSCs co-transfected with NICD plasmid and *Mgat3* siRNA (25nM) or the scrambled control for 48 h at 37ºC. Data are presented as the ratio of expression relative to the negative control sample co-transfected with empty vector plasmid and a non-targeted (scrambled) siRNA. Error bars based on SEM. Data representative of n=3. * $p < 0.05$. ns – $p > 0.05$.

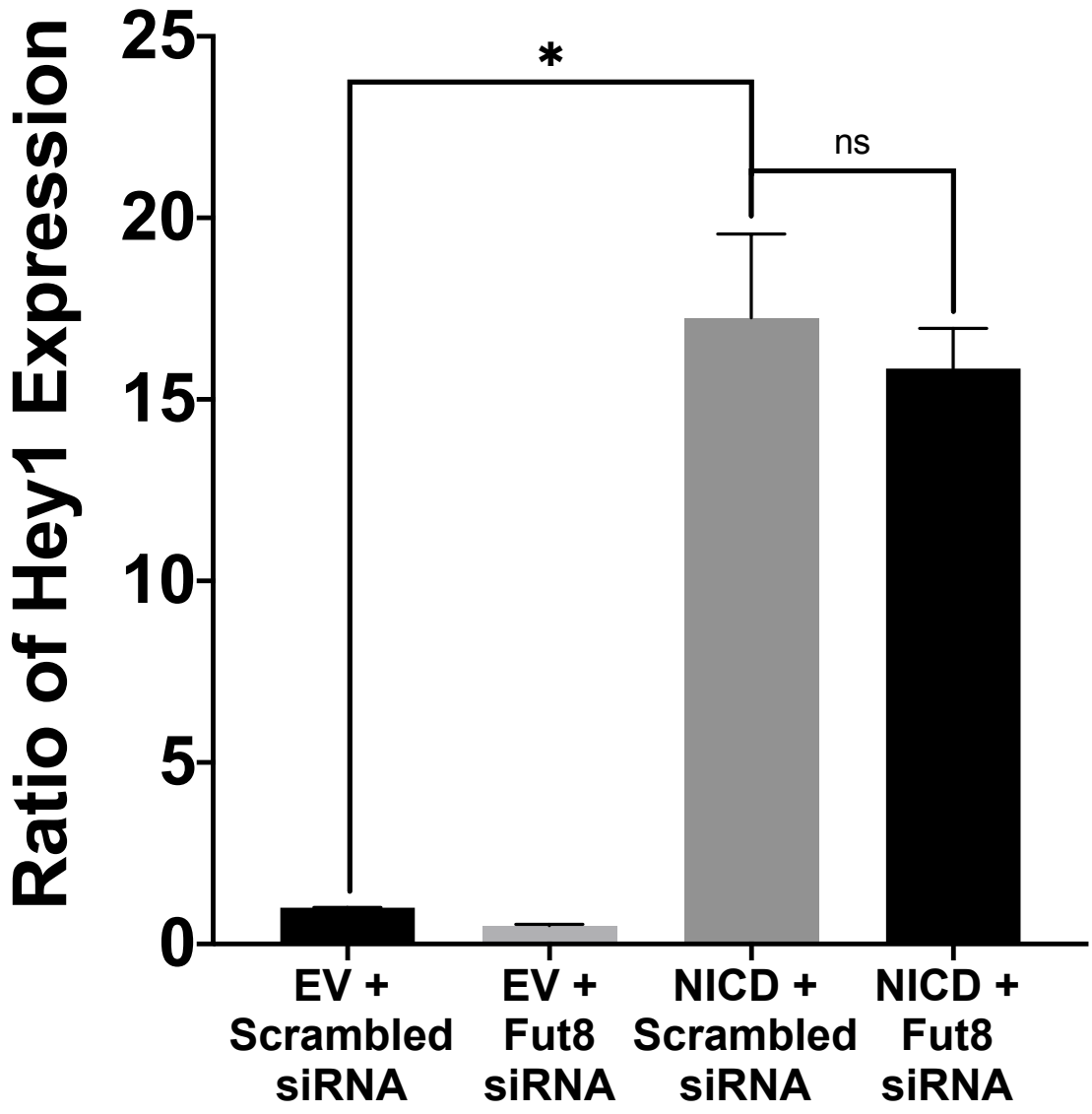


Fig.5.18 Effect of *Fut8* knockdown on NICD-activated *Hey1* expression in MVSCs. The relative expression of NICD stimulated *Hey1* mRNA levels by qRT-PCR in MVSCs co-transfected with NICD plasmid and *Fut8* siRNA (25nM) or the scrambled control for 48 h at 37°C. Data are presented as the ratio of expression relative to the negative control sample co-transfected with empty vector plasmid and a non-targeted (scrambled) siRNA. Error bars based on SEM. Data representative of n=3. * $p < 0.05$. ns – $p > 0.05$.

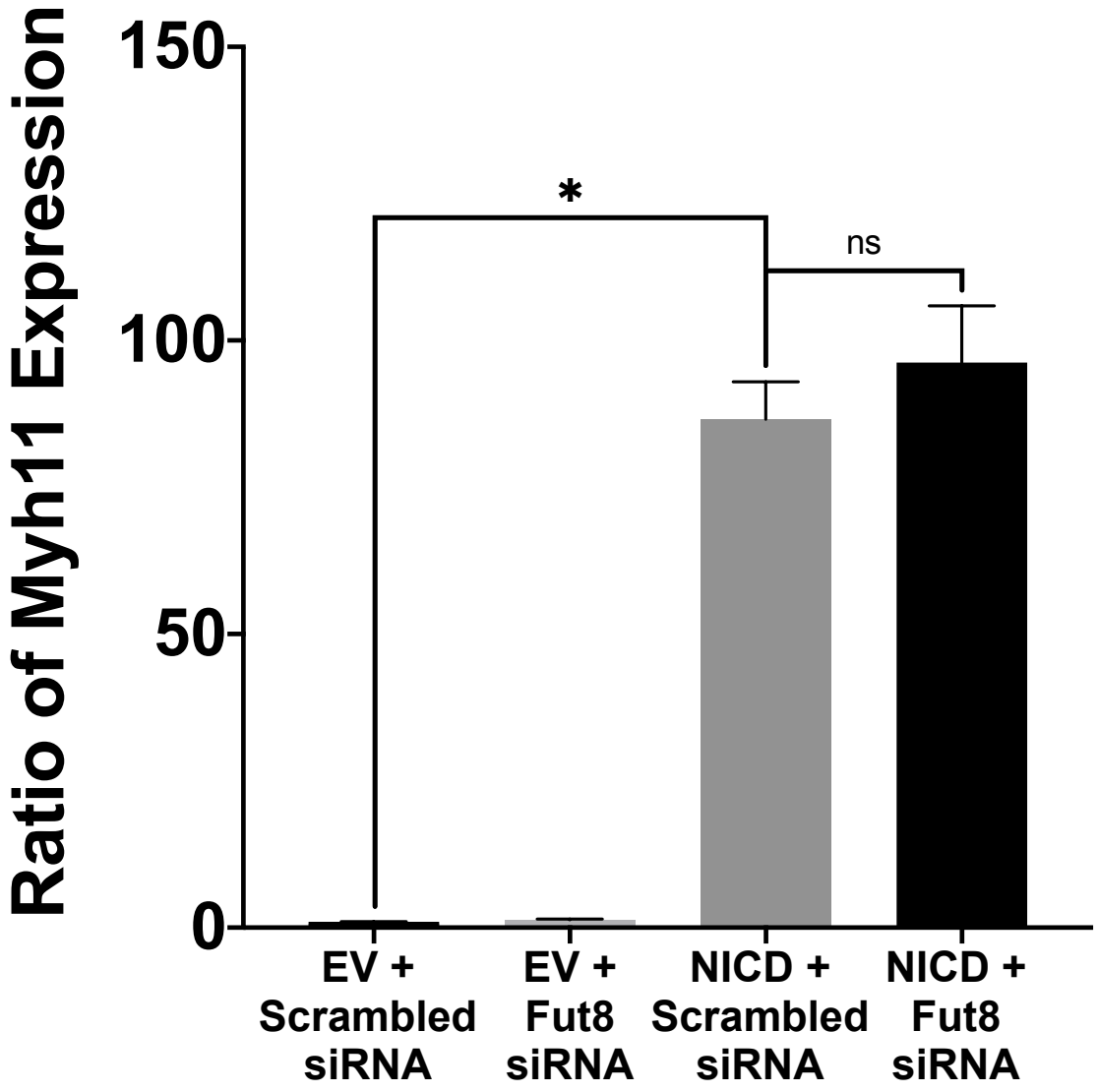


Fig.5.19 Effect of *Fut8* knockdown on NICD-activated *Myh11* expression in MVSCs. The relative expression of NICD stimulated *Myh11* mRNA levels by qRT-PCR in MVSCs co-transfected with NICD plasmid and *Fut8* siRNA (25nM) or the scrambled control for 48 h at 37^{o}C. Data are presented as the ratio of expression relative to the negative control sample co-transfected with empty vector plasmid and a non-targeted (scrambled) siRNA. Error bars based on SEM. Data representative of n=3. * $p < 0.05$. ns – $p > 0.05$.

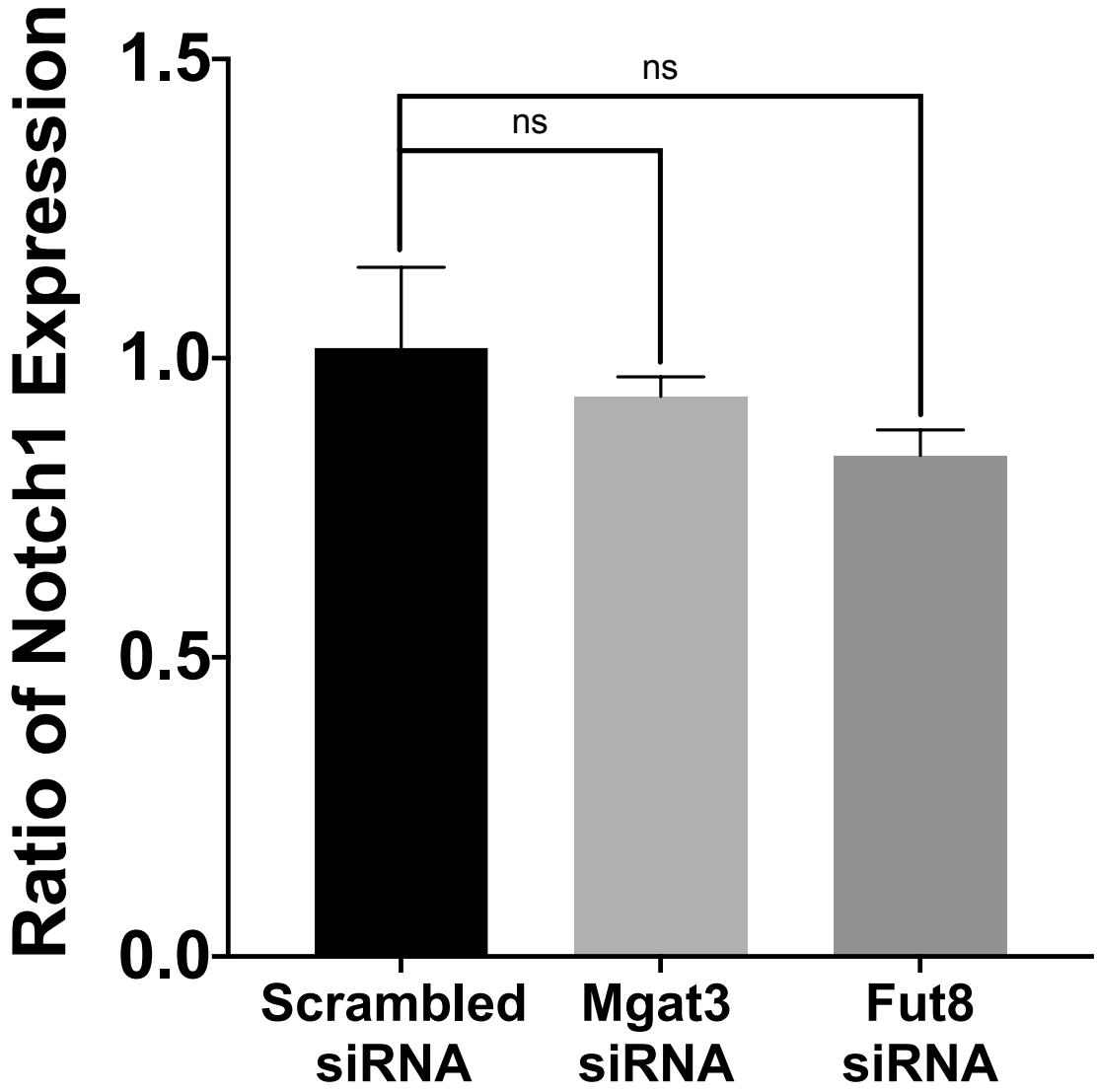


Fig.5.20 Effect of *Mgat3* and *Fut8* knockdowns on *Notch1* transcript expression in MVSCs. The relative expression of *Notch1* mRNA levels by qRT-PCR in MVSCs transfected with *Mgat3* or *Fut8* siRNA (25nM) and the scrambled control for 48 h at 37ºC. Data are presented as the ratio of expression relative to the negative control sample transfected with a scrambled siRNA. Error bars based on SEM. Data representative of n=3. ns – $p > 0.05$

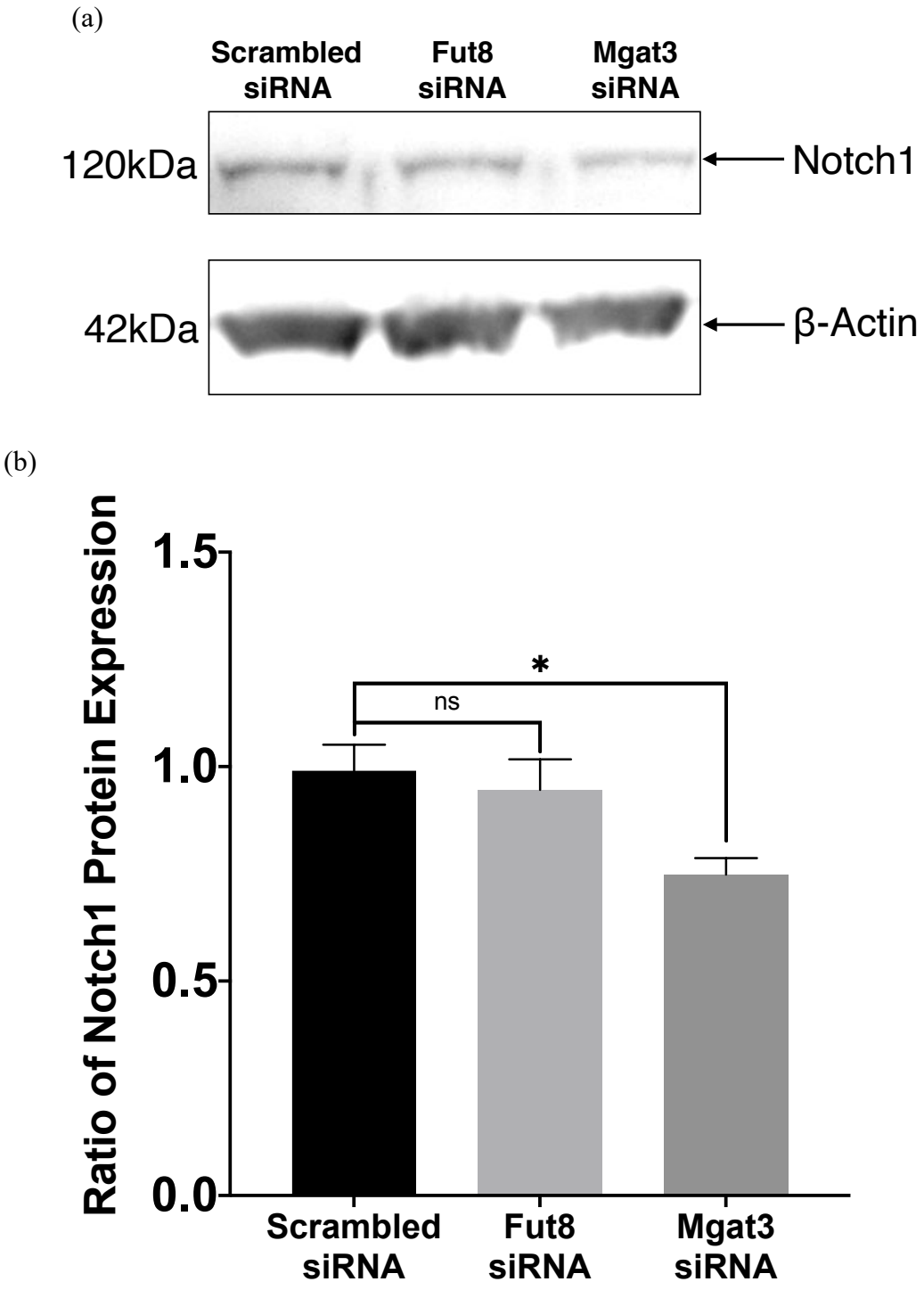


Fig.5.21 Effect of *Mgat3* and *Fut8* knockdowns on Notch1 protein expression in MVSCs. Notch 1 receptor protein expression in MVSCs transfected with *Mgat3*, *Fut8* siRNA (25nM) or the scrambled control for 48 h at 37ºC. HRP-conjugated secondary antibody and chemiluminescent staining used to visualise bands on the blot. (a) Representative immunoblot image of Notch1 bands at 120kDa and β-actin bands at 42kDa. Densitometry was carried out on western blot samples to measure intensity of Notch1 bands normalised to the β-actin loading control. (b) Notch1 protein levels are presented as the ratio of expression relative to the negative control sample transfected with a scrambled siRNA. Error bars based on SEM. Data representative of n=3. * $p < 0.05$. ns – $p > 0.05$

5.3.8 Effect of *Mgat3* and *Fut8* Knockdowns on Membrane Localisation of Notch1

Membrane fractionation was used to determine whether knockdown of *Mgat3* and *Fut8* were affecting Notch1 localisation to the membrane. MVSCs were transfected with either *Mgat3* siRNA, *Fut8* siRNA or Scrambled control siRNA. A control sample was treated with 1X Brefeldin A (BFA). Cells were incubated at 37^{o}C for 48 h before being harvested. Membrane fractions were isolated from all four samples using the Mem-PER™ Plus Membrane Protein Extraction Kit. Protein concentration in the membrane fractions was measured by BCA Assay. Western blot was then carried out and samples were immuno-probed using an anti-Notch1 antibody (ab52627). Chemiluminescent staining was used to visualise immunoblotting. Bands at the 120kDa mark represent the Notch1 transmembrane protein. The bands in both the Scrambled siRNA sample and the *Fut8* siRNA sample are of a similar size, while those in the *Mgat3* siRNA and especially the BFA-treated sample are less distinct and robust in comparison. Densitometry was carried out using ImageJ to measure the intensity of Notch1 bands. Notch1 band intensities were calculated relative to the Ponceau S stain of the corresponding lane (refer to Section 4.3.11 for rationale). A significant decrease in band intensity was recorded in the *Mgat3* knockdown sample and in the BFA-treated sample compared to the Scrambled siRNA control, indicating a reduction in Notch1 receptor at the plasma membrane in each case. Meanwhile, no significant change in band intensity was measured following *Fut8* knockdown (Fig 5.22).

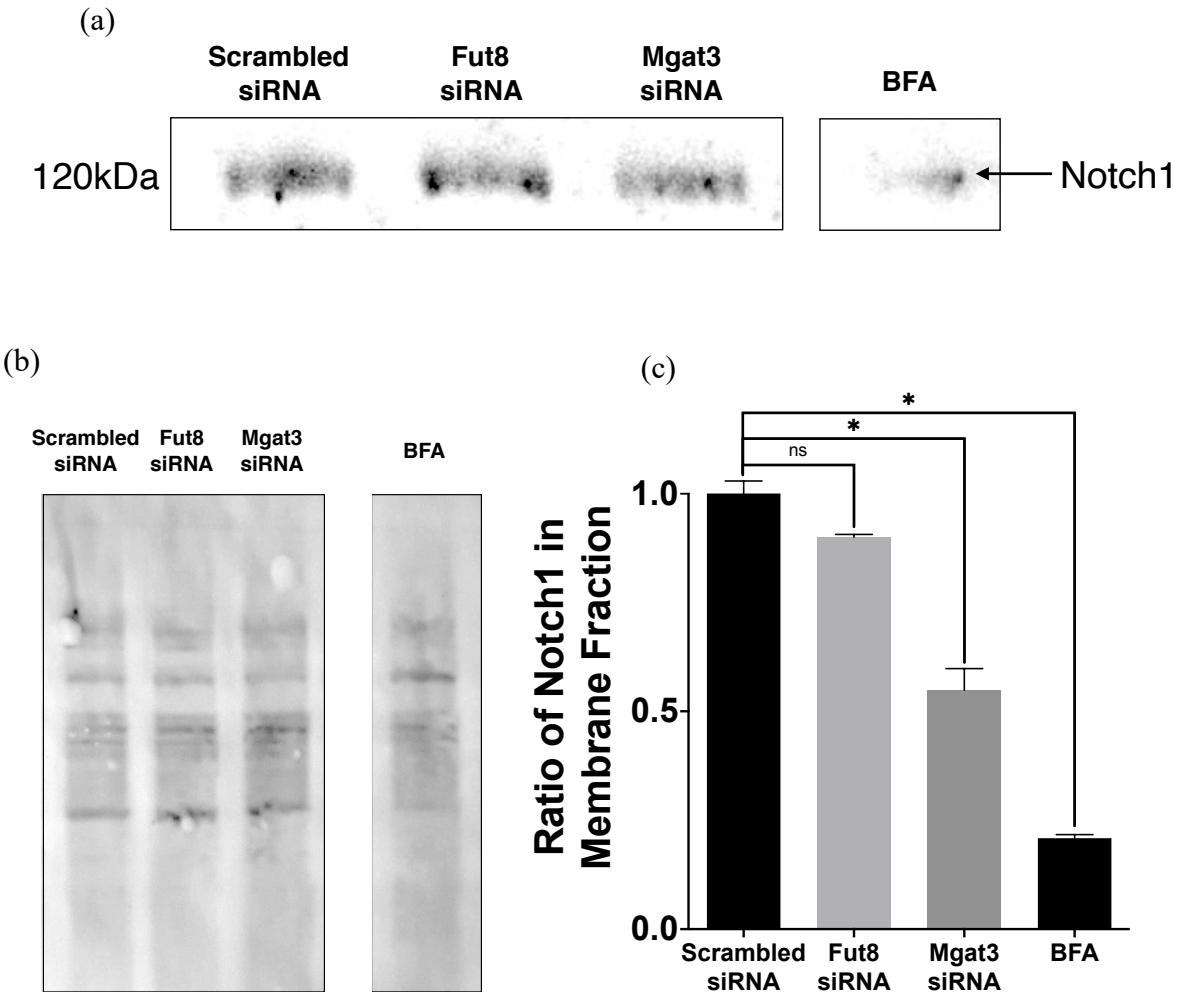


Fig.5.22 Effect of *Mgat3* and *Fut8* knockdowns on Membrane Localisation of Notch1. Notch 1 receptor protein expression in MVSCs transfected with *Mgat3*, *Fut8* siRNA (25nM), scrambled control or treated with 1X BFA for 48 h at 37°C. Membrane fractionation was carried out on cell lysates using Mem-PER™ Plus Membrane Protein Extraction Kit. HRP-conjugated secondary antibody and chemiluminescent staining was performed to visualise bands on the blot. (a) Representative immunoblot image of Notch1 bands at 120kDa. (b) Ponceau S staining displays protein band profiles in each fraction. Densitometry was carried out on western blot samples to measure intensity of Notch1 bands normalised to the Ponceau S loading control. (c) Notch1 protein levels in the membrane fraction are presented as the ratio of expression relative to the negative control sample transfected with a scrambled siRNA. Error bars based on SEM. Data representative of n=3. * $p < 0.05$. ns – $p > 0.05$

5.3.9 Effect of *Mgat3* and *Fut8* Knockdowns on Trafficking of Notch1 Receptor

Fluorescent microscopy was used to explore whether Notch1 trafficking was being affected by knockdown of *Mgat3* or *Fut8*, as any effect on trafficking would influence the activation of Notch target genes and myogenic differentiation. MVSCs were seeded at 5,000 cells/well onto sterile cover slips and transfected with either *Mgat3* siRNA, *Fut8* siRNA or Scrambled control siRNA. A control sample was treated with 1X BFA. Cells were incubated at 37^{o}C for 48 h before being fixed with 3.7% formaldehyde. Immunocytochemistry was then carried out as per Section 2.2.6 and samples were stained using an anti-Notch1 antibody (ab52627). A control sample was also stained with an anti-Golgin-97 antibody (PA530048) to visualise the subcellular location of the GA. Nuclei were also stained with DAPI. One sample was only stained with an IgG control secondary antibody to account for background fluorescence. Samples were imaged using a fluorescent microscope. ImageJ was used to calculate the mean fluorescence intensity and the integrated density of fluorescence at both the cell membrane and in the perinuclear region (adjacent to nucleus, ie. where the GA is located). Samples were graphed as a ratio of the fluorescence at the membrane to the fluorescence in the perinuclear region.

There was no significant change in the ratio of either the fluorescence intensity or density following *Mgat3* or *Fut8* knockdown (Fig.5.23a and 5.23b). Meanwhile, both ratios decreased significantly following treatment BFA. Lower ratios indicate a higher level of fluorescence in the perinuclear region compared to that at the membrane. Representative images, including the subcellular location of the GA (Fig.5.23a).

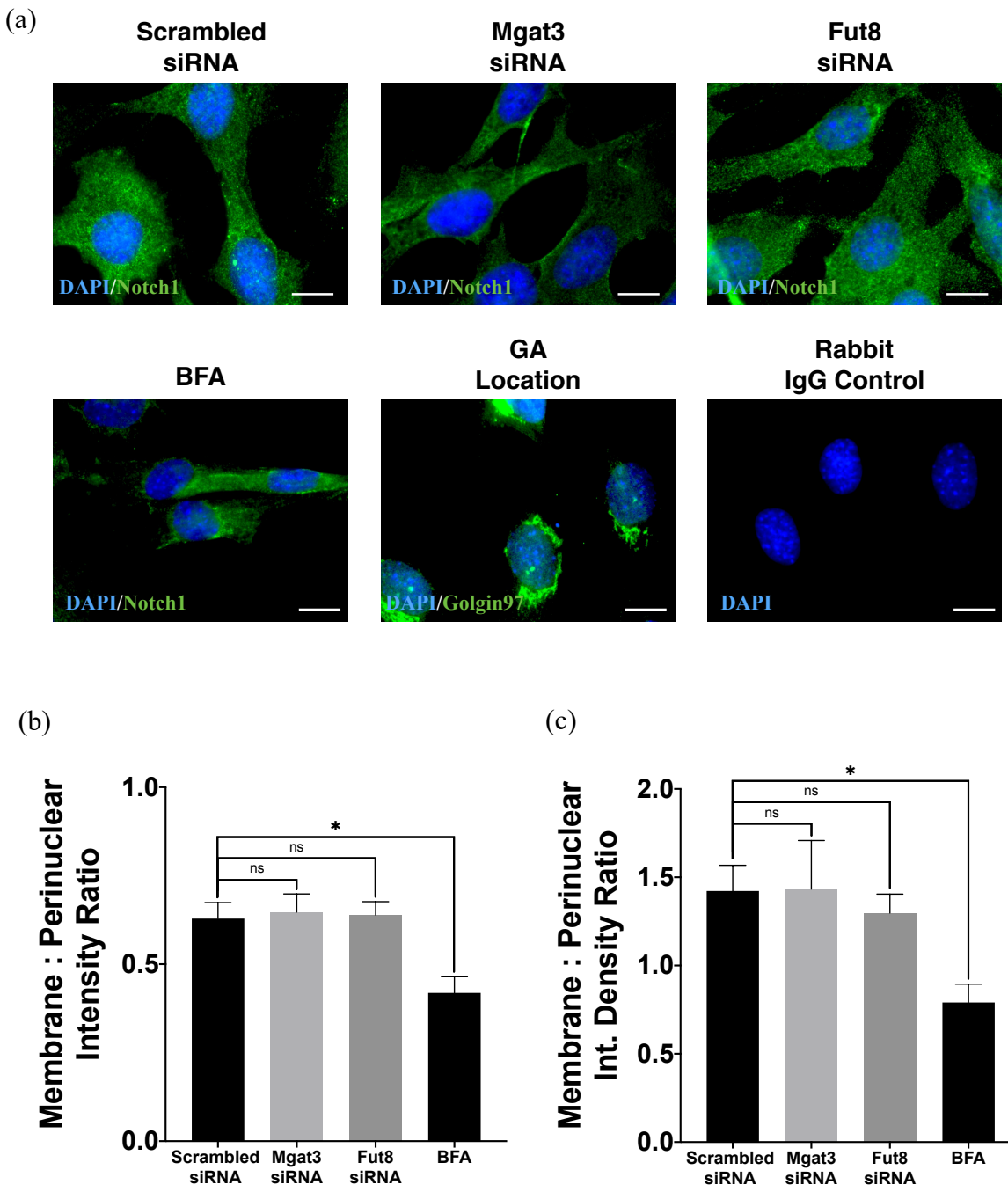


Fig.5.23 Effect of *Mgat3* and *Fut8* knockdowns on Notch1 Receptor Trafficking. Notch 1 receptor protein expression in MVSCs transfected with *Mgat3*, *Fut8* siRNA (25nM), scrambled control or treated with 1X BFA for 48 h at 37°C. ICC and fluorescence microscopy was performed to image the localisation of Notch1 in each sample. Nuclei stained with DAPI. AlexaFluor 488 secondary antibody was used to visualise primary antibody staining. (a) Representative images at 60X magnification of both treated and untreated samples, including a control sample showing the location of the GA (using GA marker Golgin-97) and a rabbit IgG secondary antibody control. Scale bar = 10µm. ImageJ used to calculate ratio of Membrane : Perinuclear fluorescence using (b) integrated density and (c) mean fluorescence intensity values. Error bars based on SEM. Data representative of n=3. * $p < 0.05$. ns – $p > 0.05$

5.4 Discussion

Glycosyltransferases are the primary enzymes responsible for the addition of sugar moieties in the process of oligosaccharide synthesis (Coutinho *et al.*, 2003). They are highly selective with regard to the type of monosaccharide they transfer, the donor molecule they transfer to and the linkages that they form (Chang *et al.*, 2011). Therefore, inhibition of specific glycosyltransferases can yield vital information regarding the role of specific glycans in molecular processes. The most common method of glycosyltransferase inhibition is through the use of targeted siRNA transfection to knock down the transcript of a particular glycosyltransferase. This method has been previously employed by many research groups to elicit information regarding oligosaccharide function in the cell. For example, it was reported in 2012 that sialyation of N-glycans plays a central role in directing proteins to the apical surface of canine kidney cells. This was achieved through siRNA knockdown of a number of glycosyltransferases such as ST6Gal-I and ST6Gal-III (Mo *et al.*, 2012).

GnT-III (coded by the *Mgat3* gene) is a member of the N-acetylglucosaminyltransferase (GnT) family of glycosyltransferases and is responsible for the formation of bisecting N-glycans (Narasimhan, 1982). Fut8 is a member of the fucosyltransferase (FUT) family of enzymes and facilitates the synthesis of core fucosylated N-glycans (Wilson, Williams and Schachter, 1976). Data from Section 4.3.3 indicated the presence of both complex bisecting N-glycans and core fucosylated N-glycans on the Notch1 receptor. While GnT-III has previously been reported to have an impact on Notch signalling, Fut8 has only been loosely associated with Notch (Pakkiriswami *et al.*, 2016; Allam *et al.*, 2017). The next aim for this project, therefore, was to examine the role of both GnT-III and Fut8 in Notch signalling and myogenic differentiation in MVSCs.

In order to assess the role of GnT-III and Fut8, a strategy of siRNA knockdown of the *Mgat3* and *Fut8* transcripts was devised. Transient transfection of both MVSCs and C3Hs with targeted siRNA was carried out and transcript knockdown was confirmed for both *Mgat3* and *Fut8* using qRT-PCR. The functional effect of these knockdowns was also confirmed by ELLA. This data revealed that a reduction in *Mgat3* expression led to a decrease in ConA and E-PHA binding to glycoproteins in the sample lysate. This corresponds to a significant drop in both total N-glycosylation and, more specifically, in the formation of bisecting N-glycans. This result is consistent with the function of the GnT-III glycosyltransferase. Similarly, *Fut8* knockdown resulted in a significant decrease in the binding of LCA, a lectin

known to have high affinity for core fucosylated N-glycans. The lack of a significant change in ConA binding following *Fut8* knockdown indicates that the proportion of N-glycans in the sample lysate which are core fucosylated may be relatively low. Many previous studies which carried out siRNA knockdown of *Mgat3* or *Fut8* confirmed the functional effect of this inhibition through altered binding of LCA or E-PHA, mostly by incorporating these lectins into western blot, flow cytometry and immunofluorescence techniques (Pinho *et al.*, 2012; Guo *et al.*, 2013; Xiang *et al.*, 2017; Tan *et al.*, 2018). However, this is the first time that ELLA has been used to confirm the functional effect of knocking down either of these glycosyltransferase genes.

The ability of *Mgat3* and *Fut8* knockdowns to affect Notch1 N-glycosylation was also assessed. MVSCs were transfected with *Mgat3* or *Fut8* siRNA for 48 h and the native Notch1 was immunoprecipitated using an anti-Notch1 antibody. ELLA was used to detect changes in N-glycosylation in treated samples compared to a control sample transfected with a non-specific (scrambled) siRNA. ConA binding was significantly reduced by both knockdowns, while LCA binding was only decreased by the *Fut8* knockdown and E-PHA binding was attenuated following the *Mgat3* knockdown. This data suggests that a substantial proportion of the N-linked oligosaccharides present on the Notch1 receptor are core fucosylated or bisecting N-glycans. This is in line with previously published data which found that *Mgat3* knockdown led to reduced binding of E-PHA to Notch1 (Allam *et al.*, 2017), and is also supported by data from Section 4.3.3 which confirmed the presence of core fucosylated and bisecting N-glycans on the Notch1 receptor.

Mgat3 and *Fut8* knockdown were subsequently used to inhibit N-glycosylation in Jag-1 treated MVSCs and C3Hs. In both cell lines, Jag-1 treatment substantially increased transcript expression of both *Hey1* and *Myh11*, but this response was significantly reduced following either knockdown. This indicates that bisecting and core fucosylated N-glycans have some effect on the processes of Notch signalling and myogenic differentiation. This may be due to functions related to their presence on the Notch1 receptor, but it is also possible that their effect is indirect as the GnT-III and Fut8 glycosyltransferases modify a vast array of proteins in the cell, many of which could have an impact on the aforementioned processes. For example, Nicastrin is a subunit of the γ-secretase complex which performs a critical cleavage step to release the NICD following Notch receptor activation (Taylor Kimberly *et al.*, 2002). Sixteen potential N-glycosylation sites have been identified along the extracellular domain of Nicastrin (Morais *et al.*, 2006), and while it is not known exactly

how many of these sites are in fact glycosylated, it has been confirmed that N-glycans are indeed present on this transmembrane protein and that a proportion of these oligosaccharides contain a complex bisecting structure (Yu *et al.*, 2000; Wollscheid *et al.*, 2009; Allam *et al.*, 2015). While some groups have reported that the glycosylation of Nicastrin is not essential for its function in the γ-secretase complex (Herreman *et al.*, 2003; Urano *et al.*, 2020), others have found that correct Nicastrin N-glycosylation is required for the formation of the γ-secretase complex, its catalytic activity and substrate preference, including the proteolysis of Notch receptors (Yu *et al.*, 2000; Yang *et al.*, 2002; Moniruzzaman *et al.*, 2018). Therefore, attenuation of *Hey1* and *Myh11* expression following *Mgat3* knockdown could be a result of altered Nicastrin glycosylation. Crosstalk from other pathways related to Notch signalling may also be influenced by glycosyltransferase knockdown. It has been previously demonstrated that TGF-β signalling is downregulated in *Fut8* knockout mouse models (Wang *et al.*, 2005). Altered components of this pathway may have an impact on Notch signal transduction. Furthermore, it must be noted that glycosyltransferases are highly inter-regulated, meaning that the activity of one can inhibit many others (Schachter, 1986; Zhao *et al.*, 2006). Consequently, knockdown of *Mgat3* and *Fut8* likely results in dramatic changes in glycosylation across other glycoproteins.

In order to investigate the possibility of downstream elements of the Notch signalling pathway being affected by glycosyltransferase inhibition, NICD ectopic expression was carried out in MVSCs in conjunction with *Mgat3* and *Fut8* knockdown. Ectopically expressed NICD successfully activated Notch target gene (*Hey1*) and myogenic marker (*Myh11*) expression. Transfection with *Mgat3* or *Fut8* siRNA incurred no significant change to this response. This evidence suggests that Notch pathway components downstream of receptor cleavage are not affected by a reduction in synthesis of bisecting or core fucosylated N-glycans.

Analysis of Notch1 expression was also carried out following Mgat3 and Fut8 knockdown in an attempt to investigate whether these knockdowns were altering the activity of transcription or translation machinery. qRT-PCR and western blot were performed on MVSCs transfected with *Mgat3* or *Fut8* siRNA for 48 h. No change in *Notch1* transcript was detected, indicating that *Notch1* transcription was not being altered and was therefore not the cause of the reduction in signalling. *Fut8* knockdown also had no effect on Notch1 protein expression. However, *Mgat3* knockdown led to a significant reduction in the level of Notch1 protein measured in the cell population. The two most likely explanations for this

decrease are: translation of Notch1 has been inhibited by the knockdown; or the rate of Notch1 degradation has been increased. Data from previous studies supports the latter explanation. Bisecting N-glycans have been reported to protect a number of membrane-bound proteins, such as BACE-1 and E-Cadherin, from lysosomal degradation (Yoshimura *et al.*, 1996; Kizuka *et al.*, 2016). Moreover, Notch1 has been shown to re-direct to the lysosome and undergo degradation following *Mgat3* knockdown (Allam *et al.*, 2017).

To further explore the possibility of either knockdown affecting Notch1 trafficking and degradation, two additional methods of analysis were employed: measurement of protein levels in the membrane fraction of an MVSC lysate; and visualisation of Notch1 localisation in the cell using ICC. Firstly, membrane fractionation and western blot were carried out on MVSCs transfected with *Mgat3* or *Fut8* siRNA, or treated with the Golgi trafficking inhibitor Brefeldin A (BFA). Significant decreases in Notch1 band intensity were observed in membrane fractions following treatment with BFA and knockdown of *Mgat3*. This implies that in each instance, the amount of Notch1 on the membrane was decreased by the treatment. *Fut8* knockdown had no significant effect on the level of Notch1 at the membrane. Due to the mechanism of BFA action, it can be surmised that, in the case of that sample, the observed attenuation is a result of Notch1 trafficking from the Golgi Apparatus (GA) to the plasma membrane being inhibited. The knockdown of *Mgat3* may give rise to a similar effect, but data from Section 5.3.7 indicates that this reduction is more likely due to a decrease in total Notch1 protein in the cell population. This theory is further supported by ICC data from Section 5.3.9 which shows a significant decrease in the ratio of Membrane : Perinuclear localisation of Notch1 in the BFA sample, but not in the *Mgat3* or *Fut8* knockdown samples. This data is based upon analysis of ICC images using integrated density (the sum of all pixel intensities in a defined area) and mean fluorescence intensity (the average intensity of all pixels in a defined area), which indicates an accumulation of Notch1 in the perinuclear region of the cell in response to BFA treatment, while there is no significant change in Notch1 trafficking from the GA to the membrane following *Mgat3* or *Fut8* knockdown.

In summary, data in this chapter confirms that the knockdown of the *Mgat3* and *Fut8* glycosyltransferase-coding genes reduces the level of certain N-glycan structures on cellular glycoproteins. This includes Notch1 as both knockdowns had a significant effect on the N-glycosylation profile of the purified receptor, supporting previous data from this study which detected the presence of both bisecting and core fucosylated N-glycans on Notch1. *Mgat3*

and *Fut8* knockdown can also reduce the level of Jag-1 mediated Notch signalling and myogenic differentiation in both MVSCs and C3Hs, although it is not certain whether this is due to their effect on Notch1 or on other cellular proteins. However, it was demonstrated that function of downstream components of the Notch and myogenic differentiation pathways were not altered by *Mgat3* or *Fut8* knockdown. Furthermore, *Notch1* transcript levels were not affected by either knockdown, but Notch1 protein expression was significantly reduced by *Mgat3* siRNA transfection. This data, combined with previously published reports and results from Notch1 trafficking analysis, suggests that bisecting N-glycans may have a role in preventing the degradation of the Notch1 receptor. The function of core fucosylated N-glycans is more difficult to decipher as reduction of their synthesis through *Fut8* knockdown seemed to have no effect on Notch1 protein expression or on receptor trafficking, but caused a significant attenuation of Notch signalling and myogenic differentiation. There may be an alternative function for core fucosylated N-glycans on the Notch1 receptor, such as regulating cleavage events, or the observed effect may be due to alterations of indirect contributors to the Notch signalling pathway.

Table 5.1 Summary of findings from small-molecule inhibitor and siRNA knockdown experiments

Experiments		Interventions: Small-molecule inhibitors	Interventions: Glycosyltransferase siRNA Knockdown	Conclusions
	Jag-1-induced Target Gene Expression	**TNC** - Hey1 ↓ Myh11 ↓	**Mgat3** - Hey1 ↓ Myh11 ↓	N-glycans, particularly bisecting and core fucosylated N-glycans, influence Notch signalling and Notch-mediated myogenic differentiation
		DMJ - Hey1 ↓ Myh11 ↓	**Fut8** - Hey1 ↓ Myh11 ↓	
	NICD-induced Target Gene Expression	**TNC** - Hey1 = Myh11 ↓	**Mgat3** - Hey1 = Myh11 =	N-glycosylation of proteins downstream of Notch is not essential for target gene expression. Bisecting and core fucosylated N-glycans on downstream proteins are not essential for myogenic gene expression, but other forms of N-glycosylation are required
		DMJ - Hey1 = Myh11 ↓	**Fut8** - Hey1 = Myh11 =	
	Notch1 Transcript Expression	**TNC** - Notch1 =	**Mgat3** - Notch1 =	N-glycosylation is not required for Notch1 transcription
		DMJ - Notch1 =	**Fut8** - Notch1 =	
	Notch1 Protein Expression/Degradation	**TNC** - Notch1 =	**Mgat3** - Notch1 ↓	Bisecting N-glycans are essential for protection of Notch1 against degradation. Core fucosylated N-glycans do not impact this process
		DMJ - Notch1 =	**Fut8** - Notch1 =	
	Notch1 Membrane Expression	**TNC** - Membrane-bound Notch1 ↓	**Mgat3** - Membrane-bound Notch1 ↓	Bisecting N-glycans do not affect Notch1 trafficking from the ER-Golgi complex but certainly protect against degradation. Core fucosylated N-glycans do not affect Notch1 trafficking. Other forms of N-glycosylation, either on Notch1 or other cellular proteins, impact Notch1 trafficking to the membrane
		DMJ - Membrane-bound Notch1 ↓	**Fut8** - Membrane-bound Notch1 =	
	Notch1 Localisation	**TNC** - Perinuclear Notch1 ↑	**Mgat3** - Perinuclear Notch1 =	
		DMJ - Perinuclear Notch1 ↑	**Fut8** - Perinuclear Notch1 =	

Chapter 6:

Effect of N-glycosylation site mutation on Notch1 signalling and myogenic differentiation

6.1 Introduction

As previously described in Section 1.6.1, N-linked glycosylation involves the addition of a 14-sugar dolichol oligosaccharide to an asparagine (Asn) residue in the polypeptide sequence (Walsh, 2009). This process cannot occur at any Asn residue, only at those located in a specific polypeptide consensus sequence of N-X-S/T where N denotes an asparagine, S is a serine and T is a threonine. The residue denoted by X can be any amino acid other than Proline which has an extremely rigid structure that induces a conformational change in the polypeptide, rendering the site unsuitable for glycosylation (Yan and Lennarz, 2004; Ghazarian, Idoni and Oppenheimer, 2011). Amino acid residues flanking the consensus sequence have also been shown to influence whether or not a site is glycosylated and what type of glycan is synthesised at the site (Mellquist *et al.*, 1998). As noted in Section 1.7.2, six N-glycosylation consensus sequences have been identified on the extracellular domain of the Notch1 receptor: four along the EGF repeat domains and one each in the LNR region and hydrophobic domain (Takeuchi and Haltiwanger, 2014).

Site-directed mutagenesis of a single nucleotide base has been used in countless studies to investigate the importance of specific DNA sequences in a vast range of cellular mechanisms. The most common method of single base substitution is to mutate a plasmid-encoded gene using PCR. This is achieved by designing primers that are complementary to the target sequence but which contain the desired sequence alteration (Hemsley *et al.*, 1989). To express this mutated plasmid in mammalian cells, transfection is often carried out and successfully transfected cells can be selected for using antibiotic resistance (Dedkova *et al.*, 2012). Puromycin is an example of an antibiotic used in this selection process. Puromycin causes cell cytotoxicity by inhibiting protein synthesis in the ribosome (Aviner, 2020).

Using the PCR method of site-directed mutagenesis, many research groups have targeted the N-X-S/T consensus sequence in order to prevent N-glycosylation at that site and determine the role of that particular N-glycan in a cellular process (Flack *et al.*, 1994; Ferlinz *et al.*, 1997). Previous reports have concluded that, in some cases, the serine/threonine residue is dispensable for N-glycosylation, but the asparagine residue is always essential, and so it has been the most regularly targeted amino acid in N-glycan site mutation (Schwarz and Aebi, 2011).

6.2 Strategy

Advancements in recombinant DNA technology have experienced an exponential growth in the last two decades. There are now a large number of methods being used to carry out genetic engineering of mammalian cell lines. The development of technologies such as CRISPR (clustered regularly interspaced short palindromic repeats) have made it relatively straightforward to obtain reliable stable mutations in genomic DNA. However, techniques such as those are still quite time-consuming, especially due to the clone screening process, and time constraints for this project did not allow for such a lengthy undertaking. Instead, site-directed mutagenesis of plasmid-encoded Notch1 was chosen to complete this section of the study.

Due to the fact that mutant Notch1 would be ectopically expressed in the cell population and not stably transfected into the genomic DNA, this would mean that cells would still be expressing the native wild-type Notch1 receptor. Therefore, it was imperative to ensure that a high enough percentage of the population were successfully transfected with the plasmid in order to make any change in Notch signalling detectable. For this reason, puromycin selection was used to maximise the proportion of transfected cells in a given population.

To ensure that puromycin would reliably eliminate the majority (>80%) of non-transfected cells in a population, the optimum concentration was determined in both MVSCs and C3Hs. This was achieved by treatment of cells with a range of puromycin concentrations before DAPI staining and subsequent viable cell counting.

Large quantities of naked plasmid DNA can be toxic when transfected into mammalian cells (Emerson *et al.*, 2003; Lesueur, Mir and André, 2016). Therefore, it was vital to also establish the optimum concentration of DNA to transfect into MVSC and C3H cells in order to achieve the best balance between proportion of plasmid-expressing cells and total number of viable cells in a transfected population. A green fluorescent protein (GFP)-coding plasmid was transfected into cells at a range of concentrations (Section 2.2.6.1). The number of viable cells and percentage of GFP-expressing cells could then be quantified by fluorescent microscopy.

Once the optimum concentrations of both puromycin and plasmid DNA had been ascertained, the method of puromycin selection was validated by transfecting cells with a

plasmid encoding a puromycin resistance gene and subsequently treating the cells with the puromycin antibiotic. Viable cells could then be counted using DAPI staining. This strategy was used to confirm that transfected cells could survive the combined toxicity of the plasmid DNA and puromycin.

At this point, a cell line was established that could exhibit a high plasmid transfection efficiency, was amenable to puromycin selection and therefore was suitable for ectopic expression of mutant Notch1 receptors. However, the plasmids required to code for these mutant receptors would first need to be generated and validated. Primers were designed to target the six N-glycosylation sites of Notch1, with each set containing a single base alteration in the codon for the essential asparagine residue. Several different amino acids have been used over the years as substitutes for asparagine in N-glycan site mutation studies including glutamine, alanine, threonine, isoleucine, serine and aspartate (Brunner *et al.*, 1992; Van Berkel *et al.*, 1996; Bühlmann *et al.*, 2000; Niu *et al.*, 2000; Ramanujam *et al.*, 2001; Lee *et al.*, 2003). In this study, isoleucine was used as the replacement amino acid for asparagine. This was due to two main factors: isoleucine contains a non-reactive side-chain, negating the possibility of unwanted reactions with other amino acids; and two of the nucleotide triplets which code for isoleucine (ATT and ATC) are very similar to those which code for asparagine (AAT and AAC) and have high codon usage (both almost 50%) in *E.coli*, meaning that the likelihood of correct base substitution, plasmid replication and gene transcription would be very high. Therefore, using primers designed to substitute asparagine for isoleucine, PCR was carried out to separately mutate all six N-glycosylation sites in the plasmid-encoded Notch1 (Section 2.2.18). Large quantities of mutant plasmids were then generated by transforming each one into bacterial cells which were then grown up in liquid culture. Plasmid DNA was then purified (Section 2.2.4.2) and sent for sequencing to confirm that the correct single base substitutions had been incorporated.

The entire objective behind mutating these asparagine residues was to ensure that N-glycosylation did not occur at that site. It was necessary then to investigate whether each one of these mutations would actually give rise to a change in Notch1 N-glycosylation. To achieve this, immunoprecipitation of the myc-tagged Notch1 proteins from the lysates of transfected cells was carried out (Section 2.2.15) and ELLA was used to detect changes in N-glycosylation on the purified mutant receptors (Section 2.2.17).

In order to examine the effect of each mutation on Notch1 signalling and myogenic differentiation, Jag-1 stimulated cells were transfected with each mutant plasmid. The expression levels of Notch target gene *Hey1* and the myogenic marker *Myh11* were then measured using qRT-PCR (Section 2.2.11). It is important to note that although expression of the native Notch1 would still continue, most of the Notch1 at the membrane should be replaced by the mutant Notch1. This assumption is based on estimated turnover rates for the Notch1 receptor. Although measurements of Notch1 half-life have not yet been described in the literature (most studies regarding Notch1 half-life concentrate on the NICD), the range of turnover rate of proteins in mammalian cells has been estimated at 0.5-35 hours (Toyama and Hetzer, 2013). In particular, membrane proteins and proteins containing phosphorylation sites or PEST domains usually have turnover rates at the lower end of this range (Rechsteiner and Rogers, 1996; Cambridge *et al.*, 2011). Therefore, in the 48 hours post-transfection, it is highly likely that the overexpressed mutant Notch1 would replace the majority of native Notch1 receptors on the membrane.

Changes in *Hey1* or *Myh11* expression could very easily be attributed to a discrepancy in efficiency of plasmid transfection across mutants. Therefore, qPCR was carried out on plasmid DNA isolated from transfected cells to measure the amount of *Notch1*-coding plasmid in each sample. Similarly, western blot (Section 2.2.16) was carried out on protein isolated from transfected cells to decipher whether changes in ectopically expressed Notch1 protein levels could be influencing changes in target gene expression.

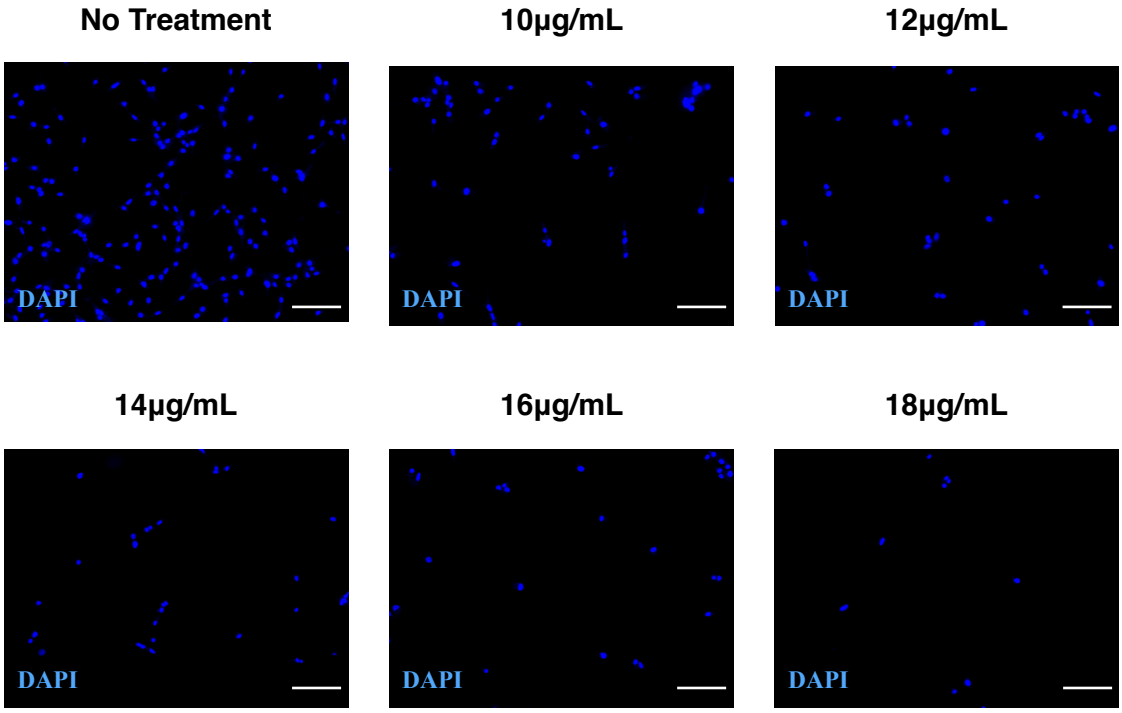
Data for all experiments in this section was gathered over at least three biological replicates. Normality tests were used to determine if data followed a parametric distribution pattern. Variation across samples was analysed by calculating p-values. The type of test used to calculate this was governed by the outcome of the normality test. Statistical significance was assigned to p-values less than 0.05 (Section 2.2.19).

6.3 Results

6.3.1 Puromycin Cytotoxicity Titration in MVSCs and C3Hs

When using a selective antibiotic, it is important to establish a concentration that finds a middle ground between not being toxic enough to eliminate the majority of non-resistant cells and being too toxic for even resistant cells to survive. Therefore, concentration of the antibiotic was titrated in both relevant cell lines in a bid to achieve elimination of 80-90% of cells in a given population. MVSCs and C3Hs were seeded at 200,000 cells/well onto sterile cover slips in 6-well plates. Cells were treated with a number of puromycin concentrations ranging from 10 - 18µg/mL in MVSCs and from 0.5 - 4µg/mL in C3Hs, followed by incubation at 37^{o}C for 24h. Formaldehyde at 3.7% was used to fix cells and nuclei were subsequently stained with DAPI. Samples were imaged using a fluorescent microscope and cell numbers were counted using ImageJ software to calculate the percentage of cell death in each sample compared to the non-treated control. In MVSCs, the optimum concentration of puromycin was deemed to be 14µg/mL, as cell death in this sample reached a level of 82.5% (Fig.6.1). Meanwhile, in C3Hs, 3µg/mL was identified as the optimum concentration of puromycin as this eliminated around 89.8% of cells after 24 hours (Fig.6.2). All increases in cell death were statistically significant across both cell lines compared to the non-treated control.

(a)



(b)

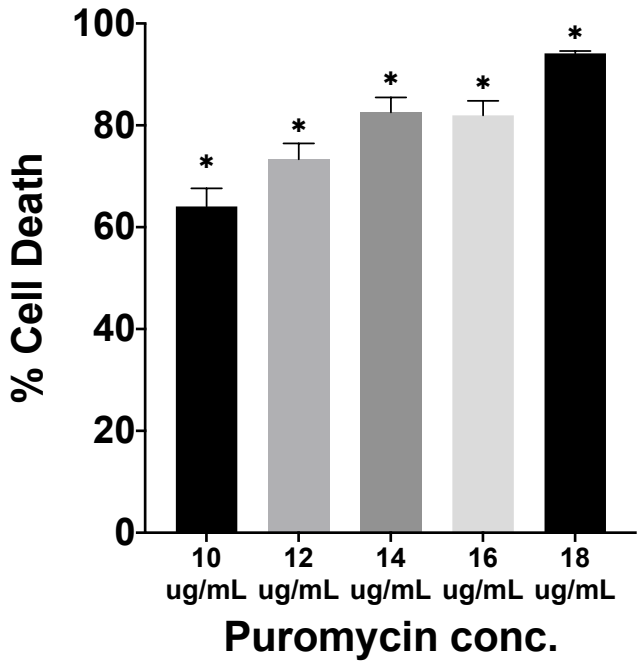
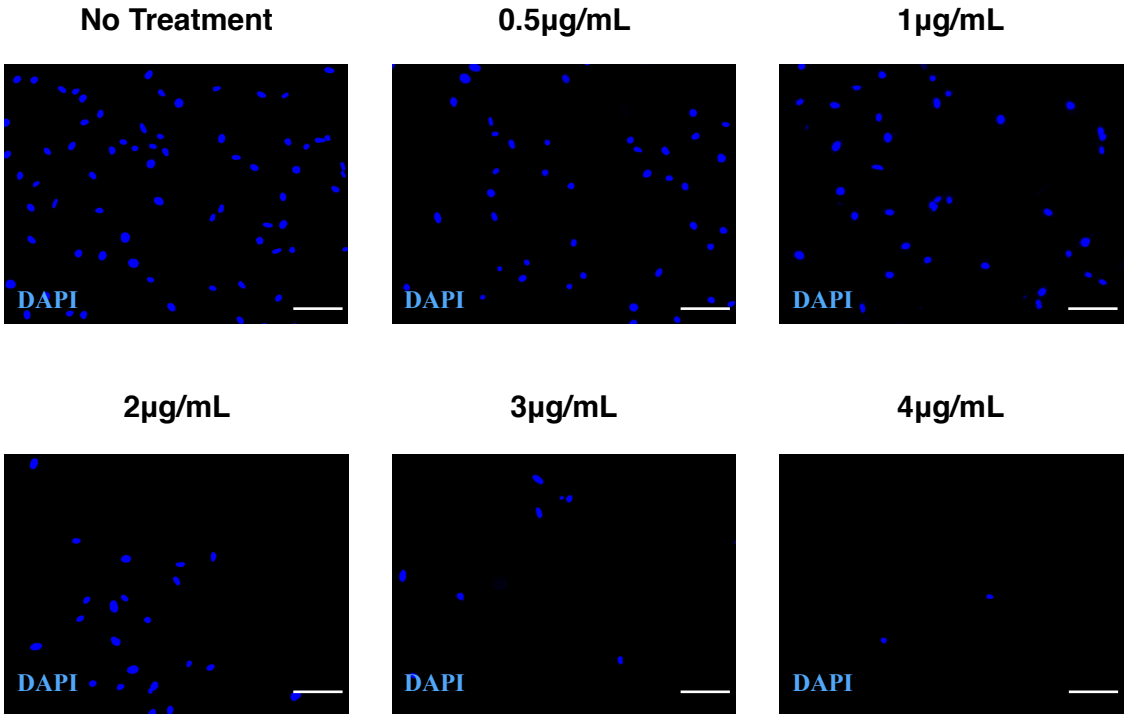


Fig.6.1 Puromycin cytotoxicity titration in MVSCs. MVSCs treated with a range of puromycin concentrations and incubated for 24 h at 37°C. Cells were fixed and nuclei stained with DAPI. Olympus DP-50 fluorescent microscope used to image samples. 10 images taken per sample. (a) Representative images at 20X magnification of all samples. Scale bar = 25µm. (b) Cells counted using ImageJ and data graphed as percentage cell death compared to the non-treated control. Error bars based on SEM. Data representative of n=3. * $p < 0.05$ compared to non-treated control.

(a)



(b)

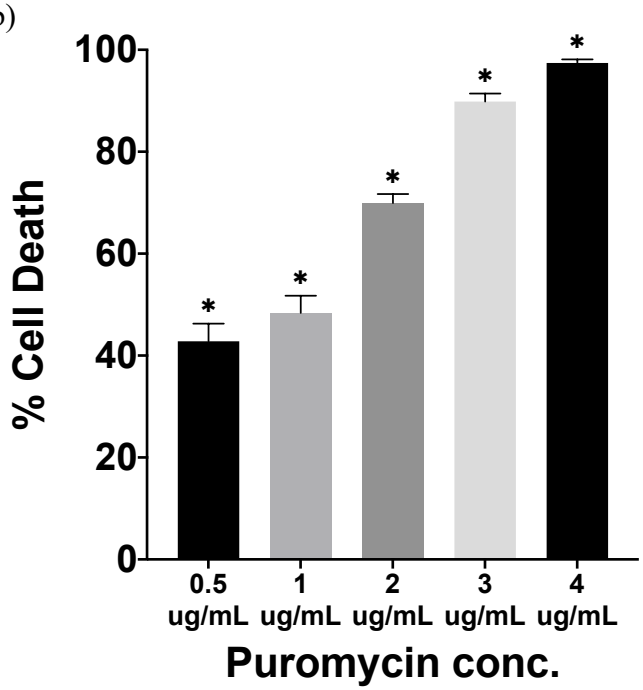
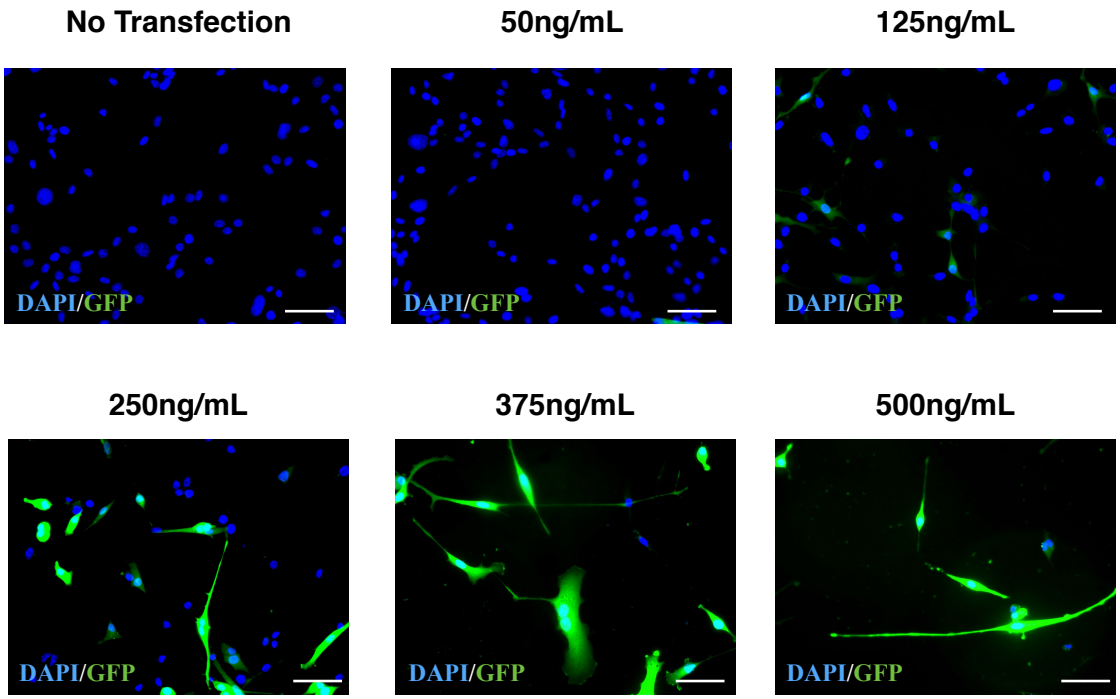


Fig.6.2 Puromycin cytotoxicity titration in C3Hs. C3Hs treated with a range of puromycin concentrations and incubated for 24h at 37°C. Cells were fixed and nuclei stained with DAPI. Olympus DP-50 fluorescent microscope used to image samples. 10 images taken per sample. (a) Representative images at 20X magnification of all samples. Scale bar = 25µm. (b) Cells counted using ImageJ and data graphed as percentage cell death compared to the non-treated control. Error bars based on SEM. Data representative of n=3. * $p < 0.05$ compared to non-treated control.

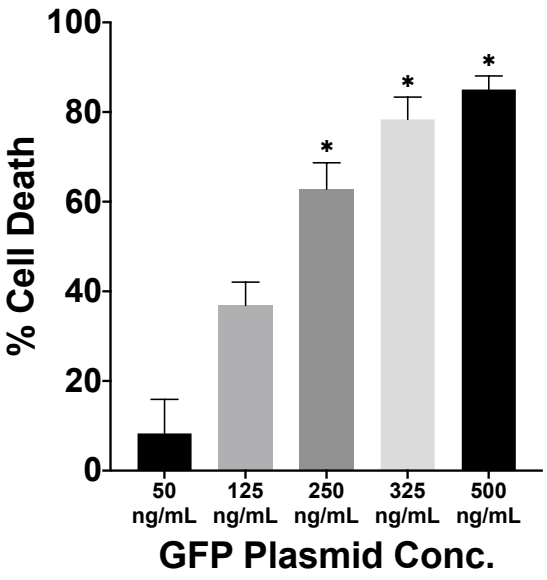
6.3.2 Plasmid Transfection Optimisation in MVSCs and C3Hs

Plasmid DNA can be toxic to cells when transfected at high concentrations. It was necessary then to determine the optimum concentrations of plasmid DNA for transfection into both relevant cell lines. To achieve this, MVSCs and C3Hs were seeded at 200,000 cells/well onto sterile cover slips in 6-well plates. Cells were transfected with a number of concentrations of GFP-coding plasmid, ranging from 50 – 500ng/mL and were then incubated at 37^{o}C for 48 h. Formaldehyde at 3.7% was used to fix cells and nuclei were subsequently stained with DAPI. Samples were imaged using a fluorescent microscope. DAPI nuclei and GFP-expressing cells were counted using ImageJ software to calculate the percentage of cell death and the plasmid transfection efficiency in each sample compared to the non-transfected control. In both MVSCs and C3Hs a higher concentration of plasmid DNA generally resulted in an increase in cell death (Fig.6.3b and 6.4b). A similar trend was observed with transfection efficiency as the proportion of GFP-positive cells increased with higher concentrations of plasmid DNA (Fig.6.3c and 6.4c). In C3Hs, this seemed to plateau at the 250ng/mL concentration. Based on requirements for downstream applications, limits were set whereby a cell cytotoxicity rate above 50% and a transfection efficiency below 70% were deemed unacceptable. One sample of C3H cells met these criteria with the 250ng/mL concentration leading to a cell cytotoxicity rate of only 39% and yielding a transfection efficiency rate of 72%. None of the MVSC samples reached an acceptable standard of plasmid transfection and therefore a decision was made to proceed with only the C3H cell line for subsequent experiments involving Notch1 mutant plasmid transfection.

(a)



(b)



(c)

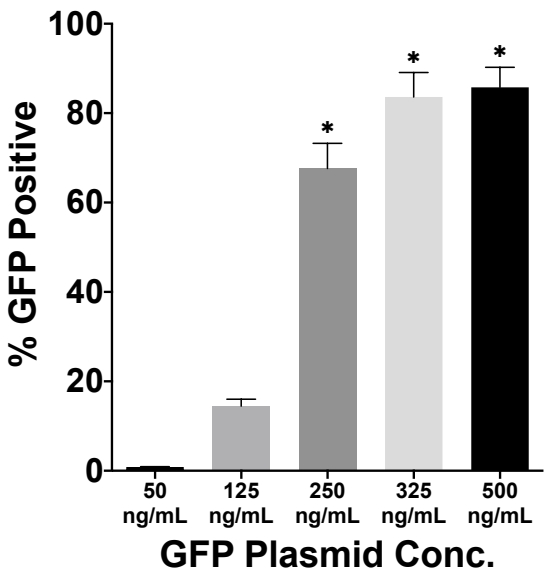
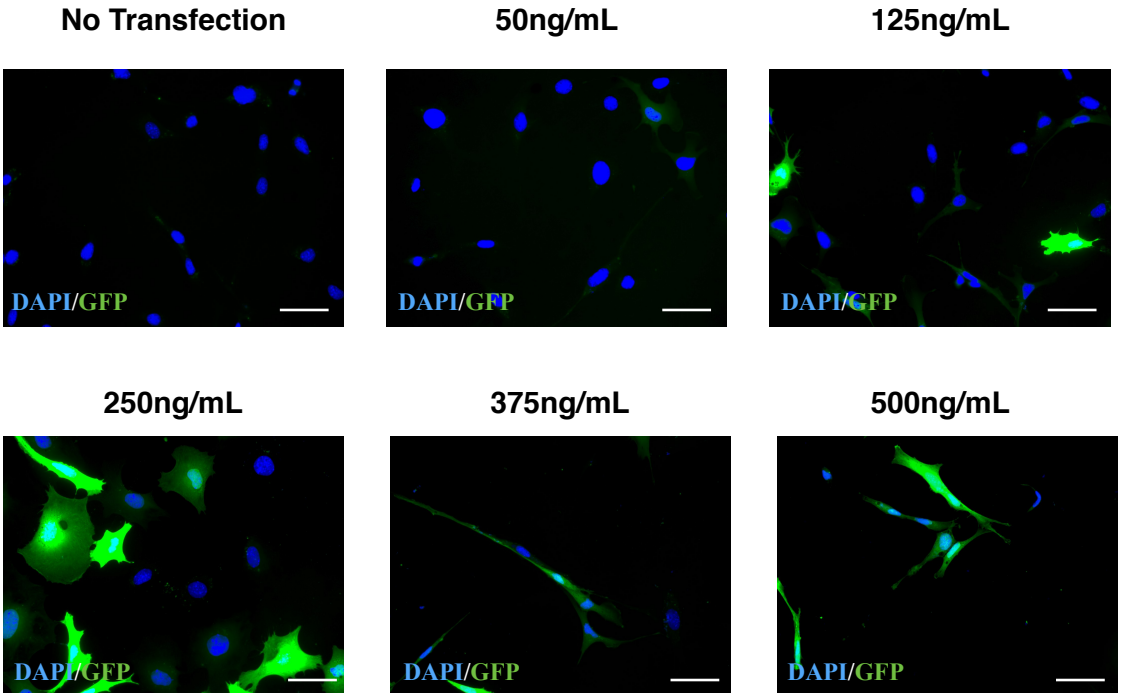
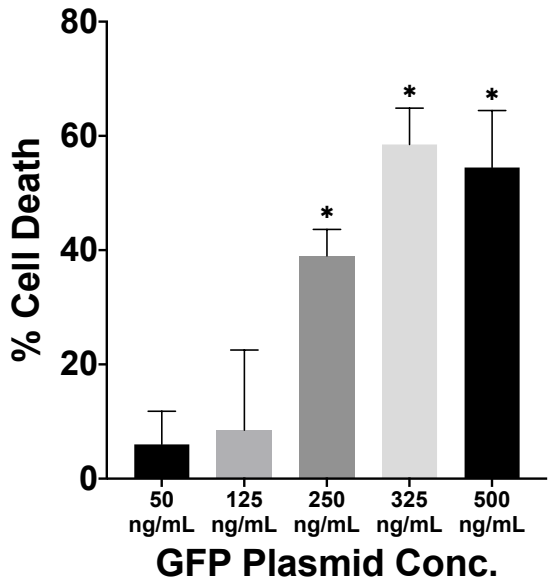


Fig.6.3 Plasmid transfection efficiency in MVSCs. MVSCs transfected with a range of concentrations of GFP-coding plasmid DNA and incubated for 48 h at 37ºC. Cells were fixed and nuclei stained with DAPI. Olympus DP-50 fluorescent microscope used to image samples. 10 images taken per sample. (a) Representative images at 20X magnification of all samples. Scale bar = 25µm. (b) Cells counted using ImageJ and data graphed as percentage cell death compared to the non-transfected control. (c) GFP-positive cells counted and graphed as a percentage of total cell number. Error bars based on SEM. Data representative of n=3. * $p < 0.05$ compared to non-transfected control.

(a)



(b)



(c)

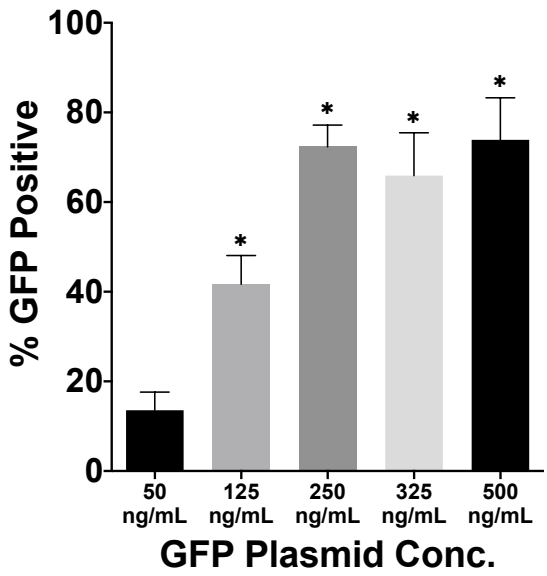


Fig.6.4 Plasmid transfection efficiency in C3Hs. C3Hs transfected with a range of concentrations of GFP-coding plasmid DNA and incubated for 48 h at 37°C. Cells were fixed and nuclei stained with DAPI. Olympus DP-50 fluorescent microscope used to image samples. 10 images taken per sample. (a) Representative images at 20X magnification of all samples. Scale bar = 25µm. (b) Cells counted using ImageJ and data graphed as percentage cell death compared to the non-transfected control. (c) GFP-positive cells counted and graphed as a percentage of total cell number. Error bars based on SEM. Data representative of n=3. * $p < 0.05$ compared to non-transfected control.

6.3.3 Validation of Puromycin Selection in C3Hs

Puromycin selection is a useful method of increasing the proportion of transfected cells in a given population by eliminating non-transfected cells. To validate the method of puromycin selection for this study, C3Hs were seeded onto six sterile cover slips of a 6-well plate at 200,000 cells/well. They were subsequently transfected with a plasmid (pPGKpuro) encoding a puromycin resistance gene at either 125ng/mL (referred to as P125) or 250ng/mL (referred to as P250) using the TransIT-X2 Dynamic Delivery System and incubated overnight at 37^{o}C. The following day, samples were treated with puromycin (Puro) at 3µg/mL and incubated at 37^{o}C for another 24h. Formaldehyde at 3.7% was used to fix cells and nuclei were subsequently stained with DAPI. Samples were imaged using a fluorescent microscope. Cells were counted using the ImageJ software and average cell counts were compared against a non-transfected control and against samples transfected with the same concentration of plasmid but which were not treated with puromycin. Survival rate following puromycin treatment in the non-transfected sample was only around 7%. This increased dramatically to 51% in P125 but was still a statistically significant level of cell death. In P250, the survival rate increased again to 88% and the level of cell death became statistically insignificant (Fig.6.5c – 6.5e). However, even with such a high survival rate compared to its non-Puro-treated counterpart, the average cell count for the Puro-treated P250 was still lower than that of the Puro-treated P125 (Fig.6.5b). Therefore, pPGKpuro was used at a concentration of 125ng/mL for all subsequent puromycin selection experiments.

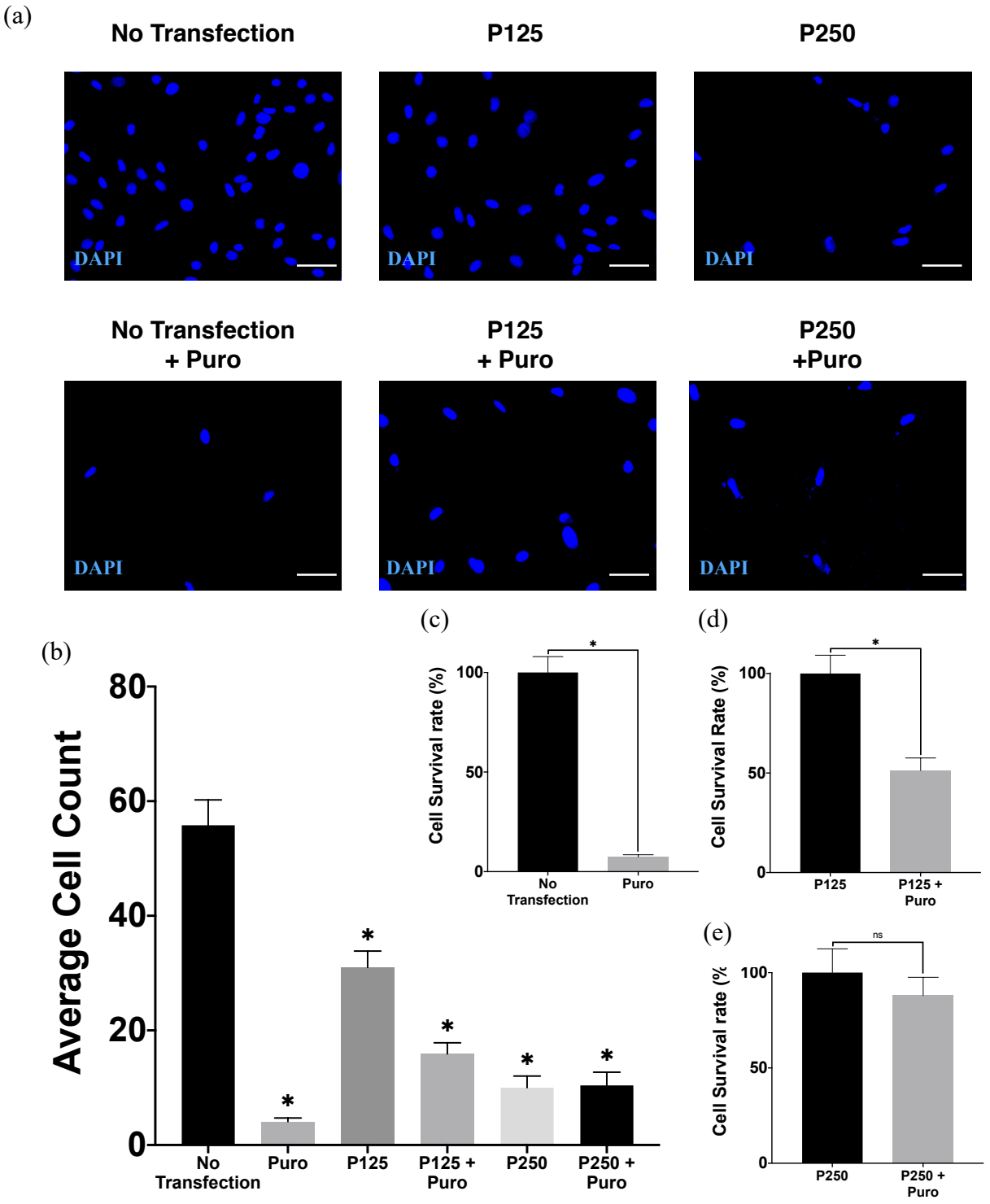


Fig.6.5 Validation of Puromycin Selection in C3Hs. C3Hs transfected with a range of concentrations of puromycin resistance-coding plasmid DNA ± puromycin (3µg/mL). Cells were fixed and nuclei stained with DAPI. Olympus DP-50 fluorescent microscope used to image samples. 10 images taken per sample. (a) Representative images at 20X magnification of all samples. Scale bar = 25µm. (b) Cells counted using ImageJ and data graphed as mean cell number. * $p < 0.05$ compared to non-treated control. (c-e) Cell survival rate against puromycin was calculated for each concentration of plasmid DNA and compared to the equivalent non-puromycin-treated control. Error bars based on SEM. Data representative of n=3. * $p < 0.05$. ns – $p > 0.05$.

6.3.4 Site-directed Mutagenesis of Plasmid-encoded Notch1

Once a cell line had been established which was highly amenable to both plasmid transfection and puromycin selection, the plasmid mutation process could begin. Using the pCS2 Notch1 Full Length-6MT plasmid from Addgene (41728), six single base substitutions were carried out separately on the *Notch1* gene to alter asparagine residues at amino acid positions 888, 959, 1179, 1241, 1489 and 1587 to isoleucine residues. This was carried out as per Section 2.2.16. Briefly, PCR reactions were set up using the Agilent QuikChange Lightning Site Directed Mutagenesis Kit and primers containing the desired mutation. PCR products were then transformed into ultracompetent XL10-Gold bacterial cells via heat-shock at 42ºC. After a period of recovery, bacterial cells were spread on LB Agar plates containing the selective antibiotic ampicillin and incubated overnight at 37ºC. Colonies were picked and grown in liquid culture before plasmid purification was carried out as per section 2.2.8. Mutant plasmids were then sent for sequencing with Source Biosciences along with specially designed sequencing primers. The resulting sequences were aligned with the wild-type plasmid sequence using Multalin (an online local alignment tool) to confirm that the correct single base substitution had been incorporated in each case. Fig. 6.6 shows the result of these alignments where in each case an essential adenine base was correctly converted to a thymine base. Chromatograms were also generated by Source Bioscience during sequencing. Chromatograms are used to determine the quality of both the sequencing read and the sample plasmid. High quality samples produce clearly defined peaks, indicating that no contaminating DNA is present. All of the chromatograms generated for the mutant Notch1 plasmid samples were of a high quality and the sections shown in Appendix B verify that no wild type plasmid remained in the sample.

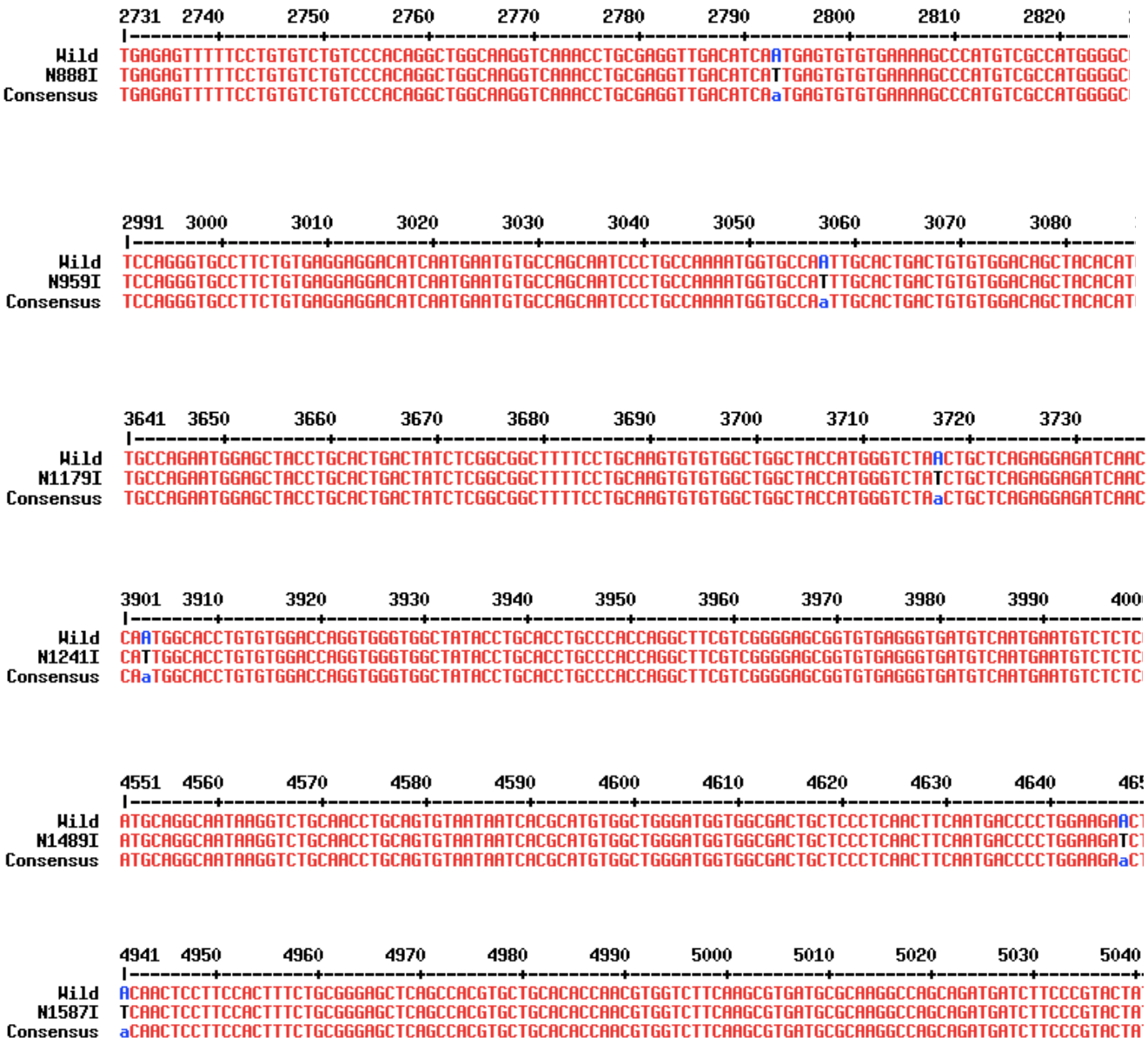


Fig.6.6 Mutant plasmid sequence alignment. Mutant plasmids sequenced by Source Biosciences. Sequences aligned to wild-type *Notch1* plasmid sequence using Multalin online sequence alignment tool. Image shows screenshots of the sections of the alignments containing the desired single base substitutions. Red letters indicate mutual consensus between wild-type and mutant plasmid. Blue or black letters indicate discrepancy between wild-type and mutant plasmids.

6.3.5 Effect of Asparagine Mutations on Notch1 N-glycosylation

As stated previously, it is not currently known which if the six N-glycosylation sites are actually glycosylated on Notch1. Therefore, having mutated all of these sites, the next logical step was to investigate whether these mutations were affecting the lectin binding profile of Notch1 compared to the wild-type. This would provide some indication as to whether each site is glycosylated and, if so, what type of N-glycan is synthesised at that site. C3Hs were grown to ~80% confluence in eight wells of 6-well plates. One of the wells was left untreated while the other seven were co-transfected with a plasmid encoding a puromycin resistance gene and one of the seven different types of Notch1 plasmid, ie. the wild type plasmid and the six mutant plasmids. Cells were incubated at 37ºC for 24h before transfected samples were treated with puromycin (3µg/mL). After another 24h incubation at 37ºC, cells were harvested and lysed to isolate protein. BCA assay was used to quantify the concentration of protein in each sample. IP was carried out on all samples using Protein G-conjugated magnetic beads and an anti-Myc-tag mouse monoclonal antibody from Abcam (ab32). The non-transfected sample was immunoprecipitated with a mouse IgG control antibody. Following elution and neutralisation, using Glycine and Tris buffers respectively, another BCA assay was carried out to quantify protein concentration in the eluted fraction. ELLA was then used to detect N-glycans in all eight samples. Control wells containing PBS rather than a protein sample were used to determine the baseline for non-specific absorbance, while the mouse IgG control sample acted as the baseline for non-specific lectin- or antibody-binding to the IP eluate. Both of these baseline values were subtracted from sample absorbance values to decipher the true level of specific lectin binding. TBST acted as the vehicle control for all lectins. The results of this ELLA can be seen in Fig.6.7. The N888I, N1489 and N1587 mutations all resulted in a significant decrease in ConA, LCA and E-PHA binding compared to that observed in the wild-type plasmid, but did not significantly alter WGA binding. N959I led to a significant reduction only in ConA binding, while N1179 caused a significant attenuation in only the binding of LCA.

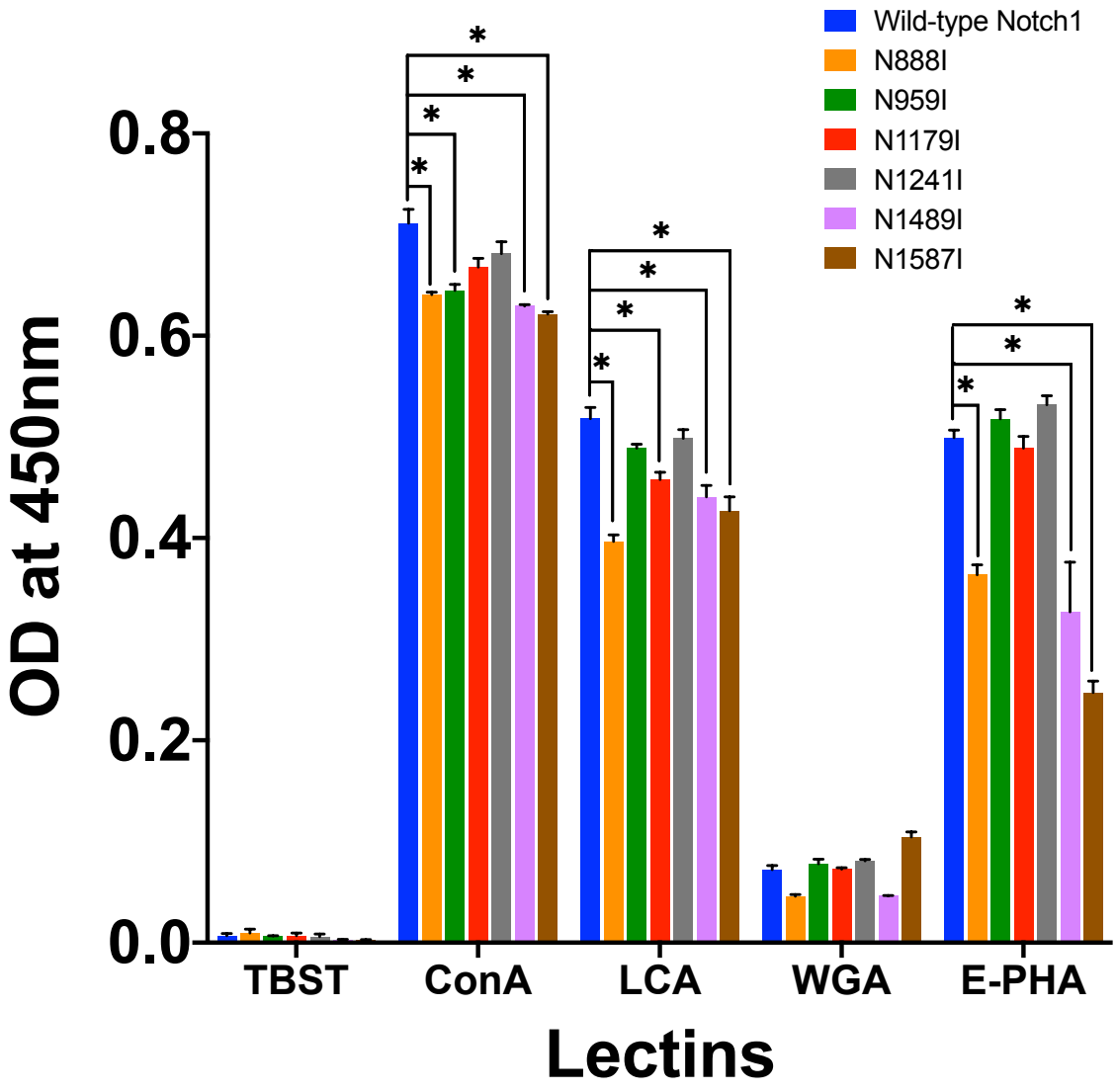


Fig.6.7 Effect of asparagine mutations on N-glycosylation of Notch1. ELLA analysis of N-glycan specific lectin binding of the Notch1 receptor from C3Hs co-transfected with puromycin resistance plasmid and either the wild-type Notch1 plasmid or one of the six mutant Notch1 plasmids for 48 h at 37°C, with puromycin treatment (3µg/mL) for the final 24 h. The Myc-tagged Notch1 was then purified from sample lysates using protein G-conjugated magnetic beads before ELLA analysis. Data are presented as the mean absorbance value at 450nm normalised to the negative control PBS sample and the IgG immunoprecipitation control. Error bars based on SEM. Data representative of n = 3,
* $p < 0.05$

6.3.6 Effect of Asparagine Mutations on Jag-1 activation of C3Hs

Changes in protein glycosylation can have a variety of effects on protein stability, activity, function and much more. For a membrane-bound receptor such as Notch1, these effects can lead to marked alterations in downstream signalling. It was important therefore, to investigate whether mutation of N-glycosylation sites on Notch1 would have an effect on the activation of Notch target genes and myogenic markers following Jag-1 stimulation. C3Hs were seeded into Jag-1- or Fc-coated wells and incubated overnight at 37ºC. The following day cells were co-transfected with a plasmid encoding a puromycin resistance gene and one of the seven different types of Notch1 plasmid, ie. the WT plasmid and the six mutant plasmids. Cells were incubated at 37ºC for 24h before transfected samples were treated with puromycin (3µg/mL). After another 24h incubation at 37ºC, cells were harvested and RNA was isolated from each sample as per Section 2.2.7. To evaluate the change in expression of *Hey1* and *Myh11,* qRT-PCR was carried out. Jag-1 significantly increased the expression of *Hey1* in the sample transfected with the WT plasmid (Fig.6.8). This response was then significantly attenuated by mutations N888I, N1241I and N1587I. Furthermore, the increase in *Myh11* expression resulting from Jag-1 treatment was significantly reduced by all six mutations compared to the WT control (Fig.6.9).

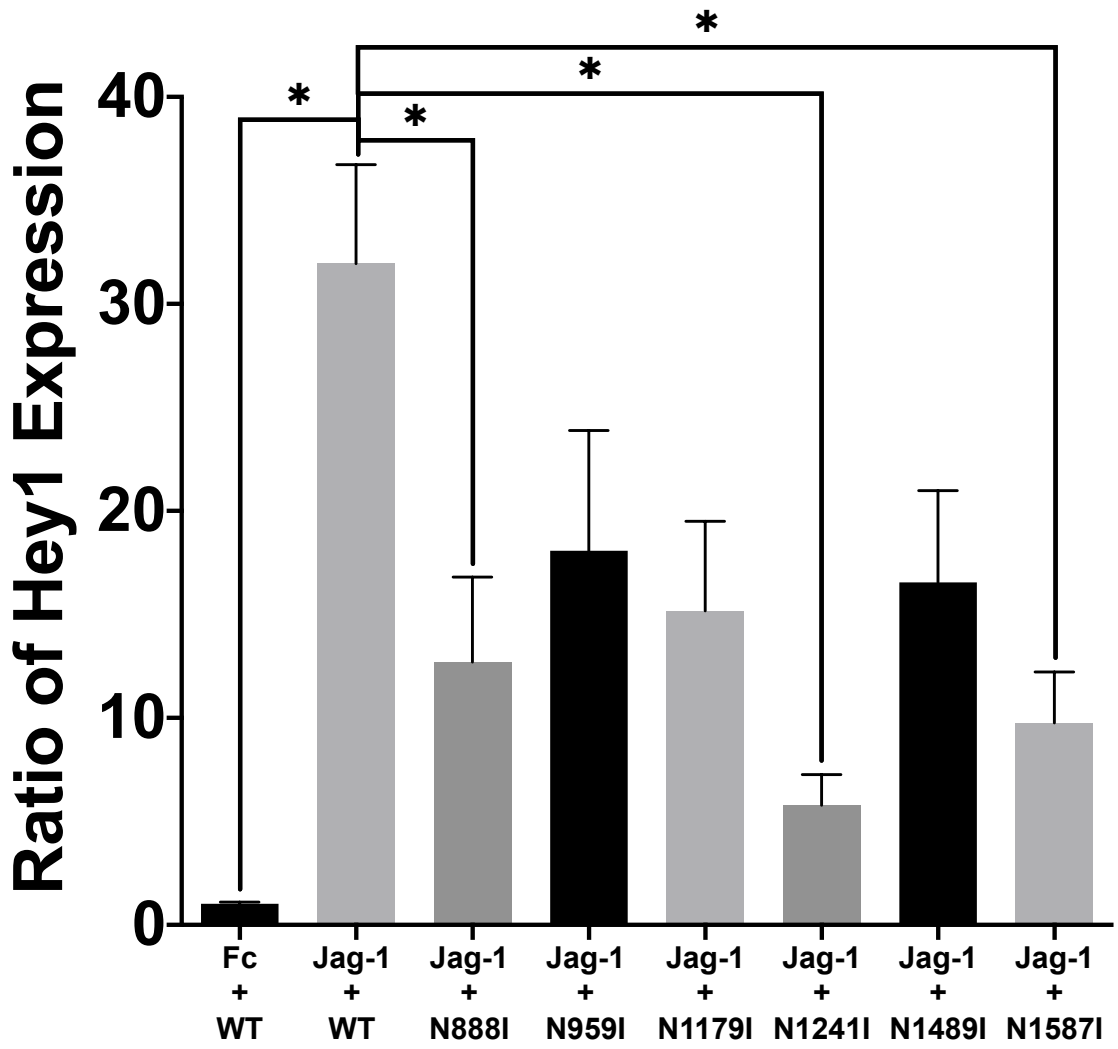


Fig.6.8 Effect of asparagine mutations on *Hey1* expression in Jag1-treated C3Hs. The relative expression of Jag-1 (1μg/mL) stimulated *Hey1* mRNA levels by qRT-PCR in C3H cells co-transfected with puromycin resistance plasmid and either the wild-type Notch1 plasmid or one of the six mutant Notch1 plasmids and incubated for 48 h at 37ºC, with puromycin treatment (3μg/mL) for the final 24 h. Data are presented as the ratio of expression relative to the negative control sample treated with Fc and transfected with the wild-type Notch1 plasmid. Error bars based on SEM. Data representative of n=3, * $p < 0.05$

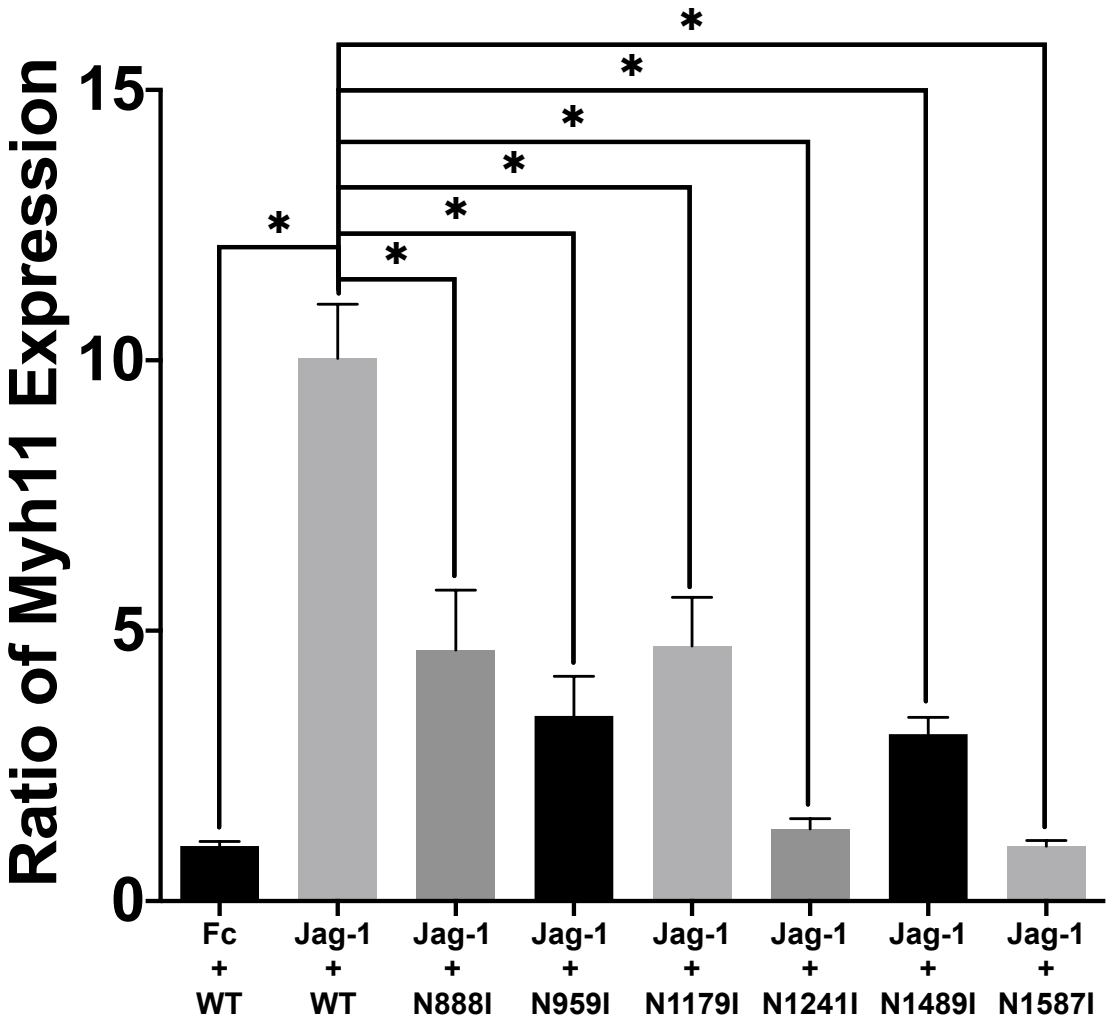


Fig.6.9 Effect of asparagine mutations on *Myh11* expression in Jag1-treated C3Hs. The relative expression of Jag-1 (1μg/mL) stimulated *Myh11* mRNA levels by qRT-PCR in C3Hs co-transfected with puromycin resistance plasmid and either the wild-type Notch1 plasmid or one of the six mutant Notch1 plasmids and incubated for 48 h at 37°C, with puromycin treatment (3μg/mL) for the final 24 h. Data are presented as the ratio of expression relative to the negative control sample treated with Fc and transfected with the wild-type Notch1 plasmid. Error bars based on SEM. Data representative of n=3, * $p < 0.05$

6.3.7 Effect of Asparagine Mutations on Plasmid Transfection Efficiency

The expression of Notch1 target gene expression can be heavily influenced by the amount of Notch1 present in a given cell. Therefore changes in target gene expression in a cell population where Notch1 is being ectopically expressed may depend on the amount of *Notch1*-coding plasmid present in that population. For this reason, it was important to determine if the single base substitutions carried out on the plasmid-encoded Notch1 gene were having an effect on the amount of plasmid being transfected into a cell population. C3Hs were co-transfected with a plasmid encoding a puromycin resistance gene and either an empty vector (EV) control or one of the seven different types of Notch1 plasmid, ie. the wild type plasmid and the six mutant plasmids. Cells were incubated at 37ºC for 24h before transfected samples were treated with puromycin (3μg/mL). Cells were harvested after another 24h incubation at 37ºC. The Promega Reliaprep^{TM} RNA Miniprep System is very efficient at removing genomic DNA from a cell lysate but is unable to degrade plasmid DNA due to its small size. Therefore, this kit was used (as described in Section 2.2.8) to isolate both the RNA and plasmid DNA from each sample. PCR was then carried out to measure the amount of *Notch1*-coding plasmid DNA in each sample. This was performed as per Section 2.2.11, except the Reverse Transcriptase was omitted from the mastermix to ensure that no RNA was converted to cDNA. This meant that while plasmid DNA could be amplified and measured, mRNA transcript could not. There was no significant difference between levels of *Notch1*-coding plasmid DNA across all mutant plasmid samples compared to the WT (Fig.6.10).

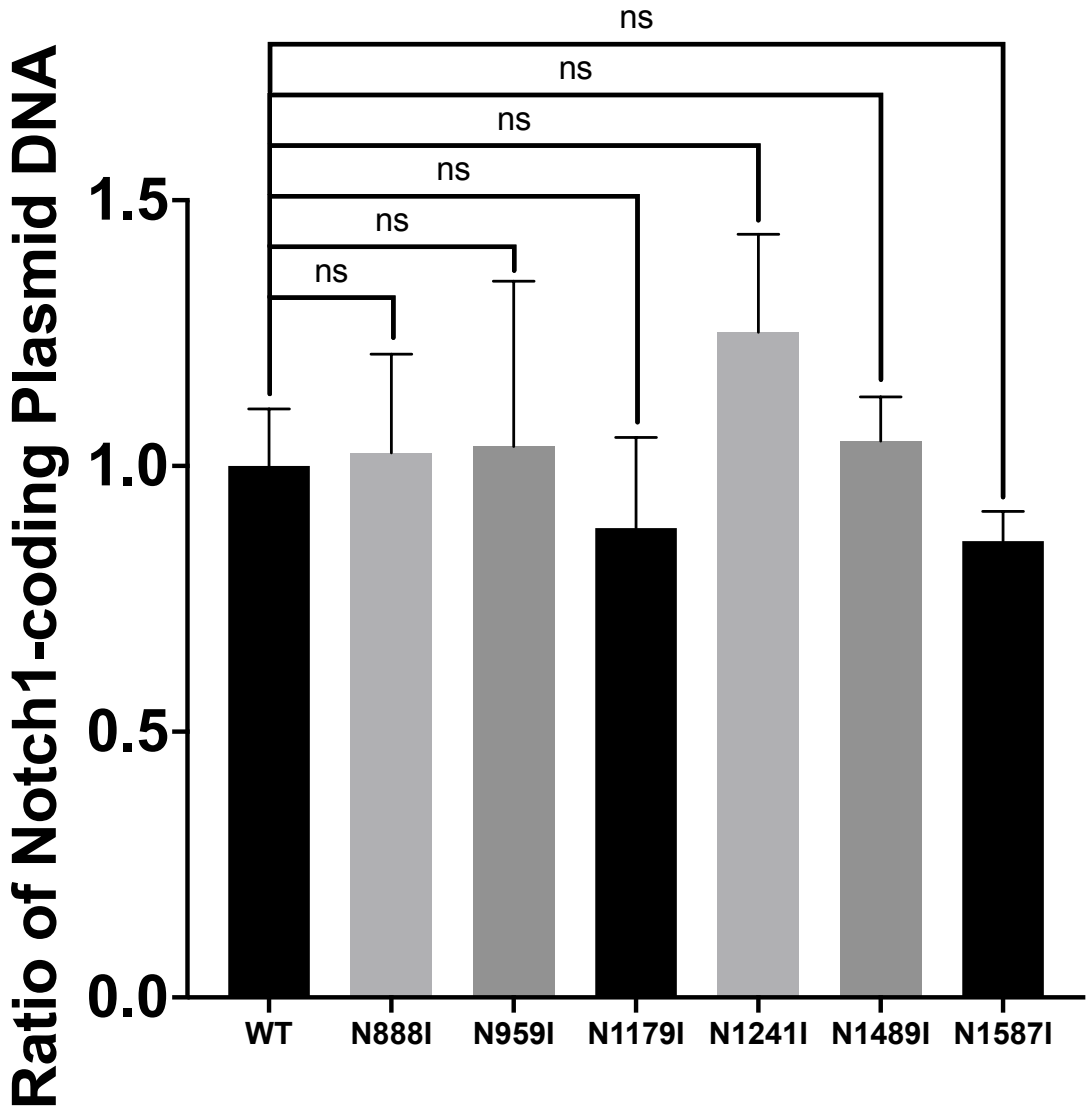


Fig.6.10 Effect of asparagine mutations on Plasmid Transfection Efficiency in C3Hs. The relative levels of *Notch1*-coding plasmid DNA by PCR in C3Hs co-transfected with puromycin resistance plasmid and either the wild-type Notch1 plasmid or one of the six mutant Notch1 plasmids and incubated for 48 h at 37°C, with puromycin treatment (3µg/mL) for the final 24 h. Data are presented as the ratio of expression relative to the wild-type control. Error bars based on SEM. Data representative of n=3, ns – $p > 0.05$

6.3.8 Effect of Asparagine Mutations on Notch1 Protein Levels

Changes in Notch target gene expression may also result from a discrepancy in the level of ectopically expressed Notch1 protein across different mutants. This may be due to changes in protein expression, processing or degradation. To investigate the effect of asparagine mutations on Noth1 protein levels, C3Hs were co-transfected with a plasmid encoding a puromycin resistance gene and one of the seven different types of Notch1 plasmid, ie. the wild type plasmid and the six mutant plasmids. Cells were incubated at 37^{o}C for 24h before transfected samples were treated with puromycin (3μg/mL). Cells were harvested after another 24h incubation at 37^{o}C. Protein was isolated as per Section 2.2.10 and BCA assay was used to quantify protein concentrations. Western Blot was carried out as described in Section 2.2.16 and an anti-myc-tag antibody from Abcam (ab32) was used to probe for myc-tagged Notch1 in each sample. Densitometry was carried out using the ImageJ software to measure intensity of Notch1 bands relative to the β-actin loading control. A significant decrease in Notch1 protein levels was observed in the samples transfected with the N1241I plasmid and the N1587I plasmid. No significant change was detected across all other mutant plasmid samples compared to the WT control (Fig.6.11).

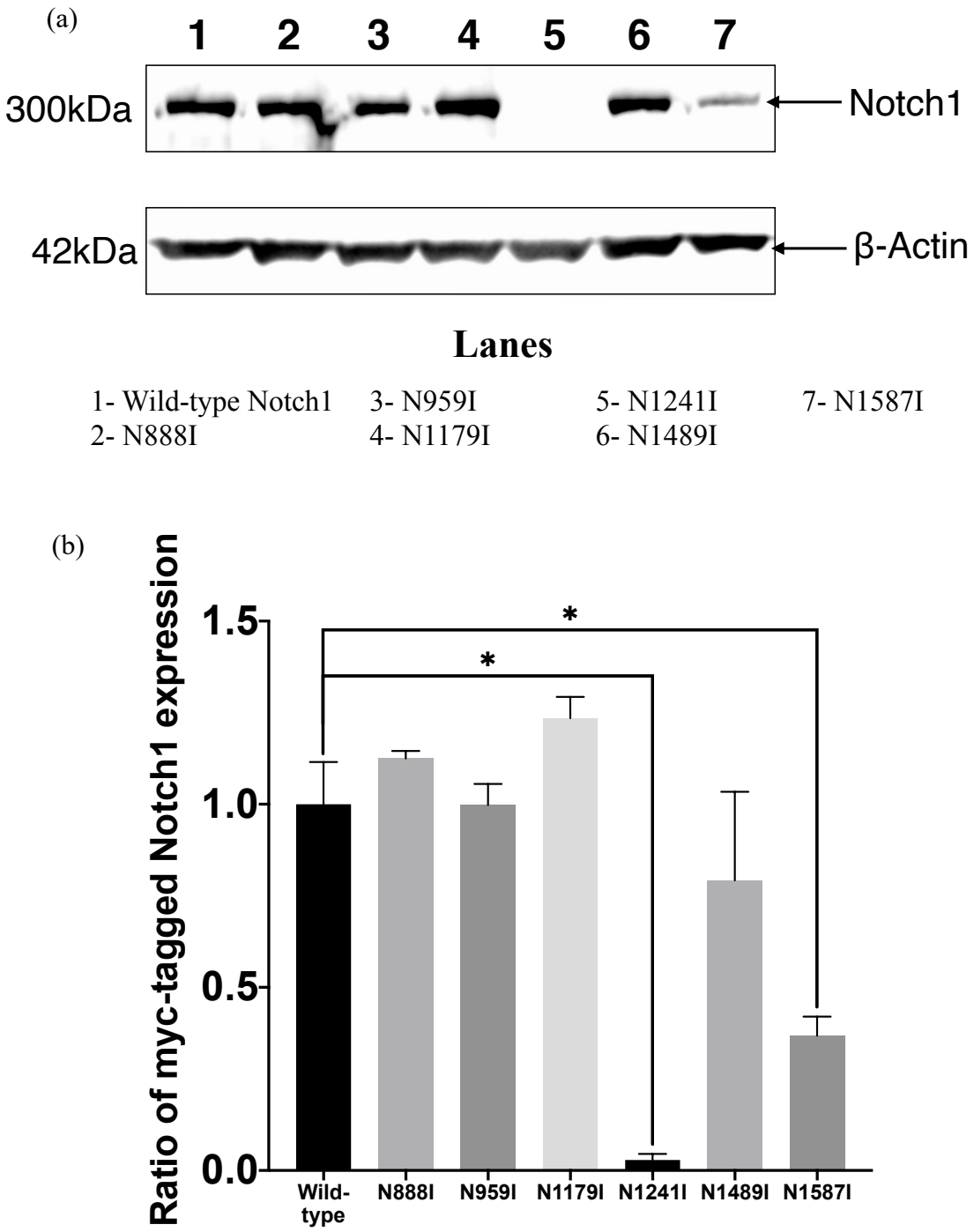


Fig.6.11 Effect of asparagine mutations on Notch1 protein levels. Notch 1 receptor protein expression in C3Hs co-transfected with puromycin resistance plasmid and either the wild-type Notch1 plasmid or one of the six mutant Notch1 plasmids and incubated for 48 h at 37°C, with puromycin treatment (3µg/mL) for the final 24 h. Western blot used to measure ectopic expression of myc-tagged Notch1. (a) Representative immunoblot image of full-length Notch1 bands at 300kDa and β-actin bands at 42kDa. Densitometry was carried out on western blot samples to measure intensity of Notch1 bands normalised to the β-actin loading control. (b) Full-length Notch1 protein levels presented as the ratio of expression relative to the negative control sample transfected with the wild-type Notch1 plasmid. Error bars based on SEM. Data representative of n=3, * $p < 0.05$

6.4 Discussion

Small-molecule inhibition and glycosyltransferase knockdown are excellent tools for gaining an overall understanding of the importance of N-glycosylation in a particular cellular process or molecular mechanism. However, their main drawback is their broad specificity, as this leads to caveats whereby detected changes often cannot be definitively attributed to alteration or removal of a particular oligosaccharide. Currently, the most specific method for removing one individual N-glycan on a particular glycoprotein is to carry out site-directed mutagenesis of the asparagine (N) residue in the N-X-S/T consensus sequence required for N-linked glycosylation at the target site. These mutations can be stably inserted into the cell genome by reliable technologies such as CRISPR. However, the most simple and rapid method of single base substitution is to mutate the target gene in a plasmid vector by using a PCR which incorporates mutant primers. The plasmid produced from this reaction can then be transfected into the cell line of interest which subsequently expresses the mutant protein. This method has been extensively used to elicit information regarding the role of individual N-glycans on specific glycoproteins (Flack *et al.*, 1994; Ferlinz *et al.*, 1997). The overall aim of this chapter was to utilise this technique to mutate the asparagine residues of the six N-glycosylation consensus sequences along the Notch1 extracellular domain, and then to express these mutant receptors in MVSCs and observe the effect of the mutation on the response to Jag-1 stimulation.

Before generating any of the mutant plasmids, it was first essential to ensure that the cell line of interest could exhibit a high enough level of plasmid uptake and expression to make any change in response detectable. This would be dependent on the susceptibility of the cell line to puromycin selection, its sensitivity to plasmid DNA cytotoxicity and the proportion of cells in a population that would take up and express the plasmid DNA. Puromycin cytotoxicity titration was carried out on both the MVSC and C3H cell lines to determine the concentration of puromycin required to kill 80-90% of cells in a population. Data from this experiment showed that the C3H cell line was much more sensitive to puromycin cytotoxicity than the MVSC cell line as the concentration required to reach optimum cell death was much lower in C3Hs.

Optimisation of plasmid DNA concentration for transfection was subsequently performed. This was to ensure that both the mutant Notch1 plasmid and the puromycin resistance plasmid (required for puromycin selection) could be transfected into a large proportion of

the cell population without causing high levels of cytotoxicity. In order to visualise the cells which had taken up the plasmid and expressed the encoded genes, a GFP-coding plasmid was transfected into both MVSCs and C3Hs at a range of different concentrations. Across multiple DNA concentration ranges and several modifications to the transfection process, no conditions could be manufactured with the MVSC cell line to yield a high enough rate of plasmid transfection efficiency (>70%) while maintaining an acceptable level of cell death (<50%) to facilitate downstream applications. Many stem cell lines, both embryonic and adult, have been previously reported to be quite difficult to transfect (Lakshmipathy, 2004; Walczak *et al.*, 2005; Han *et al.*, 2015). In particular, stem cells from a neuroectodermal lineage regularly exhibit very low levels of transfection efficiency (Sapet *et al.*, 2011; Bertram, Wiese and von Holst, 2012; Adams *et al.*, 2016). As MVSCs come from a neuroectodermal origin, they may be inherently difficult to transfect with plasmid DNA. Additionally, this level of cell death was observed with transfection of the GFP-coding plasmid, which is only ~4.7kb in length. The *Notch1*-coding plasmid, meanwhile, is over 11kb in length and as it has been reported that larger plasmids cause higher levels of cell death and lower levels of transfection efficiency (Lesueur, Mir and André, 2016), these issues would only become more prominent in downstream experiments. Therefore, all subsequent experiments involving the transfection of Notch1 mutant plasmids would be carried out in the C3H cell line which met the criteria required for transfection efficiency and cell death at a concentration of 250ng/mL plasmid DNA, and was subsequently shown in Section 6.3.3 to be amenable to puromycin selection of transfected cells. The suitability of this C3H cell line for plasmid transfection has been widely reported in the literature as it has an excellent track record for exhibiting high levels of transfection efficiency (Jackson *et al.*, 2005; Yamano, Dai and Moursi, 2010; Kim *et al.*, 2013; Son *et al.*, 2020). Furthermore, C3H cells should closely mimic the response of MVSCs in Notch signalling and Notch-dependent myogenic differentiation. While C3H cells are mesoderm-derived embryonic fibroblasts, as opposed to the neuroectodermal-derived adult MVSCs, previous data in the current study has demonstrated that they express some of the same CVD-relevant markers (Sca1 and S100β) as MVSCs; they have the capacity to undergo Notch-mediated myogenic differentiation; and they have exhibited an almost identical response to MVSCs when treated with small-molecule inhibitors of N-glycosylation and glycosyltransferase-specific siRNAs.

Having identified a cell line which could display high levels of plasmid uptake with relatively low levels of cell death, the next objective was to generate the necessary mutant plasmids. PCR was carried out using the full-length Notch1 plasmid as the template DNA

and primers which had been designed to insert a single base substitution in all copies of the template. Once these mutant plasmids had been generated, they were transformed into competent bacterial cells to be amplified before purification and sequencing. The sequencing data confirmed that the correct mutation had been incorporated into each of the six N-glycosylation sites on the *Notch1* gene. These mutations should alter the asparagine residue at that site to an isoleucine residue, thus preventing the addition of an N-glycan. Hence any changes in Notch1 function or downstream signalling in subsequent experiments could be in part due to the lack of an N-glycan at a particular site. However, it should be noted that changes in the polypeptide sequence could also lead to altered mechanisms such as protein folding and cleavage thereby impacting on Notch1 functionality.

To confirm that each mutation was indeed having an effect on the glycosylation of the Notch1 receptor, ELLA was carried out on the purified mutant Notch1 proteins. From the binding profiles of each sample in this data set, some information can be obtained regarding the structure of N-glycans at each position. The mutation at amino acid site N1241 did not lead to a significant change in binding with any of the lectins. This may indicate that no N-glycan actually resides at this site. However it is possible that this site does contain an N-glycan whose structure does not fall under the specificity of the LCA, WGA or E-PHA lectins, and whose absence is not detected by ConA due to issues with the sensitivity of the assay. As stated previously, lectins have a very high level of binding affinity *in vivo*, but their binding affinity *in vitro* is considerably reduced (Weis and Drickamer, 1996; Bewley and Otero-Quintero, 2001). This low level of binding affinity, coupled with the fact that the difference in binding between statistically significant and insignificant samples is quite small, means that the possibility that ConA did not detect the presence of a glycan at N1241 cannot be ruled out. This is further emphasised by the fact that the N1179 mutation did not lead to a significant change in ConA binding, but did significantly reduce the level of LCA binding, indicating that a core fucosylated oligosaccharide may be present at this site which was not detected by ConA.

The mutation at N959, meanwhile, resulted in a significant decrease in ConA binding, but no significant changes to binding with the other three lectins. This suggests that although there may be an N-glycan present at this site, it does not possess any of the structural characteristics required for binding to LCA, WGA or E-PHA. Mutations at N888, N1489 and N1587 significantly decreased the level of binding with ConA, LCA and E-PHA, suggesting that glycans at those sites are both core fucosylated and have a bisecting structure.

However, this is unlikely as it has previously been demonstrated that GnT-III modification of an oligosaccharide actively inhibits the addition of a fucose by Fut8 (Zhao *et al.*, 2008). This discrepancy may be explained by the alternative binding specificities of certain lectins. E-PHA predominantly binds to N-glycans containing a bisecting structure, but has also been shown to have affinity for oligosaccharides with terminal galactose residues (Yamamoto *et al.*, 2005; Nagae *et al.*, 2014). Similarly, LCA has very high binding affinity for α1,6-fucosylated glycans, but can also bind the mannose core of an N-glycan in the absence of core fucosylation (Maupin, Liden and Haab, 2012). These alternative binding affinities may resolve the apparent contradiction in this data. Comprehensive studies into the nature and structure of Notch1 N-glycans have not previously been carried out and therefore these findings provide novel insights into the profile of N-glycosylation along the extracellular domain of the Notch1 receptor.

Once the effect of each mutation on Notch1 N-glycosylation had been confirmed, all six mutated plasmids were then separately transfected into Jag-1 treated C3Hs for 48 h to investigate how these alterations would impact the Jag-1 response. To quantify this impact, changes in *Hey1* or *Myh11* expression resulting from the asparagine mutations were measured by qRT-PCR. In the sample transfected with the wild-type Notch1 plasmid, Jag-1 substantially increased the expression of both *Hey1* and *Myh11*. The increase in *Hey1* expression was significantly reduced by mutations at amino acid sites N888, N1241 and N1587, indicating that N-glycans at these three sites may have an important role in Notch signalling. *Myh11* expression was significantly attenuated by all six mutations. For the mutations at N888, N1241 and N1587, this is most likely related to their effect on *Hey1* expression and indicates that alterations at these sites directly impact the expression, processing or activation of the Notch1 receptor. With regard to the mutations at N959, N1179 and N1489, it may be the case that their effect on the myogenic differentiation process is more indirect and related to a possible role for Notch1 in this process outside of its initial activation by Jag-1. Non-canonical Notch signalling independent of ligand activation or Notch target gene expression, which occurs mainly in stem/progenitor cells (Andersen *et al.*, 2012), has been reported on multiple occasions to influence other cellular pathways such as Wnt/β-catenin signalling (Sanders *et al.*, 2009; Acosta *et al.*, 2011; Kwon *et al.*, 2011). Membrane-bound Notch can inhibit Wnt/β-catenin signalling by reducing the levels of active β-catenin at the membrane, likely by directing it for lysosomal degradation (Hayward *et al.*, 2005; Kwon *et al.*, 2009). In addition, Wnt/β-catenin signalling has been regularly identified as a stimulator of myogenic differentiation in a number of different adult

stem cell types (Polesskaya, Seale and Rudnicki, 2003; Shang *et al.*, 2007; Ling, Nurcombe and Cool, 2009; Tanaka, Terada and Nohno, 2011). It is thought that this stimulation is intrinsically linked to, and regulated by, Notch signalling (Brack *et al.*, 2008). Another example of non-canonical Notch signalling involves the regulation of cell junction assembly by the Notch1 transmembrane domain (TMD). Following cleavage and release of the NICD, the TMD can recruit proteins such as VE-cadherin and the protein tyrosine phosphatase LAR to form a complex and activate junction assembly (Polacheck *et al.*, 2017). This further demonstrates the many ways in which Notch can regulate other signalling pathways outside its direct transcription activation role. Therefore, it is possible that mutations at N-glycosylation sites N959, N1179 and N1489 inhibit myogenic differentiation by altering the regulatory functions of non-canonical Notch signalling. It is also conceivable that, although their reduction of *Hey1* expression may not be statistically significant, it may be enough to bring signalling under the threshold required for the activation of myogenic differentiation.

Although all mutant plasmids were the same size and only differed by a single nucleotide, it was possible that changes in Notch signalling and myogenic differentiation were being caused by altered plasmid transfection efficiency. PCR was carried out on plasmid DNA from C3Hs transfected with each Notch1 plasmid. The resulting data showed that there was no significant change in the amount of *Notch1*-coding plasmid DNA in any of the samples transfected with a mutant plasmid compared to the sample transfected with the wild-type plasmid. This indicates that the transfection efficiency of the plasmid was not being altered by the single base mutation and therefore this was not the cause of the changes observed in the Jag-1 response.

Another possible reason for the changes detected in *Hey1* and *Myh11* expression, may be that the amount of Notch1 protein being expressed or degraded could be altered by the mutation, leading to different levels of Notch1 protein in the cell. Western blot data showed significant decreases in myc-tagged Notch1 protein levels in samples transfected with the N1241I and N1587I mutant plasmids compared to the wild-type control. This suggests that either the mutation of the asparagine codon at these two sites has inhibited the proper transcription or translation of Notch1, or that the Notch1 protein is being rapidly degraded as a result of either the change in N-glycosylation or the change in amino acid sequence. Previous site-directed mutagenesis studies have found that removal of a single N-glycosylation site can have a profound effect on the trafficking and degradation of a particular glycoprotein. This was demonstrated on multiple occasions with proteins such as

dipeptidylpeptidase IV(DPPIV), lecithin:cholesterol acyltransferase (LCAT) and cathepsin V (L2), where in each case the mutation of a single N-glycosylation site led to a dramatic increase in protein degradation, often due to incorrect folding and/or trafficking (Qu *et al.*, 1993; Fan *et al.*, 1997; Niwa *et al.*, 2012). It has also been demonstrated by a number of research groups that mutation of the asparagine residue in an N-glycosylation consensus sequence can inhibit the production and processing of glycoproteins such as EPO, glucoamylase and sphingomyelinase, especially when the glycosylation site is located adjacent to important processing motifs such as cleavage sites (Yamaguchi *et al.*, 1991; Chen, Ford and Reilly, 1994; Ferlinz *et al.*, 1997). Therefore, combining evidence from this section with previously published data, it is highly likely that N-glycans on the Notch1 protein, particularly those at sites N1241 and N1587, serve some role in the production, processing or degradation of the receptor.

In summary, data in this chapter showed that the MVSC cell line was not suitable for these site-directed mutagenesis experiments due to its low plasmid transfection efficiency and high level of sensitivity to DNA cytotoxicity. The C3H cell line was more amenable and was therefore used as a substitute for MVSCs. This slightly reduces the impact of some of the subsequent data but, as previously detailed, the C3H cell line has many similar characteristics to MVSCs, and exhibited a response that was almost identical to MVSCs in every other major experiment in this project. Mutant plasmids were generated and validated by sequencing. Most of the mutations incorporated into the *Notch1* gene had a measurable effect on receptor glycosylation, while one mutation, at N1241, elicited no significant change. ELLA data indicated the presence of a range of different N-glycan structures on the Notch1 extracellular domain, including core fucosylated and bisecting N-glycans, and also some structures that could not be identified with the limited range of lectins used. Mutation of asparagine residues at Notch1 N-glycosylation sites reduced *Hey1* expression (N888, N1241 and N1587) and *Myh11* expression (all mutations) following Jag-1 stimulation of C3Hs. This did not seem to be a result of altered plasmid transfection efficiency. In the case of N1241 and N1587, evidence suggests that the attenuation of the Jag-1 response may have been due to altered expression or degradation of Notch1, while in the case of the other four mutations, there is no data to indicate a change in Notch1 protein levels and therefore it is likely that the role of N-glycans at those sites may influence another aspect of Notch1 processing or signalling, such as receptor cleavage or trafficking; or through indirect effects on processes such as non-canonical signalling of Notch and its regulation of the Wnt/β-catenin pathway.

Chapter 7:

Final Discussion

The uncertainty surrounding the origin of SMC-like cells in an arteriosclerotic lesion and the exact molecular mechanisms by which they arise, has plagued the world of vascular biology for decades and limited the potential for development of highly effective therapies. For many years, the generally accepted model was that of differentiated SMCs in the medial layer of the artery undergoing phenotypic switching and de-differentiating to become SMC-like cells in the developing neointima (Owens, Kumar and Wamhoff, 2004). However, this model has been challenged by a wave of studies in recent years which have provided evidence to suggest that a number of other cell types may be responsible for this process of arterial remodelling. Some publications have reported the involvement of circulating bone marrow-derived stem cells (Sata, 2003), and many others have cited the transition of endothelial cells to mesenchymal stem cells as the primary mode of neointima formation (Cooley *et al.*, 2014). However, the most compelling evidence to date comes from studies which describe the myogenic differentiation of resident vascular stem cells in response to vessel injury. Stem cell populations have been identified in both the medial and adventitial layers of the artery and data from lineage tracing studies, scRNA-Seq and single cell photonics has bolstered the argument that neointimal cells are derived from a stem cell parent population in the vessel wall which is $S100\beta^{+}$ and/or $Sca1^{+}$ (Torsney, Hu and Xu, 2005; Tang *et al.*, 2012; Roostalu *et al.*, 2018; Molony *et al.*, 2020; Di Luca *et al.*, 2021).

Many research groups have sought to determine the molecular pathways by which these stem cell populations may undergo myogenic differentiation to SMC-like cells. The Notch signalling pathway, and the Notch1 receptor in particular, has been reported to have an important role in both the process of arterial remodelling and the myogenic differentiation of stem cells (Kurpinski *et al.*, 2010; Redmond *et al.*, 2014). This pathway is known to be tightly regulated by a number of cellular mechanisms, one of which is the glycosylation of the Notch receptor itself. Numerous studies have demonstrated the importance of O-linked glycosylation in processes such as receptor-ligand binding and receptor trafficking (Xu *et al.*, 2007; Matsumoto *et al.*, 2016). However, the extracellular domain of the protein also harbours N-linked glycans about which very little is known. Although it has been shown that there are six highly conserved N-glycosylation sites on the Notch receptor (Takeuchi and Haltiwanger, 2014), there is currently no data available to determine how many of these sites are actually glycosylated and what type of N-glycans reside on the receptor, other than one study from 2017 which suggested that Notch1 contains complex bisecting N-glycans (Allam *et al.*, 2017). Therefore, the overall aim of this study was to investigate the role of Notch1 in the myogenic differentiation of a resident vascular stem cell population, define the profile

of N-glycosylation on the Notch1 receptor and explore the impact of this N-glycosylation on Notch signalling and Notch-mediated myogenic differentiation.

7.1 Notch1 mediates myogenic differentiation in S100β$^+$ MVSCs

An essential element of this study is the choice of stem cell population used to investigate the role of Notch and its N-glycans in the process of myogenic differentiation. Previous publications have detailed the importance of S100β$^+$ resident vascular stem cells and S100β itself in arterial remodelling following vessel ligation (Tang *et al.*, 2012; Cao *et al.*, 2017). Images from a lineage tracing study carried out by our own research group were analysed in this project and the resulting data confirmed the presence of neointimal cells in an injured vessel which were derived from an S100β$^+$ parent population. Moreover, this lineage tracing model, which used an inducible S100β-controlled Cre system, was the first of its kind to incorporate a 4-week Tamoxifen washout period to ensure that the potential for mislabelling neointimal cells was kept to a minimum. These findings supported previous evidence from our research group which used both lineage tracing and single cell photonics to identify a subpopulation of multipotent vascular stem cells (MVSCs) which are S100β$^+$ and, following vascular injury, can migrate and differentiate to become SMC-like cells in the neointima (Molony *et al.*, 2020; Di Luca *et al.*, 2021). Use of an MVSC population for subsequent experiments involving Notch and its N-glycans would therefore give added relevancy to the data and provide more meaningful insights into the molecular mechanisms of fibromuscular intimal thickening.

MVSCs were then isolated from the arch region of a mouse aorta. They were characterised first by their protein expression profile and found to be negative for SMC markers Cnn1 and Myh11, but positive for S100β, Sca1 and the neuroectodermal marker Nestin. A high level of telomerase activity compared to differentiated SMCs confirmed their stemness. Finally, their capacity to differentiate down both an osteogenic and adipogenic lineage, along with their previously reported myogenic differentiation ability (Tang *et al.*, 2012), was testament to the multipotency of this cell line.

The Notch signalling pathway has been shown on a number of occasions to drive myogenic specification of a range of stem cells, including S100β$^+$ resident vascular stem cells (Doi *et al.*, 2006; High *et al.*, 2007; Kurpinski *et al.*, 2010; Tang *et al.*, 2012). While previous reports used OP-9-Delta1 feeder cells to activate Notch signalling in MVSCs, this study confirmed

that immobilised Jag-1 could activate the Notch receptor and stimulate the expression of both Notch target genes and myogenic markers in MVSCs isolated from the mouse aortic arch. Data from this study also demonstrated that this activation was mediated by canonical Notch signalling as the γ-secretase inhibitor DAPT could effectively abrogate the response. Canonical Notch signalling operates via the NICD-RBP-Jκ complex which, along with other transcription factors, activates target gene expression (Bray, 2006). It has previously been demonstrated that the NICD-RBP-Jκ complex is essential in the stimulation and regulation of myogenic differentiation (Morrow *et al.*, 2008). One of the mechanisms by which the NICD-RBP-Jκ complex may activate the transcription of SMC genes is via interaction with the SRF-myocardin transcription activator complex (Noseda *et al.*, 2006). However, several studies have described the ability of Notch target genes, such as *Hey1* and *Hey2*, to inhibit myocardin-induced myogenic differentiation, although many of these studies differ in their description of the mechanism of inhibition, with some citing a direct interaction between Notch target genes and SRF, while others suggest that this occurs via an independent parallel pathway (Doi *et al.*, 2005; Proweller, Pear and Parmacek, 2005). Therefore, the primary mode of Notch-mediated myogenic differentiation observed in this study may arise from a myocardin-independent pathway. While it has been well documented that Notch target genes such as *Hey1* and *Hes1* contain RBP-Jκ binding domains at specific GTGGGAA consensus sequences (Maier and Gessler, 2000; Chang *et al.*, 2010; del Bianco *et al.*, 2010), recent bioinformatic analysis by our research group has revealed the presence of similar consensus sequences in the *Myh11* and *Cnn1* promoter regions (Appendix C), indicating that transcription of myogenic genes may be directly activated by the NICD-RBP-Jκ complex. It has also been previously reported that CBF1 (the human form of RBP-Jκ) interacts with SMAD2/3 in the TGF-β signalling pathway to promote transcription of SMC genes such as Calponin1 and SM22α (Tang *et al.*, 2010). Therefore, further research would be required to determine the exact mechanisms by which Notch signalling activates the process of myogenic differentiation in stem cells.

Mammalian cells express four different types of Notch receptor and each one has the capacity to initiate Notch signal transduction (Weinmaster, Roberts and Lemke, 1992; Lardelli, Dahlstrand and Lendahl, 1994; Uyttendaele *et al.*, 1996). It has been reported by a number of research groups that Notch1 in particular plays a role in the process of arterial remodelling (Li *et al.*, 2009; Redmond *et al.*, 2014; Q. Chen *et al.*, 2015). In the current study, knockdown of the *Notch1* transcript through siRNA transfection significantly attenuated the Jag-1 response of MVSCs. This demonstrates a novel finding that Jag-1-

induced Notch signalling, mediated by the Notch1 receptor, stimulates myogenic differentiation in an S100β^{+} resident vascular stem cell population. Future studies that selectively delete the Notch1 receptor in resident S100β stem cells using S100β-CreERT2 transgenic mice crossed with Notch1 floxed mice will reveal the consistency of this data *in vivo* in addition with studies that explore the role of the other three Notch receptors in this process. Nevertheless, these findings highlight the potential of Notch1 as a therapeutic target for arteriosclerosis.

7.2 N-glycosylation Profile of the Notch1 Receptor

Glycosylation is an essential regulator of many cellular processes and Notch signalling is no different. O-glycosylation has been reported on multiple occasions to influence the folding, trafficking, activation and cleavage of Notch1 (Acar *et al.*, 2008; Boskovski *et al.*, 2013; Matsumoto *et al.*, 2016; Ogawa *et al.*, 2020). However, as previously mentioned, the N-glycosylation of the Notch1 receptor is poorly understood. The only concrete evidence currently available regarding the profile of N-linked glycans is that six consensus sites are present and highly conserved along the extracellular domain (ECD), and at least some of the N-glycans at these sites contain a bisecting structure (Takeuchi and Haltiwanger, 2014; Allam *et al.*, 2017). In the current study, ELLA analysis of the purified Notch1 receptor confirmed the presence of N-glycans, and of bisecting N-glycans in particular, whilst also revealing the existence of oligosaccharides with a fucose residue bound to the core GlcNAc by an α-1,6 linkage (referred to as core fucosylation). Treatment with global N-glycosylation inhibitors tunicamycin (TNC) and 1-deoxymannojirimycin (DMJ) further supported these findings as each inhibitor effected a reduction in binding of the E-PHA (specific for bisecting structures) and LCA (specific for core fucosylated structures) lectins to the purified Notch1 protein. However, many lectins have weak affinity for oligosaccharide structures other than their main binding target, including both E-PHA and LCA (Maupin, Liden and Haab, 2012; Nagae *et al.*, 2014). Therefore, in order to further confirm the type of structures being bound by these lectins, a strategy of siRNA knockdown was implemented to inhibit the expression of the glycosyltransferases responsible for the formation of bisecting and core fucosylated N-glycans. These are GnT-III and Fut8 respectively. Knockdown of the *Mgat3* transcript (which codes for the GnT-III protein) led to a reduction in E-PHA binding, while *Fut8* knockdown resulted in a decreased level of LCA binding. These findings further confirm the presence of both complex bisecting and core fucosylated N-glycans on the Notch1 receptor.

The final strategy for analysis of the N-glycan profile of Notch1 was the most specific and comprehensive. Six Notch1 mutant proteins were expressed and purified for ELLA analysis. Each one contained a single base substitution at one of the six N-glycosylation sites which would block the addition of an oligosaccharide at that site. A reduction in binding of a given lectin to a mutant receptor would mean that the N-glycan missing from that receptor contained the structural properties necessary for binding to that lectin. In this way, key information regarding the specific structures of each N-glycan on the ECD of Notch1 was obtained. This data indicated that the amino acid site N1241 may not be glycosylated at all, but from analysis of other binding profiles in this assay and evidence from later experiments in this study, it is more likely that the N-glycan at this site was not detected due to the limited range of lectins used and the low binding affinity of some lectins *in vitro*. It is also possible that, due to steric hindrance, this glycosylation site was not accessible to ConA. Analysis of the N959 mutant indicated that an N-linked oligosaccharide is present at this site but does not contain structures required for binding to LCA, WGA or E-PHA. Meanwhile, the glycan at site N1179 was found to contain a core fucosylated structure. Finally, it is noteworthy that N-glycans at N888, N1489 and N1587 shared a similar lectin binding profile and therefore it is likely that they share similar structural characteristics. However, further investigation would be required to decipher which structures they possess as data from the ELLA suggests the presence of either a core fucosylated N-glycan with a possible terminal galactose residue, or a bisecting N-glycan. Data from previous publications (Allam *et al.*, 2017), along with glycosyltransferase knockdown and small-molecule inhibition experiments in this study, suggests that at least one of these three sites contains an N-glycan with a bisecting structure, with the most likely candidate being N1587 as mutation of this residue resulted in the greatest reduction in E-PHA binding.

The full impact of this data is somewhat limited by the range of available lectins which are specific for N-linked oligosaccharides. The vast majority of commercially available lectins exhibit their highest affinity for a particular monosaccharide in a specific branching/linkage format. However, many of these structures can be found in both O-linked and N-linked glycans. For example, the *Erythrina critagalli* lectin (ECL) binds strongly to the terminal galactose of an N-acetyllactosamine-containing N-glycan, but will also bind to a terminal β1,4-galactose in O-glycans (Itakura *et al.*, 2007; Iskratsch *et al.*, 2009). Using lectins such as ECL could therefore lead to misinterpretation of data and incorrect identification of glycan structures. For this reason, future research would benefit from the incorporation of techniques such as mass spectrometry to accurately assess individual oligosaccharide

structures on the Notch1 receptor. However, the key findings in this study still provide an excellent basis for further investigation of these structures. From a starting point of knowing only the possible N-glycosylation sites and the presence of bisecting N-glycans, a preliminary profile for Notch1 N-glycosylation has been formed, detailing the presence and location of N-glycans on the extracellular domain, as well as some of their basic structural patterns which may provide insights into their individual roles.

7.3 N-glycans on Notch1 Regulate its Degradation and its Control of Myogenic Differentiation

There has been a distinct lack of research directed towards the role of Notch1 N-glycans in the context of receptor expression, processing, trafficking and signal transduction. As well as revealing information about the presence and structure of N-glycans on the Notch1 receptor, the intervention strategies adopted in the current study were used to address this issue and develop an understanding of the function of these oligosaccharides with regard to Notch1 and their wider role in Notch-mediated myogenic differentiation.

TNC and DMJ treatment of MVSCs revealed that cellular N-glycosylation is an essential aspect of both Notch signalling and of myogenic differentiation following Jag-1 stimulation. The data obtained from these treatments did not necessarily implicate Notch1 N-glycosylation directly in the process, as many other glycoproteins would be modified by the small-molecule inhibitors. In fact it was discovered that while activation of Notch target genes by the ectopically expressed NICD was not affected by these interventions, components of the myogenic differentiation pathway downstream of Notch activation may have been altered, leading to inhibition of that process. However, further investigation into the manner by which TNC and DMJ attenuated the Jag-1 response revealed the main obstacle they created was preventing Notch1 trafficking out of the ER-Golgi complex to the plasma membrane. A study from 2008 reported a similar effect on Notch3, where TNC treatment resulted in accumulation of the receptor in the ER-Golgi complex (Stahl *et al.*, 2008). While this may be due to changes in the glycosylation of the numerous proteins involved in receptor trafficking, multiple previous reports have demonstrated that inhibiting the N-glycosylation of developing proteins can block their transport to the membrane (Skrenkova *et al.*, 2018; Janezic *et al.*, 2020; Sun *et al.*, 2020). Therefore it may be the case that some of the N-glycans on the extracellular domain of the Notch1 receptor are required for correct trafficking of the protein to the plasma membrane.

Knockdown of the GnT-III and Fut8 glycosyltransferases provided a more specific insight into how two particular groups of N-glycans (bisected and core fucosylated) contributed to Notch signalling and myogenic differentiation. Evidence from this study demonstrated that both of these groups of N-glycans play a major role in activation of both Notch target gene expression and myogenic marker expression following Jag-1 activation of MVSCs. However, as with the small-molecule inhibition strategies used in this study, this siRNA knockdown strategy would also alter the N-glycosylation of proteins other than the Notch1 receptor and it was possible that this would influence its signalling capacity. Nicastrin, for example, is part of the γ-secretase complex which cleaves the NICD from the Notch1 transmembrane domain (TMD) following receptor activation, and it contains bisecting N-glycans which may be crucial for its role in the cleavage process (Yu *et al.*, 2000; Allam *et al.*, 2015). Therefore, the reduction in Notch target gene and myogenic gene expression following *Mgat3* knockdown may have been due, at least in part, to removal of these glycans. For this reason, it was important to further explore the mechanisms by which core fucosylated and bisecting N-glycans were affecting the Notch signalling process.

Unlike TNC and DMJ treatment, knockdown of GnT-III and Fut8 did not affect downstream elements of either the Notch signalling or myogenic differentiation pathways, indicating that bisecting and core fucosylated N-glycans exert their influence on the Jag-1 response either at the point of Notch receptor activation or before it takes place. Analysis of receptor trafficking revealed that glycosyltransferase knockdowns did not result in accumulation of Notch1 in the ER-Golgi complex, as was seen with small-molecule inhibition of N-glycosylation. This suggests that the inhibition of trafficking observed following TNC and DMJ treatment was either due to altered glycosylation of transport proteins or removal of N-glycans on the Notch1 receptor which do not contain bisecting or core fucosylated structures. Through combination of receptor trafficking data and measurement of Notch1 protein levels, the cumulative data revealed that bisecting N-glycans prevent the accelerated degradation of the Notch1 receptor. This supports previously published work that reported Notch1 receptor co-localisation with lysosomal degradation proteins following *Mgat3* knockdown (Allam *et al.*, 2017). The role of core fucosylated N-glycans may be more directly related to the activation of the Notch1 receptor as knockdown of the Fut8 glycosyltransferase inhibited Notch signalling and myogenic differentiation but did not affect Notch1 expression, trafficking, degradation or downstream signalling. More specific

targeting of individual glycans was required to further define the function of both bisecting and core fucosylated N-glycans.

This greater degree of specificity was achieved through mutation of the six N-glycosylation consensus sequences along the Notch1 ECD. Due to issues with plasmid transfection efficiency, analysis of the effect of these mutations was carried out in C3H cells rather than in MVSCs. While this means that the relevancy of the subsequent findings is obviously decreased somewhat, it must be kept in mind that the C3H cell line (which is also S100β^{+} and Sca1^{+}) exhibited the same response as MVSCs throughout many of the seminal experiments in this study. Importantly, myogenic differentiation could be initiated in C3H cells by Jag-1 treatment, and this response was inhibited by TNC and DMJ treatment, and also by *Mgat3* and *Fut8* knockdown. Therefore, the C3H cell line proved to be a suitable substitute for MVSCs in these experiments.

All six mutations resulted in a reduction of the myogenic differentiation capacity of C3Hs in response to Jag-1 stimulation. This further supports ELLA data in this study by confirming that N-glycans reside at each of the six consensus sites and also reinforces data from small-molecule inhibition and glycosyltransferase knockdown experiments by demonstrating that all of these glycans are involved in the process of Notch-mediated myogenic differentiation. However, only the mutations at sites N888, N1241 and N1587 significantly attenuated the expression of the Notch target gene *Hey1*. This indicates that the other three mutations at sites N959, N1179 and N1489 have an indirect effect on myogenic differentiation which is independent of canonical Notch signalling. In addition, none of these three mutations led to significant changes in the levels of the Notch1 receptor protein in the cell. Their effect on myogenic differentiation may be related to non-canonical Notch signalling pathways. For example, the Wnt/β-catenin pathway is heavily involved in the myogenic differentiation of stem cells and is regulated by non-canonical Notch signalling (Brack *et al.*, 2008; Acosta *et al.*, 2011; Tanaka, Terada and Nohno, 2011). The Notch1 receptor has been shown to interact with activated β-catenin at the membrane (Hayward *et al.*, 2005). While this interaction occurs at the intracellular C-terminal of the Notch1 receptor and it is unlikely that any direct interaction takes place between these glycans and β-catenin, it is possible that their absence leads to altered processing/folding of the receptor which results in dysregulation of Wnt signalling and myogenic differentiation. However, further research is required to fully define the role of these N-glycans.

With regard to the mutations at sites N888, N1241 and N1587, their effect specifically prevents canonical Notch signalling. ELLA data suggests that the N-glycan at N888 possessed either a bisecting or core fucosylated structure and combining this with evidence from glycosyltransferase knockdown experiments, this means that its absence does not lead to accumulation of Notch1 in the ER-Golgi complex. Furthermore, since the mutation at this site did not result in any change to Notch1 protein levels in the cell, *i.e,.* did not accelerate Notch1 degradation, this suggests that it is most likely a core fucosylated N-glycan (possibly with a terminal galactose residue), rather than a bisecting N-glycan. All of this evidence suggests that the N-glycan at N888 has a direct influence on Notch1 signal activation at the membrane. This may occur through regulation of processes such as receptor folding or cleavage, mechanisms which are regularly affected by loss of an individual N-glycan on other membrane-bound proteins (Branza-Nichita *et al.*, 2000; Hsiao *et al.*, 2009; West *et al.*, 2011). The N1241I mutation resulted in a dramatic decrease in Notch1 protein levels in the cell, implying that the Notch1 receptor was rapidly degraded, and as a result, Notch target gene expression was inhibited. ELLA data suggested that there may have been no N-glycan present at N1241 but evidence from this mutation experiment is a strong indication that an N-glycan does indeed reside at this site, but does not contain bisecting or core fucosylated structures. Removal of the N-glycan at N1587 also reduced Notch1 protein levels, most likely through receptor degradation. Combined with ELLA data and evidence from siRNA knockdown experiments, the cumulative data suggests that the oligosaccharide which resides at this site contains a complex bisecting structure.

While mutation of asparagine residues is a highly specific method for investigating the role of individual N-glycans, a major limitation to this strategy is the fact that not only is the N-glycan being removed, but another amino acid is taking the place of the asparagine residue. A single change in nucleotide or amino acid sequence can have a dramatic effect on the expression, processing and/or function of the target protein (Delorme *et al.*, 1992; Ding *et al.*, 2015). Moreover, these effects are quite difficult to predict, and also difficult to investigate. Research groups who employ this technique are faced with the difficult decision of which amino acid to use as the substitute for Asn in order to incur the lowest possible level of adverse side effects. The majority of studies which have mutated N-glycosylation sites have used glutamine as a substitute since its structure is the most similar to asparagine, but this substitution comes with the caveat that the polar amide group of the glutamine residue may lead to unwanted molecular reactions (Van Berkel *et al.*, 1996; Fan *et al.*, 1997; West *et al.*, 2011). Isoleucine was chosen as the substitute for this study due the ease of

mutation (only a single base substitution required for each Asn site) and the non-reactive nature of the side chain. However, the drastic change in side-chain composition may alter the conformation of the receptor or result in issues with steric hindrance (Ishikawa *et al.*, 2001; Suga and Maeshima, 2004; Doering *et al.*, 2018). In previous studies, the main strategy used to combat this issue has been to carry out additional mutations to the N-glycosylation site. This usually involves mutating the Asn residue to a number of different amino acids, mutating the serine/threonine residue in the consensus sequence, or mutating a proximal amino acid which is not part of the consensus sequence (Flack *et al.*, 1994; Moharir *et al.*, 2013). Investigations of this nature would be required to confirm that the effects of mutations carried out in this study were in fact due to the absence of N-glycans and not a result of the altered amino acid in the N-glycosylation consensus sequence. However, while these limitations highlight the necessity of further research, they do not negate the relevancy of the findings in this study.

7.4 Future Work

While evidence from this study reinforces the theory that S100β$^+$ resident vascular stem cells contribute significantly to the formation of an arteriosclerotic lesion, the topic of neointimal cell origin will remain widely disputed. Further investigation is required to define the exact location of these S100β$^+$ stem cells and decipher the extent of their role in neointima formation. Genetic lineage tracing, scRNA-Seq and single cell photonics have all yielded promising results on their own in recent years (Molony *et al.*, 2020; Tang *et al.*, 2020; Di Luca *et al.*, 2021), but in order reconcile the conflicting data that has arisen around this research area, a strategy is required which combines these technologies to compensate for the limitations of each one individually. Furthermore, the signalling pathways which drive neointima formation must be more thoroughly dissected in order to gain greater understanding of the process of injury-induced myogenic differentiation and to identify reliable therapeutic targets. This study was limited to unravelling the mechanics and impact of Jag-1-induced Notch1 signalling *in vitro*, but this scope must be expanded in future studies. In particular, an inducible Notch1 knockout mouse model, driven by an S100β-controlled Cre system, would provide valuable insights into the importance of Notch1 in stem cell contribution to vascular lesion development *in vivo*. Similar studies have already been carried out using mouse models with a Notch2 knockout controlled by a Myh11 promoter to examine the role of Notch signalling in SMCs following vessel ligation and neointima formation (Peterson *et al.*, 2018). In addition to exploring the *in vivo* role of

Notch1 in arteriosclerosis, future work would investigate the involvement of the other three Notch receptors and also Notch ligands such as DLL-1 in myogenic differentiation of MVSCs.

Very little was previously known about the nature of N-glycosylation on the Notch1 receptor. This study used a lectin based method to identify both the presence and structure of N-glycans on Notch1. However, N-linked oligosaccharides can be highly complex with a variety of monosaccharides linked in very specific branching patterns (Walsh, 2009). The first port of call for future analysis of these structures would be to expand the lectin catalogue used for ELLAs. Alternatives such as *Solanum tuberosum* lectin (STL) and *Erythrina cristagalli* lectin (ECL) could be incorporated to further characterise the composition of Notch1 N-glycans (Itakura *et al.*, 2007; Guo *et al.*, 2017). To avoid complications surrounding the dual affinities of these lectins for both N- and O-glycans, it may be necessary to first inhibit O-glycosylation in the cells producing the Notch1 receptor. This could be achieved through use of small molecule inhibitors such as Ac5GalNTGc and α-OBn GalNAc (Patsos *et al.*, 2009; Wang *et al.*, 2021). More in-depth analysis of Notch1 N-glycans could eventually be carried out using advanced techniques such as mass spectrometry (MS). This would require specialised equipment and expertise in data interpretation, but it has been demonstrated on a number of occasions that MS can determine discrete oligosaccharide structures in samples of glycans which have been chemically stripped from their glycoproteins (Xia *et al.*, 2013; Keser *et al.*, 2018; Guan *et al.*, 2021).

The two principle methods of N-glycosylation inhibition used in this study were small-molecule inhibition via TNC and DMJ treatment, and siRNA knockdown of the glycosyltransferases GnT-III and Fut8. In future work, these strategies would be expanded to include a more diverse range of targeting methods. Alternative small-molecule inhibitors such as swainsonine, which blocks α-mannosidase-II activity, would provide greater insights into the role of N-glycans in Notch signalling, while knockdown of additional glycosyltransferases such as GnT-IV and ST3Gal1 could be useful in deciphering the exact structures of N-linked oligosaccharides on the Notch1 receptor (Jacob, 1995; Esko, Bertozzi and Schnaar, 2015; Stanley, 2016). Further research would also be required to determine the exact effect of these interventions on Notch signalling and myogenic differentiation of MVSCs. *Hey1* and *Myh11* expression were used as the respective indicators for changes in these two processes. It would be essential, therefore, to expand the scope of analysis to investigate the impact of N-glycosylation inhibition on expression of alternative Notch target

genes such as *Hey2*, *HeyL* and *Hes1*, and myogenic genes such as *Cnn1* and *SM22-α*. Lastly, to fully define the effect of these interventions on Notch signalling, the next logical step for this research would be to perform in-depth analysis of the processing, trafficking, degradation and activation of Notch1. Lysosomal co-localisation studies and receptor cleavage analyses have previously been carried out to examine these mechanisms and similar strategies could be implemented to established where N-glycosylation fits into the equation (Allam *et al.*, 2017; Alabi *et al.*, 2021).

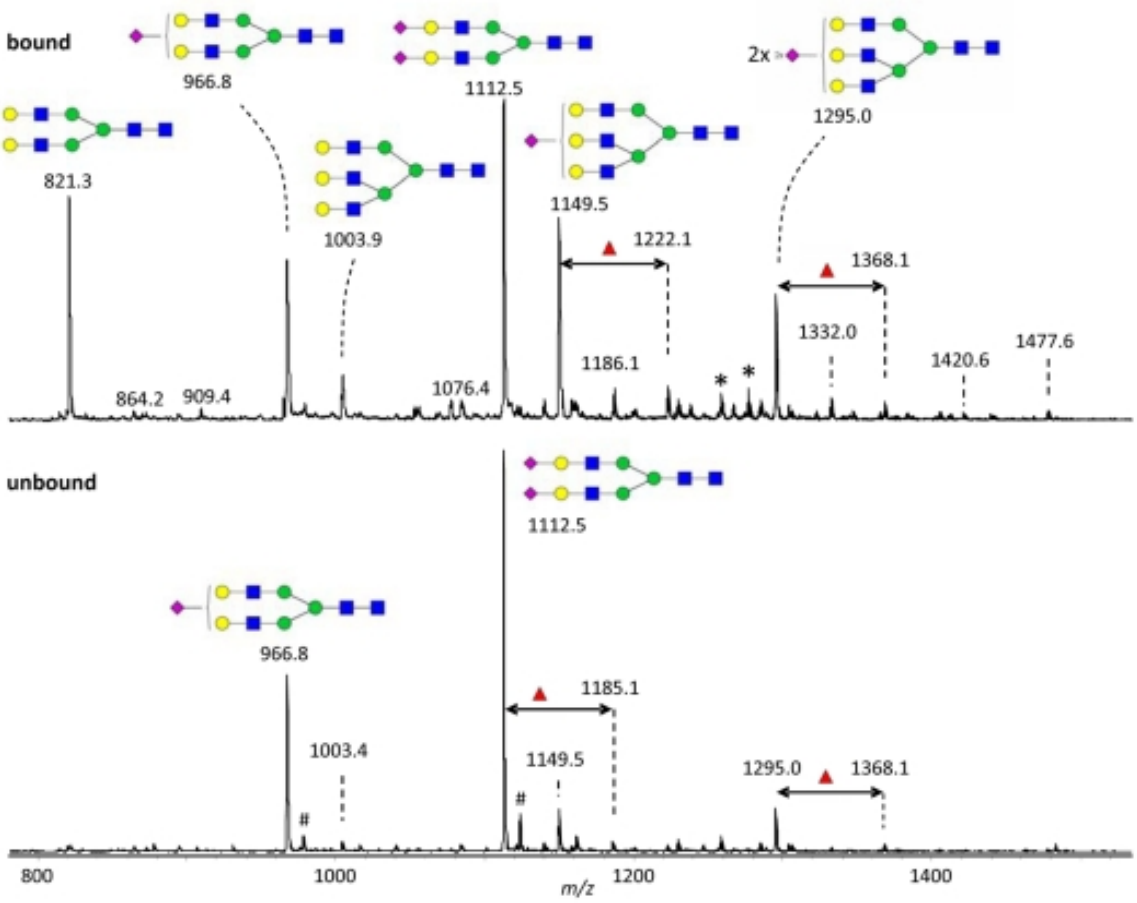


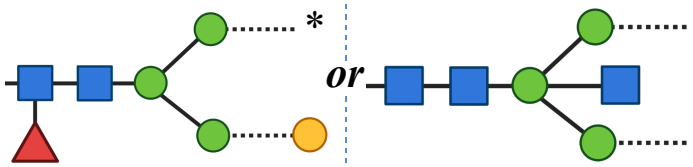
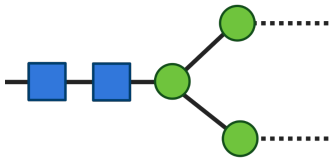
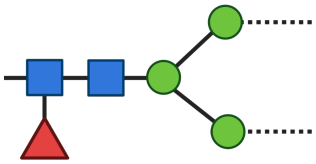
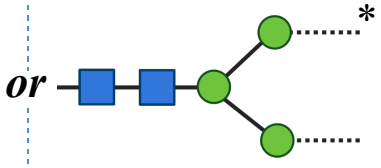
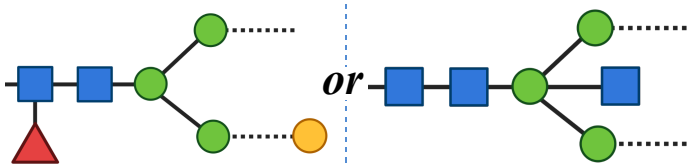
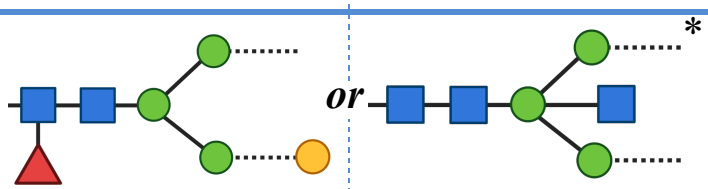
Fig.7.1 Example of Glycan Structural Analysis by MS. Data output from nano-LC-ESI-ion trap-MS where N-glycans with different structures are separated based on their mass-to-charge (m/z) ratio (Carlsson *et al.*, 2011).

The site-directed mutagenesis section of this study yielded a lot of very promising evidence regarding both the structure of N-glycans on the Notch1 receptor and the role of these glycans in Notch signalling and myogenic differentiation. However, this is also the section with the greatest scope for expansion and further research. As previously mentioned, additional mutations would need be carried out on both the essential asparagine residue and

on other proximal non-essential residues to investigate the impact of the amino acid alteration on protein expression, function and stability (Flack *et al.*, 1994; Moharir *et al.*, 2013). Many studies which involve the mutation of N-glycosylation sites on a glycoprotein also use simultaneous multi-site mutation to investigate whether the combined impact of losing two or more N-glycans differs from the effect observed following loss of a single N-glycan (Lee *et al.*, 2003; Ding *et al.*, 2015; Janezic *et al.*, 2020). This is a strategy that could reveal crucial information about the synergistic roles of N-glycans on the Notch1 ECD.

Finally, the ectopic expression of mutant Notch1 receptors in this study gives rise to a number of limitations. One such limitation is that the effect of the mutation can only be observed in a small time frame (about 48 hours post-transfection) before the proportion of plasmid-expressing cells in the population is dramatically reduced as a result of cell division. Another issue with this strategy is the fact that the receptor is overexpressed, which may lead to responses that differ significantly to that of a population expressing normal levels of Notch1. Therefore, the development of a stable mutant cell line, using CRISPR technology, would provide more accurate insights into how the loss of a single N-glycan would impact regular levels of Notch signalling. CRISPR-Cas9 has been used to incorporate stable single base substitutions in a range of different mammalian cell lines in recent years (Zhang *et al.*, 2017; Okamoto *et al.*, 2019; Yang and Huang, 2019). However, its only published application for mutation of an N-glycosylation site so far has been in a viral genome (Shi *et al.*, 2021). Stable mutation of Notch1 N-glycosylation sites in a mammalian cell line would therefore have a profound impact not only on Notch research, but also on the wider application of CRISPR.

Table 7.1 N-Glycan Structures and Possible Roles on the Notch1 Receptor

Asn Site	N-Glycan Structures	Possible Role of Glycan
N888		Regulation of receptor folding/cleavage
N959		Impacts non-canonical Notch signalling
N1179		Impacts non-canonical Notch signalling
N1241	No N-glycan present 	Regulation of receptor degradation
N1489		Impacts non-canonical Notch signalling
N1587		Regulation of receptor degradation



* Indicates most likely structure based on Notch1 expression and signalling data

7.5 Conclusions

The cumulative data in this study provides novel insights into the molecular mechanisms which give rise to arterial remodelling events. This evidence strengthens the hypothesis that S100β^{+} multipotent vascular stem cells (MVSCs) which reside in the vessel wall undergo differentiation and migration to become SMC-like cells in the developing neointima. Clearly, the process of myogenic differentiation in cultured MVSCs, isolated from a mouse aortic arch, is mediated by activation of the Notch1 receptor. Analysis of the Notch1 receptor using ELLA, in conjunction with several N-glycosylation inhibition strategies, revealed that N-glycans reside at all six consensus sequences along the extracellular domain of the receptor, and that while the structures of some of these N-glycans are not entirely clear, a number of them most certainly contain bisecting or core fucosylated structures.

Further implementation of inhibition strategies, most notably the mutation of individual N-glycosylation sites, illustrated the impact of all of these N-glycans on the process of myogenic differentiation. In the case of some, this impact may relate to non-canonical modes of Notch signalling, possibly via regulation of the Wnt/β-catenin pathway, while others exhibit a more direct influence on the Notch1 receptor. With regard to the latter group, their roles appear to mainly centre around the degradation of the Notch1 receptor and the transduction of Notch signalling. In particular, this study found strong evidence to indicate that bisecting N-glycans (most likely at the N1587 site) have a crucial role in the protection of Notch1 against accelerated lysosomal degradation. These findings highlight the importance of Notch1 N-glycosylation in Notch signalling and myogenic differentiation, and underscore the potential of Notch1 and its N-glycans as important therapeutic targets in arteriosclerosis.

Bibliography

Abdullahi, A. *et al.* (2017) 'MODELING ACUTE ER STRESS in VIVO and in VITRO', *Shock*. Lippincott Williams and Wilkins, 47(4), pp. 506–513. doi: 10.1097/SHK.0000000000000759.

Acar, M. *et al.* (2008) 'Rumi Is a CAP10 Domain Glycosyltransferase that Modifies Notch and Is Required for Notch Signaling', *Cell*, 132(2), pp. 247–258. doi: 10.1016/j.cell.2007.12.016.

Acosta, H. *et al.* (2011) 'Notch destabilises maternal β-catenin and restricts dorsal-anterior development in Xenopus', *Development*. Development, 138(12), pp. 2567–2579. doi: 10.1242/dev.061143.

Adams, C. *et al.* (2016) 'Development of Multifunctional Magnetic Nanoparticles for Genetic Engineering and Tracking of Neural Stem Cells', *Advanced Healthcare Materials*. Wiley-VCH Verlag, 5(7), pp. 841–849. doi: 10.1002/adhm.201500885.

Alabi, R. O. *et al.* (2021) 'Analysis of the Conditions That Affect the Selective Processing of Endogenous Notch1 by ADAM10 and ADAM17', *International Journal of Molecular Sciences*. MDPI AG, 22(4), p. 1846. doi: 10.3390/ijms22041846.

Allam, H. *et al.* (2015) 'Glycomic Analysis of Membrane Glycoproteins with Bisecting Glycosylation from Ovarian Cancer Tissues Reveals Novel Structures and Functions', *Journal of Proteome Research*, 14(1), pp. 434–446. doi: 10.1021/pr501174p.

Allam, H. *et al.* (2017) 'The glycosyltransferase GnT-III activates Notch signaling and drives stem cell expansion to promote the growth and invasion of ovarian cancer', *Journal of Biological Chemistry*, 292(39), pp. 16351–16359. doi: 10.1074/jbc.m117.783936.

Ambrosi, M., Cameron, N. R. and Davis, B. G. (2005) 'Lectins: tools for the molecular understanding of the glycocode', *Organic & Biomolecular Chemistry*, 3(9), p. 1593. doi: 10.1039/b414350g.

Andersen, P. *et al.* (2012) 'Non-canonical Notch signaling: Emerging role and mechanism', *Trends in Cell Biology*. NIH Public Access, pp. 257–265. doi: 10.1016/j.tcb.2012.02.003.

Anderson, K. M. *et al.* (1991) 'Cardiovascular disease risk profiles', *American Heart Journal*. Mosby, 121(1 PART 2), pp. 293–298. doi: 10.1016/0002-8703(91)90861-B.

Andersson, J., Libby, P. and Hansson, G. K. (2010) 'Adaptive immunity and atherosclerosis', *Clinical Immunology*, 134, pp. 33–46. doi: 10.1016/j.clim.2009.07.002.

Aoyagi, Y. *et al.* (1998) 'The fucosylation index of ?-fetoprotein as a possible prognostic indicator for patients with hepatocellular carcinoma', *Cancer*. John Wiley & Sons, Ltd, 83(10), pp. 2076–2082. doi: 10.1002/(SICI)1097-0142(19981115)83:10<2076::AID-CNCR5>3.0.CO;2-L.

Artavanis-Tsakonas, S., Rand, M. D. and Lake, R. J. (1999) 'Notch signaling: Cell fate control and signal integration in development', *Science*. Science, pp. 770–776. doi: 10.1126/science.284.5415.770.

Aviner, R. (2020) ‘The science of puromycin: From studies of ribosome function to applications in biotechnology’, *Computational and Structural Biotechnology Journal*. Elsevier B.V., pp. 1074–1083. doi: 10.1016/j.csbj.2020.04.014.

Bacakova, L. *et al.* (2018) ‘The Role of Vascular Smooth Muscle Cells in the Physiology and Pathophysiology of Blood Vessels’, in *Muscle Cell and Tissue - Current Status of Research Field*. InTech. doi: 10.5772/intechopen.77115.

Bagriaçik, E. Ü., Kirkpatrick, A. and Miller, K. S. (1996) ‘Glycosylation of native MHC class Ia molecules is required for recognition by allogeneic cytotoxic T lymphocytes’, *Glycobiology*. Oxford University Press, 6(4), pp. 413–421. doi: 10.1093/glycob/6.4.413.

Baron, M. (2003) ‘An overview of the Notch signalling pathway’, *Seminars in Cell and Developmental Biology*. Elsevier Ltd, pp. 113–119. doi: 10.1016/S1084-9521(02)00179-9.

Basmanav, F. B. *et al.* (2014) ‘Mutations in POGLUT1, Encoding Protein O-Glucosyltransferase 1, Cause Autosomal-Dominant Dowling-Degos Disease’, *The American Journal of Human Genetics*, 94(1), pp. 135–143. doi: 10.1016/j.ajhg.2013.12.003.

Berdnik, D. *et al.* (2002) ‘The endocytic protein α-adaptin is required for numb-mediated asymmetric cell division in Drosophila’, *Developmental Cell*. Cell Press, 3(2), pp. 221–231. doi: 10.1016/S1534-5807(02)00215-0.

Berk, B. C. *et al.* (2008) ‘Endothelial Atheroprotective and Anti-inflammatory Mechanisms’, *Annals of the New York Academy of Sciences*. New York Academy of Sciences, 947(1), pp. 93–111. doi: 10.1111/j.1749-6632.2001.tb03932.x.

Van Berkel, P. H. C. *et al.* (1996) ‘Heterogeneity in utilization of N-glycosylation sites Asn624 and Asn138 in human lactoferrin : A study with glycosylation-site mutants’, *Biochemical Journal*. Portland Press Ltd, 319(1), pp. 117–122. doi: 10.1042/bj3190117.

Bertram, B., Wiese, S. and von Holst, A. (2012) ‘High-efficiency transfection and survival rates of embryonic and adult mouse neural stem cells achieved by electroporation’, *Journal of Neuroscience Methods*. Elsevier, 209(2), pp. 420–427. doi: 10.1016/j.jneumeth.2012.06.024.

Bewley, C. A. and Otero-Quintero, S. (2001) ‘The potent anti-HIV protein cyanovirin-N contains two novel carbohydrate binding sites that selectively bind to Man8 D1D3 and Man9 with nanomolar affinity: Implications for binding to the HIV envelope protein gp120’, *Journal of the American Chemical Society*. J Am Chem Soc, 123(17), pp. 3892–3902. doi: 10.1021/ja004040e.

del Bianco, C. *et al.* (2010) ‘Notch and MAML-1 Complexation do not detectably alter the DNA binding specificity of the transcription factor CSL’, *PLoS ONE*. PLoS One, 5(11). doi: 10.1371/journal.pone.0015034.

Bigge, J. C. *et al.* (1995) ‘Nonselective and Efficient Fluorescent Labeling of Glycans Using 2-Amino Benzamide and Anthranilic Acid’, *Analytical Biochemistry*, 230(2), pp. 229–238. doi: 10.1006/abio.1995.1468.

Blanpain, C. *et al.* (2006) 'Canonical notch signaling functions as a commitment switch in the epidermal lineage', *Genes and Development*. Cold Spring Harbor Laboratory Press, 20(21), pp. 3022–3035. doi: 10.1101/gad.1477606.

Blaumueller, C. M. *et al.* (1997) 'Intracellular cleavage of Notch leads to a heterodimeric receptor on the plasma membrane', *Cell*. Cell Press, 90(2), pp. 281–291. doi: 10.1016/S0092-8674(00)80336-0.

Blokzijl, A. *et al.* (2003) 'Cross-talk between the Notch and TGF-β signaling pathways mediated by interaction of the Notch intracellular domain with Smad3', *Journal of Cell Biology*. Rockefeller University Press, 163(4), pp. 723–728. doi: 10.1083/jcb.200305112.

Borggrefe, T. and Oswald, F. (2009) 'The Notch signaling pathway: Transcriptional regulation at Notch target genes', *Cellular and Molecular Life Sciences*. Springer, pp. 1631–1646. doi: 10.1007/s00018-009-8668-7.

Boskovski, M. T. *et al.* (2013) 'The heterotaxy gene GALNT11 glycosylates Notch to orchestrate cilia type and laterality', *Nature*. Nature Publishing Group, 504(7480), pp. 456–459. doi: 10.1038/nature12723.

Brack, A. S. *et al.* (2008) 'A Temporal Switch from Notch to Wnt Signaling in Muscle Stem Cells Is Necessary for Normal Adult Myogenesis', *Cell Stem Cell*. Cell Press, 2(1), pp. 50–59. doi: 10.1016/j.stem.2007.10.006.

Brandish, P. E. *et al.* (1996) 'Modes of action of tunicamycin, liposidomycin B, and mureidomycin A: Inhibition of phospho-N-acetylmuramyl-pentapeptide translocase from Escherichia coli', *Antimicrobial Agents and Chemotherapy*. American Society for Microbiology, 40(7), pp. 1640–1644. doi: 10.1128/aac.40.7.1640.

Branza-Nichita, N. *et al.* (2000) 'Mutations at critical N-glycosylation sites reduce tyrosinase activity by altering folding and quality control', *Journal of Biological Chemistry*. American Society for Biochemistry and Molecular Biology Inc., 275(11), pp. 8169–8175. doi: 10.1074/jbc.275.11.8169.

Bray, S. (1998) 'Notch signalling in Drosophila: Three ways to use a pathway', *Seminars in Cell and Developmental Biology*. Elsevier Ltd, 9(6), pp. 591–597. doi: 10.1006/scdb.1998.0262.

Bray, S. J. (2006) 'Notch signalling: a simple pathway becomes complex.', *Nature reviews. Molecular cell biology*, 7(9), pp. 678–89. doi: 10.1038/nrm2009.

Brockhausen, I. (2014) 'Crossroads between bacterial and mammalian glycosyltransferases', *Frontiers in Immunology*. Frontiers Media S.A. doi: 10.3389/fimmu.2014.00492.

Brooks, S. A. (2009) 'Strategies for analysis of the glycosylation of proteins: Current status and future perspectives', *Molecular Biotechnology*, 43(1), pp. 76–88. doi: 10.1007/s12033-009-9184-6.

Brückner, K. *et al.* (2000) 'Glycosyltransferase activity of Fringe modulates Notch-Delta interactions', *Nature*, 406(6794), pp. 411–415. doi: 10.1038/35019075.

Brunner, A. M. *et al.* (1992) 'Site-directed mutagenesis of glycosylation sites in the transforming growth factor-beta 1 (TGF beta 1) and TGF beta 2 (414) precursors and of cysteine residues within mature TGF beta 1: effects on secretion and bioactivity.', *Molecular Endocrinology*. Oxford Academic, 6(10), pp. 1691–1700. doi: 10.1210/mend.6.10.1448117.

Bühlmann, N. *et al.* (2000) 'Glycosylation of the calcitonin receptor-like receptor at Asn ^{60} or Asn ^{112} is important for cell surface expression', *FEBS Letters*. John Wiley & Sons, Ltd, 486(3), pp. 320–324. doi: 10.1016/S0014-5793(00)02259-6.

Bulman, M. P. *et al.* (2000) 'Mutations in the human Delta homologue, DLL3, cause axial skeletal defects in spondylocostal dysostosis', *Nature Genetics*. Nature Publishing Group, 24(4), pp. 438–441. doi: 10.1038/74307.

Cambridge, S. B. *et al.* (2011) 'Systems-wide proteomic analysis in mammalian cells reveals conserved, functional protein turnover', *Journal of Proteome Research*. UTC, 10(12), pp. 5275–5284. doi: 10.1021/pr101183k.

Campbell, C. T. and Yarema, K. J. (2005) 'Large-scale approaches for glycobiology', *Genome Biology*, 6(11), pp. 1–8. doi: 10.1186/gb-2005-6-11-236.

Cao, T. *et al.* (2017) 'S100B promotes injury-induced vascular remodeling through modulating smooth muscle phenotype', *Biochimica et Biophysica Acta - Molecular Basis of Disease*. Elsevier B.V., 1863(11), pp. 2772–2782. doi: 10.1016/j.bbadis.2017.07.002.

Cao, Y. *et al.* (2015) 'Autophagy Sustains Hematopoiesis Through Targeting Notch', *Stem Cells and Development*, 24(22), pp. 2660–2673. doi: 10.1089/scd.2015.0176.

Caolo, V. *et al.* (2011) 'Soluble jagged-1 inhibits neointima formation by attenuating notch-herp2 signaling', *Arteriosclerosis, Thrombosis, and Vascular Biology*. Lippincott Williams & WilkinsHagerstown, MD, 31(5), pp. 1059–1065. doi: 10.1161/ATVBAHA.110.217935.

Caplice, N. M. *et al.* (2003) 'Smooth muscle cells in human coronary atherosclerosis can originate from cells administered at marrow transplantation', *Proceedings of the National Academy of Sciences of the United States of America*. National Academy of Sciences, 100(8), pp. 4754–4759. doi: 10.1073/pnas.0730743100.

Carlson, M. E. and Conboy, I. M. (2007) 'Regulating the Notch pathway in embryonic, adult and old stem cells', *Current Opinion in Pharmacology*. Elsevier, pp. 303–309. doi: 10.1016/j.coph.2007.02.004.

Carlsson, M. C. *et al.* (2011) 'Galectin-1-binding glycoforms of haptoglobin with altered intracellular trafficking, and increase in metastatic breast cancer patients', *PLoS ONE*. Public Library of Science, 6(10). doi: 10.1371/journal.pone.0026560.

Chamley-Campbell, J., Campbell, G. R. and Ross, R. (1979) 'The smooth muscle cell in culture', *Physiological Reviews*. Physiol Rev, pp. 1–61. doi: 10.1152/physrev.1979.59.1.1.

Chang, A. *et al.* (2011) 'Glycosyltransferase structural biology and its role in the design of catalysts for glycosylation', *Current Opinion in Biotechnology*. Elsevier Current Trends, pp. 800–808. doi: 10.1016/j.copbio.2011.04.013.

Chang, P. J. *et al.* (2010) 'Binding of RBP-Jκ (CSL) protein to the promoter of the Kaposi's sarcoma-associated herpesvirus ORF47 (gL) gene is a critical but not sufficient determinant of transactivation by ORF50 protein', *Virology*. Virology, 398(1), pp. 38–48. doi: 10.1016/j.virol.2009.11.022.

Chappell, J. *et al.* (2016) 'Extensive Proliferation of a Subset of Differentiated, yet Plastic, Medial Vascular Smooth Muscle Cells Contributes to Neointimal Formation in Mouse Injury and Atherosclerosis Models', *Circulation Research*. Lippincott Williams & WilkinsHagerstown, MD, 119(12), pp. 1313–1323. doi: 10.1161/CIRCRESAHA.116.309799.

Chen, D. *et al.* (2021) '<scp>miRNA</scp> -200c- <scp>3p</scp> promotes endothelial to mesenchymal transition and neointimal hyperplasia in artery bypass grafts', *The Journal of Pathology*. John Wiley and Sons Ltd, 253(2), pp. 209–224. doi: 10.1002/path.5574.

Chen, G. *et al.* (2007) 'Brain-derived neurotrophic factor suppresses tunicamycin-induced upregulation of CHOP in neurons', *Journal of Neuroscience Research*. John Wiley & Sons, Ltd, 85(8), pp. 1674–1684. doi: 10.1002/jnr.21292.

Chen, H., Ford, C. and Reilly, P. J. (1994) 'Substitution of asparagine residues in Aspergillus awamori glucoamylase by site-directed mutagenesis to eliminate N-glycosylation and inactivation by deamidation', *Biochemical Journal*. Portland Press Ltd, 301(1), pp. 275–281. doi: 10.1042/bj3010275.

Chen, P. Y. *et al.* (2015) 'Endothelial-to-mesenchymal transition drives atherosclerosis progression', *Journal of Clinical Investigation*. American Society for Clinical Investigation, 125(12), pp. 4514–4528. doi: 10.1172/JCI82719.

Chen, Q. *et al.* (2015) 'miRNA-34a reduces neointima formation through inhibiting smooth muscle cell proliferation and migration', *Journal of Molecular and Cellular Cardiology*. Academic Press, 89, pp. 75–86. doi: 10.1016/j.yjmcc.2015.10.017.

Chen, Z. *et al.* (2013) 'Dynamic evaluation of cell surface N-glycan expression via an electrogenerated chemiluminescence biosensor based on concanavalin A-integrating gold-nanoparticle-modified Ru(bpy)32+-doped silica nanoprobe', *Analytical Chemistry*. American Chemical Society, 85(9), pp. 4431–4438. doi: 10.1021/ac303572g.

Cheung, C. *et al.* (2012) 'Generation of human vascular smooth muscle subtypes provides insight into embryological origing-dependent disease susceptibility', *Nature Biotechnology*. Nature Publishing Group, 30(2), pp. 165–173. doi: 10.1038/nbt.2107.

Chiba, S. (2006) 'Concise Review: Notch Signaling in Stem Cell Systems', *Stem Cells*. Wiley, 24(11), pp. 2437–2447. doi: 10.1634/stemcells.2005-0661.

Chillakuri, C. R. *et al.* (2012) 'Notch receptor-ligand binding and activation: Insights from molecular studies', *Seminars in Cell and Developmental Biology*. Elsevier Ltd, 23(4), pp. 421–428. doi: 10.1016/j.semcdb.2012.01.009.

Christiansen, M. N. *et al.* (2014) 'Cell surface protein glycosylation in cancer', *PROTEOMICS*, 14(4–5), pp. 525–546. doi: 10.1002/pmic.201300387.

Conboy, I. M. and Rando, T. A. (2002) 'The regulation of Notch signaling controls satellite cell activation and cell fate determination in postnatal myogenesis', *Developmental Cell*. Cell Press, 3(3), pp. 397–409. doi: 10.1016/S1534-5807(02)00254-X.

Contessa, J. N. *et al.* (2008) 'Inhibition of N-linked glycosylation disrupts receptor tyrosine kinase signaling in tumor cells', *Cancer Research*. American Association for Cancer Research, 68(10), pp. 3803–3809. doi: 10.1158/0008-5472.CAN-07-6389.

Cooley, B. C. *et al.* (2014) 'TGF-β signaling mediates endothelial-to-mesenchymal transition (EndMT) during vein graft remodeling.', *Science translational medicine*. American Association for the Advancement of Science, 6(227), p. 227ra34. doi: 10.1126/scitranslmed.3006927.

Cordle, J. *et al.* (2008) 'A conserved face of the Jagged/Serrate DSL domain is involved in Notch trans-activation and cis-inhibition', *Nature Structural & Molecular Biology*, 15(8), pp. 849–857. doi: 10.1038/nsmb.1457.

Cornier, A. S. *et al.* (2008) 'Mutations in the MESP2 Gene Cause Spondylothoracic Dysostosis/Jarcho-Levin Syndrome', *American Journal of Human Genetics*. Cell Press, 82(6), pp. 1334–1341. doi: 10.1016/j.ajhg.2008.04.014.

Coutinho, P. M. *et al.* (2003) 'An evolving hierarchical family classification for glycosyltransferases', *Journal of Molecular Biology*. Academic Press, 328(2), pp. 307–317. doi: 10.1016/S0022-2836(03)00307-3.

D'Souza, B., Meloty-Kapella, L. and Weinmaster, G. (2010) *Canonical and non-canonical notch ligands*, *Current Topics in Developmental Biology*. Academic Press. doi: 10.1016/S0070-2153(10)92003-6.

Dang, T. P. *et al.* (2000) 'Chromosome 19 Translocation, Overexpression of Notch3, and Human Lung Cancer', *JNCI Journal of the National Cancer Institute*. Oxford University Press, 92(16), pp. 1355–1357. doi: 10.1093/jnci/92.16.1355.

Das, R. N. and Yaniv, K. (2020) 'Discovering new progenitor cell populations through lineage tracing and in vivo imaging', *Cold Spring Harbor Perspectives in Biology*. Cold Spring Harbor Laboratory Press, 12(10), pp. 1–25. doi: 10.1101/cshperspect.a035618.

Davies, M. G. and Hagen, P. O. (1995) 'Pathophysiology of vein graft failure: A review', *European Journal of Vascular and Endovascular Surgery*. W.B. Saunders, pp. 7–18. doi: 10.1016/S1078-5884(05)80218-7.

Dedkova, L. M. *et al.* (2012) 'β-puromycin selection of modified ribosomes for in vitro incorporation of β-amino acids', *Biochemistry*. UTC, 51(1), pp. 401–415. doi: 10.1021/bi2016124.

Delaby, C. *et al.* (2005) 'Presence of the iron exporter ferroportin at the plasma membrane of macrophages is enhanced by iron loading and down-regulated by hepcidin', *Blood*. American Society of Hematology, 106(12), pp. 3979–3984. doi: 10.1182/blood-2005-06-2398.

Delorme, E. *et al.* (1992) 'Role of Glycosylation on the Secretion and Biological Activity of Erythropoietin', *Biochemistry*. American Chemical Society, 31(41), pp. 9871–9876. doi: 10.1021/bi00156a003.

Dennis, J. W. *et al.* (2009) 'Adaptive regulation at the cell surface by N-glycosylation', *Traffic*, 10(11), pp. 1569–1578. doi: 10.1111/j.1600-0854.2009.00981.x.

Dennis, J. W., Granovsky, M. and Warren, C. E. (1999) 'Protein glycosylation in development and disease', *BioEssays*, 21(5), pp. 412–421. doi: 10.1002/(SICI)1521-1878(199905)21:5<412::AID-BIES8>3.0.CO;2-5.

DeRuiter, M. C. *et al.* (1997) 'Embryonic endothelial cells transdifferentiate into mesenchymal cells expressing smooth muscle actins in vivo and in vitro.', *Circulation research*, 80(4), pp. 444–51. doi: 10.1161/01.RES.80.4.444

Diaconu, C. *et al.* (2019) 'Beta-blockers in Cardiovascular Therapy: A Review', *Journal of Mind and Medical Sciences*. Valparaiso University, 6(2), pp. 216–223. doi: 10.22543/7674.62.p216223.

Ding, Y. *et al.* (2015) 'Effects of N-Glycosylation Site Removal in Archaellins on the Assembly and Function of Archaella in Methanococcus maripaludis', *PLOS ONE*. Edited by F. Lisacek. Public Library of Science, 10(2), p. e0116402. doi: 10.1371/journal.pone.0116402.

Dobnikar, L. *et al.* (2018) 'Disease-relevant transcriptional signatures identified in individual smooth muscle cells from healthy mouse vessels', *Nature Communications*. Nature Publishing Group, 9(1), pp. 1–17. doi: 10.1038/s41467-018-06891-x.

Doering, J. A. *et al.* (2018) 'In Silico Site-Directed Mutagenesis Informs Species-Specific Predictions of Chemical Susceptibility Derived From the Sequence Alignment to Predict Across Species Susceptibility (SeqAPASS) Tool', *Toxicological Sciences*. NLM (Medline), 166(1), pp. 131–145. doi: 10.1093/toxsci/kfy186.

Doi, H. *et al.* (2005) 'HERP1 inhibits myocardin-induced vascular smooth muscle cell differentiation by interfering with SRF binding to CArG box', *Arteriosclerosis, Thrombosis, and Vascular Biology*. Lippincott Williams & Wilkins, 25(11), pp. 2328–2334. doi: 10.1161/01.ATV.0000185829.47163.32.

Doi, H. *et al.* (2006) 'Jagged1-selective notch signaling induces smooth muscle differentiation via a RBP-Jκ-dependent pathway', *Journal of Biological Chemistry*, 281(39), pp. 28555–28564. doi: 10.1074/jbc.M602749200.

Domenga, V. *et al.* (2004) 'Notch3 is required for arterial identity and maturation of vascular smooth muscle cells', *Genes and Development*. Genes Dev, 18(22), pp. 2730–2735. doi: 10.1101/gad.308904.

Dongre, A. *et al.* (2014) 'Non-Canonical Notch Signaling Drives Activation and Differentiation of Peripheral CD4+ T Cells', *Frontiers in Immunology*. Frontiers Research Foundation, 5(FEB), p. 54. doi: 10.3389/fimmu.2014.00054.

Dzau, V. J. (1990) 'Mechanism of Action of Angiotensin-Converting Enzyme (ACE) Inhibitors in Hypertension and Heart Failure: Role of Plasma versus Tissue ACE', *Drugs*. Springer, 39(2), pp. 11–16. doi: 10.2165/00003495-199000392-00004.

Elbein, A. D. (1987) 'Inhibitors of the Biosynthesis and Processing of N-Linked Oligosaccharide Chains', *Annual Review of Biochemistry*. Annual Reviews, 56(1), pp. 497–534. doi: 10.1146/annurev.bi.56.070187.002433.

Ellisen, L. W. *et al.* (1991) 'TAN-1, the human homolog of the Drosophila Notch gene, is broken by chromosomal translocations in T lymphoblastic neoplasms', *Cell*. Cell, 66(4), pp. 649–661. doi: 10.1016/0092-8674(91)90111-B.

Emerson, M. *et al.* (2003) 'Transfection efficiency and toxicity following delivery of naked plasmid DNA and cationic lipid-DNA complexes to ovine lung segments', *Molecular Therapy*. Academic Press Inc., 8(4), pp. 646–653. doi: 10.1016/S1525-0016(03)00233-8.

Esapa, C. T. *et al.* (2003) 'The effects of post-translational processing on dystroglycan synthesis and trafficking [1]', *FEBS Letters*. Elsevier, 555(2), pp. 209–216. doi: 10.1016/S0014-5793(03)01230-4.

Esko, J. D., Bertozzi, C. and Schnaar, R. L. (2015) *Chemical Tools for Inhibiting Glycosylation*, *Essentials of Glycobiology*. Cold Spring Harbor Laboratory Press. PMID: 20301258

Fan, H. *et al.* (1997) 'Domain-specific N-glycosylation of the membrane glycoprotein dipeptidylpeptidase IV (CD26) influences its subcellular trafficking, biological stability, enzyme activity and protein folding', *European Journal of Biochemistry*. Blackwell Publishing Ltd, 246(1), pp. 243–251. doi: 10.1111/j.1432-1033.1997.00243.x.

Farooq, V., Gogas, B. D. and Serruys, P. W. (2011) 'Contemporary Reviews in Interventional Cardiology Delineating the Numerous Causes of Drug-Eluting Stent Restenosis', pp. 195–205. doi: 10.1161/CIRCINTERVENTIONS.110.959882.

Ferlinz, K. *et al.* (1997) 'Functional characterization of the N-glycosylation sites of human acid sphingomyelinase by site-directed mutagenesis', *European Journal of Biochemistry*. Blackwell Publishing Ltd, 243(1–2), pp. 511–517. doi: 10.1111/j.1432-1033.1997.511_1a.x.

Fernández-Friera, L. *et al.* (2017) 'Normal LDL-Cholesterol Levels Are Associated With Subclinical Atherosclerosis in the Absence of Risk Factors', *Journal of the American College of Cardiology*. Elsevier USA, 70(24), pp. 2979–2991. doi: 10.1016/j.jacc.2017.10.024.

Fishbein, G. A. and Fishbein, M. C. (2009) 'Arteriosclerosis: Rethinking the Current Classification', *Archives of pathology & laboratory medicine*, 133, pp. 1309–1316.

Flack, M. R. *et al.* (1994) 'Site-directed mutagenesis defines the individual roles of the glycosylation sites on follicle-stimulating hormone', *Journal of Biological Chemistry*. Elsevier, 269(19), pp. 14015–14020. doi: 10.1016/s0021-9258(17)36748-0.

Fortini, M. E. (2009) 'Notch Signaling: The Core Pathway and Its Posttranslational Regulation', *Developmental Cell*. Elsevier Inc., 16(5), pp. 633–647. doi: 10.1016/j.devcel.2009.03.010.

Fortini, M. E. (2012) 'Introduction—Notch in development and disease', *Seminars in Cell & Developmental Biology*. Academic Press, 23(4), pp. 419–420. doi: 10.1016/J.SEMCDB.2012.03.001.

Frid, M. G., Kale, V. A. and Stenmark, K. R. (2002) 'Mature vascular endothelium can give rise to smooth muscle cells via endothelial-mesenchymal transdifferentiation: in vitro analysis.', *Circulation research*, 90(11), pp. 1189–96. DOI: 10.1161/01.res.0000021432.70309.28

Galkina, E. and Ley, K. (2009) 'Immune and Inflammatory Mechanisms of Atherosclerosis', *Annual Review of Immunology*. Annual Reviews , 27(1), pp. 165–197. doi: 10.1146/annurev.immunol.021908.132620.

Gazave, E. *et al.* (2009) 'Origin and evolution of the Notch signalling pathway: An overview from eukaryotic genomes', *BMC Evolutionary Biology*. BioMed Central, pp. 1–27. doi: 10.1186/1471-2148-9-249.

Geyer, H. and Geyer, R. (2006) 'Strategies for analysis of glycoprotein glycosylation', *Biochimica et Biophysica Acta - Proteins and Proteomics*, 1764(12), pp. 1853–1869. doi: 10.1016/j.bbapap.2006.10.007.

Ghazarian, H., Idoni, B. and Oppenheimer, S. B. (2011) 'A glycobiology review: Carbohydrates, lectins and implications in cancer therapeutics', *Acta Histochemica*. Elsevier, 113(3), pp. 236–247. doi: 10.1016/j.acthis.2010.02.004.

Gilda, J. E. and Gomes, A. V. (2013) 'Stain-Free total protein staining is a superior loading control to b-actin for Western blots', *Analytical Biochemistry*. Academic Press Inc., 440(2), pp. 186–188. doi: 10.1016/j.ab.2013.05.027.

Gimbrone, M. A. *et al.* (2000) *Endothelial Dysfunction, Hemodynamic Forces, and Atherogenesis a*. Boston, Massachusetts 02115-5817, USA.

Gomez, D., Swiatlowska, P. and Owens, G. K. (2015) 'Epigenetic Control of Smooth Muscle Cell Identity and Lineage Memory', *Arteriosclerosis, Thrombosis, and Vascular Biology*. Lippincott Williams and Wilkins, 35(12), pp. 2508–2516. doi: 10.1161/ATVBAHA.115.305044.

Gordon, W. R., Arnett, K. L. and Blacklow, S. C. (2008) 'The molecular logic of Notch signaling--a structural and biochemical perspective.', *Journal of cell science*, 121(Pt 19), pp. 3109–19. doi: 10.1242/jcs.035683.

Greenwald, I. (1998) 'LIN-12/Notch signaling: Lessons from worms and flies', *Genes and Development*. Cold Spring Harbor Laboratory Press, pp. 1751–1762. doi: 10.1101/gad.12.12.1751.

Gridley, T. (2010) *Notch signaling in the vasculature*, *Current Topics in Developmental Biology*. Curr Top Dev Biol. doi: 10.1016/S0070-2153(10)92009-7.

Grimm, J. J. *et al.* (2004) *Novel Nanosensors for Rapid Analysis of Telomerase Activity*, *CANCER RESEARCH*. DOI: 10.1158/0008-5472.can-03-2798

Gu, J. *et al.* (1993) 'Purification and Characterization of UDP-N-Acetylglucosamine: -6-D-Mannoside ß-6N-Acetylglucosaminyltransferase(N-Acetylglucosaminyltransferase V) from a Human Lung Cancer Cell Line1', *The Journal of Biochemistry*. Oxford University Press, 113(5), pp. 614–619. doi: 10.1093/oxfordjournals.jbchem.a124091.

Guan, Y. *et al.* (2021) 'Comparative Analysis of Different *N* -glycan Preparation Approaches and Development of Optimized Solid-Phase Permethylation Using Mass Spectrometry', *Journal of Proteome Research*. American Chemical Society, p. acs.jproteome.1c00135. doi: 10.1021/acs.jproteome.1c00135.

Guo, J. *et al.* (2017) 'Conditioned Medium from Malignant Breast Cancer Cells Induces an EMT-Like Phenotype and an Altered N-Glycan Profile in Normal Epithelial MCF10A Cells', *International Journal of Molecular Sciences*. MDPI AG, 18(8), p. 1528. doi: 10.3390/ijms18081528.

Guo, M., Jan, L. Y. and Jan, Y. N. (1996) 'Control of daughter cell fates during asymmetric division: Interaction of Numb and Notch', *Neuron*. Cell Press, 17(1), pp. 27–41. doi: 10.1016/S0896-6273(00)80278-0.

Guo, R. *et al.* (2013) 'Glycogenes mediate the invasive properties and chemosensitivity of human hepatocarcinoma cells', *International Journal of Biochemistry and Cell Biology*. Pergamon, 45(2), pp. 347–358. doi: 10.1016/j.biocel.2012.10.006.

Guruharsha, K. G., Kankel, M. W. and Artavanis-Tsakonas, S. (2012) 'The Notch signalling system: Recent insights into the complexity of a conserved pathway', *Nature Reviews Genetics*. Nature Publishing Group, 13(9), pp. 654–666. doi: 10.1038/nrg3272.

Haab, B. B. (2012) 'Using lectins in biomarker research: Addressing the limitations of sensitivity and availability', *Proteomics - Clinical Applications*. NIH Public Access, 6(7–8), pp. 346–350. doi: 10.1002/prca.201200014.

Haery, C., Sachar, R. and Ellis, S. G. (2004) 'Drug-eluting stents: The beginning of the end of restenosis?', *Cleveland Clinic Journal of Medicine*, 71(10), pp. 815–824. doi: 10.3949/ccjm.71.10.815.

Hamilton, A. J. and Baulcombe, D. C. (1999) 'A species of small antisense RNA in posttranscriptional gene silencing in plants', *Science*. Science, 286(5441), pp. 950–952. doi: 10.1126/science.286.5441.950.

Han, J. *et al.* (2019) 'Laser cleavable probes for: In situ multiplexed glycan detection by single cell mass spectrometry', *Chemical Science*. Royal Society of Chemistry, 10(47), pp. 10958–10962. doi: 10.1039/c9sc03912k.

Han, X. *et al.* (2015) 'CRISPR-Cas9 delivery to hard-to-transfect cells via membrane deformation', *Science Advances*. American Association for the Advancement of Science, 1(7), p. e1500454. doi: 10.1126/sciadv.1500454.

Hayward, P. *et al.* (2005) 'Notch modulates Wnt signalling by associating with Armadillo /β-catenin and regulating its transcriptional activity', *Development*. Development, 132(8), pp. 1819–1830. doi: 10.1242/dev.01724.

Heifetz, A, Keenan, R. W. and Elbein, A. D. (1979) 'Mechanism of action of tunicamycin on the UDP-GlcNAc:dolichyl-phosphate Glc-NAc-1-phosphate transferase.', *Biochemistry*, 18(11), pp. 2186–92. DOI: 10.1021/bi00578a008

Heifetz, Aaron, Keenan, R. W. and Elbein, A. D. (1979) 'Mechanism of Action of Tunicamycin on the UDP-GlcNAc:Dolichyl-Phosphate GlcNAc-1 -Phosphate Transferase', *Biochemistry*. American Chemical Society, 18(11), pp. 2186–2192. doi: 10.1021/bi00578a008.

Helenius, A. and Aebi, M. (2002) 'Intracellular Functions of N-Linked Glycans', *Science*, 291(5512), pp. 2364–2369. doi: 10.1126/science.291.5512.2364.

Hempleman, S. C. and Warburton, S. J. (2013) 'Comparative Embryology of the Carotid Body', *Respiratory Physiology and Neurobiology*. Elsevier B.V., pp. 3–8. doi: 10.1016/j.resp.2012.08.004.

Hemsley, A. *et al.* (1989) 'A simple method for site-directed mutagenesis using the polymerase chain reaction', *Nucleic Acids Research*. Oxford Academic, 17(16), pp. 6545–6551. doi: 10.1093/nar/17.16.6545.

Herreman, A. *et al.* (2003) 'γ-Secretase activity requires the presenilin-dependent trafficking of nicastrin through the Golgi apparatus but not its complex glycosylation', *Journal of Cell Science*. The Company of Biologists Ltd, pp. 1127–1136. doi: 10.1242/jcs.00292.

Herring, B. P. *et al.* (2014) 'Previously differentiated medial vascular smooth muscle cells contribute to neointima formation following vascular injury Previously differentiated medial vascular smooth muscle cells contribute to neointima formation following vascular injury', *Vascular Cell*, 6(21). doi: 10.1186/2045-824X-6-21.

Hicks, C. *et al.* (2000) 'Fringe differentially modulates Jagged1 and Delta1 signalling through Notch1 and Notch2', *Nature Cell Biology*, 2(8), pp. 515–520. doi: 10.1038/35019553.

High, F. A. *et al.* (2007) 'An essential role for Notch in neural crest during cardiovascular development and smooth muscle differentiation', *Journal of Clinical Investigation*. J Clin Invest, 117(2), pp. 353–363. doi: 10.1172/JCI30070.

Higuchi, M. *et al.* (2014) 'GFP-expressing S100β-positive cells of the rat anterior pituitary differentiate into hormone-producing cells', *Cell and tissue research*. Springer, 357(3), pp. 767–779. doi: 10.1007/s00441-014-1890-0.

Hirabayashi, J. and Arai, R. (2019) 'Lectin engineering: The possible and the actual', *Interface Focus*. Royal Society Publishing. doi: 10.1098/rsfs.2018.0068.

Hoffmann, R. *et al.* (1996) 'Patterns and Mechanisms of In-Stent Restenosis', *Circulation*. Lippincott Williams & Wilkins, 94(6), pp. 1247–1254. doi: 10.1161/01.CIR.94.6.1247.

Hoofnagle, M. H. *et al.* (2006) 'Origin of Neointimal Smooth Muscle', *Arteriosclerosis, Thrombosis, and Vascular Biology*. Lippincott Williams & Wilkins, 26(12), pp. 2579–2581. doi: 10.1161/01.ATV.0000249623.79871.bc.

Hsiao, C. C. *et al.* (2009) 'Site-specific N-glycosylation regulates the GPS auto-proteolysis of CD97', *FEBS Letters*. No longer published by Elsevier, 583(19), pp. 3285–3290. doi: 10.1016/j.febslet.2009.09.001.

Ihrie, R. A. and Alvarez-Buylla, A. (2008) 'Cells in the astroglial lineage are neural stem cells', *Cell and Tissue Research*. Springer, pp. 179–191. doi: 10.1007/s00441-007-0461-z.

Ishikawa, H. *et al.* (2001) 'Ligand migration human myoglobin: Steric effects of isoleucine 107(G8) on O2 and CO binding', *Biophysical Journal*. Biophysical Society, 80(3), pp. 1507–1517. doi: 10.1016/S0006-3495(01)76123-1.

Iskratsch, T. *et al.* (2009) 'Specificity analysis of lectins and antibodies using remodeled glycoproteins', *Analytical Biochemistry*. Academic Press Inc., 386(2), pp. 133–146. doi: 10.1016/j.ab.2008.12.005.

Iso, T., Kedes, L. and Hamamori, Y. (2003) 'HES and HERP families: Multiple effectors of the Notch signaling pathway', *Journal of Cellular Physiology*, 194(3), pp. 237–255. doi: 10.1002/jcp.10208.

Itakura, Y. *et al.* (2007) 'Systematic Comparison of Oligosaccharide Specificity of Ricinus communis Agglutinin I and Erythrina Lectins: a Search by Frontal Affinity Chromatography', *Journal of Biochemistry*. Oxford Academic, 142(4), pp. 459–469. doi: 10.1093/jb/mvm153.

Iwata, Y. *et al.* (2017) 'Activation of the Arabidopsis membrane-bound transcription factor bZIP28 is mediated by site-2 protease, but not site-1 protease', *The Plant Journal*. Blackwell Publishing Ltd, 91(3), pp. 408–415. doi: 10.1111/tpj.13572.

Jackson, A. *et al.* (2005) 'Gene array analysis of Wnt-regulated genes in C3H10T1/2 cells', *Bone*. Elsevier Inc., 36(4), pp. 585–598. doi: 10.1016/j.bone.2005.01.007.

Jacob, G. S. (1995) 'Glycosylation inhibitors in biology and medicine', *Current Opinion in Structural Biology*. Elsevier Current Trends, 5(5), pp. 605–611. doi: 10.1016/0959-440X(95)80051-4.

Jafar-Nejad, H., Leonardi, J. and Fernandez-Valdivia, R. (2010) 'Role of glycans and glycosyltransferases in the regulation of Notch signaling', *Glycobiology*, 20(8), pp. 931–949. doi: 10.1093/glycob/cwq053.

Janezic, E. M. *et al.* (2020) 'N-glycosylation of α1D-adrenergic receptor N-terminal domain is required for correct trafficking, function, and biogenesis', *Scientific Reports*. Nature Research, 10(1), pp. 1–12. doi: 10.1038/s41598-020-64102-4.

Jhappan, C. *et al.* (1992) 'Expression of an activated Notch-related int-3 transgene interferes with cell differentiation and induces neoplastic transformation in mammary and salivary glands', *Genes and Development*. Cold Spring Harbor Laboratory Press, 6(3), pp. 345–355. doi: 10.1101/gad.6.3.345.

Kakuda, S. and Haltiwanger, R. S. (2017) 'Deciphering the Fringe-mediated Notch Code: Identification of activating and inhibiting sites allowing discrimination between ligands', *Developmental Cell*, 40(2), pp. 193–201. doi: 10.1177/0333102415576222.Is.

Kalluri, A. S. *et al.* (2019) 'Single-Cell Analysis of the Normal Mouse Aorta Reveals Functionally Distinct Endothelial Cell Populations', *Circulation*. Lippincott Williams and Wilkins, 140(2), pp. 147–163. doi: 10.1161/CIRCULATIONAHA.118.038362.

Kebarle, P. (2000) 'A brief overview of the present status of the mechanisms involved in electrospray mass spectrometry', *Journal of Mass Spectrometry*, 35(7), pp. 804–817. doi: 10.1002/1096-9888(200007)35:7<804::AID-JMS22>3.0.CO;2-Q.

Kennedy, E., Mooney, C. J., *et al.* (2014) 'Adult vascular smooth muscle cells in culture express neural stem cell markers typical of resident multipotent vascular stem cells', *Cell and Tissue Research*, 358(1). doi: 10.1007/s00441-014-1937-2.

Kennedy, Eimear *et al.* (2014) 'Adult vascular smooth muscle cells in culture express neural stem cell markers typical of resident multipotent vascular stem cells', *Cell and Tissue Research*. Springer Berlin Heidelberg, 358(1), pp. 203–216. doi: 10.1007/s00441-014-1937-2.

Kennedy, E., Hakimjavadi, R., *et al.* (2014) 'Embryonic rat vascular smooth muscle cells revisited - A model for neonatal, neointimal SMC or differentiated vascular stem cells?', *Vascular Cell*, 6(1). doi: 10.1186/2045-824X-6-6.

Keser, T. *et al.* (2018) 'Comparison of 2-Aminobenzamide, Procainamide and RapiFluor-MS as Derivatizing Agents for High-Throughput HILIC-UPLC-FLR-MS N-glycan Analysis', *Frontiers in Chemistry*. Frontiers Media S.A., 6(JUL), p. 324. doi: 10.3389/fchem.2018.00324.

Kester, L. and van Oudenaarden, A. (2018) 'Single-Cell Transcriptomics Meets Lineage Tracing', *Cell Stem Cell*. Cell Press, pp. 166–179. doi: 10.1016/j.stem.2018.04.014.

Kidd, S. *et al.* (1989) 'Structure and distribution of the Notch protein in developing Drosophila.', *Genes & development*. Cold Spring Harbor Laboratory Press, 3(8), pp. 1113–1129. doi: 10.1101/gad.3.8.1113.

Kim, E. J. *et al.* (2013) 'MiR-433 mediates ERRγ-suppressed osteoblast differentiation via direct targeting to Runx2 mRNA in C3H10T1/2 cells', *Life Sciences*. Pergamon, 92(10), pp. 562–568. doi: 10.1016/j.lfs.2013.01.015.

Kizuka, Y. *et al.* (2016) 'Bisecting GlcNAc modification stabilizes BACE1 protein under oxidative stress conditions', *Biochemical Journal*. Portland Press Ltd, 473(1), pp. 21–30. doi: 10.1042/BJ20150607.

Klaver, E. *et al.* (2019) 'Selective inhibition of N-linked glycosylation impairs receptor tyrosine kinase processing', *DMM Disease Models and Mechanisms*. Company of Biologists Ltd, 12(6). doi: 10.1242/dmm.039602.

Kolodgie, F. D. *et al.* (2007) 'Is pathologic intimal thickening the key to understanding early plaque progression in human atherosclerotic disease?', *Arteriosclerosis, Thrombosis, and Vascular Biology*. Arterioscler Thromb Vasc Biol, pp. 986–989. doi: 10.1161/ATVBAHA.0000258865.44774.41.

Kooh, P. J., Fehon, R. G. and Muskavitch, M. A. T. (1993) 'Implications of dynamic patterns of Delta and Notch expression for cellular interactions during Drosophila development', *Development*, 117(2), pp. 493–507.

Kopan, R. and Ilagan, M. X. G. (2009) 'The Canonical Notch Signaling Pathway: Unfolding the Activation Mechanism', *Cell*, 137(2), pp. 216–233. doi: 10.1016/j.cell.2009.03.045.

Korshunov, V. A. and Berk, B. C. (2003) 'Flow-Induced Vascular Remodeling in the Mouse: A Model for Carotid Intima-Media Thickening', *Arteriosclerosis, Thrombosis, and Vascular Biology*. Lippincott Williams & Wilkins, 23(12), pp. 2185–2191. doi: 10.1161/01.ATV.0000103120.06092.14.

Kramann, R. *et al.* (2016) 'Adventitial MSC-like Cells Are Progenitors of Vascular Smooth Muscle Cells and Drive Vascular Calcification in Chronic Kidney Disease', *Cell Stem Cell*. Cell Press, 19(5), pp. 628–642. doi: 10.1016/j.stem.2016.08.001.

Kretzschmar, K. and Watt, F. M. (2012) 'Lineage tracing', *Cell*. Cell Press, pp. 33–45. doi: 10.1016/j.cell.2012.01.002.

Kuroda, K. *et al.* (2003) 'Regulation of marginal zone B cell development by MINT, a suppressor of Notch/RBP-J signaling pathway', *Immunity*. Cell Press, 18(2), pp. 301–312. doi: 10.1016/S1074-7613(03)00029-3.

Kurpinski, K. *et al.* (2010) 'Transforming growth factor-β and notch signaling mediate stem cell differentiation into smooth muscle cells', *Stem Cells*, 28(4), pp. 734–742. doi: 10.1002/stem.319.

Kwon, C. *et al.* (2009) 'A regulatory pathway involving Notch1/β-catenin/Isl1 determines cardiac progenitor cell fate', *Nature Cell Biology*. Nat Cell Biol, 11(8), pp. 951–957. doi: 10.1038/ncb1906.

Kwon, C. *et al.* (2011) 'Notch post-translationally regulates β-catenin protein in stem and progenitor cells', *Nature Cell Biology*. Nat Cell Biol, 13(10), pp. 1244–1251. doi: 10.1038/ncb2313.

Lakshmipathy, U. (2004) 'Efficient Transfection of Embryonic and Adult Stem Cells', *Stem Cells*. Wiley, 22(4), pp. 531–543. doi: 10.1634/stemcells.22-4-531.

Lanzer, P. *et al.* (2014) 'Medial vascular calcification revisited: review and perspectives', *European Heart Journal*, 35(23), pp. 1515–1525. doi: 10.1093/eurheartj/ehu163.

Lardelli, M., Dahlstrand, J. and Lendahl, U. (1994) 'The novel Notch homologue mouse Notch 3 lacks specific epidermal growth factor-repeats and is expressed in proliferating neuroepithelium', *Mechanisms of Development*. Elsevier, 46(2), pp. 123–136. doi: 10.1016/0925-4773(94)90081-7.

Lavie, C. J., Milani, R. V. and Ventura, H. O. (2009) 'Obesity and Cardiovascular Disease. Risk Factor, Paradox, and Impact of Weight Loss', *Journal of the American College of Cardiology*, pp. 1925–1932. doi: 10.1016/j.jacc.2008.12.068.

Lee, C.-T. *et al.* (2014) 'Calcification of the Aortic Arch Predicts Cardiovascular and All-Cause Mortality in Chronic Hemodialysis Patients', *Cardiorenal Medicine*. S. Karger AG, 4(1), pp. 34–42. doi: 10.1159/000360230.

Lee, T. K. *et al.* (2003) '*N* -glycosylation controls functional activity of Oatp1, an organic anion transporter', *American Journal of Physiology-Gastrointestinal and Liver Physiology*. American Physiological Society, 285(2), pp. G371–G381. doi: 10.1152/ajpgi.00358.2002.

Legler, K. *et al.* (2018) 'Reduced mannosidase MAN1A1 expression leads to aberrant N-glycosylation and impaired survival in breast cancer', *British Journal of Cancer*. Nature Publishing Group, 118(6), pp. 847–856. doi: 10.1038/bjc.2017.472.

Lesueur, L. L., Mir, L. M. and André, F. M. (2016) 'Overcoming the Specific Toxicity of Large Plasmids Electrotransfer in Primary Cells In Vitro', *Molecular Therapy - Nucleic Acids*. Elsevier Inc, 5(3), p. e291. doi: 10.1038/mtna.2016.4.

Lewis, J. (1998) 'Notch signalling and the control of cell fate choices in vertebrates', *Seminars in Cell and Developmental Biology*. Elsevier Ltd, 9(6), pp. 583–589. doi: 10.1006/scdb.1998.0266.

Li, L. Bin *et al.* (2004) 'The role of N-glycosylation in function and surface trafficking of the human dopamine transporter', *Journal of Biological Chemistry*. American Society for Biochemistry and Molecular Biology Inc., 279(20), pp. 21012–21020. doi: 10.1074/jbc.M311972200.

Li, M. *et al.* (2013) 'Mutations in POFUT1, Encoding Protein O-fucosyltransferase 1, Cause Generalized Dowling-Degos Disease', *The American Journal of Human Genetics*, 92(6), pp. 895–903. doi: 10.1016/j.ajhg.2013.04.022.

Li, Y. *et al.* (2009) 'Smooth muscle notch1 mediates neointimal formation after vascular injury', *Circulation*. NIH Public Access, 119(20), pp. 2686–2692. doi: 10.1161/CIRCULATIONAHA.108.790485.

Liang, M. *et al.* (2019) 'Notch signaling in bone marrow–derived FSP-1 cells initiates neointima formation in arteriovenous fistulas', *Kidney International*. Elsevier B.V., 95(6), pp. 1347–1358. doi: 10.1016/j.kint.2018.11.027.

Lindner, V. *et al.* (2001) 'Members of the Jagged/Notch Gene Families Are Expressed in Injured Arteries and Regulate Cell Phenotype via Alterations in Cell Matrix and Cell-Cell Interaction', *The American Journal of Pathology*, 159(3), pp. 875–883. doi: 10.1016/S0002-9440(10)61763-4.

Ling, L., Nurcombe, V. and Cool, S. M. (2009) 'Wnt signaling controls the fate of mesenchymal stem cells', *Gene*. Elsevier, pp. 1–7. doi: 10.1016/j.gene.2008.12.008.

Ling, Y. H. *et al.* (2009) 'Activation of ER stress and inhibition of EGFR N-glycosylation by tunicamycin enhances susceptibility of human non-small cell lung cancer cells to erlotinib', *Cancer Chemotherapy and Pharmacology*. Cancer Chemother Pharmacol, 64(3), pp. 539–548. doi: 10.1007/s00280-008-0902-8.

Link-Lenczowski, P. *et al.* (2018) 'The glycomic effect of N-acetylglucosaminyltransferase III overexpression in metastatic melanoma cells. GnT-III modifies highly branched N-glycans', *Glycoconjugate Journal*. Springer New York LLC, 35(2), pp. 217–231. doi: 10.1007/s10719-018-9814-y.

Lis, H. and Sharon, N. (2002) 'Lectins: Carbohydrate-Specific Proteins That Mediate Cellular Recognition', *Chemical Reviews*, 98(2), pp. 637–674. doi: 10.1021/cr940413g.

Liu, W. *et al.* (2011) 'Differential effects of daily-moderate versus weekend-binge alcohol consumption on atherosclerotic plaque development in mice', *Atherosclerosis*. Atherosclerosis, 219(2), pp. 448–454. doi: 10.1016/j.atherosclerosis.2011.08.034.

Liu, W. *et al.* (2020) 'Moderate Alcohol Consumption Targets S100β+ Vascular Stem Cells and Attenuates Injury-Induced Neointimal Hyperplasia', *Alcoholism: Clinical and Experimental Research*. Blackwell Publishing Ltd, 44(9), pp. 1734–1746. doi: 10.1111/acer.14415.

Liu, Z.-J. *et al.* (2003) 'Regulation of Notch1 and Dll4 by Vascular Endothelial Growth Factor in Arterial Endothelial Cells: Implications for Modulating Arteriogenesis and Angiogenesis', *Molecular and Cellular Biology*. American Society for Microbiology, 23(1), pp. 14–25. doi: 10.1128/mcb.23.1.14-25.2003.

Logeat, F. *et al.* (1998) 'The Notch1 receptor is cleaved constitutively by a furin-like convertase', *Proceedings of the National Academy of Sciences of the United States of America*. National Academy of Sciences, 95(14), pp. 8108–8112. doi: 10.1073/pnas.95.14.8108.

Longmore, G. D. and Schachter, H. (1982) 'Product-identification and substrate-specificity studies of the GDP-l-fucose: 2-acetamido-2-deoxy-β-d-glucoside (fuc→asn-linked GlcNAc) 6-α-l-fucosyltransferase in a golgi-rich fraction from porcine liver', *Carbohydrate Research*. Elsevier, 100(1), pp. 365–392. doi: 10.1016/S0008-6215(00)81049-6.

Lu, Y. *et al.* (2006) '1-Deoxymannojirimycin, the α1,2-mannosidase inhibitor, induced cellular endoplasmic reticulum stress in human hepatocarcinoma cell 7721', *Biochemical and Biophysical Research Communications*. Academic Press Inc., 344(1), pp. 221–225. doi: 10.1016/j.bbrc.2006.03.111.

Di Luca, M. (2019) *The embryological origin of resident vascular stem cells – implications for vascular disease*, *PhD thesis, Dublin City University.* Dublin City University. School of Biotechnology.

Di Luca, M. *et al.* (2021) 'The calcium binding protein S100β marks hedgehog-responsive resident vascular stem cells within vascular lesions', *npj Regenerative Medicine*. Nature Publishing Group, 6(1), p. 10. doi: 10.1038/s41536-021-00120-8.

Luca, Vincent C *et al.* (2017) 'Notch-Jagged complex structure implicates a catch bond in tuning ligand sensitivity.', *Science (New York, N.Y.)*. American Association for the Advancement of Science, 355(6331), pp. 1320–1324. doi: 10.1126/science.aaf9739.

Luca, Vincent C. *et al.* (2017) 'Notch-Jagged complex structure implicates a catch bond in tuning ligand sensitivity', *Science*. American Association for the Advancement of Science, 355(6331), pp. 1320–1324. doi: 10.1126/science.aaf9739.

Mackenzie, N. C. W. *et al.* (2011) 'MOVAS-1 cell line: A new in vitro model of vascular calcification', *International Journal of Molecular Medicine*. Spandidos Publications, 27(5), pp. 663–668. doi: 10.3892/IJMM.2011.631.

Madhavan, M. V *et al.* (2014) 'Coronary Artery Calcification Pathogenesis and Prognostic Implications', *Journal of the American College of Cardiology*, 63(17), pp. 1703–1714. doi: 10.1016/j.jacc.2014.01.017.

Madsen, C. S. *et al.* (1998) 'Smooth muscle-specific expression of the smooth muscle myosin heavy chain gene in transgenic mice requires 5'-flanking and first intronic DNA sequence', *Circulation Research*. Lippincott Williams and Wilkins, 82(8), pp. 908–917. doi: 10.1161/01.RES.82.8.908.

Maier, M. M. and Gessler, M. (2000) 'Comparative analysis of the human and mouse Hey1 promoter: Hey genes are new Notch target genes', *Biochemical and Biophysical Research Communications*. Academic Press Inc., 275(2), pp. 652–660. doi: 10.1006/bbrc.2000.3354.

Malecki, M. J. *et al.* (2006) 'Leukemia-Associated Mutations within the NOTCH1 Heterodimerization Domain Fall into at Least Two Distinct Mechanistic Classes', *Molecular and Cellular Biology*, 26(12), pp. 4642–4651. doi: 10.1128/MCB.01655-05.

Manabe, I. and Owens, G. K. (2001) 'CArG elements control smooth muscle subtype-specific expression of smooth muscle myosin in vivo', *Journal of Clinical Investigation*. The American Society for Clinical Investigation, 107(7), pp. 823–834. doi: 10.1172/JCI11385.

Martínez-Milla, J. *et al.* (2019) 'Role of Beta-blockers in Cardiovascular Disease in 2019', *Revista Espanola de Cardiologia*. Ediciones Doyma, S.L., 72(10), pp. 844–852. doi: 10.1016/j.recesp.2019.02.024.

Martini, F. H. and Nath, J. L. (2011) *Fundamentals of Anatomy and Physiology*. 8th edn. Pearson.

Martos, C. J. *et al.* (2020) 'Fibrous caps in atherosclerosis form by Notch-dependent mechanisms common to arterial media development', *bioRxiv*. Cold Spring Harbor Laboratory, p. 2020.09.28.316984. doi: 10.1101/2020.09.28.316984.

Mašek, J. and Andersson, E. R. (2017) 'The developmental biology of genetic Notch disorders', *Development*, 144(10), pp. 1743–1763. doi: 10.1242/dev.148007.

Matsumoto, K. *et al.* (2016) 'Dual Roles of O-Glucose Glycans Redundant with Monosaccharide O-Fucose on Notch in Notch Trafficking *'. doi: 10.1074/jbc.M115.710483.

Matsuura, A. *et al.* (2008) 'O-linked N-acetylglucosamine is present on the extracellular domain of notch receptors', *Journal of Biological Chemistry*, 283(51), pp. 35486–35495. doi: 10.1074/jbc.M806202200.

Maupin, K. A., Liden, D. and Haab, B. B. (2012) 'The fine specificity of mannose-binding and galactose-binding lectins revealed using outlier motif analysis of glycan array data', *Glycobiology*. Oxford Academic, 22(1), pp. 160–169. doi: 10.1093/glycob/cwr128.

McCoy, J. P., Varani, J. and Goldstein, I. J. (1983) 'Enzyme-linked lectin assay (ELLA): Use of alkaline phosphatase-conjugated Griffonia simplicifolia B4 isolectin for the detection of α-d-galactopyranosyl end groups', *Analytical Biochemistry*. Academic Press, 130(2), pp. 437–444. doi: 10.1016/0003-2697(83)90613-9.

McNeil, J. J. *et al.* (2018) 'Effect of Aspirin on Cardiovascular Events and Bleeding in the Healthy Elderly', *New England Journal of Medicine*. New England Journal of Medicine (NEJM/MMS), 379(16), pp. 1509–1518. doi: 10.1056/NEJMoa1805819.

Mellquist, J. L. *et al.* (1998) 'The amino acid following an Asn-X-Ser/Thr sequon is an important determinant of N-linked core glycosylation efficiency', *Biochemistry*. Biochemistry, 37(19), pp. 6833–6837. doi: 10.1021/bi972217k.

Meloty-Kapella, L. *et al.* (2012) 'Notch Ligand Endocytosis Generates Mechanical Pulling Force Dependent on Dynamin, Epsins, and Actin', *Developmental Cell*. Cell Press, 22(6), pp. 1299–1312. doi: 10.1016/j.devcel.2012.04.005.

Mender, I. and Shay, J. W. (2015) 'Telomerase Repeated Amplification Protocol (TRAP).', *Bio-protocol*. NIH Public Access, 5(22). Available at: http://www.ncbi.nlm.nih.gov/pubmed/27182535

Meng, L. *et al.* (2016) 'DLL4+ dendritic cells: Key regulators of Notch Signaling in effector T cell responses', *Pharmacological Research*. Academic Press, pp. 449–457. doi: 10.1016/j.phrs.2016.09.001.

Mizuno, H. *et al.* (2002) 'Myogenic differentiation by human processed lipoaspirate cells.', *Plastic and reconstructive surgery*, 109(1), pp. 199–209; discussion 210-1. DOI: 10.1097/00006534-200201000-00030

Mizutani, K. I. *et al.* (2007) 'Differential Notch signalling distinguishes neural stem cells from intermediate progenitors', *Nature*. Nature Publishing Group, 449(7160), pp. 351–355. doi: 10.1038/nature06090.

Mo, D. *et al.* (2012) 'Sialylation of N-linked glycans mediates apical delivery of endolyn in MDCK cells via a galectin-9–dependent mechanism', *Molecular Biology of the Cell*. Edited by K. E. Mostov. American Society for Cell Biology, 23(18), pp. 3636–3646. doi: 10.1091/mbc.e12-04-0329.

Moharir, A. *et al.* (2013) 'The Role of N-Glycosylation in Folding, Trafficking, and Functionality of Lysosomal Protein CLN5', *PLoS ONE*. Edited by C. Beh. Public Library of Science, 8(9), p. e74299. doi: 10.1371/journal.pone.0074299.

Mohr, O. L. (1919) ‘Character Changes Caused by Mutation of an Entire Region of a Chromosome in Drosophila.’, *Genetics*. Genetics Society of America, 4(3), pp. 275–82. PMID: 17245926

Moloney, D. J., Panin, V. M., *et al.* (2000) ‘Fringe is a glycosyltransferase that modifies Notch’, *Nature*, 406(6794), pp. 369–375. doi: 10.1038/35019000.

Moloney, D. J., Shair, L. H., *et al.* (2000) ‘Mammalian Notch1 Is Modified with Two Unusual Forms of O -Linked Glycosylation Found on Epidermal Growth Factor-like Modules’, *Journal of Biological Chemistry*, 275(13), pp. 9604–9611. doi: 10.1074/jbc.275.13.9604.

Molony, C. *et al.* (2020) ‘Disease-relevant single cell photonic signatures identify S100β stem cells and their myogenic progeny in vascular lesions’, *bioRxiv*. Cold Spring Harbor Laboratory, p. 2020.05.13.093518. doi: 10.1101/2020.05.13.093518.

Moniruzzaman, M. *et al.* (2018) ‘Glycosylation status of nicastrin influences catalytic activity and substrate preference of γ-secretase’, *Biochemical and Biophysical Research Communications*. Elsevier B.V., 502(1), pp. 98–103. doi: 10.1016/j.bbrc.2018.05.126.

Moonen, J.-R. A. J. *et al.* (2015) ‘Endothelial-to-mesenchymal transition contributes to fibro-proliferative vascular disease and is modulated by fluid shear stress’, *Cardiovascular Research*. Oxford University Press, 108(3), pp. 377–386. doi: 10.1093/cvr/cvv175.

Mooney, C. J. *et al.* (2015) ‘Hedgehog and Resident Vascular Stem Cell Fate’, *Stem Cells International*. Hindawi Publishing Corporation. doi: 10.1155/2015/468428.

Morais, V. A. *et al.* (2006) ‘N-glycosylation of human nicastrin is required for interaction with the lectins from the secretory pathway calnexin and ERGIC-53’, *Biochimica et Biophysica Acta - Molecular Basis of Disease*. Elsevier, 1762(9), pp. 802–810. doi: 10.1016/j.bbadis.2006.06.018.

Mori, H. *et al.* (2018) ‘Coronary Artery Calcification and its Progression: What Does it Really Mean?’, *JACC: Cardiovascular Imaging*. Elsevier Inc., pp. 127–142. doi: 10.1016/j.jcmg.2017.10.012.

Mori, K. *et al.* (2004) ‘Engineering Chinese hamster ovary cells to maximize effector function of produced antibodies using FUT8 siRNA’, *Biotechnology and Bioengineering*. John Wiley & Sons, Ltd, 88(7), pp. 901–908. doi: 10.1002/bit.20326.

Moritz, C. P. (2017) ‘Tubulin or Not Tubulin: Heading Toward Total Protein Staining as Loading Control in Western Blots’, *PROTEOMICS*. Wiley-VCH Verlag, 17(20), p. 1600189. doi: 10.1002/pmic.201600189.

Morrow, D. *et al.* (2005) ‘Notch-mediated CBF-1/RBP-Jκ-dependent regulation of human vascular smooth muscle cell phenotype in vitro’, *American Journal of Physiology - Cell Physiology*, 289(5 58-5). doi: 10.1152/ajpcell.00198.2005.

Morrow, D. *et al.* (2008) ‘Notch and Vascular Smooth Muscle Cell Phenotype’, *Circulation Research*. Lippincott Williams & Wilkins, 103(12), pp. 1370–1382. doi: 10.1161/CIRCRESAHA.108.187534.

Muto, A. *et al.* (2010) 'Mechanisms of vein graft adaptation to the arterial circulation - Insights into the neointimal algorithm and management strategies', *Circulation Journal*. Circ J, pp. 1501–1512. doi: 10.1253/circj.CJ-10-0495.

Nacev, B. A. *et al.* (2011) 'The antifungal drug itraconazole inhibits Vascular Endothelial Growth Factor Receptor 2 (VEGFR2) glycosylation, trafficking, and signaling in endothelial cells', *Journal of Biological Chemistry*. Elsevier, 286(51), pp. 44045–44056. doi: 10.1074/jbc.M111.278754.

Nagae, M. *et al.* (2014) 'Phytohemagglutinin from Phaseolus vulgaris (PHA-E) displays a novel glycan recognition mode using a common legume lectin fold', *Glycobiology*. Oxford University Press, 24(4), pp. 368–378. doi: 10.1093/glycob/cwu004.

Nakayasu, M. *et al.* (1980) 'Induction of differentiation of human and murine myeloid leukemia cells in culture by tunicamycin', *Proceedings of the National Academy of Sciences of the United States of America*. Proc Natl Acad Sci U S A, 77(1), pp. 409–413. doi: 10.1073/pnas.77.1.409.

Nam, D. *et al.* (2009) 'Partial carotid ligation is a model of acutely induced disturbed flow, leading to rapid endothelial dysfunction and atherosclerosis', *American Journal of Physiology - Heart and Circulatory Physiology*. Am J Physiol Heart Circ Physiol, 297(4). doi: 10.1152/ajpheart.00510.2009.

Narasimhan, S. (1982) 'Control of glycoprotein synthesis. UDP-GlcNac:Glycopeptide β4-N-acetylglucosaminyltransferase III, an enzyme in hen oviduct which adds GlcNAc in β1-4 linkage to the β-linked mannose of the trimannosyl core of N-glycosyl oligosaccharides', *Journal of Biological Chemistry*. Elsevier, 257(17), pp. 10235–10242. doi: 10.1016/s0021-9258(18)34010-9.

Nemenoff, R. A. *et al.* (2011) 'SDF-1 ␣ Induction in Mature Smooth Muscle Cells by Inactivation of PTEN Is a Critical Mediator of Exacerbated Injury-Induced Neointima Formation', *Arteriosclerosis, Thrombosis, and Vascular Biology*, 31(6), pp. 1300–1308. doi: 10.1161/ATVBAHA.111.223701.

Nguyen, A. T. *et al.* (2012) 'Smooth Muscle Cell Plasticity', *Circulation Research*, 112(1), pp. 17–22. doi: 10.1161/circresaha.112.281048.

Nicolas, M. *et al.* (2003) 'Notch1 functions as a tumor suppressor in mouse skin', *Nature Genetics*. Nature Publishing Group, 33(3), pp. 416–421. doi: 10.1038/ng1099.

NIH (2014) *Coronary Artery Bypass Grafting | National Heart, Lung, and Blood Institute (NHLBI)*. Available at: https://www.nhlbi.nih.gov/health-topics/coronary-artery-bypass-grafting

Niu, L. *et al.* (2000) 'High-affinity binding to the GM-CSF receptor requires intact N-glycosylation sites in the extracellular domain of the β subunit', *Blood*. W.B. Saunders, 95(11), pp. 3357–3362. doi: 10.1182/blood.v95.11.3357.

Niwa, Y. *et al.* (2012) 'Determination of cathepsin v activity and intracellular trafficking by N-glycosylation', *FEBS Letters*. No longer published by Elsevier, 586(20), pp. 3601–3607. doi: 10.1016/j.febslet.2012.08.001.

Noseda, M. *et al.* (2004) 'Notch Activation Results in Phenotypic and Functional Changes Consistent with Endothelial-to-Mesenchymal Transformation', *Circulation Research*. Lippincott Williams & Wilkins, 94(7), pp. 910–917. doi: 10.1161/01.RES.0000124300.76171.C9.

Noseda, M. *et al.* (2006) 'Smooth muscle α-actin is a direct target of Notch/CSL', *Circulation Research*. Lippincott Williams & Wilkins, 98(12), pp. 1468–1470. doi: 10.1161/01.RES.0000229683.81357.26.

Ogawa, M. *et al.* (2020) 'Contribution of extracellular O-GlcNAc to the stability of folded epidermal growth factor-like domains and Notch1 trafficking', *Biochemical and Biophysical Research Communications*. Elsevier B.V., 526(1), pp. 184–190. doi: 10.1016/j.bbrc.2020.03.066.

Ogen-Shtern, N. *et al.* (2016) 'Mannosidase IA is in Quality Control Vesicles and Participates in Glycoprotein Targeting to ERAD', *Journal of Molecular Biology*. Academic Press, 428(16), pp. 3194–3205. doi: 10.1016/j.jmb.2016.04.020.

Ohtsubo, K. and Marth, J. D. (2006) 'Glycosylation in Cellular Mechanisms of Health and Disease', *Cell*, 126(5), pp. 855–867. doi: 10.1016/j.cell.2006.08.019.

Okajima, T. *et al.* (2008) 'Contributions of chaperone and glycosyltransferase activities of O-fucosyltransferase 1 to Notch signaling', *BMC Biology*, 6, pp. 1–10. doi: 10.1186/1741-7007-6-1.

Okamoto, S. *et al.* (2019) 'Highly efficient genome editing for single-base substitutions using optimized ssODNs with Cas9-RNPs', *Scientific Reports*. Nature Publishing Group, 9(1), pp. 1–11. doi: 10.1038/s41598-019-41121-4.

Okazaki, A. *et al.* (2004) 'Fucose Depletion from Human IgG1 Oligosaccharide Enhances Binding Enthalpy and Association Rate between IgG1 and FcγRIIIa', *Journal of Molecular Biology*. Academic Press, 336(5), pp. 1239–1249. doi: 10.1016/j.jmb.2004.01.007.

Oliver, E., Mayor Jr, F. and D'Ocon, P. (2019) 'Beta-blockers: Historical Perspective and Mechanisms of Action', *Revista Española de Cardiología (English Edition)*. Elsevier BV, 72(10), pp. 853–862. doi: 10.1016/j.rec.2019.04.006.

Osumi, D. *et al.* (2009) 'Core fucosylation of E-cadherin enhances cell-cell adhesion in human colon carcinoma WiDr cells', *Cancer Science*. John Wiley & Sons, Ltd, 100(5), pp. 888–895. doi: 10.1111/j.1349-7006.2009.01125.x.

Otsuka, F. *et al.* (2015) 'Natural progression of atherosclerosis from pathologic intimal thickening to late fibroatheroma in human coronary arteries: A pathology study', *Atherosclerosis*. Elsevier Ireland Ltd, 241(2), pp. 772–782. doi: 10.1016/j.atherosclerosis.2015.05.011.

Owens, G. K., Kumar, M. S. and Wamhoff, B. R. (2004) 'Molecular Regulation of Vascular Smooth Muscle Cell Differentiation in Development and Disease', *Physiology Reviews*, 84(3), pp. 767–801.

Pakkiriswami, S. *et al.* (2016) 'Glycosylated Notch and Cancer', *Frontiers in Oncology*, 6(February), pp. 1–8. doi: 10.3389/fonc.2016.00037.

Panelos, J. and Massi, D. (2009) 'Emerging role of Notch signaling in epidermal differentiation and skin cancer', *Cancer Biology and Therapy*. Landes Bioscience, pp. 1986–1993. doi: 10.4161/cbt.8.21.9921.

Panin, V. M. *et al.* (2002) 'Notch ligands are substrates for protein O-fucosyltransferase-1 and Fringe.', *The Journal of biological chemistry*, 277(33), pp. 29945–29952. doi: 10.1074/jbc.M204445200.

Panyam, J. and Labhasetwar, V. (2003) 'B iodegradable nanoparticles for drug and gene delivery to cells and tissue', 55, pp. 329–347. doi: 10.1016/S0169-409X(02)00228-4.

Patsos, G. *et al.* (2009) 'O-Glycan inhibitors generate aryl-glycans, induce apoptosis and lead to growth inhibition in colorectal cancer cell lines', *Glycobiology*. Oxford Academic, 19(4), pp. 382–398. doi: 10.1093/glycob/cwn149.

Penton, A. L., Leonard, L. D. and Spinner, N. B. (2012) 'Notch signaling in human development and disease', *Seminars in Cell and Developmental Biology*. Elsevier Ltd, pp. 450–457. doi: 10.1016/j.semcdb.2012.01.010.

Perdigoto, C. N. and Bardin, A. J. (2013) 'Sending the right signal: Notch and stem cells', *Biochimica et Biophysica Acta - General Subjects*. Elsevier, pp. 2307–2322. doi: 10.1016/j.bbagen.2012.08.009.

Peterson, S. M. *et al.* (2018) 'Notch2 and proteomic signatures in mouse neointimal lesion formation', *Arteriosclerosis, Thrombosis, and Vascular Biology*. Lippincott Williams and Wilkins, 38(7), pp. 1576–1593. doi: 10.1161/ATVBAHA.118.311092.

Pinho, S. S. *et al.* (2012) 'Loss and Recovery of Mgat3 and GnT-III Mediated E-cadherin N-glycosylation Is a Mechanism Involved in Epithelial-Mesenchymal-Epithelial Transitions', *PLoS ONE*. Edited by S. Deb. Public Library of Science, 7(3), p. e33191. doi: 10.1371/journal.pone.0033191.

Pinho, S. S. and Reis, C. A. (2015) 'Glycosylation in cancer: Mechanisms and clinical implications', *Nature Reviews Cancer*. Nature Publishing Group, pp. 540–555. doi: 10.1038/nrc3982.

Polacheck, W. J. *et al.* (2017) 'A non-canonical Notch complex regulates adherens junctions and vascular barrier function', *Nature*. Nature Publishing Group, 552(7684), pp. 258–262. doi: 10.1038/nature24998.

Polesskaya, A., Seale, P. and Rudnicki, M. A. (2003) 'Wnt signaling induces the myogenic specification of resident CD45+ adult stem cells during muscle regeneration', *Cell*. Elsevier B.V., 113(7), pp. 841–852. doi: 10.1016/S0092-8674(03)00437-9.

Potter, C. M. F. *et al.* (2014) 'Role of biomechanical forces in stem cell vascular lineage differentiation', *Arteriosclerosis, Thrombosis, and Vascular Biology*. Lippincott Williams and Wilkins, 34(10), pp. 2184–2190. doi: 10.1161/ATVBAHA.114.303423.

Poulson, D. F. (1937) ‘Chromosomal Deficiencies and the Embryonic Development of Drosophila Melanogaster’, *Proceedings of the National Academy of Sciences*. Proceedings of the National Academy of Sciences, 23(3), pp. 133–137. doi: 10.1073/pnas.23.3.133.

Proweller, A., Pear, W. S. and Parmacek, M. S. (2005) ‘Notch signaling represses myocardin-induced smooth muscle cell differentiation’, *Journal of Biological Chemistry*, 280(10), pp. 8994–9004. doi: 10.1074/jbc.M413316200.

Pucella, J. N., Upadhaya, S. and Reizis, B. (2020) ‘The Source and Dynamics of Adult Hematopoiesis: Insights from Lineage Tracing’, *Annual Review of Cell and Developmental Biology*. Annual Reviews Inc., pp. 529–550. doi: 10.1146/annurev-cellbio-020520-114601.

Qiu, R., Zhang, X. and Regnier, F. E. (2007) ‘A method for the identification of glycoproteins from human serum by a combination of lectin affinity chromatography along with anion exchange and Cu-IMAC selection of tryptic peptides’, *Journal of Chromatography B: Analytical Technologies in the Biomedical and Life Sciences*, 845(1), pp. 143–150. doi: 10.1016/j.jchromb.2006.08.007.

Qu, S. J. *et al.* (1993) ‘Effects of Site-Directed Mutagenesis on the N-Glycosylation Sites of Human Lecithin: Cholesterol Acyltransferase’, *Biochemistry*. Biochemistry, 32(34), pp. 8732–8736. doi: 10.1021/bi00085a002.

Rademacher, T. W., Parekh, R. B. and Dwek, R. A. (1988) ‘Glycobiology’, *Annual Review of Biochemistry*. Annual Reviews 4139 El Camino Way, P.O. Box 10139, Palo Alto, CA 94303-0139, USA , 57(1), pp. 785–838. doi: 10.1146/annurev.bi.57.070188.004033.

Rahmani, M. *et al.* (2006) ‘Allograft vasculopathy versus atherosclerosis’, *Circulation Research*. Lippincott Williams & Wilkins, pp. 801–815. doi: 10.1161/01.RES.0000246086.93555.f3.

Ramanujam, M. *et al.* (2001) ‘Effect of site-directed asparagine to isoleucine substitutions at the N-linked E1 glycosylation sites on rubella virus viability’, *Virus Research*. Elsevier, 81(1–2), pp. 151–156. doi: 10.1016/S0168-1702(01)00374-4.

Rand, M. D. *et al.* (2000) ‘Calcium Depletion Dissociates and Activates Heterodimeric Notch Receptors’, *Molecular and Cellular Biology*. American Society for Microbiology, 20(5), pp. 1825–1835. doi: 10.1128/mcb.20.5.1825-1835.2000.

Rechsteiner, M. and Rogers, S. W. (1996) ‘PEST sequences and regulation by proteolysis’, *Trends in Biochemical Sciences*. Elsevier Ltd, pp. 267–271. doi: 10.1016/S0968-0004(96)10031-1.

Redheuil, A. *et al.* (2010) ‘Reduced ascending aortic strain and distensibility: Earliest manifestations of vascular aging in humans’, *Hypertension*. Lippincott Williams & Wilkins, 55(2), pp. 319–326. doi: 10.1161/HYPERTENSIONAHA.109.141275.

Redheuil, A. *et al.* (2011) ‘Age-related changes in aortic arch geometry: Relationship with proximal aortic function and left ventricular mass and remodeling’, *Journal of the American College of Cardiology*, 58(12), pp. 1262–1270. doi: 10.1016/j.jacc.2011.06.012.

Redmond, E. M. *et al.* (2014) 'Perivascular Delivery of Notch 1 siRNA Inhibits Injury-Induced Arterial Remodeling', *PLoS ONE*. Edited by C. Chatziantoniou. Public Library of Science, 9(1), p. e84122. doi: 10.1371/journal.pone.0084122.

Reilly, I. A. G. and FitzGerald, G. A. (1988) 'Aspirin in Cardiovascular Disease', *Drugs*. Springer, pp. 154–176. doi: 10.2165/00003495-198835020-00005.

Reinert, R. B. *et al.* (2012) 'Tamoxifen-Induced Cre-loxP Recombination Is Prolonged in Pancreatic Islets of Adult Mice', *PLoS ONE*. Edited by K. Maedler. Public Library of Science, 7(3), p. e33529. doi: 10.1371/journal.pone.0033529.

Rensen, S. S. M., Doevendans, P. A. F. M. and van Eys, G. J. J. M. (2007) 'Regulation and characteristics of vascular smooth muscle cell phenotypic diversity.', *Netherlands heart journal : monthly journal of the Netherlands Society of Cardiology and the Netherlands Heart Foundation*. Springer, 15(3), pp. 100–8. DOI: 10.1007/BF03085963

Reznikoff, C. A., Brankow, D. W. and Heidelberger, C. (1973) 'Establishment and Characterization of a Cloned Line of C3H Mouse Embryo Cells Sensitive to Postconfluence Inhibition of Division', *Cancer Research*, 33(12).

Ribeiro, J. P. *et al.* (2018) 'Tailor-made Janus lectin with dual avidity assembles glycoconjugate multilayers and crosslinks protocells', *Chemical Science*. Royal Society of Chemistry, 9(39), pp. 7634–7641. doi: 10.1039/c8sc02730g.

Robbins, S. L. (Stanley L. and Cotran, R. S. (2010) *Robbins and Cotran Pathologic basis of disease.* Saunders/Elsevier.

Roboti, P. and High, S. (2012) 'The oligosaccharyltransferase subunits OST48, DAD1 and KCP2 function as ubiquitous and selective modulators of mammalian N-glycosylation', *Journal of Cell Science*. The Company of Biologists Ltd, 125(14), pp. 3474–3484. doi: 10.1242/jcs.103952.

Romero-Calvo, I. *et al.* (2010) 'Reversible Ponceau staining as a loading control alternative to actin in Western blots', *Analytical Biochemistry*. Academic Press Inc., 401(2), pp. 318–320. doi: 10.1016/j.ab.2010.02.036.

Roostalu, U. *et al.* (2018) 'Distinct cellular mechanisms underlie smooth muscle turnover in vascular development and repair', *Circulation Research*. Lippincott Williams and Wilkins, 122(2), pp. 267–281. doi: 10.1161/CIRCRESAHA.117.312111.

Roostalu, U. and Wong, J. K. (2018) 'Arterial smooth muscle dynamics in development and repair', *Developmental Biology*. Elsevier Inc., 435(2), pp. 109–121. doi: 10.1016/j.ydbio.2018.01.018.

Ross, R. (1999) 'Atherosclerosis - An Inflammatory Disease', *The New England Journal of Medicine*, 340(2), pp. 115–126. doi: 10.1056/NEJM199901143400207.

Ross, R. and Glomset, J. A. (1973) 'Atherosclerosis and the arterial smooth muscle cell', *Science*. Science, pp. 1332–1339. doi: 10.1126/science.180.4093.1332.

Roth, Z., Yehezkel, G. and Khalaila, I. (2012) 'Identification and Quantification of Protein Glycosylation', *International Journal of Carbohydrate Chemistry*. Hindawi, 2012, pp. 1–10. doi: 10.1155/2012/640923.

Rothman, R. J. *et al.* (1989) 'Antibody-dependent cytotoxicity mediated by natural killer cells is enhanced by castanospermine-induced alterations of IgG glycosylation', *Molecular Immunology*. Mol Immunol, 26(12), pp. 1113–1123. doi: 10.1016/0161-5890(89)90055-2.

Rudd, P. M. *et al.* (2005) 'Glycoforms modify the dynamic stability and functional activity of an enzyme', *Biochemistry*, 33(1), pp. 17–22. doi: 10.1021/bi00167a003.

Sainz, J. *et al.* (2006) 'Isolation of "Side Population" Progenitor Cells From Healthy Arteries of Adult Mice', *Arteriosclerosis, Thrombosis, and Vascular Biology*. Lippincott Williams & Wilkins, 26(2), pp. 281–286. doi: 10.1161/01.ATV.0000197793.83391.91.

Sakamoto, A. *et al.* (2018) 'Pathologic intimal thickening: Are we any closer to understand early transitional plaques that lead to symptomatic disease?', *Atherosclerosis*. Elsevier Ireland Ltd, pp. 227–229. doi: 10.1016/j.atherosclerosis.2018.04.033.

Sala, E. *et al.* (2012) 'Endocytosis in Notch Signaling Activation', in Ceresa, B. (ed.) *Molecular Regulation of Endocytosis*. IntechOpen, pp. 331–376. doi: 10.5772/32009.

Saliba, A. E. *et al.* (2014) 'Single-cell RNA-seq: Advances and future challenges', *Nucleic Acids Research*. Oxford University Press, pp. 8845–8860. doi: 10.1093/nar/gku555.

Sanchez-Irizarry, C. *et al.* (2004) 'Notch Subunit Heterodimerization and Prevention of Ligand-Independent Proteolytic Activation Depend, Respectively, on a Novel Domain and the LNR Repeats', *Molecular and Cellular Biology*, 24(21), pp. 9265–9273. doi: 10.1128/MCB.24.21.9265-9273.2004.

Sanders, P. G. T. *et al.* (2009) 'Ligand-independent traffic of notch buffers activated armadillo in Drosophila', *PLoS Biology*. PLoS Biol, 7(8). doi: 10.1371/journal.pbio.1000169.

Sapet, C. *et al.* (2011) 'High transfection efficiency of neural stem cells with magnetofection', *BioTechniques*. Future Science Ltd London, UK , 50(3), pp. 187–189. doi: 10.2144/000113628.

Sartore, S. *et al.* (2001) 'Contribution of Adventitial Fibroblasts to Neointima Formation and Vascular Remodeling', *Circulation Research*. Lippincott Williams & Wilkins, 89(12), pp. 1111–1121. doi: 10.1161/hh2401.100844.

Sata, M. (2003) 'Circulating Vascular Progenitor Cells Contribute to Vascular Repair, Remodeling, and Lesion Formation', *Trends in Cardiovascular Medicine*. Elsevier, 13(6), pp. 249–253. doi: 10.1016/S1050-1738(03)00106-3.

Savi, P. *et al.* (2002) 'Clopidogrel: a review of its mechanism of action', *Platelets*, 9(3–4), pp. 251–255. doi: 10.1080/09537109876799.

Schachter, H. (1986) 'Biosynthetic controls that determine the branching and microheterogeneity of protein-bound oligosaccharides.', *Advances in experimental medicine and biology*. Springer, Boston, MA, pp. 53–85. doi: 10.1007/978-1-4684-5209-9_2.

Schwarz, F. and Aebi, M. (2011) 'Mechanisms and principles of N-linked protein glycosylation', *Current Opinion in Structural Biology*. Elsevier Current Trends, pp. 576–582. doi: 10.1016/j.sbi.2011.08.005.

Schweisguth, F. (2004) 'Regulation of Notch Signaling Activity', *Current Biology*. Elsevier BV, 14(3), pp. R129–R138. doi: 10.1016/j.cub.2004.01.023.

Seri, B. *et al.* (2004) 'Cell types, lineage, and architecture of the germinal zone in the adult dentate gyrus', *Journal of Comparative Neurology*. John Wiley & Sons, Ltd, 478(4), pp. 359–378. doi: 10.1002/cne.20288.

Sethi, M. K. *et al.* (2010) 'Identification of Glycosyltransferase 8 Family Members as Xylosyltransferases Acting on O-Glucosylated Notch Epidermal Growth Factor Repeats', *Journal of Biological Chemistry*, 285(3), pp. 1582–1586. doi: 10.1074/jbc.C109.065409.

Shalel Levanon, S. *et al.* (2018) 'An efficient method to control high mannose and core fucose levels in glycosylated antibody production using deoxymannojirimycin', *Journal of Biotechnology*. Elsevier, 276–277(April), pp. 54–62. doi: 10.1016/j.jbiotec.2018.04.006.

Shang, Y. C. *et al.* (2007) 'Activated β-catenin induces myogenesis and inhibits adipogenesis in BM-derived mesenchymal stromal cells', *Cytotherapy*. Elsevier, 9(7), pp. 667–681. doi: 10.1080/14653240701508437.

Shankman, L. S. *et al.* (2015) 'KLF4-dependent phenotypic modulation of smooth muscle cells has a key role in atherosclerotic plaque pathogenesis', *Nature Medicine*. Nature Publishing Group, 21(6), pp. 628–637. doi: 10.1038/nm.3866.

Shao, L., Moloney, D. J. and Haltiwanger, R. (2003) 'Fringe Modifies *O* -Fucose on Mouse Notch1 at Epidermal Growth Factor-like Repeats within the Ligand-binding Site and the Abruptex Region', *Journal of Biological Chemistry*, 278(10), pp. 7775–7782. doi: 10.1074/jbc.M212221200.

Shi, J. *et al.* (2021) 'Efficient influence of ssDNA virus PCV2 replication by CRISPR/Cas9 targeting of the viral genome', *Molecular Immunology*. Elsevier Ltd, 133, pp. 63–66. doi: 10.1016/j.molimm.2021.01.024.

Shimizu, K. *et al.* (2001) 'Host bone-marrow cells are a source of donor intimal smooth-muscle–like cells in murine aortic transplant arteriopathy', *Nature Medicine*. Nature Publishing Group, 7(6), pp. 738–741. doi: 10.1038/89121.

Sinclair, A. M. and Elliott, S. (2005) 'Glycoengineering: The effect of glycosylation on the properties of therapeutic proteins', *Journal of Pharmaceutical Sciences*, 94(8), pp. 1626–1635. doi: 10.1002/jps.20319.

Singh, R. *et al.* (2003) 'Androgens Stimulate Myogenic Differentiation and Inhibit Adipogenesis in C3H 10T1/2 Pluripotent Cells through an Androgen Receptor-Mediated Pathway', *Endocrinology*. Oxford Academic, 144(11), pp. 5081–5088. doi: 10.1210/en.2003-0741.

Sjöqvist, M. and Andersson, E. R. (2019) 'Do as I say, Not(ch) as I do: Lateral control of cell fate', *Developmental Biology*. Elsevier Inc., pp. 58–70. doi: 10.1016/j.ydbio.2017.09.032.

Skrenkova, K. *et al.* (2018) 'N-Glycosylation Regulates the Trafficking and Surface Mobility of GluN3A-Containing NMDA Receptors', *Frontiers in Molecular Neuroscience*. Frontiers Media S.A., 11, p. 188. doi: 10.3389/fnmol.2018.00188.

Snippert, H. J. *et al.* (2010) 'Intestinal crypt homeostasis results from neutral competition between symmetrically dividing Lgr5 stem cells', *Cell*. Cell Press, 143(1), pp. 134–144. doi: 10.1016/j.cell.2010.09.016.

Solá, R. J. and Griebenow, K. (2009) 'Effects of glycosylation on the stability of protein pharmaceuticals.', *Journal of pharmaceutical sciences*. NIH Public Access, 98(4), pp. 1223–45. doi: 10.1002/jps.21504.

Son, H. E. *et al.* (2020) 'Fat Mass and Obesity-Associated (FTO) Stimulates Osteogenic Differentiation of C3H10T1/2 Cells by Inducing Mild Endoplasmic Reticulum Stress via a Positive Feedback Loop with p-AMPK', *Molecules and cells*. NLM (Medline), 43(1), pp. 58–65. doi: 10.14348/molcells.2019.0136.

Song, Y. *et al.* (2010) 'The bisecting GlcNAc on N-glycans inhibits growth factor signaling and retards mammary tumor progression', *Cancer Research*. American Association for Cancer Research, 70(8), pp. 3361–3371. doi: 10.1158/0008-5472.CAN-09-2719.

Spana, E. P. and Doe, C. Q. (1996) 'Numb antagonizes Notch signaling to specify sibling neuron cell fates', *Neuron*. Cell Press, 17(1), pp. 21–26. doi: 10.1016/S0896-6273(00)80277-9.

Stahl, M. *et al.* (2008) 'Roles of Pofut1 and O-fucose in mammalian Notch signaling', *Journal of Biological Chemistry*. Elsevier, 283(20), pp. 13638–13651. doi: 10.1074/jbc.M802027200.

Stanley, P. (2007) 'Regulation of Notch signaling by glycosylation', *Current Opinion in Structural Biology*, 17(5), pp. 530–535. doi: 10.1016/j.sbi.2007.09.007.

Stanley, P. (2016) 'What Have We Learned from Glycosyltransferase Knockouts in Mice?', *Journal of Molecular Biology*. Academic Press, pp. 3166–3182. doi: 10.1016/j.jmb.2016.03.025.

Stary, H. C. (1992) 'Composition and classification of human atherosclerotic lesions', *Virchows Archiv A Pathological Anatomy and Histopathology*. Springer-Verlag, pp. 277–290. doi: 10.1007/BF01660974.

Staudacher, E. *et al.* (1999) 'Fucose in N-glycans: From plant to man', *Biochimica et Biophysica Acta - General Subjects*. Elsevier, pp. 216–236. doi: 10.1016/S0304-4165(99)00181-6.

Stittrich, A. B. *et al.* (2014) 'Mutations in NOTCH1 Cause Adams-Oliver Syndrome', *American Journal of Human Genetics*. The American Society of Human Genetics, 95(3), pp. 275–284. doi: 10.1016/j.ajhg.2014.07.011.

Stowell, S. R. *et al.* (2008) 'Galectin-1, -2, and -3 exhibit differential recognition of sialylated glycans and blood group antigens', *Journal of Biological Chemistry*. Elsevier, 283(15), pp. 10109–10123. doi: 10.1074/jbc.M709545200.

Suga, S. and Maeshima, M. (2004) 'Water Channel Activity of Radish Plasma Membrane Aquaporins Heterologously Expressed in Yeast and Their Modification by Site-Directed Mutagenesis', *Plant and Cell Physiology*. Oxford Academic, 45(7), pp. 823–830. doi: 10.1093/pcp/pch120.

Sukarawan, W. *et al.* (2016) 'Effect of Jagged-1 and Dll-1 on osteogenic differentiation by stem cells from human exfoliated deciduous teeth', *Archives of Oral Biology*. Pergamon, 65, pp. 1–8. doi: 10.1016/J.ARCHORALBIO.2016.01.010.

Sun, X. *et al.* (2020) 'Glycans function as a Golgi export signal to promote the constitutive exocytic trafficking', *Journal of Biological Chemistry*. American Society for Biochemistry and Molecular Biology Inc., 295(43), pp. 14750–14762. doi: 10.1074/jbc.RA120.014476.

Takahata, Y. *et al.* (2009) 'Functional expression of β_2 adrenergic receptors responsible for protection against oxidative stress through promotion of glutathione synthesis after Nrf2 upregulation in undifferentiated mesenchymal C3H10T1/2 stem cells', *Journal of Cellular Physiology*. John Wiley & Sons, Ltd, 218(2), pp. 268–275. doi: 10.1002/jcp.21594.

Takatsuki, A. and Tamura, G. (1985) 'Brefeldin a, a specific inhibitor of intracellular translocation of vesicular stomatitis virus G protein: Intracellular accumulation of high-mannose type G protein and inhibition of its cell surface expression', *Agricultural and Biological Chemistry*, 49(3), pp. 899–902. doi: 10.1080/00021369.1985.10866826.

Takeuchi, H. and Haltiwanger, R. S. (2014) 'Significance of glycosylation in Notch signaling', *Biochemical and Biophysical Research Communications*, 453(2), pp. 235–242. doi: 10.1016/j.bbrc.2014.05.115.

Talora, C. *et al.* (2008) 'Notch signaling and diseases: An evolutionary journey from a simple beginning to complex outcomes', *Biochimica et Biophysica Acta - Molecular Basis of Disease*, 1782(9), pp. 489–497. doi: 10.1016/j.bbadis.2008.06.008.

Tan, Z. *et al.* (2018) 'Bisecting N-Acetylglucosamine Structures Inhibit Hypoxia-Induced Epithelial-Mesenchymal Transition in Breast Cancer Cells', *Frontiers in Physiology*. Frontiers Media S.A., 9(MAR), p. 210. doi: 10.3389/fphys.2018.00210.

Tanaka, S., Terada, K. and Nohno, T. (2011) 'Canonical Wnt signaling is involved in switching from cell proliferation to myogenic differentiation of mouse myoblast cells', *Journal of Molecular Signaling*. Ubiquity Press Ltd, 6(1), pp. 1–17. doi: 10.1186/1750-2187-6-12.

Tang, J. *et al.* (2020) 'Arterial Sca1+ Vascular Stem Cells Generate De Novo Smooth Muscle for Artery Repair and Regeneration', *Cell Stem Cell*. Cell Press, 26(1), pp. 81-96.e4. doi: 10.1016/j.stem.2019.11.010.

Tang, Q. Q., Otto, T. C. and Lane, M. D. (2004) 'Commitment of C3H10T1/2 pluripotent stem cells to the adipocyte lineage', *Proceedings of the National Academy of Sciences of the United States of America*. National Academy of Sciences, 101(26), pp. 9607–9611. doi: 10.1073/pnas.0403100101.

Tang, Y. *et al.* (2010) 'Notch and transforming growth factor-β(TGFβ) signaling pathways cooperatively regulate vascular smooth muscle cell differentiation', *Journal of Biological Chemistry*. Elsevier, 285(23), pp. 17556–17563. doi: 10.1074/jbc.M109.076414.

Tang, Y., Urs, S. and Liaw, L. (2008) 'Hairy-related transcription factors inhibit notch-induced smooth muscle α-actin expression by interfering with notch intracellular domain/CBF-1 complex interaction with the CBF-1-binding site', *Circulation Research*. Lippincott Williams & Wilkins, 102(6), pp. 661–668. doi: 10.1161/CIRCRESAHA.107.165134.

Tang, Z. *et al.* (2012) 'Differentiation of multipotent vascular stem cells contributes to vascular diseases', *Nature Communications*. Nature Publishing Group, 3(1), pp. 1–13. doi: 10.1038/ncomms1867.

Taylor Kimberly, W. *et al.* (2002) 'Complex N-linked glycosylated nicastrin associates with active γ-secretase and undergoes tight cellular regulation', *Journal of Biological Chemistry*. Elsevier, 277(38), pp. 35113–35117. doi: 10.1074/jbc.M204446200.

Tesauro, M. *et al.* (2017) 'Arterial ageing: from endothelial dysfunction to vascular calcification', *Journal of Internal Medicine*. Blackwell Publishing Ltd, 281(5), pp. 471–482. doi: 10.1111/joim.12605.

van Tetering, G. and Vooijs, M. (2011) 'Proteolytic cleavage of Notch: "HIT and RUN".', *Current molecular medicine*, 11(4), pp. 255–69. DOI : 10.2174/156652411795677972

Thacker, J. S. *et al.* (2016) 'Total protein or high-abundance protein: Which offers the best loading control for Western blotting?', *Analytical Biochemistry*. Academic Press Inc., 496, pp. 76–78. doi: 10.1016/j.ab.2015.11.022.

Thompson, R. *et al.* (2011) 'Optimization of the enzyme-linked lectin assay for enhanced glycoprotein and glycoconjugate analysis', *Analytical Biochemistry*. Elsevier Inc., 413(2), pp. 114–122. doi: 10.1016/j.ab.2011.02.013.

Tintut, Y. *et al.* (2003) 'Multilineage Potential of Cells From the Artery Wall', *Circulation*. Lippincott Williams & Wilkins, 108(20), pp. 2505–2510. doi: 10.1161/01.CIR.0000096485.64373.C5.

Tommasone, S. *et al.* (2019) 'The challenges of glycan recognition with natural and artificial receptors', *Chemical Society Reviews*. Royal Society of Chemistry, pp. 5488–5505. doi: 10.1039/c8cs00768c.

Tordai, A., Brass, L. F. and Gelfand, E. W. (1995) 'Tunicamycin inhibits the expression of functional thrombin receptors on human T-lymphoblastoid cells', *Biochemical and Biophysical Research Communications*. Academic Press, 206(3), pp. 857–862. doi: 10.1006/bbrc.1995.1122.

Torsney, E., Hu, Y. and Xu, Q. (2005) 'Adventitial Progenitor Cells Contribute to Arteriosclerosis', *Trends in Cardiovascular Medicine*. Elsevier, 15(2), pp. 64–68. doi: 10.1016/J.TCM.2005.02.003.

Toyama, B. H. and Hetzer, M. W. (2013) 'Protein homeostasis: Live long, won't prosper', *Nature Reviews Molecular Cell Biology*. NIH Public Access, pp. 55–61. doi: 10.1038/nrm3496.

Traustadóttir, G. Á. *et al.* (2019) 'The imprinted gene Delta like non-canonical Notch ligand 1 (Dlk1)is conserved in mammals, and serves a growth modulatory role during tissue development and regeneration through Notch dependent and independent mechanisms', *Cytokine and Growth Factor Reviews*. Elsevier Ltd, pp. 17–27. doi: 10.1016/j.cytogfr.2019.03.006.

Turnpenny, P. D. *et al.* (2003) 'Novel mutations in DLL3, a somitogenesis gene encoding a ligand for the Notch signalling pathway, cause a consistent pattern of abnormal vertebral segmentation in spondylocostal dysostosis', *Journal of Medical Genetics*. BMJ Publishing Group, 40(5), pp. 333–339. doi: 10.1136/jmg.40.5.333.

Urano, Y. *et al.* (2020) 'Curcumin Derivative GT863 Inhibits Amyloid-Beta Production via Inhibition of Protein N-Glycosylation', *Cells*. NLM (Medline), 9(2). doi: 10.3390/cells9020349.

Uyttendaele, H. *et al.* (1996) 'Notch4/int-3, a mammary proto-oncogene, is an endothelial cell-specific mammalian Notch gene', *Development*, 2259, pp. 2251–2259.

Virmani, R. *et al.* (2000) 'Lessons from sudden coronary death: A comprehensive morphological classification scheme for atherosclerotic lesions', *Arteriosclerosis, Thrombosis, and Vascular Biology*. Lippincott Williams and Wilkins, 20(5), pp. 1262–1275. doi: 10.1161/01.ATV.20.5.1262.

Wadhera, R. K. *et al.* (2016) 'A review of low-density lipoprotein cholesterol, treatment strategies, and its impact on cardiovascular disease morbidity and mortality', *Journal of Clinical Lipidology*. Elsevier Ltd, pp. 472–489. doi: 10.1016/j.jacl.2015.11.010.

Walczak, P. *et al.* (2005) 'Instant MR labeling of stem cells using magnetoelectroporation', *Magnetic Resonance in Medicine*. John Wiley and Sons Inc., 54(4), pp. 769–774. doi: 10.1002/mrm.20701.

Walsh, G. (2009) *Post-translational Modification of Protein Biopharmaceuticals*. Weinheim, Germany: Wiley-VCH Verlag GmbH & Co. KGaA. doi: 10.1002/9783527626601.

Wang, D. *et al.* (2018) 'Adult stem cells in vascular remodeling', *Theranostics*, 8(3), pp. 815–829. doi: 10.7150/THNO.19577.

Wang, G. *et al.* (2015) 'Origin and differentiation of vascular smooth muscle cells', *The Journal of Physiology*. Blackwell Publishing Ltd, 593(14), pp. 3013–3030. doi: 10.1113/JP270033.

Wang, S.-S. *et al.* (2021) 'Efficient inhibition of O-glycan biosynthesis using the hexosamine analog Ac5GalNTGc', *Cell Chemical Biology*. Elsevier BV, 0(0). doi: 10.1016/j.chembiol.2021.01.017.

Wang, X. *et al.* (2005) 'Dysregulation of TGF-β1 receptor activation leads to abnormal lung development and emphysema-like phenotype in core fucose-deficient mice', *Proceedings of the National Academy of Sciences of the United States of America*. National Academy of Sciences, 102(44), pp. 15791–15796. doi: 10.1073/pnas.0507375102.

Wang, Y. *et al.* (2020) 'Tunicamycin induces ER stress and inhibits tumorigenesis of head and neck cancer cells by inhibiting N-glycosylation', *American Journal of Translational Research*. E-Century Publishing Corporation, 12(2), pp. 541–550.

Wasley, L. C. *et al.* (1991) 'The importance of N- and O-linked oligosaccharides for the biosynthesis and in vitro and in vivo biologic activities of erythropoietin', *Blood*. Elsevier, 77(12), pp. 2624–2632. doi: 10.1182/blood.v77.12.2624.2624.

Weinmaster, G., Roberts, V. J. and Lemke, G. (1992) 'Notch2: A second mammalian Notch gene', *Development*, 116(4), pp. 931–941.

Weis, M. and Von Scheidt, W. (1997) 'Cardiac allograft vasculopathy: A review', *Circulation*. Lippincott Williams and Wilkins, pp. 2069–2077. doi: 10.1161/01.CIR.96.6.2069.

Weis, W. I. and Drickamer, K. (1996) 'Structural basis of lectin-carbohydrate recognition', *Annual Review of Biochemistry*. Annual Reviews Inc., pp. 441–473. doi: 10.1146/annurev.bi.65.070196.002301.

Wen, F. *et al.* (2014) 'Induction of Myogenic Differentiation of Human Mesenchymal Stem Cells Cultured on Notch Agonist (Jagged-1) Modified Biodegradable Scaffold Surface', *ACS Applied Materials & Interfaces*. American Chemical Society, 6(3), pp. 1652–1661. doi: 10.1021/am4045635.

Wesley, C. S. and Saez, L. (2000) 'Analysis of notch lacking the carboxyl terminus identified in Drosophila embryos.', *The Journal of cell biology*. The Rockefeller University Press, 149(3), pp. 683–96.

West, M. B. *et al.* (2011) 'Autocatalytic cleavage of human γ-glutamyl transpeptidase is highly dependent on N-glycosylation at asparagine 95', *Journal of Biological Chemistry*. Elsevier, 286(33), pp. 28876–28888. doi: 10.1074/jbc.M111.248823.

Wexler, L. *et al.* (1996) 'Coronary artery calcification: Pathophysiology, epidemiology, imaging methods, and clinical implications. A statement for health professionals from the American Heart Association', *Circulation*. Lippincott Williams and Wilkins, pp. 1175–1192. doi: 10.1161/01.CIR.94.5.1175.

Whittock, N. V. *et al.* (2004) 'Mutated/MESP2 causes spondylocostal dysostosis in humans', *American Journal of Human Genetics*. University of Chicago Press, 74(6), pp. 1249–1254. doi: 10.1086/421053.

Williams, S. E. *et al.* (2011) 'Asymmetric cell divisions promote Notch-dependent epidermal differentiation', *Nature*. Nature Publishing Group, 470(7334), pp. 353–358. doi: 10.1038/nature09793.

Wilson, J. R., Williams, D. and Schachter, H. (1976) 'The control of glycoprotein synthesis: N-acetylgluocosamine linkage to a mannose residue as a signal for the attachment of L-fucose to the asparagine-linked N-acetylglucosamine residue of glycopeptide from α1-acid glycoprotein', *Biochemical and Biophysical Research Communications*. Academic Press, 72(3), pp. 909–916. doi: 10.1016/S0006-291X(76)80218-5.

Wollscheid, B. *et al.* (2009) 'Mass-spectrometric identification and relative quantification of N-linked cell surface glycoproteins', *Nature Biotechnology*. NIH Public Access, 27(4), pp. 378–386. doi: 10.1038/nbt.1532.

World Health Organisation (2020) *The top 10 causes of death*. Available at: https://www.who.int/news-room/fact-sheets/detail/the-top-10-causes-of-death

Wright, W. E. *et al.* (1996) 'Telomerase activity in human germline and embryonic tissues and cells', *Developmental Genetics*. John Wiley & Sons, Ltd, 18(2), pp. 173–179. doi: 10.1002/(SICI)1520-6408(1996)18:2<173::AID-DVG10>3.0.CO;2-3.

Wu, J. *et al.* (2018) 'Tunicamycin specifically aggravates ER stress and overcomes chemoresistance in multidrug-resistant gastric cancer cells by inhibiting N-glycosylation', *Journal of Experimental and Clinical Cancer Research*. BioMed Central Ltd., 37(1), p. 272. doi: 10.1186/s13046-018-0935-8.

Wu, Y. *et al.* (2019) 'S100B is required for maintaining an intermediate state with double-positive Sca-1+ progenitor and vascular smooth muscle cells during neointimal formation', *Stem Cell Research and Therapy*. BioMed Central Ltd., 10(1), p. 294. doi: 10.1186/s13287-019-1400-0.

Xia, B. *et al.* (2013) 'Serum N-glycan and O-glycan analysis by mass spectrometry for diagnosis of congenital disorders of glycosylation', *Analytical Biochemistry*. Academic Press Inc., 442(2), pp. 178–185. doi: 10.1016/j.ab.2013.07.037.

Xiang, T. *et al.* (2017) 'Alteration of N-glycan expression profile and glycan pattern of glycoproteins in human hepatoma cells after HCV infection', *Biochimica et Biophysica Acta - General Subjects*. Elsevier B.V., 1861(5), pp. 1036–1045. doi: 10.1016/j.bbagen.2017.02.014.

Xiao, H., Smeekens, J. M. and Wu, R. (2016) 'Quantification of tunicamycin-induced protein expression and: N -glycosylation changes in yeast', *Analyst*. Royal Society of Chemistry, 141(12), pp. 3737–3745. doi: 10.1039/c6an00144k.

Xu, A. *et al.* (2007) 'In vitro reconstitution of the modulation of Drosophila Notch-ligand binding by Fringe.', *The Journal of biological chemistry*. American Society for Biochemistry and Molecular Biology, 282(48), pp. 35153–62. doi: 10.1074/jbc.M707040200.

Xu, K. *et al.* (2012) 'Lunatic Fringe Deficiency Cooperates with the Met/Caveolin Gene Amplicon to Induce Basal-like Breast Cancer', *Cancer Cell*, 21(5), pp. 626–641. doi: 10.1016/j.ccr.2012.03.041.

Xu, Q. (2008) 'Stem cells and transplant arteriosclerosis', *Circulation Research*. Lippincott Williams & Wilkins, pp. 1011–1024. doi: 10.1161/CIRCRESAHA.108.171488.

Yagita, M. and Saksela, E. (1990) 'Swainsonine, an Inhibitor of Glycoprotein Processing, Enhances Cytotoxicity of Large Granular Lymphocytes', *Scandinavian Journal of Immunology*. John Wiley & Sons, Ltd, 31(3), pp. 275–282. doi: 10.1111/j.1365-3083.1990.tb02769.x.

Yamaguchi, K. *et al.* (1991) 'Effects of site-directed removal of N-glycosylation sites in human erythropoietin on its production and biological properties', *Journal of Biological Chemistry*. Elsevier, 266(30), pp. 20434–20439. doi: 10.1016/s0021-9258(18)54942-5.

Yamamoto, K. *et al.* (2005) 'Measurement of the carbohydrate-binding specificity of lectins by a multiplexed bead-based flow cytometric assay', *Analytical Biochemistry*. Academic Press Inc., 336(1), pp. 28–38. doi: 10.1016/j.ab.2004.09.030.

Yamano, S., Dai, J. and Moursi, A. M. (2010) 'Comparison of transfection efficiency of nonviral gene transfer reagents', *Molecular Biotechnology*. Springer, 46(3), pp. 287–300. doi: 10.1007/s12033-010-9302-5.

Yan, A. and Lennarz, W. J. (2004) 'Unraveling the Mechanism of Protein N-Glycosylation*'. doi: 10.1074/jbc.R400036200.

Yang, D. S. *et al.* (2002) 'Mature glycosylation and trafficking of nicastrin modulate its binding to presenilins', *Journal of Biological Chemistry*. Elsevier, 277(31), pp. 28135–28142. doi: 10.1074/jbc.M110871200.

Yang, G. and Huang, X. (2019) 'Methods and applications of CRISPR/Cas system for genome editing in stem cells', *Cell Regeneration*. KeAi Communications Co., pp. 33–41. doi: 10.1016/j.cr.2019.08.001.

Yin, R. X., Yang, D. Z. and Wu, J. Z. (2014) 'Nanoparticle drug- and gene-eluting stents for the prevention and treatment of coronary restenosis', *Theranostics*, 4(2), pp. 175–200. doi: 10.7150/thno.7210.

Yodoi, J., Hirashima, M. and Ishizaka, K. (1981) 'Lymphocytes bearing Fc receptors for IgE. VI. Suppressive effect of glucocorticoids on the expression of Fc receptors and glycosylation of IgE-binding factors', *The Journal of Immunology*, 127(2), pp. 471–476.

Yoshida, T., Kaestner, K. H. and Owens, G. K. (2008) 'Conditional deletion of Krüppel-like factor 4 delays downregulation of smooth muscle cell differentiation markers but accelerates neointimal formation following vascular injury', *Circulation Research*. Lippincott Williams & Wilkins, 102(12), pp. 1548–1557. doi: 10.1161/CIRCRESAHA.108.176974.

Yoshimura, M. *et al.* (1995) 'High expression of udp-n-acetylglucosamine: β-d mannoside β-1, 4-n-acetylglucosaminyltransferase III (GnT-III) in chronic myelogenous leukemia in blast crisis', *International Journal of Cancer*. John Wiley & Sons, Ltd, 60(4), pp. 443–449. doi: 10.1002/ijc.2910600404.

Yoshimura, M. *et al.* (1996) 'Aberrant glycosylation of E-cadherin enhances cell-cell binding to suppress metastasis', *Journal of Biological Chemistry*. Elsevier, 271(23), pp. 13811–13815. doi: 10.1074/jbc.271.23.13811.

Yu, G. *et al.* (2000) 'Nicastrin modulates presenilin-mediated notch/glp-1 signal transduction and βAPP processing', *Nature*. Nature, 407(6800), pp. 48–54. doi: 10.1038/35024009.

Yuan, F. *et al.* (2017) 'Contribution of Vascular Cells to Neointimal Formation', *PLoS One*, 12(1), pp. 1–11. doi: 10.1371/journal.pone.0168914.

Yusuf, S. *et al.* (2020) 'Modifiable risk factors, cardiovascular disease, and mortality in 155 722 individuals from 21 high-income, middle-income, and low-income countries (PURE): a prospective cohort study', *The Lancet*. Lancet Publishing Group, 395(10226), pp. 795–808. doi: 10.1016/S0140-6736(19)32008-2.

Zagouras, P. *et al.* (1995) 'Alterations in Notch signaling in neoplastic lesions of the human cervix', *Proceedings of the National Academy of Sciences of the United States of America*. National Academy of Sciences, 92(14), pp. 6414–6418. doi: 10.1073/pnas.92.14.6414.

Zhang, S. *et al.* (2014) 'Tumor-Suppressive Activity of Lunatic Fringe in Prostate through Differential Modulation of Notch Receptor Activation', *Neoplasia*, 16(2), pp. 158–167. doi: 10.1593/neo.131870.

Zhang, Z. *et al.* (2017) 'CRISPR/Cas9 Genome-Editing System in Human Stem Cells: Current Status and Future Prospects', *Molecular Therapy - Nucleic Acids*. Cell Press, pp. 230–241. doi: 10.1016/j.omtn.2017.09.009.

Zhao, Y. *et al.* (2006) 'N-Acetylglucosaminyltransferase III antagonizes the effect of N-acetylglucosaminyltransferase V on α3β1 integrin-mediated cell migration', *Journal of Biological Chemistry*. Elsevier, 281(43), pp. 32122–32130. doi: 10.1074/jbc.M607274200.

Zhao, Y. *et al.* (2008) 'Branched N-glycans regulate the biological functions of integrins and cadherins', *FEBS Journal*. John Wiley & Sons, Ltd, 275(9), pp. 1939–1948. doi: 10.1111/j.1742-4658.2008.06346.x.

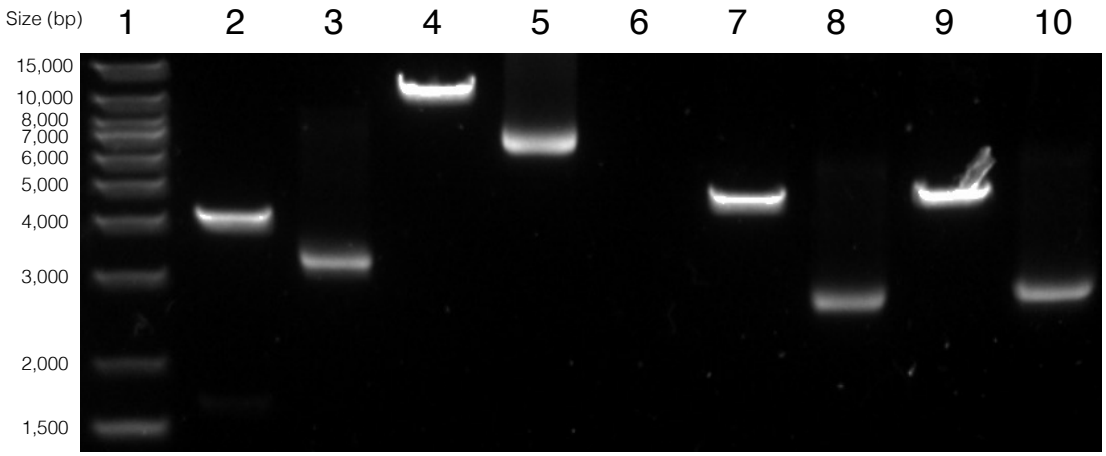
Zhou, J. *et al.* (2009) 'Functional analysis of an α-1,2-mannosidase from Magnaporthe oryzae', *Current Genetics*. Springer, pp. 485–496. doi: 10.1007/s00294-009-0261-y.

Zhou, Y. *et al.* (2015) 'SIRT1 inhibits adipogenesis and promotes myogenic differentiation in C3H10T1/2 pluripotent cells by regulating Wnt signaling', *Cell and Bioscience*. BioMed Central Ltd., 5(1), p. 61. doi: 10.1186/s13578-015-0055-5.

Zou, Y. *et al.* (1998) 'Mouse model of venous bypass graft arteriosclerosis', *American Journal of Pathology*. American Society for Investigative Pathology Inc., 153(4), pp. 1301–1310. doi: 10.1016/S0002-9440(10)65675-1.

Appendices

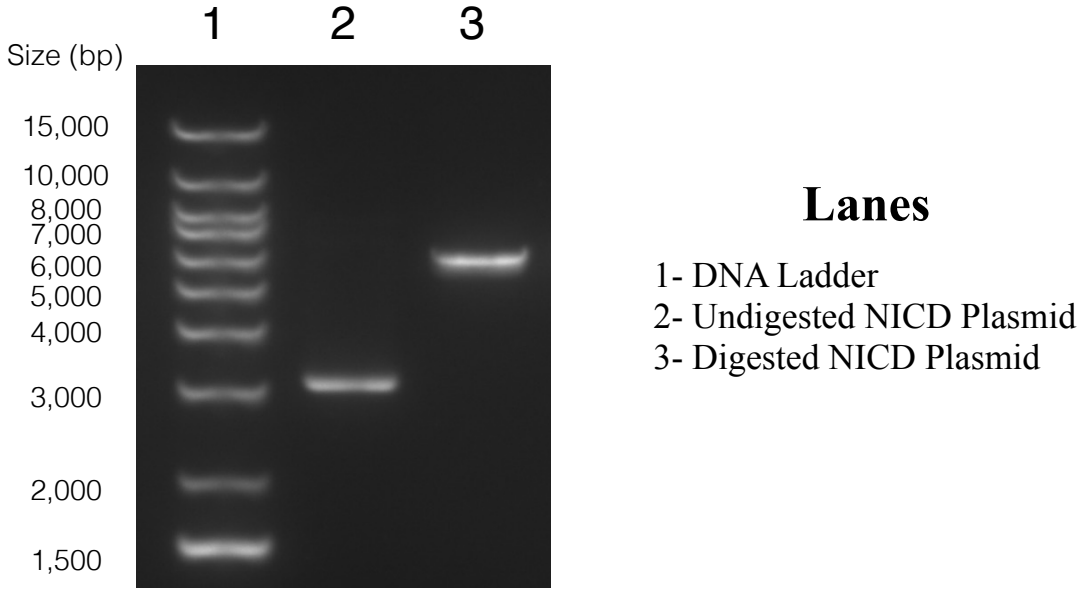
Appendix A



Lanes

1- DNA Ladder
2- Digested NICD Plasmid
3- Undigested NICD Plasmid
4- Digested Notch1 Plasmid
5- Undigested Notch1 Plasmid
6- Blank
7- Digested GFP Plasmid
8- Undigested GFP Plasmid
9- Digested Puro Resistance Plasmid
10- Undigested Puro Resistance Plasmid

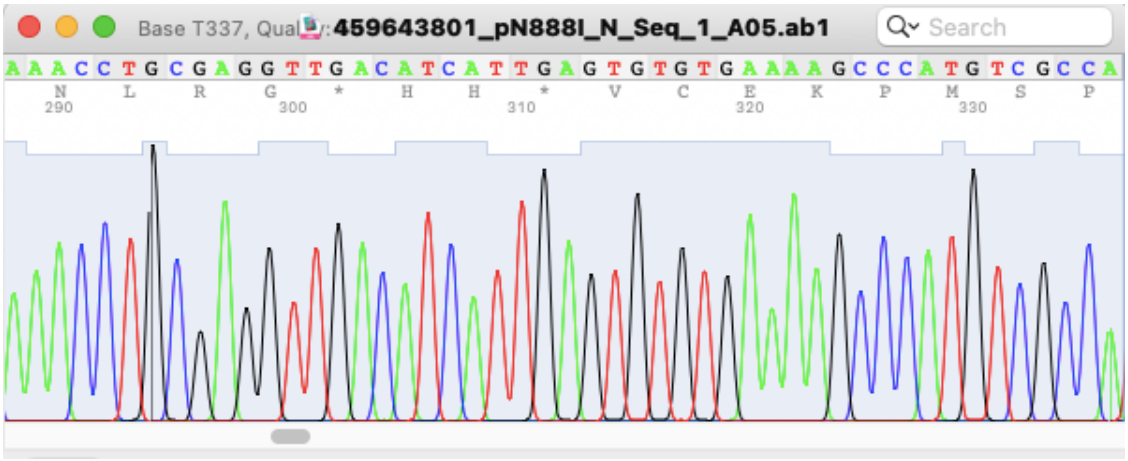
Supplementary Fig.1 Plasmid Validation. NICD, Notch1, GFP and Puromycin (Puro) Resistance Plasmids were purified from bacterial cultures and digested with an appropriate restriction enzyme (BamHI or EcoRI) to linearise DNA. Digested and undigested samples were run on a 1% Agarose Gel and visualised under UV light to validate plasmid purity and length. Data representative of n=3. Note: Incorrect restriction enzyme used for NICD plasmid resulting in incorrect plasmid length.

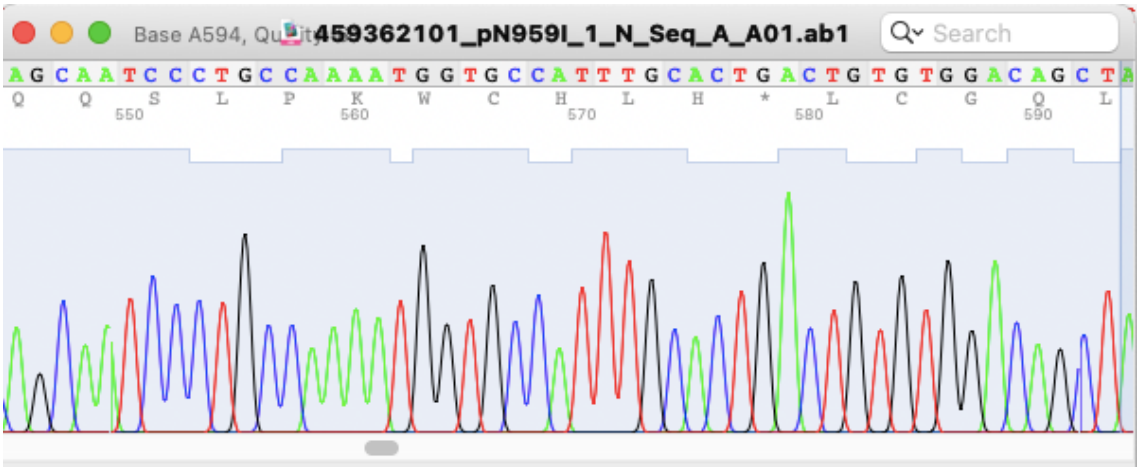


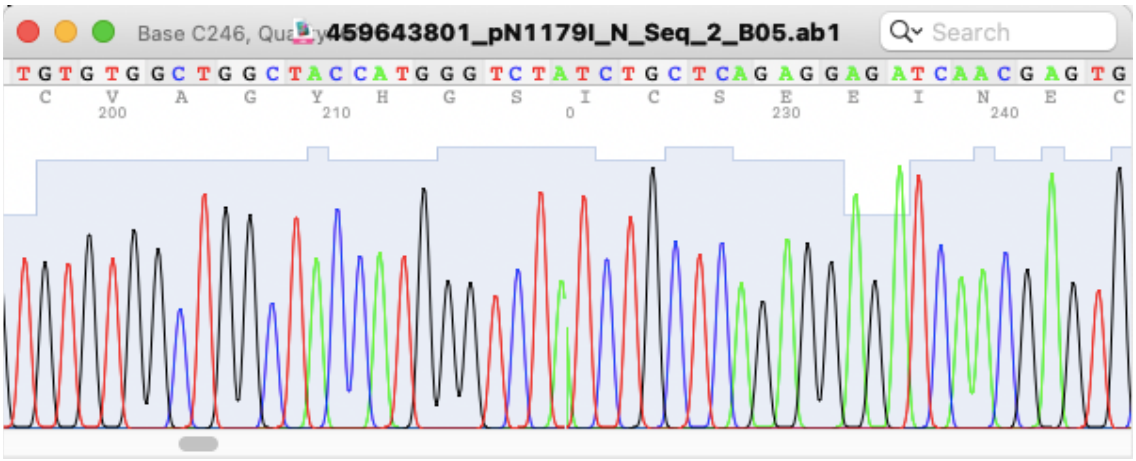
Supplementary Fig.2 NICD Plasmid Validation Repeat. NICD Plasmid was purified from bacterial culture and digested with EcoRI restriction enzyme to linearise DNA. Digested and undigested samples were run on a 1% Agarose Gel and visualised under UV light to validate plasmid purity and length. Data representative of n=3.

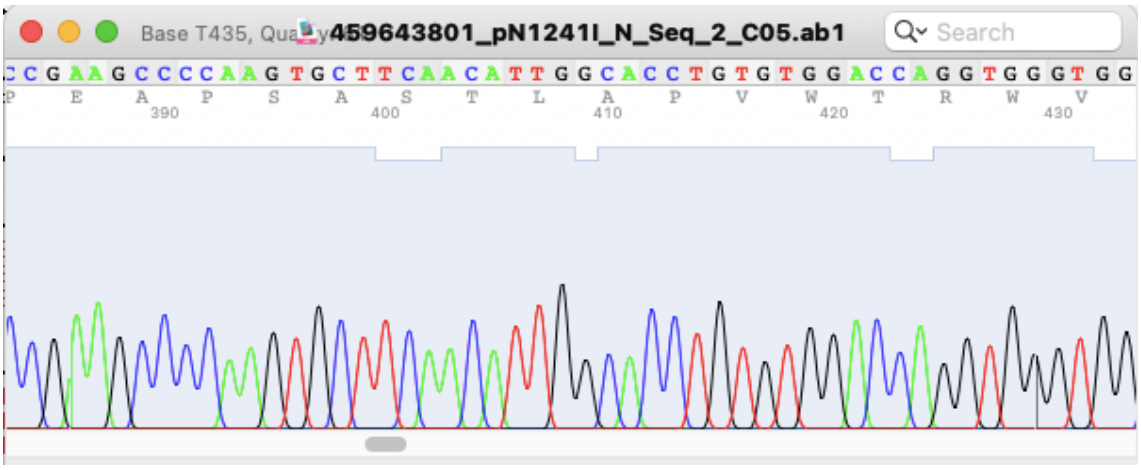
Appendix B

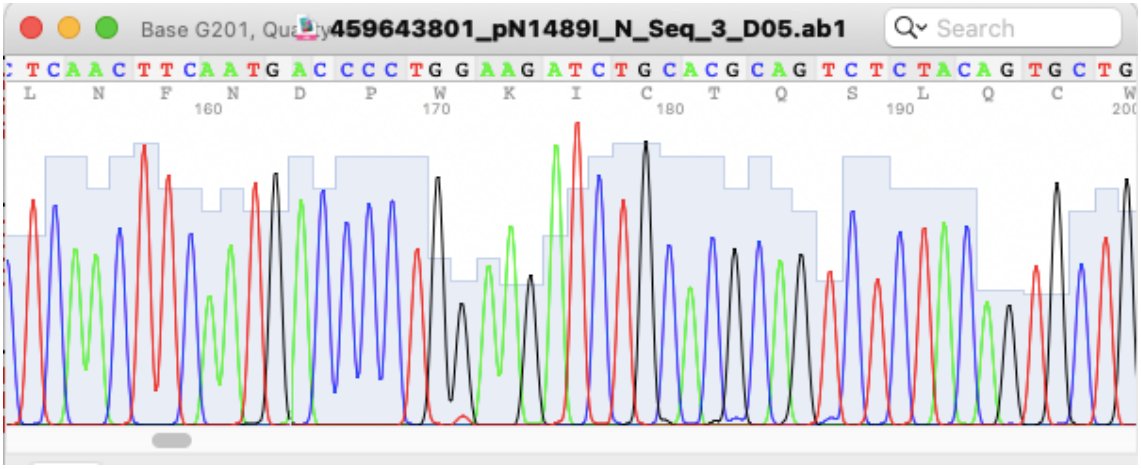
Chromatograms from Source Bioscience validating the quality of sequencing reads at the site of each Notch1 N-glycosylation site mutation:

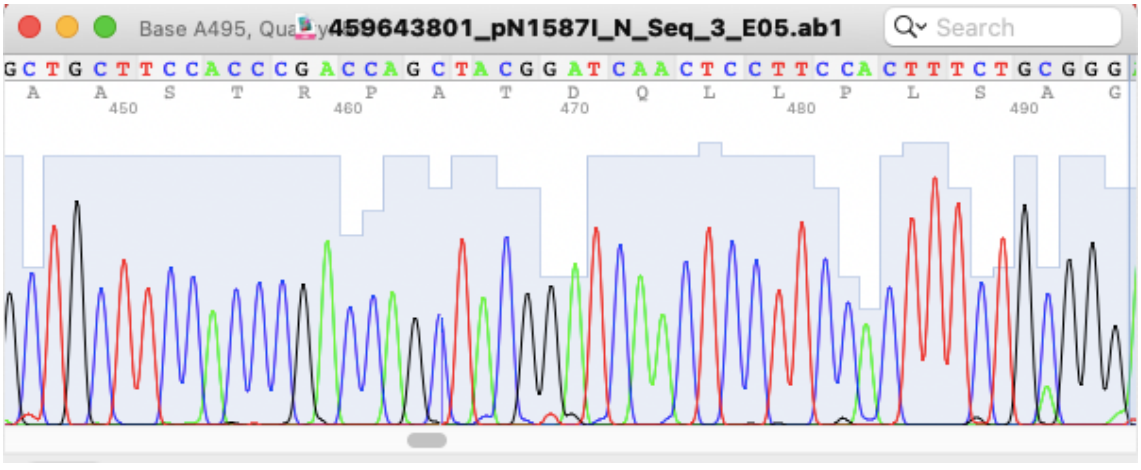







Base T435, Qua
459643801_pN1241l_N_Seq_2_C05.ab1
Search


Base G201, Qua
459643801_pN1489l_N_Seq_3_D05.ab1
Search


Base A495, Qua
459643801_pN1587l_N_Seq_3_E05.ab1
Search

Appendix C

RBP-Jκ-binding sites in promoter regions of Notch target genes *Hey1*, *Hey2* and *HeyL* and myogenic genes *Cnn1* and *Myh11*:

Mouse Hey1 promoter from -10kbp to 100bp TSS

```
>FP003555 Hey1_1 :+U EU:NC; range-10000 to 100.
acaccagcctcctcttcatccagaggcagtcctctgtctctctgccccaggacaaatacc
ccttccccttctcccttgttccttttccctcctccttcatctatgtcttgccttctgcct
ttgttcatctggagaaaataactctttgtgctgagaattaggtcttggggtgtcttgtgc
caatatcagccccttacttcaagttatagagatctacctggagcaagacatgagctgtg
tctcaaagtatgctcctgggaaattgaacatctggtccactgtattgggaagactattct
tgcaaagacagctataactataaacctggagaaaggaatcctgctagcagtgcattctgg
ggaattaatacggtacagcaagtagagggagctgaaatcttagagggagggtcctggtct
catgtaatgtacagccagaggctgaagggccagttttataaagtgggatacctagcagag
agaaactggccatccattcctctgctcaagtggagaaagaaagaagaaaatgtgtgggct
gaaaactcgaactacttttaagcagagatgtaagaaataccatcatctgtgtcatttata
tagaaagaaagttgtcctagttcattaacttgtaatccctaaaggatttgaaaagtcatt
gaaaaattaaaaaaaaaaaagaaaaaaaccagactttctctgaaaataaggcctttaaca
tgcaaaacagtatgtcctttgctcagcccagtcaattatatataaaatagtccatttcaa
tgatgttttcaaaagtaattatatatatatatgtatatacatatacatatatcacttctt
ttacaatggaaaaataagtttattgatacatacacacatatatatatacatacacatgta
tttgtgtgtgtgtgtatatatatatatatgtgtatgtatatatctccttttcactctaat
gagcattaaagagagctatgacaaaatcttccagagaatgaacaacagaattgaagataa
ggtttgggggatcatctatttcaaaacttctgtaacatcctaatacatcctcataagtag
acagaccagctcacaaaggtgctttgcccagcaattgaaaagtgttccactgggggggtag
agtgtcttctgtctctttgtctgtctggggtggggtgggtatgtgcacagggtgcaggtg
ctgggcctggggagcccagaagcatcagaatcacgggagctggaattaagagaaggttgt
gaccatgctcaatattctggaaaccaaacttgggtcttctgcaagtatgtacccttaacc
actgagccatctcttcaccccacacacacatatatgtgtgtgtatgtatgtacatatata
tgtatatgtgtgtgtctgaataaacttatttttttccatttaaaagagctcatacatatgg
taatataaagaataaagcatgtatagaatttcataactactaaagagttctaaatcttga
gagaacaagctgaatgtgttatacaatataatctgaatcattaagtaatagaatgatttt
ctaaatataaatttctaatatgaatatggaaaataagaaaaaattaatatctaactttaa
acattgaatttattagtaagaacactgttgtgtatctcagatttaaaaaaaagttttgca
acaggaattatcttacctctagccatcatcagttcagtcctacagactgagtcacgtaga
caataagaatcccattttagccttggagacactgtcttagttagggttttactgctgtga
acagacaccatgaccaaggcaagtcttataaaaaacaacatttaattggggctggcttac
aagttcagaggttcagtccattatcatcaaggtgggagcatggcagcatccaggctgtca
tggtgcaggcagagctgagggttctatgtcttcatccaaaggctgctagtggaagactga
cttccaggcaactggggtgagagtcttaagcccacatccacagtgacacacctactccaa
ccaggtcacacctattccaacaaggccacagctccaaatggtgccactccctggtccaag
aatatacaaaccatcacagacaggaagtgtgagaggaggaccccagcatgatggggtgcc
aatgagccacccccacttatggtcttgcagatgtctggctactgtctgctgtggtcggta
caaaaagaggaggaagagggagagtaaagaaggatgtggggaaaggagtggggaggaggg
aagagctctagtttcctggtatcttctcttaccaaagcaccagtttcaccatgatggccc
cctcttcctccaaacctaattacttcccaagggccctgacttagagttactaccactgtg
gtgaaacaccaggccaaaagcaaataaaagaggaaaggattattttgcttatacttcca
tatcacggttcatcatctaaggcagtcaggacagaaagtagaacagagcaggagcctgga
tgcagagctgacaatgaggagcggacaatgcagagctgacatggggtcacagagggtgct
tctaatggttaatcccatggcgtgctcctctctctctctctctctctctctctctctc
tctctctctctctctctctctctctctctctctctctctctctctctctctctctctc
ttcccatgggaaacttacagggttatttaacaaaataactgttcagggcttacagcccag
aggtttctctgtgcaggcttgtccctagggccccaactggagagggagccccagtctggc
cttagctgtctcttcttcccctttgtccactggaattgatcaccaagttgcaggaaccaaa
gaaaaaaaccatgtgatctcctgctttgcctgcccccctgaaaggggtctgggtgctgg
tggtgggagtttgggggcttcttacctgtgagggtgccccgcccatacctcattccagtt
gtcagacttggatgctccagggctatgacagatgggccatggatttgagttctggtcttc
cacaaggtcctttacaaggcatcccagccgcccttcctggaagaagggataacttctgcc
gcctctttggccctgtgttttctgtttgtggttcgttttcttcttctttagtacagagaa
gcagcgacacacaagactgtttttctgtcctgttgtcagcgctcaggtattccaagtgct
tcagtgggtacagttttgttgatcaatttgcttccaaaagggttccatggtgacagcaac
atccaccctgctgcagccatgctgcagatgtcatgcgggtcaccttactccaggtgtcac
actgtccagaaaagtgtggccattgcagcctccgaggacgtacatcctgccttggtgcac
ggtaatcccaagcgcactgcggggaagcttcatgggggctatgaaagtccaggtctctgt
```

ctccatgtctaagcgctccccgctattcagctggtcctgcccatcgtagccccctgctga
atagatacagttgtgcggcactcagcccgctaaagggaagcctcggcctgctttcttata
gcacccaggatcaccagcctagagatggcaccacccacaacgggctgggccctaccccat
caatcactagttaagaaaaggccccataggcttgcctatagcctaatcttctgaaggcat
tttctcagttgaggttctctcctctcagatgactctagcttgtgccaagttgacataaaa
accagccagcagaggccccttctccaaacatgatttcttcaggctatggagctattacac
ttgctgcttttcccccttctgtagcacaaggttgcagagtcccagtagatattgaataca
aacgaggccacatctatgctcacactgcgatggagatccagctcagtggttattagaact
tatcttgtagaggacccgggttcatttcccgggatccacatggcagctcataactgtgtg
taactccagtttcaggggtcaagcatgcatatagtgtacaggcatacattcaggcaaaa
cactcatgtgcattgtggtggtttgaatagatttggccccatagattcaagtgtttgaat
gcttggcccataaggagtggcactattaggaggcatggccttgttggagtaggtgtggcc
ttggtggctctacacttgtatatcacagtgttggcagggcttggagctttctttcctaag
ttcaagctgtacccagtgtgccagttcccttctgctgcctgtggatcaagatgtagaact
ctcagctccttctccagcaccatgtctgcctgcacactgccatgtttcccaccatgatga
taatggactaaacctctgaaactgtaagccagtcccaattaaatgttttccttttataaga
gttgccttggtcatagtgtctctttacagcaataaaaccctaagatatgcataaaagtaa
gtaataaataataaataaatctaaacaacaagaaaatacctcctccaagctacagtgagt
cagtcttcctacttggcttagattctgccttgttctaggctctcgactcacctggggagg
acctgtccatactggggaggacctgtccatactgtggatcaggttgagcacacctgggga
ggacctgtccatactgtggatcaggttgagcactgtttgttaacttcatccatattccca
ggaaggctctggcttctgtccctagttgttcccaagatgccgtgtggtagggagtgtgag
cacccgtgtggcccggcgtgtgttggtgatggggacagggtttacagagcaaacaatgct
tcctttcccctcccaaatcatctattggctccctcagactctgctcttaacttttttgt
ctgctaagaatatccgtacctgcaattctcttttcttcttcatctctaccctgtgctttt
gaataaaataaagaaagccttttgactctaaaatcaaagctccaggaagtatcaattcta
gccaataggcagtgggttagaagctggttagtttcaaagccatagacttccatgtgactt
ccagtctggggatcacctagaacctcctatatttggcctttcaaaattggatttattttg
tctcactttgctgtttgttgctgtgatgaaacaccatgaccaaaagcaagttgaggaaag
aaacgactaattttgatcttgctctttgcagtccagcattaggtgaagccaaggctggag
cccagcaagcgggctcttgtgtctgaactgaagcagagaccatggagaaacagtggtcag
tagttgatctcatggcttatccaggtcacttccttataccacccaggaccacttgcttag
gggtgccactgcccagagcggggttctggaacctctcacattaaccatcaaccaagagct
taccctacagacctgctaacaggactatctaatggaggtgtttcttaaatttaggttttc
ctttcccagatgaccctagcgagtatcaagccaacaagaaccaaaaccaagacccaacta
accatcacatatttattataataatctgttgctgtattagttgtggtcctctagagtgac
aagaacttataggatgaatttctctctggattcattctctctcccggacacttctctttt
cttgttgtttatgaagcagcgtctaatatattccaggttagctctcaacttctcatgtag
ccgaggatggccttgcactgatcctcctgccatgatctccatagtgttgggaccacaggc
actgtcaccatcccaacagatgctgtgatgcatcgttcttactgatgaagaaactgaggc
ccatgggactgaggtgtgggcatggctaaggactagctcactgtgactcgaacccaagca
agtgacttatctcccctccttgcccactgtccacggtgtcctgtggggtttacaactaaa
cacgcctgtccaacaaacaccatggcacattaggagagctgagatggacatgcgcttgtc
tgtggcatggcatggcacaaggctgtgtgatgtatgcagggtttctgggggtcaatgcat
atagtgggtagaggaaaatggctgtggagtcaagactctctgtgacagtttggggccatt
gtgcttcgattctgacaagcaaaagctgaactctctgagtgtgaagcttatttatatacc
tagttatagcatttgtgctcaggggatgtctcttaagaagagactaaaaatgaactgct
gctttaaataggtagcaccaattacctctcacaatgctgaaactcctctgctttctagag
atgctatgctaatatatctggttactagattatgctgcataatctcagcagttgtgagat
atatcagaagaagatgctgaggtcacctatggctacattcaccaacagaccggacacatc
agtatccgggtgttatttagtgttggtcaatggccacactgatataatcaatgctcttta
tgtaactggcttttgatggtgattattatcaatatccttatgtcacagataatagagatg
tagaggttaaataatgtgcccagtgtcgggaagttctgaggagatggatgtagactatgg
cttttcagtctctttgctccaggcctgactcagtgcctaccatgtaggcatgaattttta
aatcaaccaaaccctagaggtttcaaatacgtcacctgctgcctcacctcagaatttctt
ggttatttttttgcatttcaagacaggatttatgtagcttgagttgtcctgaaacattca
ctcctcctgtctcaggactgggattacaggcctgtcccaccatgagttattctaacacaa
aactgttttggagacagggatagcactggcctggaactctgtttgatcaggctggcctca
catttgagatgtgactgactcagcgtcttgagagctgaggtaggctgtcccaaagccgtt
ttgcttcacagtgaatccaagctgactggagcagccctttcctctttctgagctgcagat
gacgcctctgccttctgatgtcaactccagcagcagtcggtgagatctcctgcgctgata
tcactgtgcagagcaagggtctcttgcagagccccgagtagggacttcagcctacaaagg
cctttcccttaaaggccaggcctggggcacccctattcactttacaagaagccccaagtc
tcctagaaaaaaaattgcctttagctggcagcc**cgtgggaa**aagagcctgatgccgtcag
cctctcagaccccactacccaagggaagccgtcaccacccttccttcctggcctccgat
tacatctccatctaacactcagggtcagctctgaaaacgtccccagacctcataaaagtg
ttcccattctctcccttctccttatcagaaggtgccactaggcttcgggacacctatggc
taccccatttgtgtatcagcttattgtgtattgtctcccgcggacttctatagctacccc
acttatgtatcagcttattgtgtgttgtctcccgaggctgtgagttcagagacagtgtgg
agcttatcacctcttgtcacctttatctctcaggtgccggcattgtgccaggcatgcaga
agacactttggaagtactgggtagacggtcagaaagagatggacagacagataagcattg

gtattctttttttagtgctaaacaagtgttgggtcccagagttctagcatttgttttgta
caaggtcttgctatacatacaattcaggagaacctatgtgcatagactggactggaactc
atgaaattttgcctctactttgcaagttctatgattagaggcacacagtaccacatgccc
accaggatagcctcattttccacagtaaatttgaggaatattggtatctaaaaccaagca
ccctcaatgtaaaccgtttctttttaccagccaatctgctgctagtttctttctctgcac
aacggccaacattggctaaagcaaacaagaccttactgtaggtgccactgacccagaaaa
cttaaaagctatgcagtagaggtcatgctggttcaggtgcagggtgctccgtcactttag
ggggaaacatgggatggcgtcaagggaggcaggtgatatgaggctctgaagatggagaag
atggatgaagagaggggtctggaggtgagcttccagcttgtgacaggagcgaagcgagct
gtgaacatggagagggaagcaggcagtgagccttggcttgaccactcctaagctgtgtgg
tgggatatgtgcactaggaaaaaacaaagccaagatggagggacctcacctttcagagg
agctgtgagggctgaggctctgaacagtagggtgaagtgcaatgagaactttaaaaggac
ccaggatgtggtctaaagtgtgtggatggagaactggacctgggaactcggtttagtctg
catttatggaacccatcatgtctagaaacagaattgcttgcaaaggtgttgagtttcttt
tattcttctcaacggttatgaagttttgcttcatagacgggattgcaggctccaagagtg
gggcaggataaagactgggctttctccaggttgtctacttctgtgaacgctgaactaggg
aaacaatccataagatttaaactatttttttaaagtcgcccttcttggtgggggagaggg
gagagcggtgtgcagaacttcatatagcaccccaaacgcccctcccaactgagaccaacg
ggtgtgtgtgtgtgtccgcgcgcgcgcgatgcgggccagaaacgtgcatcctcgcacaga
tgatcgcacagcctcagaagcaaacacccaggccgccaccctgtcgcctgctaagaggat
ctggccgccaacactaggggggaagggaggacaaaaacaaaacaaaacaacagcaaaaatc
ccaacataatgaatgtctcgggggatagctactcctccctcaagctaacccagaaaacaa
gcgctctacttccccggaaatgacatgcatagggcatgcatttcgtcccaaagctgaga
agccttgcaggattagctttagaggctcctagaacccaaaaagcagcatcccttgagtct
ctcaggctctgctcccagagctggtggccaccatccaaaggagcggcgccccaggcgact
gttcctgtaggacccgccaactacgcccgcctccagccgcggggcaccggcagcagtgca
gagaacgggacgcgggcggtggcttccggggcccgccggcgcccggactccgattacagg
ttcacaccaggagcccggcaggcgcgccctcgtgcagcccggctccccgcctggctatt
cttctccattcatgcagccgcccagagcagccgcccagagcagccgccgccgccgccgcc
accgtcgccgccgccgtcgccgtccgtccggattggctggcggccggggcgccggcactt
tcccacggcccgcggcgcgtgcggctcaccggcggcgctgcaggcgcggccctggcacac
ggccaggccaatccgggcgcgcggggtggggctgggcggggcggtggctatcgccgggct
ggtgtcccgggccggccccccatttctgcccgccgccggcccaccgccgcccgcggcccc
cagccgaactcctgcggagccgacgcactgccgccgggcaggggcgggctccgggggcgg
ggagcagccagcctcggcctccgctcgtcccgcccccatgcggctgccaatctgcgcagc
gaggcgccaattggccggggcacgcggttacccgggagccgtggccccgcccctgcccca
acctctccgccttccccgccctcccctatccatgggaaggggcgcaggcgtgggaaaggg
atggttgagttttaaccggagactgagcgtgagtgtgggatcAGTGTGCACGCACCTCCCGC
AGCCGAGCGCTGAGCGGCCACTGCAGTTAACTCCTCCTTGCCCGCCGCGCGACCCTCCTC
GGAGCCCACGCTCCGCCACCA

Mouse Hey2 promoter from -10kbp to 100bp TSS

>FP013903 Hey2_1 :+U EU:NC; range-10000 to 100.
tcattccccaaaaatattcattttaagatagtaggtgattcactcctatctatccagtgc
taatcacaaaacacatatcaactacgctttccattcacagatgtcatgaccatcattacc
atgggaagaatcctaaaactaaagaaaatctgtagattcctcagtgaaaataggagacgg
gtagggacaggcatagctttggaaactgtgtatggacagccaacatgaaagccaacccta
aaccaaaaaatatgtcacttgtgtgcatacttaaattgctaaagatttggttctgcataa
ttccgtacaattctgatatactgagccaggtgtgttagtgcacacttgcaatctcagcat
tttagggcatgagtaattaagtgcatccttgccttactattacttattaagatgcattgc
tgtaaaattataacaaattattgaggtactgacagatgtaaaaaaaaatagataaaactg
aatttaaaaaaaaaaagacagtaagcagatgcaatgtacagaatgaagtaaactctcagt
tcataatgcttggtcattgacaggaagtctgaggccaggcctgagccatttgaaaacttа
gtgacttcttgaaggcataaattctgatagtgtcatttatcactcacacacctaagagtg
ttttacccagaatatcatgggcatctagataatatgggggggggtgtgaattcactcct
acatataaaatatgatacaataaattccaagctgaataaagtttttaaaatgggaaaaat
agaaaacatagaacagggcaaatggaagtagccataatctttgctactataatattagaa
tagtaaattctccaggggcactgtgttgctttctactaccaaaagacaaaagcacacta
gatggttcattggcaaagtaaaacttagaataaaataatttctgaagaaaaggtctttgt
gaggcagatgcacttctctgatttgagaagcactgtctagcttgcctctgtctcttaaca
ggaatacttatttgctctcaggtgacaagaataaagctttaattctgccttacattttct
cactgagcatcatggctactttccaaatacatagccaatatttaaatacaagttacatcc
attttagcaaggtctttgtgtagaaggatgtaagtggttgttgcctaacagtaactggat
gaacgatgtaaggggctgttgtctaacatagctggatgacacatgagttataaaattcat
ggatgtttgaaaataaaagacttctgtaacaaaggcgaatttaattcagtcattctaaac
ctgtaggtgggacccatttcataggcgtcactaggctcaatcaaaatagcagatataca
cattatgatttataacagtagcaaaatcacagttatgaattagcagtgaaaataatttta
tgactgggggtcaccacaacatgagcaactgtattaaagagtcacagtgttaggagagtt
gagaaccactgccgtaacctctgagcaagtagcaagaaagagtcatagttcaacctttta

ctgtgatatttaagctggacaaatccagggatagctagctgtgttgctgtactttgtgtt
actttgaagtcaatgaagcttaaaaatcttactttaagacgttttcttaatcattgaggg
tataaccatattctggctttaattatgacatgatgaatttttaaacaaatctataaatac
ttgtatgcatgttgtgaagtaattatgtaagtattccacagagcaggtgtgtgtgtgtgt
gtgtgtgtgtgtgtaattatcttatattaaggaaaactaaagaactcaatcaaaagtagt
gttccgtgggcagagttccacctgacaatactcttccatattagtttttcattgctgtaa
tgaatacttgacatgggcctccatgagttaaagaggcatattacatctcacaggtcaatt
ggtttaaacccatggatacttggcctgttgctttgaacccatgatggcatggcaggagca
catggtacaggagatctatcacgttttggaggccaggaatcacaaagtcaagaagaggtt
gggtgttaaaattccattcgtgggcataagcattaatgaccttacttccttctgtatgac
tctatttcccaactgtctaaacacctctcagttgtgccacaggctgcagaccaagctttc
aacacatggacccttggagatatttaacattcacaatatcccaccctcactcaataggga
aatgcactgagacacaatccccatcaaatatcccactttccagaactggagtgatggctc
aggggttaagtgcttgctgctcttgcagatgacccacaattcagttccctgcacctactt
ctggctcacaacctttgtaactacaattctgggggttctgatgtccctttggcttctac
aggcactgtacacatgtggtacagacatatgcaggcaaaatactcacagataaaaataag
caagtcttttaaaaatgctcccatttctgaggctggtgagatgtctctatgagtaaaggt
attttctgtgtaagcagaaagatctgagtttaatctccaacacccatctaaaaagccaag
catgccatctgagatctttaacccaacactggggttagggcatgggcagagacaggaaga
ttgtgggagctcacagtcagcctagccaaacagtgagcttccaggtcattaagagaccct
cattcaaagtaataagatagatagatataaaggaagatgctgatgttcgtctctggtccc
ctctagacttccatgcatataatagggcacaagcatccataaacatactcacatgcttgt
aacacacacacacacacacacacacacacacacacatcccatttcccaagacacatctaaga
acatgccattaagctagctaagtaaaagcaatatgcttattatttaaatttaacttgaag
acaaaagttcttaggtgatctctacccttaaaagtctttttttcctctggattgaagttgc
tgctacaaaatgccctccacccacccccttaagtgaatctttgctgtctttgtgtgcaca
gcatatagttttctgtctactggggtcttgactttgtcgaactttatttaacagttgttt
gcgcagagttcccctattatttttcttactatttcagggagaaagcattaaatctagctca
ccacgcctcacccacgttgctcagtggaacattggtcacaggagccattcagtatcttag
tgggcaggaagcaaacaaaggggaactgtccaaaaaaattctatgatgattaataaaga
ctgatttgtctactctcagcatgtaaactacagttctatgagtattctgacccatagctc
tttagtttcatttttagattattcccactaccaccagcagctacccacacacgtacagtc
ctatctatctagtctctactgtgctgttctcagtccacacactataaaatagggagaaaag
catttcatggttaaaattaaaatacagatattcttttcccagttgattcctccaaaataa
ctctatggttagaacttttaaatttttgttcaaaactccattgtcttaaccagagtcagtg
cacataaacataactgagcaacatactatcagtttccgtggctttcctggggcaccattt
aaacaccaaaaaaagaaccactttcctctgttatccctcttgttttatttcaatttcact
gagaggttcgaagtactaagatatgatttttctaaggttctgcgttttaaaaactgcata
attcaactgccttaaaatgtggtttatagagtaaacaaaagataatgagttacagattct
aaagtatgatgatgttttttaagaacaaatgtcctaccagatatacaaacgctataaatt
ccactgtgcaagtgatagtcaactagaaagcactctctcagattgtagctgctggtttgt
attagtactaccaaagcctttcaaatgctaacaactaagtcatggcaactttcaaacttt
caattctgtaccatatttgtgtacagatacttgtatttgcagaatgacttatacatgcat
gcatacccacataaatcatttatatatttttagtaacattttgtcttccaaagtcaggct
ttcaaatctttctggtcttgtagctcctgaatgctaggagtttggattcataaattaata
atgttctcaattaaaagtgccatggaaacacatagtgtgcttttcttgcataggcaaggc
acagtgtactactggttcatatgtcgcagctgatcttggagctgtctgtgaagtccaatg
acatactgttgccaaagtgtcattgtcctggtcaacaaacaaactgttatcttctttaaa
gtatttatttgctagaagcctattcagcagaacaccagatccatctctttaaaaatgctt
agtctagtatttccaatatattcccaagctattaaatgattttgatgcctccactcagga
aacacaaacttccatgctttgtatttaaccaacagatacagagaactagccaaagactta
tccagtagaacaaatttagctccatctagggtgaaaaacaaacaaaaagcgttctttctc
tgtttcttatattgtccatattttgacaggtttataaagtactgaggcctgaaatagctt
gtgcctttccctccgtcttaagtctaaaattagtgagttattttcagtcaatatgggttt
tctttttttaaagccgcctaccacgttagtaatatgacgaggctatgaatgtgaacaca
tctaatggaaatgttctgacagatattctaagaaaatgtagacattggtttgtattctgt
gggcaaataattttaatgtttccgtggcagttaatatttcaaaatgttttactgtcttct
ggtaatgccagcctcacagattcagggatccttatcttgcatgatttgcttctttaaaga
gaaagcaagtgtttttgcccccagagactctccatttgttggagtactgttgaagaccct
ggttctgttaaagttaattaattaatactgacagcttactggatggtttgctcagcaact
tagagctattgttttcatggatatatcctgccagtgttatttttcctgctataactaata
cagatacttaggaaagaattttagacaaggaaaacaattgtttcaaattattcaaacttt
caagcctgtaatctagacagccagggaactaggttagaatatacttgatgaagcttcttt
aagttttgaaatactaagtgtgaacacttttctgattataaaaattagaggttcattgta
gttcttttcagccttggccaccaggatacgccagactatgagagcccattcatagccagt
gttttcctgctttcctgcccaggcttagtcactatgtatcttcacagtcttttcatgttg
tttattctattattccactataactaagctcagtgtttatcagacacagtagagagttca
ttgcttttgatgagaaattcattccacgccatctattttgtacccactacctgccaggca
tcatcttagaagatggagatatagttaagaatcatattcatgatagaagtgaacatattt
ccctatcaggggaggggaagagctgctagtcaaaccagcatcaaggacagagaaatttat
agacatccatttacagaaaaacttgaggccatcaatttggcctcctggagaaatttagtt

aatacagtgagtgctgacgtcctctgactattgcttacttggttttgaaaaactcattcc
ttgctgcccaaccctcttttcaaggctcctataattaagccagccttcaaccctgggtct
gtgctgagtactaaaaacaataagctctcaggaaggaaaagcttttatgaagattgcctc
tttgtggcacaaatcagcctaaataacacaatttccaggaaagggagtttggggtcttgg
gtttcctcccttgcaatctttaatattgtaacaagcaattgcacctagaagggctagcca
taaataccatccacactgtgcaactaacctggcaagaatacttgctaaatggaaacattg
ttgaagagatgatttcaagattggtgggcctggatttttcccttgctttcagctttgtgc
tgttttactggcttggctattcctatcacaaagtgaccctagattggcctgcttgctgcc
tgcctgaggttcaaaagggtattgaaatttacaaggatcttgcccttgtcaccaactccc
agggcacagcattctcacacttttaagatgatgcctgctcccaatagccctgaagtcaa
gcaagactgctcaacaaagctgcccacagattagtacatgcttatcacctaccaggcaat
tgcaaatatccttcctctgagaaagagagagacagagatagagagatagagaaacagaga
gacagagactggcttctggatgcttgcatttcaaaaggggcaaagccctgggcttcctag
tttgaactgtgtgcgtgtcgacttctcagacttaaagttctttcaatatcagaattgccc
taacttcacaaattatatataccttgctgagacaagcaaatgctctagtaggtcgtgtgt
tttgttttggtttgttttaagaaactgtgagcgacatctcaattcaaataaagaaaacac
cacagtactccctatgagagaagaaagcagcccaagaactatgtatatatccaattcatt
ccaaacttcttcaggagaatttttagaagagcggcaaagaaaaaaaatcaattagtttgt
gagctaaagtttccagtttatgggacaaggtaagacttgctcaagatcgccaaacttaat
gtaagtaggaaaactcacagtgtaataacgggtagatctcgtccggaggaatatcaaaac
gactacatttggtcgccaaaaaaatctctgcttttcccaacttcctctgctactcagtga
gctaaatcacttaagcaccaaggaccaatttagggaggggcggcaagtctacatctccct
ttcccctttagatttgttggccagcagcctgatctttctttcctaatggcatttcgtttc
taggacagtccctcctccccgtatctatctgtctaattatcccattgttcaaatctttca
aaaggaaaacgcagatagctctatgcaaagaacatttttttcttttaccctggttcttagc
cttccagtaactcactctttctttctctgaaaccagtgtcgcagagaggagatggggctt
aaagttccaaagttctctttctttctccctgcttatgccaccccagttcctccccactcc
acccacgctcaattatttttttaaataggttgaagcgcttgcaagagtttattctgtttct
acctctgacccagacgtaggacatagaaaaggtgtgtctagacaggagacaggaaaaagg
gatgcttgagaacaaccaatataaaagaaaactactctaactgggattaagtattttaaa
gattaacaaggagactttaaaattctgtcttctgccttatttgttcttcttaacacacat
gtttggcgtagcaggctctattctaaacgcttttaatatatgccccttgttgattaaaaa
gcattcaaaccaactttaaatccgtgcgtgctttctgaacgtctcctccatattctttta
tgacactgcatggcagttaagccttcaaagacaaaatggaaaaactttaaccagttgcta
ctttattacaagcaaaccatttcccgctgcaatttttgcaaccagtataattaaatgca
ctggtgtagtgagagagaaaaaaatctcttagggttgtgccaccccagctccacacgcct
ataatgatttcaggtcttgcttccggcgtttggaagattccattaattgtgtgctcgcgt
ggcaaaccttaacttcaaggggtgggggagtgaagccatcactaagcgctgggaactctc
gctcctgccccctactctagctgagaaagcgaggcctggagagctcacactcagctcaaa
cactggataaccgcagggtgcaggcctggattggacagggccagcaagcctcgggctgtc
tgctctgtccctgaggaaaagccatgctgtccgtgagcacccaggtgcccgcccagagac
tgagtgcagagctgggaagttcgccacccacggttctgcggccaagcagtgctgacccca
tcctgcctcgccaggccccgcccggccccgatgatcctgtgatttgcctggagttgagt
ttcagaagtcaggacagaaagtttcagatttctgttcacacggttattgaagacaccgcg
gtgaggaccgcacaaaagaggccagggcctgtagggaaggggttttgtgttttaacgaca
cgctggctgcagatccttggcgttactccggctccttcccactccccatcaacccaatct
gcgcccagtccagtcagtcttttgctgtctctttttctcttgtcctttcccgctgcaccg
gtctagtgtaaccaaggaatggagtttggaaagggtgccttagtcagatttccagaaaga
taattatctgtgtaaggtggagggtctcggtgattgatggatgtcttcttttctcaaagg
ccttttccaccaagcacaaagagcaccatgtggagtctctagacctccactaacccacc
cagcgctacagcgccagatggtctagctcacgccagactccccgagactgtcttgctcac
ttcctgagcgcgcggaaaagtcggcagagcctgctaaaaaatccccacagtatgcagaga
gagacagagacttaaaaacggagtctgaacaccacacctggagtttacacaatccatgct
gtacgtgcactaagaactagcgatctgggcaaactttacaaaacaaatacagtgtacaag
taaatacaaatcctctccccggatgctaaagaactccgtggctgcacacaccggagaaac
tggagggatgactgggacatttaatttggataatccaaatccgagaactttgaactcgaa
aacctactcagatttgtgtcctacaatccctcttcccatcagtaggaagaccactcaagc
ctgccatttaccgagatagttacacccccctccctccagtttctgtgtccagagatacaaa
ggaagtaaccagaggtgactaatccaacaatgcacggggacaacctcctgcagttaggca
cctggaccggtgagcgggcgtcctttatctgaccacaaccctagaggctggggagctggca
gggtgaaaaaaaaaaaaaaaaaaactttgacttaaagctttcaaaatcccctgagggtcaa
catgaccgctccggtcagccactcagcagcttgatccagaagagggacagcccagagggg
tgggtcgccgagcctagcactcccaccctagacgtcacacacgctcactcgcactcagcc
acgcgctagcggttattctttaaaccgagggtagaaactcggcgggagagatcacggctt
gcaggtgatggcccaaaacccaggagccctcgcccgacacgcccgccccatgcgctctcg
cgcctgcgcccgctcccgccgccggcggtcaaccccagcgctccactcccggctcccagg
tgcgcggtggcattcccacgcctctgccaacgcctctcggcagccattggccagcgcggg
tccgcccctccatattaaccaatagaaagccacaccgtcccagggaggcggggcctggag
agtggccagggcgggcacacgaagaagcggaggggccccgcccgcgctgggggcgtggc
cagtaccgggtcttgcgccctggctgggctgcagcgtgggAAAGAACCTCCAGGAGCCGA

CCGCGCCGCCGAGGGAGCGGCGCCTGCAGAAGCCGGGCAGGGAGGGAGGGAGGAAGCCCG
CGGGGAGCGCGCTGCGTTCCG

Mouse HeyL promoter from -10kbp to 100bp TSS

>FP005724 Heyl_1 :+U EU:NC; range-10000 to 100.
ctcttcctgtctttttcttttttcctccctccctccttccctccctccctccctccttcctt
ccttccttcctttcttcctttcttcctttcttccttccttccttgacaggttcttagtac
atatccctaactaacctggaactcccctacacagaccaggctggtcttgaactccgactg
ccttggcctcctgagggctgagattaaaggtatggcttcaaaaacaaatcttaaaaccct
cagaaaatttgagctgccatttacttagtttgcacaatgtgtctccagacctcaggagtg
gtgacttcctcttcatctgagtgactctgggcagaagtgtgtggagtggtctcctatggt
actttcaagagaagcagggctctctgtatagagacaaaaatagtgatttttctttaaccc
actatttttttcctgagttggagatagaagtggggttttctatttacatcttgcagagaa
aagaaagatgtttgtctgacacagaaaggaaattggagcactaaactgttgctccaggtt
ggaaccattccctctgggatgtcgtgttttgcctgattccatgcatgtgttggtctgctc
tagctgctataacaaacgaccataaactgagcagcatagaaacttatttctcaggccagg
catggtggtgcatgcctttaatcccagcactcaggagtcagatacaagaggaactcttgt
gagttcaaggccgccccatctacataacaagttcctagatggccaggactctaatagaga
gatgtggtctcaaagaacaaacaaatgaatgagcaaagaaccaaaaagaaaaagctcaaa
ctccttggggcagaaatccagaatcaaggattgggccctttggtgtctgctgagtatcct
ttctgtctcatcagaggccacctcactgtggggtagagggacaaagaggctgtctcgctc
tcttctccaaagacactggccacattcatgagggcagaccctcatgagctatttcctctc
acaggccgcacagtctaatattatccacagctgattgtcatcataggaatcaggggtggg
ggtggacacagaagtcagagtctccctttctttctctgctccagcaaagtcctgtcttgaa
gccttgggcgttccatgtgttatagagctcaccccaccaagaggatagcgcagccataac
tccaggtgtgaactcgtcacctgcttgctgggtgaccttgtaaagcacacctccaccgga
gccaagaggacatgctccggggatctctctgccagagaacctgcttccggagagaatgcc
accgcctctcggctgcagggatcacaccttcagagctgccgtggaatacatttccctgag
attattgccagagtgaccgggcatgctaaggacacaaacgccacgcatttcttttctttt
catttttttcttttaaataaaaataactggggctagagaggtggctcggtggttaagagc
actgactgctcttctgaaggtcctgagttcaaatcccagcaaccacatggtggctcacaa
ccatccgtaataagatctgatgccctcttctggggtgtctgaagacagctacagtgtact
cacatacatgaaataaatctttataaaaacaaaacaaaactatgtctgtgtgtctgtagt
agaggtgtggtgtgtgtgtgtgtgcaagcatgtacaactaaaccaaaggaagtcatca
ggtgttcttctctgtcacaccctgtcttattccctgaagacagtgcctctcactgaatct
cagctcagtgtcaaaaagctccagggctagaattacaagggtgagtgactgtgccctgct
tcttatctgggtattggagattgtacctgggacctcatacataaaccacaagaacactca
cctattgagccacatccccaggcacaacacatggctctctctgcagtaaggaagactctc
ctgtctaccttggaccaaggctccctcagaaccgaacgattgccagtggctcttattatg
caaggcaccttcctctccccttttccttcagaggtcagagttccatattgtgtcacgcaat
tcccgggagaccagaacgaacatctatcaccctaaattaggaagcgatgacaggcttaaa
agtaaggacaccaccagagtccaacctggtgatccagtgagtgtcactggggttgtttac
aggagtatgggtgagggattacaggagcagaaatgagtcatatgcagacagctgcatcac
cagagcccacccccaccatgagtgacacctcatggaaactgggaacccagagcgcactgca
cagcctgcaggcagctcagcgtgggggagggagatgacatttttcaggcagctggtctgg
tctgagtatcttccaggcagctgggctggatggactctgcctcttccagacagctcagat
ggtgcatttcttccaggtggcttggctggtcttggccccttcgaggcagctcagcttgtc
gaaggagtgcttcccccatagaatggactgttttgccttcccttggaacagcgtgtgtctg
aacaaacttccctccaagatggaaagttttaagctcatggaaactgctccatggcacgcc
accagccactcttcctccctcccgtctatccttccaagctagttctccaggaaatctctt
gtctctctaactggattcagtctctgtctccgagaagcgctaatacaacacagtctttct
gggccattggctcatgtctggccacactcaggagagcacgtgagtggggcttgtgttctt
aaacatctccatcatcactaagaagtgaagaagaagtgtggtttccctgacaacataagg
acccagcaggctccaatttcaaccacatcaactacttcccaaggcctggaccctcacccc
attgagctccatataaaagcatcagagaggggtttggaggcagaggagagagcctttgg
ctgggtcctaacccagtccctggttctgacattcatgtcctgggctgtttctactccatg
tgcccagtgggggcggaaccttggtgggcaaaggcagaaatggctgctttggggccttag
tgaatgatttaatttggggccagcaagacagctcagcaggttaaggcacctgctgccaag
ccggatccccagaatttatgtggtgaaaagaatcaacagcatgtttctctttcacttcca
cacatgtgtgcacttgtacacacacagacacacacacacacgcacacacacacacacatg
cacacacacacacacatgcacaccagacacacacacacacacccccataaaacaggaggaa
ggattccttaatggcctgggaacggagctcagtttatataatacttaaccgggcatgcat
aaagccctgggtttggtcaccagcataaagcaaggtatggtggtacacacctgtaatctt
atgacttgagaagtggaggcaggatgatcatcttcagccacacagttagttaaagaccag
cctaggttacatgagaccctgaaccctctaccactccaccccccccccaaaagtaaaaagg
atttaattatggtggtaggacttaattattggggtggtacacacctataataccagctct

cagggatgctaaggaggaaggatgacaagcttaaagccagcctgagctgcacagcaaagt
cctatctgaggaaaagagaaatcaaaaaggaccataccagatagtctgtatgcagggaaa
tactttcccctgtgctacagataaggcccaggtttgaggagagctgggcagggtttgggg
acccagttaggcctgagagctagggagggagccatctatcatcgtgtgtgagcatggtaa
gagccagcttctccctctatccctgcccccactcccacaaccatctgacttcaggaagcg
aagcccttccctgcctcccacagtgtcctggtcctactgacatcatgaacacatggaaga
gaaatctgtgagattccagcggggccagagtgtgggaaccaggacagatgctactggcac
tgccccaggcagagactactccagagcccctgggtgctgccaaggggctctggaatgtg
tctggagcctctggcttcctccacagaaggctgtctcgtggggcctgggaaagctgagga
ggttctgaaggccattccagctctgagcagccatttcaggacttgtactctttcaacatg
ggagtggggacgtggctgagcaccagcatcggggcttcaggtcactctcaggaaccttcc
caagggacagtacaaccaccataacctctatagcccagggctaagaaaaaaagaatcaag
cccatattgtcacccatattatacagacaagaaacagagtgtgtgtgtgtatctttgttc
atgtgtatatgttacagacagacagacagacaaagacagatggtctcactctcatcccca
ccagccccaggggaagctgtgcactgcctgtccacacatgtggctcccagcagctgcaca
ttccgtcagtgaccagctgtggtggcagctgtggaggtggagagtgagctctgatgggtc
ccaggagggacggggagggcaggaagaacctgagatgagcaggggtcagggagtgagaca
aggaagctcagagtgttctcaggctggaacacagcagaaaagcagctgctaggaagctga
catctggaccttggcacagagagtctggggaggtcagggcagccccagagtgccctaact
agcacttggcatgagtaagacgagaaagactacacagtgagataatacatggggctaaat
ctcaggcctcacaagagacacaactttgagaatgaccggcttgtaggaggtgaagccatg
ggtgtgaatgaaccacctagggagagaggacagacagagacaagggctgaccataaggga
caccctctggacaccaggcatggtgtgtcatgtcatcctcatgagcctatggcagcaaga
gtgttactagcccatttttataggtgtgaaaaccaaagttccactgtgtgcaccgggaagt
atacctgccccctctgaagatgtcattgcctcagacgcaaagggagcacagcggcaaggca
ccgcagagaagccacgtggcccaaacacgtcccgacaaagggaagtcctggttgacatta
tgctgtcttcccagggatcccagcactgcctcatccacaggaaaggtagaggccttcagg
gaccctcctgtctctcttatcactagactttgagccagcctgtaccaaacacctacgatg
tgccagactgccagacggcgggagttaacagcaacaagcccgacacagttcctgctttta
tggggattccgaagctgtccccaagacagatgtaaattattgcacaattcttaactagct
agccgctgccagagcttctctcacaccccaccctgagatccatctccaccgcagcgtgag
aggccccgtggtcaccccagcagagggccctggaaagttggttccctggatggcagccac
accatggatgctaaccatttagagcctgggccacatctgtttggtgatctaagagaagac
gggactgacctagtgtggctttggagactgccagagctgaaacccgtccctgaatgtccc
ctatttgctcagggccagagtgtagtgaccgtctgacactctgcaggagccgtctgttgg
ccaatggtgaagggctcagaagcaagcagaggggtaaatctgggcggcccttggtatgtc
agacagcctcagtctaagaggagggagacagagaaaggactgctcttctccacacttccc
ttctcaccctcattggcctggaacttgctgtgtagactaggcaggccttgaactcataga
gatccaccatgctcagcttggaagccttttcaatgcctacccatatggggcatggacag
tgaataagtagacatgtctaagataatgtaaactatgttgttggatgctgaggaaaggct
atggagaggtagcaggcacagactgatgggggggggtggctactttggggcagtcaggat
agtcctctctggggatgtgacaacaaagaactggataaagtgagatctgatatgatctga
cacaaatgaagatcctggggagaaaaagtagcagagccaagactcagaatgagagacaag
catggagcaccggcagggaggaaggcaggaagactggggtctctgcagaagtgaggcaga
agctggcagaagatgaagcttgagaggtacctagagacaagtattcactaggtggtcata
cctgtgtaccctggaccattggggaataagaactagtattgcctcccttcaatcttaagg
atactgaggcttagataatagattacacacttgccctgtgtagctgcgtgaggagcagct
agcatttggtttaggatgtgatggggaggctgggggtgatgctgagtgggaggtgacatg
ctctggtggcattgtaaaggctcacagccaagtccgggcagcgttctctgggcccccgct
gagcattcttggttctcccagccttctgagtatccttccttccttcctaggcttcccgc
tagcaacctgagtcttctcccgaaccttccaggtgtgcccagtcttttacacttttacat
tgccacacggcactgtttctacaaggtttatactcaagaactatgcaaaagagttgttga
tgtttctttctaaacacacacacacactcaatgttttaagtaagttttcagttttatgtt
gggtgcaagtggcccatggtctgcaggttttactcgcctgtaagcagttgctttgagcag
tacatctcaactggggccaatttctcccgtttggtgttacccgtagatttttctggaaaa
tactgcttgcatctagtgggaagtggttagcatttaactttctataggccacagaataac
cccaagctgcagttacccagccccgattattactagtataaaggttgagaaggccgttct
gggtttgtactagccagtgagaacatcatgggagctgtttatacaaccaaagatgttcta
ggagccacagtagggcaagaaaaaaaaaaagcaagatgtaattaatgtctcacacctataa
tcttggtgttcaggaggctgtggctagaggctcttgagttcaatatcagcctgggctaca
atactgacattaaaaataggaaaaaggagctgggcagtggtggtgcacgcctttaatccc
agcacttgggaggcagaggcaggcagatttctgagtttgaggccagcctggtctacagag
tgagttccaggacaggaagggctatatagagaaaaaaaaccaaaaaagaaaaaagaagaa
aaaaagtaaaaaaaagaatagggtgaaagaagagggtgaaataaaaaagatgaattgaaa
tatatgtattttaaatttttgtggatatatatatacatatatatgaattttaattaaatt
gaatttgaattaaaatatatgtattttaaagagatggctcacacataaaggtgctttcca
ccaaacctgagttgaaacacacactaaataaataaatagatgtaatttttttaaaattctg
ttgtgttgcaatcagaaattcaagccaattaggtttcaatttctttaggcgtgtgtgtga
aggccactgaactgacagcatagcactaggcttagagctagagtgcatggcctaatgtct
gagagctctataagataataaagccaagttatttgcctctgaaatcaaactgccttgtgg
aattccagctctccttcttcttctgccggagttgctctaactacccatctcctttcgctt

ggccaattgagggttaaatgaattaaaatttacagaacacttagaataacagttctcaac
ctgtgggctgagacccttggggattgaacaaccttctcacaagggttgcctaagaccat
aaaagaaaacacagatatttacattatgattcataacagtagcaaaattatagttatgaa
gtagcaatgaaaataatttttatggttgggggtcaccacagcatgaagctttgtattaaag
ggtcacagcactaagaaggctgagaaccactggcttaggtacctttccagctgctgtgag
aagcactcaccaaacagtaactaacaggctccgccgcctctccatccatttgccctctcc
caaagctttaaaggccgtccattacctaatgacttccaaacttaaatctctttgccgaac
cccatagtccctatttaactgtgcagtgtattttgaggacctgggacgtctctcgagaac
atgcctacctcagagcccttaccttcccctgcaaatctgccagccctttctctctcagcc
aatcacatagagcaaacaagtatctgcctttctaggaaatgcctagtgcacacattgggc
actcttcacactggttgaggttctcactgttttggcaggtgcccacagaaattatgtgag
tgctgagggcatttggaacaggagaattggtgcttgcggctgcggtggccagcagagttt
cctgatggcgaccgttcatgccagtcctatctggtcatctatgagcatgataagtttctg
tgcttggccaagtggttacgtgtgggtctgagtggcaagaggcctgttctttcccatcag
gaagtatctgcaagcagagctgactatggtgaaagtgtgtgtagtcagcttcaggtgacc
aaccccacttccctacaccaaaagctggctttcttttgtgcctgtcccagtgagcagaac
aaagggagaggactcctctggtgccctgcccaccacacccacctccaccatctccctgcc
gcccctgcaagaagtttgctctcctccctcagcttccctctgcacttctctgcgtacgat
gacctgggaggatggcagctgaatctctaggcacaaggacaggaactctcactgactaaa
tagttgtctgtggtcagacaggctcccccagaaagagaagccgaaggctcctttcctctc
ttcctctccctggtgcctgccaggacagctgtcattaaatgaactggggtgactcccagg
gataccccaccaaccaccacaccctacctaccttctccattcctgtgctccctcccacaa
gtcagaagctcaaagatcttggccactgtaaagtcagcacttgggatgcagaggcaggag
ggtcagggatcagtagttcaaggtcatcttctgctacacatcaagttcaatgccactttg
ggttctatgaccctgtctcccctcctccagccttctcagctggcaagcagcagccacccc
tttgggggttcaccaaaggacttcgaagttctgagcatcccacagtgcacgtagcttccc
caatacacacacacacacacacacaccacaaactttggtcccctatagaaggagtgac
tgaagaattacttccaaggggtcacaggcacccccagtaacctttccaaacctatctgcc
ctccctgcatgccctggagcaggaaggtacaggtctgacccttataaaaagctgaggcac
tgcaaagcgaagtctgtcgcacagaactagggacagatccggattctctgggcttccccg
tggggcctcccagggcacctgcccaaggccacccagagcgccagcccaggcagcgccggt
ggagcggagccggacctcccagcggccgatgggggcggtgaccgccccggggccttcccac
ggttcggtggcgcgtcaccgcgggggcgagggggcgccggggcgccccgggctgcggtgc
aggaaagggccctgggaaagggcggcgtcggctcccgggccggggcggggctgaggcggg
gcccaacaaccaactccagggatcgcagggctgggaccccGCAGCCAGCTTTCGGCATGA
AGCGGCCCAGGGCGCCCAGTGGCTCCGACGGCGAGTCTGATGGACCCATCGATGTGGGTC

Mouse Hes1 promoter from -10kbp to 100bp TSS

>FP020995 Hes1_1 :+U EU:NC; range-10000 to 100.
tatgttttctatttgtgtttgtgtgtgtaagaaaattgaattactatgaattactatgtc
acacagctagaaatcacctaagttccaacttgaactcaggcagcctgtctcctaaggaag
tcagccttgcaggtactctgctcgcccgattttcctgagcacatacacagtctatgccca
acattcctaatgcgagtaatcatcgggccaatcaaacctcagctggagatcactcgccac
tcccagaggaaggctctatttaaatagcaggacattgcccctgtgactttacagcctcct
ttatcactcggcaccataaaaccacaggtgtgttgggctgctctataaaaacaggtgttc
tgtgtgccccagtcacacttcacccagtgtgtcgggataggattactatctacttcttga
ctgcacagaatctcccacgaggagctggcaggaaaagagaagcaggacggtaggggacgc
aagaagtagggtctcagctcccaggcatctgctgcccttgtgcatggcctgggtgagggc
ccactggggtcacctgtcccagctgcccttctcgttttctctgccagtcttccaggagga
tgcctggcctacccactggcacttttaccctttctatctgcgttgccatgatgggacctg
cctgcttaaatcttacttattaactttacaaagatatggcaggctgcgattacaggagaa
ttgtttgagagtgcagtatctcgctccttcccacgtaccttacccgggaattgctttgt
acctgcacattgctgtgtgctggtgtgtgtttaataaccatcaataaagataggcctggg
aaaacacggacagacacagattcctcaggaaacgagtatccaggagggtgctggctgccc
acaggtgatcactgggcgtggtcaaaggtaaacccacccctctgactaagcagttaaaag
tttggaaagtaagtgtggcctgaggatcccttaactgcccatacaactgatctccttaaa
tcgaagctgattcctgtgtttatgatccagatatcagagtgtctactctgcaggaggtta
tttcccaaatagctcatttactagagaatcaagggaaattgggagtgtgagatgcagctt
agcatatatagcttaactgtacactgcttgcctagggagcacctggttccaattcttggc
accatacacacacacacacacacacacacacacacacacacacacaaataataattaagtaa
ataaataatgaaatgaacattcaataataataaaatagaggaagtgtgtgtgtgtcgggt
ggcatttctgaactatgaacttggaatgtcaccattccaaacagatgaataacatttgta
tagtgggaagatatggaagtaactgtcgaatagatacataactctgactcccgcatacta
ggtgctcaaaaagtttgttgtgcagaattaatcaactaaccagaaatggaaaaatctaac
cttcactctattcacagtcaacagcattcattagaaacaaggcaaactgactaggagcct
tccaccaaggcaacagaccagtccagaaaccaagtcgctggctgtccccagcagcaggcc

tttgagagtaactgaggagggtatagatcatgcaggacagtacttgaacttgggtacttg
gttcctaagtgactgtgggagcctgctgagattaaggcccagctggatatttgtgcaagt
cacacagtgcctggcaacctcctccaggagctaacaacatacttgatcaagaggcctctc
ctgtgaggtcaggccagcttggcatgcgccagcatgtttccagagagctcattttccatg
ggccttctaggatagcagccaagattggccctgttgcagttcagtcccacaaaaggaaaa
actcagttcatactccacacaatgtccacatactgagcaaccccaaggggacccaaaata
gtctccaccacacccacagaagttgaagggatgacagagattaaagtttggtcctgagtc
tccctttgtcctgaaccatcccgtgacctctcgggaacctcttccccccatgcggacccc
agagcaggatgcagtctctccaccccattccctggcgccatgaaaacccacttccattct
gtgagatttgatctatgactacagtgctacagaccacacagggcagatgactaaccactg
agaaagggaacaagttctagaattctttcaaggaacctcagtgggaaagccgatgtcacg
ttctaagatcttccgagggagactatagcagacagttgtgccatctccctggactctctt
cctgaactgttctctaagttcagcatcccaaaggaaaatatatagttcacacacaagcat
catctctcagcaacttgggaaatcattatttgtcttacccatcccttggataaatgtggt
attagcccaaagctcaagcaaggtctctctctctgtgtgttctctcccctaaagtcatgt
ttctgagagaaaaacttagcatctgaagattcaaattccagggacagaactattctctct
ccccatcttcctgtcccagcaatggttctcaaccttacaacgctgtgacccctttaataca
gatccttgtgttgaggtcactcctaaccataaaattatttcattgctacttcataactgt
aattttgctagttatgagtcatcatgtaaatatgtagggtatctgatatgcaacccccatg
aaagggttgactgacccccctagagcagtctctacccacaggttgggagccattgttttag
tgcataaagattaaccctaagagagaaggccaagtggcttggcttagcttggatggctgg
gaggggccaggctgcctgtacttgtggctcctttctgtctcctggaactgaggagtcaag
attccttccctcacagagaagacaggatgataagcaaacctgggcaagacagtccagaaa
actcagggatgtctgttaaaagctccatgcttcagattacccaaggtgcaccgcagcagg
gcctcttcctcctcagctgaaataccgggtaatgcagtgacccaaagtgttcttctccta
tagagagggtagggcgagtttctagatcgaaaggtggagagcctgaggctggtccaggat
tggctactccttctctagagaggcaaccacggacttgtacaagccatttcctcctggcct
gtttcctcacttgttacatgaacgaagaatctctttccgtggtgcctggagcctgtggct
tcctataatctgagataaactggaggatggagcggagcagaggagattgaaaatatgttg
tatgtattcacccattacacacacacacatacacacacacacacacacacacacacac
acaccctgctgaggtactgggagtggtatgtaaggtctcatatatgctagacagggcctc
ctaagactaagctgtatccccagccctcgactttctgagacacgatctaagttaccaagg
ctggtcttgaactctttaactcgggtgggtcttgaccttgtaatcttccagcctcagagg
gatttatagaccagcatcaccaggcccagcgcatatcatatccattcttgaattttactc
aattgatttttctgggcagttatatttatttttggttttgatttttagagagacttcgggt
ctgatgtcaccatttgagtggcttatctgcaagccacataatttcaggtcgtgggttttg
agggccctagcttcacccccacattcctaaccttcccagagcccttgagcctgtcctcac
atgcctcagtcattaacccagctggaacctttcttgccctcagtcctgaggtagcatccc
atggtgcctggaaatgccttccccacctctgagccttcaggcttacctcacagaagtctc
actgagggttaggctattggctatgagcacagttagggcctcctgagtcccccatgcctc
agccaagtgggagagttgagcagaccgtgggcaccccaccccccaccctgctgaggaaggt
cttcttggcagccaccctcctccagagcccattagggaagtgcacattcccttggtctcg
ctggctccagtgagtgttaggggcgggggagcattacaggctattagccaatgttgaaa
gcctctgttttccacccccctcccgacttctcttagcaccgtctgggcttggccaggaatc
aagccttttttttttttttgttcagaagtggcgacttatttttatcaaagatggaatgc
agtctcgcagttgtttccagtgcctctgcatggcaaccaaactcttgttccaagcattcc
cgaacctgcttttcccagtagacatctctctccttttctccatctaaatgctggccaggga
tcagcttaggtttctggggttgcagaaattaagactcattattaatatctctactttaaa
atacaggccctggctggtgaccggaactctgtaaatcccaccctaaaacaacctgagggc
cacagtactaccgaagtgggtaagcctgggctatgcctcctccacccccacaactcacc
ccttgcctcaaggcttacattgctgtatttcctccagctagcccttccctctctggaggt
tagggtgcccactaggaggcacagattgcctaaacctttctgaccccaaaatctgggggt
catccttgggtaagaaggtgaggcacttgttcgtttgagacatatttattagatagacac
aaaggggacataaagacatatagaggaacaatttcgaattcattttgagggttatgagaa
gttctctttggggattctgtgatgagctcaaagactcttatctaagaagacatcatgatg
acgatggtgatgatgatttcagtaaaggatactgatgccagatgccatctaaatgcctgc
ctgagatcaggctaaaaaagaggccacaggaaaatgatctccagcttccttcttgccccc
ggtctcgccaggaggcacccacagacaaacatgcaagtacaggatgcctggaatgtcaaa
tgtgtttctggacactcccagctgcaaggagctagctggctgccaccccaggggaaaggc
aaacacgtctcttctctcctaggctttatttttctcacggtgtctgaaagggctgtgatc
aggtgatatgtgtagggctgctcccagtacaggtgcggggcaggtaggaggggaggtgag
cgatccaccccgcccagtgtgtgcttactctgagctctttcaatagccctaccaggagag
ctcttggcaaggcagcaacctccatctctggcaggctgcagggaatccgagtgtgagaaa
gtcagtcatgcgagggagaaagaaaaaaaagctttgagtcctcgggcaaaataccaccac
caccacccctccctagctctaaaccaaacccacaaaacagtcccaaaaaccgagtgggga
aaggggagtctctcccaggctacagatacttgttttatgctttaaaagccaacaggtgat
aaagcaagacagagaagtcagaccctcacgggtggtgggttacactggggacaggcaggg
agaagcccccgttacaactgattactgggcacaaagcagtgtttaagattctgttttatt
gacaccataatgggagccaaaagacctccactcaaaacatccccactgaggcacaggact
ccgtcttcctcctgcttgtgggagtaggggaagatatgactgaaaaacattccttggaact
tttcaagtcgaaaaagcctttctggatattgagttcactgccctcgttggcgttggtggg

tggacagcaccaatttgacaaaccttctctgtccagagtaagagactaaaacctcatcta
tggggtctgtctgcaaagcgaccttgttcttgaatacttagcagagtcaagactcaggac
ctccatggcttcttaacactatttcaagagggcagtgcagaggcacaaacatatacataa
tgtttgatcacatgggtctgctgtccctctacttagaactgtgtatgtgaagtcagttgc
tcactctagcgggtaaatgttctaaagtgacagttaaggagttgtggttaactccctgac
ccatgggacagcatgaggctgcactgggagaccctatgtgacttattcatcctccacaca
ctttcttggtttgccaggaaccaaagcccaagaggcaatagaatcagactagagaaacgt
tagaagggacgatggtatcctaggttggggcatgagggcttaagagcagacagcagtcaa
agtcataacagaccttattgcctaagaagggtcttggagggaacctggagaggggtaaa
cgccccccaccccacccactgggagaatgttgttgttgagggtttttgttttgttttgttt
tgtttttaaatagctttcaaagaagcctaagaaggttattggggttgaaaagaaggtaa
ccccacctttcacctaaaggattttcaaacatacaggaaaaccccactgtttaaaaagca
accgattttctttcagcagccactactttcccatctgtttaggacatgaaaggagtgccc
aaactcattggtccaggttgcagggtaacaaagaaggcattgtttatcatttcttcaaac
aagatagggaccggcccactctgcagcatatatatattctctctctctctctccctct
ccctctctctccctctctcccaaaaggcaagtcaaacactgaggtaaaggtttatctgc
aaactctggggagggctgtcctggcgggtagaagagaggcttagaagataaaaatggtta
gaagcctgtgaaataatagacaacagctcgcccagggcaaacaagtttctaactcaagtc
agtggagtgtgtggttagtggtcaggtaacctgaaccaagtaggtagcatgtcagcctac
ctgtgccacttaggagccctctctactagtctgattcccttagatggcctgtgtctccaa
gccctgcagtccgctcttgacactttcctcagggtcacctaaggagagccctgatgtctt
ttctccactgcgaacctcctttgtggctcttcattgtcttaagggaaggttcagagtcct
tcataaagcaggatgcccaagggtcttgtgtgtggtgatctcaaatttcttacatgtcca
tttacacccgctgtgagtgttctataactgaggacatcaggttctgtgccttaaacgcca
tcggtagctcccttcctctccatccccatgactcagcatatttccaacacctcagccata
tttttctgaggtacagaatacagatcctctccaccagtagccctactagaagcttaacgt
atgactaattgttctggattctctacatccttttacttctgtctactgcctcttttaaag
gcactcccaggggaatcttgtggggaatctatagatggcagccataccacacagatacct
ggcaacgagctttctaaaggcactgttaatgaactacacccgatgaaggcttcatgacct
aaaggcacccctccggattcaacccccgcaacacgatctaagcccccaaagggaaaaac
agaatccccaagcattgtccagaaagcccggttctgtgcgcccctgcagtaggttggaga
ataaatactccgtgggagcggccactctatctctcatcgtggtaatcccagggtttaaca
gtgtctggcgttccatcacaaaggggggtgggggggcttgcccaaggtcatgcagtcaa
ggaagcaccacctcgtccgggaccagagctggagaaatctttcacatgatctcagtggga
ggttgggggaggggacgaagggacgagccggtgcgccttgtgtgccaggcctcccggacg
cgggaaagactgggggcggggatcaaacaacgcgctgggatcccgagctgccccgagttc
acggcggcgggaaaactgaggggtctggggcacccgggtggaggccagggcaggcaggag
ggaggcaggcagccgcccgggcagtgcgcaccgcccgcgccgcgcggcaaatcccccagg
gaggccgccgccagagccctggcgctcccggcccggcgcccgccacgtggcacccggcgg
cggcggcgactcccggcgcgcagccccggccagccggcagcacgcagccgcccgtctctt
cccagccgtccgccggcagcctcctggacgcagcgagggacccggggaaggggcgggcgg
cagcgaagccgctggaaccgcaagccgccgagcggaggcaggaggctgacccggccgctt
cctaagtgcggtcaggcatctcgtgaccgcggcgggcgcccggacccctccccgccgca
gtcacccgggtggtttcggccacgctcagatccccaagcccggagtcccggcgggctggg
ggtgggggggtggcgatgggggggtggggacggggaaggggggcccacgaattccccgatcgc
caccccttgggcgtgcgctccctgcccggaaggattgaccttggccggggcgggggaaggg
aggccagcgcgggggctcagctttcgggccgccgcccccgcggattcctggctcgcccgg
gccggaggaggggggccccggacacacggacgcacgcacacaccccacacgcagcgcgcgc
caatgagccctggccaggcgcaggggggcggggttttcccaggctcgagcacagcagctgc
tatttaccttcttggcttctcccggggaccagaggcggcccccgctccctcccggccggc
cgccgccggcccccgcctccctgcccccggggcgcgcgcacacacactcacacacgcacg
cacacacacacatcctctgggccccggccgcagccgcggcggcaataaaacatcctggca
cgtgctccgactccaggcgcgccctcgccggccggctgatgtcaaactgcagctcggctg
gtggagctcttaaagggctcgcgcgcgggggcgccgaggccgccttggccgcccgcggggt
gaggaggggagagccccgactcccttgcccgccgtctatccgtattgccaactgggagcc
tgcggggagaaaggtagagagagtggcggaggaacgagcgcgcccctcctgtcgcattgc
tatcaaagccccccttgttcatttttttttcgtttgaaattccatttccttctgccca
gtaggaaattattctgattgttttctggagaagcgtgaggtccaaggttgcaattccaag
agaggaatgaatgggctagagggagacaagcatccaaaagacaccttgctccgaaaaccc
tggctgtgaaggcatttgggggacggtaagggcatgtttagcgtgtggggtttagtatc
tccccaacctcatgagcagttttgactcccctaaacatacagagttcgagcgggaattcc
ggaagacattagagtaacacatcctctttaccttgttccctccttttttcaatcactaaa
ttttgtcttggcctatatctgttcaaaatatttttcaaatgaacttattatacaaagtag
ttatattgcatgcagcaagaacaataaaaaccaaaggcctggccacaaaagaaatagact
agactaaaactaagcaaagcccagaggaaagagttagcaaagggttaaaatccttttgat
tgacgttgtagcctccggtgccccgggctcaggcgcgcgccattggccgccagaccttgt
gcctagcggccaatgggggggcgcagtccacgagcggtgccgcgtgtctcttcctcccat
tggctgaaagttactgtgggaaagaaaagttgtgggaagtttcacacgagccgttcgcgtgc
agtcccagatatatatagaggccgccagggcctgcggatcACACAGGATCTGGAGCTGGT
GCTGATAACAGCGGAATCCCCTGTCTACCTCTCTCCTTGGTCCTGGAATAGTGCTACCGA
TCACTAAGTAGCCCTAAGACA

Mouse Hes2 promoter from -10kbp to 100bp TSS

>FP006286 Hes2_1 :+U EU:NC; range-10000 to 100.
atgcccgaccagaagcttcagcgaggggaggtctcctttggcggcagcgtagtggatagg
cagggcgcccgtgtctgtggtgatggccgaatttgcaccgccctggtacagcagccactt
caccacatccgggtggccaaagcgggcagccagatgcaggactgtggcaccagagttatc
tttttcctgtggaggagagccagttagaaccctatagtccaaacctgttcttgccaggtg
ctcagtccattcactgccagcctctttcaggcagggggaagaccgtgtgcttgagctaag
cttagtgtagcgggcttttggggtgaactggaacctaggcttgtgaatcccgcctctgtc
ctttagcaactgctggctggctttgcccctcaggtcacaggcagcagcgccatgaaggtc
tcttggaggccttcagggcatgaaggcaagctgcaagagactccctcccaaaaacacagc
atcatagcaggagtctgggctcaggcctggcacccaggaaacacttgagcgaatgagaac
gttgtggggctgagtaaggccaggagagatgaccaggtcaggctccaccaggctggtatc
aagatccccctgctcctaacctttgttcttcttcttcctcattcccaggtgtcccttgaa
agggacaaaggcttccatcctggtacacctctaaacccgcctccccccccccccccaga
aagaagttgccctcttgtcgactcccatgcacatggcttcaggaacaagctgtgttcttg
tgctgtagaggaggaggtcacagggcactggtgggcagggcctggggcagacagccaatg
gtgtaggtgtgtactagcagcaggctccttgagaggctaggtaaaaccctacagacacc
ctctgggttcagacctgttcttcatatatatatatatacctactgtgtctctctttgggg
aaggggctgttcatgggcagggagaaaagctcccagcagcaccccgaatctctggatcta
ggctgctgcatttgagattggcattatcccaggatctgagagcatccagcacacattcat
cagagatggctgggattaggagaaagtgtgaagcagctgtgagaggcaacgggaagtaag
gcctctcctcctctccctgtagagagaggataccacagagacacaagtggccgagattca
gacaatctgagctacgggaatctcagcaggaaggccctagagcctcctgataggagaaaa
ggatgcaggggctagcatggcatccatcaggctctggaggcagagaggaccatgggaca
gaaagtaacaggcaagaagggaccgaggaagacaccagagttccctgctgtggggtgcag
gtgcaggcgtgtgtaggcgtatgcagtctgttccctggagctcaggcataggcagctaga
ggtggcctaagcaagaccacagcgatgaaggtcgggtaccttagttcttgagaacagcct
tctcttcccactggccttaggatatgggcctgaggctctagggcatccctatagctcgag
gcttctgcataatgatggcactatgaagtcagtggcctgagttcaaggtgccatcagctg
gacaggccctgggagccttgtgtgctggggcccacattctaagctgtttatctctgggcc
agatagaaccagagattgaggtcaaccctcaggccctgttctgcccctagcttcctgggga
gtagaggataggacacttgataaaccgggcacaaggttactctttccttccacctcctcc
attggtgataaaggaggcttccggccagtgctgggcttagaatcggggaggcaggaacct
cccaagagacaggaggagtggaccatgtggctgcaggccacatggccaggaactcctgat
aacaaggccaagagataagggaaggagagactcttccagaaagatgggaggtggagcttg
cccccaaggacagcaggtgggagctgtattggcttttgctaggctactgcagatgagact
gaaactggccctcagcccttcgatttgcagctaacccaggggtttgtttttgtttgcctg
gttgattttgtttttttttttttttgtttttttttttttaagatagggtctcactctgt
acccccaggctgacttcaaactcacaacaattctcctgcctcagtctcccaagtgctgtg
gttacagatatgagccattcagtggtcactgtcagctggaaatcagcttccctttctcagc
tggttgctgggcaaccagagcgtcatcccagttccttaccttggcctaggagaccctcta
ggcctggcctgggtggccttctaccctatccctcgctatcactctggtctccccagcct
tcctccagcacatcacagagcgtttcccttctttttctctgtgctgagggctctgatcca
ctcggcagccaggactccccttggcaggtcacacccctcaacgtcaccaggcacaaagat
gccaggtggggctgagaagtgatttcgagttggaagggcccaaagttgctcatgttctta
ggtccacttattccctgaggagaactccctcacctcatgtcccactacctttgtctctga
cttagtggtatctgcatcttggcctggggtgatgtctgagaccctatttattctcactcc
agacctgaacctggtggctatgggcttctaatttggcagccaaggcccatcactgcccca
ccttcttccgccctgggccactccctccagcgagtgctttgcctactctaggagatatca
gcctaacagagtccagcttccccccaaccccacccccgggttctcctaatatcacgcagc
caggtatctaccccagtcctcaatctcaggggcccactttatctaaagccttttggaaag
agcacaaggctcagcttagccacgaccatgtctattccacccgtctttgagccgcaggag
ggctggagtcctctctgggcccaaactgtctcttagagtggactcacctgcaccctgcag
ccaccctgtgtgagcagccactgcaggcaagagaggtagcctgtggcggcggcgtcatgg
gctggtgtggcgccgttgcgcgcgcgggacacggctgggagggcaacctcctccaccaag
tagcgcagacagtgcagcttgcctgagcgggccgcatggtgcaccggcagggcgtctagc
gagtcgcgcagagaaggccccagcaggccggcggcgtgcagggacctcagcacgtccagg
tcgccccgccgtgccgcctgcagcgcctgctccagggccatggtgtcgccctcggcgccg
cgatccggcgctcagtgggctccccggggcgtcatgcgggtggtcccaggctccaggagc
aacctcgccgtgcagccgtcggaggagtgcggacccgggatgcagagagcctgccagccg
gctctgcgatcccggggactcaactccagctctgcagcgctctggggcggggaccccgaa
gagtgcccacttaagcctgggtcccgcccccgccacgcctcctctctgccccgcctcccc
tgccctgagccctcccctatccccggcggccagcaagggttggtgcgcacttttctaatt
tgctgcgcacaaaacctgaataggattctactaccctccaaacacagacccgttcactca
gctgcccagtggcctctatgttttgttttaggttgctggggacacaagccagcaagtgac

ggcaattacaaggagagacaaatgtcactagaacctggcaaatgtgagttagaaaatatt
ttgtcgggctggagagatggctcagcgatgaagagcactgactgctcttcccaaggtcct
gagttcaattcccagcaaccacatggtggctcacagccatgtataatggggatccgatgc
cctcttcctgtgtgtctgaagacagcaacaatgtactcacatacatgaaataaattattt
taaaaaagaaagaaagaaaatattttgtcacaggcatcaagaaggtgcccgatgcttggt
ctggttggtaagaagggacgttcaaagccagggaactagacgccactgcccagaagttta
aaaagtcccaccaagtgcagaatgcaactgccctcatgctcaggacttcaaggttcctct
agagtacaaagtctagacccaagaaaaagatgggagatgggagaaagcagaaagagaaag
taaggagggagtcagcaaaatgactgggtaaaggggcttgctgccaagcctaacaacctg
agttcgatcccagggacccacatgatggaaggagagcctgagctaccgaaagttgtcttc
tgcccccacatgcgcagtgtagcaatggcccccaagtaaataaacacaatgattagaggg
ggggaccctcaaaactcatatgatctatttctttcttaagtaaaaggaagttaggactta
gaactgtttggaccagggtgtggatgactctgattactcaggttggtgtgtgtgtgtgtg
tgtgtgtgtgtgtgtgtgtgtgtggtggtggtggtggtggtggtggggagtggacttgaa
ggcctgggcctgccaaactaaggaccagaaaaggaggacgtgagggctggaggctattgg
agagacgctccagcgccttcgtgcaaagaatcgctattgtgagtgaggaccctgggaagt
gctggagggtccaggcaggtaagcactagggtcaaactaccttaaggggcagagctggaa
acaggtcatgggagctggagaaggcaaggcctgctgggctgaagcagaggctcccagaaa
ggaggggttgtgcaagctgtgggagcgcagcaagcatatcgggcaatcttgaaactgctc
gcgttcttcctcttcgtctcccacgcacagcggaggtcagtcagaacccagccccactcc
ccgggcgttgtttccatcactgcctagctcctaccagccagggcggtgctggaaatgtaa
acggaagctgtttgcagaacgcaaagagtgggtctcggggcagtctcagataccattccc
gttttcaccacatggtggcgccatgcacggtgtccgcctgagctcccgggtgagctcaaa
cttcgtcgctgttcgcggcatgctcagttgagtttccaaccacttccgcctagctggtaa
ggcctcattcctccagaggacctgcggttactgggacctgtagtttcttttcagaggttt
ccagattcctcacagtgccatagcttcgctgccgctatgtacttttgaactaagtacat
tagcataccccaacaggcaggtgccccttaagaccaacaagtgtcagggaaccaaactaa
gatgctggacctggcttctactcccctgtagcttctttgacagaagtcttgaaattcttc
caccctacaaagttggtgccttgaccctggatactttgcgtgtttttgtttgtttgttta
ttgtttgttgtttttgtttattgttttgttttgtttttgtatggctcctacgtcaaatgc
ctctgagtcggtaccaactcggccagggacaacgacatgagacaggtgttactacacatc
ctggctgaccgatctctcagattccccgaggacacagctaatattcagactgggagccag
gccctttcagctgtctgtcctccctatctgactcttctactccaccaagtcctttccagc
agtcttaaagggccctgtcgtcagagacacagtataaaaccccttaccactacccaggcat
ggtgggtgccaggctcttcattcaaatagttaatccttaaggatgtttttgtttcgtttt
ggtcttttgtttttttgtttttgtttttgttttttttcagtagctggccttgaacttgctag
catctcaggctcatcctatttcttccttatgatgctagcattacaggcaagaaccacctc
cagaggggtccaactctcattttatagctgtggaaacagaggcatgagtggtttattttg
tggtgtgtgtgtatgtgtgtgtgtgtgtgtgtgtgtgtgtgtgtgtgtgtggtgtcacaatg
ctcatggatgtcagaggacagcttgcgtgagttggttttctccttccactaagtgtatcc
tggggattgaactcaggtcgtcaggttagtgggaggtgcccttacccgacaagccatttc
acagtctttttaaaaattaattaatttttaattacttaatttagttaatttatatgagta
cagtgtaactggcttcagacacaccagaagagggcatcagatcccattacagatggttgt
gagccaccatgtggctgttgctgggaattgaactcagggacttctggaagagcagtcagt
gctcttaaccactgagccatctctccagccctcacatggtctttttttttaagcttaaggt
gacacagatgagaagagacaaacgtgaccgtccagtgtacttccttcctctacatcccag
ggtggaattttctcttccggaagctccctctgtctctgccccctctgggagtgagcttag
ggcctccctcctctcctctgagggtctcttcttatctccttctgctggacgcatcaatgc
cctcacctccaagctgggtgaaaattaattctcaggcatctcccatggccaaggactggt
acctttctcagtaccctaggaaggaccggggtagagcatgtccccatggtactgaggatc
accctagatcccctagagcctgagccccactttctgaacaccctactacctcaccaggtt
ctcctgcttctaaagaactccatcttccagatccctagcaaactcccagaatcctttggt
tgaagagaggggtgcattacctaggttaaaatcctttgctgggtgtcgtggcgcacgcct
ttaatcccagcactcgggaggcagaggcaggaggatttctgagtttgccagcctggccaa
caaagtgagttccaggacagccagggctatacagagaaacccttttctcgaaaaaaaaaaa
tcttttatagcgggggtgagcaggatagagacttaaaattgaggtatctggtatagcaca
gggagagtttgctttctgccctagggccttttttttttttttttgaatatactttctttat
tgaggggtgacaaacaaaaacaaaaagagcaaacatgtaaaaacccagggtgctagaaat
acaaactcgggggctggtgagatggctcagtgggtaagagcacccgactgctcttccgaa
ggtccggagttcaaatcccagcaaccacatggtggctcacaaccatctgtaacaagatct
gactccctcttctggagtgtctgaagacagctacagtgtacttacatataataaataaat
aaatcttaaaaaaaaaagaatacttaaaaataaaaaaaaaaaaaaaaaaaagaaatacaa
actcaattcagactcaagctcgtctagaccctggtcataatccccagtgaggtgcctgtg
aacaccaagccagggacggggacaggagtgaattggaagccaagagaaagggcaggaagg
gatctcctaggtctcccggtgtcacccctgcagtggcatctccatcttcccaatgactga
agatctgccaggccctgtcctcttggccccaacctcaccctaaccagagcatgaaggctg
atggcagtcggtcctcccttcccttgcttagtcctcacttgctctggcctccagccttat
tctttcccttcacattcttctccttgattagtagcaggttaggtactgtagaaagccaca
gtgaggggctggtgagatggctcagtggttaagagcaccgactgctattccaaaggtcct
gagttcaaatcccagcaaccacatggtgactcacaaccatccgtaacaaaaatctgatgc
cctcttctggagtgtctgaagatagctacagtgtacacacatataataaataaattaatt

taaaaaaaaaaagaaagccacagtgaggctgggggtcagaagaggtggggtggagacggg
gtgaagacgagggaagagctgtcctagggcccctctcttcatgggatcccaaactgtaca
accagctcttctttctcgtccacgcagatctgagaaagtgcactataggcatatgcagct
atcttagagacctgctgcaagtcagagaaggggataggctcgctggccagcacttggtgg
ggctggctggtgagagatggcagcggtggcagcttcttccaatgggtcagactgctgcta
agcacagccaagcgggtactgtactgccttgctcggtccgtgtactcatgctgttccatg
ccctgggagtctgcggcagacacatcaatgatgttgctagctgtcttggcaaggatggag
gaaagcagggcctactcatctgtgggagctgaaggtaggctatggtagttgggcttggct
ccattgagggctttggtaggggtgctactggggtccagcaacagcttcctctcctcccga
tcctggtccgagtcttcatttttgctgctatagcagcaccccatggcaggggttgggccg
ggcactcaggcggtgctgaggagggacagcgtctgtcaggagcctttctggtcacatgcc
attgggccttcaaatagtggaagccctgggaaggaatgtttccacactcaccctcggggc
tacgagcagtctttgatcagtgtagggtgggcttggggacactggactgagttgggggca
agggacccacacaacccctccatccccagacagggtttccctctgtagccttggcgtcct
ggaactgaccatgtagaccaggctggcctcaaattccaagatccacctgcccctgcctct
caagtgctgggattaaaagcgtgtgccaccactatcaggctacacaattctttttttaaaa
atgaaaattcacttttctttttaactgtttttttaactgtttttttgtccgtgtgtgaattt
gtgcatatgactgccatgcccgagaagtccagaaggggggcgctagatgccccagaactgg
agatgtaggtagttttgcgtgcgcaatccgatctgaaacgcaggtctctgcaagagcaat
acttgcttttaagcactgagccttgtaaactcctctttgagctcttaaaagataattaat
gactgagaatggtagcacactcctttaatcccagcgctcgggaggcagagtttggctgct
ctttgtgaattcgaaactggcctggtctacatattgagaggctagcccacaggcatgcta
gacccgactgtgggggggaatcaggcagccccaaggcctgctgcgacaaatcctcatagtt
aggactgttgggttggtggaaatgaggaagcgaaggccgaaaacagcgagttcggagctt
gtacaaagtaactccttggaggttgtactgggggttcttgcatgccacagagagaaata
gggctgagcgctcctgtccaggctgccctgggccccttccctggtacactggttccactg
tttccgaatgtctgccgtgggagccccttccaggaatttggggttagtgaagggaatgggg
ctcgatggcaggagggaggggtcctcccagtaccctggacagagccctccctggctccgc
tcctcaagcacctcctactggctctggttgttcgggtctcgccttcggagcccaagactg
tcccaaaattgcaacagggtccgtggaggtagccgttgccctgtcagccgacccagggag
gggagcccgcagcagatgggcgggggacgcctgccagtttgcagcagcaacggccacgcg
ttgtggaggcgtgtctgggcccgctggggcccagaggagcagccggggcacacgcccagg
accgcctccactcgtctgtcatgtgaccttcgtctgtcccACAGGTGGAATCTGGAGTCC
AGAGCAAGTTGAAAATGAGATGAACTCCGAGGACCCCGGGGGTTGCCTCTTCTTGGGAAG
CGGAGCTACGGTTTCTTTTTC

Mouse Cnn1 promoter from -10kbp to 100bp TSS

>FP012536 Cnn1_1 :+U EU:NC; range-10000 to 100.
tattattattattattgactatgaatccctgactagcctggaacttgctatgtagactag
actggccttgaactcactgagattcacctgcttcttcctcccaagtacttggattaaagg
cctgggctaccatgctcagatagtttgattatttttatgtgtgtgtgtgtgcgcgcgcgc
gcgcacttgtgtacaatgcctgtaaaggccagaagagggcattgagtctgaaactggagt
cacaggcagttgtgagctgcctgccacatgggtgctgggaactaaacttgctcttgctgg
ctttgaaggcacatgtgacacttaagtgcaagcaaaacactcatgcacataaaactttaa
aaagaataaagtctttaaaatgaaaaggtaccgtggggcttaatgtgtagttcagtggta
gagtgcttaatcagcatgcataaaagtcccgaggttcagttctcatgccagccccagagc
agtgaggtagtggtgtgacccatgtcagtgcgtttgcaacccccagagctgccttggattc
ctgggactcgcgggggaagggagaacagattcccacatgttttccttgctcttttttgta
tgtgttttagcttgtgcttggatgcactcacacaagtatatgaatgtaataaacatttaa
aaacaaacagggctgaggaatgcagccccaagtggctgatttaaacaagtgctttcactg
acacctgtgtccctgtgtcagtcctacgtggtctagaacacaatagtatatttgaggccc
caggtgtccctctttatcatgaggtccttaacataaccctaggaaaatagtggagagtgc
tggcagacctcctggcagccagaggaccatgcttcccatcaccagccatgagtcaccgtg
acaacacataccctgggtatgacgcacacagaaggcatactgtcacctctcctgtgctct
tcccaaaacgcttcagtcagggccaactacatagagaatcactgctgaggggttggcacg
ggggtcaggctcacagacgactgaaggacaaccagtggagagtctatagaggcgtgagac
tgaaggcacactctacttgcctataatccccagacttaggaagctgaagcaggagacttg
tgaatttgaggccggcctcgactacataatgaaatccagtctcaaccaactaaacaaaca
agccaaaaagttcatttatttttttacagcagttaacattaagggctggagagagagctc
aggagttaagaacacttactgttcttactctgctcttgcagagaacctgagctcagtttg
caggacccatgtgatagcttgtaactccagctccatggatccaacccctctgaatactgca
tacacatacatacactcatgtgtacatgcaaacacaagggagcacatatacacatgtact

actttaaaaaaaaatgttaacactggggctggagaggtggctcagcagtttcttaagagc
accaactgcttttccaaaggtccttcttgcgcgcgctcgactggccaggaagaacgacgc
tgcaacaggatccttctgcagatgtttattgggagagcttgattgtagaggcgaagagac
ctcgagcccagaactggtgctgcttttataggcctaggaggggcgtgtctcacacccgga
ttggttatgcactaagccttatttgcatgttcctcatctgattggctactctctctcagt
accttacagaacctcattatcatacctcatttgcatgtctcacatctgattggttatact
ctcagtaccttacagaacctcattatcatacctcatttgcatgtctcacatctgattggt
tatactctctctcagtaccttacagaacctcattatcatacctcatttgcatgtctcaca
tctgattggttatactctcagtaccttacagaacctcattatcatgcccgggccaggcag
tgtctttgcaaaaaactttactgcatatgtacacattggttgtttgtccaaacttatgcg
tggtggccagcagtagtcagtgccactctgcaaccgcacatgtggcttcccacaggtcct
gaatacaattcccagaaaactcatggtggctcacaactatctgtaatggaatccaatgcc
ctcttcttgtgagtctgaagacagctacggtatactcatatacattaaatttttaaaaat
gttaacataagcatctaggaataagtatacaggagaactctgtaactagtttcacaactc
ttttctaaaaattaccagttgtgtgtgtgtgtgtgtgtgtgtgtgtgtatgtgtgatatg
tatgtgtaagtaaatgtgtgtcaaggtgcctgtgccctgtatgtgccctgaggagtccag
gggaggacatctggtgtctttctttattgctgtcttattccctgaccacgaagcctctca
atgaacctgactcctgttgtcgggaggctggcttactcagccagcttccaggacccttcc
tgtctctgccccagctcctagcccatgctgggctcacaggcgcaggcagctctgcctggc
ttttatttatttgttttgttgctgttttgagacaggctatctctgttatgtagccttcac
tgtcctggaactcaatgtatagggtaggctggccttgaactcacagagatccatctgatt
ctgcctcccaagtgctgggattaaacgtgtgcaccaccacactcagctgcttttttttt
ttttaacatggtgtactggctggttttgtttgtcaacttgacacaagctggagttgtcac
agagaaaggagcttcagttgaggaaatgcctccatgagatccaactgtaaggcattttct
caattagtgatcaaaggtgaaaggccccttgtgggtgggaccatctctgggctggtagtc
ttgggttctataagagagcaggctgagcaagccagtggaagcaagctagtaaggaacatc
cctccatggcctctgcatcagctcctgctttctgacctgcttgagttccagtcctgactt
cctttggtgatgaacagcagtatggaagctgaataaacccttcctccccaactgcttct
tggtcatggtgtttgtgcaggaacggaaaccctgactgagacagatgggttctagggatt
cgaatccagcccctcattcttagtgggtatgaatgcttgcacccacttcaagatggcgtt
gctcgtgccattgaaggagaagaagctcatgggagtcagacttggagagcttctgagctg
gataatgatgcgggatttcacccccagtggcattgcaggagcctttcggagagggtatga
ccggtattacaagtacatcaacgtttgaaaggcagcatctcagggattagcatggtcctg
gcagcctacgtggttttcagctactgcatttcttacaaggaactcaaacatgagcggcga
cgcaaataccactgaagaggggtcactggagggcattgcatggccgagcataactgcctg
ccccactccgacctaggaagaattcaactggctgaaccttcataccctgactgagaacta
gtgcccaataaaaggtgactgattcacaaaaaaaaaaaaaaaaaaaaaaaaaaaaaaaa
aaatgcttgcacccactagaccagtttataaatgcttgcacccaggaggccgggagatga
gtcagcaggtaaggcacttgccaccaatcctgagggcccaagtcccattcctgtgactcc
cataatggaaggagaaaacatttctgcaagttgtcctatgacctccacatatactggcac
acaaatacaaatgaatgaatgaatgaatgaatgaatgaatgaataaataaataaatgtta
aaaacgagcaagcctcagaagaacaatttcagtgcccattacagaagggatggaggttca
taaatgtgaggacagctgtccagagccaaggaggtggccgtggggtgggggggtgagggtg
tgtgcacatgccagctgtcatcccatcactcagaagacacaggatcaaaagcttaagtct
ctcctgaactacatgttaagttacgtttaaaaagtatttgactttatctgtgtgggtcat
gtgtgccttggtgtggatgtggaagccggaggacattaaataagttggtcttctcagggg
tcctaaggaaaagtttgaggtcttcaggcttcgtatcaaaccactgagtcatttcagtga
cccccacattgacttcttaatcagctacctgagacatgtatttttttttaaaggcaatcc
agaataaagtcaacctgtctaaggccaggaagccaggaagcattggctcacgtcctcatc
ttagtagcggttttattgctgtgaagagacaccatgcaaggcaacttataaaagagagca
tttacttgcggagcttgcttacagtctcacagggtgaggccatgaccagcatggcgggag
tatggcgggagcatggtgggagctcggcggcagacaggcaaacatgatgctggagcagca
gctgagtgctcatatctgacccaaaagttggagtcagagggacaaagtctgacatggact
tttgaacccacatctaaggacacatctccaacaaggccatgcctcctagtccttcctaaa
tagcccaccaactaaggaccaaacattcaaatgtatcagcagatggatgggggaggcggg
acatcctcatgcaaaccaccgcagccccagagagagcaaacggtgaggagttctgcactt
accatctctgtctggctgcagcggaggctgcatgcagtgggagaatgtgagacccgcatc
ttttctcttctcttcttcttcttcttcttcttcttcttcttcttcttcttcttcttcttct
cttcttcttcttcttcttcttcttcttcttcttcttcctctctctctctctctctctctc
tctctccctccctccctccctccctccctccctccctccctccctccttccttccttcc
ttccatccttttttttctttttctttttttttgattttcgagacagggtttctctgtgta
gccctggctgtcctggaactcactctgtagaccaggctggccttgaactcagaaatccgc
ctgcctgcctcccaagtgctggggttaaaggcatgtatcaccactgccaggcaacccgga
tcttccactgctcttgtgtttagggatgaaatctccctctattttcccccaatttgatcc
tgccccatcctagcccctccccacccacccccttccacccatctgatccatctgatgt
ctattctatttccccttctgagtgggattcaggcatgaccccatgggctctccttgttac
ttagtttctttgggtctctggattgtagcatggttatcctgtaatttatggctactattc
acttacaagtgagtacattccatgtttgtctttctgagtctgggttacctcactcaggat
gatattctcaagctccatccatttgcctgaaaatttcatgatgtcattgtttttaatagc
tatgtcataatattccattgtgtaaatgtaccacattttctttatctgttcttcgtttga
gggacatctgtgttgtttccagtctccattacaaataaagctactatgaacatagttgag

tcctcgtcgtatggttaagcatcttttgggtatatgcccatcagtggtatagctgggtct
tgatgtagaactattcccagttttctgagaaactgccaaattggcttccaaagtggctat
ataagtttgcaatccaccagcaatggaggagtgttcctcttgctccacatcctcgccagc
atctgctgtcacctgagtttttgatcttagctattctgacaggtgtaaggtggaatctca
gagtcgttttgatttgcatttccctggtgactaaggatgttgaacatttctttaagagag
ggctgccaagaaaaactggtgtagtggagtttaatcactcatgccaacatacaaaggtat
tgaaatgtgtggggaagtgttttagggagtcccctcaagcttagggaaacaccagtttta
ccttttccttctttcctatttgtttgtttgtttgtttaatatttatttatttaacttttta
ttttttgacacagggtttctctgtgtagccctcgctgtcctgtaacttgctttgtagacc
ttgaattcagagatctgcctgctgatgtgcaccaccactgcctggcttatttaaaaagtt
ttgtttgtttgtttgtttttttgttttgctttgttttgtttttcgagacagggtttctctg
tatagccctggctgtcctggaactcactttgtagaccaggctggcctcgaactcagaaat
ctgcctgcctctgcctcccgagtgctgggattaaaggcatgcgccaccatgcccggctta
aaaaaagttattaattaaatttttttgttttgttttgagacaggttatcatgtagcccagg
ctagcctggaactcagtctgtagtccatgttgacctgaactcctgatgcccctgctccac
ctccgagtgctaacctcacagctgtatatcggcaaacttgaaagattcccgcgtttcttg
taggagtgggaaacaggcactgtgggcctgtggttaggtggtctgagactaggatgggac
cagcgacgaactccaggatcaggatgccaagggaggcccatagagcaccgcccctggggt
acccgggctccccacccactgccccctcggccggccgtgcctgcgctctgacttcagagc
tcccagggattctataaatggccaagccgcggcggactcgggagccccgcgagtgagtca
gcgctgacgtcagccgctcgcctcggcgcagtgccctggccaccaggggtaccagacct
tgctgtagcaatagctctcttggtggaagaagcttttggttatgaattaattcaaattcc
actctacttccttcaggctgtatgacctgtacaaccgactacacttctctgttcctcctt
agggctgttgggaggcacgggttgctacgttatttgatgcttagcccaatgggtctgtct
gtctgtctctcactctcttgctatctttgtctctgtttctgtctctgtctctcctttccc
actccctctctccttctcttcctcctgtccagactctcactgtgtagccctgtcaggcct
gtgtgtgtgtgtgtgtgtgtgtgtgtgtgtgtgtgtgtactcacaaattatatata
tatacatatatacatacaaagatatatatatatatatatatacatatactatatatatat
agagagagagagagagcccatgataacagcattgataatagcattggttgtagaggtgca
gtgagtatcgagcaggctatatggtcacagattagacaatgcatgcctgtaatcccagct
acatagaaggtagagagaggcagattctagttcaagtccagcctgggaatttagtgagac
cgtgtctcaaacaaggttttctttttttctgtgtctatgtttgtgtgtgcagtgcccttaa
aggccaggccagtgtatcagatcccctgaatctggagttacaagagattgtgagccaccg
gatacgggagccaggaactgagttcaggccctctgcaagaacagtgtgctcttagccacg
gagccagctccccagcctgagaagttttgtgtgtttgtttgtttaatattctatatggtg
tgaaagcagacatggggccaactggggagagaaagacaatctaatataaaaaggggagc
agggaggaggagtggtgggggactggttgacagcgtgcctgggtgtggttgtccatgatg
gacatgtcagggctgggagttgaggaaggagaatcaggagttcaaggtcatcattggcta
gattgcaagtttgatatcagcctgagccacattagacattgtctcactcaccacctagaa
atgttagaataaacacttgtatttcactctgtgtgtgtgtgtgtgtgtgtgtgtgtgtat
gtgtgtgtgtgtgtatgtgtgttcatacatatgtggaggtcagggaacaactttcagatt
tctccttccatcatggaggtcccagaaatcaaactcaggtagtcaggcttggtggcaagt
tccttcacctgccaggccacctcatcagcccttctgttcactgatctgttcagcatctgg
aagcatcttcagtctacactgtttgcttgcagtggacagtgagttatacttgaagattgt
cacatgctgggtaagggcttgtcactgaggcttgtccactgacatgtgtccccaacccat
accaaaaaccaaacttattattatttattattgttgagacagggtcttgccatgcaactt
tggcttgtctggaactccctgtgatctgcctgcctctgcctcctgagtgctgggattaat
ggtgtggccctccatgccttgccagatgtgccctttatatatggccaacaaattgcaggt
tctaaagtgccattaatgcatagaagactgatgtcatgtccttgacatgatgtgggtgga
gcatccaactccatggtccagatgagagctgtctagatctgtacttacagaccagcctga
tttggatagagataggggcgtgttcgtggcccaagacctgttaacctggccccaggggct
caggtggccagtgaatggatattggaaccagatccaggatatttccttgtttgttttttc
atttcaaatagcccagactggtcttgaactcatgtagctaaggatgaccttgtacttctg
agcatcctgcctattcctcctgggtgctgggattacacacacaaattaccaggcttggtt
tatgtggtcctggggattgagcctagggtttgtggatggaaatgctctactaacaaatct
atgtcctagcctcacccttaaaaatgtctcattacatgtgtgtgtgtgtgtgtgtgtgt
gtgtgtgcgtgcatgtgtggcttgttctctcattctattgagtcccggagttcaaactct
agacatcaaacttgttggtaaacaccttaccattttaaactaatgtgtgtgtgtgtgtgt
gtgtgtgtgtgtgtgtgtgtgtgtgtgagagagagagagagagagagagagagagaga
gagtcagtctcaaggccaggctgtgctggaattctgtgtagcccaggctggccccaaact
ctcaggcatccttttgcttcaggttctcaagtgctaggattgcaggcacgggtcatctac
gagcttagatctaggttctttgctgttccaattccttatgagtgactggagaggacagaa
ctgggtactagattcttcaaagaaataaagctttgctgaagttctccttttgtgccagctt
tcatactgggcaccctggaggtgacatttcctccctgccctttactgcacccttgtgagg
caagcacagttgttagcccctctagagatttggcaatagggtcccatagaggggaaggct
ctgtgtagagggttggtgaatggaggtctgtcagatcatcttgctatgctaggggcttgg
gtgggggtgcagcggttctgtctgtggactgaagaaggagatcaatgacctctgagataa
ggagtctcagagacgggacagttggcatggggagaagggtggaaaaggggtgggctgtat
gagaacccctctcccagaataaggcattcagccccctaggtggaaacaatgacacagtca
gctcccaataccaaggctctgacatcaggaggtgggggtggccagagtatgtgtggggtg
ccacgcctcttggcagcccccgtggccaatgggacaggcttggaagagcccagggctggc

ttctggagcttcaaaaacgtgtgaggagggaagagggtgcAGACGGAGGCTCGGCTGCCT
GTTGCGCTTGTCTGTGTCATCTGCACCTCTGCTTTGCCAGAGCCCCCTGGCCAGCATGTC
TTCTGCACATTTTAACCGAGG

Mouse Myh11 promoter from -10kbp to 100bp TSS

>FP020792 Myh11_1 :+U EU:NC; range-10000 to 100.
cctcgtgcatgcctggtgtcttaggaagccagaagatggcatcagatttccagaaactag
acttatagaccattatgagctgccatgtgtccagtgggaactgaacgtgggttctctagc
agcaagttctgtgaaccactggactatccctccagcgtggcatgtgtacctgtaacccag
catgggtggagcagagccaggcagatctcagtgtggatcaggatggcatttattattcta
cctcagcctcccaagggatggtcttaaaggtgtatctccccatgcccagcttatctttgg
attttattttatttagttatcacttttattacacttatatctatttgtgcatgcatggac
catagtgcatatgtgggggtaagggacaacgtgtaggagtcagttctgtccttccatgta
agttttaaagatcaaagttggagtcagactttgtggcagcatctttactccctgagccat
cttgcaggctttaaaagtactttctaccatttcctggatagtgttacaatagatacaaaa
caaccccctttttgtgttccacaggagggctcagctaacaggcaatcatagtggttttg
ttggccctacaatgctgattgcacacttgtccttcctcctgagtccattccttatatctg
agatagtggcttacagggctccacgctgcacttcactccaaggggaaaaaagaaaaaaga
aaagctgagcctgtgcttgaagcctgtgacatcagcactcaagctgaggcagaaggccag
cctgggctaaacagtgagaccctcttgttcctctaccctccaaatgaagaaacacttgaa
ttattacagttagtctctaataccaaacagttatgatttcttcagtgatgcttaagacat
gagtagagttcacaaagatagttcagcaggtttgctgccaagcctcatgacccgagttca
atacctggacacacatggtagaaggaaagcactgattctctcaagttgtcctctgacttc
tgcatgcatggtagtacagtacatgttgtaaggaaaactcataaagtactaacacaatgc
cctataacataagtgcttgcttgtctgcctgttgggatttgcagtgaatattgacacctg
tgtgttttctctagatgaccacgtgaggaaggacacagggccaagaaccacaactgaaga
gcttcctgctgctgcacaagcagtcagcagatgatgcgatgcatacaccaggctcatcac
ctcagctgtgtgtggagtaaccgacgtattattcccaatgccatcaattagaccaccact
gcttgtaaatgtttgagtgtctgcattcagccactcatggtttactgcatctgtggaaag
ctgatctgtcgtctcgcttgctggatgccactggggaaaatttattgttttcaggatgta
tttttaaagttctcatttgtgaaatctgaaagggctttttagtactttgtatagggtttt
gttttgggtttttttggccagctctaagggctgttgctatgctgctggtaaagcacttccc
tccctatgcaaggtcctgggttcagtcctagcactgaagaaagaaagcacaagaacaggt
ctttgtccatgtgctctgctcattaaacttttttcagctagaagtatatggacctatggg
gaaagtcattcatgttttgaaaaaatatctaaaggaatattaaaaccagaacttaattta
tatgaagtttgatttttttaaaaaatacctgaattattattgcctgccctggctagtttta
tatcaacttgatacaagctagagtcatttggggagagggactctgaattgagaaaatccc
tccatcagattggcttatgggcaaacctgtagtacatttttcttgattcatgattgatat
gggagggtccagcccacagtgggtggtgtcacccctgggcaggtgatcctgggttcagta
agaaagactgagcaagccatggggagcaagccactaagtagcactcctctgtggcctctg
cattaacttctgccgtgatttctctcagtgacaaactgtgatgttgaactgtaagctgaa
ataaaccttcttcttcccaagttgcttatggtcatggtctgtctgtctttctttccttcc
ttctctctctctctctctctctctctctctctttctttctttctttctttctttctttct
ttctttctttcttcctttctttctttctttttttcaagacagggtttctctgtgtagccat
ggcggtcctggaactcactctgtagactcagaaatccacctgcctctgcctcccgagtgc
tgggattaaaggcgtgcatcaccacgcccagcggtcatggtctttataacatcaatgaaa
actctaatgttgatctttaaactagataacaatactctttccccaagaacagtttagctt
ctactagggaatttaatgaaaaggtaaaggggggaaataattattttaactttgctttaag
taaaacagtttgttagataaataatgcaaaactaaaagtctgggctggactctgagcatt
cagaacaggtgcgcaggttcctggactcagtgtgctcatcacagggttgctgggttcaga
gtgcatctctcagcttctagcactgtgactcatgcaggccaccaatgcctaaagctgcac
acatccccgtttccgttttaagtctgcactgactagagttataaattccattgtgttctc
tgttcagatataaataccagcttctcccggagggcttggttaatgttcagaagtgtcagc
tatggatgctatgctatcttaggaattgcagttatgtagggccagatgaagggaaaatat
tggtgtttataattttggatatggatgtgaaatcattaaagtggaagctacacagaaatg
cagctttatgcattccttttttattttttatttatttatttttaaatttttatttatta
ttttaaataagtacactgtaactgtcttcagatgcaccagaagagggcgtcagatctcat
tacaggtggttgtgagccaccatgtggttgctgggatttgaactcgaaaccttcggaaga
gcagttggtgctcttacccaccttacccactgagccatctcaccagccctttttttttt
tttttaagatttattattataaataagtacactgtcgctgtctttagacgcaccagaaga
gggcatcagatctcattgcaggtggttgtgagccaccatgtagttgttgggatttgaact
caggtccttcggaagagcagtcagtcttacccactgaaccacctcaccatcccagcctta
tgcattcctgagtcttgattctaacctgttttactctgaataatcatttaatgcagctca
gctcatctctgtgtagattgtcacgtcactatcttgtcatccagaggggggatgactggg
gctgaagcactgggcacgtggggtctttgaaggcaggcctggtacatatgtgcacttgat

atccaccattcttacagactgccacaacctgaggaccaggtatatttgaagagctacttt
aaagaggggaaaaccatctatttttaaaccatgttaccatttttgttttttttaattatcc
aaagaaagaaccattttgtattcctaaaagctgaagaagtgccaggtcatggtgaaatat
gcctgtaatccagtaaagtacctgggaggcccagacaggaagattggagattggtagttc
taagctagccctgactgtgtagccagaccttgtgtccaaagaaagaatcaaggggctgga
gagatggctcagtgtttctcacttttgcttcttcagaggctctgatggcctcttctgagc
tctgagcatctgctctcacatgttcctatgcatacaacatagctaaccagaaaccctgag
gatctcacagacaacaacaaagagttgagacagtctactgtagctgtctatttgtgcagg
atttataaacactgtcagctgatttacttcctacggcttcttaaaaaggtttgtaagctg
gaacatttggtttcaagacaacttgtcactatatagaccagatggcctaaaactcgtaga
tctctgtgcctctgtcttccagagagctgtaattatgcaccatgcctggctacgctgaaa
aaaactcccaagaaaggaaaacacaggtctagaagacccctttactatcctcacaaacagt
attggtatctcactgtctgtttcttgaggttagggcaagttatcttctagaaataacaag
ggaagtttatgggaaaacttgaagtcacacaaaacaggatgggaataggaccagatggct
gtaggagactgggttattcaaaacttgggggaaaaaatgtctatcaagcctagggctgac
ttctggagatcataagtttaagactagtgtatatgcttgtgtagaataaacagatagctt
tattattatgtgcaagaacatgtttgtatatgatttgcatgcctggctgattatgtaaac
ctgattgttcctttagcaaaaagccaagtgtctggaggattgatggttaagaatgtgcct
ttaaaggcatctggaacactgcttctcagacacttagcattctatgtttgtggcaaccac
catatgaggaccgtggtctgcatgtaatacttcaaataaaagtgagaccaaactcctgga
ggcggctcagtcagggaaagtgctttccatgcaaacatgatgaaatccccagatacccag
gcacctaagaaacagggcacagctgtagcttccttctatcacagagctgggaaggtggca
gcagggtgatccttggacattgtgggccaatctgtccagtcattttagtgaaccctgggt
tcagtgagggaccctgtctcaaaaagtaaaattgtagtttggcagcatatacttttgtct
cagtactctgaaagtagacacaagcagattttggagtttgaggccagcctggtctacata
gcaaattgcaggcctgtcagggctatgtagtgttgtgttgtctcagaaaagagagagaga
gagagagagagagagagagagagagaactttcagttgcccgactaacagaagtggggagc
actgagtgccctcactctcctcccacaggccctgtcttctcccactgtctgaatctgttt
gagagctgcagttgtcacagaagagccttctttgtcacctgacaaagcatggtgatgaga
gttcatggtggcagtacctgacacctttgcccacctttcccaggacaccatgtggcttca
accacttcaaccttctaggattggcatacctcccatagctttgtggtttgttagctttct
agaaagtgcagaatcctgccttttttattagctatctgtatacctactaaaaaccggccta
gctgccttcaggtgcttgcagttaacaaagctgctgagctggaggtgtgatggtcagttt
taaaggtctgggctacttggtgagaccatgtcttaaaaaaacaataacaaaaccatgctc
ctataaatgcccacgcacagaacttcatgagataagtccatctcttagggtaaatttccc
agtagtgtcttagttacttttctattgctatggcaaagtattactactaagatattacta
acttaaataagaaaggatttattgggggcttacagttccagaggactagaagctatggcc
atctggcagataggcaggcatggtaatggagctgtagccaggagcttacatactgatcca
cacgcaggaggcagagagtactagttgtgggaatggcatgatctctagaaacctgaaagtcc
accccagtgactcacttcctccaaaagaccacagctccaacaaggctacagctcctatac
cgtcccagttctaccaagtggggaccaaagattgaaacatatgagcctctggggacattc
tcattcaacccaccacccagaacatgtgtaggtttatgaaaatgcaaagcttctgaccat
tccctatggaggcctttccaatagagacatcatctgtagttataggaagaccagaatggg
acatgagtgaagaggaaacagcacagcaggtgcagtctcctgccttgagacccagtggtg
accagtgcctgggcttggaacagttcccactgatctgtgagacagatcttccatggacct
gggatgaaactgtgtgtgtctgagtgtctgtgtctgtgtgcgtacgcacacatgcatttg
aggccagaggagaatgtcaggtggcctgtcactgtgctctattccctcgagacaggagtc
tctcactgaacctgttggagctaggctggtagccagcaagccccggtgagcctcctgtct
ctgtctcacagcacacccgttaaaggtatgtgtggccatgtcccacttttacacgggtg
ttgtacagtgagcagcagcactcttacccactgagccatctcctcaggccagctgatata
gttttaaatgattaaatctttagcacctgcaagagtcagccatgcttggatacaatcttt
gattttcctaaagctagagggcatcacatactgaggcttttacaagccaatagctattta
aaactatttgctagaaaaaaaaaaaaaagaccccaaagagaaatttccccttcatcgtcca
cttcccatcacagaaaaacatacaatttatttgacaccacccaaaggagcattttgttaa
gtgacttttctcctcttcttacaataaatgacctcttcaaccacaagaaaaatagaagcc
tctaccctgttctaggtagaacttccttctgaagacttcagatatcggaacttctcacag
tggacagaaacttcccaagtgactgtgaagtgaacatactgtccctgggtactgcccaag
catgccaggaggggatgggtggtttatacaaggccggcactgtcattaacaacccagcaa
ggtgggggaaggcagaaagcctttcctaaggcagtgtcacataaggacatggataacccc
agaggttcttggctagtgcttagcagggctgagatcagacttttgggcctcagtgggaca
gcgcttgcctattgtgagcaacactcaagactcgggggaacagtaagttggtctggggag
atggctcagtagttacagcaagaatcccaacactgggaagacagacagagggggtccct
gggctttgctgtccggctctgcagtctagcagcctagcagaatcaacaagctccatgtgc
agtgagagatgctcataaaataaaatggaggggcaacttatggacacaatgttgacgccc
acactcgagaatgtatacacagacacagtgtaaccaccagccatgccatgaatggaccca
ggttggaatctcagctcctctgttaaccttgctcttattggccagatgatatatactctt
tcaaacctggatcctcagcagtagatgctgacgaacctacttcatgccatcattctgggc
attagatgtaaagaaagcagtaaagtttccccttttcttgactgaggtgatgaggtctgaa
ttccatctctaacacttatataaagacacccagacggcactggacaacagacacactgta
accaccaagcatcccagcccagctgtgagagactgtctcaaaaacaaagtaaaaacaaca
aaatcaatgtcagatgtgcacacattggatcccagcatgtgtaaagcaagtttgttgcca

gcctggtttacacagagtttgaggccaacgagctagaactgtgtatacagtgagaccctg
tggtagatgggtcctgagaactgacatctgcgattgacgggtgtgcacatctaccacatg
cacaacacagtttccattaaaaaaaaatgctaacactaattgattggggagcagggtgcc
ctactgcttacacgtgaaagtcagagaatgatgtgttccattcagtcacgtggctcctaa
ggatggaactcaaggcagtcttgggcagcaagtgcttttgaccagtcttactgacccagt
ctctccttgtactgaaattagttttgtttcaaaattgataccattctttaaaactcagct
gtgctccttggaattgacttcactgaggcctgctgcgggagtgcccttccttcctaacac
ggggatggcaagctctgggctggttccagactggga taggtgcaggtgggtcctgggctt
ccctcttccattcctcctgggctcaatgcccagacggtttccattccttttacgtgcagc
tgcgaagaggctttggggaagcagcctcgtccatcatgtggagggctcctccccacctc
tacatcgaggcagccaagctgctgtccttggctctgtgtattgctgcccagtgaggctgg
gatggggttaggaatggggatggggaggaccaagatccagatgttttcaagtctgagaag
caggtgagcttggtcctggacggatatggaaggggtccagatgggctgggatatgaaagg
ccacacagcacccctgttggctttgtacacagtgatccgtaactcagctctccagagtga
acattggtattaaacagtactgagcttgctaaggaccctcacaggactcagtcttctggc
ctgcaaaatagggctggggcaggtttggccagaatcatccttgggttggaagaaccagct
gcacctgggtctggagctcctgtctgagcactggggtccctataccgccccgcgggctca
gcgggaggctgcgcgggaccatatttagtcaggggagccagagccccgctggtatgcca
cgctgggaattcctgtttcgagaattgcgcctggccttttgggttgtctcccgcccagg
cccaggagggaggaccagcccgggacctcgagggtccgcgcgcggggagcgaggcgtccc
cggtctggcgtggggccagctctgcctcgacttccttttatggcctgagtggtgtgtgtg
caaggggggggggagggggagggagagagagagagagagagaaagaaactgactttag
ggacataacagatgaaatgatagagacagaacaaaaatcgtcacagggaaatcaaagcta
gagtgtaatggagagtgtgtcaggtccgacaaaagagacagggagacagggacctagatc
catacagggctaagggaaagagattgagaagtatcccttgctgaggggggacagctgtga
acttgcgggggaccagcaagtaccccgcattctcttagggtcttagcacgcatcctccaa
gtgccataatgcactctttctccagcagcaccccgcttttcaacgatgttcagagaaacc
acgttattggttccaggcaccctgggattatatttaattttggttgtagcatgaatggaa
ctgcaaagaacaagttaggaaaaacaagtttccctttctttcccacacattcccagcag
tcactggaggatatgcggtgacctgctttgcaccttgcagagttcaaaaaaaaaaaaaaa
aaatcacctttcccctccctttgctaaacacaaccgccctcagatctaagaggtggcagg
tgaatgaagaggggatgaaggagagtgtgggaggtatcaagcctccagtatgtatgaacagg
aagaggttaaaatccagctggaatggacctaggggagaaattctcacgtttccctacag
actctgtataccggattccttttctgtaaggacccaggatctgggtggctacagggagcg
aagcctgaggctgtgggtcagtgcggctctgttcctcacctgcaggggcgccgcgaagg
gaagaggatcctcccactctcggacgtccgacagccacctccccttccactctcagata
gcgctgactctataaagccaggcgtccgaagcttacagagAGATTTGGACCATCCCAGCC
TGGGATCAGTGCCAGATCCGAGCTCTCCATCCGGTGTCCTCCTGCTAATCCACCCCCGGA
GTAGATCTGTAAGTAGAGTTG

Appendix D

MVSCs treated with Fc or Jag-1 ± DAPT or DMSO for 48 hours

